THE 13TH RESCEU INTERNATIONAL SYMPOSIUM

JGRG31

October 24 - 28, 2022

The 31st Workshop on General Relativity and Gravitation
Koshiba Hall, The University of Tokyo
(Online-hybrid style)

Volume II: Contributed Talks 1

Contributed talks

C01 – C40

C01

Starobinsky Model Revisited

Shi Pi (皮石)
Institute of Theoretical Physics, Chinese Academy of Sciences
Based on arXiv:2209.14183 with Jianing Wang

JGRG 31, 2022-10-23
RESCEU, University of Tokyo, Japan

Contents

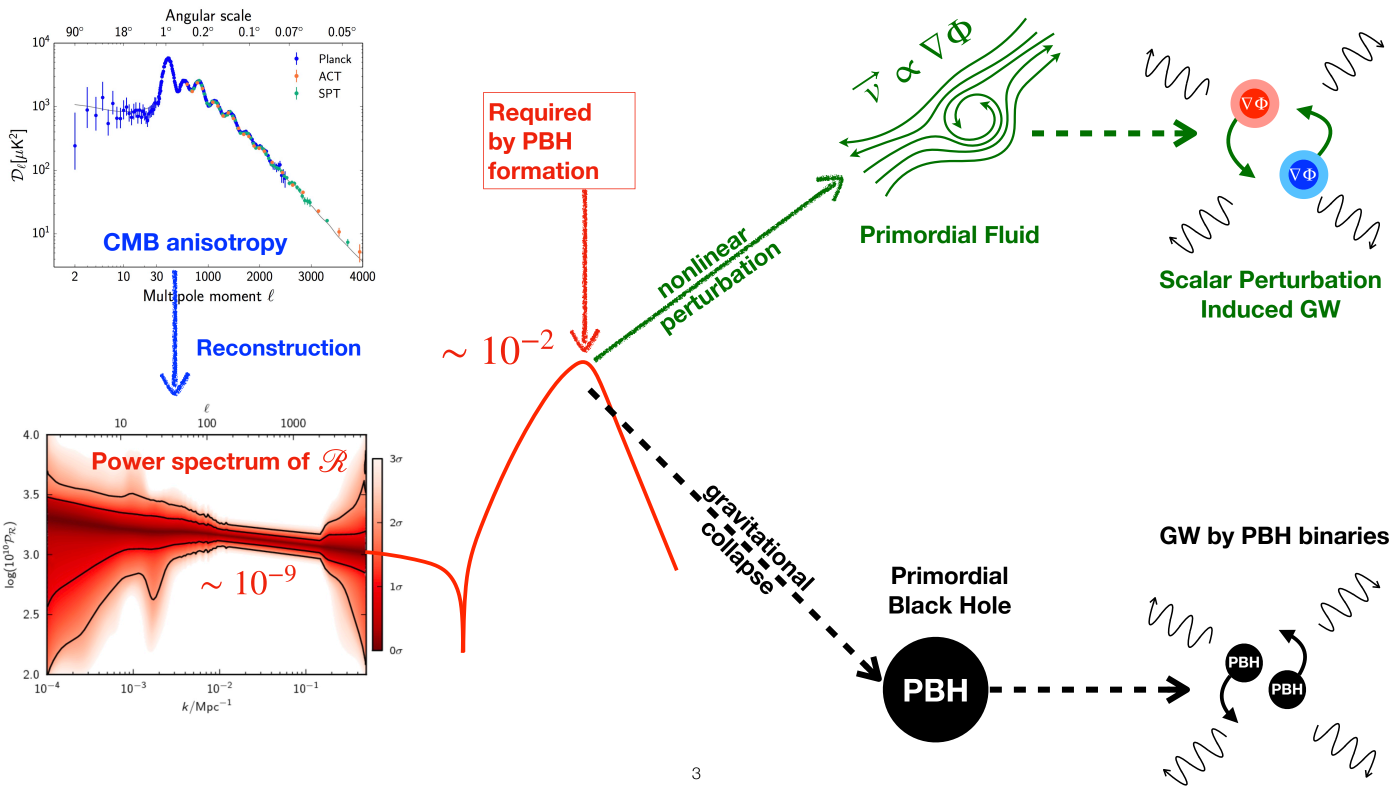

Ultra-slow-roll Inflation

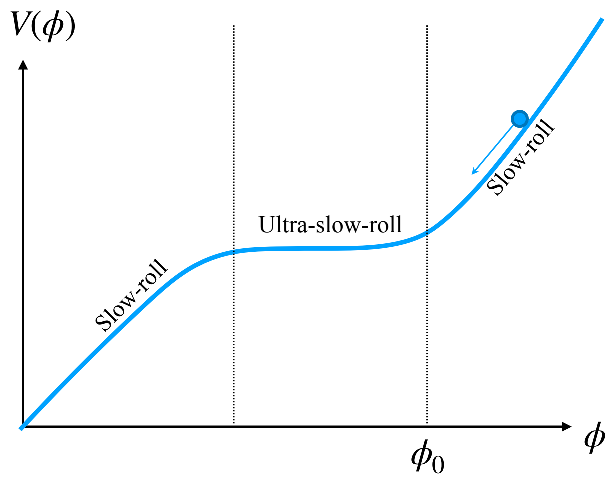

Leach and Liddle, hep-th/0010082;
Tsamis and Woodard, astro-ph/0307463;
Kinney, gr-qc/0503017

Ultra-slow-roll Inflation

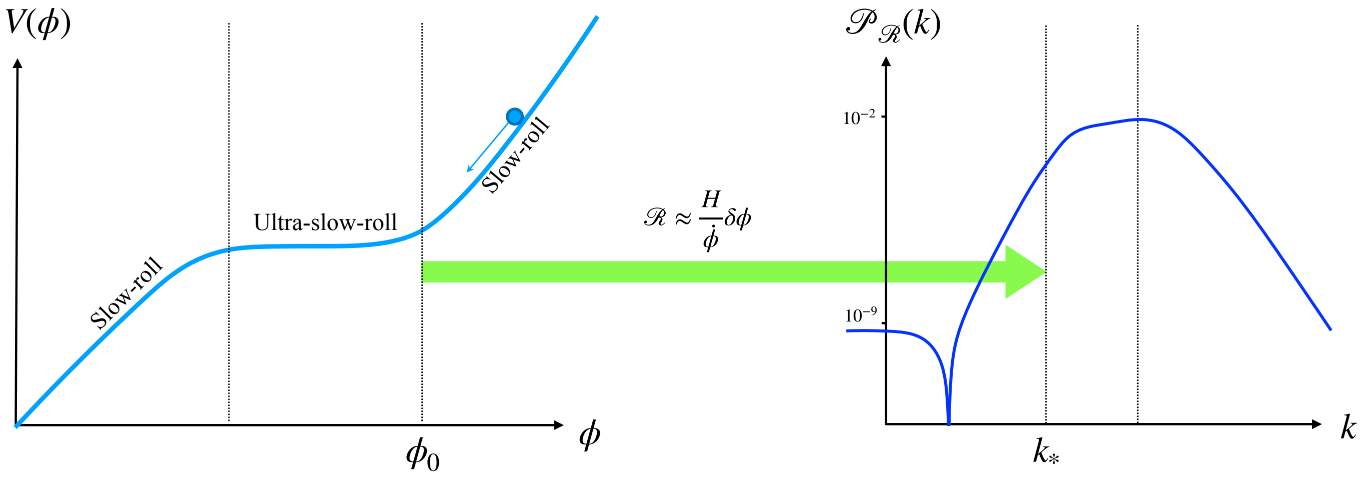

Leach and Liddle, hep-th/0010082;
Tsamis and Woodard, astro-ph/0307463;
Kinney, gr-qc/0503017

PBH abundance

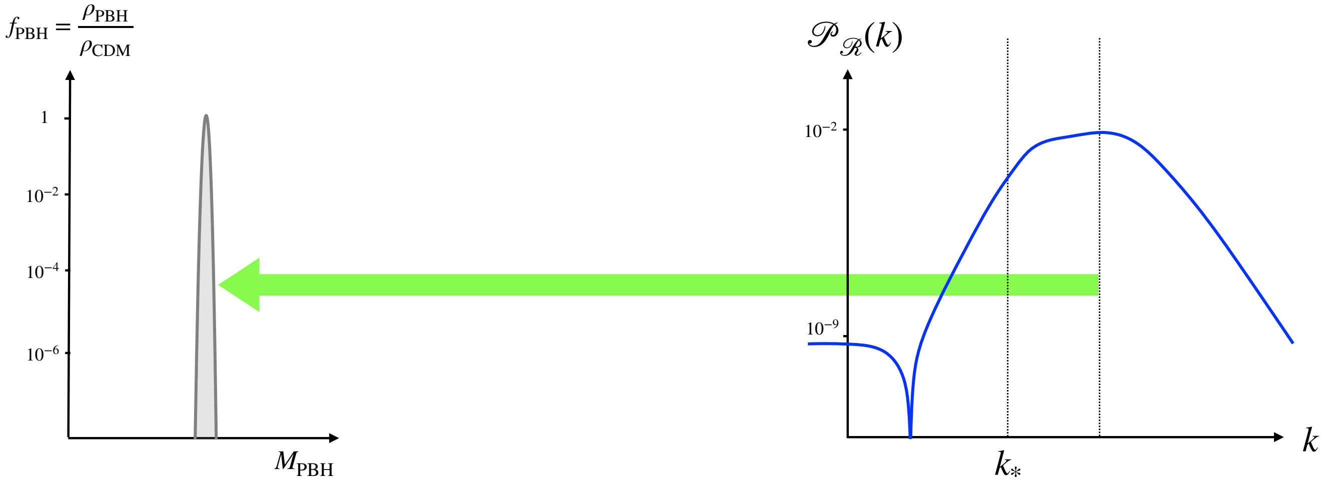

Press and Schechter, ApJ 187, 425 (1974);
Carr et al., 1607.06077

Starobinsky Model

Starobinsky's linear potential model is a ``prototype'' of the ultra-slow-roll inflation.

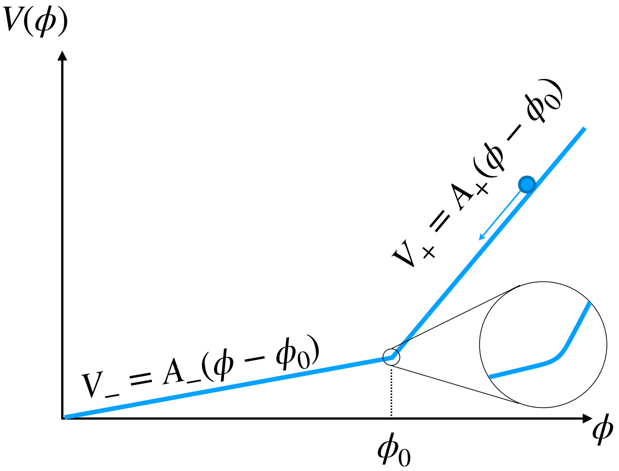

Spectrum of adiabatic perturbations in the universe when there are singularities in the inflaton potential

A. A. Starobinskiĭ
L. D. Landau Institute of Theoretical Physics, Russian Academy of Sciences, 117334, Moscow

(Submitted 9 April 1992)
Pis'ma Zh. Eksp. Teor. Fiz. **55**, No. 9, 477–482 (10 May 1992)

If the potential of the effective scalar which controls the de Sitter (inflationary) stage in the early universe has a singularity consisting of a rounded change in slope, a step of a universal form arises in the spectrum of adiabatic perturbations. Along with this step, there are superimposed modulations. If the singularity in the potential is instead a rounded jump, a hump appears in the spectrum.

Starobinsky, JETP Lett. 55, 489 (1992)

Enhancement and modulations are the characteristic features of a sharp transition.

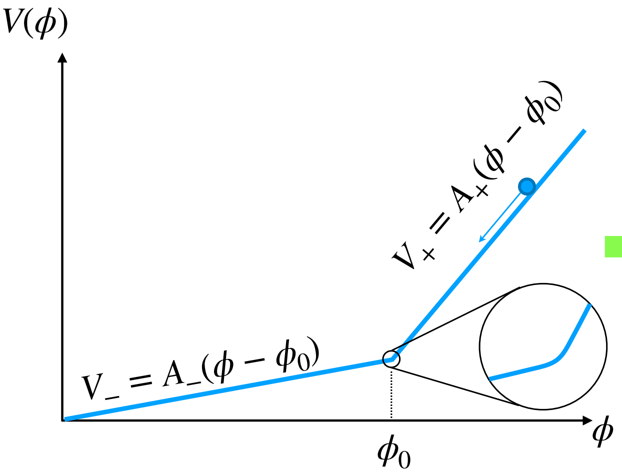

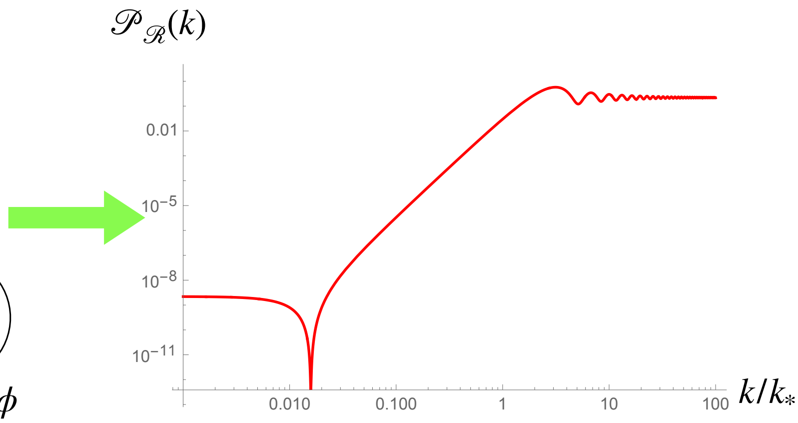

Leach, Sasaki, Wands, Liddle, astro-ph/0101406;
Byrnes, Cole, Patil, 1811.11158

Enhancement and modulations are the characteristic features of a sharp transition.

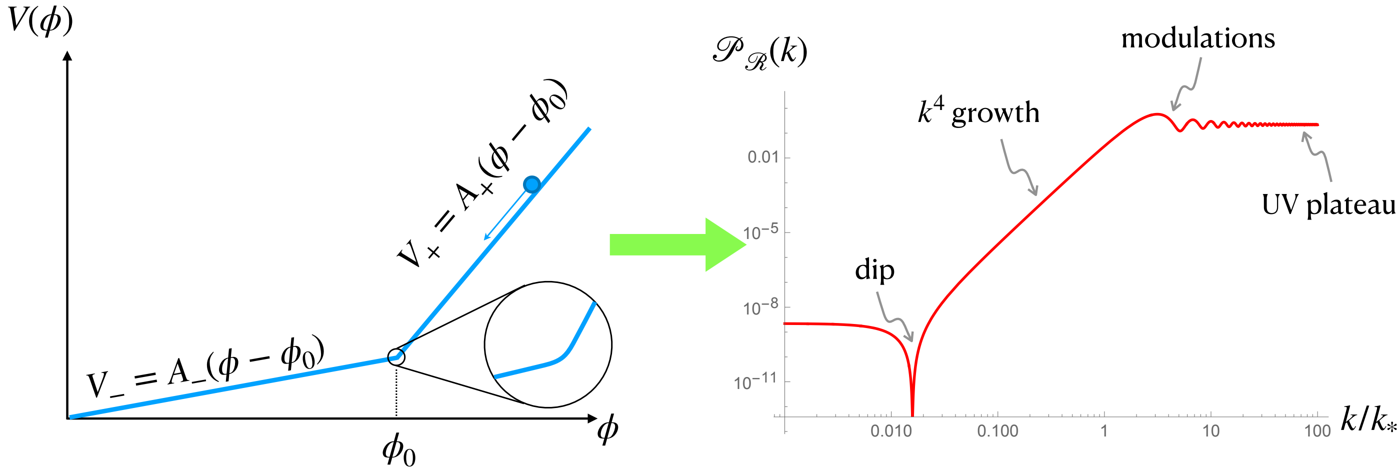

Leach, Sasaki, Wands, Liddle, astro-ph/0101406;
Byrnes, Cole, Patil, 1811.11158

The main enhancement is given by the suppression of slow-roll parameter ϵ.

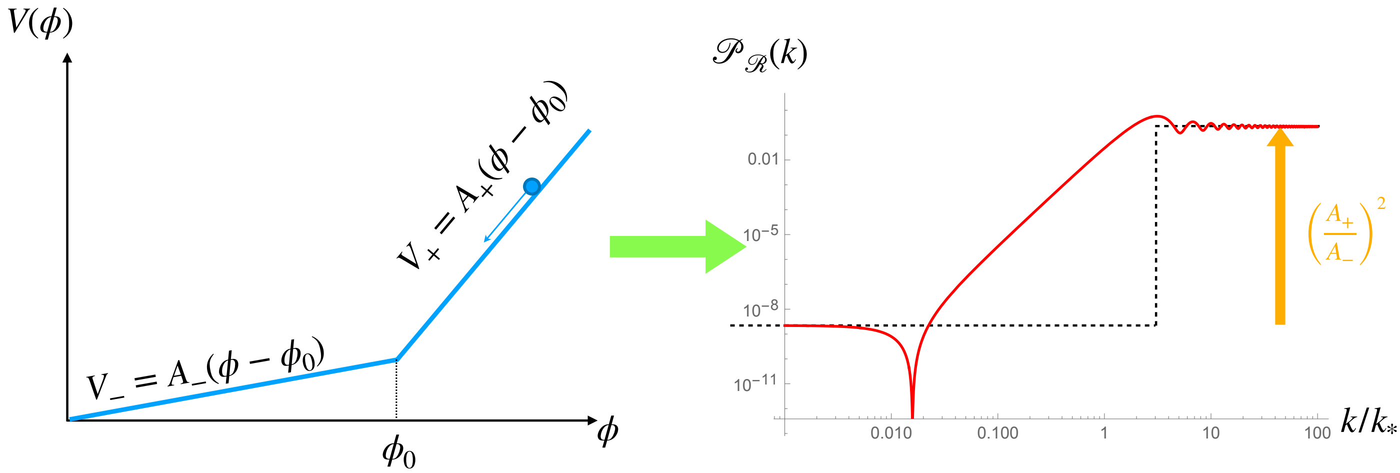

But the modulated oscillations are crucial to determine the height and position of the peak.

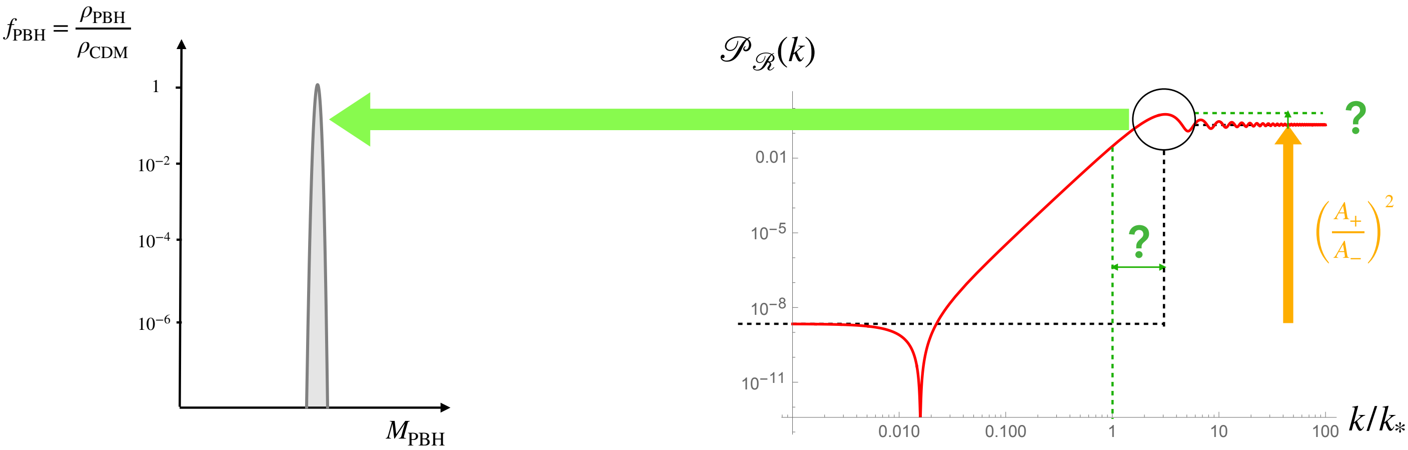

Therefore it is important to determine the position and height of the modulations

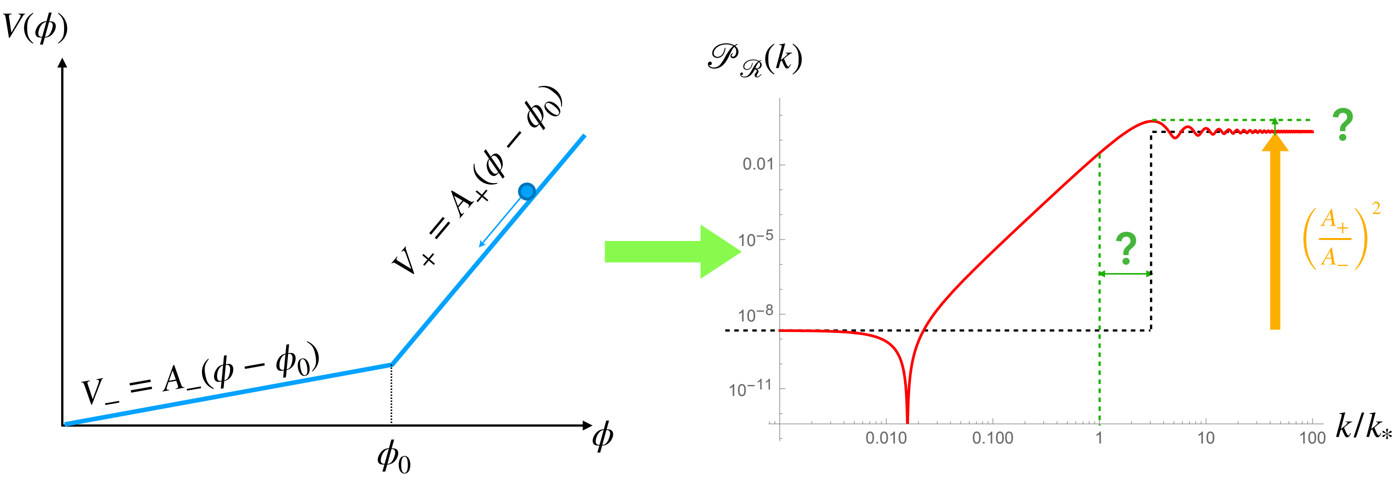

Contents

Method

- Numerical
- Matching the solutions of Mukhanov-Sasaki eqn
- Gradient-expansion

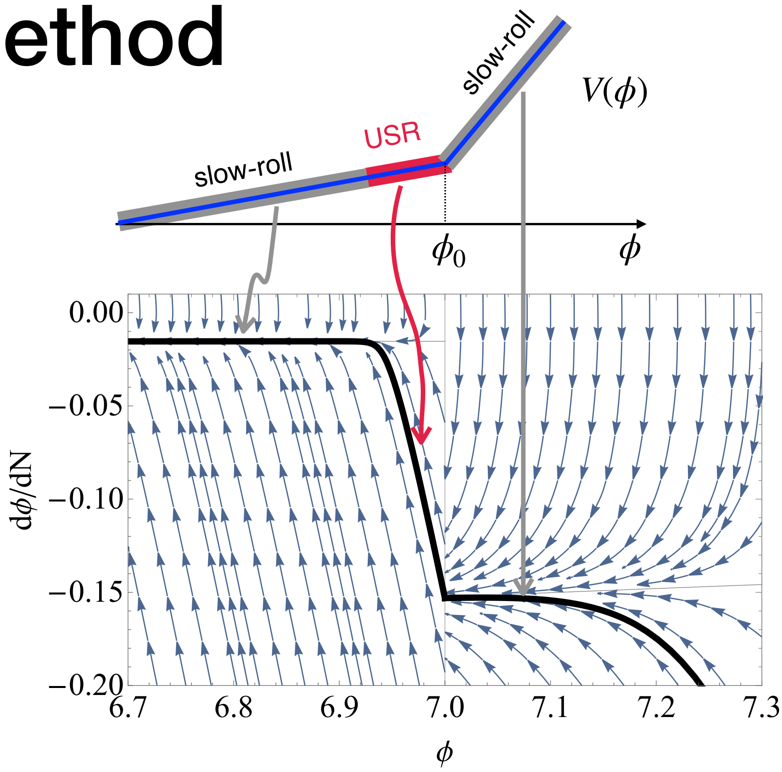

SP and J. Wang, 2209.14183

Matching the MS equation

- Define $\mathscr{R} = v/z$, then the eqn becomes
$$v_k'' + \left(k^2 - \frac{z''}{z}\right) v_k = 0$$
- with $z''/z = 2/\tau^2$ for both stages
- Then we match $\mathscr{R}$ and $\mathscr{R}'$ at ϕ_0

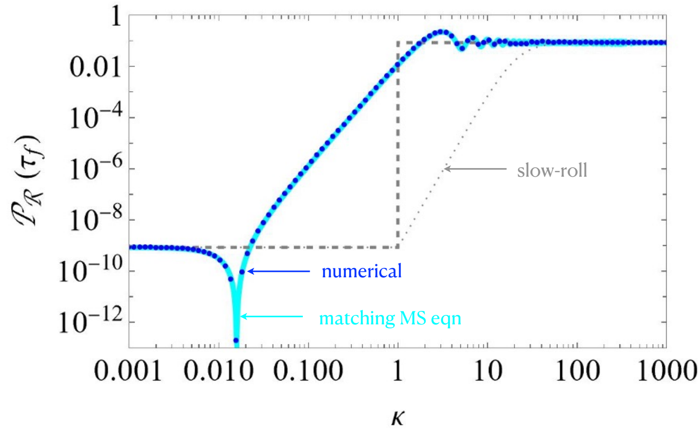

$$\frac{\mathscr{P}_\mathscr{R}(\kappa)}{\mathscr{P}_\mathscr{R}^{(\mathrm{IR})}} = \frac{9(\Lambda-1)^2}{\kappa^6}\left(\sin\kappa - \kappa\cos\kappa\right)^4 + \left\{\Lambda + \frac{3(\Lambda-1)}{2\kappa^3}\left[(\kappa^2-1)\sin 2\kappa + 2\kappa\cos 2\kappa\right]\right\}^2$$
$$(\Lambda \equiv A_+/A_-, \quad \kappa \equiv k/k_0)$$

SP and J. Wang, 2209.14183

Gradient Expansion

Leach, Sasaki, Wands, Liddle, astro-ph/0101406

- $\mathscr{R}$ does not approach constant right after the horizon exit, so we define
$$\mathscr{R}_k(\tau) = \alpha_k u(\tau) + \beta_k v(\tau)$$
- where $\alpha_k = 1 + \mathcal{O}(k^2) \gg 1$ is the superhorizon enhancement factor.
- Then neglecting the decaying mode
$$\mathscr{P}_\mathscr{R}(\tau_f) = |\alpha_k|^2 \mathscr{P}_\mathscr{R}(\tau_k)$$
- The peak is mainly contributed by superhorizon enhancement.

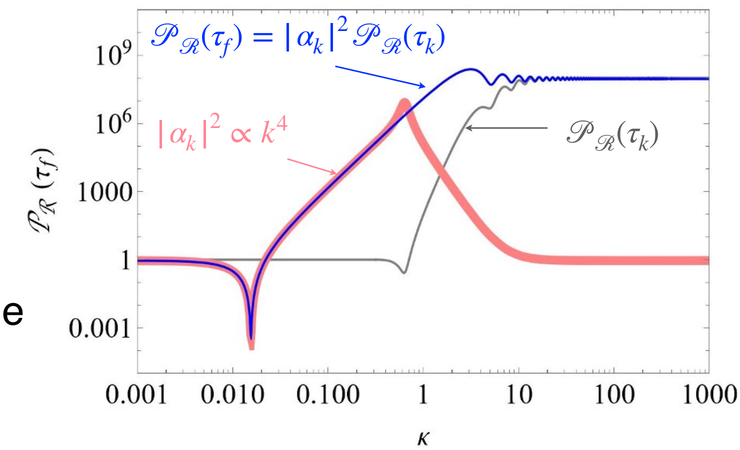

SP and J. Wang, 2209.14183

Modulations

$$\frac{\mathscr{P}_{\mathscr{R}}(\kappa)}{\mathscr{P}_{\mathscr{R}}^{(\mathrm{IR})}} = \frac{9(\Lambda-1)^2}{\kappa^6}\left(\sin\kappa - \kappa\cos\kappa\right)^4 + \left\{\Lambda + \frac{3(\Lambda-1)}{2\kappa^3}\left[(\kappa^2-1)\sin 2\kappa + 2\kappa\cos 2\kappa\right]\right\}^2$$

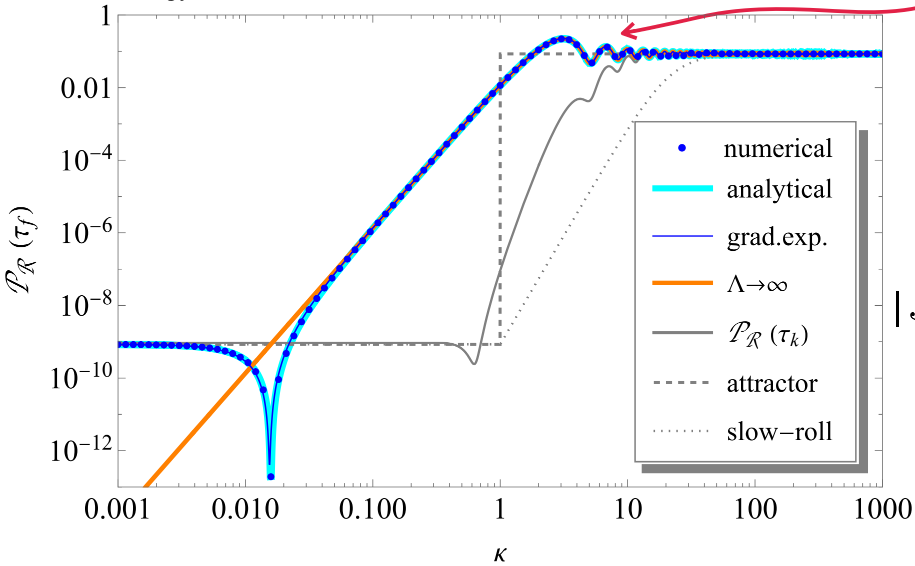

Modulations are given by sinusoidal oscillations of period π, which originates in the mode mixing.

$$|\mathscr{R}| \sim |a_k e^{ik\tau} + b_k e^{-ik\tau}| \sim |a_k| \left| 1 + \frac{b_k}{a_k} e^{-2ik\tau} \right|$$

SP and J. Wang, 2209.14183

Modulations

π

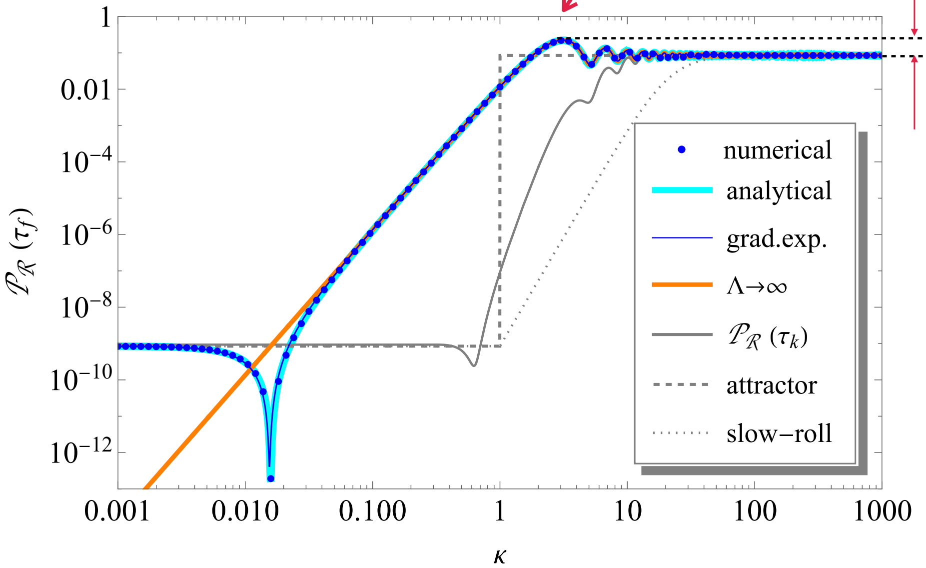

$$1 + \frac{15}{\pi^2} + \frac{9}{\pi^4} \approx 2.61$$

SP and J. Wang, 2209.14183

Contents

PBH

This extra enhancement is not enough to evade the γ-ray constraints.
So a further suppression is required, like in the constant-roll model.

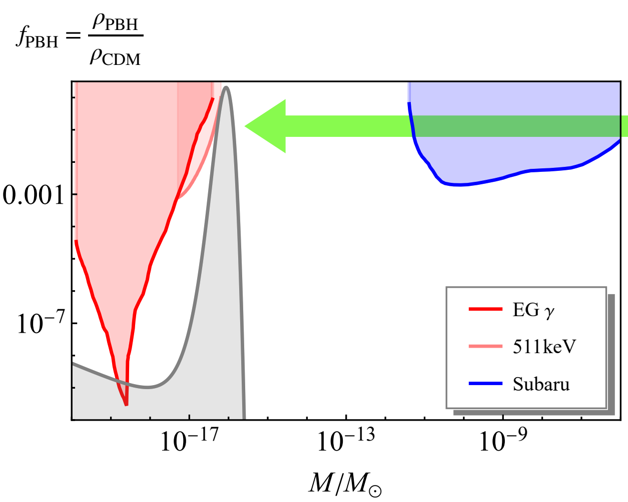

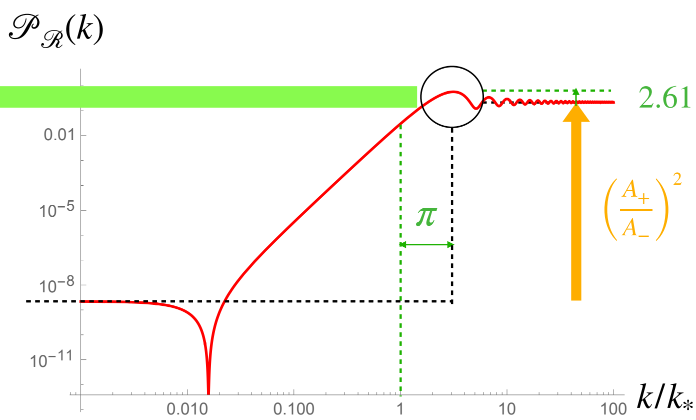

Constant-roll

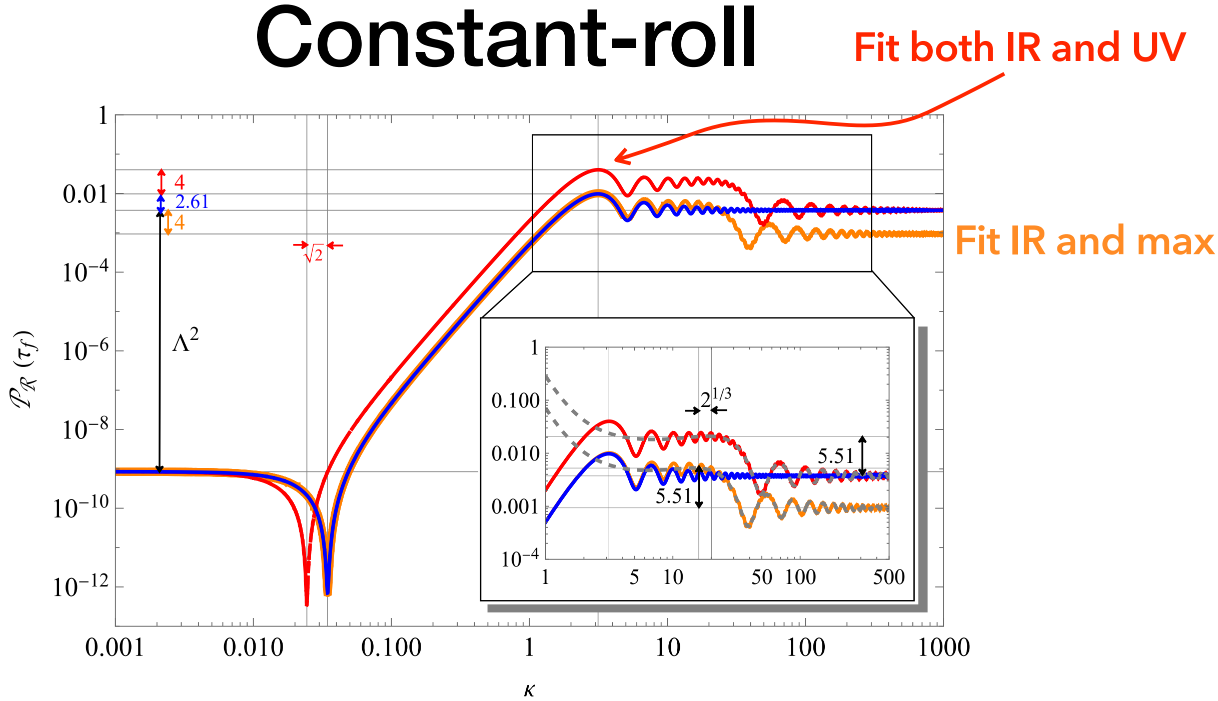

PBH

For given IR and max values,
constant-roll suppresses UV plateau 4 times further.

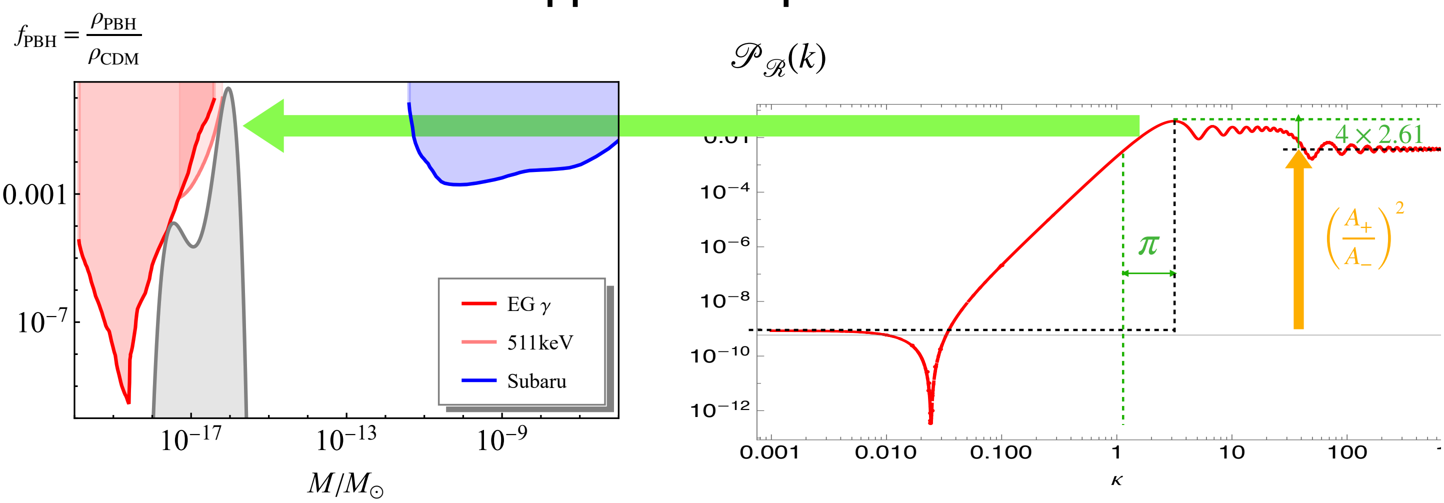

Induced GWs

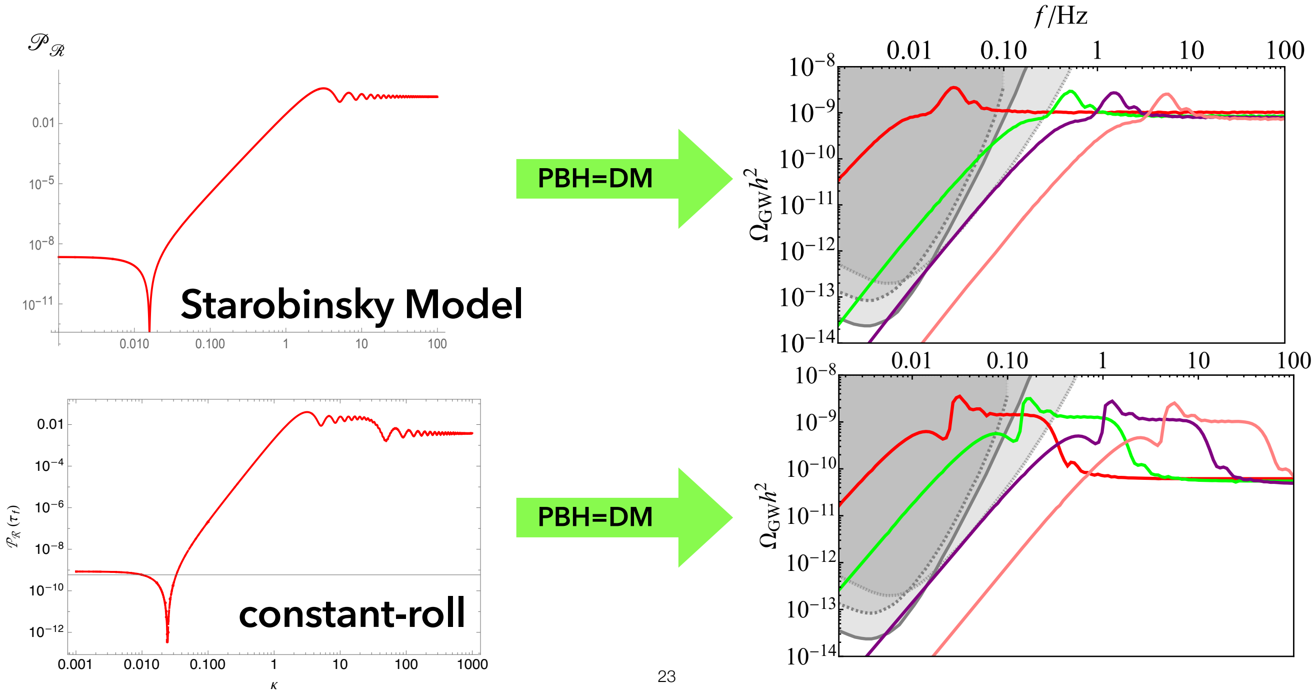

Contents

- Introduction
- Starobinsky model revisited
- Applications to PBH and IGW
- Discussion

Non-Gaussianity

- We only focus on the NG near the peak, which is generated in the USR stage.
- It is known that for smooth transitions, the NG should be proportional to V''/V.

Cai et. al, 1712.09998

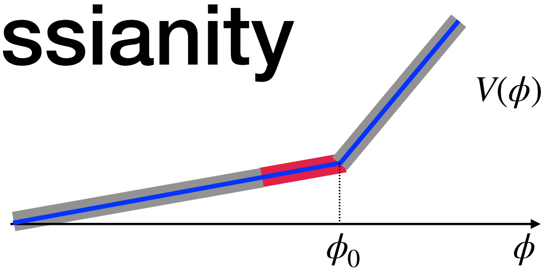

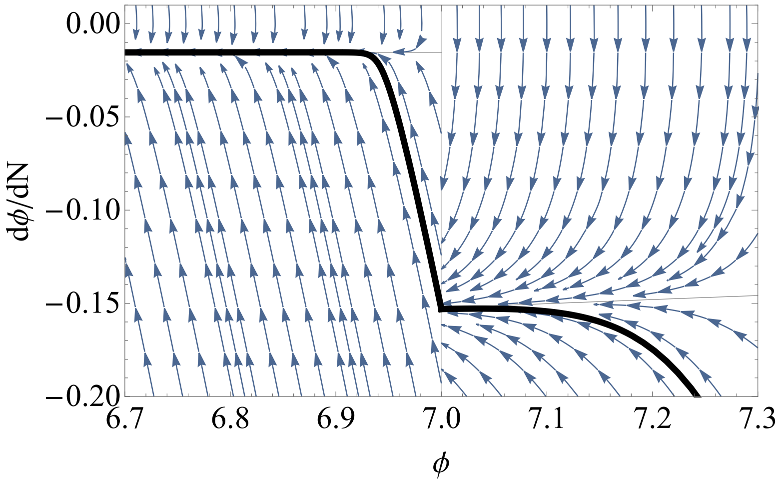

Non-Gaussianity

$$N = \frac{H_0^2}{A_-}\Big((\pi + 3\phi) - (\pi_* + 3\phi_*)\Big)$$

$$\zeta = \delta N \approx \frac{3H_0^2}{A_-}\delta\phi$$

- Non-Gaussianity can be calculated by δN formalism.
- When fixing the endpoint, the equal-N lines are parallel to the USR trajectories, which implies no NG generated duration USR stage.

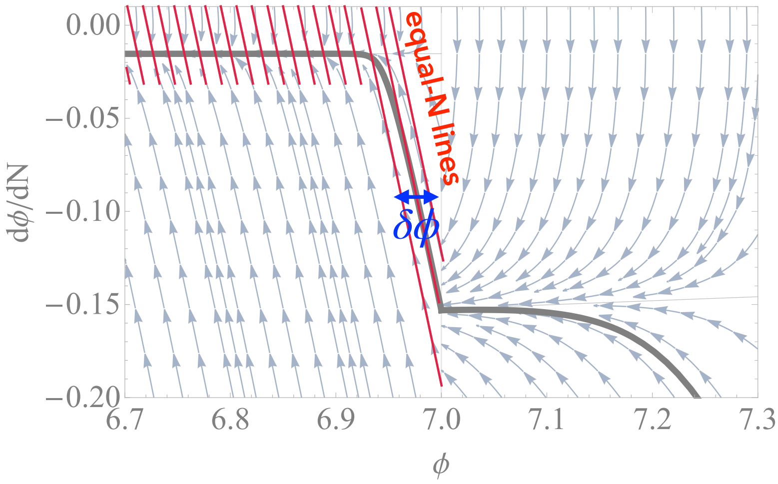

SP and J. Wang, in preparation

Non-Gaussianity

- On the other hand, the non-Gaussianity in the constant-roll model might be very large.
- This is because USR ends abruptly.

Passaglia, Hu, and Motohashi, 1812.08243

SP and J. Wang, in preparation

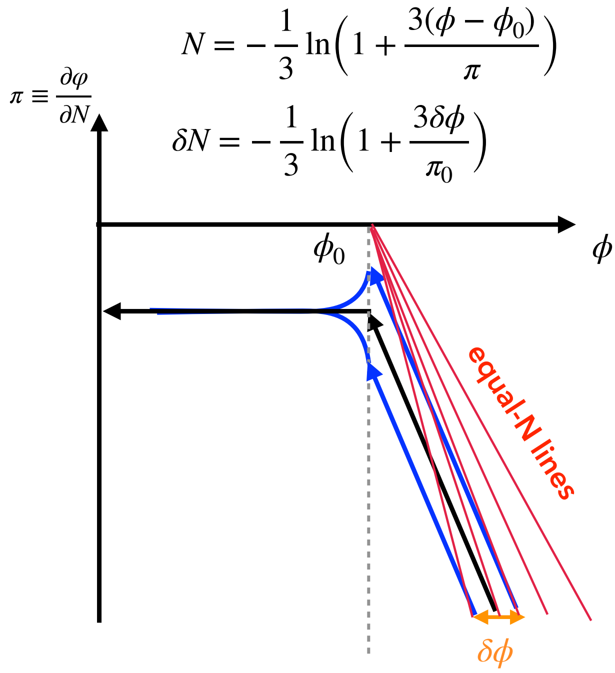

Conclusions

- The power spectrum has a maximum at π, which gives an extra enhancement of ~ 2.61, originating from mode mixing.
- "Global" Starobinsky model generates too many tiny PBHs.
- Starobinsky model and constant-roll model have characteristic features in induced GWs, both of which comes from the abrupt transition of slow-roll to ultra-slow-roll.
- The non-Gaussianity is negligible in Starobinsky model, while for constant-roll model, it might be large.

Thank you for your attendance!
ご出席ありがとうございました。
Happy birthday to Yokoyama san!
横山先生お誕生日おめでとうございます!

C02

Distance dependence of auto-pulsar correlations in pulsar timing arrays

Oct. 24th 2022

JGRG31

C02: Hiroaki Tahara (Rikkyo University)

with Yosuke Mishima (Rikkyo University)

Pulsar timing array (PTA) & HD curve

PTAs may give the next detection of gravitational waves.

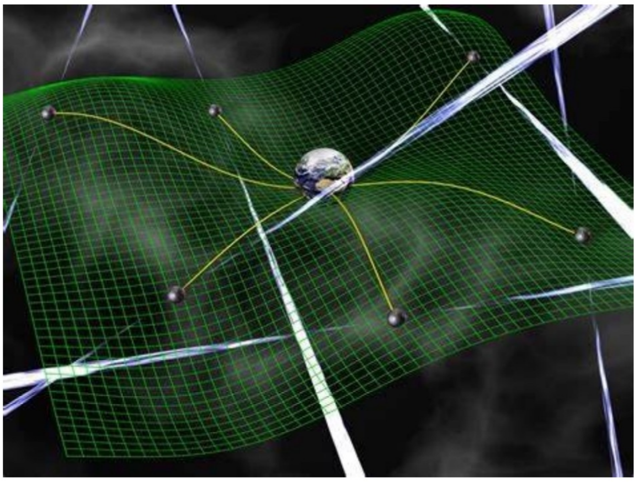

To verify that their signal is actually (tensor) GWs:

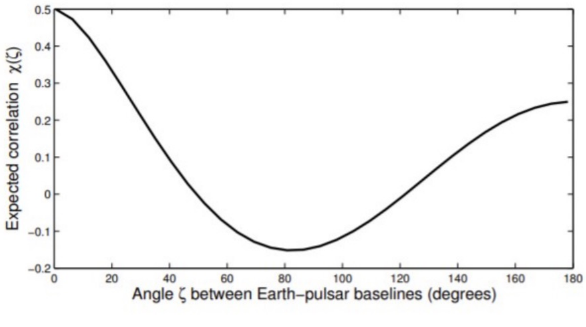

Hellings and Downs 1983

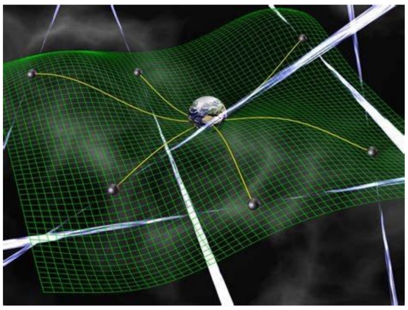

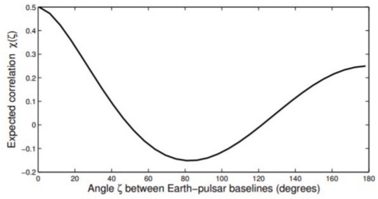

Hellings and Downs 1983

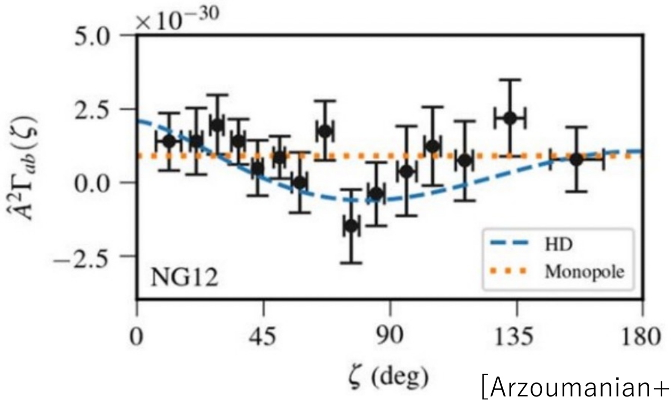

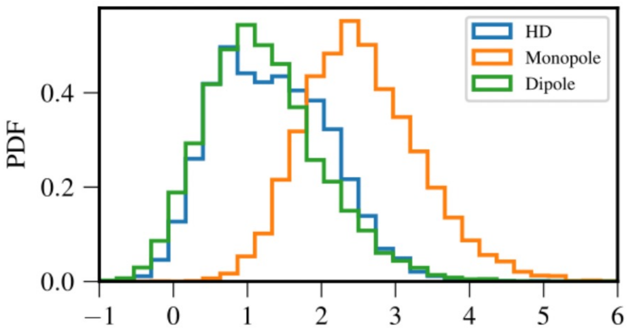

[Arzoumanian+ 2020 (NANOGrav 12.5yr)]

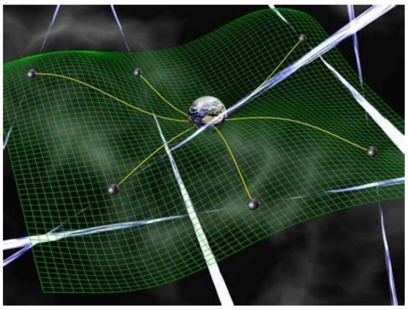

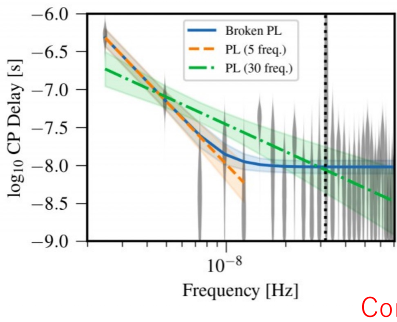

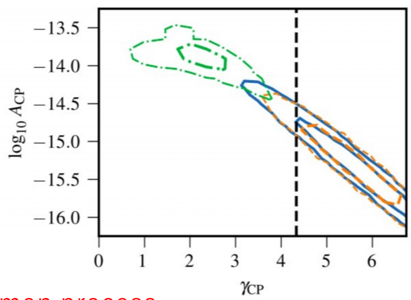

Common process

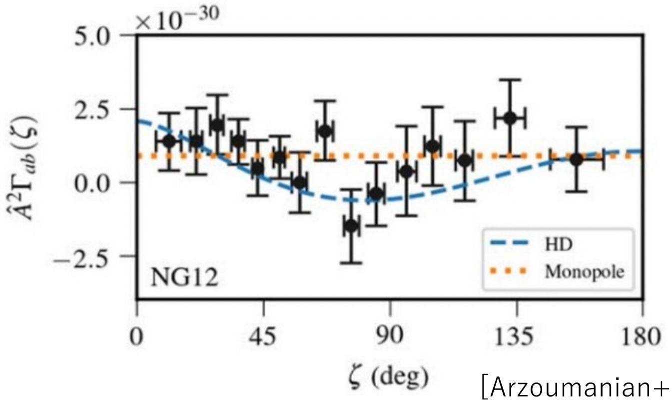

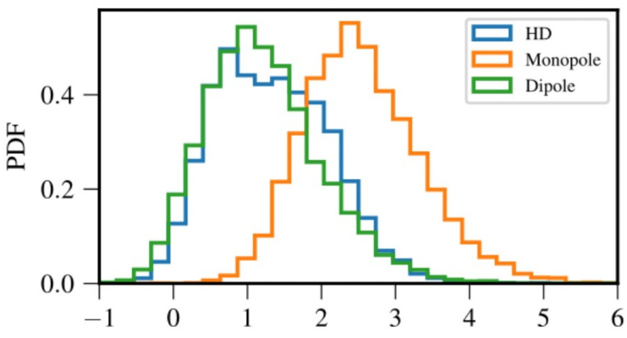

[Arzoumanian+ 2020 (NANOGrav 12.5yr)]

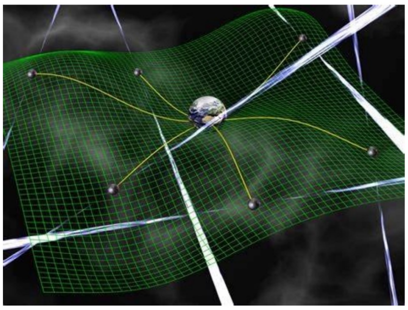

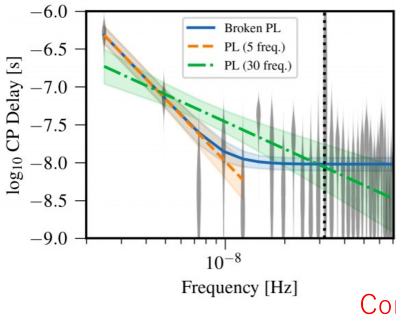

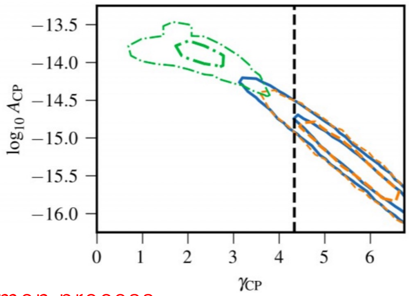

Common process

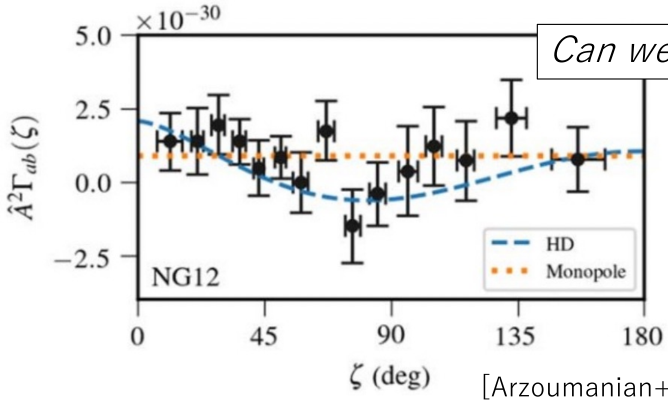

Can we say anything from common process?

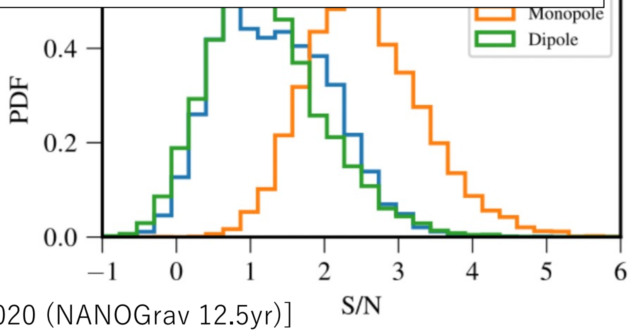

[Arzoumanian+ 2020 (NANOGrav 12.5yr)]

Testing modified gravity from PTAs

- Inter-pulsar correlation
  - Superluminal phase speed in f(R) [Qin, Boddy, Kamionkowski (2021)]
  - Massive gravity (Superluminal phase speed) [Liang, Trodden (2021)]

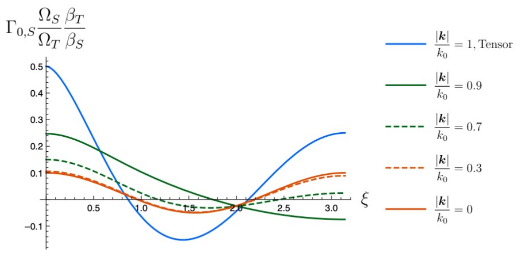

- Auto-pulsar correlation?
  - Surfing effect [Polnarev, Baskaran (2008)]

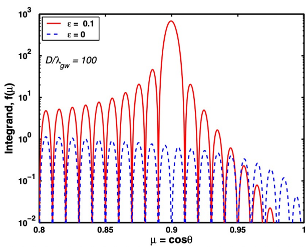

→ Amplification of timing residuals

Surfing effect

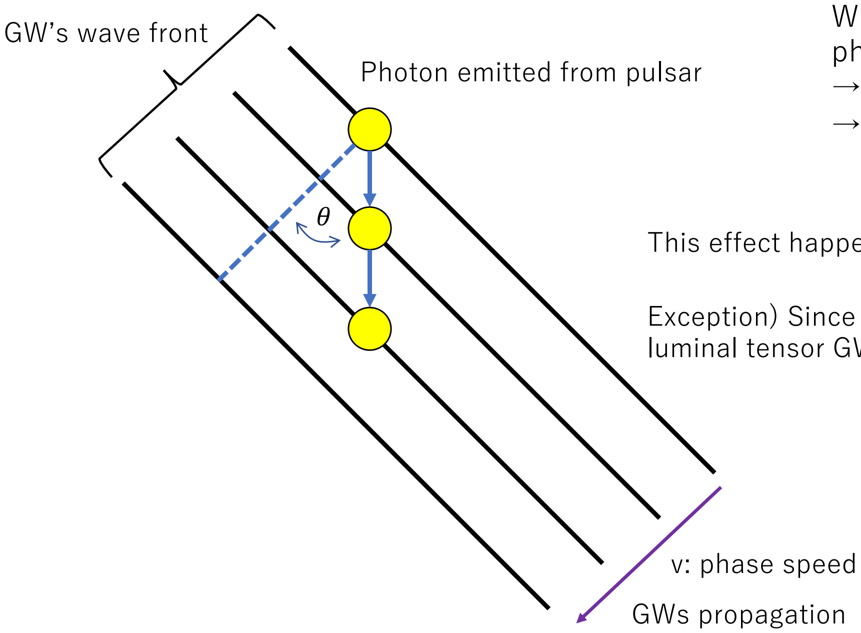

When $c\cos\theta = v$,
photon stays at GW's wavefront.
→ Signal gets amplified.
→ We need $v \le c$.

This effect happens if GW has (sub)luminal phase speed.

Exception) Since tensor modes are transverse,
luminal tensor GW propagation makes no effect (as in GR).

Pulsar Timing Arrays (PTAs)

- Observe timing residuals from milli-second pulsars

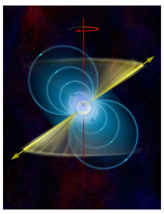

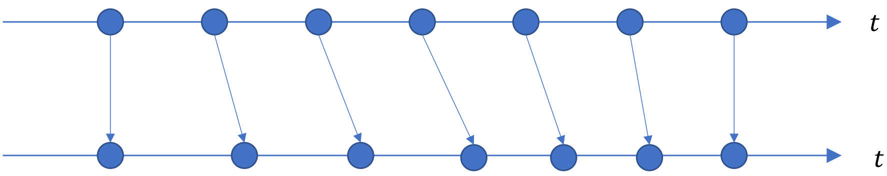

If pulsars emit pulses with the same period, GWs can delay them.

Timing Residuals

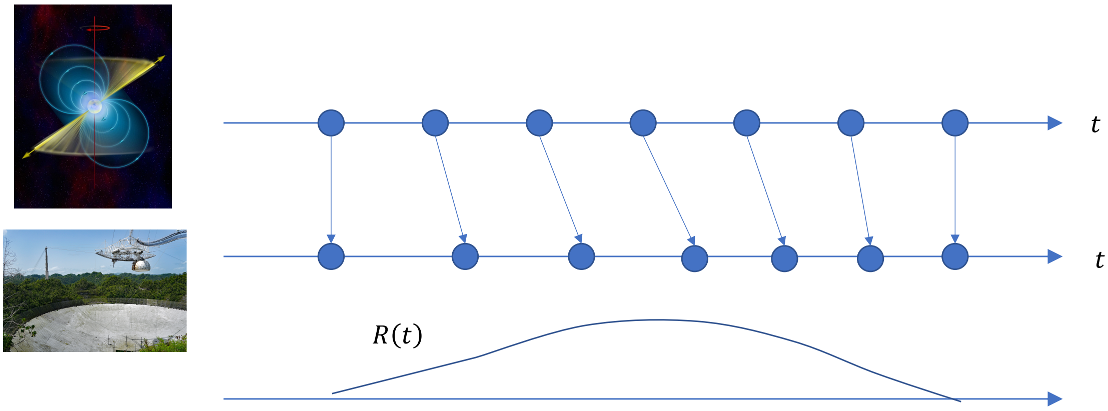

Variation of R(t) is slower than pulse interval and we get its time derivative

$$z(t) \coloneqq \dot{R}(t)$$

z(t) induced by GWs

- Delay of arrival time due to GWs

$$ds^2 = -dt^2 + \left(\delta_{ij} + h_{ij}\ (t, \mathbf{x})\right) dx^i dx^j$$

$$t_{obs} = t_{em} + d_a + \frac{n_a^i n_b^j}{2} \int_{t_{em}}^{t_{em}+d_a} dt' h_{ij}\ \left[t', (t_{em} + d_a - t')\ \mathbf{n}_a\right].$$

- z(t) induced by plane wave $h_{\mu\nu}^{(\lambda)}(x)$ with wavenumber k_μ, pol λ.

$$z_A^\lambda = \frac{1}{2} \frac{k_\sigma u^\sigma}{k_\rho n_A^\rho} n_A^\mu n_A^\nu \{h_{\mu\nu}^{(\lambda)}(x_{\rm obs}) - h_{\mu\nu}^{(\lambda)}(x_A)\}.$$

n_A : null vector parallel to photon trajectory
u : 4-velocity vector of observer
x_{obs}, x_A : positions of the observer and pulsar named A

Stochastic GWs

- Stochastic homogeneity and isotropy (unpolarized)

$$\langle \tilde{h}_k \tilde{h}^*_{k'} \rangle = P_h(\omega)\delta^{(3)}(\mathbf{k}-\mathbf{k}'),$$

- From this, we get

$$\begin{aligned}\langle zz\rangle_{AB}(\omega) &= \int d^2\Omega_k \int d^2\Omega_{k'} \langle z_A(\tilde{h}_k) z_B(\tilde{h}^*_{k'})^* \rangle, \\ &= C^\lambda_{AB}(\theta_{AB})P_h(\omega)\end{aligned}$$

This C have information of polarization and speed of GW.

(If A=B → auto-pulsar   if A≠B → inter-pulsar)

Polarization tensors

- polarizations $\quad \Pi_{\mu\nu} = \sum_{\lambda=+,\times,X,Y,T,L} f_\lambda \Pi^{(\lambda)}_{\mu\nu},$

tensor modes
$$\begin{cases}\Pi^{(+)}_{\mu\nu} = l_\mu l_\nu - m_\mu m_\nu, \\ \Pi^{(\times)}_{\mu\nu} = l_\mu m_\nu + m_\mu l_\nu,\end{cases}$$

vector modes
$$\begin{cases}\Pi^{(X)}_{\mu\nu} = l_\mu n_\nu + n_\mu l_\nu, \\ \Pi^{(Y)}_{\mu\nu} = m_\mu n_\nu + n_\mu m_\nu,\end{cases}$$

scalar modes
$$\begin{cases}\Pi^{(T)}_{\mu\nu} = l_\mu l_\nu + m_\mu m_\nu, & \text{(transverse)} \\ \Pi^{(L)}_{\mu\nu} = \sqrt{2} n_\mu n_\nu & \text{(longitudinal)}\end{cases}$$

basis

$$\begin{aligned} l_\mu &= (0, \sin\phi, -\cos\phi, 0), \\ m_\mu &= (0, \cos\theta\cos\phi, \cos\theta\sin\phi, -\sin\theta), \\ n_\mu &= (0, \sin\theta\cos\phi, \sin\theta\sin\phi, \cos\theta). \end{aligned}$$

Calculation

- After integration with respect to ϕ, we get a integrand

$$4c_\lambda^2\pi\left((f_T-f_+)\sin^2\theta-2f_Y\sin\theta\cos\theta+\sqrt{2}f_L\cos^2\theta\right)^2\times\frac{\sin^2[\frac{D_A}{2v}(v+\cos\theta)]}{(v+\cos\theta)^2}$$

- Integrating this with respect to θ, we get $C^\lambda(v, D_A)$

v : phase speed of GWs ($\omega = v\,k$)
D_A : phase change from pulsar A ($D_A = d_A\,\omega$)
(Dimensionless distance)

$$\langle zz\rangle_{AB}(\omega)=\int d^2\Omega_k\int d^2\Omega_{k'}\langle z_A(\tilde{h}_k)z_B(\tilde{h}^*_{k'})^*\rangle,$$
$$=C^\lambda_{AB}(\theta_{AB})P_h(\omega)$$

- In GR ($v = 1, f_+ = 1$), we take $\sin^2[\,] \to \frac{1}{2}$ (assuming $D_A \to \infty$).
- If $f_Y \neq 0$ or $f_L \neq 0$, we cannot take this limit at $\theta = \cos^{-1}(-v)$.

Results

- tensor or scalar transverse

$$\frac{C^\lambda_A}{2\pi}=(f_T-f_+)^2[I_2(\mu=1)-I_2(\mu=-1)],$$

where

$$I_s=v^{5-2s}(v^2-1)^sD_A\Theta-4v^3(v^2-\tfrac{s}{2})\Lambda+\tfrac{v^2+1-s}{v^2-1}\xi+2\zeta,$$

- vector

$$\frac{C^\lambda_A}{2\pi}=-4f_Y^2[I_1(\mu=1)-I_1(\mu=-1)]$$

- scalar longitudinal

$$\frac{C^\lambda_A}{2\pi}=2f_L^2[I_0(\mu=1)-I_0(\mu=-1)]$$

Tensor or Scalar transverse modes

- subluminal

superluminal

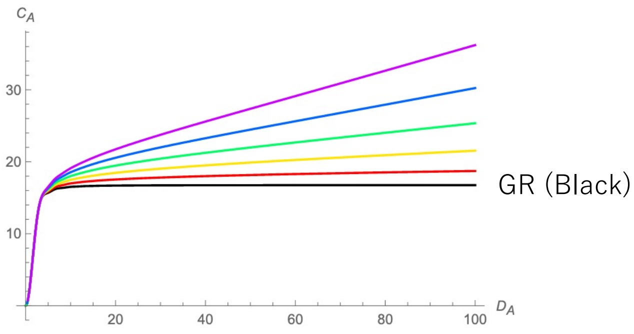

FIG. 3. Subluminal tensor mode is plotted. $v = 1$, 0.99, 0.98, 0.97, 0.96, and 0.95.

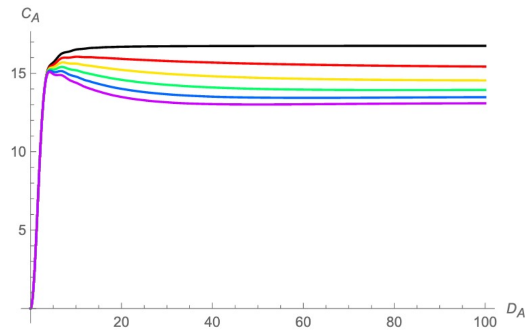

FIG. 4. Superluminal tensor mode is plotted. $v = 1$, 1.01, 1.02, 1.03, 1.04, and 1.05.

Vector modes

- subluminal

superluminal

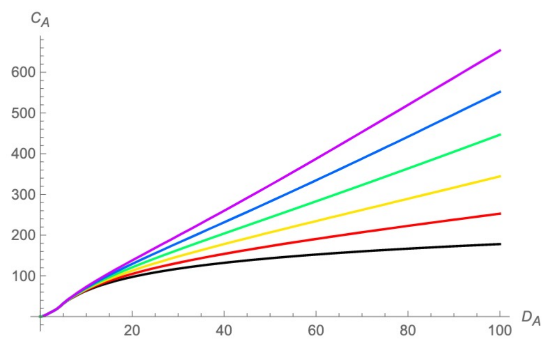

FIG. 5. Subluminal vector mode is plotted. $v = 1$, 0.99, 0.98, 0.97, 0.96, and 0.95.

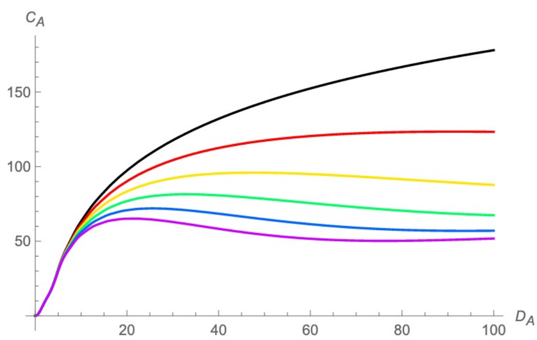

FIG. 6. Superluminal vector mode is plotted. $v = 1$, 1.01, 1.02, 1.03, 1.04, and 1.05.

Scalar longitudinal mode

- subluminal superluminal

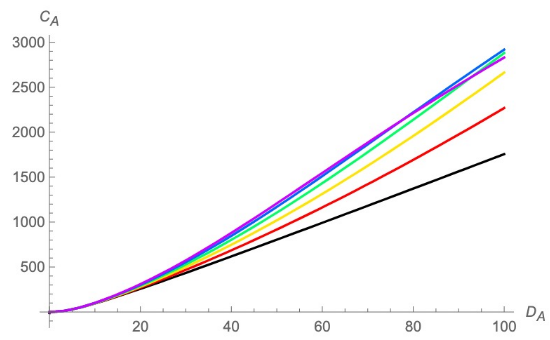

FIG. 7. Subluminal longitudinal mode is plotted. $v = 1$, 0.99, 0.98, 0.97, 0.96, and 0.95.

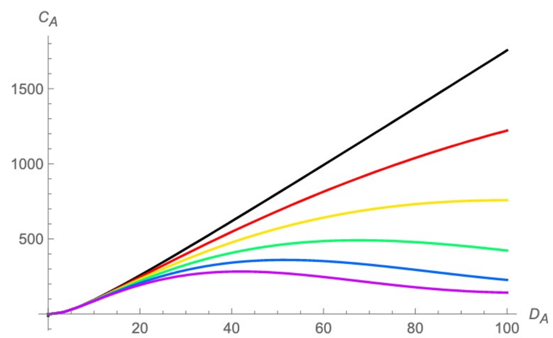

FIG. 8. Superluminal longitudinal mode is plotted. $v = 1$, 1.01, 1.02, 1.03, 1.04, and 1.05.

We study two easy cases:

- Massless dof (e.g. tensor dof in ST theory)
  - $\omega(k)^2 = c_{\mathrm{T}}^2\, k^2$ (massless, not always luminal)
  - $\to v = c_{\mathrm{T}}$ (constant phase speed)
- Massive dof (e.g. Massive gravity)
  - $\omega(k)^2 \approx\ k^2 + m^2$ (not exact but approximately correct)
  - $\to v = v(k) = \sqrt{k^2 + m^2}/k$ (superluminal phase speed)
- In both cases, we assume one polarization mode dominates.

Although our setup is too simple and unrealistic,
we can immediately apply it to more realistic models.

IPTA second data release

[Antoniadis+ 2022]

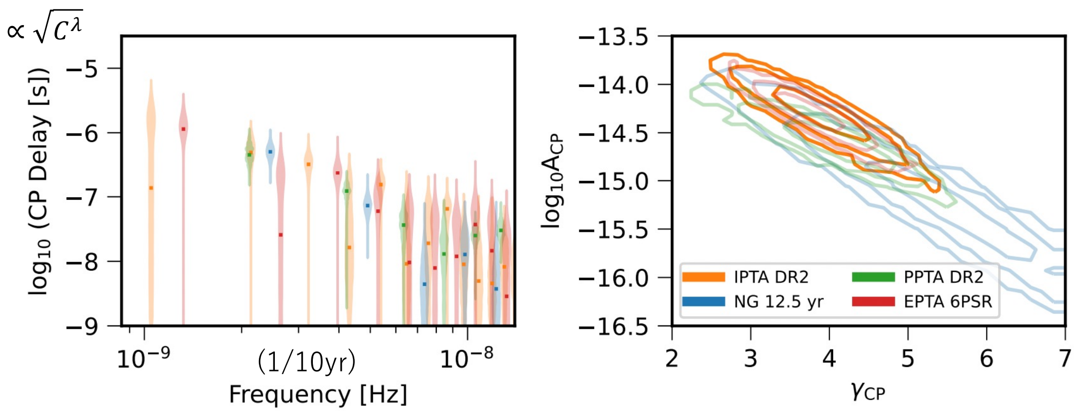

Figure 9. Comparison of IPTA DR2 to other recent data sets. *left:* Free spectral common-spectrum process model. The inclusion of legacy data not used in recent PTA analyses allows IPTA DR2 to reach lower frequencies despite missing the most recently collected data. *right:* 2D posterior for CP parameters log-amplitude and spectral index, where the contours represent the 1–, 2–, and 3–σ confidence intervals. All recent data sets are in broad agreement on the characteristics of a common-spectrum process.

At $10^{-9} - 10^{-8}$ Hz, uncertainty is factor of $\sqrt{10} \approx 3$ within 2 σ level.

Pulsar distances

[Antoniadis+ 2022]

Pulsar distance: 0.28 kpc – 2.4 kpc

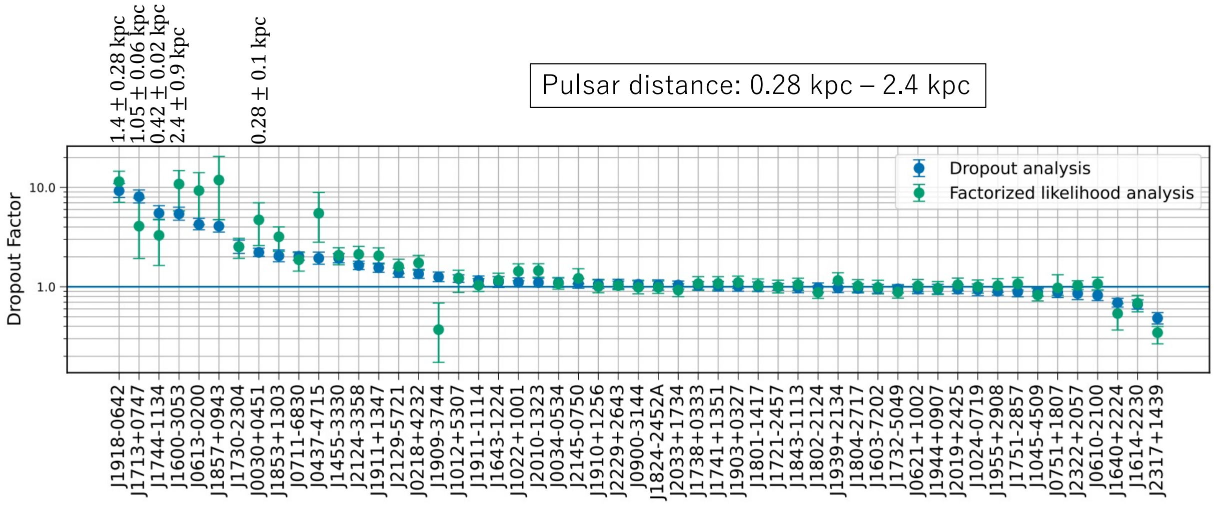

Figure 7. Individual pulsar consistency with common-spectrum process, error bars represent 95% credible intervals. Pulsars with dropout factors > 1 contribute to the detection of the CP. Dropout factors of ∼ 1 correspond to no evidence for or against the CP, usually due to higher white noise levels and/or shorter observation timespans. Pulsars with dropout factors < 1 are in tension with the CP.

Massless case (subluminal phase speed)

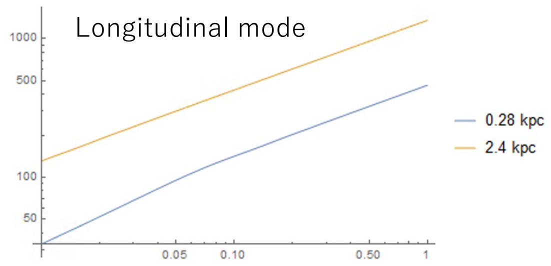

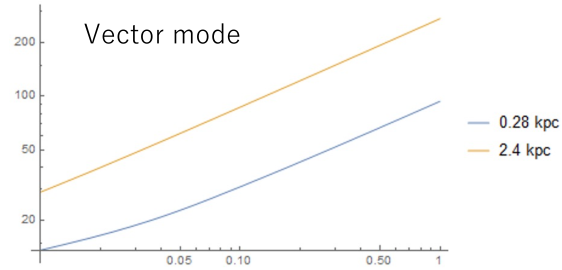

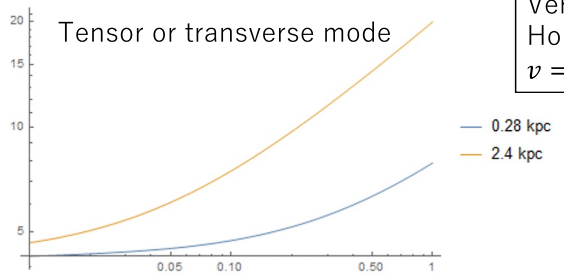

Vertical : $\sqrt{C^\lambda}$
Horizontal : f $[\mathrm{yr}^{-1}]$
$v = 1 - 10^{-2}$

Surfing effect give difference seen in these plots.
Pure SL modes contradicts the current observations.
Other mods contradicts when $v < 1 - 10^{-2}$.

Massive case $\left(v(k) = \sqrt{k^2 + m^2}/k\right)$

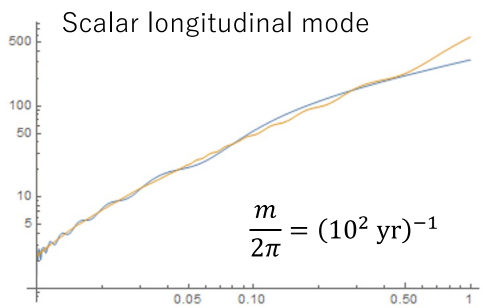

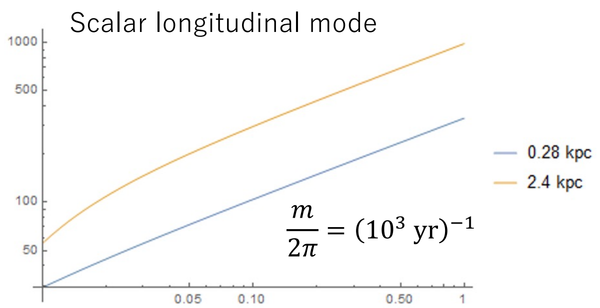

Vertical : $\sqrt{C^\lambda}$
Horizontal : f $[\mathrm{yr}^{-1}]$

Smaller m gives larger distance dependence.
If $\mathrm{m} < 2\pi \cdot 10^{-3}\mathrm{yr}^{-1}$, pure SL mode contradicts the current observations.
pure vector modes contradicts if uncertainty is constrained up to ~10%.
pure tensor or ST modes contradicts if uncertainty is constrained up to ~0.25%.

Summary

- We focused on distance dependence of auto-pulsar correlation.
  - Inter-pulsar correlation has been well studied in many literatures.
  - We proposed a possibility to check consistency by using auto-corr.

- The PTAs have reported common process in autocorrelation.
  - at frequency band 10^-9 Hz ~10^-8 Hz
  - pulsar at a distance 0.28-2.4 kpc
  - uncertainty of the order of 3

  This current constraint suggests:
  → If SL mode dominates, $v \geq 1$ or $m > 2\pi \cdot 10^{-3}\mathrm{yr}^{-1}$.
  → If other mode dominates, $v > 1 - 10^{-2}$.

Although our setup is too simple, we can immediately apply it to more realistic models.
In future, PTAs would find (1)farther pulsars and observe (2)longer period, which give more stringent constraint.

C03

Deep learning for intermittent gravitational wave signals

Takahiro S. Yamamoto (Nagoya U.)

w/ Sachiko Kuroyanagi (IFT UAM-CSIC, Nagoya U.), Guo-Chin Liu (Tamkang U.)

arXiv: 2208.13156

24th-28th October, 2022, JGRG31 @ RESCEU

GW astronomy

We have detected 91 compact binaries.

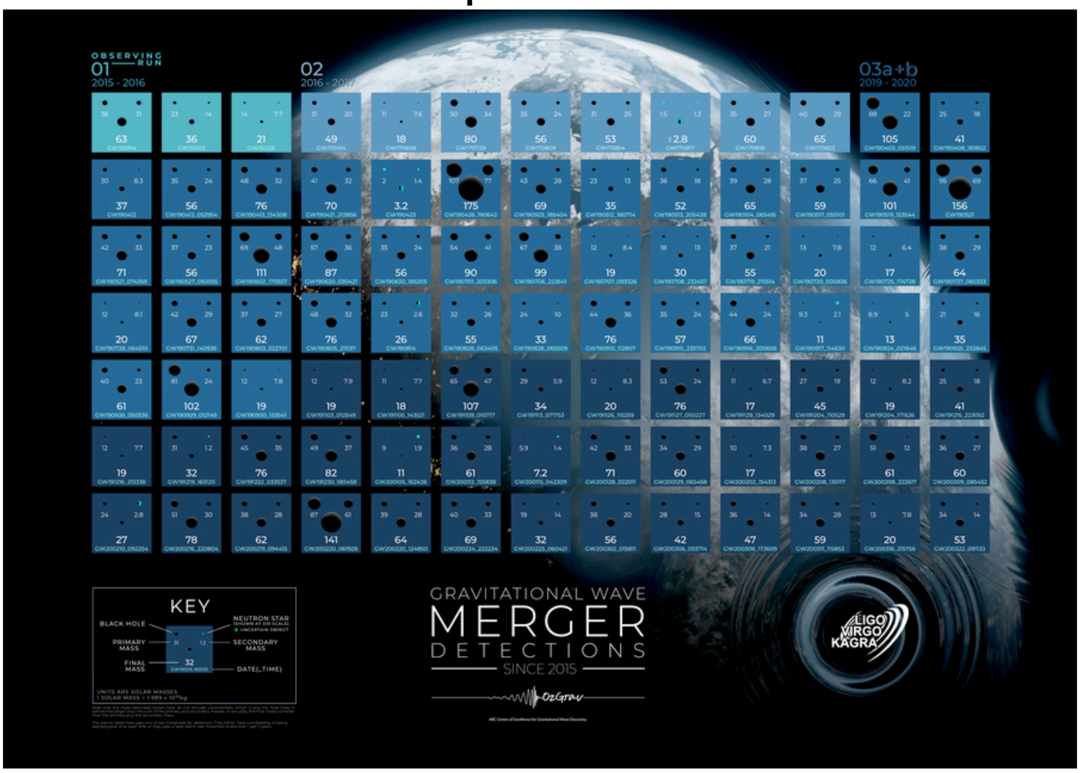

https://www.ligo.caltech.edu/gallery

Various types of GWs

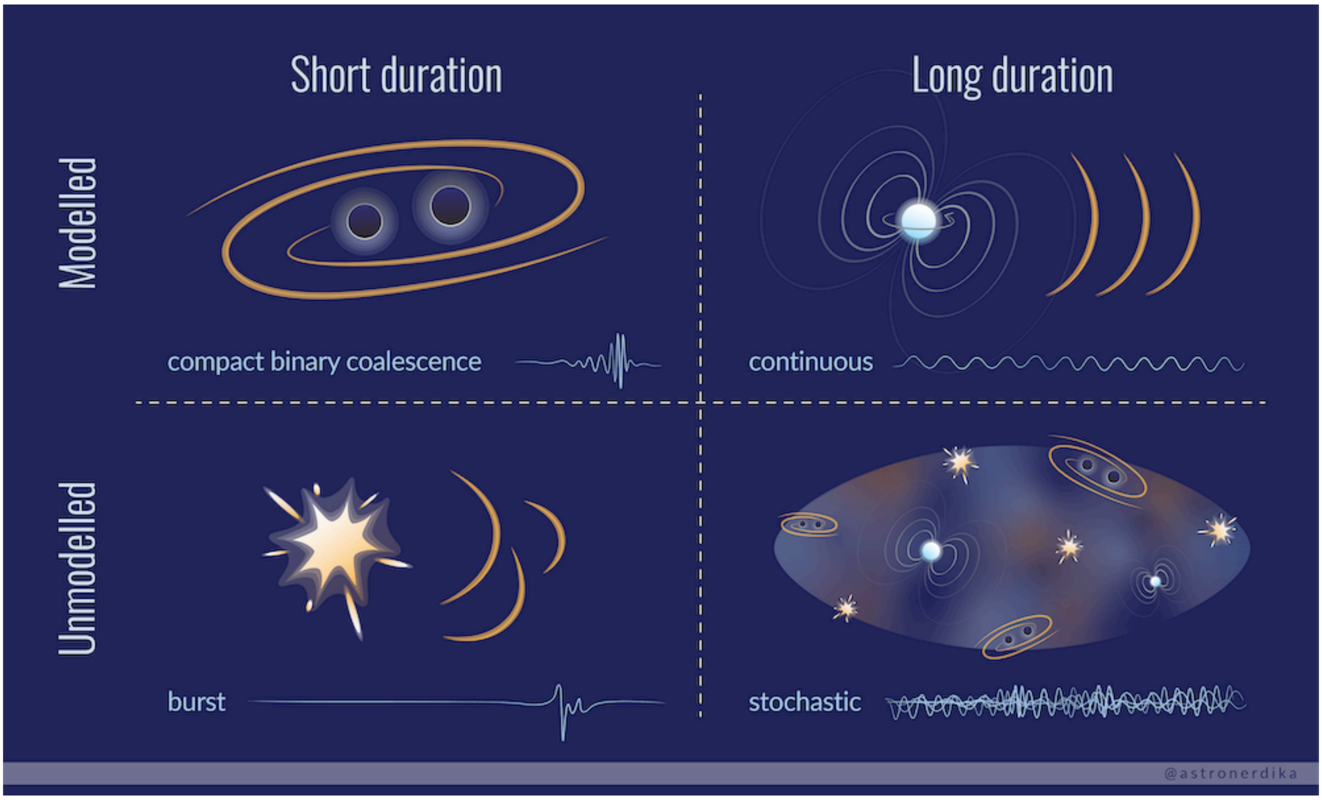

https://spaceaustralia.com/news/cosmic-lighthouses-and-continuous-gravitational-waves credit: Shanika Galaudage

Stochastic GW background (SGWB)

◉ SGWB have no deterministic waveforms.

◉ Sources

- Quantum fluctuations in inflation era ("primordial SGWB")
- phase transition in early Universe
- Ensembles of (merging) compact binaries ("astrophysical SGWB") **Our target**
- Cosmic strings

Astrophysical SGWB

Continuous or intermittent

Ensemble of BBH signals is considered to emerge as stochastic background.

Ensembles of BBH signals have intermittency. (Rarely overlapped)

Considering the intermittency is expected to improve the detection efficiency.

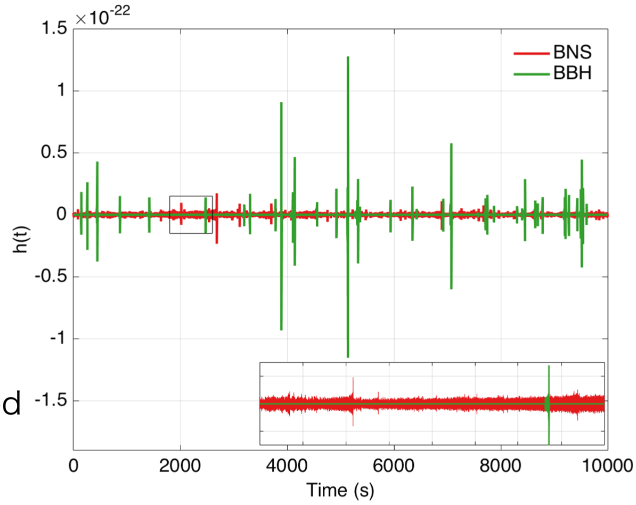

LIGO/Virgo, PRL120, 091101 (2018)

Duty cycle

Measuring non-Gaussianity

LIGO/Virgo, PRL120, 091101 (2018)

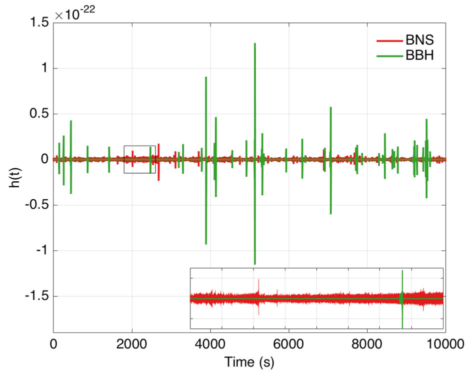

Duty cycle

$$\xi \sim R_{\mathrm{event}} T_{\mathrm{dur}}$$

R_{event} :event rate, T_{dur} :burst duration

$\xi \gtrsim 1$: bursts overlap -> Gaussian SGWB

$\xi \to 0$: non-Gaussian

BBH $\xi \simeq 0.06$, BNS $\xi \simeq 15$

Duty cycle provides us with the merger rate.

$\to$ useful for distinguishing the SGWB source

• Final goal

- To infer the population of compact binaries from non-Gaussian SGWB, we develop deep learning methods that is computationally efficient.

• This work's motivation

- Check the detection efficiency of the deep learning method by using a toy model.
- Study whether deep learning can estimate duty cycle.

Toy model of SGWB

Noise model

Drasco & Flanagan, PRD67, 082003 (2003)

- Co-aligning and co-locating two detectors

$$h_i^k = s^k + n_i^k$$

k: index of time bin, $i = 1,2$: detector

- White, Gaussian, and stationary detector noise
- Noise model

$$p(n_i^k \,|\, \sigma_i^2) = \frac{1}{\sqrt{2\pi\sigma_i^2}} \exp\left[-\frac{(n_i^k)^2}{2\sigma_i^2}\right]$$

(in this work $\sigma_1 = \sigma_2 = 1$)

Toy model of SGWB

Signal model

Drasco & Flanagan, PRD67, 082003 (2003)

- A burst is modeled by a peak at one time bin
- Signal model

$$p(s^k\,|\,\xi,\alpha^2) = \xi\frac{1}{\sqrt{2\pi\alpha^2}}\exp\left[-\frac{(s^k)^2}{2\alpha^2}\right] + (1-\xi)\delta(s^k)$$

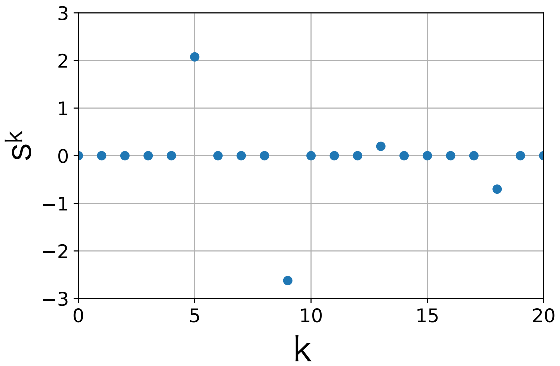

$\xi \in [0,1]$:duty cycle, ($\xi \to 1$: Gaussian)

α^2 : amplitude variance of each burst

Examples of toy model

SNR $\rho := \frac{\xi\alpha^2\sqrt{N}}{\sigma_1\sigma_2} = 100 \quad (N = 10000\,,\ \sigma_1 = \sigma_2 = 1)$

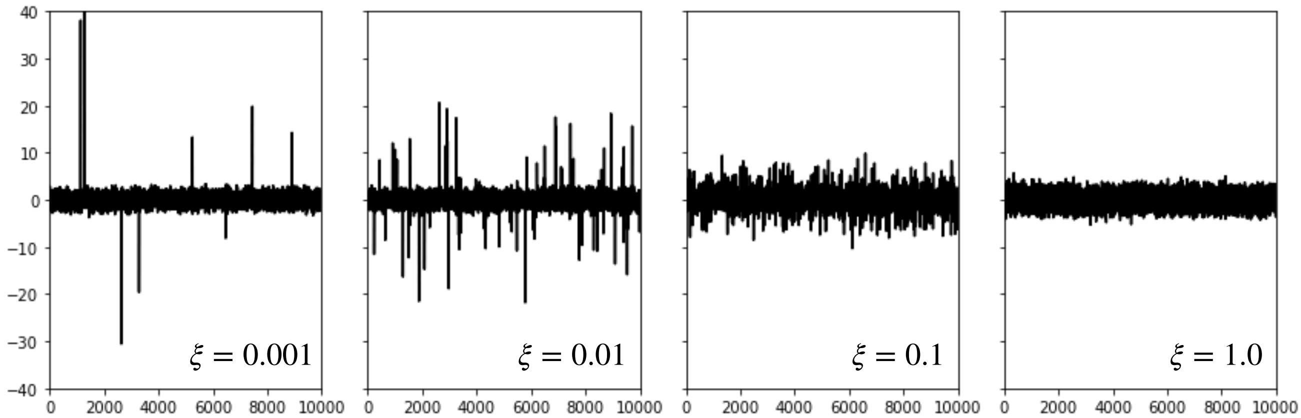

Duty cycle

non-Gaussianity

Maximum likelihood statistic

as a reference

Drasco & Flanagan, PRD67, 082003 (2003)

$$\Lambda_{\mathrm{ML}}^{\mathrm{NG}} := \max_{0<\xi\leq 1} \max_{\alpha^2\geq 0} \max_{\sigma_1^2\geq 0} \max_{\sigma_2^2\geq 0} \lambda_{\mathrm{ML}}^{\mathrm{NG}}(\alpha^2, \xi, \sigma_1^2, \sigma_2^2)$$

$$\lambda_{\mathrm{ML}}^{\mathrm{NG}}(\alpha^2, \xi, \sigma_1^2, \sigma_2^2) := \prod_{k=1}^{N} \left\{ \frac{\bar{\sigma}_1 \bar{\sigma}_2 \xi}{\sqrt{\sigma_1^2 \sigma_2^2 + \sigma_1^2 \alpha^2 + \sigma_2^2 \alpha^2}} \exp\left[\frac{(h_1^k/\sigma_1^2 + h_2^k/\sigma_2^2)^2 \alpha^2}{2(\alpha^2/\sigma_1^2 + \alpha^2/\sigma_2^2 + 1)} - \frac{(h_1^k)^2}{2\sigma_1^2} - \frac{(h_2^k)^2}{2\sigma_2^2} + 1 \right] + \frac{\bar{\sigma}_1 \bar{\sigma}_2}{\sigma_1 \sigma_2} (1-\xi) \exp\left[-\frac{(h_1^k)^2}{2\sigma_1^2} - \frac{(h_2^k)^2}{2\sigma_2^2} + 1 \right] \right\},$$

$$\bar{\sigma}_i^2 := \frac{1}{N} \sum_{k=1}^{N} (h_i^k)^2 .$$

- approximated version of likelihood ratio
- parameter search required
  (in this work, grid search is carried out)

Setup for comparison

Maximum likelihood vs deep learning

- # of data points in a strain = 10000
- False alarm probability = 5%
- Using 500 noise data, we determine the threshold for detection statistics
- Estimate a signal SNR that is detectable with 90% efficiency
- Maximum likelihood is calculated by the grid search on four dimensional parameter space $(\xi, \alpha^2, \sigma_1^2, \sigma_2^2)$.
  # of grid points ~ 10^6.
- SNR $\rho := \frac{\xi \alpha^2 \sqrt{N}}{\sigma_1 \sigma_2}$ (N: data length)

Setup of neural network

Structure, data generation

- Three networks with different structures
  - Shallower CNN, deeper CNN, residual net
  - # of tunable params: shallower CNN << deeper CNN ~ residual net
- Predict the probability that a GW signal exists in strain.
- Training data are randomly generated at each iteration step.
- Implemented with PyTorch

Paszke et al. 1912.01703

- GPU Quadro GV100 (some part of calculation is done by GTX1080Ti at Kyoto)

Results: detection

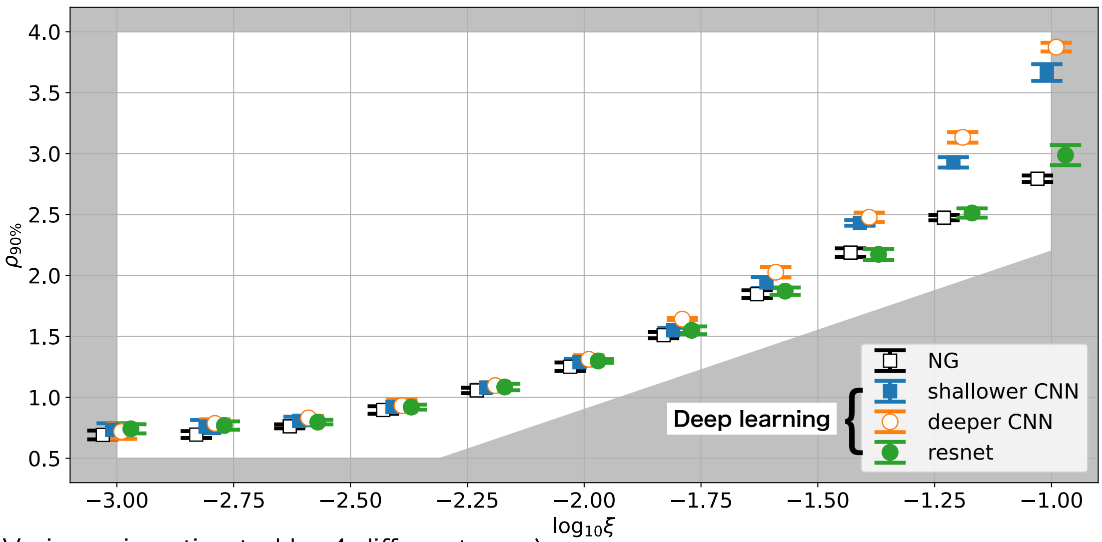

(* Variance is estimated by 4 different runs)

(** White is the region that we used for training.

・Residual network shows comparable performance to the maximum likelihood statistic.

・CNNs also work for low duty cycle, $\log_{10}\xi \lesssim -2$.

Result: computational speed

method	time [sec]	ratio
non-Gaussian statistic	1.13×10^{4}	1
shallower CNN	2.54×10^{-2}	2.25×10^{-6}
deeper CNN	7.96×10^{-2}	7.04×10^{-6}
residual network	7.66×10^{-2}	6.78×10^{-6}

NN: GPU Quadro GV100
ML: CPU Intel(R) Xeon(R) CPU E5-1620 v4 @ 3.50GHz
Based on elapsed time to process 500 data

Speed up by $O(10^5)$

Results: parameter estimation

- Residual network trained on $\log_{10}\xi \sim U[-2,0], \rho \sim U[1,60]$
- ResNet can recover the duty cycle and SNR.

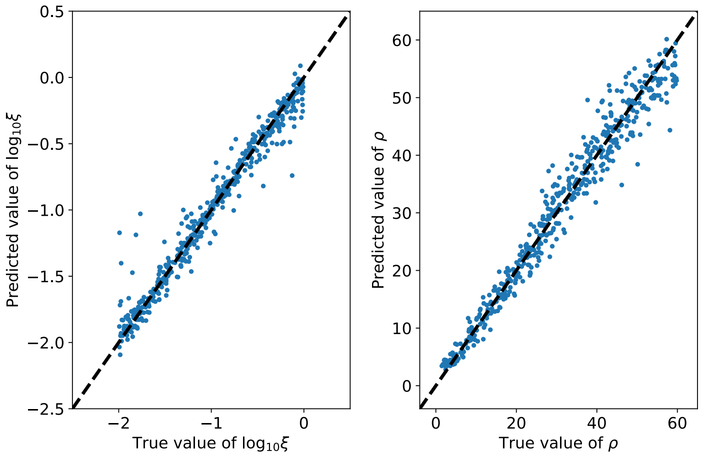

TABLE IV: Averages and standard deviations of errors in $\log_{10}\xi$ and ρ.

$\overline{\delta \log_{10}\xi}$	$\sigma[\delta \log_{10}\xi]$	$\overline{\delta\rho}$	$\sigma[\delta\rho]$
-1.29×10^{-5}	0.11	-8.90×10^{-2}	2.97

$$\overline{\delta Q} = \frac{1}{N}\sum_{n=1}^{N}(Q_n^{\mathrm{pred}} - Q_n^{\mathrm{true}})$$

$$\sigma[\delta Q] = \sqrt{\frac{1}{N}\sum_{n=1}^{N}(Q_n^{\mathrm{pred}} - Q_n^{\mathrm{true}})^2}$$

Conclusion

- Non-Gaussianity is one of the keys to determine the source of SGWB.
- We try to apply deep learning for search of non-Gaussian SGWB. In this work, we demonstrate it with a toy model that is originally proposed by Drasco & Flanagan (2003).
- The residual network performs comparable to the maximum likelihood statistic.
- NN can well recover the duty cycle.
- The computational time is reduced by O($10^{5\text{-}6}$).

Future work

- Taking into account various factors:
  - Considering the waveform of BBH
  - Simultaneously detect Gaussian and non-Gaussian background c.f. Biscoveanu et al. 2020
  - Detector's geometrical information
  - Realistic noise properties (glitch noise, non-stationarity)
- Preprocess the strain data
  - 1yr data is too long to analyze without preprocessing it.

C04

Stochastic gravitational wave background phenomenology beyond Einstein

(2206.01056, 2208.12538, 2209.14834)

Reggie Bernardo, Kin-Wang Ng

Institute of Physics, Academia Sinica

JGRG31 @ 24 October 2022

Outline

1. **The stochastic gravitational wave background**
2. **Pulsar timing array**
3. **SGWB phenomenology (tensor, off-lightcone, etc.)**
4. ***Looking out for the Galileon**
5. **Outlook**

Accessed 031022
https://www.ligo-india.in/wp-content/uploads/2016/02/gw-spectrum-1024x450-1.png

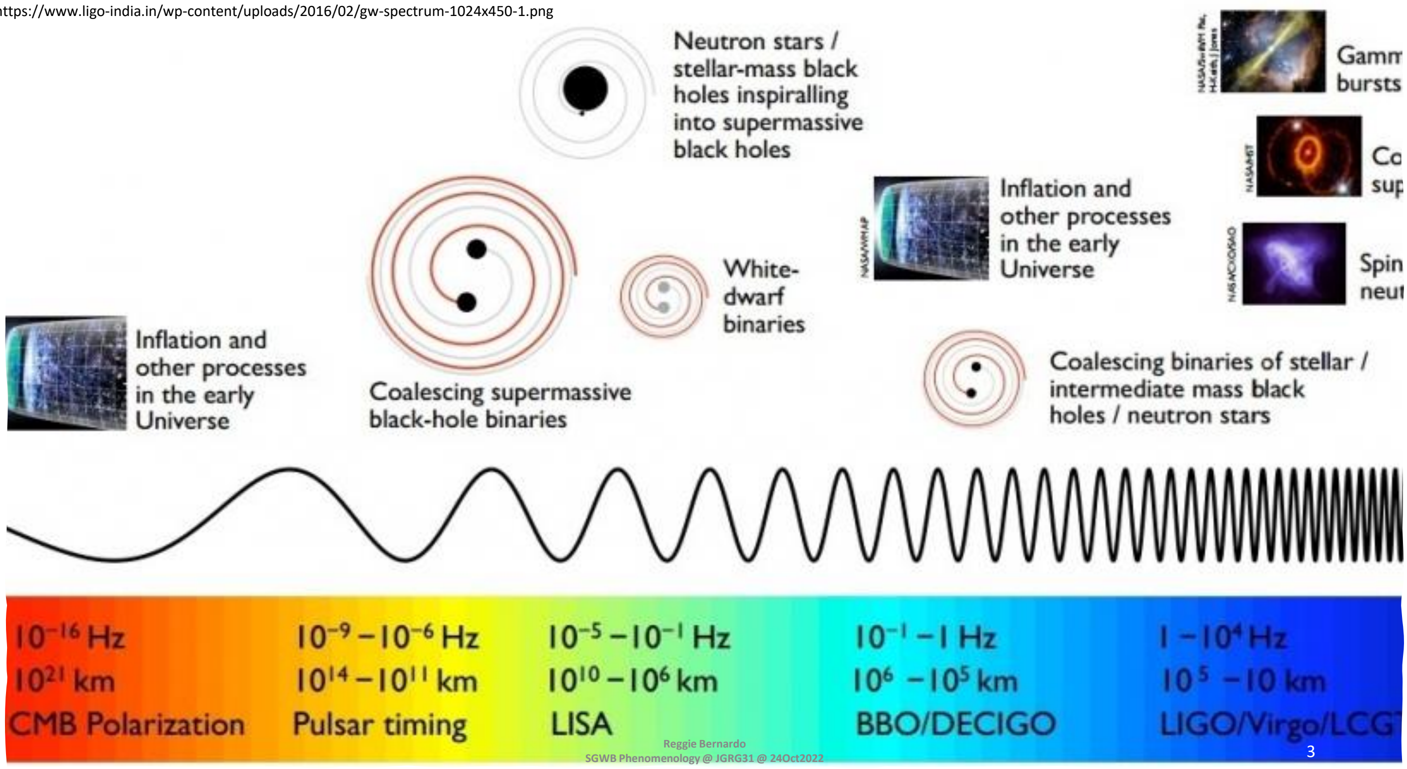

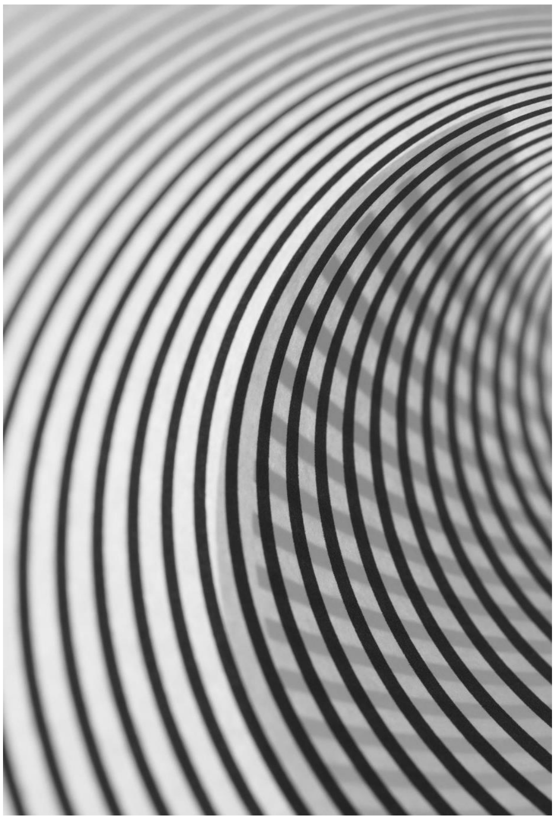

Gravitational Waves

- Spacetime distortions/perturbations

$$ds^2 = -dt^2 + (\delta_{ab} + \boldsymbol{h_{ab}})dx^a dx^b$$

- Wave properties:

  Carry energy, momentum, $v \sim 1$ @ 10^{1-3} Hz

- Tells about its sources

  e.g., BBH/BNS (LVK), IMRI/EMRI (LISA/TianQin)

- Challenge:

$$\boldsymbol{h_{ab} \sim G_{\mathrm{N}} \rightarrow \text{GW strains: } h \ll 1}$$

Stochastic Gravitational Wave Background

- Results from many GWs from various sources;
- Sources tied to early cosmos.

THE ASTROPHYSICAL JOURNAL, 234:1100–1104, 1979 December 15

PULSAR TIMING MEASUREMENTS AND THE SEARCH FOR GRAVITATIONAL WAVES

STEVEN DETWEILER
Department of Physics, Yale University
Received 1979 June 4; accepted 1979 July 6

ABSTRACT

Pulse arrival time measurements of pulsars may be used to search for gravitational waves with periods on the order of 1 to 10 years and dimensionless amplitudes $\sim 10^{-11}$. The analysis of published data on pulsar regularity sets an upper limit to the energy density of a stochastic background of gravitational waves, with periods ~ 1 year, which is comparable to the closure density of the universe.

Subject headings: cosmology — gravitation — pulsars — relativity

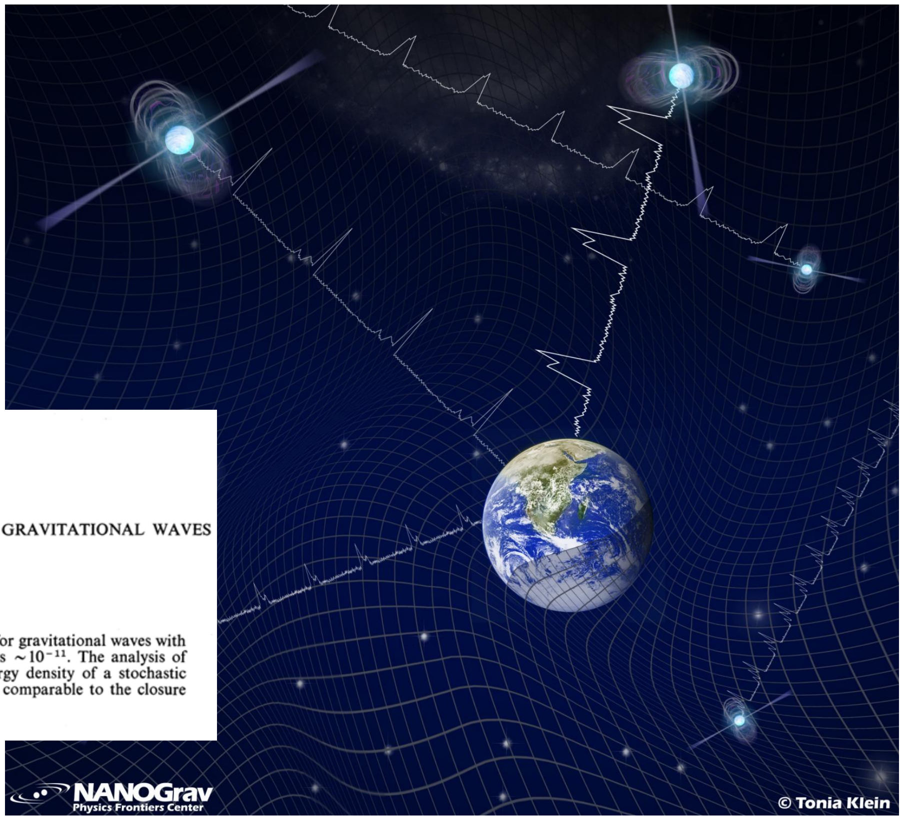

6

Galactic lighthouses

- Neutron Star:
  $M \sim 10^{0-1}\, M_{\odot}, D \sim 10^{0-1}$ km
- Pulsar = NS + magnetic field
- Millisecond pulsar
  - spins at ~100x per sec

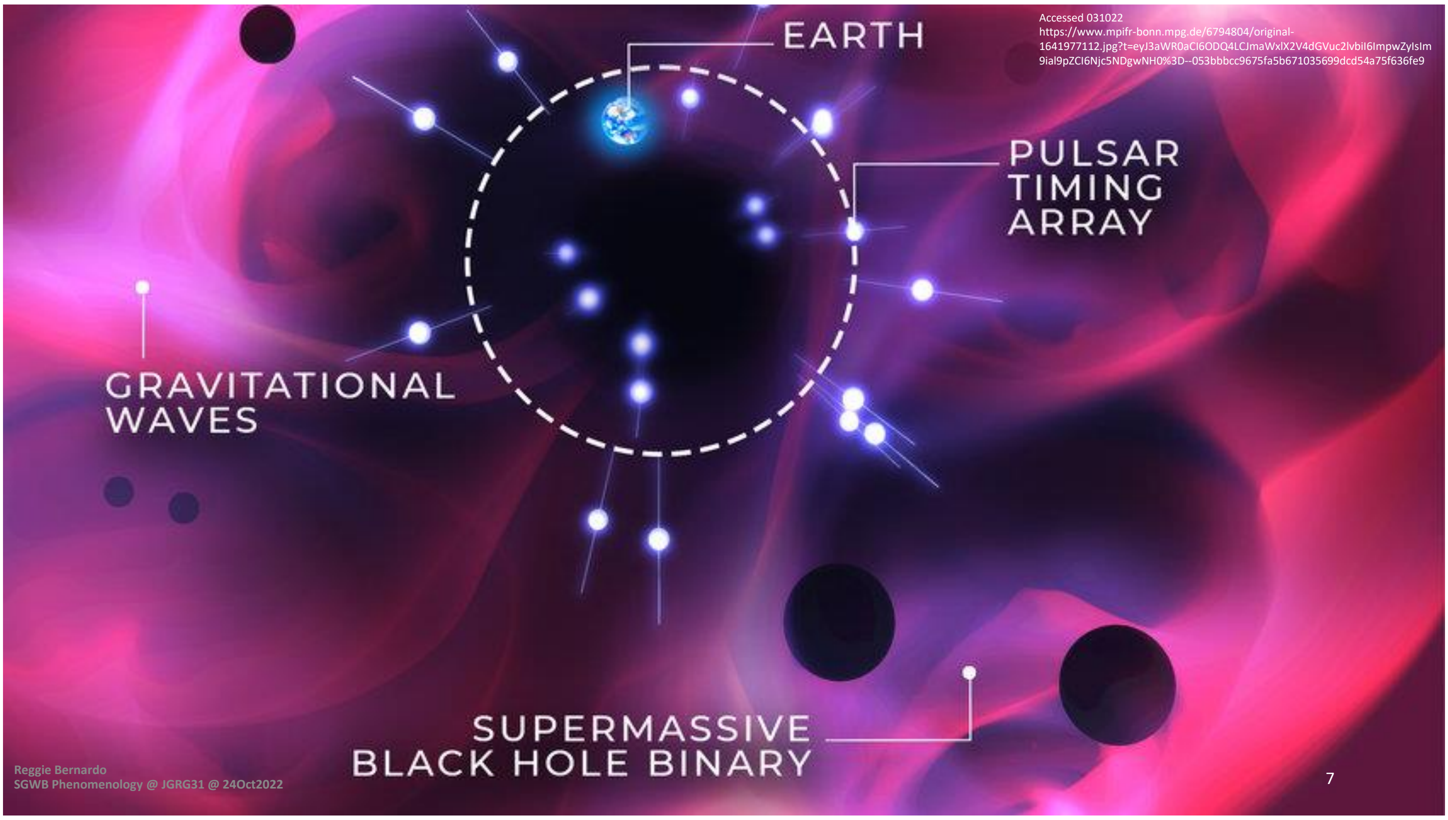

Pulsar Timing

- The **timing residual** – observable

$$r(t) = \int dt' \, z(t')$$

- Redshift fluctuation from **GW $\boldsymbol{h_{ij}(t)}$**:

$$z(t) = \frac{\left(\hat{e}^i \otimes \hat{e}^j\right)}{2\left(1 + v\hat{k}\cdot\hat{e}\right)}\left(h^e_{ij} - h^p_{ij}\right)$$

$$\boxed{z(t) = -\frac{1}{2}\int d\eta \, \hat{e}^i \otimes \hat{e}^j \, \partial_\eta \boldsymbol{h_{ij}(\eta)}}$$

- **Two point function**

$$\langle r_a(t) r_b(t)\rangle = \sum a_{lm} Y_{lm}(\hat{e}_a \cdot \hat{e}_b)$$

Gravitational Wave Polarizations

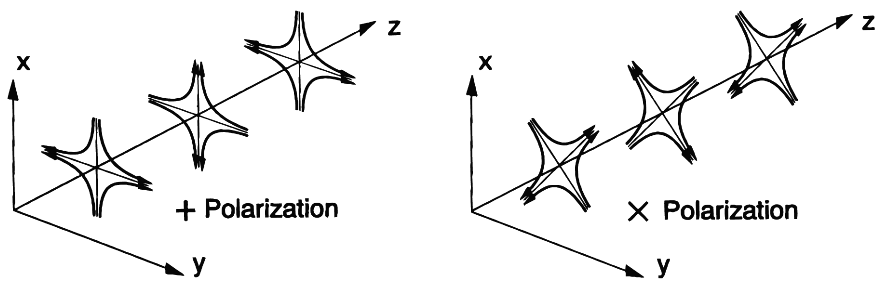

Accessed 30 June 2022: https://i.stack.imgur.com/IW50W.png

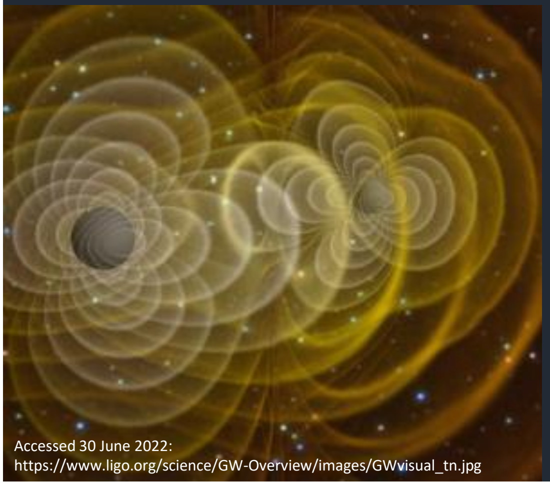

Accessed 30 June 2022:
https://www.ligo.org/science/GW-Overview/images/GWvisual_tn.jpg

GW amplitude

$$h_{ij}(\eta,\vec{x}) = \sum_A \int df \int d\hat{k}\; \tilde{h}_A\left(f,\hat{k}\right) \boldsymbol{\varepsilon}^{\boldsymbol{A}}_{\boldsymbol{ij}}\, e^{-2\pi i f(\eta - v\hat{k}\cdot\vec{x})}$$

velocity

polarization basis tensor

GW Polarizations: Beyond Einstein

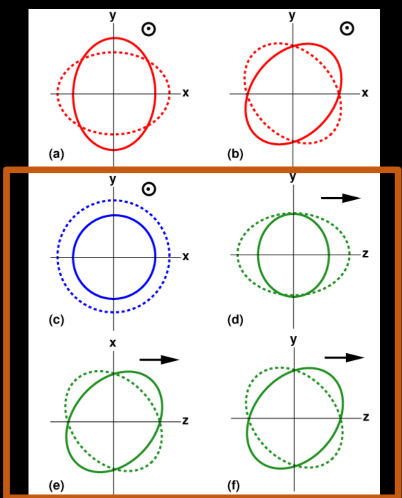

Accessed 30 June 2022:
https://www.ligo.org/science/Publication-GW170814/images/figure5.png

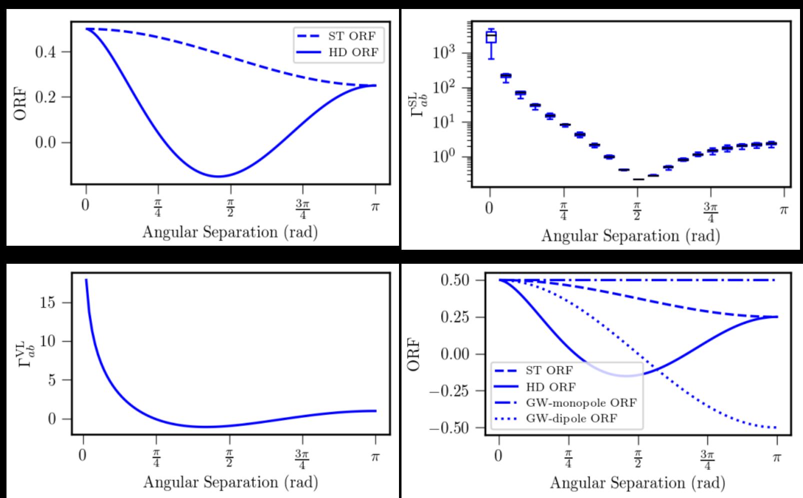

NANOGrav: arXiv:2109.14706

The ORF of Isotropic SGWB: technical

- **Overlap Reduction Function (ORF)** γ_{ab} is given by:

$$\gamma_{ab}(\zeta) = \sum_{l} \frac{2l+1}{4\pi} C_l P_l(\cos\zeta)$$

$$C_l^A = \frac{J_l^A(fD_a) J_l^{A*}(fD_b)}{\sqrt{\pi}}$$

- Polarization A = tensor, vector, scalar (**2208.12538, RCB, KWN**)

$$\boxed{J_l^A = N_l \int_0^{2\pi \boldsymbol{fDv}} \frac{dx}{v}\, \boldsymbol{e^{ix/v}}\, \partial_x^{\boldsymbol{p=0,1}} \left(\frac{\boldsymbol{j_l(x)}}{x^{\boldsymbol{q=0,1,2}}} \right)}$$

Progress on Uncertainty

2205.05637 (Allen)
- Theory uncertainty of the HD

2209.14834 (RCB & KWN)
- Theory uncertainty of general GW polarizations using PSF

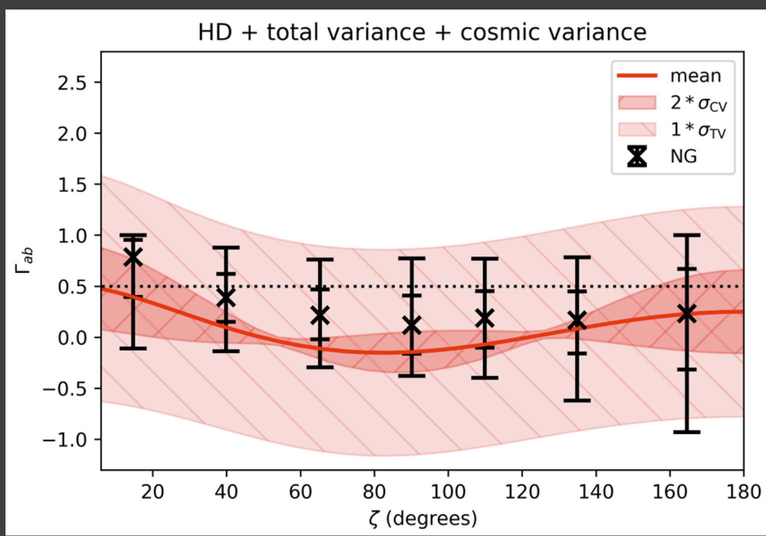

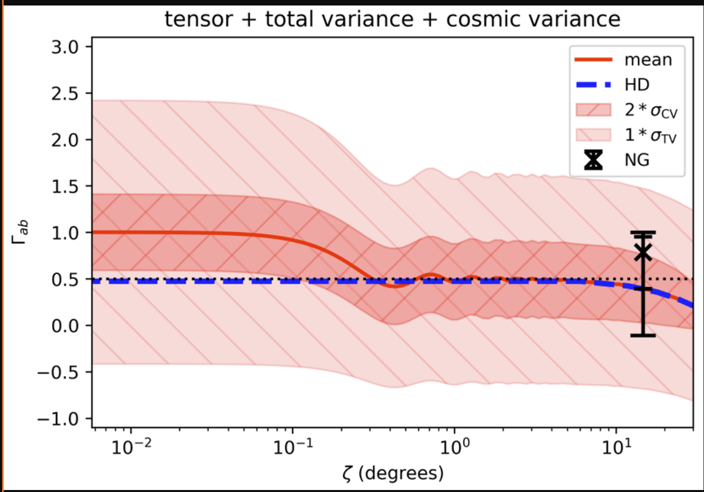

Finite pulsar distance

- At $fD \sim 100$, HD outside 2σ of the CV;
- Accounts for power at small scales;
- Easy to accommodate using PSF.

arXiv:1606.02532 (Bishop & Rezzolla)

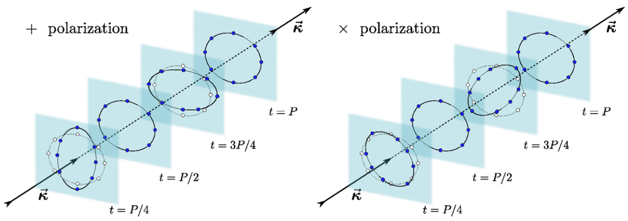

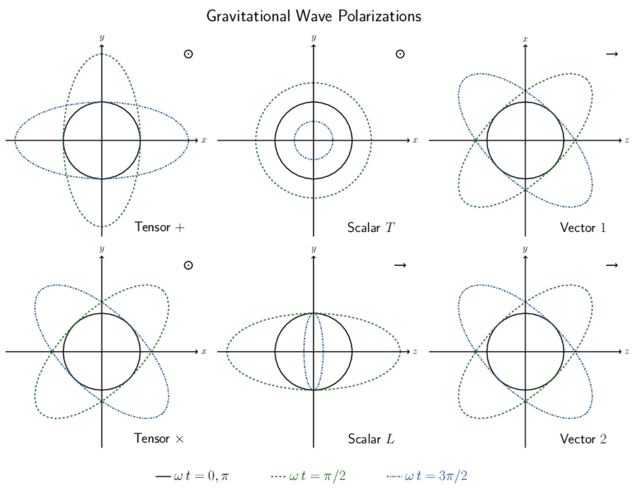

Accessed 041022:
https://cds.cern.ch/record/2632389/files/GW_Polarizations.png

Tensor PS and ORF ($v = 1/2$, half luminal)

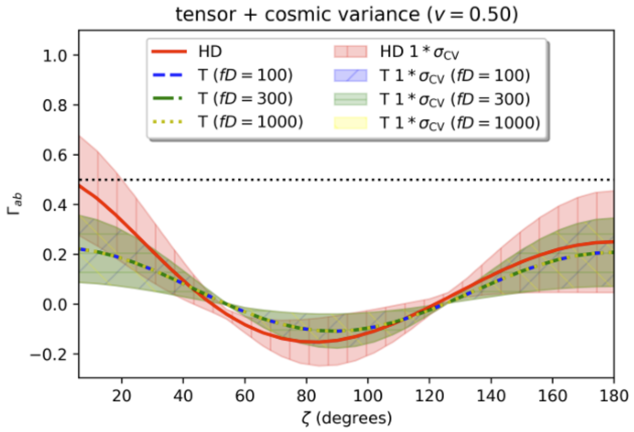

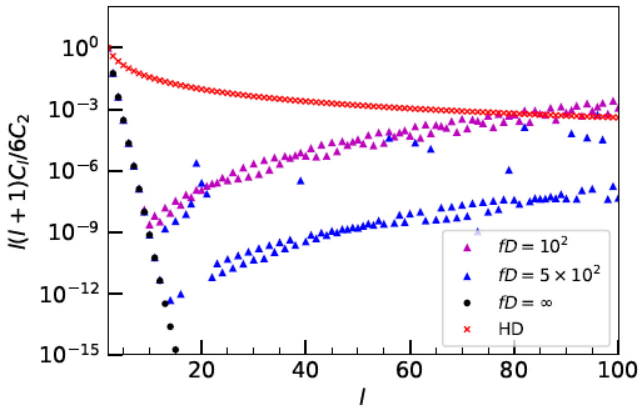

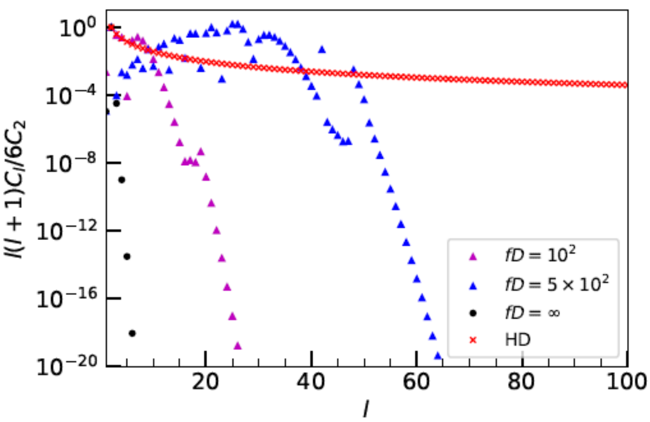

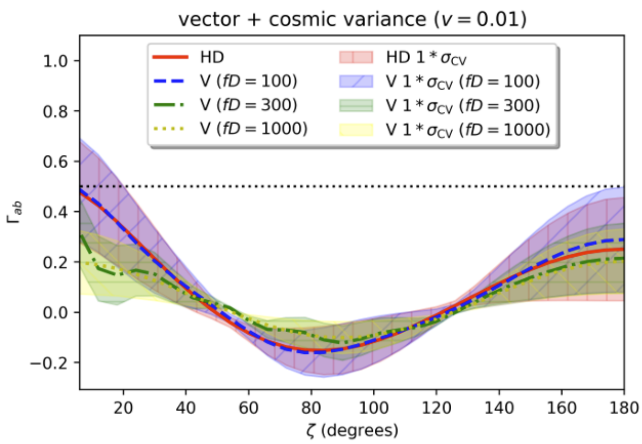

Vector PS and ORF ($v \ll 1$, near static)

The covariant Galileon

$$S_G[g_{ab},\phi] = \int d^4x\sqrt{-g}\left(\left(1+\frac{\alpha\phi}{M_{\rm P}}\right)\mathrm{EH} - \Lambda - \lambda^3\phi + X + \frac{X}{\kappa^3}\partial^2\phi + \frac{\mu^2\phi^2}{2}\right)$$

- **EH** = Einstein-Hilbert term
- $\boldsymbol{\Lambda}$ = cosmological constant
- $\boldsymbol{\kappa}$ = braiding -> Vainshtein mechanism/ϕ suppression at $R \ll L$
- $\boldsymbol{\mu}$ = *bare* mass -> chameleon screening/ϕ suppression at dense environments
- $\boldsymbol{\alpha}$ = conformal coupling -> mixes the tensor and scalar modes
- $\boldsymbol{\lambda}$ = tadpole -> self tuning mechanism (**2202.08672, Appleby, RCB**)

Best fit in NG12.5

$$v = 0.44^{+0.15}_{-0.42}\,c \;\rightarrow m_{\rm eff} \sim 10^{-22}\ \mathrm{eV}\ (\mathrm{Galileon})$$

Marginalized statistics for the ST, SL, and the Galileon ($\boldsymbol{\varphi}$) constrained by NG12.5. The performance statistics (chi-squared, AIC, and BIC) are relative to the systematic monopole, or that a positive value means statistical preference over the systematic monopole.

mode	v	A^2 $[\times 10^{-30}]$	$\Delta\chi^2$	ΔAIC	ΔBIC
ST	0.46 ± 0.24	$5.0^{+1.4}_{-1.6}$	1.47	-0.53	-1.24
SL	< 0.44	$7.9^{+2.8}_{-3.4}$	3.92	1.92	1.21
ϕ	$0.44^{+0.15}_{-0.42}$	3.8 ± 1.2	2.91	0.91	0.20
HD	$v = 1$	3.9 ± 1.1	-1.66	-1.66	-1.66
GW mon.	$- - -$	1.94 ± 0.48	0	0	0

2206.01056 (RCB & KWN)

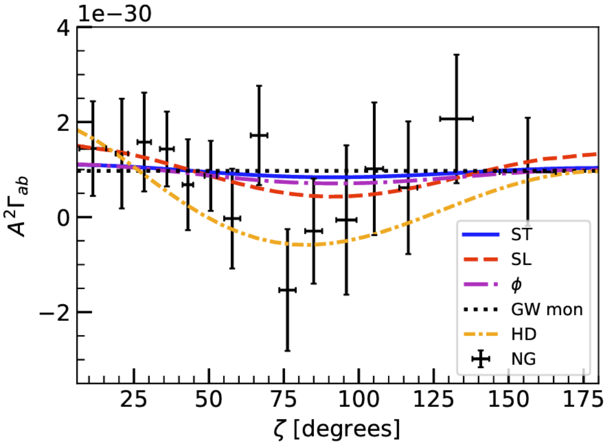

Outlook

In 2206.01056, 2208.12538, 2209.14834 (RCB & KWN), we:

- presented **PS formalism** for calculating the overlap reduction function;
- studied **PTA phenomenology** of **subluminal metric polarizations** for **finite pulsar distances**.

- analysis of tensor polarizations off the light cone;
- alternative gravity constraints;
- anisotropies.

Extra Slides

PSF for variances

(2209.14834, RCB & KWN)

- Mean ORF

$$\gamma_{ab}^{A}(\zeta) = \sum_{l} \frac{2l+1}{4\pi} C_l^A P_l(\cos\zeta)$$

- Total variance [1 PP]

$$\Delta\gamma_{ab}^{2}(\zeta) = \left(\gamma_{ab}^{A}(\zeta)\right)^2 + \gamma_{aa}^{2}$$

- Cosmic variance [Gaussian ensemble]

$$\Delta\gamma_{ab}^{2}(\zeta) = \sum_{l} \frac{2l+1}{8\pi^2} C_l^2 P_l(\cos\zeta)$$

arXiv:2206.01056 (RCB & KWN)

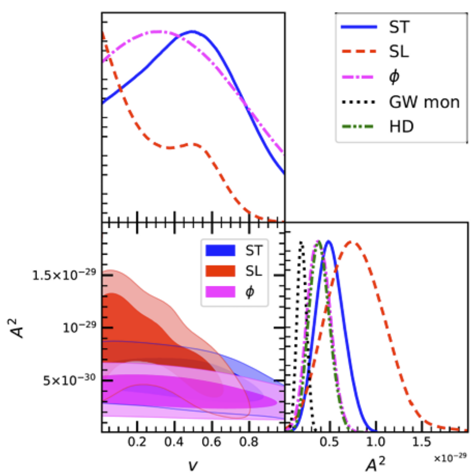

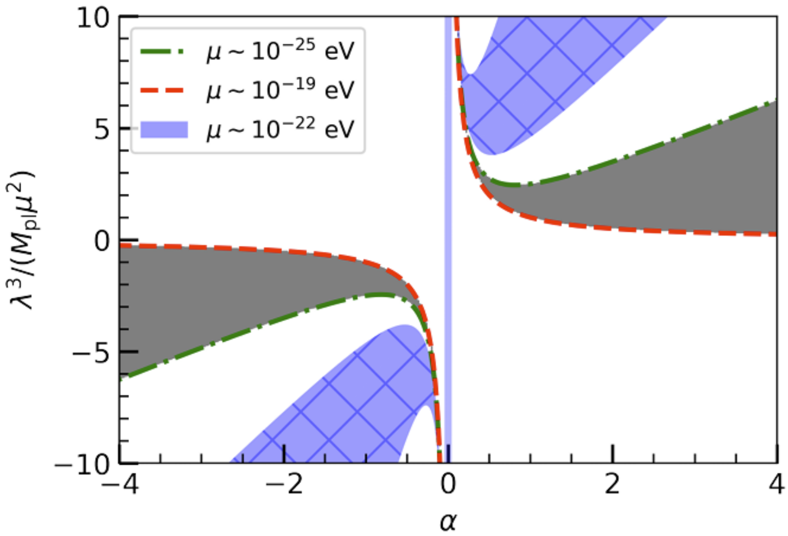

C05

Cosmic strings and GWs from pure Yang-Mills theory

Masaki Yamada

Tohoku University

in collaboration with

Kazuya Yonekura (Tohoku Univ.)

Based on hep-th/2204.13123, hep-th/2204.13125

Oct. 24th, 2022 - JGRG

Cosmic strings from SSB of U(1) symmetry

- Cosmic strings form after the spontaneous symmetry breaking of U(1) symmetry.

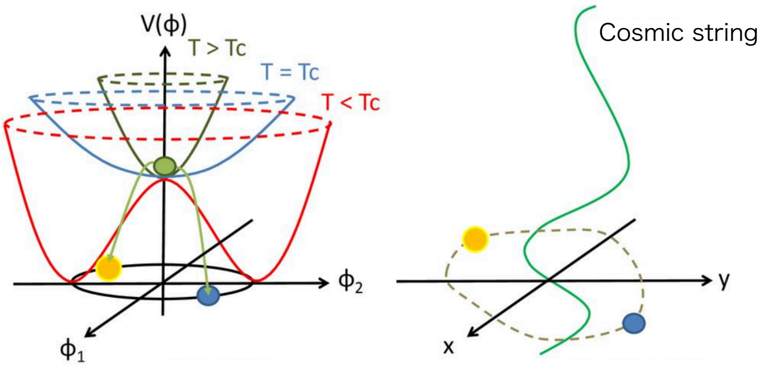

Figure from Daisuke Yamauchi's slide

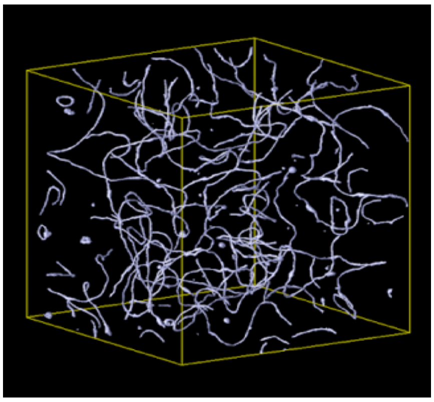

Hiramatsu, Sendouda, Takahashi, Yamauchi, Yoo, '13

Cosmic strings from SU(N) confinement

- Let us consider an SU(N) gauge theory.
- After the confinement phase transition, quark and anti-quark are connected by a color flux tube.

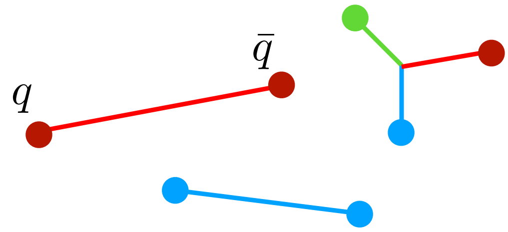

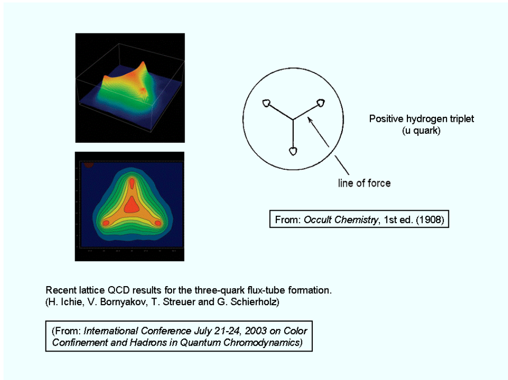

Cosmic strings from SU(N) confinement

- According to the duality between strong and weak coupling theories, the color flux tube can be identified as a cosmic string.

Strong coupling theory

high T: Deconfinement phase
low T: Confinement phase

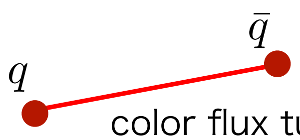

Duality ⟷

Weak coupling theory

high T: Symmetric phase
low T: Higgs phase

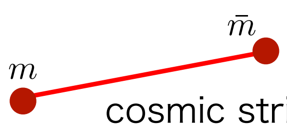

Seiberg, Witten '94

- The duality implies that the color flux tubes form even without quarks.

Properties of cosmic strings

- According to the electric-magnetic duality, cosmic strings (macroscopic color flux tubes) should form at the confinement phase transition.
- The string tension is of order the dynamical scale squared, $\mu \sim \Lambda^2$.
- According to the large N limit argument, the reconnection probability of two cosmic strings is suppressed by $P \sim N^{-2}$.

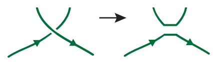

- According to the holographic dual descriptions, those cosmic strings correspond to fundamental (F-) strings in gravity side.

See, e.g., Witten '98, Polchinski, Strassler '00, Klebanov, Strassler '00, Maldacena, Nunez '00, Vafa '00

Dynamics of cosmic strings: VOS model

- Long strings lose their energy via small loop production.

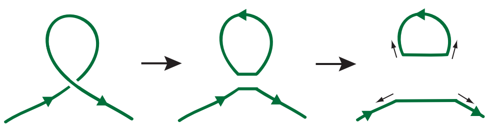

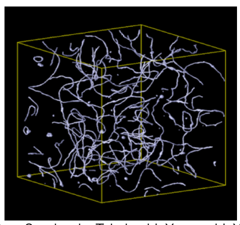

Hiramatsu, Sendouda, Takahashi, Yamauchi, Yoo, '13

- The statistical properties of cosmic string network can be described by the following equations. This is known as the one-scale model.

Energy density: $$\frac{d\rho_\infty}{dt} = -\left(2H(1+\bar{v}^2)\right)\rho_\infty + \left(\frac{d\rho_\infty}{dt}\right)_{\rm loop}, \qquad \rho_\infty \propto P^{-1}$$

Velocity dispersion: $$\frac{d\bar{v}}{dt} = (1-\bar{v}^2)\left(\frac{k(\bar{v})}{R} - 2H\bar{v}\right),$$

$$-P\, n_\infty(\tilde{c}\mu\xi)\frac{n_\infty \xi^3 \bar{v}}{\xi}$$

curvature ~ H^{-1}

Kibble '85, Martins, Shellard '95, '96, '00
MY and Yonekura '22

Gravitational waves from cosmic strings

- Long strings lose their energy via small loop production.

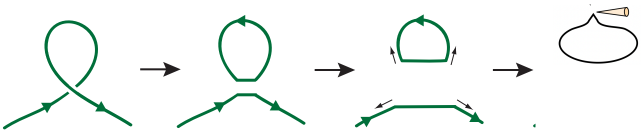

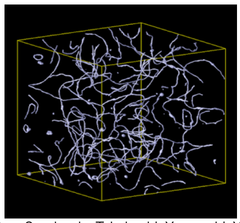

Hiramatsu, Sendouda, Takahashi, Yamauchi, Yoo, '13

- Gravitational waves are produced from the dynamics of string loops.

Vilenkin '81, Vachaspati, Vilenkin '85

$$\frac{d\rho_{\rm GW}}{df}(t) = \int_{t_i}^{t} dt' \left(\frac{a(t')}{a(t)}\right)^3 \int_0^l dl\, n_{\rm loop}(l,t')\, h\left(f\frac{a(t)}{a(t')}, l\right)$$

$$(\Omega_{\rm GW}h^2)^{(\rm peak)} \simeq 2.5\times 10^{-10} \times P_{\rm eff}^{-1}\left(\frac{G\mu}{10^{-12}}\right)^{1/2}$$

$$f^{(\rm peak)} \simeq 1.9\times 10^{-6}\,{\rm Hz}\times\left(\frac{G\mu}{10^{-12}}\right)^{-1}$$

MY and Yonekura '22

Gravitational waves from cosmic strings

- Gravitational waves are produced from the dynamics of string loops.

Peak amplitude of GW:

$$(\Omega_{\rm GW}h^2)^{(\rm peak)} \simeq 2.5\times 10^{-10} \times P_{\rm eff}^{-1}\left(\frac{G\mu}{10^{-12}}\right)^{1/2}$$

Peak frequency:

$$f^{(\rm peak)} \simeq 1.9\times 10^{-6}\,{\rm Hz}\times\left(\frac{G\mu}{10^{-12}}\right)^{-1}$$

Physical parameters in the theory:

$$\begin{cases} \mu \sim \Lambda^2 \\ P \sim N^{-2} \end{cases}$$

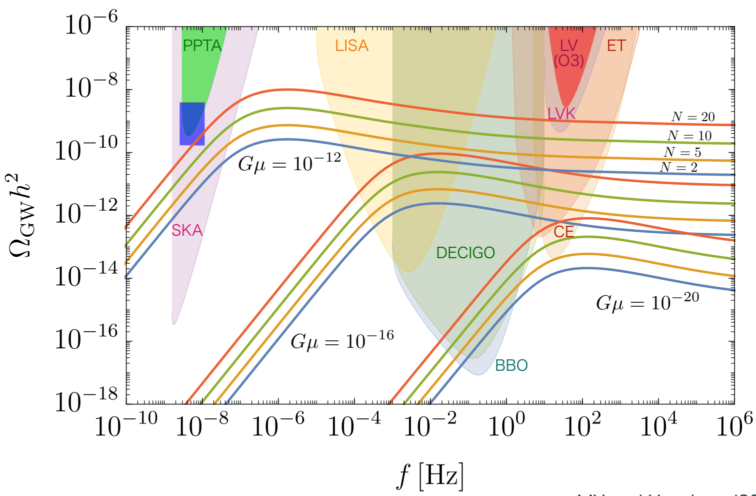

MY and Yonekura '22

Gravitational waves from cosmic strings

- Gravitational waves are produced from the dynamics of string loops.

Peak amplitude of GW:

$$(\Omega_{\rm GW}h^2)^{(\rm peak)} \simeq 2.5 \times 10^{-10} \times P_{\rm eff}^{-1} \left(\frac{G\mu}{10^{-12}}\right)^{1/2}$$

Peak frequency:

$$f^{(\rm peak)} \simeq 1.9 \times 10^{-6}\,{\rm Hz} \times \left(\frac{G\mu}{10^{-12}}\right)^{-1}$$

Physical parameters in the theory:

$$\begin{cases} \mu \sim \Lambda^2 \\ P \sim N^{-2} \end{cases}$$

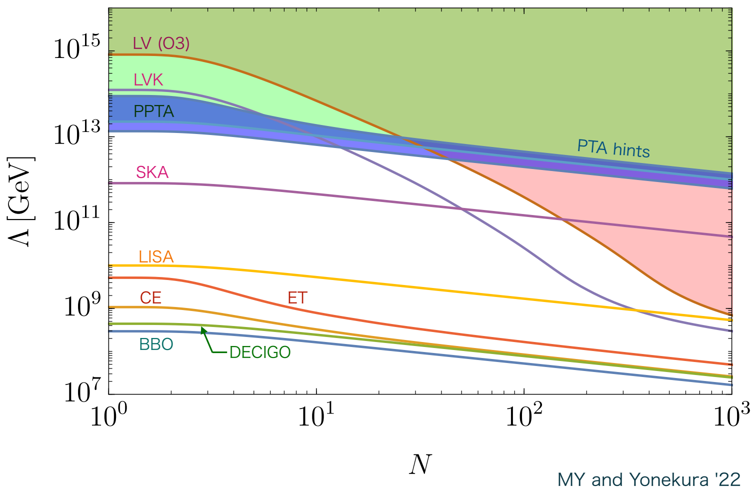

MY and Yonekura '22

Summary

- We pointed out that cosmic strings form after the confinement phase transition in pure SU(N) gauge theory.
- The string tension is $\mu \sim \Lambda^2$
- The reconnection probability is suppressed by $P \sim N^{-2}$
- We extend the VOS model to describe the dynamics of cosmic strings and calculate the GW spectrum.

C06

Temperature Profile Around a Primordial Black Hole

Speaker: Minxi He (IPNS, KEK)

2022/10/24@JGRG31, RESCEU

MH, Kazunori Kohri, Kyohei Mukaida, Masaki Yamada, arXiv: 2210.06238

Plan of the talk

- Primordial black hole (PBH) and Hawking evaporation
- Landau-Pomeranchuk-Migdal (LPM) effect and diffusion
- Temperature profile around a primordial black hole
- Summary

Hawking radiation

- Black holes emit nearly blackbody radiation with Hawking temperature

$$T_{\rm BH} = M_{\rm pl}^2/M \simeq 1.1 \times 10^4 {\rm GeV} (M/10^9 {\rm g})^{-1}$$

The typical energy of the emitted particle is therefore $\sim T_{\rm BH}$

- Mass loss rate is inversely proportional to M^2

$\Rightarrow$ evaporation process accelerates
Hawking temperature increases with time

$$-dM/dt \propto M^{-2} \qquad t_{\rm ev} \simeq 0.41 \ {\rm sec} \ \left(M/10^9 {\rm g}\right)^3$$

Hawking (1974)

Hawking radiation

- Big Bang nucleosynthesis (BBN) time $\sim 1 \ {\rm sec}$

Compare with $t_{\rm ev} \simeq 0.41 \ {\rm sec} \ \left(M/10^9 {\rm g}\right)^3$

$\Rightarrow$ A black hole with a mass $\lesssim 10^9 \ {\rm g}$ formed in the very early Universe, it completely evaporates by BBN.

- Such tiny black holes can only form in the early Universe through the collapse of large enough density perturbation, i.e. primordial black holes (PBHs).

Hawking (1974)

Primordial black holes (PBHs)

- Inflation ⟶ Quantum fluctuations, nearly scale-invariant and Gaussian

$\delta > \delta_c$

⬇

PBH

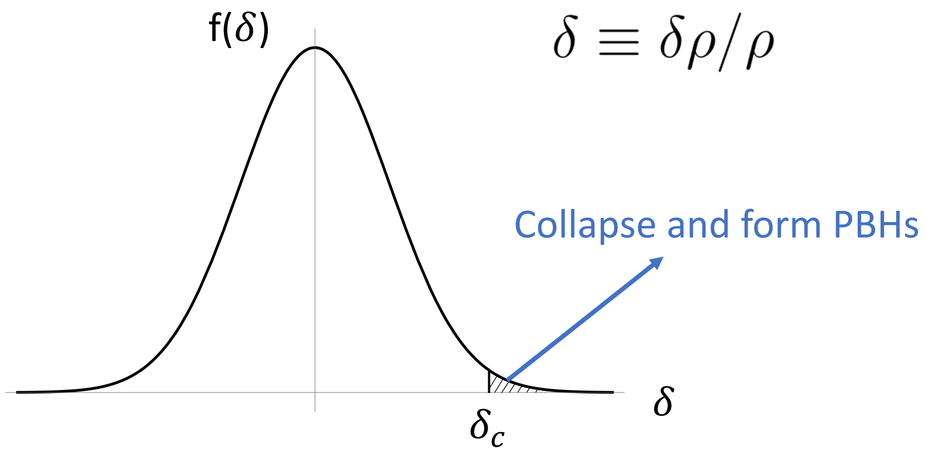

Zel'dovich, Novikov (1974), Hawking (1971), Carr, Hawking (1974), Carr (1975)

Primordial black holes (PBHs)

- PBH mass depends on formation time (here focus on the PBHs form in RD era).

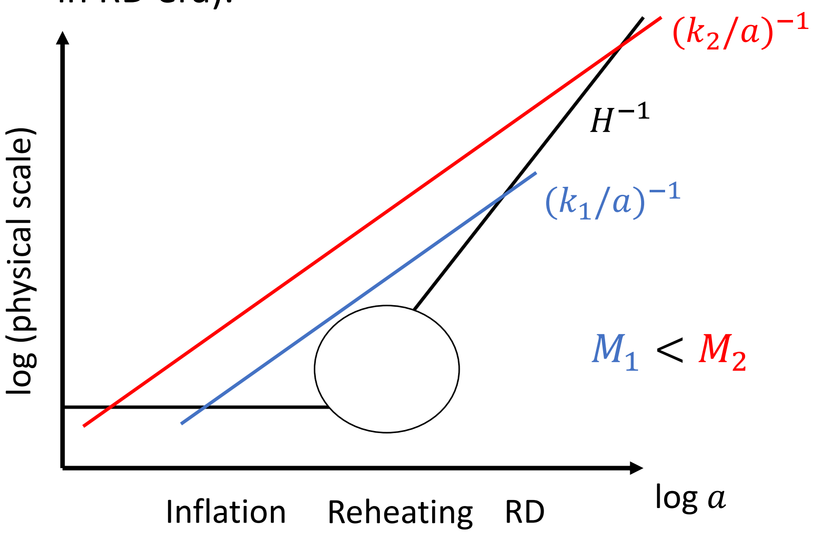

PBH mass at formation is proportional to the horizon mass

$$M_{\rm ini} = \gamma \frac{4\pi\rho}{3H_{\rm ini}^3}$$

⬇

Lower bound on PBH mass > 0.4 g

Primordial black holes (PBHs)

- Assume RD right after the PBH evaporation. Then, using the lifetime of these PBHs, one can estimate the temperature of the Universe at evaporation

$$T_{\rm ev} \simeq 1.5\mathrm{MeV}\,(M_{\rm ini}/10^9\mathrm{g})^{-3/2}$$

$$\ll \quad T_{\rm BH} = M_{\rm pl}^2/M \simeq 1.1 \times 10^4\mathrm{GeV}(M/10^9\mathrm{g})^{-1}$$

➡ Before evaporation, the Hawking temperature will become much higher than the temperature of the ambient plasma. This fact is essential for the discussion of thermalization of the Hawking radiation from these PBHs.

Landau-Pomeranchuk-Migdal (LPM) effect

- For a particle with energy much larger than the ambient plasma, the thermalization process is suppressed by the LPM effect. This process is dominated by the emission of soft daughter particles.

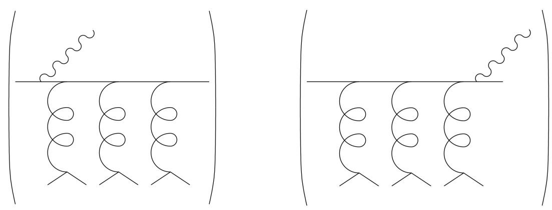

- The emitted daughter particles are almost conlinear with the hard primary, which leads to destructive quantum interference.

Landau, Pomeranchuk (1953), Migdal (1956)
Gyulassy, Wang (1994), Arnold, Moore, Yaffe (2001a,2001b,2002),
Besak, Bodeker (2010), Kurkela, Wiedmann (2014)

Landau-Pomeranchuk-Migdal (LPM) effect

- More intuitive understanding (relevant regime $p \gtrsim T/\alpha^2 \gg T$)

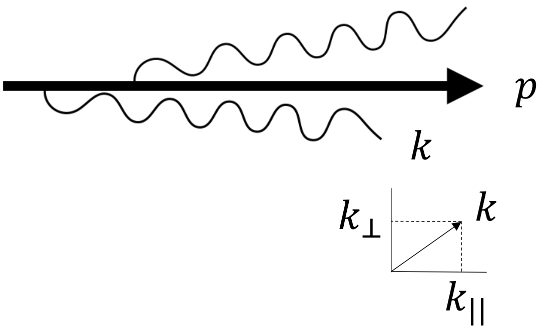

Almost colinear so cannot separate from the mother particle

Typically, it needs $t \geq k/k_\perp^2$ to form and separate, where $k_\perp$ experiences Brownian motion in the medium

$$k_\perp^2 \sim \hat{q}_{\rm el} t \sim \alpha^2 T^3 t$$

Landau, Pomeranchuk (1953), Migdal (1956)
Gyulassy, Wang (1994), Arnold, Moore, Yaffe (2001a,2001b,2002),
Besak, Bodeker (2010), Kurkela, Wiedmann (2014)

Landau-Pomeranchuk-Migdal (LPM) effect

- More intuitive understanding (relevant regime $p \gtrsim T/\alpha^2 \gg T$)

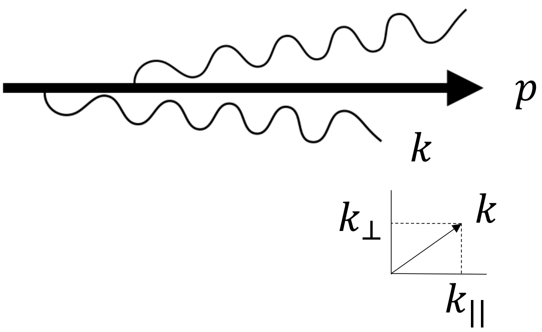

Almost colinear so cannot separate from the mother particle

$$t_{\rm form} \sim \alpha^{-1} \sqrt{k/T^3}$$

Landau, Pomeranchuk (1953), Migdal (1956)
Gyulassy, Wang (1994), Arnold, Moore, Yaffe (2001a,2001b,2002),
Besak, Bodeker (2010), Kurkela, Wiedmann (2014)

Landau-Pomeranchuk-Migdal (LPM) effect

- More intuitive understanding (relevant regime $p \gtrsim T/\alpha^2 \gg T$)

$$t_{\rm form} \sim \alpha^{-1}\sqrt{k/T^3}$$

In a weakly coupled theory, this only means that there is a probability $\sim\alpha$ to emit such a particle.

$$\Gamma_{\rm LPM}(\boxed{k}, T) \equiv \alpha\ t_{\rm form}^{-1} \sim \alpha^2\sqrt{T^3/k}$$

Momentum of the daughter particle

Landau, Pomeranchuk (1953), Migdal (1956)
Gyulassy, Wang (1994), Arnold, Moore, Yaffe (2001a,2001b,2002),
Besak, Bodeker (2010), Kurkela, Wiedmann (2014)

Landau-Pomeranchuk-Migdal (LPM) effect

- More intuitive understanding (relevant regime $p \gtrsim T/\alpha^2 \gg T$)

$$\Gamma_{\rm LPM}(k, T) \equiv \alpha\ t_{\rm form}^{-1} \sim \alpha^2\sqrt{T^3/k}$$

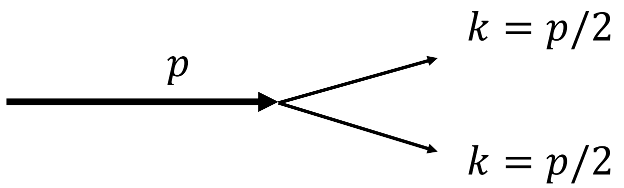

- Max energy loss
- Longest time
- But still $k \sim p \gg T$

Landau, Pomeranchuk (1953), Migdal (1956)
Gyulassy, Wang (1994), Arnold, Moore, Yaffe (2001a,2001b,2002),
Besak, Bodeker (2010), Kurkela, Wiedmann (2014)

Landau-Pomeranchuk-Migdal (LPM) effect

- More intuitive understanding (relevant regime $p \gtrsim T/\alpha^2 \gg T$)

$$\Gamma_{\rm LPM}(k,T) \equiv \alpha\; t_{\rm form}^{-1} \sim \alpha^2 \sqrt{T^3/k}$$

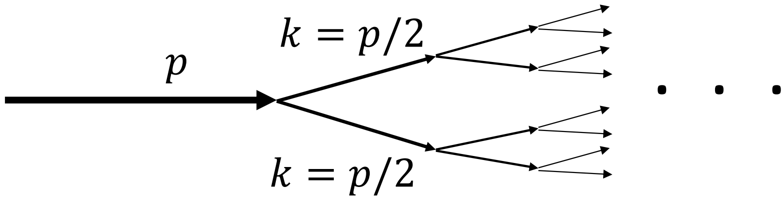

Need a series of splittings with subsequent splittings take shorter time. Estimate as $t_{\rm th}(p,T) \equiv 1/\Gamma_{\rm LPM}(p,T)$

Landau, Pomeranchuk (1953), Migdal (1956)
Gyulassy, Wang (1994), Arnold, Moore, Yaffe (2001a,2001b,2002),
Besak, Bodeker (2010), Kurkela, Wiedmann (2014)

Diffusion

- For $t \gtrsim t_{\rm th}$, the high energy particles from the PBH get thermalized and deposit their energy into the shell $r \simeq t_{\rm th}$ (before that the particle travels with speed of light). This energy will then diffuse (random walk process) into other part of the ambient plasma.

Diffusion length $r_{\rm d}(t,T) \sim \sqrt{t/(\alpha^2 T)}$

➡ Two important scales

1. $r_{\rm d}(t_{\rm d},T) = t_{\rm th}(T_{\rm BH}(M),T)$
   Time scale for diffusion to cover $t_{\rm th}$
2. $r_{\rm dec} \equiv r_{\rm d}(t_{\rm ev}(M), T(r_{\rm d}))$
   Max distance that diffusion can cover

Temperature profile around a PBH

- Regime 1: $t \lesssim t_{\rm ev}$

Black hole mass is almost unchanged.

If $t_{\rm d} < t_{\rm ev}$, the diffusion can cover $t_{\rm th}$

$\Longrightarrow$ A core in equilibrium

$M > M_* \simeq 0.8~{\rm g}$

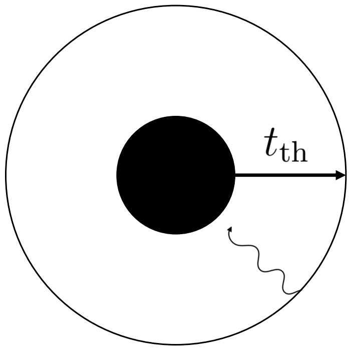

Temperature profile around a PBH

- Regime 1: $t \lesssim t_{\rm ev}$

Black hole mass is almost unchanged.

If $t_{\rm d} < t_{\rm ev}$, the diffusion can cover $t_{\rm th}$

$\Longrightarrow$ A core in equilibrium

Energy conservation

$\Longrightarrow$ $T(r \gtrsim t_{\rm th}) \propto r^{-1/3}$

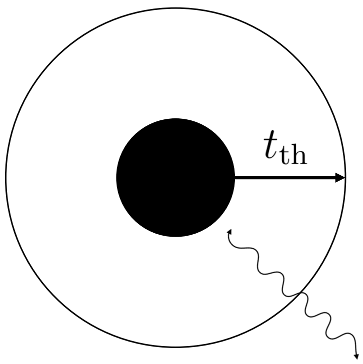

Temperature profile around a PBH

- Regime 1: $t \lesssim t_{\rm ev}$

Black hole mass is almost unchanged.

If $t_{\rm d} < t_{\rm ev}$, the diffusion can cover $t_{\rm th}$

➡ A core in equilibrium

Energy conservation

➡ $T(r \gtrsim t_{\rm th}) \propto r^{-1/3}$

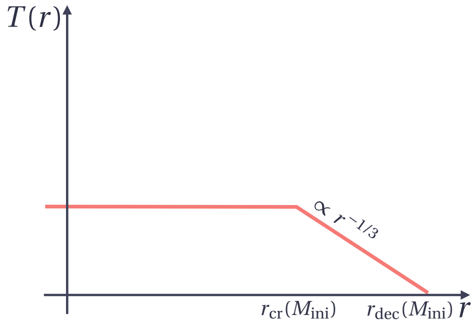

Temperature profile around a PBH

- Regime 2: $M_* \lesssim M \lesssim M_{\rm ini}$ ($M > M_* \simeq 0.8$ g still satisfied)

Change of black hole mass is not neglibile. Simply change the previous analysis by replacing the constant mass with a time-dependent mass.

➡ $r_{\rm cr} \propto M$

$r_{\rm dec} \propto M^{11/5}$

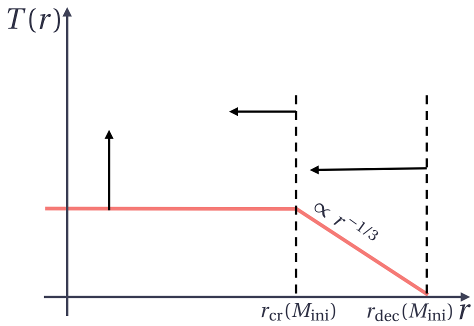

Temperature profile around a PBH

- Regime 2: $M_* \lesssim M \lesssim M_{\rm ini}$ ($M > M_* \simeq 0.8$ g still satisfied)

Change of black hole mass is not neglibile. Simply change the previous analysis by replacing the constant mass with a time-dependent mass.

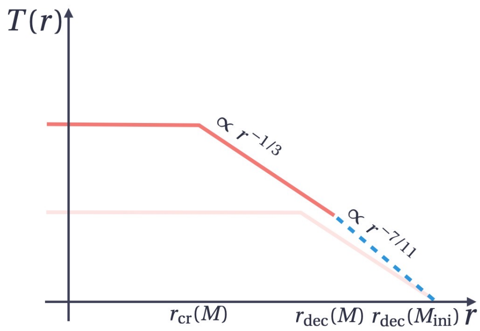

$\Rightarrow$ $r_{\rm cr} \propto M$

$r_{\rm dec} \propto M^{11/5}$

$\Rightarrow$ $T \propto r^{-7/11}$

Temperature profile around a PBH

- Regime 2: $M_* \lesssim M \lesssim M_{\rm ini}$ ($M > M_* \simeq 0.8$ g still satisfied)

Change of black hole mass is not neglibile. Simply change the previous analysis by replacing the constant mass with a time-dependent mass.

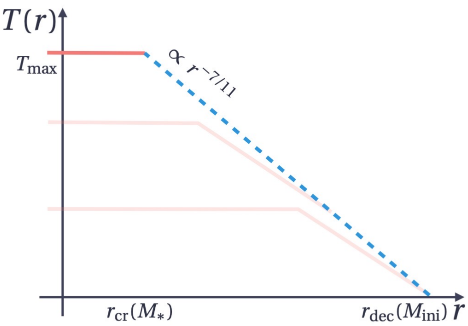

$\Rightarrow$ $r_{\rm cr} \propto M$

$r_{\rm dec} \propto M^{11/5}$

$\Rightarrow$ $T \propto r^{-7/11}$

$$T_{\rm max} \equiv T(r < r_{\rm cr})|_{M_*} \simeq 2 \times 10^9\,{\rm GeV} \left(\frac{\alpha}{0.1}\right)^{\frac{19}{3}} \left(\frac{g_*}{106.75}\right)^{-\frac{4}{3}} \left(\frac{g_{H*}}{108}\right)^{\frac{5}{6}} \quad \text{at } M = M_*$$

Independent of the initial black hole mass

Temperature profile around a PBH

- Regime 3: $M < M_*$

Diffusion can no longer cover the core.

⟹ High-temperature shell at $t_{\rm th}$?

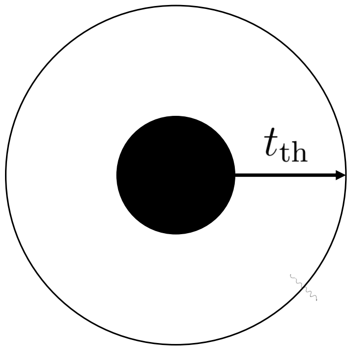

Temperature profile around a PBH

- Regime 3: $M < M_*$

Diffusion can no longer cover the core.

⟹ High-temperature shell at $t_{\rm th}$?

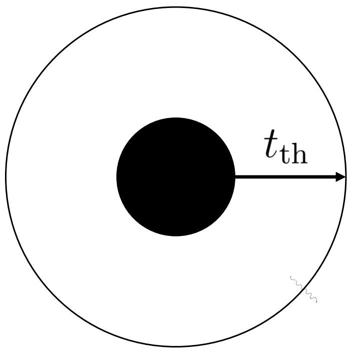

Actually no because

1. Hawking temperature is higher at later time
   ⟹ more LPM-suppressed
   ⟹ energy deposited in larger radius
2. Less total energy at later time as the black hole mass is getting smaller

⟹ Smaller energy density hence smaller $T \propto \rho^{1/4}$

Summary

- We consider the thermalization of the Hawking radiation from small PBHs in the early Universe
- Take into account the LPM effect and diffusion

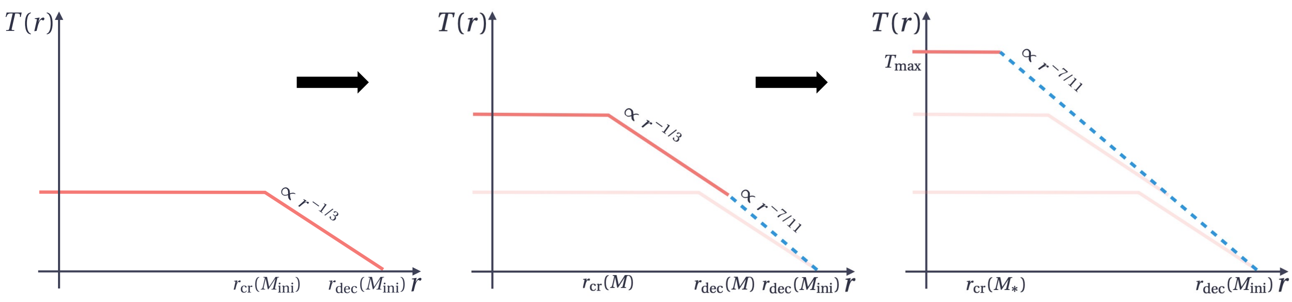

Thank you for your attention!

C07

Varying electron mass solution to the Hubble tension and Big Bang Nucleosynthesis

Theoretical Particle & Cosmological Physics Group
Hokkaido University
D1　Yo Toda

Osamu Seto, Yo Toda　arXiv:astro-ph/2206.13209

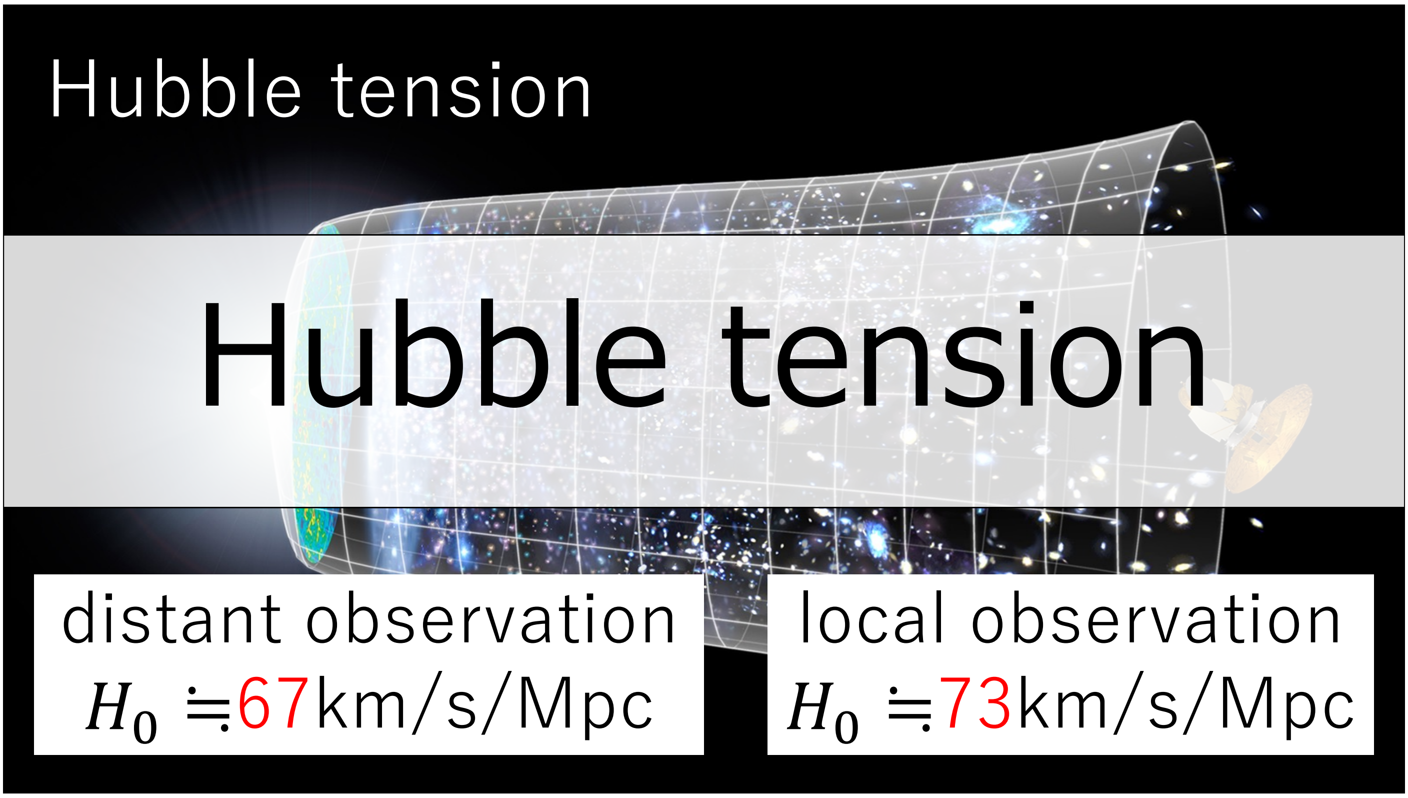

HUBBLE TENSION SOLUTION

Model	$\Delta N_{\rm param}$	$\Delta\chi^2$	Finalist
ΛCDM	0	0.00	✗
$\Delta N_{\rm ur}$	1	−6.10	✗
SIDR	1	−9.57	✓ 3
mixed DR	2	−8.83	✗
DR-DM	2	−8.92	✗
SIν+DR	3	−4.98	✗
Majoron	3	−15.49	✓ 2
primordial B	1	−11.42	✓ 3
varying m_e	1	−12.27	✓ 1
varying m_e+Ω_k	2	−17.26	✓ 1
EDE	3	−21.98	✓ 2
NEDE	3	−18.93	✓ 2
EMG	3	−18.56	✓ 2
CPL			
PED			
GPE			
DM			
DM			

varying m_e	1	−12.27	✓ 1
varying m_e+Ω_k	2	−17.26	✓ 1

varying electron mass

▼

fewer additional parameters
large improvement in $\Delta\chi^2$

In this presentation

・Consider the varying electron mass model and its consistency with BBN

・Summarize that the varying electron mass model is limited by helium abundance Yp measurements

VARYING ELECTRON MASS MODEL

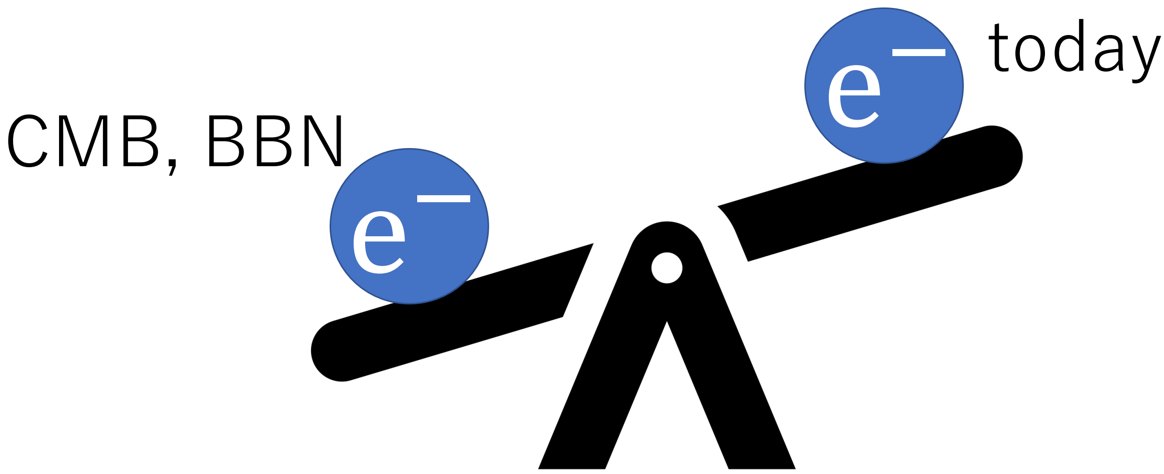

VARYING ELECTRON MASS MODEL

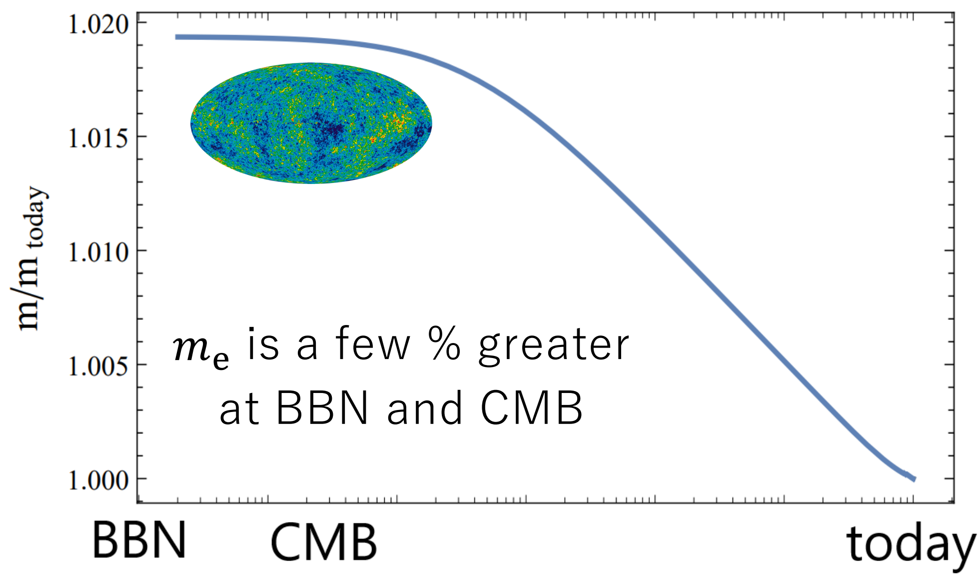

ELECTRON MASS AND CMB

Electron mass at last scattering was greater than today

$m_{\mathrm{e}\,|\mathrm{Last\ Scatter}}/m_{\mathrm{e}\,|\mathrm{today}} > 1$

Photons lose energy earlier
to excite electrons in hydrogen

$\because$ energy level of hydrogen: $E \propto m_{\mathrm{e}}$

Recombination occurs earlier

Last scattering time t_* gets shorter

ELECTRON MASS AND CMB

Angular Size : $\theta_* = \frac{r_*}{D_{M*}} = (1.0411 \pm 0.0003)\times 10^{-2}$

$r_* = \int_0^{t_*} \frac{c_s d\tilde{t}}{a(\tilde{t})}$: comoving sound horizon at recombination

$D_{M*} = \int_{t_*}^{t_0} \frac{d\tilde{t}}{a(\tilde{t})}$: comoving angular diameter distance

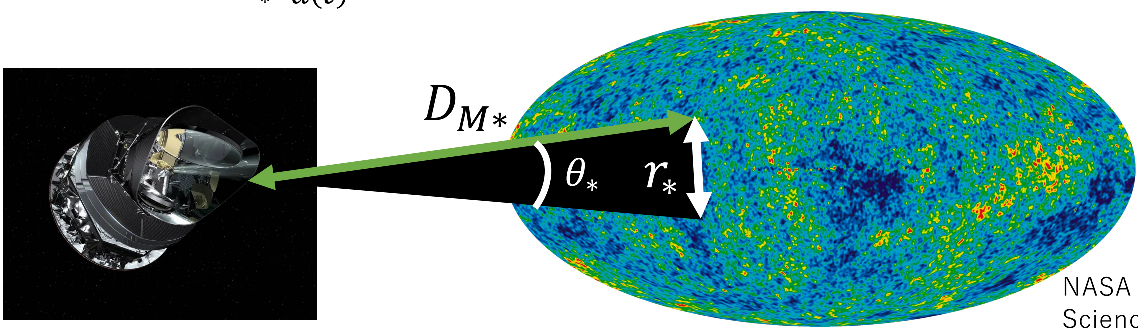

NASA / WMAP
Science Team

ELECTRON MASS AND CMB

Angular Size : $\theta_* = \frac{r_*}{D_{M*}} = (1.0411 \pm 0.0003) \times 10^{-2}$
$\propto H_0 \times r_*$

Electron mass was greater than today and
last scattering time t_* gets shorter

▼ $r_* = \int_0^{t_*} \frac{c_s d\tilde{t}}{a(\tilde{t})}$: comoving sound horizon at recombination

Horizon r_* decreases and Hubble constant H_0 increases

ELECTRON MASS AND HUBBLE H_0

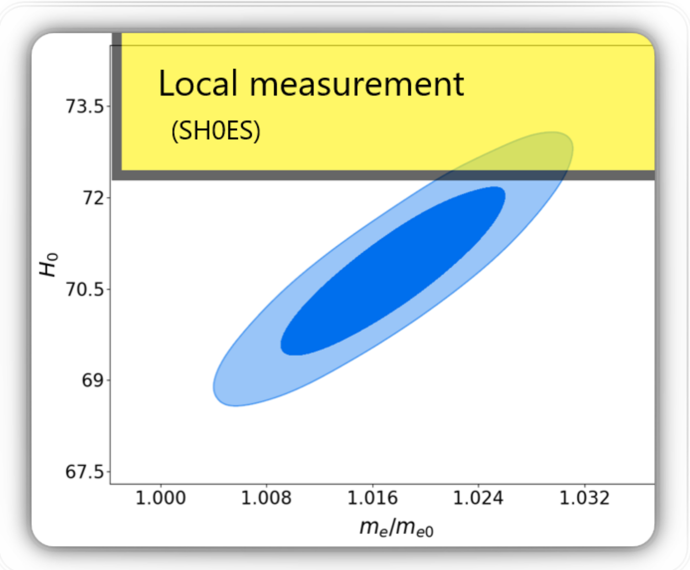

m_e/m_{e0} ↑

▼

Hubble constant H_0 ↑

Planck + Pantheon + BAO + SH0ES

BBN consistency

ELECTRON MASS AND BBN

Electron mass at BBN was larger than today

▼ $m_{\mathrm{e}\,|\mathrm{BBN}}/m_{\mathrm{e}\,|\mathrm{today}} > 1$

Neutron lifetime$(n + \nu_e \to p + e^-)$gets longer

▼

Neutron-to-proton ratio (n/p) increases

▼

Helium mass fraction Y_P increases

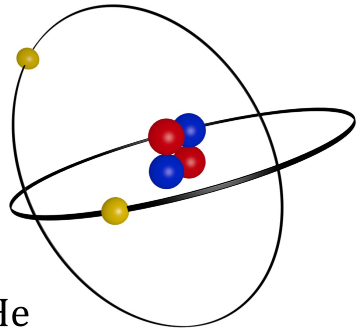

$^4\mathrm{He}$

ELECTRON MASS AND HELIUM Y_P

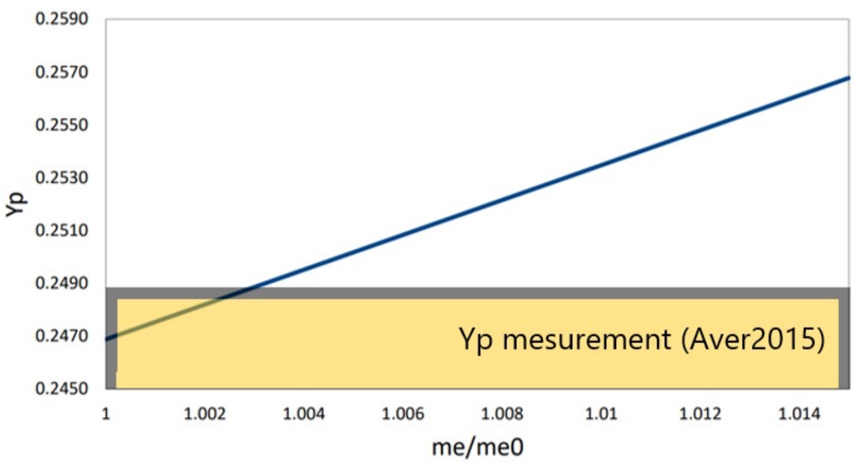

$m_{\mathrm{e}}/m_{\mathrm{e0}}$

▼

helium Y_P

BEST-FIT

Parameter	$\frac{m_e}{m_{e0}} = 1.00$	$\frac{m_e}{m_{e0}} = 1.01$	$\frac{m_e}{m_{e0}} = 1.015$
H_0[km/s/Mpc]	67.7679	68.9728	70.423
Y_P	0.246883	0.253517	0.256897
$D/H \times 10^5$	2.5081	2.48528	2.44627
χ^2_{Cooke17}	1.3691	1.99689	3.3433
χ^2_{Aver15}	0.24233	4.61371	8.95409
χ^2_{prior}	4.9674	3.98448	4.57643
χ^2_{CMB}	2776.4	2779.61	2779.36
χ^2_{BAO}	5.5765	5.27398	6.82482
χ^2_{total}	2788.56	2795.479	2803.059

Y_P measurement

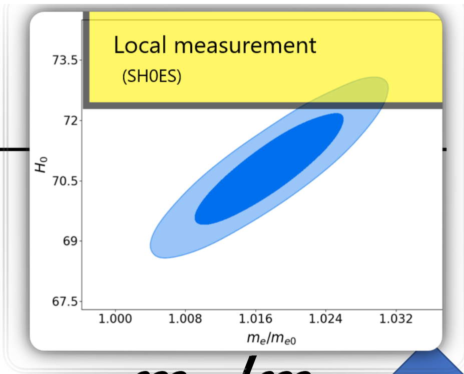

m_e/m_{e0}

worse $\chi^2_{Y_P}$

To relax this limit
neutrino degeneracy

NEUTRINO DEGENERACY

The degeneracy parameter $\xi_i = \dfrac{\mu_{\nu i}}{T_\nu}$ $(i = e, \mu, \tau)$

μ_{ν_i} : chemical potential for neutrinos ν_i

T_ν : temperature of neutrinos

distribution functions

$$f_\nu = \frac{1}{\exp(p/T_\nu - \xi_i) + 1}$$

$$f_{\bar{\nu}} = \frac{1}{\exp(p/T_\nu + \xi_i) + 1}$$

Number densities of
neutrinos and antineutrinos

$$n_{\nu_i} - n_{\bar{\nu}_i} \propto T^3_{\nu_i}(\pi^2 \xi_i + \xi_i^3) \rightarrow \text{BBN}$$

NEUTRINO DEGENERACY

Positive electron neutrino degeneracy ξ_e

$$n_{\nu_e} - n_{\bar{\nu}_e} \propto T_{\nu_e}^3 (\pi^2 \xi_e + \xi_e^3)$$

More neutrinos ν_e than antineutrinos $\bar{\nu}_e$

The process $p + \bar{\nu}_e \to n + e^+$ is more suppressed than $n + \nu_e \to p + e^-$

Neutron-to-proton ratio (n/p) and helium mass fraction Y_P decrease

BEST-FIT

Parameter	$\frac{m_e}{m_{e0}} = 1.00$	$\frac{m_e}{m_{e0}} = 1.01$	$\frac{m_e}{m_{e0}} = 1.015$	$\left(\frac{m_e}{m_{e0}}, \xi_e\right) =$ (1.015, 0.05)
H_0[km/s/Mpc]	67.7679	68.9728	70.423	70.024
Y_P	0.246883	0.253517	0.256897	0.245207
$D/H \times 10^5$	2.5081	2.48528	2.44627	2.41079
$\chi^2_{\mathrm{Cooke17}}$	1.3691	1.99689	3.3433	4.86725
χ^2_{Aver15}	0.24233	4.61371	8.95409	0.00605534
χ^2_{prior}	4.9674	3.98448	4.57643	3.24241
χ^2_{CMB}	2776.4	2779.61	2779.36	2780.3
χ^2_{BAO}	5.5765	5.27398	6.82482	5.94482
χ^2_{total}	2788.56	2795.479	2803.059	2794.361

Y_P measurement

ξ_e degenerates

χ^2 improves

TAKE-HOME MESSAGE

・The varying electron mass model is
a promising solution to the Hubble tension.
($\Delta m_{\mathrm{e}}/m_{\mathrm{e}0}$ $\gtrsim$2% can solve the Hubble tension)

・However, this model is limited
by the **helium** abundance measurement.
(Even $\Delta m_{\mathrm{e}}/m_{\mathrm{e}0}$ =1.5% doesn't fit well.)

・The combination model of varying electron mass
and neutrino degeneracy relaxes this limitation.

Thank you
for your kind attention!

Osamu Seto, Yo Toda arXiv : 2206.13209
y-toda@particle.sci.hokudai.ac.jp

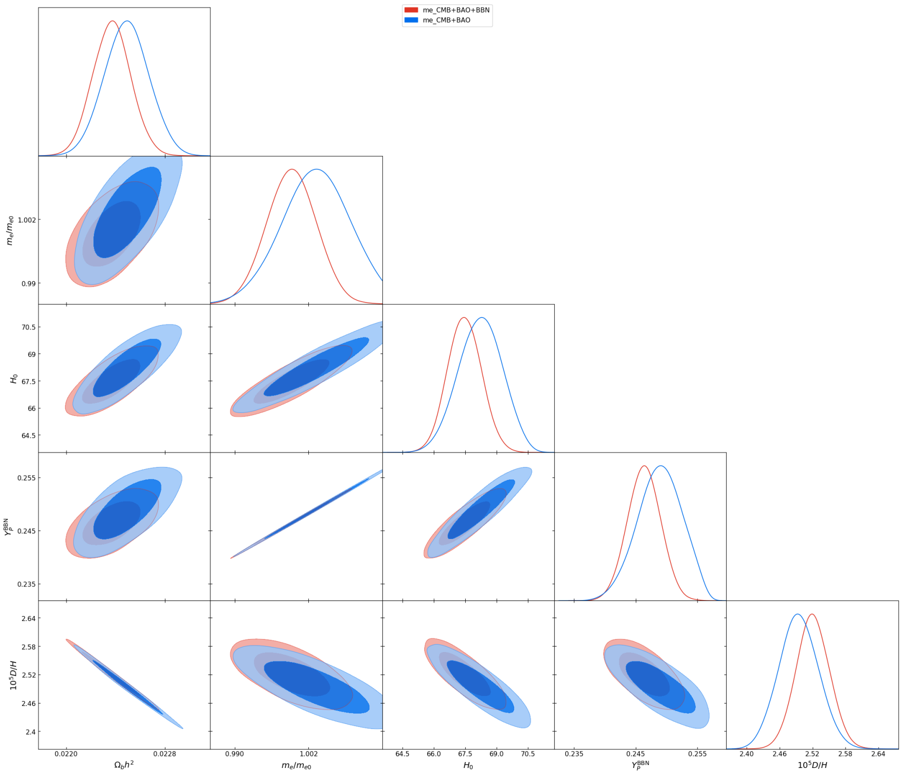

me_CMB+BAO+BBN
me_CMB+BAO
$\Omega_b h^2$
m_e/m_{e0}
H_0
Y_P^{BBN}
$10^5 D/H$

D/Hについて

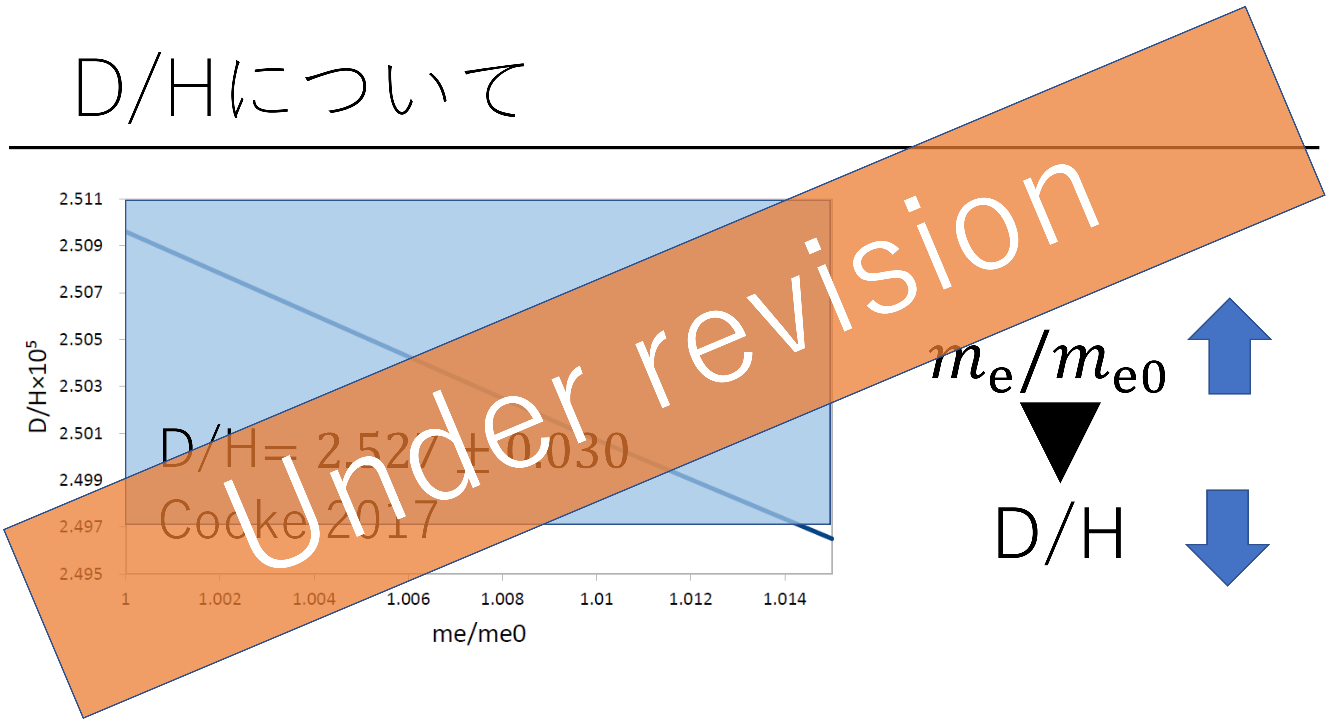

D/H×10^5
2.511
2.509
2.507
2.505
2.503
2.501
2.499
2.497
2.495
1
1.002
1.004
1.006
1.008
1.01
1.012
1.014
me/me0
D/H= 2.527 ± 0.030
Cooke 2017
Under revision
m_e/m_{e0}
D/H

VARYING ELECTRON MASS MODEL

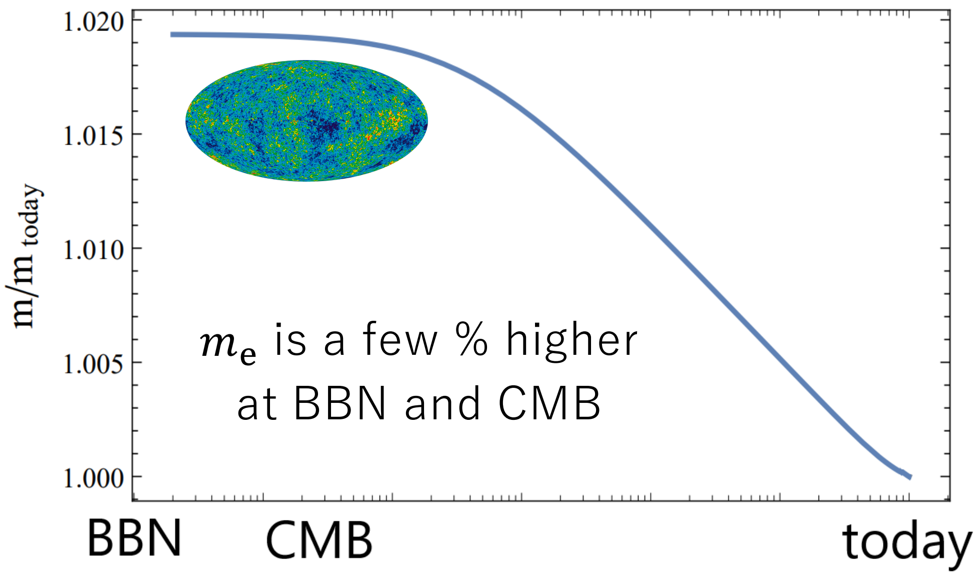

Axi-Higgs cosmology
Leo W.H. Fung *et al.*
2102.11257 [hep-ph]

Cosmological evolution
of brane world moduli
P. Brax *et al.*
Phys.Rev.D 67 (2003) 023512

EMPRESS

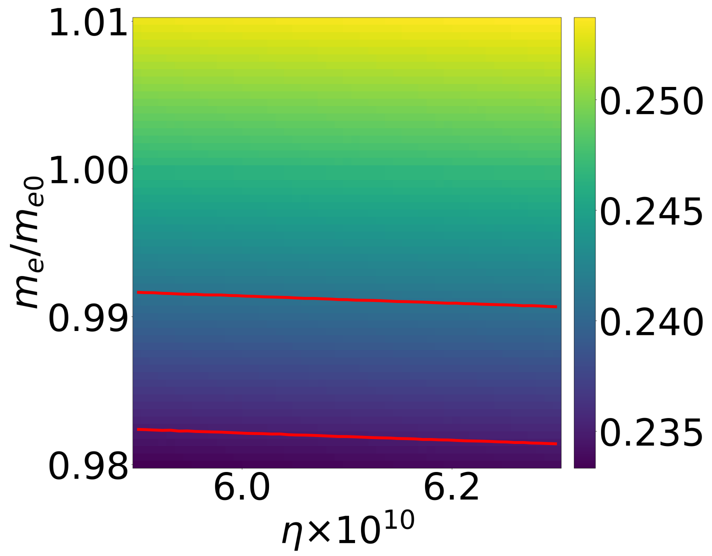

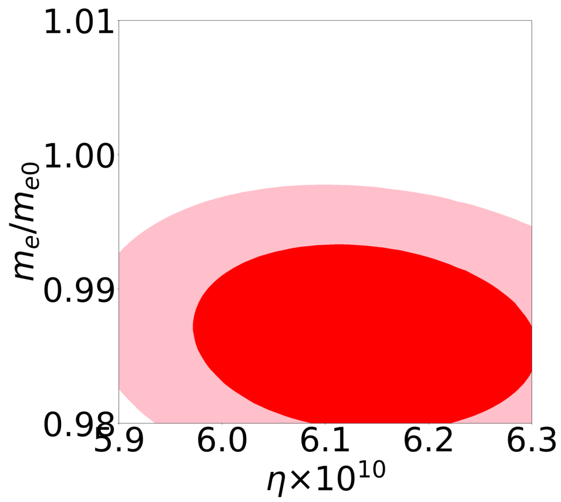

ELECTRON MASS AND r_*

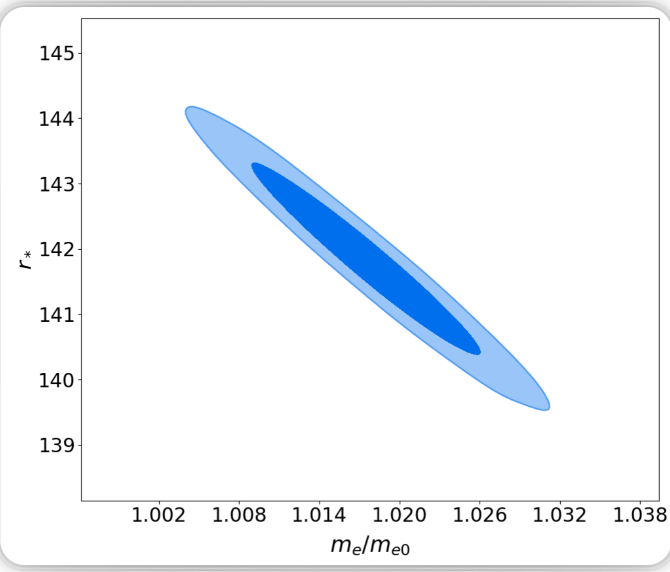

Higher m_e/m_{e0}

decrease r_*

$$\frac{m_e}{m_{e0}} = \frac{m_{e\,|\text{Last Scatter}}}{m_{e\,|\text{today}}}$$

Planck + Pantheon + BAO + R19

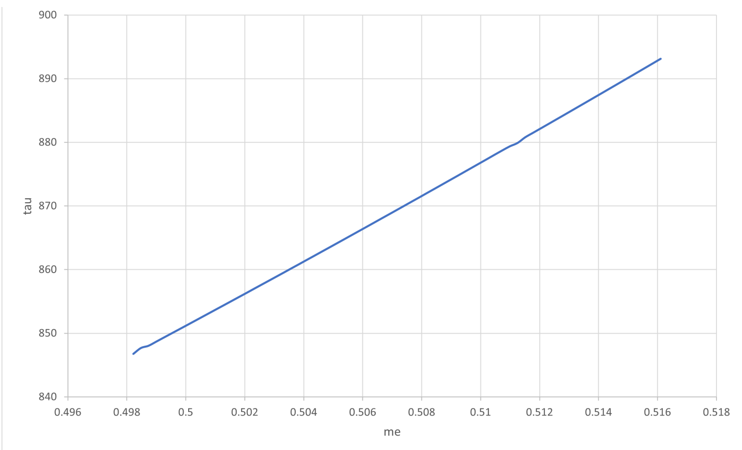

$$\Gamma(n \to p^+ e^- \nu) = \frac{G_F^2}{2\pi^3}(1 + 3g_A^2) m_e^5 \lambda_0(q),$$

$$\lambda_0(q) = \int_1^q dx x(x-q)^2(x^2-1)^{1/2},$$

ANGULAR SIZE OF THE SOUND HORIZON

Directly Measured

Angular Size : $\theta_* = \frac{r_*}{D_{M*}} = (1.0411 \pm 0.0003) * 10^{-2}$

$$= \frac{\int_0^{t_*} \frac{c_s d\tilde{t}}{a(\tilde{t})}}{\int_{t_*}^{t_0} \frac{d\tilde{t}}{a(\tilde{t})}} = \frac{H_0}{H_*} \frac{\int_{z_*}^{\infty} \frac{dz}{H_0\sqrt{\rho(z)/\rho_*}}}{\int_0^{z_*} \frac{dz}{H_0\sqrt{\rho(z)/\rho_0}}}$$

$$\because \frac{dt}{a(t)} = \frac{dz}{H_0\sqrt{\rho(z)/\rho_0}}$$

ρ : energy density

$$\boxed{\sim H_0 * \sqrt{\frac{\rho \text{ in the late universe}}{\rho \text{ in the early universe}}}}$$

COSMIC MICROWAVE BACKGROUND (CMB)

Before 375,000 yrs.,
it was hot enough
for electrons
to scatter photons

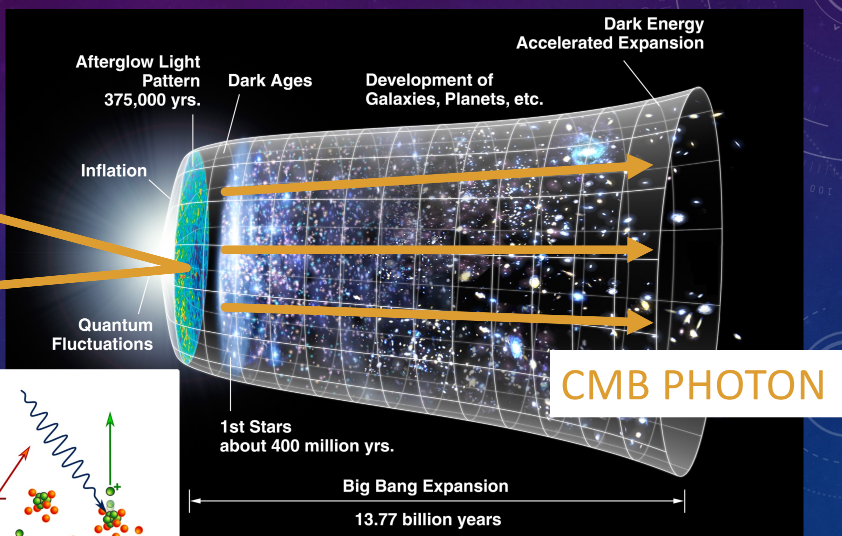

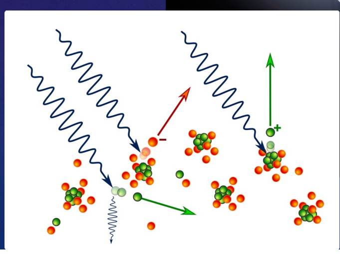

C08

Spins of primordial black holes with soft EoS parameters

Daiki Saito (Nagoya. U)
Ongoing work
with CM.Yoo(Nagoya. U), T.Harada (Rikkyo. U), Y.Koga(Nagoya. U)

2022 Oct. 24, JGRG31

Introduction

1/10

Primordial Black Hole(PBH): BH formed in the early universe

- Remnant of primordial inhomogeneity
- Candidate for DM
- Candidate for supermassive BH
- Source for GW (Binary)

- (typically) formed in the RD era
- Formed from
  e.g. density fluctuation

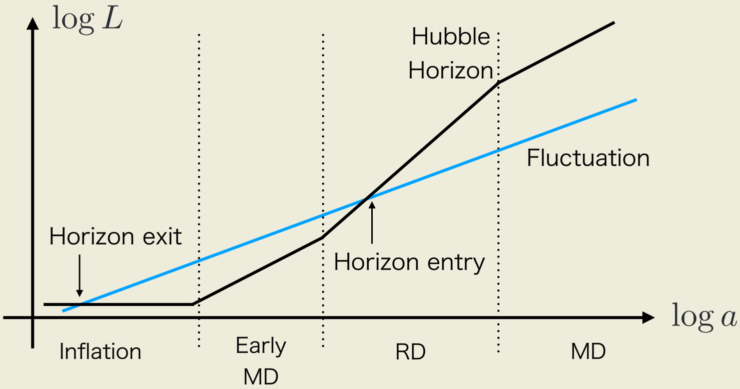

Introduction

$\delta = \dfrac{\rho - \rho_b}{\rho_b}$: density perturbation

δ_{pk} : peak of the perturbation

δ_{th} : threshold value

PBH formation due to density fluctuation

PBH is formed if $\delta_{pk} > \delta_{th}$

(if gravity overcomes pressure)

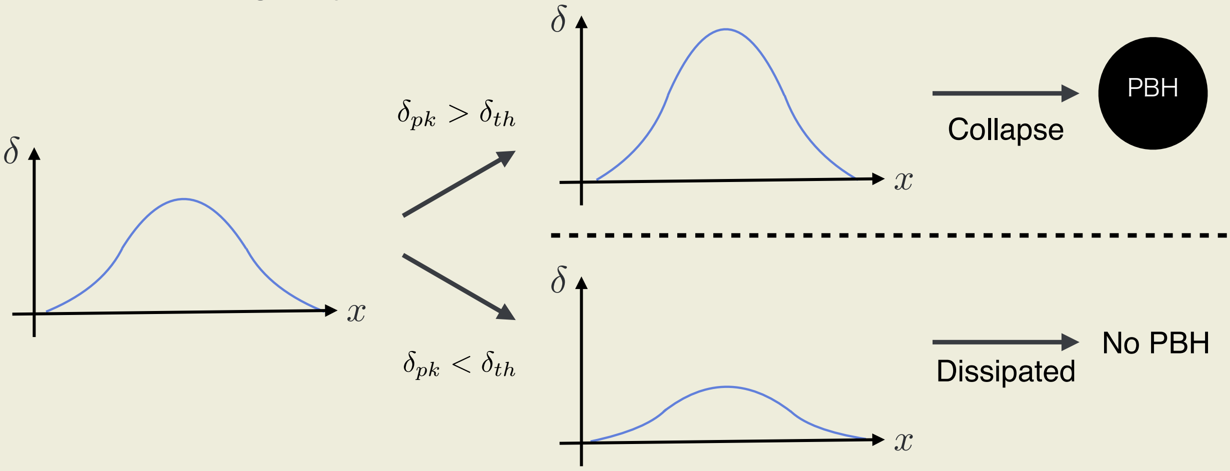

Introduction

Distribution of PBH spin: important for observations

$\longrightarrow$ Estimate spin of a single PBH

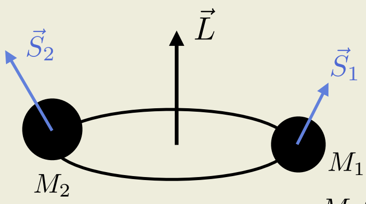

$$\chi_{\rm eff} = \frac{M_1\vec{S}_1 + M_2\vec{S}_2}{M_1 + M_2} \cdot \vec{L}$$

Previous results

- RD era $(w = 1/3)$ (Harada+ 2020) $\sqrt{\langle a_*^2 \rangle} \sim O(10^{-2})$
- MD era $(w = 0)$ (Harada+ 2017) $a_* \simeq 1$

a_* : non-dimensional Kerr parameter

Our work: compute mean value of spin for $0 < w \leq 1/3$ to

- Get a unified understanding
- Applyication: QCD phase transition $(0.2 < w < 1/3)$

Assumptions

a region which will collapse to

Goal: Evaluate spin of a PBH

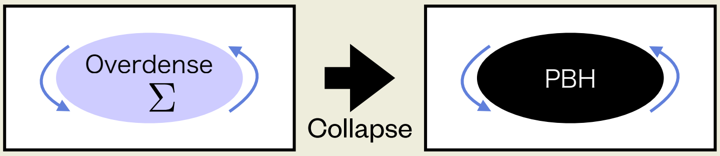

Focus on linear order effects of perturbation

Assumptions:

- BG: flat FLRW $ds^2 = a^2(-d\eta^2 + dx^2 + dy^2 + dz^2)$
- Matter: perfect fluid with $p = w\rho \qquad 0 < w \leq 1/3$
- Spacetime $ds^2 = -\alpha a^2 d\eta^2 + a^2 e^{-2\zeta}\left(dx^2 + dy^2 + dz^2\right)$
- Curvature perturbation $\zeta(\eta)$: Gaussian $\langle \zeta_{\vec{k}}(0)\zeta^*_{\vec{k}'}(0)\rangle = (2\pi)^3\delta^3(\vec{k}-\vec{k}')\dfrac{2\pi^2}{k^3}\underline{P_\zeta(k)}$

power spectrum

Spin of a closed region

Σ: region where fluid will collapse to a BH

$$\Sigma = \{\vec{x}|\delta(\vec{x}) > f\delta_{pk}\} \quad 0 < f < 1$$

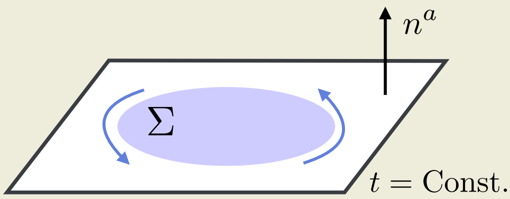

Spin (Komar integral):

$$S_i(\Sigma) := -\int_\Sigma T^{ab} n_a (\phi_i)_b d\Sigma$$

$$\simeq -(1+w)a^4\rho_b\epsilon_{ijk}\underline{v^k_{\ l}}\int_\Sigma x^j x^k d^3x \qquad (\vec{x}_{peak} = \vec{0})$$

$$= S_{\rm ref}(\eta)s_{ei}$$

n_a	: unit normal to the time slice
$(\phi_i)_b$	: rotational Killing vector
$v^k_{\ l} = \dfrac{\partial v^k}{\partial x^l}$	: velocity shear

$S_{\rm ref}(\eta)$ depends on η , independent of the peak shape

s_{ei} depends on the peak shape, independent of η

$$\Rightarrow \sqrt{\langle S^2\rangle} = S_{\rm ref}\sqrt{\langle s_e^2\rangle}$$

Peak theory

The statistics of δ and v^k_l $\longrightarrow \sqrt{\langle s_e^2\rangle}$
In long wavelength, $\delta \propto \Delta\zeta(0)$ $v_i \propto \partial^3\zeta(0)$: Gaussian (Harada+ 2015)

Peak theory (Heavens+ 1988): theory for statistics of peaks of Gaussian variables

$\longrightarrow$ Peak number density $N_{pk}(\nu, \lambda_i, w_i)d\nu d\lambda_i dw_i$

$\nu = \dfrac{\delta_{pk}}{\sigma_0}$ λ_i : eigenvalues of $-\dfrac{\partial_i\partial_j\delta}{\sigma_2}$ w_i :non-diagonal comp of v^k_l

characterized by $\sigma_j^2 := \displaystyle\int \frac{d^3\vec{k}}{(2\pi)^3} k^{2j}|\delta_{\vec{k}}|^2$

- Assume a high (rare) peak $\nu \gg 1 \longrightarrow \Sigma$ is nearly spherical

Expectation value of spin

M : PBH mass
η_H : horizon entry
M_H : Horizon mass at η_H
$\gamma = \dfrac{\sigma_1^2}{\sigma_0\sigma_2}$

Assume: $P_\zeta(k) \simeq \sigma_\zeta^2 k_0 \delta(k-k_0)$ $S_{\rm PBH} \sim S(\eta_{ta})$

At η_{ta}, Σ decouples from the expansion (turn around)
Turn around $\sim$ maximum expansion of a closed FLRW

$$\delta(\eta_{ta}) \simeq \frac{3(w+1)}{4(9w+5)}(6\pi)^{\frac{2}{3}} \simeq 1$$

$a_{i*} = \dfrac{S_{\rm ref}(\eta_{ta})s_{ei}}{M^2}$: Non-dimensional Kerr parameter

$$\longrightarrow \sqrt{\langle a_*^2\rangle} = \frac{S_{\rm ref}(\eta_{ta})}{M^2}\sqrt{\langle s_e^2\rangle}$$

$$\xrightarrow[\text{(Peak theory)}]{\sqrt{\langle s_e^2\rangle} \simeq 5.96\frac{\sqrt{1-\gamma^2}}{\gamma^6\nu}} \sqrt{\langle a_*^2\rangle} \propto \sqrt{1-\gamma^2}\left(\frac{M}{M_H}\right)^{-1/3}\frac{(1+w)^2}{5+3w}\left(\frac{a(\eta_{\rm ta})}{a(\eta_H)}\right)^{2w+1}\left(\frac{\nu}{8}\right)^{-1}$$

Expectation value of spin

M : PBH mass

η_H : horizon entry

M_H : Horizon mass at η_H

$\gamma = \frac{\sigma_1^2}{\sigma_0\sigma_2}$

Assume: $P_\zeta(k) \simeq \sigma_\zeta^2 k_0 \delta(k-k_0) \qquad S_{\rm PBH} \sim S(\eta_{ta})$

At η_{ta}, Σ decouples from the expansion (turn around)

Turn around $\sim$ maximum expansion of a closed FLRW

$$\delta(\eta_{ta}) \simeq \frac{3(w+1)}{4(9w+5)}(6\pi)^{\frac{2}{3}} \simeq 1$$

$a_{i*} = \frac{S_{\rm ref}(\eta_{ta}) s_{ei}}{M^2}$: Non-dimensional Kerr parameter

$$\longrightarrow \quad \sqrt{\langle a_*^2 \rangle} = \frac{S_{\rm ref}(\eta_{ta})}{M^2}\sqrt{\langle s_e^2 \rangle}$$

Set $\nu_{th} \propto \sin^2\left(\frac{\pi\sqrt{w}}{1+3w}\right)$

(Harada+ 2013)

$\sqrt{\langle s_e^2 \rangle} \simeq 5.96 \frac{\sqrt{1-\gamma^2}}{\gamma^6 \nu}$

(Peak theory)

$$\longrightarrow \quad \sqrt{\langle a_*^2 \rangle} \propto \sqrt{1-\gamma^2}\left(\frac{M}{M_H}\right)^{-1/3} \frac{(1+w)^2}{5+3w}\left(\frac{a(\eta_{\rm ta})}{a(\eta_H)}\right)^{2w+1} \boxed{\left(\frac{\nu}{8}\right)^{-1}}$$

Result

Expectation value of spin

$M \sim 10^{-3} \times M_H$

$\gamma = 0.85$

Decreases with w

$\sqrt{\langle a_*^2 \rangle} = 1.6 \times 10^{-2}$ for RD

$\sqrt{\langle a_*^2 \rangle} = O(0.1)$ for $w \leq 0.06$

Asymptotic form: $\sqrt{\langle a_*^2 \rangle} \propto w^{-2.48}$

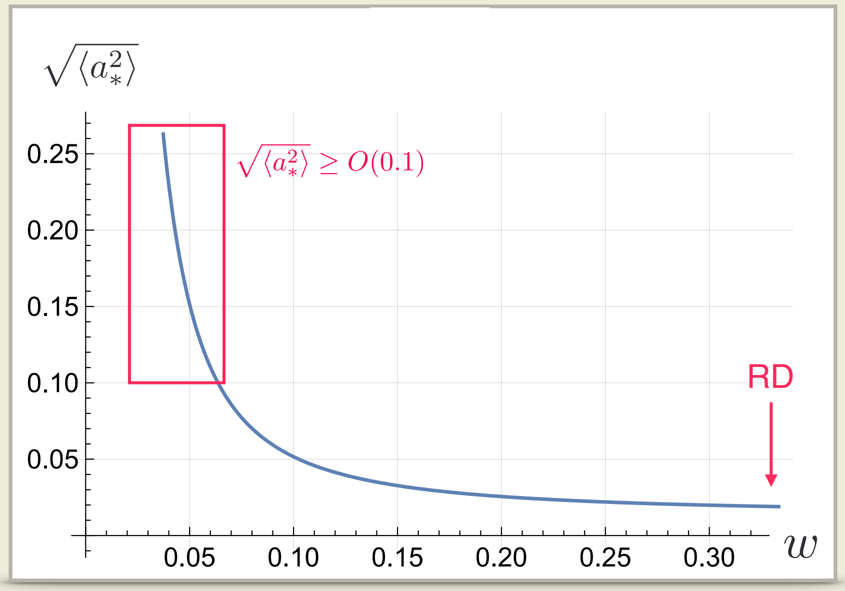

Discussion

$$\nu = \frac{\delta_{pk}}{\sigma_0}$$

$$\sqrt{\langle a_*^2 \rangle} \propto \sqrt{1-\gamma^2}\left(\frac{M}{M_H}\right)^{-1/3}\frac{(1+w)^2}{5+3w}\left(\frac{a(\eta_{\rm ta})}{a(\eta_H)}\right)^{2w+1}\boxed{\left(\frac{\nu}{8}\right)^{-1}}$$

(Threshold of) ν increases with w

$$\nu_{th} \propto \sin^2\left(\frac{\pi\sqrt{w}}{1+3w}\right)$$ (Harada+ 2013)

Weaker pressure
$\longrightarrow$ smaller fluctuation can collapse

Assumption $\nu \gg 1$: violated at $w \simeq 0$

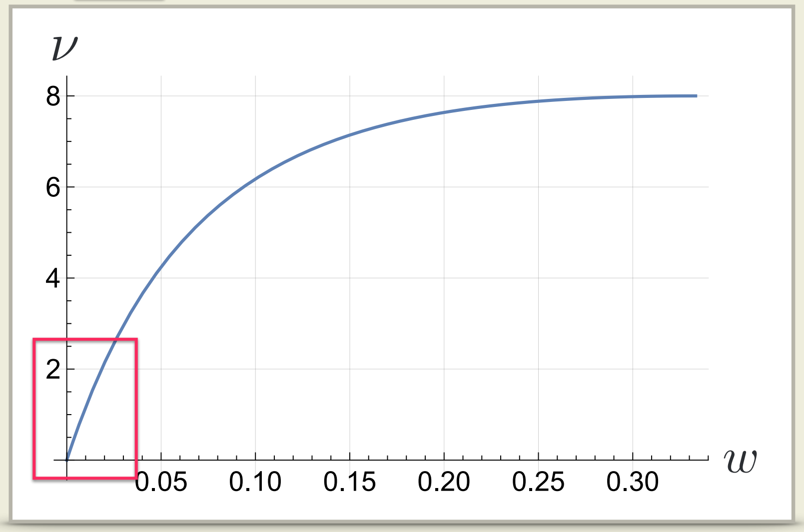

Summary

- We have estimated the PBH spin with $0 < w \leq 1/3$
- The spin decreases with w $\qquad \sqrt{\langle a_*^2 \rangle} = 1.6 \times 10^{-2}$ for RD
  $\qquad \sqrt{\langle a_*^2 \rangle} = O(0.1)$ for $w \leq 0.06$
- For $w \ll 1$, the assumption for rare peak would be violated
- Future work:

  Alternative approach for $w \ll 1$
  Effective spin for binary

Back-Up Slides

Discussion

$$\sqrt{\langle a_*^2\rangle} \simeq \frac{5.96}{8}\,\frac{9\sqrt{3}}{32\pi}\,\frac{(1+w)^2}{5+3w}\boxed{\left(\frac{a(\eta_{\rm ta})}{a(\eta_H)}\right)^{2w+1}}\sqrt{1-\gamma^2}|T_{v_{\rm CN}}(k_0,\eta_{\rm ta})|\sigma_H\left(\frac{M}{M_H}\right)^{-1/3}\left(\frac{\nu}{8}\right)^{-1}$$

$\frac{a(\eta_{ta})}{a(\eta_H)}$: growth of scale factor horizon entry → turnaround

Decreases with w

Smaller w
⟶ larger growth
⟶ larger spin

η_{ta} also decreases with w

$x_{ta} := k_0\eta_{ta}$

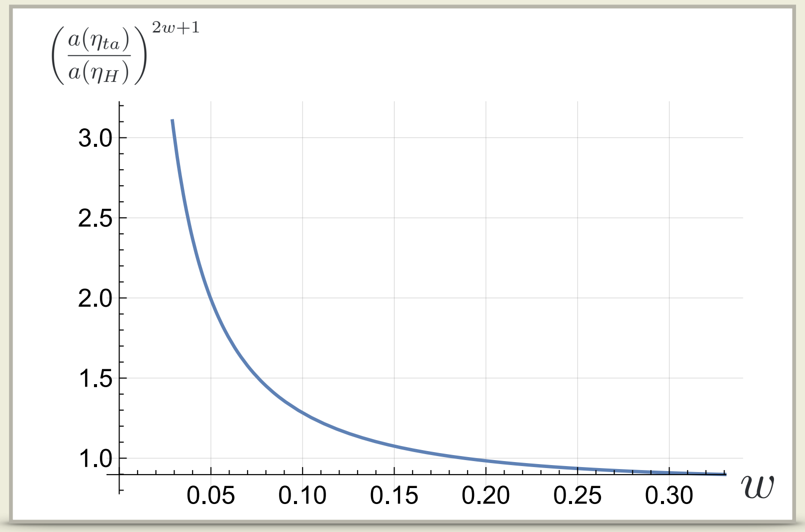

Discussion

$$\sqrt{\langle a_*^2\rangle} \simeq \frac{5.96}{8}\frac{9\sqrt{3}}{32\pi}\frac{(1+w)^2}{5+3w}\boxed{\left(\frac{a(\eta_{\rm ta})}{a(\eta_H)}\right)^{2w+1}}\sqrt{1-\gamma^2}|T_{v_{\rm CN}}(k_0,\eta_{\rm ta})|\sigma_H\left(\frac{M}{M_H}\right)^{-1/3}\left(\frac{\nu}{8}\right)^{-1}$$

$\frac{a(\eta_{ta})}{a(\eta_H)}$: growth of scale factor horizon entry → turnaround

Decreases with w

Smaller w
⟶ larger growth
⟶ larger spin

η_{ta} also decreases with w

$x_{ta} := k_0\eta_{ta}$

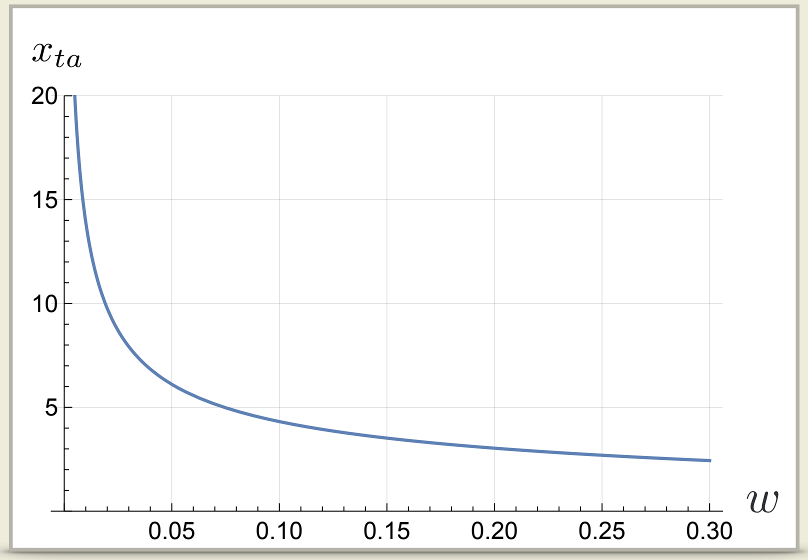

Perturbation & threshold

Narrow power spectrum $P_\zeta(k) \simeq \sigma_\zeta^2 k_0\delta(k-k_0)$

→ Typical profile: sinc type $\begin{cases}\zeta(\eta,r)=\zeta_{pk}(\eta)\psi(r)\\ \delta(\eta,r)=\delta_{pk}(\eta)\psi(r)\end{cases}$ $\psi(r)=\frac{\sin(k_0 r)}{k_0 r}$ (in the CMC slicing)

We must fix δ_{pk} so that a PBH forms

Analytic formula (Harada+ 2013) $\sin^2\left(\frac{\pi\sqrt{w}}{1+3w}\right) < \delta(\eta_H) \leq 1$

Fix $\delta_{pk}(\eta_H)$ so that $\bar{\delta}(\eta_H) = \sin^2\left(\frac{\pi\sqrt{w}}{1+3w}\right)$

η_H :horizon entry

$\bar{\delta}(\eta_H)$:ave. of δ at η_H over the overdose region

Turnaround

When should we evaluate $\sqrt{\langle S^2 \rangle}$?

Assumption: $S(\eta_{ta}) \sim S_{\rm PBH}$

At η_{ta}, Σ decouples from the expansion (turn around)

We assume that
- Linear perturbation is (approximately) valid
- Turnaround $\sim$ maximum expansion of a closed FLRW

For linear perturbation, $\delta(\eta_{ta}) \simeq \frac{3(w+1)}{4(9w+5)}(6\pi)^{\frac{2}{3}} \simeq 1$

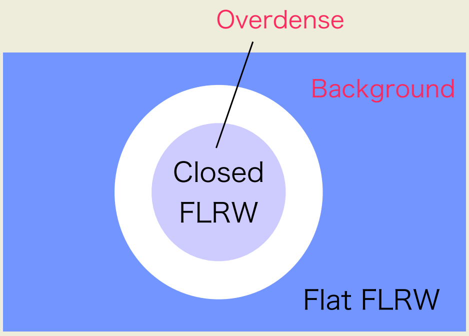

Threshold of perturbation

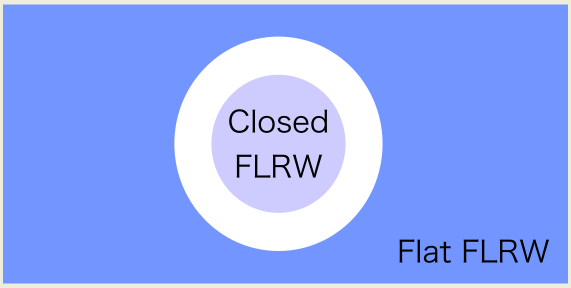

Use the analytic formula (Harada+ 2013)

Based on the discussion so called
"three-zone model"

"Sound crossing time" vs "free falling time"

Pressure Gravity

$$\delta_{th} = \sin^2\left(\frac{\pi\sqrt{w}}{1+3w}\right) < \delta(\eta_H) \leq 1$$

Threshold of perturbation

Use the analytic formula (Harada+ 2013)

Based on the discussion so called "three-zone model"

$$\delta_{th} = \sin^2\left(\frac{\pi\sqrt{w}}{1+3w}\right) < \delta(\eta_H) \le 1$$

Smaller w ⟶ small pressure

⟶ small δ_{th}

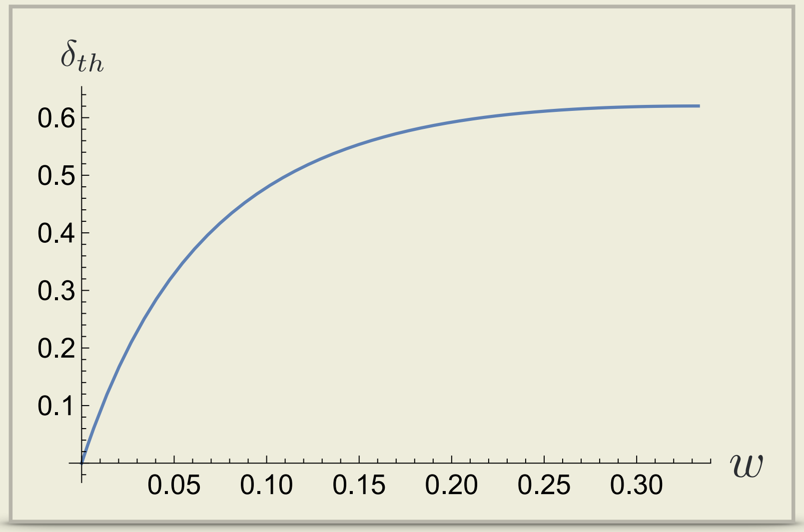

Spin

Spin with higher order effect

$$S_i(\Sigma) = -(1+w)a^4\rho_b\epsilon_{ijk}\int_\Sigma (1+\delta)x^j v^k d^3x$$

$$= \underbrace{-(1+w)a^4\rho_b\epsilon_{ijk}\int_\Sigma x^j v^k d^3x}_{} \underbrace{- (1+w)a^4\rho_b\epsilon_{ijk}\int_\Sigma \delta x^j v^k d^3x}_{}$$

1st order
: vanishes if Σ is sphere

2nd order
: doesn't vanish even if Σ is sphere

Spin is generated from 2nd order when Σ is exactly spherical!

$\vec{s}_e \propto (-\alpha_1\tilde{v}_{23}, \alpha_2\tilde{v}_{13}, -\alpha_3\tilde{v}_{12})$ $\quad \alpha_1 = \frac{1}{\lambda_3} - \frac{1}{\lambda_2}$

$\vec{s}_e = \vec{0}$ with spherical Σ $(\lambda_1 = \lambda_2 = \lambda_3)$

Axes length: $a_i = \sqrt{2\frac{\sigma_0}{\sigma_2}\frac{1-f}{\lambda_i}\nu}$

Radius of the region

$$\Sigma = \{\vec{x}|\delta(\vec{x}) > f\delta_{pk}\}$$

$$\delta \simeq \delta_{pk} + \frac{1}{2}(\partial_i\partial_j\delta)_{pk}(x - x_{pk})^i(x - x_{pk})^j$$
$$= \delta_{pk} - \frac{\sigma_2}{2}\lambda_i\{(x - x_{pk})^2\}^i$$

λ_i: eigenvalues of $-\dfrac{\partial_i\partial_j\delta}{\sigma_2}$

Ellipsoid with $a_i = \sqrt{2\frac{\sigma_0}{\sigma_2}\frac{1-f}{\lambda_i}\nu}$

High peak: $\nu \gg 1 \longrightarrow a_i \simeq r_f = \sqrt{6(1-f)}\frac{\sigma_0}{\sigma_1}$

$$S_i(\Sigma) \simeq -(1+w)a^4\rho_b\epsilon_{ijk}v_l^k \underbrace{\int_\Sigma x^j x^k d^3x}_{\propto (1-f)^{5/2}}$$

Scale factor dependence

Mass ratio

$$\frac{M_{ta}}{M_H} = \frac{(\rho_b a^3)(\eta_{ta})}{(\rho_b a^3)(\eta_H)}\left(\frac{r_f}{r_0}\right)^3 = (1-f)^{3/2}\left(\frac{a(\eta_H)}{a(\eta_{ta})}\right)^3 \quad (\because \quad \rho_b a^3 \propto a^{-3w})$$

$$\longrightarrow (1-f)^{1/2} \propto \left(\frac{a(\eta_{ta})}{a(\eta_H)}\right)^w$$

$$S_{ref}(\eta) = (1+w)\underbrace{a^4\rho_b}_{\propto (a(\eta_{ta}))^{1-3w}}\sqrt{\langle(v_l^k)^2\rangle}\underbrace{(1-f)^{5/2}}_{\left(\frac{a(\eta_{ta})}{a(\eta_H)}\right)^{5w}}\left(\sqrt{3}\frac{\sigma_1}{\sigma_2}\right)^5 \propto \left(\frac{a(\eta_{ta})}{a(\eta_H)}\right)^{2w+1}$$

Turnaround condition

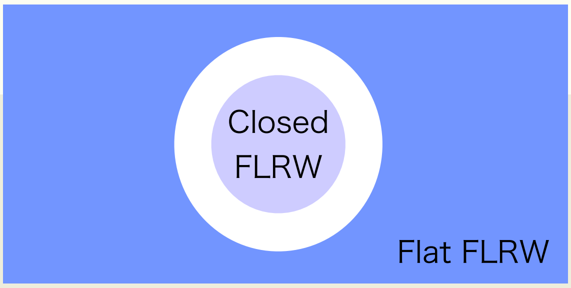

Ω_{w0} : density perturbation

Closed FLRW dominated by matter with $p = w\rho$

Friedmann eq. $\left(\dfrac{\dot{a}}{a}\right)^2 = H_0^2\left[\dfrac{\Omega_{w0}}{a^{3(1+w)}} + \dfrac{1-\Omega_{w0}}{a^2}\right]$

Solution $\tilde{a} = \dfrac{\Omega_{w0}}{2(\Omega_{w0}-1)}(1-\cos\theta)$

$$H_0\tilde{t} = \frac{\Omega_{w0}}{2(\Omega_{w0}-1)^{\frac{3}{2}}}(\theta - \sin\theta)$$

$$\tilde{a} = a^{1+3w}$$

$$d\tilde{t} = (1+3w)\tilde{a}^{\frac{3w}{1+3w}}\,dt$$

a: maximum at $\theta = \pi$ (maximum expansion/turnaround)

$$\rho = \rho_0 a^{-3(1+w)}$$

$\theta \ll 1$ expansion

$$\simeq \bar{\rho}\left\{1 + \frac{3(w+1)}{4(9w+5)}\theta^2\right\}$$

$\bar{\rho}$: energy density of flat FLRW

Turnaround condition

Linearized perturbation with $p = w\rho$

$$\ddot{\delta} + 2\frac{\dot{a}}{a}\dot{\delta} - 4\pi\bar{\rho}\delta = 0 \qquad \frac{\dot{a}}{a} = \frac{2}{3(1+w)t} \qquad \bar{\rho} = \frac{1}{6\pi(1+w)^2t^2}$$

$$\longrightarrow \quad \ddot{\delta} + \frac{4}{3(1+w)t}\dot{\delta} - \frac{2}{3(1+w)^2t^2}\delta = 0$$

Growing solution $\delta \propto \tilde{t}^{2/3}$

Nonlinear solution + small θ expansion $\rho - \bar{\rho} \simeq \dfrac{3(w+1)}{4(9w+5)}\theta^2 \propto \tilde{t}^{2/3}$

Linear approx $\delta \simeq \dfrac{3(w+1)}{4(9w+5)}\theta^2 = \dfrac{3(w+1)}{4(9w+5)}\left(\dfrac{12(\Omega_{w0}-1)}{\Omega_{w0}}H_0\tilde{t}\right)^{2/3}$

Turnaround condition $\delta = \dfrac{3(w+1)}{4(9w+5)}\left(\dfrac{12(\Omega_{w0}-1)}{\Omega_{w0}}H_0\tilde{t}(\theta=\pi)\right)^{2/3} = \dfrac{3(w+1)}{4(9w+5)}(6\pi)^{3/2}$

C09

JGRG31

From merger of primordial black holes to the primordial power spectrum of curvature perturbations

Ying-li Zhang

Tongji University

2022. 10. 24

X. Wang, YZ, Kimura and M. Yamaguchi, arXiv: 2209.12911

R. Kimura, T. Suyama, M. Yamaguchi and YZ, JCAP 04 (2021) 031 [arXiv: 2102.05280]

Happy 60 year Birthday!

お誕生日おめでとうござ
います

生日快乐！

Why Primordial Black Hole?

- BHs exist in the universe
- No need for new physics
- PBHs may dominate Dark Matter
- Detected GW events from LIGO may originate from the merger of PBH binaries

  M. Sasaki, T. Suyama, T. Tanaka, S. Yokoyama, PRL 117, no. 6, 061101 (2016)
- A possible way to probe the primordial power spectrum of curvature perturbation on small scales
- …

The formation of Primordial Black Holes

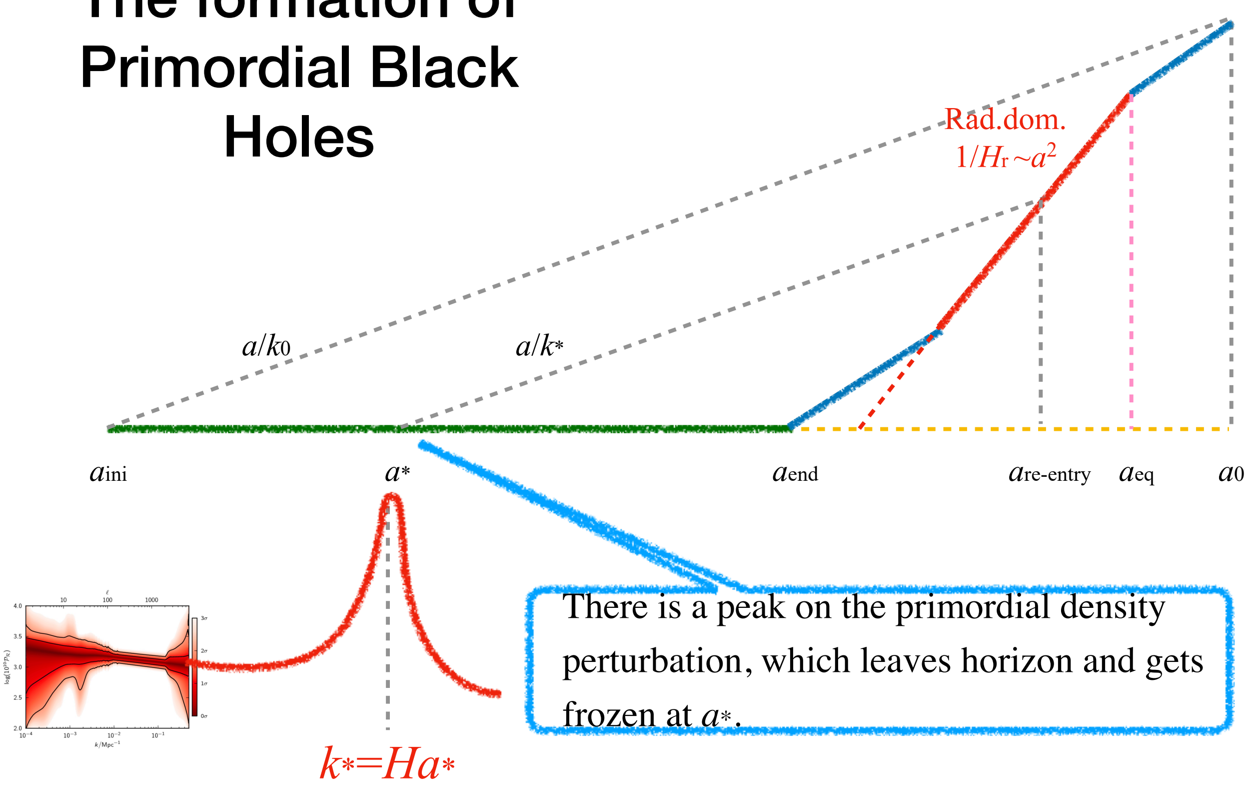

The formation of Primordial Black Holes

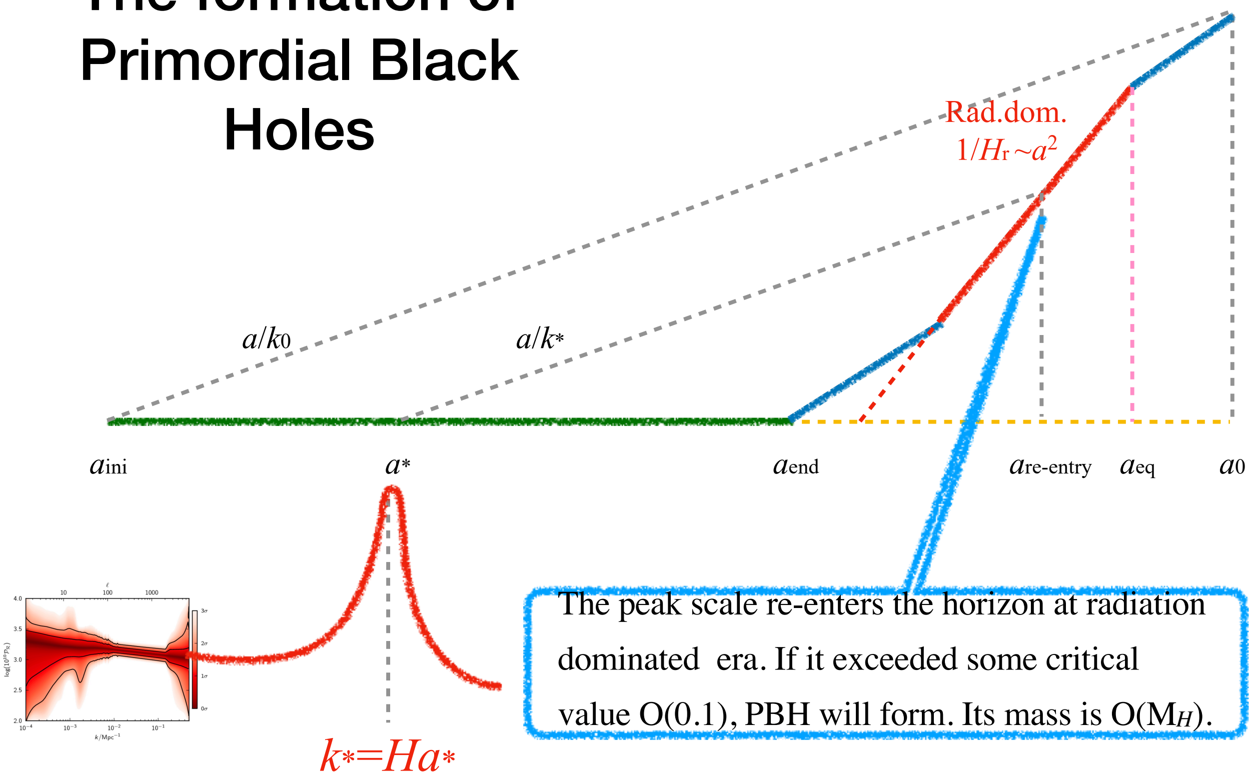

Idea

<u>PBHs from large curvature perturbations</u>

+ <u>LIGO data from mergers of PBH binaries</u>

Primordial Power Spectrum of
curvature perturbations?
(on small scales)

Assumptions

0. At least some of the BBH LIGO events are PBHs

   merger rate from observations

1. PBHs formed out of high peaks of curvature perturbations

   the simplest case

2. Window function: top-hat form

   semi-analytic expression for calculation of merger rate

3. Gaussian distribution of density perturbation

   simple relation between between power spectrum and the variance

The logic

$$\begin{tikzcd} \mathcal{P}_{\mathcal{R}}(k) & \mathcal{R}(m_1, m_2, t) \arrow[l, "?"'] \end{tikzcd}$$

$$\downarrow$$

$$\mathcal{P}_{\mathcal{R}}(k) \boxed{\overset{\text{(i)}}{\Longleftrightarrow} \sigma^2(R) \overset{\text{(ii)}}{\Longleftrightarrow} f(m) \overset{\text{(iii)}}{\Longleftrightarrow}} \mathcal{R}(m_1, m_2, t)$$

Question: can we uniquely determine $\mathcal{P}_{\mathcal{R}}(k)$?

Step (i) $\mathcal{P}_{\mathcal{R}}(k) \overset{\text{(i)}}{\Longleftrightarrow} \sigma^2(R)$

$$P(\Delta) = \frac{1}{\sqrt{2\pi}\,\sigma} e^{-\frac{\Delta^2}{2\sigma^2}}$$

$$\mathcal{P}_{\Delta}(k) \longrightarrow \sigma^2(R) = \int_0^\infty W^2(kR)\mathcal{P}_{\Delta}(k)\ \mathrm{d}(\ln k)$$

$$W(kR) = \begin{cases} 1 & ;\ 0 < k < 1/R\,, \\ 0 & ;\quad \text{otherwise}\,, \end{cases}$$

$$\mathcal{P}_{\Delta}(t,k) = \frac{16}{81}\left(\frac{k}{aH}\right)^4 \mathcal{P}_{\mathcal{R}}(k)$$

$$\frac{81}{16} R^4 \frac{\mathrm{d}}{\mathrm{d}R}\left(\frac{\sigma^2(R)}{R^4}\right)\Bigg|_{1/R=k} = -k\mathcal{P}_{\mathcal{R}}(k)$$

Step (ii) $\sigma^2(R) \overset{\text{(ii)}}{\Longleftrightarrow} f(m)$

The mass function $f(m)$ is expressed in terms of PBH abundance

$$f(m) \propto \beta \equiv \int_{\Delta_{\rm th}}^{1} P(\Delta)\mathrm{d}\Delta = \frac{1}{2}\mathrm{erfc}\left(\frac{\Delta_{\rm th}}{\sqrt{2}\sigma}\right)$$

Step (iii) $f(m) \overset{\text{(iii)}}{\Longleftrightarrow} \mathcal{R}(m_1, m_2, t)$

Mainly 2 possible process for PBH merger events: PBH binaries formed at

(a). early (radiation-dominated) epoch;

Sasaki et al., PRL 117(2016)6, 061101

Dominated

(b). late (matter-dominated) epoch.

Bird et al., PRL 116(2016)20, 201301

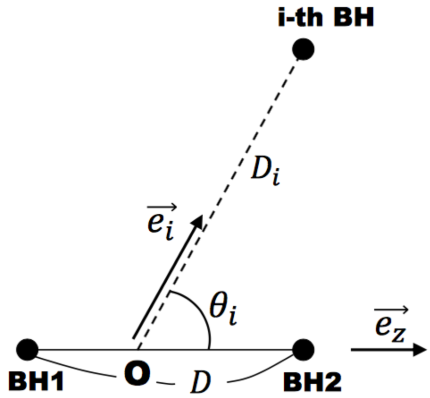

B. Kocsis, T. Suyama, T. Tanaka and S. Yokoyama, Astrophys. J. 854, no. 1, 41 (2018)

Step (iii) $f(m) \overset{\text{(iii)}}{\Longleftrightarrow} \mathcal{R}(m_1, m_2, t)$

Mainly 2 possible process for PBH merger events: PBH binaries formed at

(a). early (radiation-dominated) epoch;

$$\mathcal{R}(m_1, m_2, t) \propto \left(\frac{m_t}{M_\odot}\right)^{-\frac{32}{37}} \left(\frac{m_t^2}{m_1 m_2}\right)^{\frac{34}{37}} S[f|f_{\rm PBH}, m_t] m_1 m_2 f(m_1) f(m_2)$$

Step (iii) $\quad f(m) \overset{\text{(iii)}}{\Longleftrightarrow} \mathcal{R}(m_1, m_2, t)$

Mainly 2 possible process for PBH merger events: PBH binaries formed at

(a). early (radiation-dominated) epoch;

$$f\left(m_2\right)=f\left(m_1\right) \frac{\mathcal{R}\left(m_1, m_2\right)}{\mathcal{R}\left(m_1, m_1\right)}\left(\frac{m_1}{m_2}\right)^{\frac{3}{37}}\left(\frac{2 m_1}{m_1+m_2}\right)^{\frac{36}{37}}$$

$$\begin{aligned} f\left(m_n\right)=f\left(m_{n-2}\right) & \frac{\mathcal{R}\left(m_{n-1}, m_n\right)}{\mathcal{R}\left(m_{n-2}, m_{n-1}\right)}\left(\frac{m_{n-2}}{m_n}\right)^{\frac{3}{37}} \times \\ & \times\left(\frac{m_{n-2}+m_{n-1}}{m_n+m_{n-1}}\right)^{\frac{36}{37}}, \quad n \geqslant 3, \end{aligned}$$

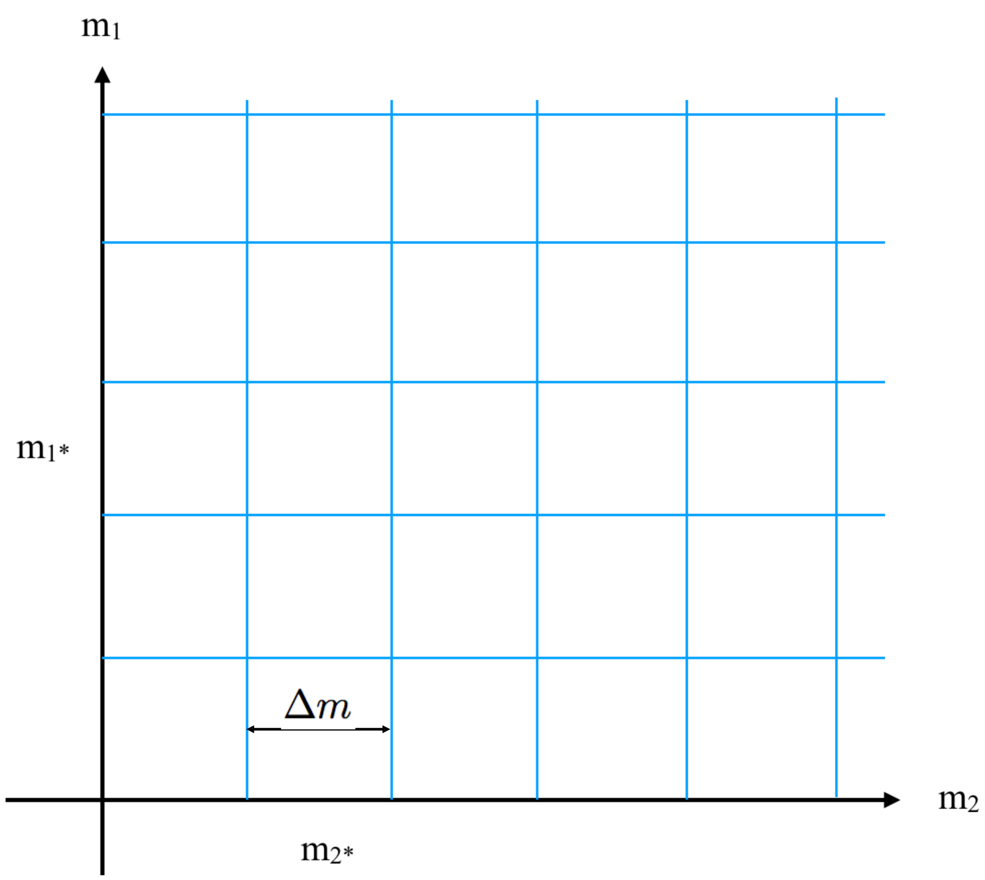

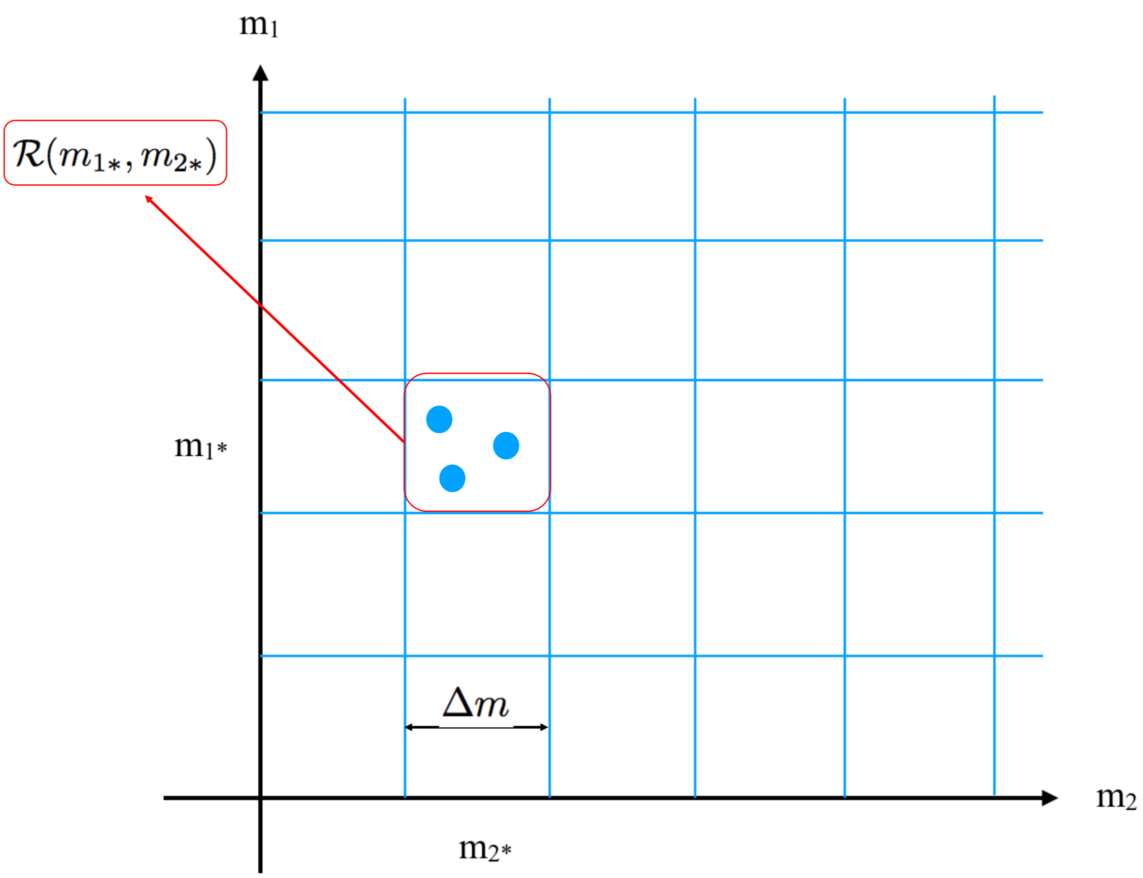

The LIGO/Virgo released data

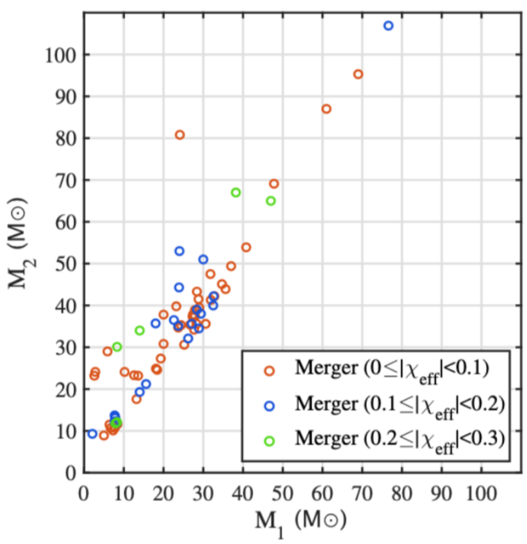

91 BBH candidates, 76 of them satisfy $m \gtrsim 1.5 M_{\odot}$ and $|\chi_{\rm eff}| \lesssim 0.3$

We simply identify these events as PBH mergers

WARN: The largest Uncertainty comes from here!

Large difference of # of points included

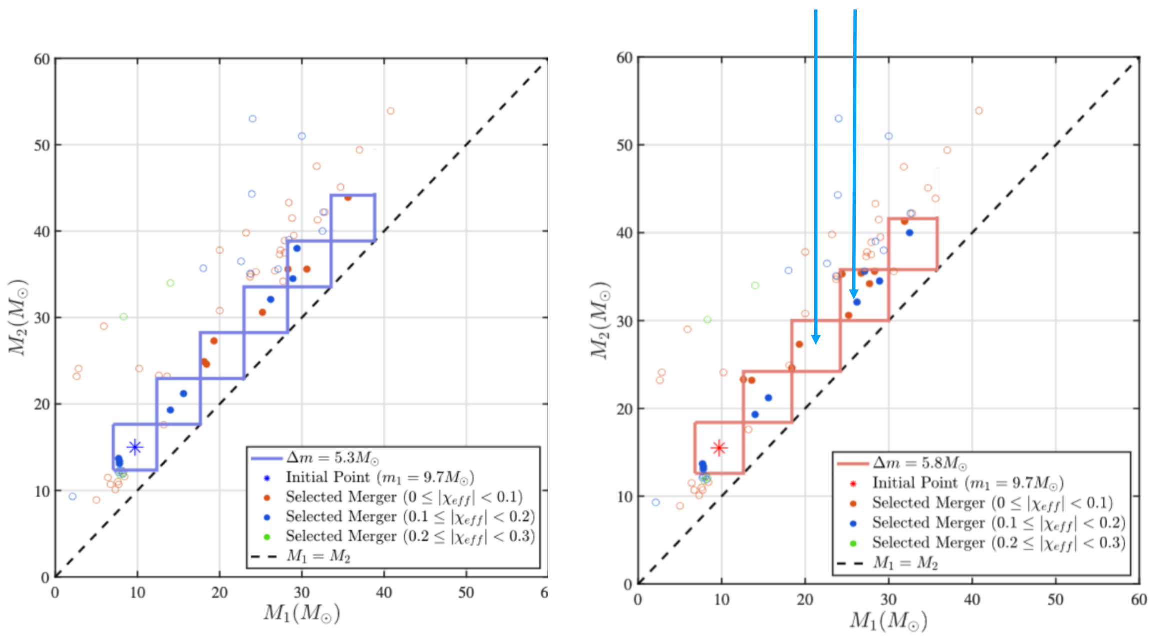

Two typical ways of division

Then it is straightforward to obtain the mass function

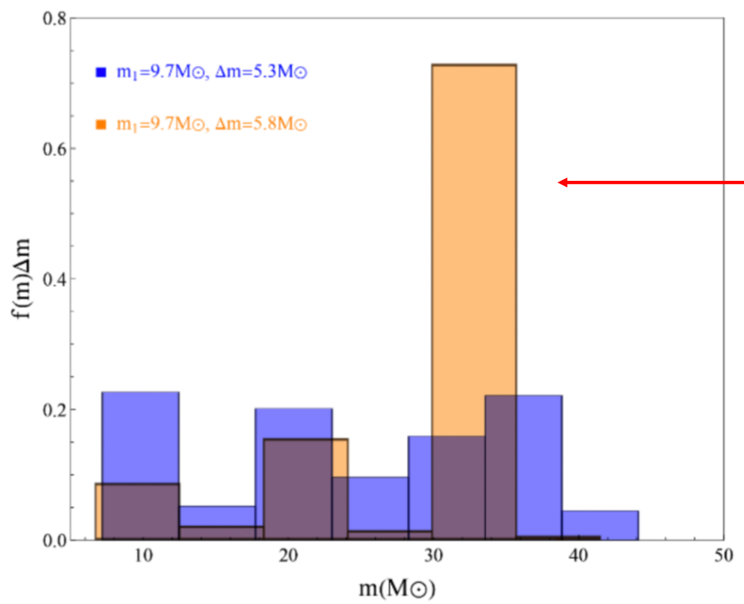

“Artificial” peak

The Power Spectrum

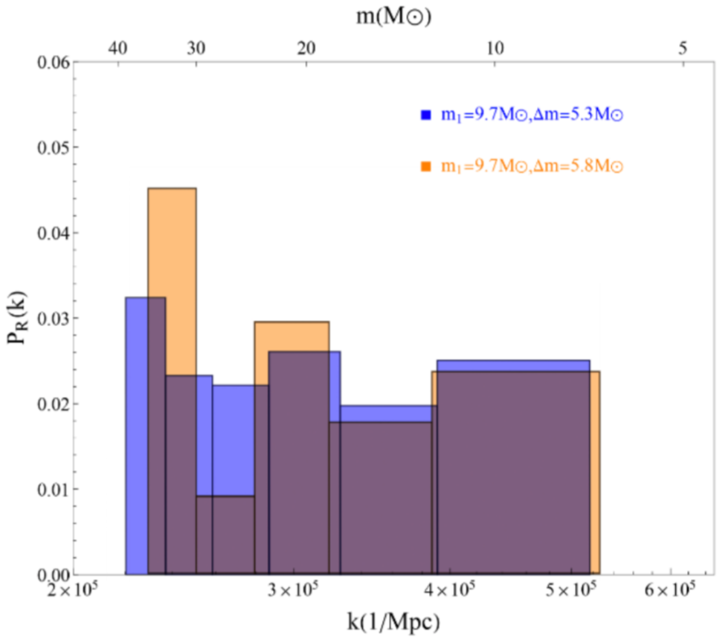

Common feature:

Amplitude of order 0.01

Consistent with PBH scenario

Main Difference:

Flat or oscillating?

Conclusion

We proposed the method to reconstruct the primordial power spectrum of curvature perturbation from the merger rate of PBH binaries

Using the GWTC-3 catalog, we reconstructed the power spectrum in practice

We need more data from LIGO, or mock data for the more realistic reconstruction process

Happy 60 year Birthday to Professor Yokoyama!

Questions: How to divide the grids?

The principle to decide initial points?

Principle: the consistency relation for PBH scenario

$$\mathcal{R}(m_1, m_2) = \left(\frac{m_1 + m_2}{2\sqrt{m_1 m_2}}\right)^{\frac{36}{37}} \sqrt{\mathcal{R}(m_1, m_1)\mathcal{R}(m_2, m_2)}$$

Check:

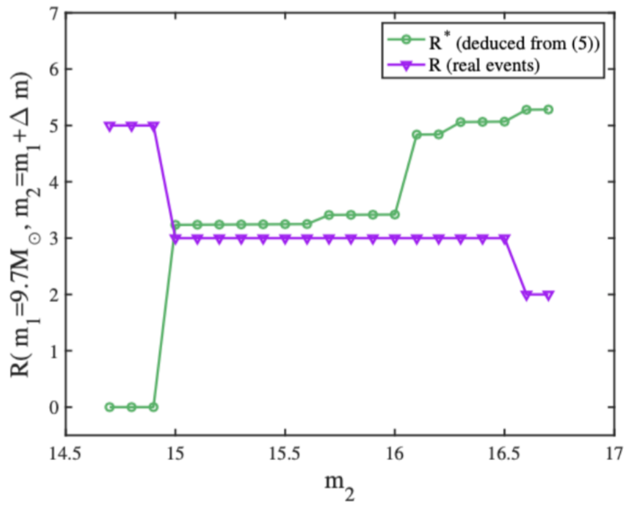

[C10]

Numerical Simulation of Type II Primordial Black Hole Formation

Koichiro Uehara
(Nagoya University)

Collaborator :
Daiki Saito, Albert Escrivà,
Tomohiro Harada
and Chulmoon Yoo

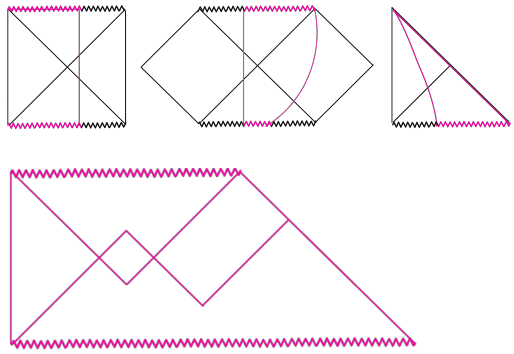

Oct 24, 2022
JGRG31

Introduction: Standard scenario of PBH formation

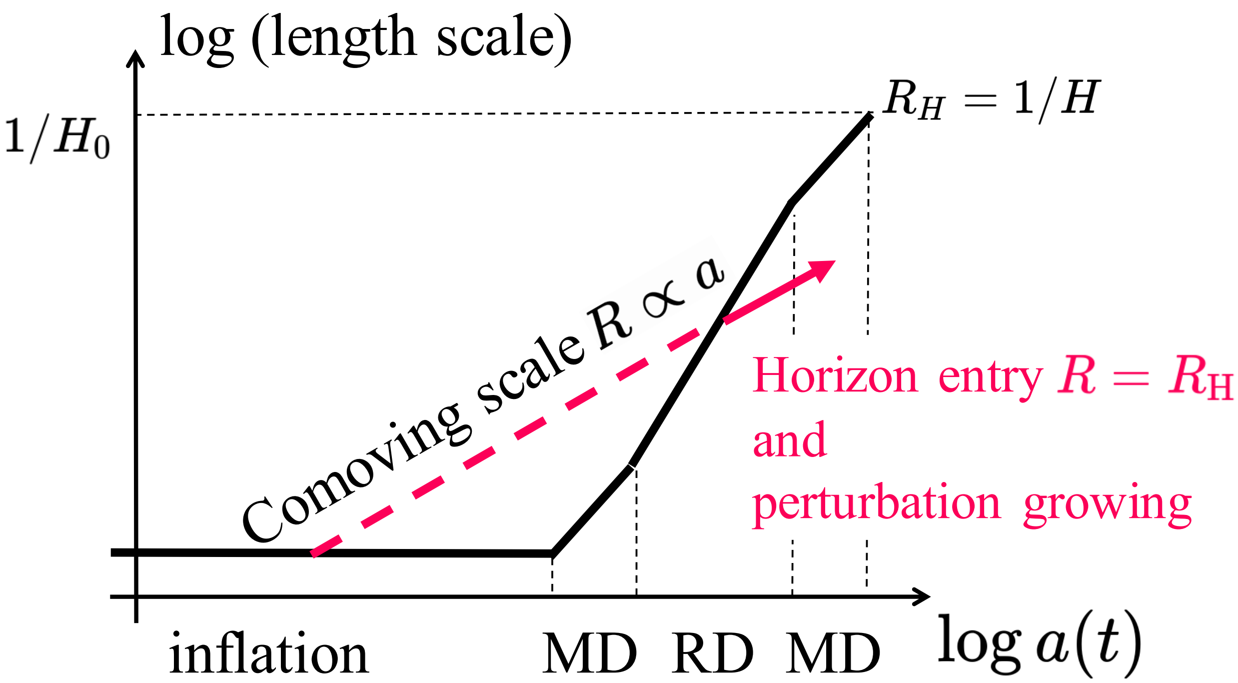

Introduction: Model of PBH formation

Carr and Hawking (1974)

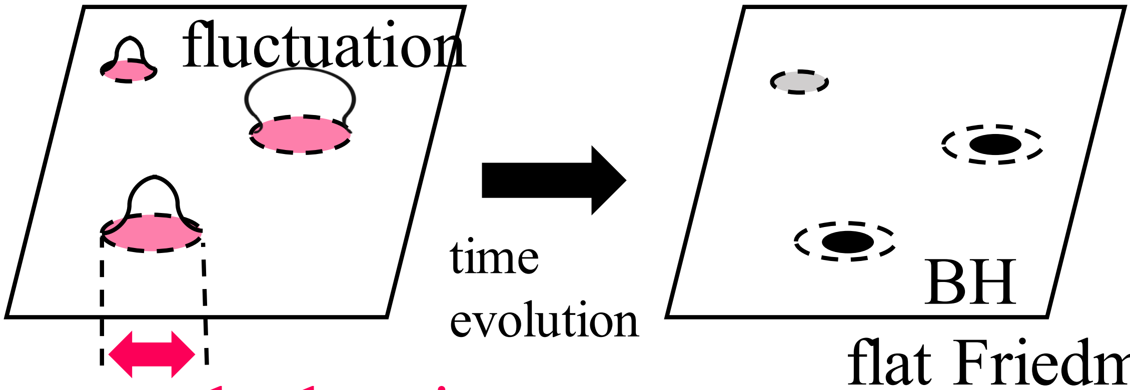

flat Friedmann background

perturbed region:
closed Friedmann universe
⇒ PBH formation
as a gravitational collapse of rad. fluid

Introduction: Schematical diagram of spacetime structure

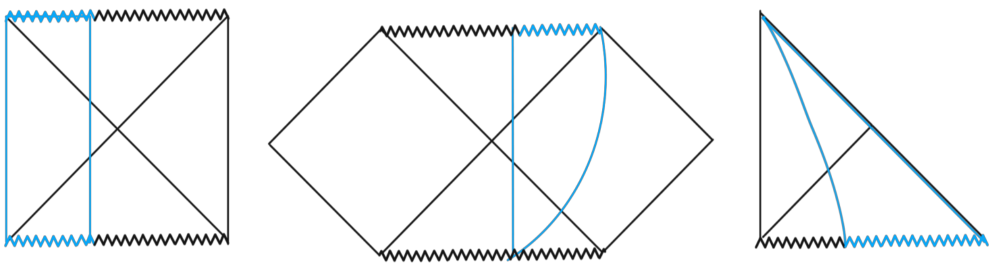

Closed Friedmann

Schwarzschild

Flat Friedmann

⇒ PBH formation

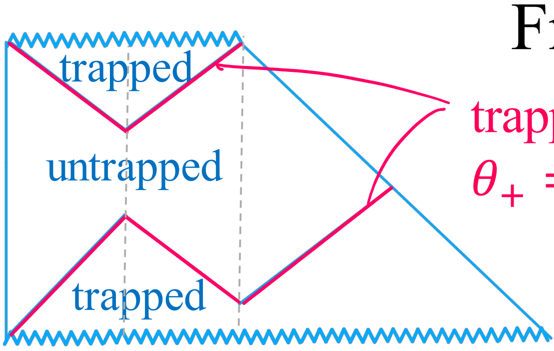

trapped surfaces
$\theta_+ = 0\,, \theta_- = 0$

Introduction: Schematical diagram of spacetime structure

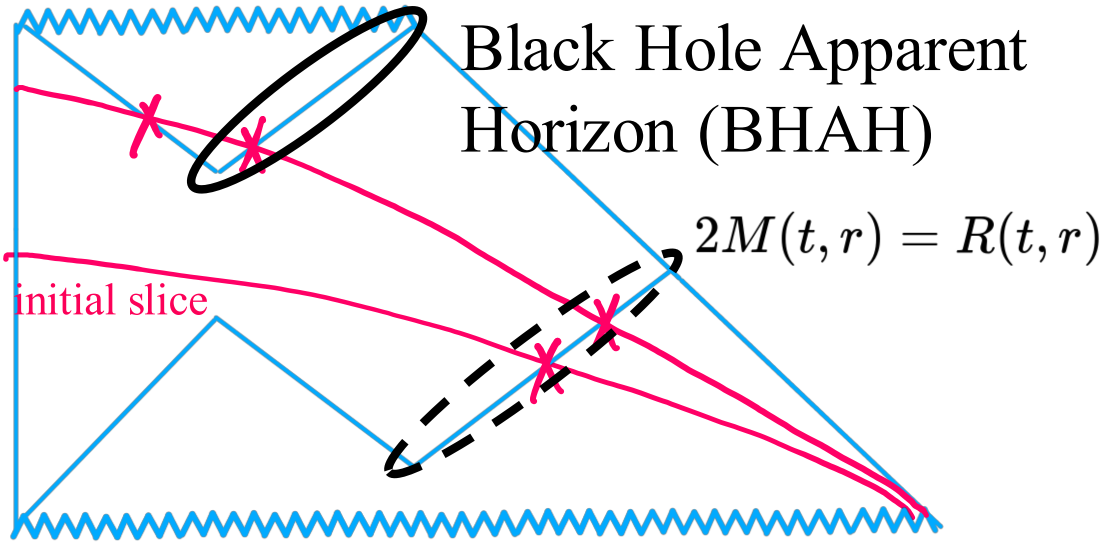

Introduction: Large amplitude of primordial fluctuations

Choptuik (1993)
Niemeyer and Jedamzik (1998)

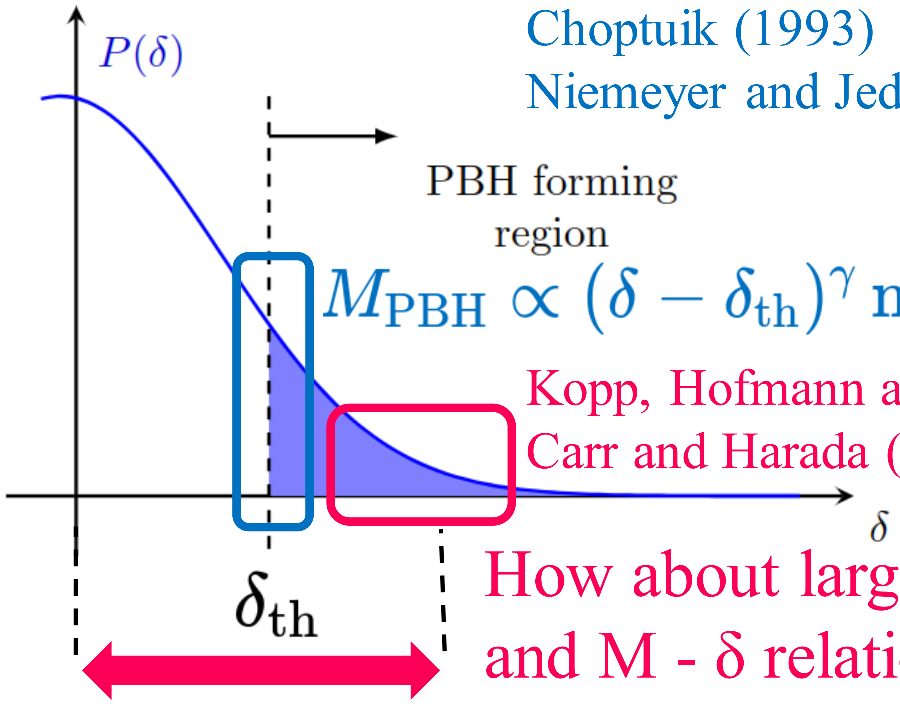

$M_{\mathrm{PBH}} \propto (\delta - \delta_{\mathrm{th}})^{\gamma}$ near δ_{th}

Kopp, Hofmann and Weller (2011)
Carr and Harada (2015)

How about large δ and M - δ relation ?

Large amplitude of primordial fluctuations

Kopp, Hofmann and Weller (2011)

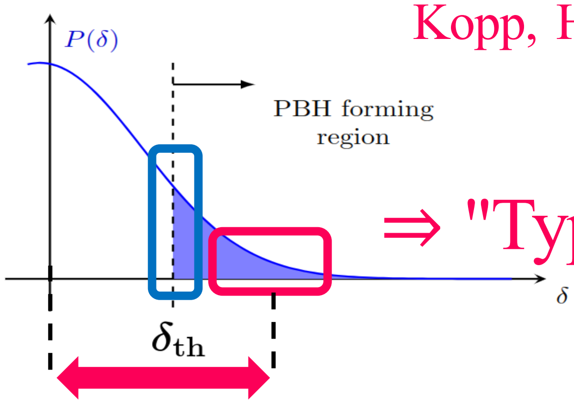

$\Rightarrow$ "Type II PBH"

☑ Analytical study for dust fluid

☐ Numerical study for radiation fluid

Spacetime structures of type II PBH formation

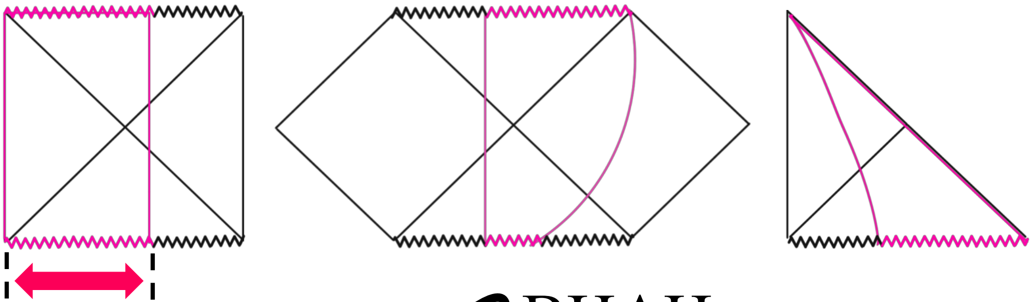

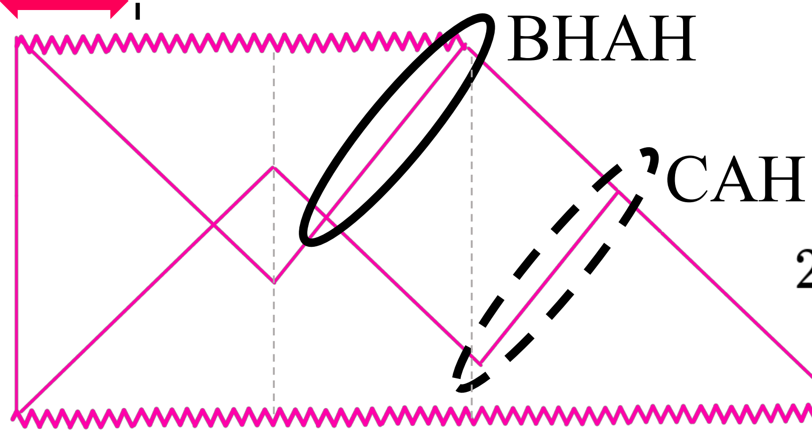

Type II PBH formation

$$2M(t,r) = R(t,r)$$

Large amplitude of primordial fluctuations

☑ Analytical study for dust fluid
☐ Numerical study for rad. fluid :

- Polnarev and Musco (2012)
- Shibata and Sasaki (1999)

⇐ We used this formulation and succeeded !!
(by using numerical code: arXiv.2112.12335
Yoo, Harada, Hirano, Okawa and Sasaki 2022)

Solving Einstein equations: Numerical simulation of PBH formation

numerical code: arXiv.2112.12335
Yoo, Harada, Hirano, Okawa and Sasaki 2022

- Spherically symmetric
- Full GR Geometry and fluid $p = w\rho, w = \frac{1}{3}$ for rad. Fluid
- Asymptotically FLRW
- Based on BSSN formalism with CARTOON method

☑ Analytical study for dust fluid

☐ Numerical study for rad. fluid :

- Polnarev and Musco (2012)
- Shibata and Sasaki (1999)

⇐ We used this formulation and succeeded !!

Kopp, Hofmann and Weller (2011)

⇐ cf. Misner-Sharp formulation:

There is a coordinate singularity

$$\dot{R}^2 = \alpha^2\left(\frac{2M}{R} + E\right) : \text{Hamiltonian constraint},$$

$$\dot{E} = -2\frac{1+E}{\rho+p}\frac{p'}{R'}\dot{R} : \text{momentum constraint},$$

$$\dot{M} = -4\pi p R^2 \dot{R} : \text{evolution equation},$$

$$(\ln\alpha)' = -\frac{p'}{\rho+p} : \text{Euler equation}.$$

Solving Einstein equations: Long-wavelength approximation and Cosmological 3+1 decomposition

super horizon size $\epsilon \sim k/aH_{\mathrm{b}} \ll 1$

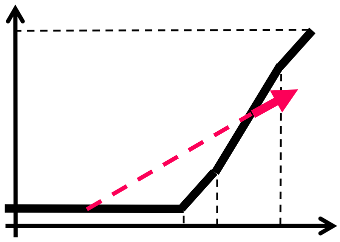

Lyth, Malik and Sasaki (2005)

Shibata and Sasaki (1999)

Harada, Yoo, Nakama and Koga (2015)

$$dl^2 = a(t)^2 \mathrm{e}^{-2\zeta(t,r)}(dr^2 + r^2 d\Omega^2) + \mathcal{O}(\epsilon^2)$$

$$= a(t)^2\left(\frac{d\tilde{r}^2}{1-K(\tilde{r})\tilde{r}^2} + \tilde{r}^2 d\Omega^2\right) + \mathcal{O}(\epsilon^2)$$

Results: Spaceime structures

Type I PBH

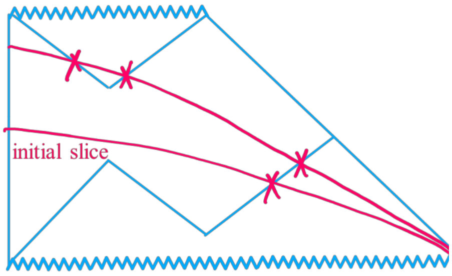

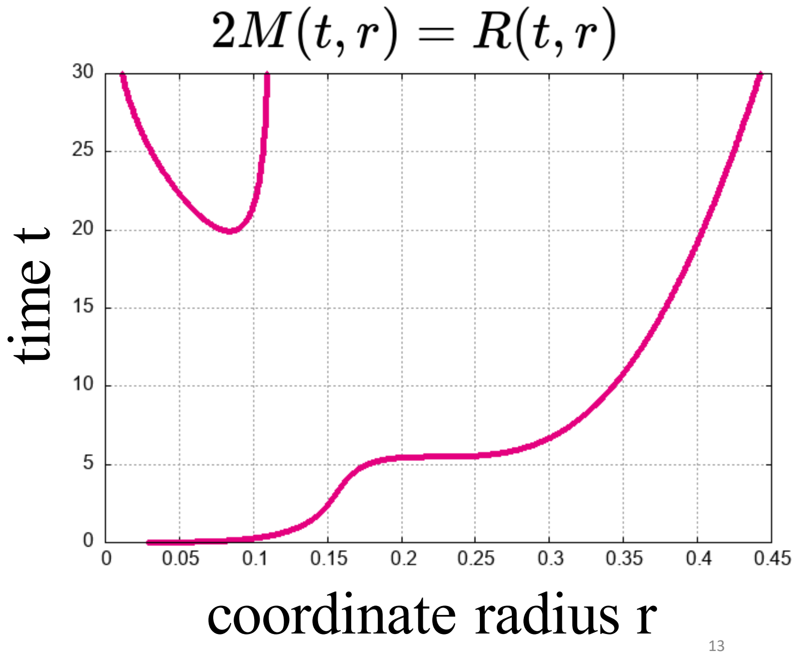

Results:
Spacetime structures of type II PBH formation

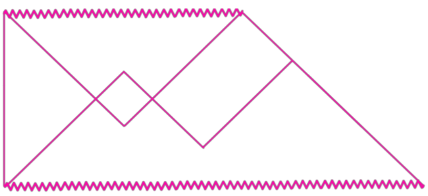

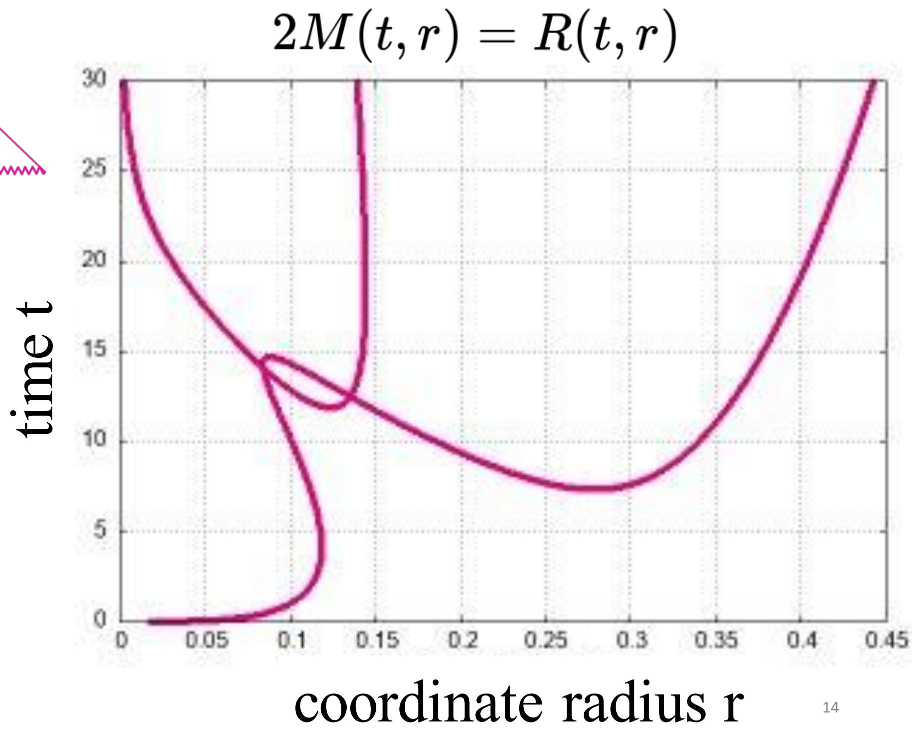

Results:

Type I PBH

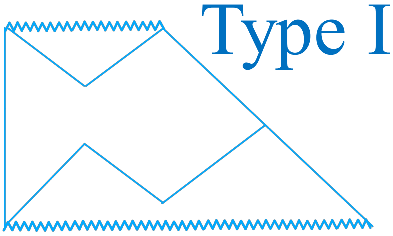

Type II PBH

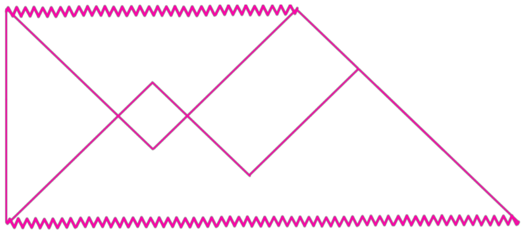

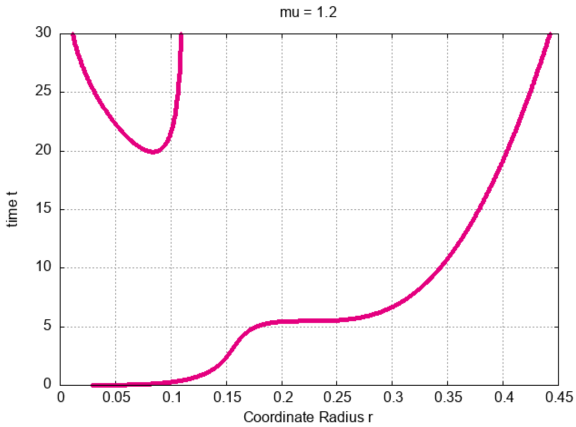

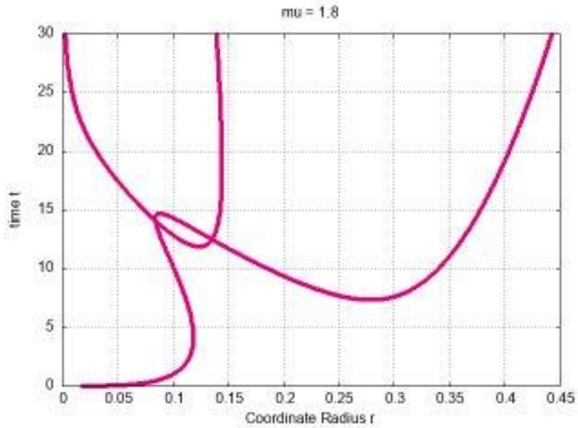

Results:

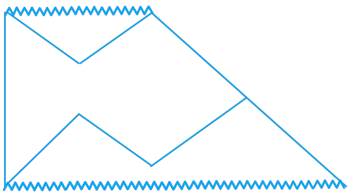

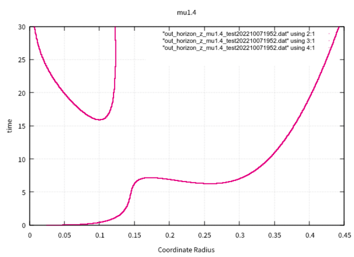

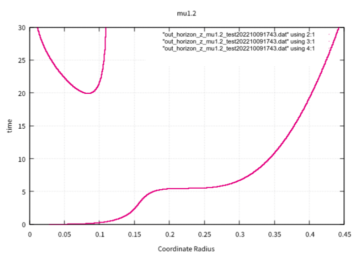

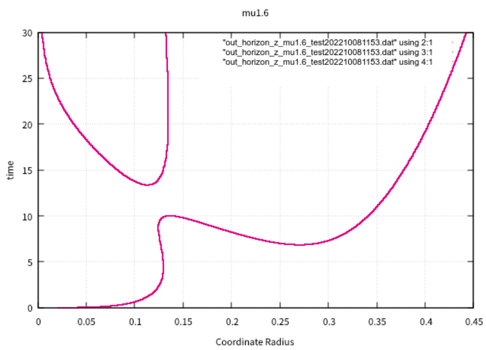

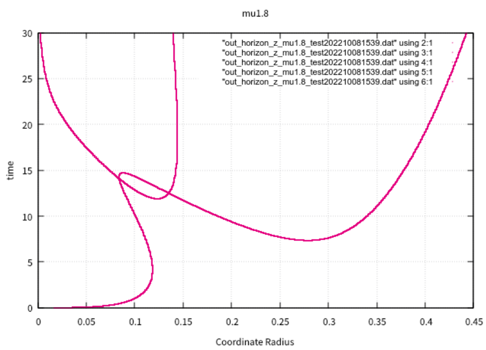

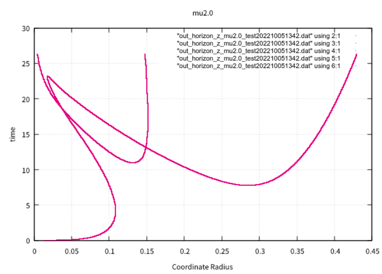

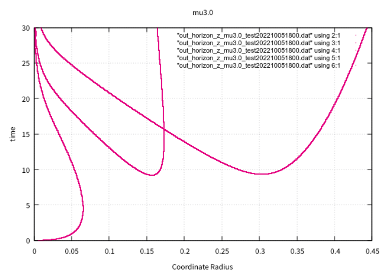

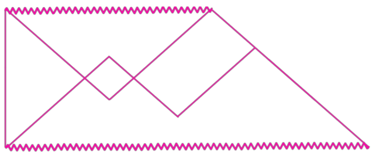

Summary and future works:
Type II PBH formation

☑ Analytical study for dust fluid

(Kopp, Hofmann and Weller ,2011)

☑ Numerical study for rad. fluid

(Our work)

- We are going to get the mass-amp. relation M(δ)

Back Up: (R, t)-plot

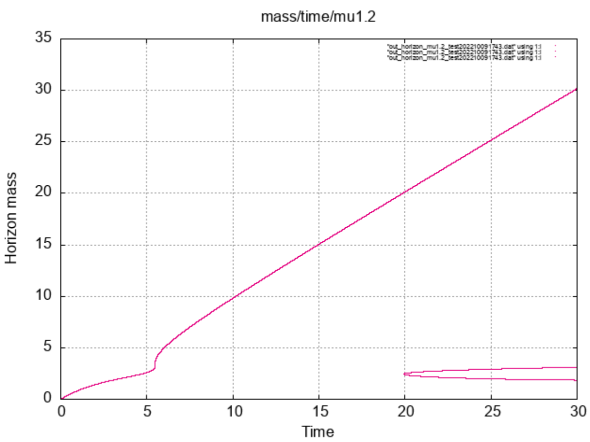

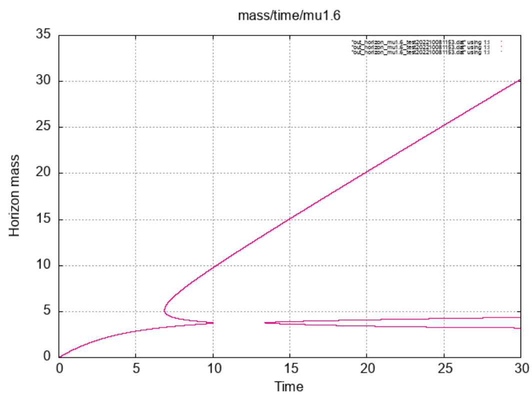

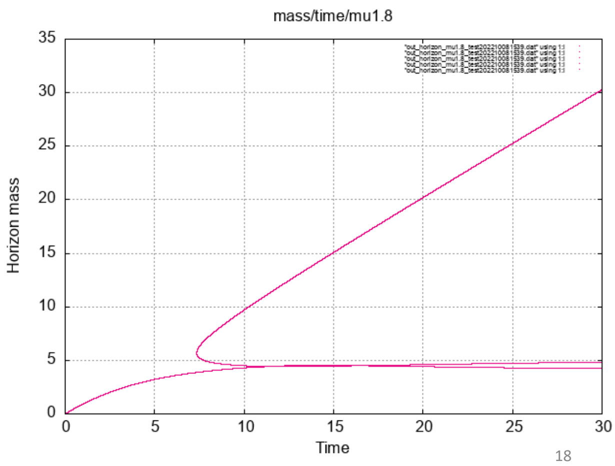

Back Up: (R, t)-plot

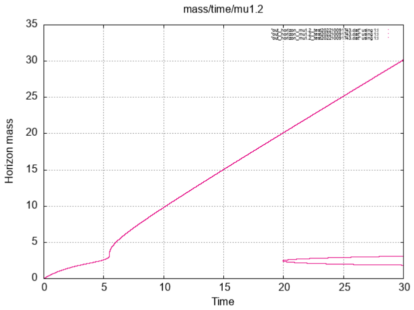

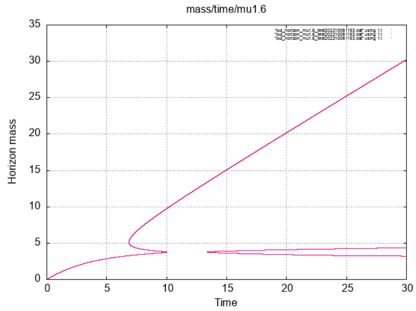

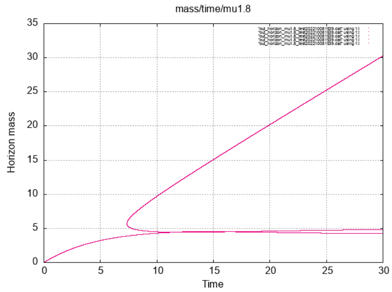

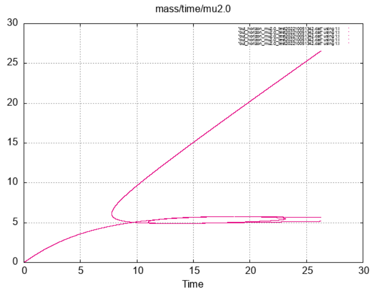

Back Up: (R, r)-plot

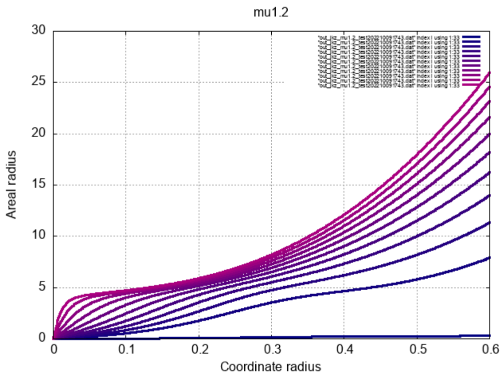

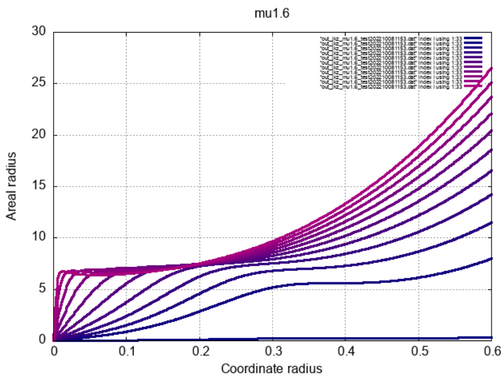

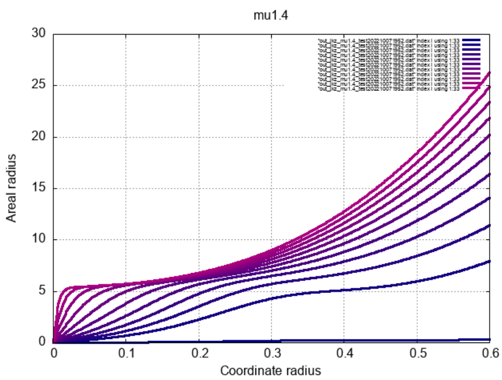

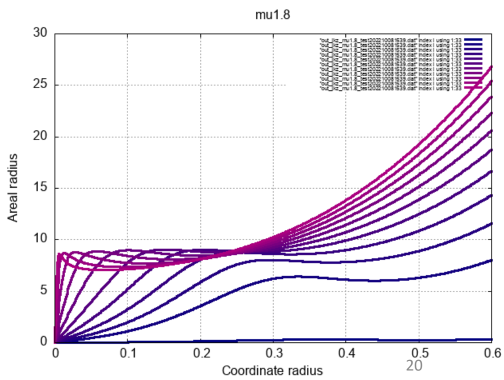

Back Up: (R, r)-plot

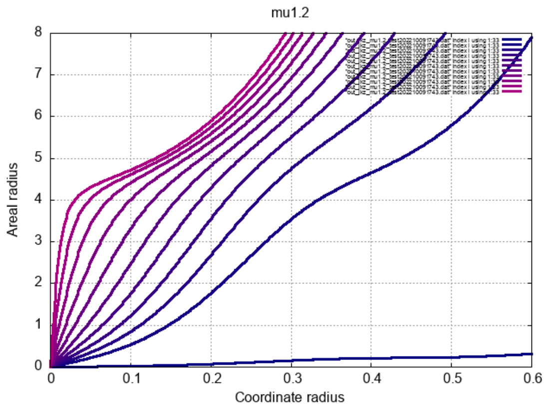

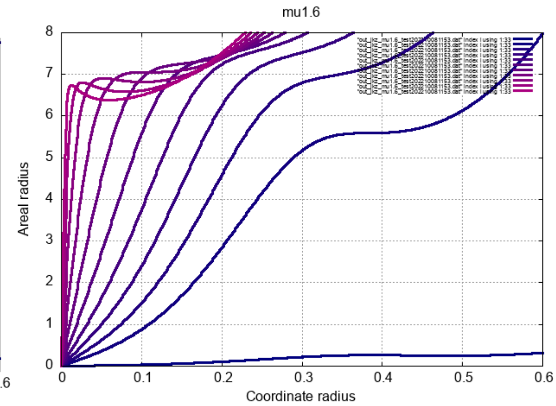

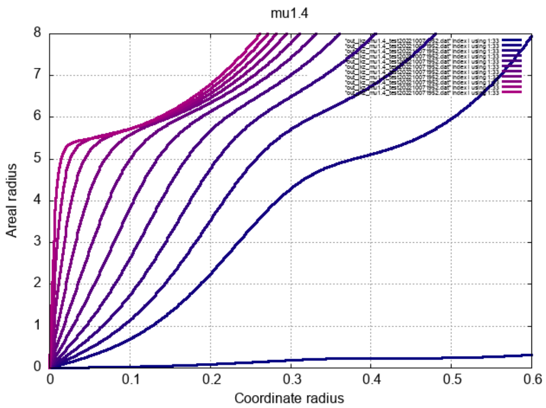

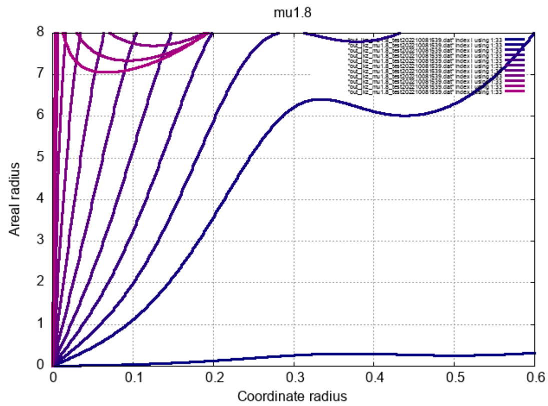

C11

Effective inspiral spin distribution of primordial black hole binaries

2022.10.24-28, JGRG31@University of Tokyo

Yasutaka Koga (Nagoya U.)
Collaborator： T. Harada (Rikkyo U.), Y. Tada, S. Yokoyama, CM Yoo (Nagoya U.)

Ref: YK, T. Harada, Y. Tada, S. Yokoyama, & C-M. Yoo, arXiv:2208.00696 (to be published in ApJ).

1. Introduction

GW from Black hole (BH) binary：

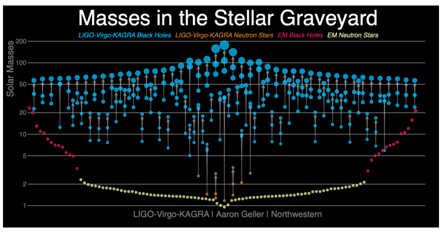

- 90 events of GWs from binary merger have been detected by LIGO-Virgo-Kagra.
- Most of the binaries consist of BHs with mass of $10 - 100 M_\odot$.
- The parameter distribution of BH binaries, e.g. effective spin $\chi_{\rm eff}$, are observationally investigated.

https://www.ligo.org/detections.php

$$\chi_{\rm eff} = \frac{M_1 a_{1,\perp} + M_2 a_{2,\perp}}{M_1 + M_2}$$

Analysis of O3 data [Callister+ (2021)]

- Effective (inspiral) spin $\chi_{\rm eff}$ & mass ratio q distribution was shown.
- Distributed around $\chi_{\rm eff} = 0$ with some width.
- $\chi_{\rm eff}$ depends on q.
- Known astrophysical models may not completely account for the result.

What is the theoretical prediction for Primordial BH binary distribution?

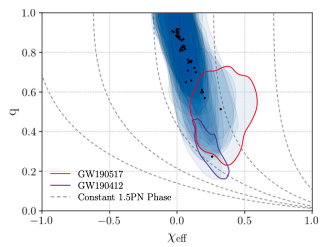

Figure 5. Effective spin and mass ratio posteriors for BBHs

1. Introduction

Primordial Black hole (PBH) = Black hole formed in the early universe:

- PBH formation by collapse of density fluctuation.

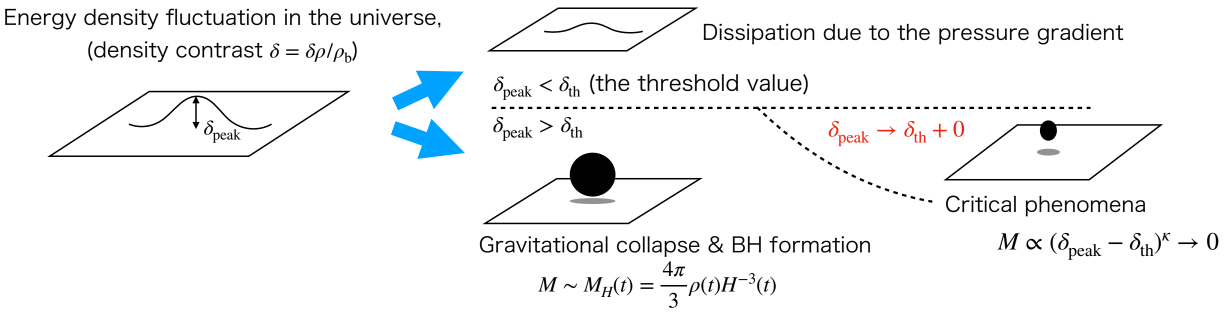

- Critical phenomena can lead to PBHs with larger spin. The interesting effect on the effective spin of PBH binary.

[Harada, Yoo, Kohri, YK, Monobe (2021)]

In radiation dom. case,	$a \sim 10^{-3} \quad (M \sim M_H)$
	$a \gtrsim 1 \quad (M \ll M_H)$

1. Introduction

Our aim:

- As the first step, we investigate a simplest model of a PBH binary and its distribution.
- Focus on the characteristic parameters in GW observation, effective inspiral spin, mass ratio, and chirp mass.

Overview:

- PBHs are formed by collapse of density fluctuation in the radiation dominated universe.
- Apply the peak theory to the density fluctuation.
- Take into account the effect of the critical phenomena.
- Two PBHs are randomly chosen and form a binary.

2. Single PBH distribution

Setup

- Background: flat FLRW spacetime,

$$ds^2 = -dt^2 + a(t)(dr^2 + r^2 d\Omega^2)$$

- Density contrast $\delta := \delta\rho/\rho_b$ is a random Gaussian field. (in CMC slicing, at an initial time before reentry)

$$P(y_1, \ldots, y_n)dy_1 \ldots dy_n = [(2\pi)^2 \det(M)]^{-1/2} e^{-Q} dy_1 \ldots dy_n, \qquad Q := \Delta y_i (M^{-1})_{ij} \Delta y_j / 2,\ M_{ij} := \langle \Delta y_i \Delta y_j \rangle,\ \Delta y_i := y_i - \langle y_i \rangle, \quad y_i = \delta(\mathbf{r}), \partial\delta(\mathbf{r}), \partial\partial\delta(\mathbf{f})$$

- Almost monochromatic power spectrum:

$$\mathscr{P}_\delta(k) \approx \sigma_0^2 k_0 \delta(k - k_0) \quad \text{->} \quad \gamma := \sigma_1^2/(\sigma_0\sigma_2) \simeq 1, \qquad \sigma_j^2 = \int d\ln k\, k^{2j} \mathscr{P}_\delta(k), \qquad \langle \delta^2 \rangle = \sigma_0^2, \ \ \langle \delta \partial_x^2 \delta \rangle = -\sigma_1^2/3, \ldots$$

- Peak theory [Bardeen, Bond, Kaiser, Szalay, 1986]

  - Distribution of normalized peak value, $\nu := \delta_{\rm peak}/\sigma_0$: $P_\nu(\nu) \simeq \dfrac{\sqrt{2/\pi}}{\mathrm{erfc}(\nu_{\rm th}/\sqrt{2})} \underbrace{e^{-\nu^2/2}}_{\text{Gaussian}}, \quad \int_{\nu_{\rm th}}^{\infty} P_\nu(\nu) d\nu = 1, \quad \nu_{\rm th} \sim 10.$ <=> $f_{\rm PBH} \sim 0.1\,\%$ [Tada+, 2019]
  - PBHs are mainly formed from nearly spherical peaks with the amplitude, $\nu \sim \nu_{\rm th}$. => Critical phenomena
  - Typical profile: $\delta \simeq \nu\sigma_0 \dfrac{\sin k_0 r}{k_0 r}$ [Yoo, Harada, Garriga, Kohri '18]

=> Necessary for specifying $\delta_{\rm th}$, or $\sigma_0 = \delta_{\rm th}/\nu_{\rm th}$, because of its profile dependence.

2. Single PBH distribution

Probability distribution of single PBHs (mass M, spin a, spin direction (θ, ϕ)) :

$$P(a, M, \theta, \phi)\, da\, dM\, d\theta\, d\phi \qquad \text{Isotropic distribution (assumption) ->} \qquad P(a, M, \theta, \phi) = \frac{1}{4\pi} P(a, M) \sin\theta$$

Distribution of spin a : [Heavens+ (1988), De Luca+ (2019), Harada+ (2021)]

- Normalized spin parameter, h:

The total angular momentum of the collapsing region Σ of the time slice of FLRW

$$S_i(\Sigma) = -\int_\Sigma T^{ab} n_a (\phi_i)_b d\Sigma \simeq \frac{4}{3} a^4 \rho_b \epsilon_{ijk} v^k{}_l \int_\Sigma (x - x_{\rm pk})^j (x - x_{\rm pk})^l d^3x,$$

$\Sigma := \{x \mid \delta(x) = f\delta_{\rm peak}\},\ 0 < f < 1,$

n_a: unit normal to the slice, $(\phi_i)^b$: rotational KV.

$$v^k{}_l := \partial v^k / \partial x^l \Big|_{x = x_{\rm pk}}, \quad v^i = (1/12\mathscr{H})\partial^i \delta.$$

(at superhorizon scale [Harada+. 2015]

The normalized spin parameter

$$h = \frac{5\gamma^6 \nu}{2^{9/2}\pi} \sqrt{1 - \gamma^2}^{-1} s_e, \qquad \sqrt{\langle S^i S_i \rangle} = S_{\rm ref} \sqrt{\langle s_e^i s_{ei} \rangle}$$

$$S_{\rm ref}(\eta) = (1 + w)\mathfrak{a}^4 \rho_b g(\eta)(1 - f)^{5/2} R_*^5,$$

$$\vec{s}_e = \frac{16\sqrt{2}\pi}{135\sqrt{3}} \left(\frac{\nu}{\gamma}\right)^{5/2} \frac{1}{\sqrt{\Lambda}} (-\alpha_1 \tilde{v}_{23}, \alpha_2 \tilde{v}_{13}, -\alpha_3 \tilde{v}_{12}),$$

$$\alpha_1 = \frac{1}{\lambda_3} - \frac{1}{\lambda_2}, \quad \alpha_2 = \frac{1}{\lambda_3} - \frac{1}{\lambda_1}, \quad \alpha_3 = \frac{1}{\lambda_2} - \frac{1}{\lambda_1},$$

$$\Lambda := \lambda_1 \lambda_2 \lambda_3, \quad R_* := \sqrt{3}\frac{\sigma_1}{\sigma_2}.$$

Distribution function (fitting formula) [Heavens & Peacock (1988)]

$$\langle (v^k{}_l(\eta))^2 \rangle = g^2(\eta) \langle (\tilde{v}^k{}_l)^2 \rangle,$$

$$P_h(h)dh = 563 h^2 \exp[-2.37 - 4.12 \ln h - 1.53 (\ln h)^2 - 0.13 (\ln h)^3] dh, \qquad \int_0^\infty P_h(h) dh = 1.$$

$$\tilde{v}^i{}_j := -\frac{1}{\sigma_0} \int \frac{d^3k}{(2\pi)^3} \frac{k^i k_j}{k^2} \delta_{\mathbf{k}} e^{i\mathbf{k}\cdot\mathbf{x}}.$$

2. Single PBH distribution

- BH spin (Kerr parameter) a:

* "turn around": decoupling from the cosmological expansion

Evaluation at the turn around time, $\eta_{\rm ta} \simeq 2.14 k_0^{-1}$, [Harada + (2021)]

$$a := \frac{S}{GM^2} = C(M,\nu)h, \quad C(M,\nu) = \frac{2^{9/2}\pi}{5\gamma^6\nu}\sqrt{1-\gamma^2}\frac{S_{\rm ref}(\eta_{\rm ta})}{GM^2} = 3.25\times10^{-2}\sqrt{1-\gamma^2}\sigma_0\left(\frac{M}{\underline{M_H}}\right)^{-1/3}\left(\frac{\nu}{10}\right)^{-1},$$

M: mass inside Σ.

$M_H \equiv M_{k_0}$.

- Conditional probability of a:

$$P(a \mid M,\nu)da = \frac{P_h\big(a/C(M,\nu)\big)}{C(M,\nu)N_a(M,\nu)}da, \qquad \int_0^1 P(a \mid M,\nu)da = 1, \qquad N_a(M,\nu) := \int_0^{1/C(M,\nu)} P_h(h)dh$$

Normalized for $a \in [0,1]$. (i.e., the spin value for BH solution)

- Critical phenomena:

power law $M(\nu) = KM_H(\sigma_0\nu - \sigma_0\nu_{\rm th})^\beta$, $K=1$, $\beta = 0.36$. [Evans & Coleman (1994), Escriva (2019)]

$$\Rightarrow P(a,M)dadM = P(a \mid M(\nu),\nu)P_\nu(\nu)dad\nu$$

Probability distribution of single PBHs:

$$\boxed{P(a,M,\theta,\phi)dadMd\theta d\phi = \frac{1}{4\pi}P(a \mid M(\nu),\nu)P_\nu(\nu)dad\nu d(\cos\theta)d\phi}$$

2. Single PBH distribution

Distribution of single PBHs:

- Single PBHs distributed as $a \lesssim 0.004$ & $0.1 \lesssim M/M_H \lesssim 0.4$.
- $\langle a\rangle = 1.77\times10^{-3}$.
- $\langle a\rangle(M)$ for each M almost scales as $\propto M^{-1/3}$ (anti-correlation).
- $\langle a\rangle(M)$ can be of order unity for $M \lesssim 10^{-8}$.

$\langle a\rangle \propto M^{-1/3}$ cf [Harada+ '21]

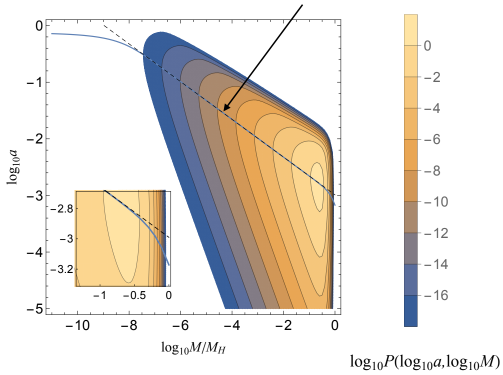

Determination of σ_0:

- Threshold in terms of max of "compaction function": $C_{\rm m,th} \simeq 2/5$ [Harada+ '15]
- Typical initial profile of a peak: $\delta \simeq \nu\sigma_0\frac{\sin k_0 r}{k_0 r}$ [Yoo+ '18]
- Relation btwn the peak & compaction func.: $\delta_{\rm peak} \simeq (24/5)C_{\rm m}$

$\Rightarrow \sigma_0 = \delta_{\rm peak,th}/\nu_{\rm th} = (24/5)C_{\rm m,th}/\nu_{\rm th} = 0.192$

- $\gamma = 0.85$. (almost monochromatic power spectrum)
- $\nu_{\rm th} = 10$. ($M = M_\odot$, $f_{\rm PBH} = 10^{-3}$, PS approx. [Tada+ '19])
- $\sigma_0 = \delta_{\rm peak,th}/\nu_{\rm th} = 0.192$. [Harada+ '15]

3. PBH binary distribution

Distribution of PBH binary

- Primary & secondary PBHs are chosen randomly. (∵ at most one PBH in each Hubble patch)
- Intrinsic parameters of PBH binary $\mathbf{x}$:

$$\mathbf{x} = (\underbrace{a_1, M_1, \theta_1, \phi_1}_{\text{PBH1 (primary)}}, \underbrace{a_2, M_2, \theta_2, \phi_2}_{\text{PBH2 (secondary)}})$$

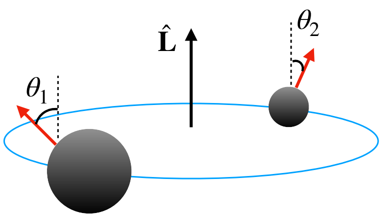

θ_1, θ_2: w.r.t the orbital angular momentum $\hat{\mathbf{L}}$

- Probability distribution of the intrinsic parameters:

$$P(\mathbf{x})d\mathbf{x} = 2 \prod_{i=1,2} P(a_i, M_i, \theta_i, \phi_i) da_i d\nu_i d\theta_i d\phi_i$$

Normalization s.t. $\int_{M_1 > M_2} P(\mathbf{x})d\mathbf{x} = 1.$

3. PBH binary distribution

Transformation to the binary's characteristic parameters:

- Effective spin $\chi_{\rm eff}$:

$$\chi_{\rm eff}(a_1, M_1, \theta_1, a_2, M_2, \theta_2) = \frac{M_1 a_1 \cos\theta_1 + M_2 a_2 \cos\theta_2}{M_1 + M_2} \in [-1, 1].$$

: weighted sum of the spin components perpendicular to the orbital plane

- Mass ratio q :

$$q(M_1, M_2) = \frac{M_2}{M_1} \in (0, 1].$$

- Chirp mass $\mathcal{M}$:

$$\mathcal{M}(M_1, M_2) = \frac{(M_1 M_2)^{3/5}}{(M_1 + M_2)^{1/5}} \in (0, \infty).$$

c.f. GW amplitude from inspiral binary [Maggiore (2008)]:

$$h_+(t) = \frac{4}{r}\mathcal{M}^{5/3}\left(\frac{\omega_{\rm gw}}{2}\right)^{2/3} \frac{1 + \cos^2\iota}{2} \cos(\omega_{\rm gw} t_{\rm ret} + 2\phi),$$

$$h_\times(t) = \frac{4}{r}\mathcal{M}^{5/3}\left(\frac{\omega_{\rm gw}}{2}\right)^{2/3} \cos\iota \sin(\omega_{\rm gw} t_{\rm ret} + 2\phi).$$

Distribution function of the binary parameters :

$$P(\mathcal{M}, q, \chi) = \frac{1+q}{2q^2\beta^2\sigma_0^2\mathcal{M}} \left(\frac{(1+q)^{2/5}\mathcal{M}^2}{q^{1/5}K^2 M_{k_0}^2}\right)^{1/\beta} \int_0^1 da_1 \int_0^1 da_2 \Theta\left(L(a_1, a_2, \chi, q)\right) L(a_1, a_2, \chi, q)$$
$$\times \frac{1}{a_1 a_2} \prod_{i=1}^{2} P\Big(a_i \mid M_i(\mathcal{M}, q), \nu\left(M_i(\mathcal{M}, q)\right)\Big) P\Big(\nu\left(M_i(\mathcal{M}, q)\right)\Big),$$

$L(a_1, a_2, \chi, q) = \min\left[a_1, q a_2 + (1+q)\chi\right] + \min\left[a_1, q a_2 - (1+q)\chi\right]$, $M_1(\mathcal{M}, q) = q^{-3/5}(1+q)^{1/5}\mathcal{M}$, $M_2(\mathcal{M}, q) = q^{2/5}(1+q)^{1/5}\mathcal{M}$, $\nu(M) = \frac{1}{\sigma_0}\left(\frac{M}{K M_{k_0}}\right)^{1/\beta} + \nu_{\rm th}$.

3. PBH binary distribution

Probability distribution of PBH binaries:

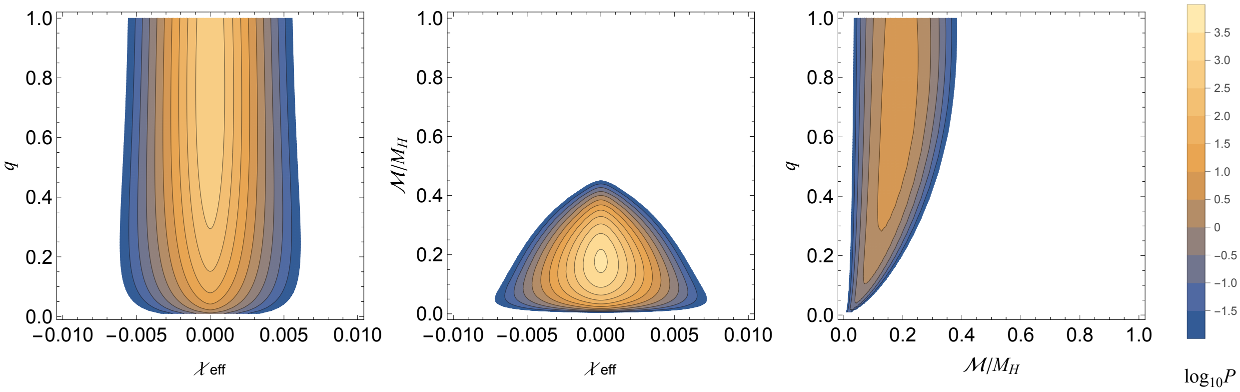

- $\sqrt{\langle\chi_{\rm eff}^2\rangle} = 8.4\times 10^{-4}$. c.f. $\langle a\rangle \sim 10^{-3}$.
- $|\chi_{\rm eff}|$ & q : no correlation. ← The contribution of a_2 to $\chi_{\rm eff} = \dfrac{a_1\cos\theta_1 + qa_2\cos\theta_2}{1+q}$ is suppressed by q.
- $|\chi_{\rm eff}|$ & $\mathscr{M}$: anti-correlation. (as well as a & M of single PBH)

4. Summary

Summary

- We investigated the probability distribution of PBH binaries focusing on the effective spin, mass ratio, and chirp mass.
- Although the critical phenomena lead to PBHs with $a\sim 1$, the effective spin is statistically very small, $\sqrt{\langle\chi_{\rm eff}^2\rangle}\sim 10^{-3}$.
- No correlation between $|\chi_{\rm eff}|$ & q. Anti-correlation between $|\chi_{\rm eff}|$ & $\mathscr{M}$.

Discussion

- Contribution from other effects?
  - Clustering of PBHs (<-> random choice of PBHs). e.g. correlation btwn peaks due to non-local non-Gaussianity
  - Evolution of spin due to accretion.
  - Temporal reduction of pressure due to the phase transition.
  - etc⋯

2. Single PBH distribution

Distribution of single PBHs:

Single PBHs distributed as $a \lesssim 0.004$ & $0.1 \lesssim M/M_H \lesssim 0.4$.

- $\langle a \rangle = 1.77 \times 10^{-3}$.
- $\langle a \rangle(M)$ for each M almost scales as $\propto M^{-1/3}$.
- $\langle a \rangle(M)$ can be of order unity for $M \lesssim 10^{-8}$.

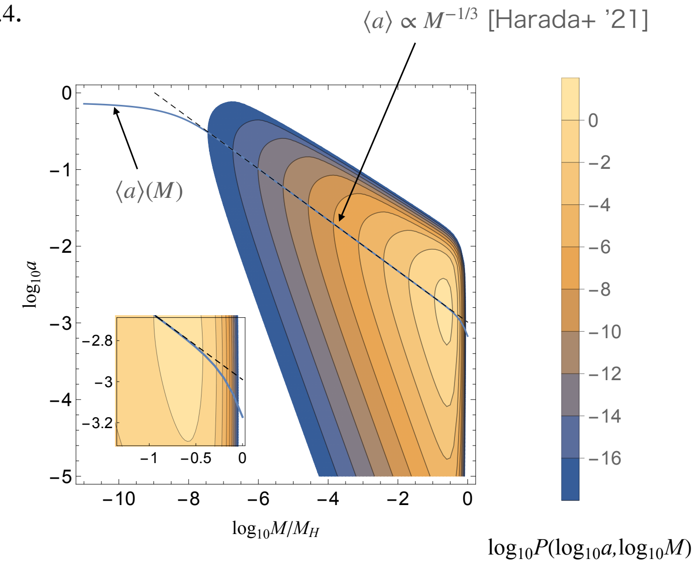

2. Single PBH distribution

Distribution of single PBHs:

- Single PBHs distributed as $a \lesssim 0.004$ & $0.1 \lesssim M/M_H \lesssim 0.4$.
- $\langle a \rangle = 1.77 \times 10^{-3}$.
- $\langle a \rangle(M)$ for each M almost scales as $\propto M^{-1/3}$ (anti-correlation).
- $\langle a \rangle(M)$ can be of order unity for $M \lesssim 10^{-8}$.

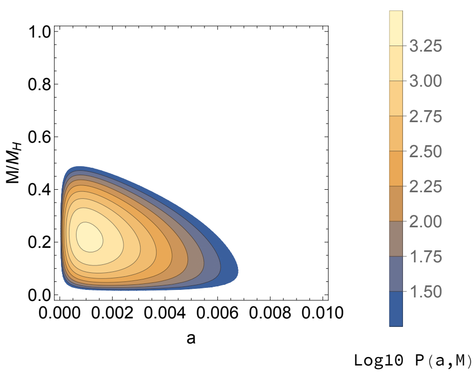

Determination of σ_0:

- Threshold in terms of max of "compaction function": $C_{\rm m,th} \simeq 2/5$ [Harada+ '15]
- Typical initial profile of a peak: $\delta \simeq \nu\sigma_0 \frac{\sin k_0 r}{k_0 r}$ [Yoo+ '18]
- Relation btwn the peak & compaction func.: $\delta_{\rm peak} \simeq (24/5) C_{\rm m}$

$\sigma_0 = \delta_{\rm peak,th}/\nu_{\rm th} = (24/5) C_{\rm m,th}/\nu_{\rm th} = 0.192$

- $\gamma = 0.85$. (almost monochromatic power spectrum)
- $\nu_{\rm th} = 10$. ($M = M_\odot$, $f_{\rm PBH} = 10^{-3}$, PS approx. [Tada+ '19])
- $\sigma_0 = \delta_{\rm peak,th}/\nu_{\rm th} = 0.192$. [Harada+ '15]

C12

JGRG 31

Primordial black holes from Affleck-Dine mechanism

Kentaro Kasai
ICRR, The University of Tokyo
Collabrator: Masahiro Kawasaki, Kai Murai

Based on: K. Kasai, M.Kawasaki, K.Murai JCAP 10 (2022) 048

Today's Talk

- Introduction
- Motivation of our scenario
  - ▶ Constraints on curvature fluctuation
- Outline of our scenario
  - ▶ Affleck-Dine mechanism
  - ▶ PBH from Affleck-Dine leptogenesis(L-balls)
  - ▶ Difficulties of Affleck-Dine baryogenesis scenario
- Conclusion

Introduction: Primordial Black Holes

■ LIGO-Virgo event : GW events of black hole (BH) binary merger with masses around $M \sim O(10)M_{\odot}$ are observed.

Ex.) R. Abbott et al., Phys. Rev. X 11 (2021) 021053

■ Supermassive black hole : BHs with masses around $M > 10^5 M_{\odot}$ are considered to exist at the center of almost all galaxies.

Ex.) J. Kormendy and D. Richstone, Ann. Rev. Astron. Astrophys. 33 (1995) 581.

■ "Primordial" black holes (PBHs): thought to be created in radiation-dominated era.

Ex.) B. J. Carr and S. W. Hawking, Mon. Mon. Not. Roy. Astron. Soc. 168 (1974) 399–415

Usual hypothesis: Curvature fluctuation

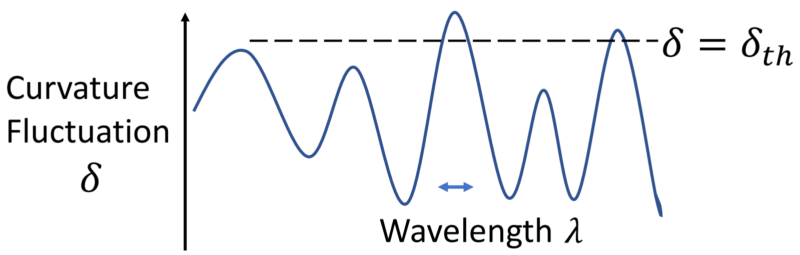

Example : J. G. Bellido, E. R. Morales *Phys.Dark Univ.* 18 (2017) 47-54

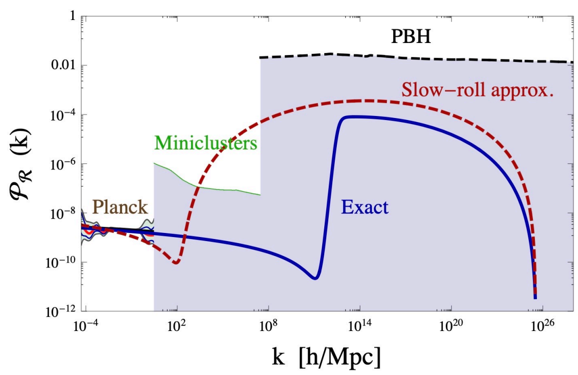

When λ becomes subhorizon scale, regions with $\delta > \delta_{th}$ gravitationally collapse and become PBHs.

Ex.) T. Harada, C.-M. Yoo and K. Kohri, Phys. Rev. D 88 (2013) 084051

Constraints on Curvature fluctuation

1. CMB μ distortion

:Non-zero chemical potential of CMB.

$\rightarrow$ density fluctuation generating PBH with

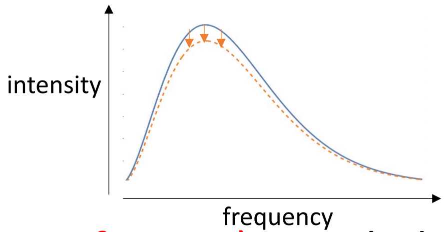

$O(10^4)M_{\odot} < M_{PBH} < O(10^9)M_{\odot}$ (← candidate of SMBH) is excluded.

Ex.) K. Kohri, T. Nakama and T. Suyama, Phys. Rev. D 90 (2014) 083514

2. Background GW

:Constrained by Pulsar-timing array experiments

$O(0.1)M_{\odot} < M_{PBH} < O(10)M_{\odot}$ is excluded.

Ex.) R. M. Shannon et al., Science 349 (2015) 1522-1525, L. Lentati et al., Mon. Not. Roy. Astron. Soc. 453 (2015) 2576–2598

Question: How do we explain LIGO-Virgo events or supermassive black holes by primordial black holes <u>without using curvature fluctuation?</u>

Question: How do we explain LIGO-Virgo events or supermassive black holes by primordial black holes without using curvature fluctuation?

Answer: Use physics of spherically collapsing nonlinear local objects whose distribution is independent of curvature fluctuation.

Question: How do we explain LIGO-Virgo events or supermassive black holes by primordial black holes without using curvature fluctuation?

Answer: Use physics of spherically collapsing nonlinear local objects whose distribution is independent of curvature fluctuation.

One idea: Inhomogeneous “Affleck-Dine baryogenesis/leptogenesis”.

Ex.) F.Hasegawa, M. Kawasaki, JCAP 01 (2019) 027

Today's Talk

- Introduction
- Motivation of our scenario
  - ▶ CMB μ-distortion
  - ▶ Second order GW
- Outline of our scenario
  - ▶ Affleck-Dine mechanism
  - ▶ PBH from Affleck-Dine leptogenesis
  - ▶ PBH from L-balls
- Conclusion

Today's Talk

- Introduction
- Motivation of our scenario
  - ▶ Constraints on curvature fluctuation
- Outline of our scenario
  - ▶ Affleck-Dine mechanism
  - ▶ PBH from Affleck-Dine leptogenesis(L-balls)
  - ▶ Difficulties of Affleck-Dine baryogenesis scenario
- Future prospects
- Conclusion

Affleck-Dine mechanism

I. Affleck, M. Dine, *Nucl.Phys.B* 249 (1985) 361-380, M. Dine, L. Randoll, S. D. Thomas, *Nucl.Phys.B* 458 (1996) 291-326

$$V(\Phi) \simeq \underbrace{m_{3/2}^2|\Phi|^2 - cH^2|\Phi|^2}_{\text{Hubble induced term}} + \underbrace{|\lambda|^2 \frac{|\Phi|^{2(n-1)}}{M_P^{2n-6}}}_{\text{Non-renormalizable term}} + \underbrace{\left(\lambda a_M \frac{m_{3/2}\Phi^n}{nM_P^{n-3}} + h.c.\right)}_{\text{A term}}$$

Φ: Affleck-Dine field(carrying lepton number)

$m_{3/2}$: Gravitino mass

Lepton number: $n_L = i\left(\Phi^*\dot{\Phi} - \dot{\Phi}^*\Phi\right) \simeq \dot{\theta}|\Phi|^2$

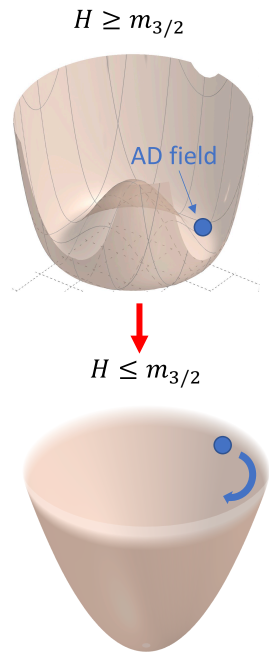

When $H \leq m_{3/2}$, the AD field is kicked in the phase direction by A term.

Then non-zero lepton number is generated.

PBH from Affleck-Dine mechanism

F.Hasegawa, M. Kawasaki (2019)

During Inflation

$$V(\Phi) = \left(m_\Phi^2 + c_I H^2\right)|\Phi|^2 + V_{NR} + V_A$$

After Inflation

$$V(\Phi) = \left(m_\Phi^2 - c_M H^2\right)|\Phi|^2 + V_{NR} + V_A + V_T(\Phi)$$

$V_T(\Phi)$: Thermal potential

Affleck-Dine mechanism

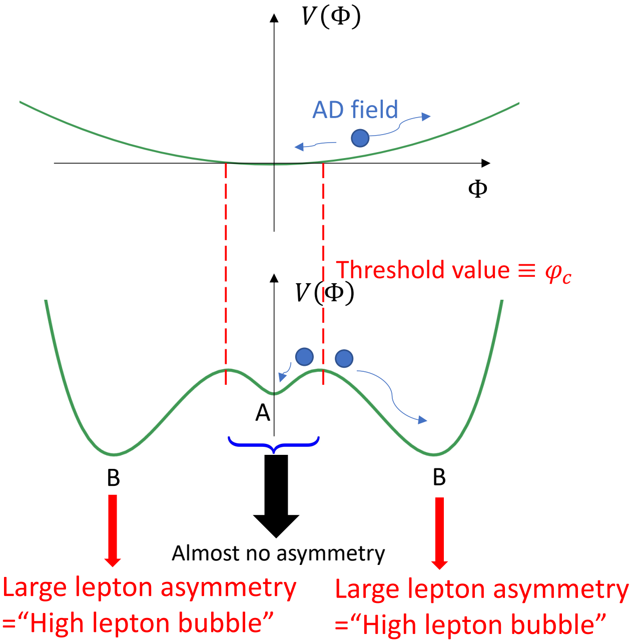

L-ball Scenario: 1.Outline

Figure: T. Hiramatsu, M. Kawasaki, F. Takahashi, JCAP 06 (2010) 008

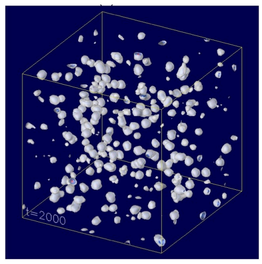

Coherent AD field oscillation (AD mechanism)

↓ (@ each high lepton bubble)

L-ball formation

L-ball(Q-ball):

$V(\Phi)$: $U(1)$ symmetric

$$\min\left(\frac{V(\Phi)}{|\Phi|^2}\right)_{|\Phi|\neq 0} < \lim_{|\Phi|\to 0}\left(\frac{V(\Phi)}{|\Phi|^2}\right)$$

→Spherically symmetric field configuration is most stable with fixed U(1) charge (: Q-ball)

In the case with lepton charge: “L-ball”

L-ball Scenario: 1.Outline

- L-balls aggregate and gravitationally collapse into PBH.

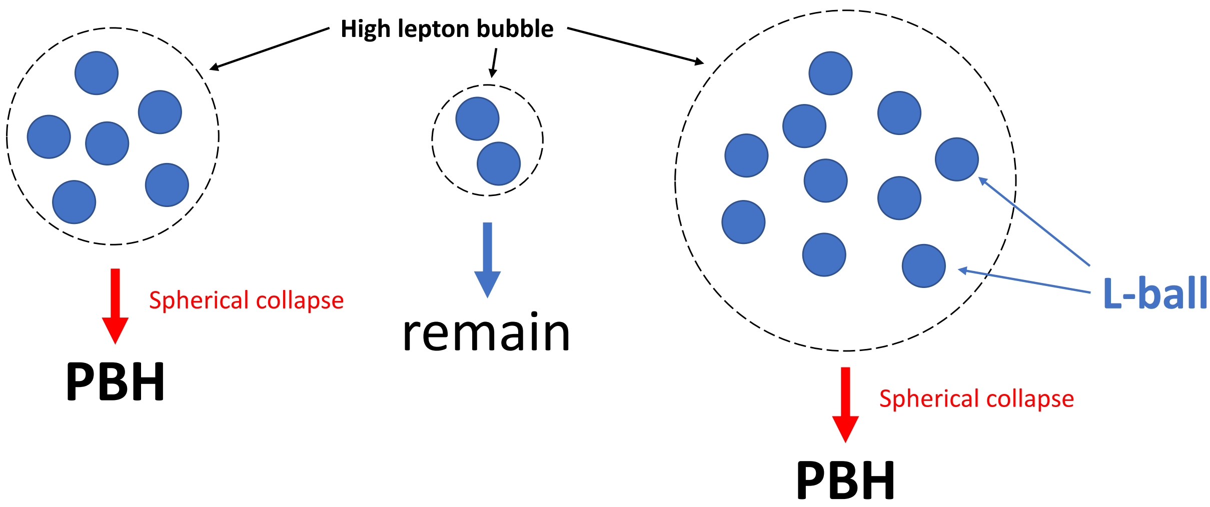

PBH from AD leptogenesis: Mass distribution

- LIGO-Virgo event

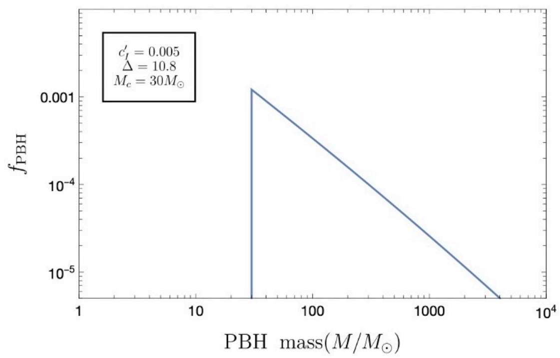

$f_{PBH} \simeq 1.1\times10^{-3}$

- Supermassive black hole

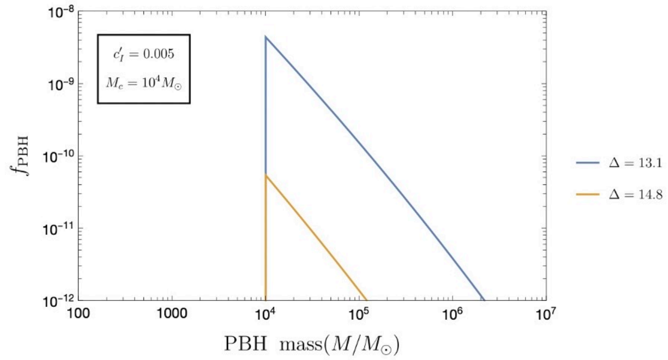

$f_{PBH} \simeq 3.1\times10^{-9}$(Blue), 3.5×10^{-11}(Orange)

L-ball scenario: 2. parameter space

L-balls decay and non-thermal neutrinos are emitted due to

$\phi\phi \rightarrow \nu\nu$ (Gaugino exchange) process.

→effects on effective number of neutrino species

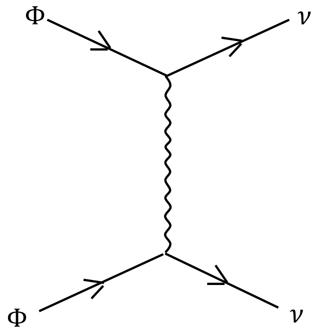

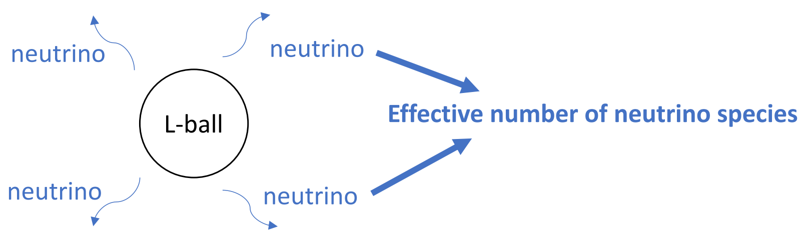

L-ball scenario: 2. parameter space

- LIGO-Virgo event

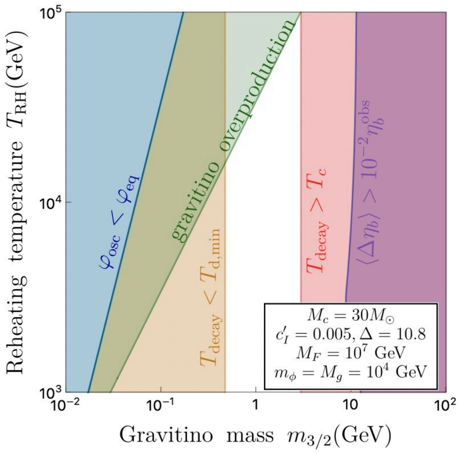

- Supermassive black hole

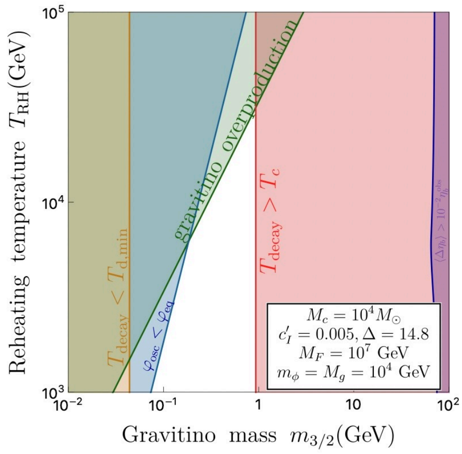

Today's Talk

- Introduction
- Motivation of our scenario
  - ▶ Constraints on curvature fluctuation
- Outline of our scenario
  - ▶ Affleck-Dine mechanism
  - ▶ PBH from Affleck-Dine leptogenesis(L-balls)
  - ▶ Difficulties of Affleck-Dine baryogenesis scenario
- Conclusion

Conclusion

- Supermassive black holes and LIGO-Virgo events can be explained by PBH using imhomogeneous Affleck-Dine leptogenesis.
- On the other hand, AD baryogenesis scenario is severely constrained by locally remaining too large baryon asymmetry.

Future prospects

This model shows strong clustering of high lepton bubbles.

(In the case of baryogenesis→ M. Kawasaki, K. Murai, H. Nakatsuka *JCAP* 10 (2021) 025)

→ This can change
- Calculation of PBH merger rate
- Constraints from CMB anisotropy spectrum

B. J. Carr, Kazunori Kohri, Yuuiti Sendouda, and Jun'ichi Yokoyama
Phys. Rev. D 81, 104019

and can also affect isocurvature perturbation.

→ We MUST further discuss clustering of high lepton bubbles and observational effects.

Generalized disformal Horndeski theories: cosmological perturbations and consistent matter coupling

Kazufumi Takahashi
(YITP, Kyoto U.)

Based on

- K. Takahashi, H. Motohashi, M. Minamitsuji, *Phys. Rev. D* 105, 024015 (2022) [arXiv: 2111.11634]
- K. Takahashi, M. Minamitsuji, H. Motohashi, arXiv: 2209.02176

Scalar-tensor theories

$$S[g,\phi] = \int \mathrm{d}^4x \sqrt{-g}\, \mathcal{L}(g, \partial g, \partial^2 g, \cdots; \phi, \partial\phi, \partial^2\phi, \cdots)$$

- Simple extension of GR, useful framework for cosmology/BHs
- Have a relatively long history
- Jordan (1955), Brans-Dicke (1961)
- Horndeski (1974) [rediscovered as Generalized Galileons (2011)]
  = The most general class of scalar-tensor theories with
  2nd-order Euler-Lagrange equations in 4D
  (No Ostrogradsky ghost associated with higher derivatives)
- DHOST [Degenerate Higher-Order Scalar-Tensor] (2015–2016)
  ⋯ known broadest class of ghost-free scalar-tensor theories so far

➢ Scalar-tensor theories

$$S[g,\phi] = \int \mathrm{d}^4x\,\sqrt{-g}\,\mathcal{L}(g,\partial g,\partial^2 g,\cdots;\phi,\partial\phi,\partial^2\phi,\cdots)$$

- Simple extension of GR, useful framework for cosmology/BHs
- Have a relatively long history
  - Jordan (1955), Brans-Dicke (1961)
  - Horndeski (1974) [rediscovered as Generalized Galileons (2011)]
    = The most general class of scalar-tensor theories with
    2nd-order Euler-Lagrange equations in 4D
    (No Ostrogradsky ghost associated with higher derivatives)
  - DHOST [Degenerate Higher-Order Scalar-Tensor] (2015–2016)
  - Generalized Disformal Horndeski [KT, Minamitsuji, Motohashi (2022)]
    ✓Novel class of ghost-free theories including known DHOST
    ✓Obtained by acting "generalized disformal trnsf." on Horndeski

➢ Disformal transformations

- Disformal transformation: field redefinition in scalar-tensor theories

$$(g_{\mu\nu},\phi) \mapsto (\bar{g}_{\mu\nu},\phi)$$

The most general trnsf. up to $\partial\phi$ (and without ∂g) is given by

$$\bar{g}_{\mu\nu} = F_0(\phi,X)g_{\mu\nu} + F_1(\phi,X)\nabla_\mu\phi\nabla_\nu\phi \quad (X \coloneqq g^{\alpha\beta}\nabla_\alpha\phi\nabla_\beta\phi)$$

✓Generalization of conformal transformations ($\bar{g}_{\mu\nu} \propto g_{\mu\nu}$)

✓The transformation is invertible in general.

$$g_{\mu\nu} = \frac{1}{F_0(\phi,X)}\left[\bar{g}_{\mu\nu} - F_1(\phi,X)\nabla_\mu\phi\nabla_\nu\phi\right]$$

with $X = X(\phi,\bar{X})$ determined from

$$\bar{X} = \frac{X}{F_0(\phi,X) + XF_1(\phi,X)}$$

so that we have $g_{\mu\nu} = g_{\mu\nu}[\bar{g},\phi]$ (at least locally).

➢ Disformal transformation of ST theories

$$S_{\rm old}[g_{\mu\nu},\phi] \mapsto S_{\rm old}[\bar{g}_{\mu\nu},\phi] =: S_{\rm new}[g_{\mu\nu},\phi]$$

■ # of DOFs is invariant under invertible transformations. [Domènech+ (2015)] [KT+ (2017)]

➢ A ghost-free theory maps to another (possibly new) ghost-free theory.

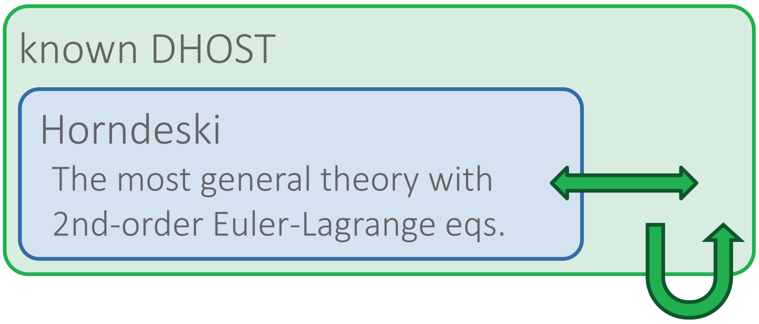

"➡" denotes disformal trnsf.

☐ More general ghost-free theory from more general transformations?

✓ We developed "generalized disformal transformation" [KT+ (2021)]

✓ Constructed a novel class of ghost-free theories [KT+ (2022)]

➢ Disformal trnsf. with higher derivatives

■ "Generalized disformal transformation"

$$\bar{g}_{\mu\nu} = F_0(\phi,X,Y,Z)g_{\mu\nu} + F_1(\phi,X,Y,Z)\nabla_\mu\phi\nabla_\nu\phi$$
$$+2F_2(\phi,X,Y,Z)\nabla_{(\mu}\phi\nabla_{\nu)}X + F_3(\phi,X,Y,Z)\nabla_\mu X\nabla_\nu X \quad \ni \nabla\nabla\phi$$

with the dependence on

$$Y \coloneqq g^{\alpha\beta}\nabla_\alpha\phi\nabla_\beta X, \qquad Z \coloneqq g^{\alpha\beta}\nabla_\alpha X\nabla_\beta X \qquad \boxed{X \coloneqq \nabla_\alpha\phi\nabla^\alpha\phi}$$

✓ The most general trnsf. with ϕ, $\partial_\mu\phi$, and $\partial_\mu X$ ($\supset$ conventional trnsf.)

✓ The group structure under the functional composition is essential for specifying the invertibility condition [KT, Motohashi, Minamitsuji (2021)]

$$F_0 \neq 0, \quad \mathcal{F} \neq 0, \quad \bar{X}_Y = \bar{X}_Z = 0, \quad \bar{X}_X \neq 0, \quad \left|\frac{\partial(\bar{Y},\bar{Z})}{\partial(Y,Z)}\right| \neq 0$$

<u>NB</u> Free funcs: $\bar{X}(\phi,X)$ and $F_{0,1,2}(\phi,X,Y,Z)$ (F_3 is not independent)

➢ Generalized disformal Horndeski (1)

■Horndeski theories described by the action

$$G_\# = G_\#(\phi, X)$$
$$\phi_{\mu\nu} := \nabla_\mu \nabla_\nu \phi$$

$$S_{\mathrm{H}} = \int \mathrm{d}^4x\sqrt{-g}\,\Big[G_2 + G_3\Box\phi + G_4 R - 4G_{4X}g^{\alpha[\mu|}g^{\beta|\nu]}\phi_{\alpha\mu}\phi_{\beta\nu} + G_5 G^{\mu\nu}\phi_{\mu\nu} + 2G_{5X}g^{\alpha[\mu|}g^{\beta|\nu|}g^{\gamma|\lambda]}\phi_{\alpha\mu}\phi_{\beta\nu}\phi_{\gamma\lambda}\Big]$$

are mapped to new ghost-free theories.

= "Generalized Disformal Horndeski" theories ("GDH" for short)

■Transformation law for each building block:

- $\sqrt{-g} \to \sqrt{-\bar{g}} = \sqrt{-g}\,\mathcal{J}$
- $R_{\mu\nu} \to \bar{R}_{\mu\nu} = R_{\mu\nu} + 2\nabla_{[\alpha}C^{\alpha}{}_{\nu]\mu} + 2C^{\alpha}{}_{\beta[\alpha}C^{\beta}{}_{\nu]\mu}$
- $\nabla_\mu\nabla_\nu\phi \to \bar{\nabla}_\mu\bar{\nabla}_\nu\phi = \phi_{\mu\nu} - C^{\lambda}{}_{\mu\nu}\phi_\lambda$

$$\mathcal{J} := F_0[F_0^2 + F_0(XF_1 + 2YF_2 + ZF_3) + (Y^2 - XZ)(F_2^2 - F_1F_3)]^{1/2}$$
$$C^{\lambda}{}_{\mu\nu} := \bar{\Gamma}^{\lambda}_{\mu\nu} - \Gamma^{\lambda}_{\mu\nu} = \bar{g}^{\lambda\alpha}\left(\nabla_{(\mu}\bar{g}_{\nu)\alpha} - \frac{1}{2}\nabla_\alpha\bar{g}_{\mu\nu}\right) \ni \partial^3\phi$$

➢ Generalized disformal Horndeski (2)

■The action of GDH theories is written as

$$S_{\mathrm{GDH}}[g,\phi] := S_{\mathrm{H}}[\bar{g},\phi] = \int \mathrm{d}^4x\sqrt{-g}\,\mathcal{J}\sum_{I=2}^{5}\tilde{\mathcal{L}}_I[g,\phi]$$

$$G_I = G_I(\phi, \bar{X}(\phi, X))$$
$$\bar{g}^{\mu\nu} = \#g^{\mu\nu} + \#\phi^\mu\phi^\nu + \#\phi^{(\mu}X^{\nu)} + \#X^\mu X^\nu$$

$$\tilde{\mathcal{L}}_2 := G_2$$
$$\tilde{\mathcal{L}}_3 := G_3\bar{g}^{\mu\nu}(\phi_{\mu\nu} - C^{\rho}{}_{\mu\nu}\phi_\rho)$$
$$\tilde{\mathcal{L}}_4 := G_4\bar{g}^{\mu\nu}\left(R_{\mu\nu} - 2C^{\alpha}{}_{\beta[\alpha}C^{\beta}{}_{\nu]\mu}\right) - 2\left(G_{4\phi}\phi_\alpha + G_{4X}\bar{X}_\alpha\right)\bar{g}^{\mu[\nu}C^{\alpha]}{}_{\mu\nu} - 4G_{4X}\bar{g}^{\alpha[\mu|}\bar{g}^{\beta|\nu]}(\phi_{\alpha\mu} - C^{\sigma}{}_{\alpha\mu}\phi_\sigma)\left(\phi_{\beta\nu} - C^{\rho}{}_{\beta\nu}\phi_\rho\right)$$
$$\tilde{\mathcal{L}}_5 := G_5\left(\bar{g}^{\mu\lambda}\bar{g}^{\nu\sigma} - \frac{1}{2}\bar{g}^{\mu\nu}\bar{g}^{\lambda\sigma}\right)\left(\phi_{\mu\nu} - C^{\rho}{}_{\mu\nu}\phi_\rho\right)\left(R_{\lambda\sigma} + 2\nabla_{[\alpha}C^{\alpha}{}_{\sigma]\lambda} + 2C^{\alpha}{}_{\beta[\alpha}C^{\beta}{}_{\sigma]\lambda}\right) + 2G_{5X}\bar{g}^{\alpha[\mu|}\bar{g}^{\beta|\nu|}\bar{g}^{\gamma|\lambda]}(\phi_{\alpha\mu} - C^{\sigma}{}_{\alpha\mu}\phi_\sigma)\left(\phi_{\beta\nu} - C^{\rho}{}_{\beta\nu}\phi_\rho\right)\left(\phi_{\gamma\lambda} - C^{\eta}{}_{\gamma\lambda}\phi_\eta\right)$$

- Contains $\partial^3\phi$ through $C^{\lambda}{}_{\mu\nu} := \bar{\Gamma}^{\lambda}_{\mu\nu} - \Gamma^{\lambda}_{\mu\nu}$
- Free functions: $G_{2,3,4,5}(\phi, X)$, $\bar{X}(\phi, X)$, $F_{0,1,2}(\phi, X, Y, Z)$.

Horndeski generalized disformal trnsf.

➢ Theory space

■ Inclusion relation among ghost-free scalar-tensor theories

generalized disformal Horndeski (GDH): up to $\partial^3\phi$

$\mathcal{L} \ni G_{2,3,4,5}(\phi, X), \bar{X}(\phi, X), F_{0,1,2}(\phi, X, Y, Z)$

New!

disformal Horndeski (DH): up to $\partial^2\phi$

(quadratic DHOST ^{2}N-I + cubic DHOST ^{3}N-I)

$\mathcal{L} \ni G_{2,3,4,5}(\phi, X), F_{0,1}(\phi, X)$

Horndeski

$\mathcal{L} \ni G_{2,3,4,5}(\phi, X)$

quadratic/cubic DHOST

$\cap$ (disformal Horndeski)^c

No viable cosmology

■ For GDH theories to be phenomenologically viable, we studied

✓cosmological perturbations

✓consistency of matter coupling

➢ Cosmology in GDH theories

$$\bar{g}_{\mu\nu} = F_0 g_{\mu\nu} + F_1 \phi_\mu \phi_\nu + 2F_2 \phi_{(\mu} X_{\nu)} + F_3 X_\mu X_\nu$$

$F_\# = F_\#(\phi, X, Y, Z)$

■ Consider an FLRW background

$$g_{\mu\nu}\mathrm{d}x^\mu \mathrm{d}x^\nu = -N(t)^2\mathrm{d}t^2 + a(t)^2\delta_{ij}\mathrm{d}x^i\mathrm{d}x^j, \quad \phi = \phi(t)$$

On this background (=BG), we have

$$X_{\rm BG} = -\frac{\dot{\phi}^2}{N^2}, \quad Y_{\rm BG} = \frac{X_{\rm BG}\dot{X}_{\rm BG}}{\dot{\phi}}, \quad Z_{\rm BG} = \frac{Y_{\rm BG}^2}{X_{\rm BG}}$$

Y & Z are not independent at BG

■ Generalized disformal trnsf. is again an FLRW background

$$\bar{g}_{\mu\nu}\mathrm{d}x^\mu \mathrm{d}x^\nu = -\bar{N}(t)^2\mathrm{d}t^2 + \bar{a}(t)^2\delta_{ij}\mathrm{d}x^i\mathrm{d}x^j, \quad \phi = \phi(t)$$

with

$$\frac{\bar{N}^2}{N^2} \coloneqq \frac{X_{\rm BG}}{\bar{X}(\phi, X_{\rm BG})} = \frac{\mathcal{F}_{\rm BG}}{F_{0,\rm BG}}, \quad \bar{a} \coloneqq F_{0,\rm BG}^{1/2} a$$

$$\mathcal{F}_{\rm BG} \coloneqq F_{0,\rm BG}^2 + F_{0,\rm BG}\left(X_{\rm BG}F_{1,\rm BG} + 2Y_{\rm BG}F_{2,\rm BG} + Z_{\rm BG}F_{3,\rm BG}\right)$$

➤ GDH theories with $c_{\mathrm{GW}}^2 = 1$

$$\bar{g}_{\mu\nu} = F_0 g_{\mu\nu} + F_1 \phi_\mu \phi_\nu + 2F_2 \phi_{(\mu} X_{\nu)} + F_3 X_\mu X_\nu$$

$$F_\# = F_\#(\phi, X, Y, Z)$$

- When applied to (late-time) cosmology, one is mostly interested in theories with $c_{\mathrm{GW}}^2 = 1$ $\left(=: c_{\mathrm{light}}^2\right)$.

  NB $|c_{\mathrm{GW}} - c_{\mathrm{light}}| \lesssim 10^{-15}$ from the almost simultaneous detection of GW170817 & GRB 170817A

- In GDH theories with $G_5 = 0$, we have

$$c_{\mathrm{GW}}^2 = \frac{X G_4(\phi, \bar{X})}{\bar{X} F_0 [G_4(\phi, \bar{X}) - 2\bar{X} G_{4X}(\phi, \bar{X})]}$$

One can make $c_{\mathrm{GW}}^2 = 1$ by setting

$$F_0 = \frac{X G_4(\phi, \bar{X})}{\bar{X} [G_4(\phi, \bar{X}) - 2\bar{X} G_{4X}(\phi, \bar{X})]}$$

✓ The other functions remain arbitrary

- ☐ Also specified the stability conditions for tensor/scalar perturbations

➤ Consistent matter coupling (1)

- The gravitational sector $S_{\mathrm{g}}[g, \phi]$ of GDH (or any DHOST) theories has no Ostrogradsky ghost thanks to degeneracy conditions.

- When coupled to a matter $S_{\mathrm{m}}[g, \Psi]$, Ostrogradsky mode can revive.

✓ Let us study the condition for consistent matter coupling.

→ Useful to move to the "Horndeski frame":

$$S[g, \phi, \Psi] = S_{\mathrm{H}}[g, \phi] + S_{\mathrm{m}}[\bar{g}, \Psi]$$

- Under the unitary gauge $\phi = \phi(t)$, the dynamics of the system is governed by the metric variables (N, N_i, γ_{ij}) and matter (Ψ).

- N is an auxiliary field in $S_{\mathrm{H}}[g, \phi]$, but $S_{\mathrm{m}}[\bar{g}, \Psi]$ contains $\dot{N}$ in general through $\bar{g}$, which revives the Ostrogradsky mode.

  NB $\bar{g} \ni \nabla\nabla\phi \supset \Gamma \supset \dot{N}$

➢ Consistent matter coupling (2)

■ Invertible generalized disformal trnsf. w/o $\dot{N}$ at the nonlinear level:

$$\bar{g}_{\mu\nu} = F_0 g_{\mu\nu} + F_1 \phi_\mu \phi_\nu + 2F_2 \phi_{(\mu} X_{\nu)} + F_3 X_\mu X_\nu$$

where F_i's have the form

$$F_0 = F_0(\phi, X, W), \quad F_3 = F_3(\phi, X, W),$$

$$F_2 = h(\phi, X, W) - \frac{Y}{X} F_3(\phi, X, W),$$

$$F_1 = \frac{\mathcal{F} - Wh^2}{\bar{X}\mathcal{F}} - \frac{F_0}{X} - \frac{2Y}{X} h + \frac{Y^2}{X^2} F_3,$$

$$\boxed{W := Y^2 - XZ}$$

with $\mathcal{F} = (XF_0 - WF_3)/\bar{X}$.

✓ For the above metric, the matter coupling would be consistent at the nonlinear level on an arbitrary BG (under the unitary gauge)

See [Naruko, Saito, Tanahashi, Yamauchi (2022)] for a complementary study (degeneracy conditions in the presence of disformally coupled canonical scalar)

➢ Summary & ongoing/future works

■ Constructed "generalized disformal Horndeski" theories by invertible generalized disformal trnsf. of Horndeski theories

✓ Specified theories with $c_{\rm GW}^2 = 1$ on a cosmological BG

✓ Condition for consistent matter coupling

□ Ongoing/future works

- Consistency of matter coupling away from unitary gauge and/or in the presence of fermions
  [Ikeda, KT, Kobayashi, in prep.] [KT, Kimura, Motohashi, in prep.]
- Embedding GDH theories into EFT of inflation/DE
  [KT, Minamitsuji, Motohashi, in prep.]

and more (CMB constraints, screening mechanism, ⋯)

UV divergence in DHOST & Its Renormalization by EFTofLSS

T. Fujita (Waseda IAS)

With S. Hirano [arXiv:2210.00772]

Executive Summary

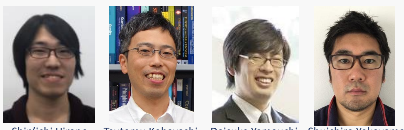

Shin'ichi Hirano Tsutomu Kobayashi Daisuke Yamauchi Shuichiro Yokoyama

$$P_\delta^{\mathrm{DHOST}} = \infty$$

Matter power spectrum in DHOST theory has a UV divergence

⇨ DHOST died?

Sin-Itiro Tomonaga Julian Schwinger Richard P. Feynman

$$\infty + \mathrm{Counterterm} = \mathrm{Finite}$$

Don't worry. UV divergence can be renormalized!

⇨ Physics converges

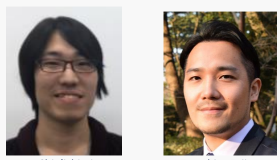

Shin'ichi Hirano Tomohiro Fujita

$$P_\delta^{\mathrm{DHOST}} = \mathrm{Finite}(C_2)$$

Counterterms in DHOST(& MG) can be found in EFTofLSS

⇨ Renormalized P_δ testable by Obs

Executive Summary

Q

What's EFTofLSS?

How to renormalize P_δ?

Why did P_δ diverge?


Shin'ichi Hirano


Tomohiro Fujita

$$P_\delta^{\mathrm{DHOST}}$$
$$= \mathrm{Finite}(C_2)$$

Counterterms in DHOST(& MG) can be found in EFTofLSS

⇨ Renormalized P_δ testable by Obs

Outline

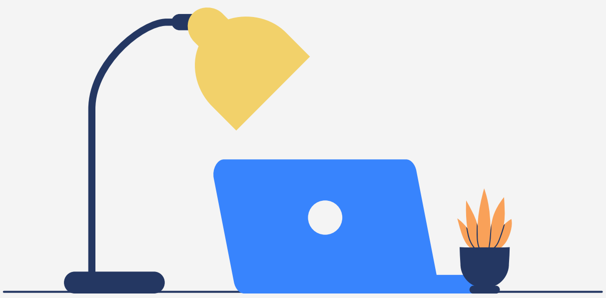

1. Introduction of LSS
2. EFTofLSS in GR
3. EFTofLSS in MG
4. Summary

Outline

1. Introduction of LSS
2. EFTofLSS in GR
3. EFTofLSS in MG
4. Summary

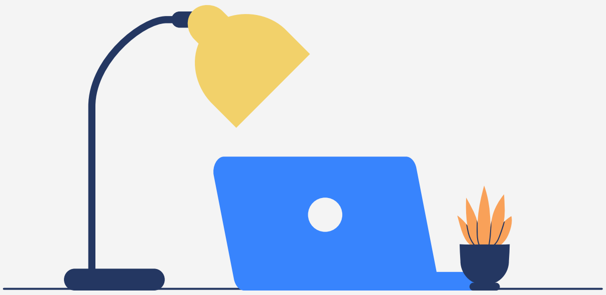

LSS in a nutshell

We know the initial condition of our universe from inflation theory or CMB obs.
e.g. primordial non-gaussianity f_{NL}

Solving the evolution of DM density fluctuation δ, one can calculate e.g. $P_{\delta\delta}$
Modified gravity, DE models
N-body, perturbation

Comparing them with LSS observations, we extract physical information
Constraints on MG, f_{NL}, w, m_ν, etc..

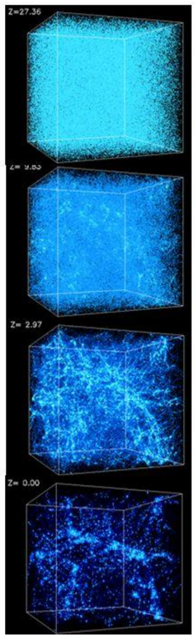

Many survey projects

We'll get unprecedent amount of data

Forecast : O(1)% precision in the growth rate

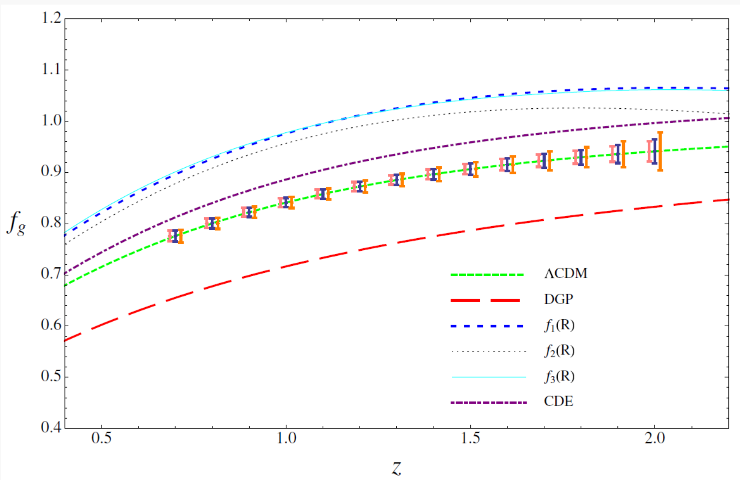

REVIEW ARTICLE

Cosmology and fundamental physics with the Euclid satellite

Luca Amendola[1] · Stephen Appleby[2] · Anastasios Avgoustidis[3] · David Bacon[4] · Tessa Baker[5] · Marco Baldi[6,7,8] · Nicola Bartolo[9,10,11] ·

z	f_g^F	σ_{f_g}		
		Ref.	Opt.	Pess.
0.7	0.76	0.011	0.010	0.012
0.8	0.80	0.010	0.009	0.011
0.9	0.82	0.009	0.009	0.011
1.0	0.84	0.009	0.008	0.011
1.1	0.86	0.009	0.008	0.011
1.2	0.87	0.009	0.009	0.011
1.3	0.88	0.010	0.009	0.012
1.4	0.89	0.010	0.009	0.013
1.5	0.91	0.011	0.010	0.014
1.6	0.91	0.012	0.011	0.016
1.7	0.92	0.014	0.012	0.018
1.8	0.93	0.014	0.013	0.019
1.9	0.93	0.017	0.015	0.025
2.0	0.94	0.023	0.019	0.037

Non-linear Calculation

- **In linearized cases,** $P_\delta^{\mathrm{DHOST}}(k) \propto P_\delta^{\mathrm{GR}}(k)$

  Only overall factor differs. Difficult to distinguish theories...

Non-linear Calculation

- **In linearized cases,** $P_\delta^{\mathrm{DHOST}}(k) \propto P_\delta^{\mathrm{GR}}(k)$

  Only overall factor differs. Difficult to distinguish theories...

- **Non-linear contributions are important**

  $\delta_{\boldsymbol{k}} = \underbrace{\delta_{\boldsymbol{k}}^{[1]}}_{\text{Linear}} + \underbrace{\delta_{\boldsymbol{k}}^{[2]} + \delta_{\boldsymbol{k}}^{[3]} + \cdots}_{\text{Non-linear}}$ in perturbative calculation.

$$P_\delta(t,k) \propto \langle \delta_{\boldsymbol{k}} \delta_{\boldsymbol{k}'} \rangle \simeq \left\langle \underbrace{\delta_{\boldsymbol{k}}^{[1]} \delta_{\boldsymbol{k}'}^{[1]}}_{\text{Linear}} + \underbrace{\delta_{\boldsymbol{k}}^{[2]} \delta_{\boldsymbol{k}'}^{[2]} + \delta_{\boldsymbol{k}}^{[1]} \delta_{\boldsymbol{k}'}^{[3]} + \delta_{\boldsymbol{k}}^{[3]} \delta_{\boldsymbol{k}'}^{[1]}}_{\text{1-loop contributions}} \right\rangle$$

$$\cancel{\propto} P_\delta^{\mathrm{GR}}(k)$$

Non-linear Calculation

- **In linearized cases,** $P_\delta^{\mathrm{DHOST}}(k) \propto P_\delta^{\mathrm{GR}}(k)$

  Only overall factor differs. Difficult to distinguish theories...

- **Non-linear contributions are important**

$$\delta_{\boldsymbol{k}} = \underbrace{\delta_{\boldsymbol{k}}^{[1]}}_{\text{Linear}} + \underbrace{\delta_{\boldsymbol{k}}^{[2]} + \delta_{\boldsymbol{k}}^{[3]} + \cdots}_{\text{Non-linear}}$$

perturbation in δ_k itself.

$$P_{\delta\delta}(t,k) \propto \langle \delta_{\boldsymbol{k}} \delta_{\boldsymbol{k}'} \rangle \simeq \left\langle \underbrace{\delta_{\boldsymbol{k}}^{[1]} \delta_{\boldsymbol{k}'}^{[1]}}_{\text{Linear}} + \underbrace{\delta_{\boldsymbol{k}}^{[2]} \delta_{\boldsymbol{k}'}^{[2]} + \delta_{\boldsymbol{k}}^{[1]} \delta_{\boldsymbol{k}'}^{[3]} + \delta_{\boldsymbol{k}}^{[3]} \delta_{\boldsymbol{k}'}^{[1]}}_{\text{1-loop contributions}} \right\rangle$$

$$= P_\delta^{\mathrm{1loop}}(k) \overset{?}{=} \infty$$

Outline

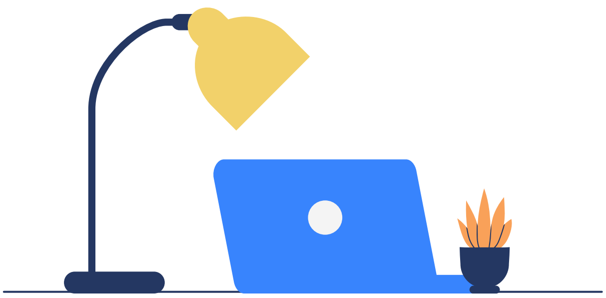

1. **Introduction of LSS**
2. **EFTofLSS in GR**
3. **EFTofLSS in MG**
4. **Summary**

Problem of Perturbative LSS

- **Standard calc.(SPT)**

  Perturbation of δ_k $(\ll 1)$

- $\boldsymbol{\delta_k \gtrsim 1}$ **for** $\boldsymbol{k \gtrsim 1\mathrm{Mpc}^{-1}}$

  Perturbation breaks down!

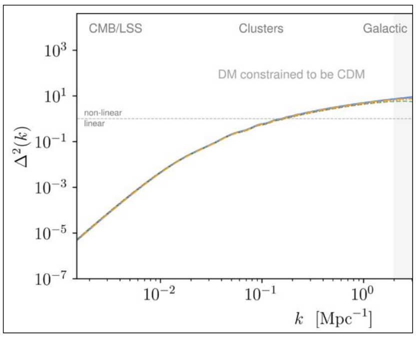

Ferreira (2021)
2005.03254

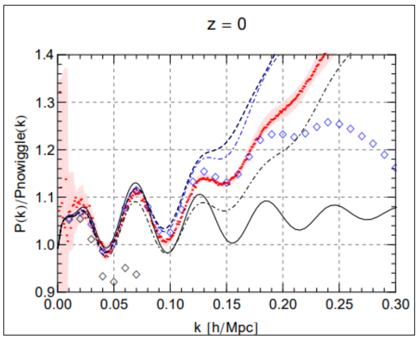

Blas+(2013)
1309.3308

Problem of Perturbative LSS

- **Standard calc.(SPT)**

  Perturbation of δ_k $(\ll 1)$

- $\boldsymbol{\delta_k \gtrsim 1}$ **for** $\boldsymbol{k \gtrsim 1\mathrm{Mpc}^{-1}}$

  Perturbation breaks down!

  resolution

- **EFT for** $\boldsymbol{\delta_k}$
  with $\boldsymbol{k < \Lambda \ll 1\mathrm{Mpc}^{-1}}$

  $\Rightarrow$ Always $\delta_k < 1$
  thus perturbation converges.

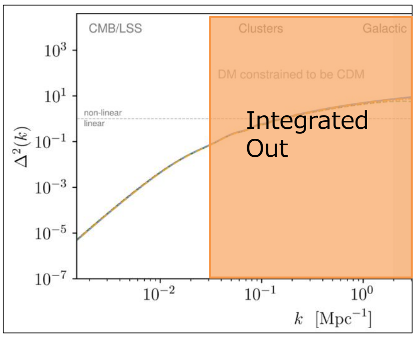

Ferreira (2021)
2005.03254

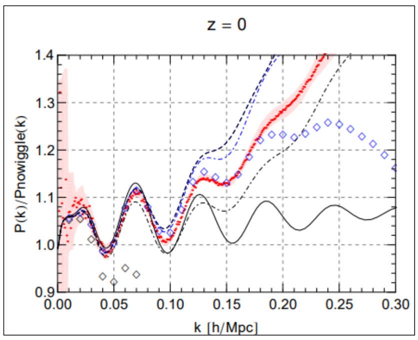

Blas+(2013)
1309.3308

Counterterms of EFT in GR

- **Integrate short modes**

  $\delta = \delta_L(k < \Lambda) + \delta_S(k > \Lambda)$, $\quad \boldsymbol{v} = \boldsymbol{v}_L + \boldsymbol{v}_S$

  integrate out δ_S and $\boldsymbol{v}_S$ to obtain EFT

- **Euler eq. has a NL term**

  $a^{-1}\partial_\eta(av^i) + \underline{v^j\partial_j v^i} = -\partial^i\Phi$

  $\rightarrow v_L^j\partial_j v_L^i + \underbrace{v_S^j\partial_j v_S^i}_{\text{Linear } v_L \text{ term}}$

$\nabla \cdot \boldsymbol{v} \propto \delta$ at linear

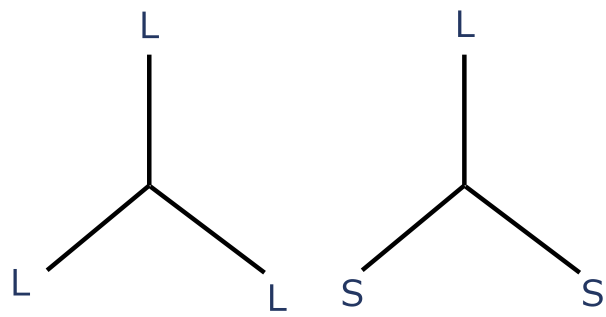

Counterterms of EFT in GR

- **Integrate short modes**

  $\delta = \delta_L(k < \Lambda) + \delta_S(k > \Lambda)$, $\quad \boldsymbol{v} = \boldsymbol{v}_L + \boldsymbol{v}_S$

  integrate out δ_S and $\boldsymbol{v}_S$ to obtain EFT

- **Euler eq. has a NL term**

  $a^{-1}\partial_\eta(av^i) + \underline{v^j\partial_j v^i} = -\partial^i\Phi$

  $\rightarrow v_L^j\partial_j v_L^i + \underbrace{v_S^j\partial_j v_S^i}_{\text{Linear } v_L \text{ term}}$

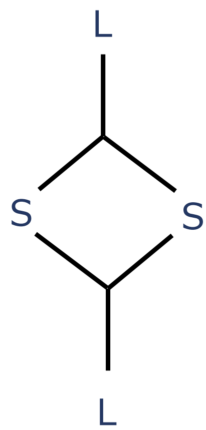

Counterterms of EFT in GR

- **Integrate short modes**

  $\delta = \delta_L(k < \Lambda) + \delta_S(k > \Lambda), \qquad \boldsymbol{v} = \boldsymbol{v}_L + \boldsymbol{v}_S$

  integrate out δ_S and $\boldsymbol{v}_S$ to obtain EFT

- **Euler eq. has a NL term**

  $a^{-1}\partial_\eta(av^i) + \underline{v^j\partial_j v^i} = -\partial^i\Phi$

  $\longrightarrow v_L^j\partial_j v_L^i + \underline{v_S^j\partial_j v_S^i}$

  Linear v_L term

- **All possible allowed terms**

  $v_S^j\partial_j v_S^i \to \partial_j\left(\boldsymbol{c_s^2}\delta_L - \boldsymbol{c_{bv}^2}\partial_k v_L^k\right)\delta^{ij}$ ⟵ Free parameters

  $+\partial_j \boldsymbol{c_{sv}^2}\left(\partial^i v_L^j + \partial^j v_L^i - \frac{2}{3}\partial_k v_L^k \delta^{ij}\right)$

EFT Power Spectrum in GR

- **Standard case:** $P_\delta = P_{11} + P_{22}^{\mathrm{SPT}} + 2P_{13}^{\mathrm{SPT}}$

  EFT adds $2P_{13}^{\mathrm{EFT}}(k) = 2C_1(t,\Lambda)\underline{k^2P_{11}}$

  $C_1^2 = c_s^2 + (c_{sv}^2 + c_{bv}^2)f$

- **Without EFT, P_δ has a UV sensitivity.**

$$P_{13}^{\mathrm{SPT}}(k) \overset{\text{hard}}{\underset{\text{loop}}{\approx}} \frac{61}{1260\pi^2}\underline{k^2P_{11}}\int_{q\gg k}^{\infty} dq\, \underbrace{P_{11}(q)}_{\propto q^{-3}\ (q\,\gg\, k_{\mathrm{eq}})} \longrightarrow \text{Converge}$$

- **If $P_{11} \propto k^{-1}$, $P_\delta \sim \infty$ even in GR. EFT would fix it.**

$$P_{13} \approx \underline{k^2P_{11}}\Big[\underbrace{\#\int_{q\gg k}^{\infty} dq\, P_{11} + C_1}_{\text{renormalize}}\Big] = C_1^{\mathrm{ren}}\underline{k^2P_{11}}$$

$\boxed{P_{13}^{\mathrm{EFT}} \text{ has the RIGHT k-dep.}}$

Short summary of EFT in GR

- In EFTofLSS, a non-linear term yields new terms with free coefficients.
- UV-sensitivity (or divergence) is renormalized by counterterm with the correct k-dependence.

Outline

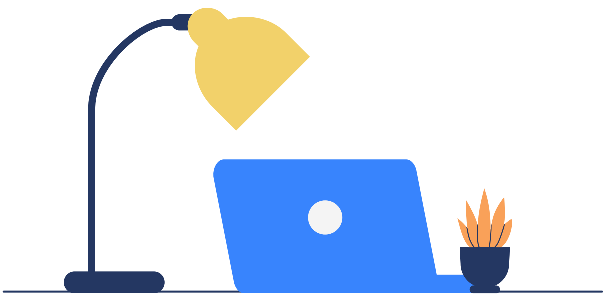

1. Introduction of LSS
2. EFTofLSS in GR
3. EFTofLSS in MG
4. Summary

New Non-linearity in MG

- **DHOST :** $P_{13}^{\mathrm{SPT}}(k) \underset{\text{loop}}{\overset{\text{hard}}{\approx}} \underbrace{Q_{13}}_{=0\text{ in GR}} P_{11} \int_{q\gg k}^{\infty} dq\, q^2 \underbrace{P_{11}}_{\propto q^{-3}\,(q\gg k_{\mathrm{eq}})}$ ⟶ **Log Div.**

- **Poisson eq. is modified in MG**

$$\partial^2\Phi + \underbrace{\sigma_{\Phi\gamma}\left[(\partial^2\Phi)^2 - \left(\partial_i\partial_j\Phi\right)^2\right] + \sigma_{\Phi\alpha}[(\partial^2\Phi)^2 + \partial_i\Phi\partial^2\partial_i\Phi]}_{} = \frac{3}{2}a^2H^2\Omega_m\delta$$

EFT ⟶ $\mathcal{O}(\Phi_L^2) + \underbrace{\mathcal{O}(\Phi_S^2)}_{}$ Linear Φ_L term

- **New terms from Φ_S^2:** $\mathcal{O}(\Phi_S^2) = c_2\partial^2\Phi_L + c_3\frac{\partial^2}{a^2\Lambda^2}\partial^2\Phi_L + \cdots$

Let's focus on c_2 term. c_3 yields the same P_{13} as c_1 in GR.

※ $\mathcal{O}(\Phi_S^2) \supset c_0\Phi\ (= m^2\Phi)$ may be relevant in e.g. Chameleon gravity.

Counterterm of EFT in MG

- $c_2\partial^2\Phi_L$ **leads to** $P_{13}^{c_2} = C_2(t,\Lambda)P_{11}$ $\boxed{\text{RIGHT k-dep.}}$

$P_{13}^{\mathrm{SPT}}(k) \approx Q_{13}P_{11}\int_{q\gg k}^{\infty} dq\, q^2 P_{11}$

- **Renormalization**

$$P_{13}^{\mathrm{SPT}}(k) \supset P_{11}\underbrace{\left[Q_{13}\int_{q\gg k}^{\Lambda} dq\, q^2 P_{11} + C_2\right]}_{\text{renormalize}} = C_2^{\mathrm{ren}}P_{11}$$

- **Result contains 2 parameters**

$$P_{\mathrm{1loop}}^{\mathrm{EFT}}(k) = P_{11} + P_{22}^{\mathrm{SPT}} + 2P_{13}^{\mathrm{ren}} + 2C_1^{\mathrm{ren}}P_{11} + 2C_2^{\mathrm{ren}}P_{11}$$

Requiring $P_{\mathrm{1loop}}^{\mathrm{EFT}} = P_{\mathrm{obs}}$ at $k = k_1^{\mathrm{ren}}\ \&\ k_2^{\mathrm{ren}}$, we fix $C_{1,2}^{\mathrm{ren}}$.

⟹ **DHOST can be tested by Obs** for $k \neq k_{1,2}^{\mathrm{ren}}$

Discussion on Screening

- Vainshtein Screening works for $k \geq k_{\rm scr}$ ➡ $Q_{13} = 0$ like GR

$$P_{13}^{\rm SPT}(k) \underset{\rm loop}{\overset{\rm hard}{\approx}} Q_{13} P_{11} \int_{q \gg k}^{\infty} dq\, q^2 P_{11} = Q_{13} P_{11} \int_{q \gg k}^{k_{\rm scr}} dq\, q^2 P_{11}$$

Converge

- This effect is overlooked in perturbative calc.
  Screening is non-linear effect ($k_{\rm scr} \sim k_{NL}$) ➡ Hard to include⋯

- EFT is agnostic to $k > k_{NL} > \Lambda$. No prediction of $P_{13}(q \gg k)$.
  ➡ Any new formalism??

- Horndeski never exhibits this UV divergence. Why??

Executive Summary

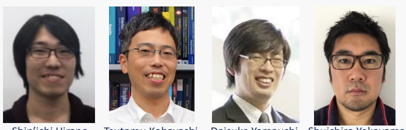

Shin'ichi Hirano Tsutomu Kobayashi Daisuke Yamauchi Shuichiro Yokoyama

$$P_\delta^{\rm DHOST} = \infty$$

Matter power spectrum in DHOST theory has a UV divergence

⇨ DHOST died?

Sin-Itiro Tomonaga Julian Schwinger Richard P. Feynman

$$\infty + \text{Counterterm}$$
$$= \text{Finite}$$

Don't worry.
UV divergence can be renormalized!

⇨ Physics converges

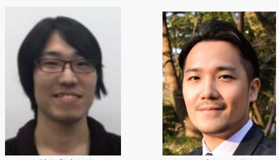

Shin'ichi Hirano Tomohiro Fujita

$$P_\delta^{\rm DHOST}$$
$$= \text{Finite}(C_2)$$

Counterterms in DHOST(& MG) can be found in EFTofLSS

⇨ Renormalized P_δ testable by Obs

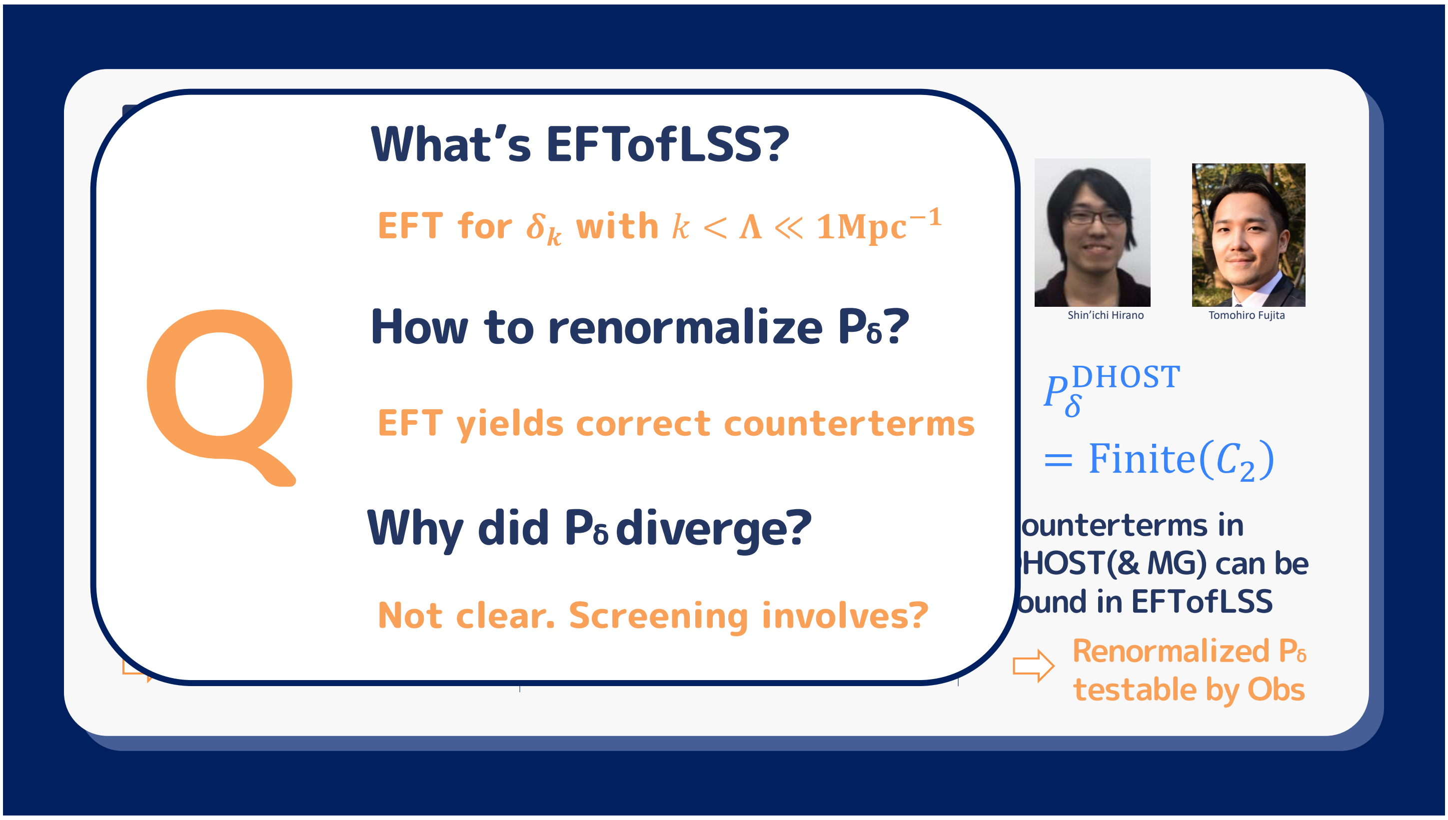
What's EFTofLSS?
EFT for δ_k with $k < \Lambda \ll 1\mathrm{Mpc}^{-1}$
Q
How to renormalize P_δ?
EFT yields correct counterterms
Why did P_δ diverge?
Not clear. Screening involves?
Shin'ichi Hirano
Tomohiro Fujita
$P_\delta^{\mathrm{DHOST}}$
$= \mathrm{Finite}(C_2)$
ounterterms in
HOST(& MG) can be
ound in EFTofLSS
Renormalized P_δ
testable by Obs

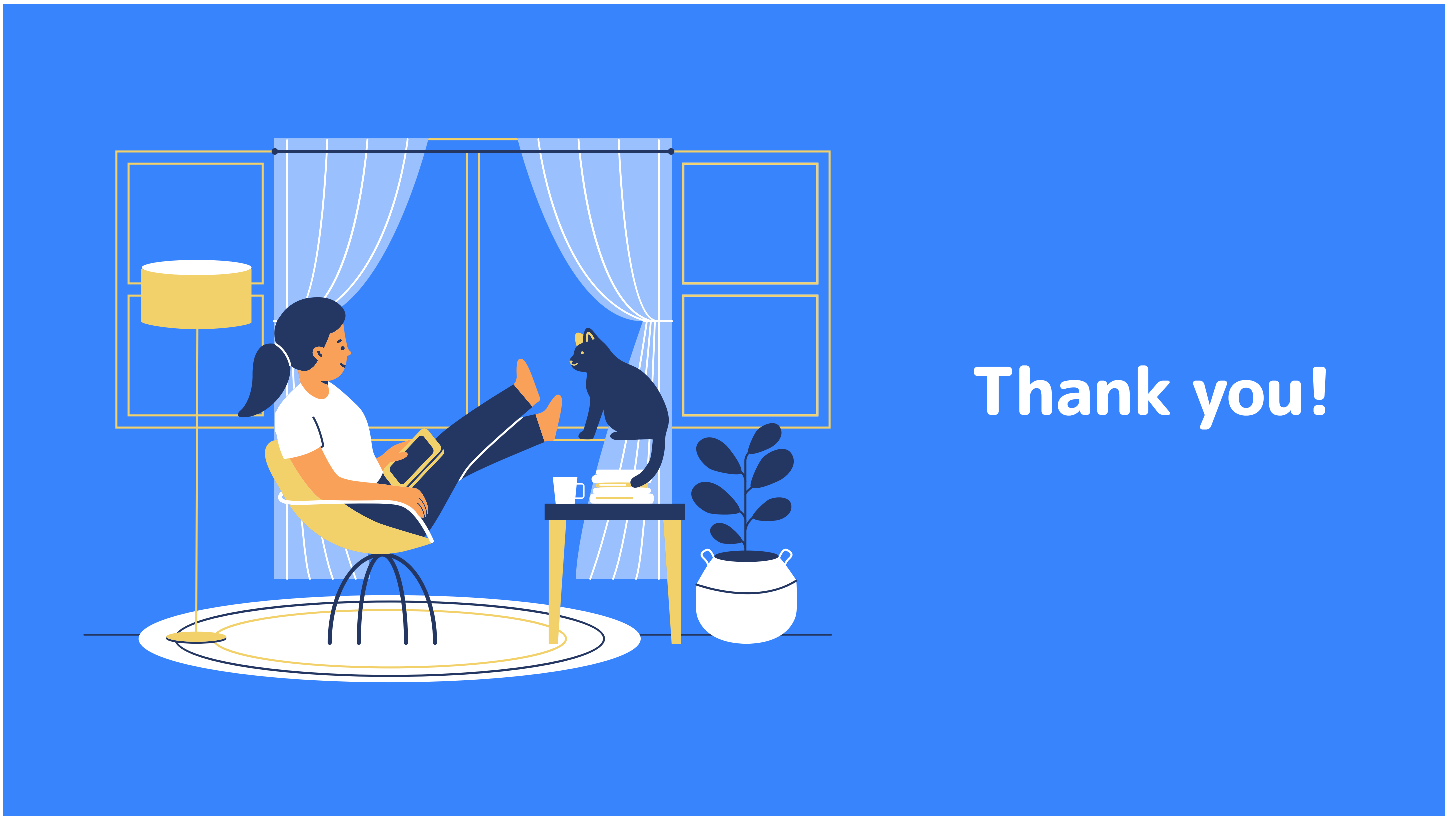
Thank you!

Any Question ?

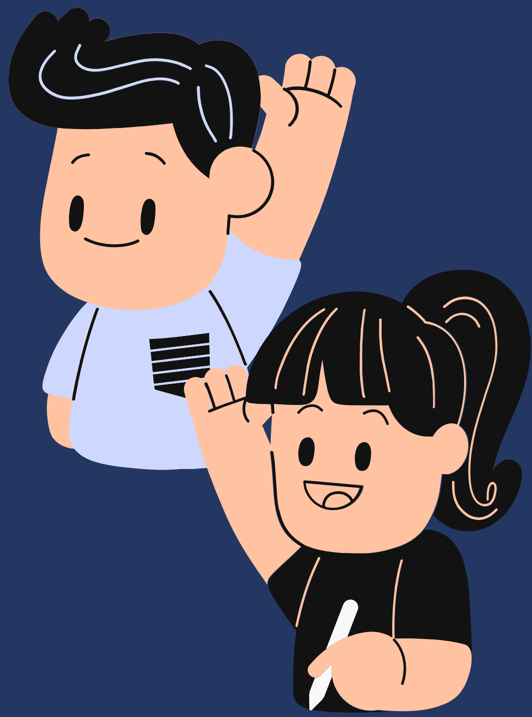

C15

At JGRG31, Oct. 24th, 2022

Revisiting TOV Problems in F(R) Gravity

Kota Numajiri (Nagoya Univ.)

Collaborators:
Yong–Xiang Cui (CCNU), Taishi Katsuragawa (CCNU),
Shin'ichi Nojiri (Nagoya U.)

Based on the upcoming paper [arXiv:2211.xxxxx]

Modified Gravity and Neutron Star

Present universe model with GR & SM still has several problems in wide range of energy-scale.

↓

Modified gravity theories can solve them or give hints!!

Probe: Neutron stars (NSs)

- Strong gravity due to its high compactness
- Many ways to observe (GWs, Pulsar X–ray, etc…)
  → **Good to test the deviation from GR!**

In theoretical point of view,

- **Background → TOV problem**
- (Static) perturbation → Tidal deformation
- Time evolution → Thermal evolution

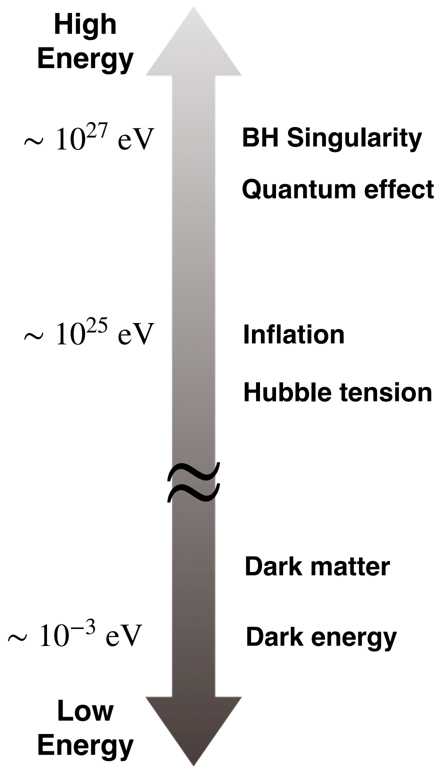

In the Previous Works

TOV problem in modified gravity has been discussed in many papers.
However **several uncleared points still exist.**

- **"Asymptotic solution" outside the star**
  "Asymptotically flat" was often assumed.
  → How do solutions become "flat"?

  E.g.) R^2 model of $F(R)$ gravity
  Exp. decay? [A. V. Astashenok+, 2018] etc…
  Power–law decay? [M. N. Callejas+, 2022] etc…
  Damping oscillation? [M. A. Resco+, 2016] etc…

- **Scalar profile inside the star**
  Scalar (=curvature) profile has not been well investigated so far.

Our Goal

Solve TOV problem in $F(R)$ gravity, paying attention on
- **Asymptotic behaviors of solutions**
- **Scalar = curvature profile**

$F(R)$ Gravity and R^2 Model

[A. A. Starobinsky, 1980] etc…

We consider $F(R)$ gravity theory that has 2+1 d.o.f. for the gravitational field.

$$\Phi \equiv F_R(R)(>0)$$
$$V(\Phi) \equiv R(\Phi)\Phi - F(\Phi)$$

Metric Description

Action: $S_F = \dfrac{1}{2\kappa^2}\displaystyle\int d^4x\sqrt{-g}F(R)$

Field equations:

$$F_R(R)R_{\mu\nu} - \frac{1}{2}F(R)g_{\mu\nu} - [\nabla_\mu\nabla_\nu - g_{\mu\nu}\Box]\,F_R(R) = \kappa^2 T_{\mu\nu}$$

Auxiliary equation:

$$F_R(R)R - 2F(R) + 3\Box F_R(R) = \kappa^2 T$$

ST Description

Action: $S_F = \dfrac{1}{2\kappa^2}\displaystyle\int d^4x\sqrt{-g}[\Phi R - V(\Phi)]$

Field equations:

$$G_{\mu\nu} = \frac{\kappa^2}{\Phi}T_{\mu\nu} + \frac{1}{\Phi}\left[\nabla_\mu\nabla_\nu\Phi - g_{\mu\nu}\left(\Box\Phi + \frac{1}{2}V\right)\right]$$

$$\Box\Phi = \frac{1}{3}\left[\Phi V'(\Phi) - 2V(\Phi) + \kappa^2 T\right]$$

To simplify and to compare with previous works, now we use **R^2 gravity.**

$$F(R) = R + \alpha R^2 \qquad \Rightarrow \qquad \Phi = F_R = 1 + 2\alpha R$$

Scalar profile can be easily read off as that of curvature.

Chameleon Mechanism in R^2 Gravity

[J. Khoury+, 2004]
[P. Brax+, 2008]
etc…

Scalar (= curvature) distribution is determined from **chameleon potential.**

→ This is helpful to understand the profile of scalar = curvature inside & outside stars.

$$\Box\Phi = \frac{\mathrm{d}V_{\mathrm{eff}}}{\mathrm{d}\Phi} = \left.\frac{\mathrm{d}V_{\mathrm{eff}}}{\mathrm{d}\Phi}\right|_{\Phi=\Phi_{\min}} + \left.\frac{\mathrm{d}^2V_{\mathrm{eff}}}{\mathrm{d}\Phi^2}\right|_{\Phi=\Phi_{\min}}(\Phi-\Phi_{\min}) + \cdots$$

$$\left.\frac{\mathrm{d}V_{\mathrm{eff}}}{\mathrm{d}\Phi}\right|_{\Phi=\Phi_{\min}} = \frac{1}{3}\left[R\left(\Phi_{\min}\right)+\kappa^2T\right] = \frac{1}{3}\left[\frac{\Phi_{\min}-1}{2\alpha}+\kappa^2T\right] = 0$$

Potential minimum corresponds to GR

$$\left.\frac{\mathrm{d}^2V_{\mathrm{eff}}}{\mathrm{d}\Phi^2}\right|_{\Phi=\Phi_{\min}} = \frac{1}{6\alpha} \equiv m_\Phi^2 \quad \Rightarrow \quad \alpha > 0$$

→ Curvature behaves as massive particle with $m_\Phi \sim \alpha^{-1/2}$

Decay exponentially for large r !!

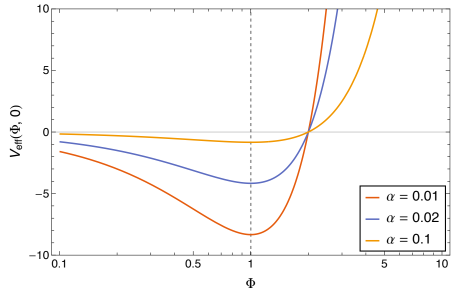

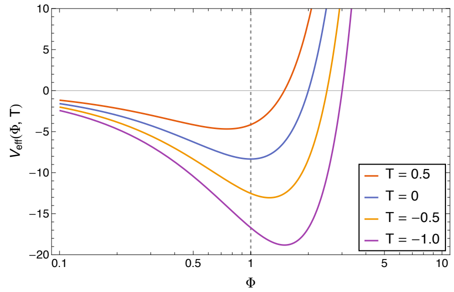

System and Equations to Solve

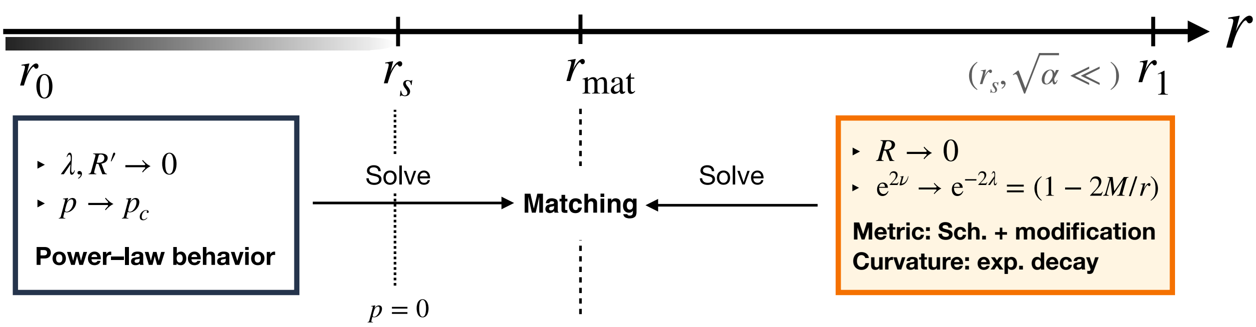

Equations to Solve

Sols.: $\lambda, \nu, R, p\ (\epsilon)$ with ansatz $ds^2 = -\mathrm{e}^{2\nu}dt^2 + \mathrm{e}^{2\lambda}dr^2 + r^2\Omega_{AB}dx^Adx^B$

Metric:

$$\lambda' = \frac{\mathrm{e}^{2\lambda}\left\{2\kappa^2r^2\epsilon + \alpha R(r^2R-4)-2\right\} + 4\alpha\left(r^2R''+2rR'+R\right)+2}{4r\left(\alpha(rR'+2R)+1\right)}$$

$$\nu' = \frac{\mathrm{e}^{2\lambda}\left\{2\kappa^2r^2p - \alpha R(r^2R-4)+2\right\} - 2\left(4\alpha rR'+2\alpha R+1\right)}{4r\left(\alpha(rR'+2R)+1\right)}$$

Curvature:
(= scalar eq.)

$$R'' = \frac{1+2\alpha R}{2\alpha}\left[\frac{1}{r}\left(3\nu'-\lambda'+\frac{2}{r}\right)+\mathrm{e}^{2\lambda}\left(\frac{1}{2}R-\frac{2}{r^2}\right)\right] + \left(\lambda'+\frac{1}{r}\right)R'$$

Matter:
(Perfect fluid)

$$p' = -\nu'\left(\epsilon+p\right) \qquad p = p(\epsilon)$$

Use tabulated SLy EOS. [J. S. Read+, 2009]

Asymptotic Conditions

Consider the asymptotic behaviors that are used for $r > r_2$.

Hint
- Conditions (**metric → Sch., curvature → 0**)
- Field equations
- **Relation** $R = \mathrm{e}^{-2\lambda}\left[-2\nu'' - 2(\nu' - \lambda')\nu' - \frac{4(\nu' - \lambda')}{r} + \frac{2\mathrm{e}^{2\lambda} - 2}{r^2}\right]$

→ Asymptotic forms are found as (C: constant, $K_1(x)$: modified Bessel func. of 2nd kind)

$$\lambda \sim -\frac{1}{2}\log\left(1 - \frac{2M}{r}\right) - 6\alpha C\, r\, K_1\left(\frac{r}{2\sqrt{\alpha}}\right)$$

correction

$$\nu \sim \frac{1}{2}\log\left(1 - \frac{2M}{r}\right) - 2\alpha C\, r\, K_1\left(\frac{r}{2\sqrt{\alpha}}\right)$$

Schwarzschild
+ exp. decaying correction

$$R \sim C\, r\, K_1\left(\frac{r}{2\sqrt{\alpha}}\right)$$

→ **Exp decay depending on $\sqrt{\alpha}$.**
Consistent with discussion on chameleon scalar.

Results – Geometrical Quantities

$\alpha = 1.0,$
$\rho_c = 10^{15.19}\ \mathrm{g/cm^3}$

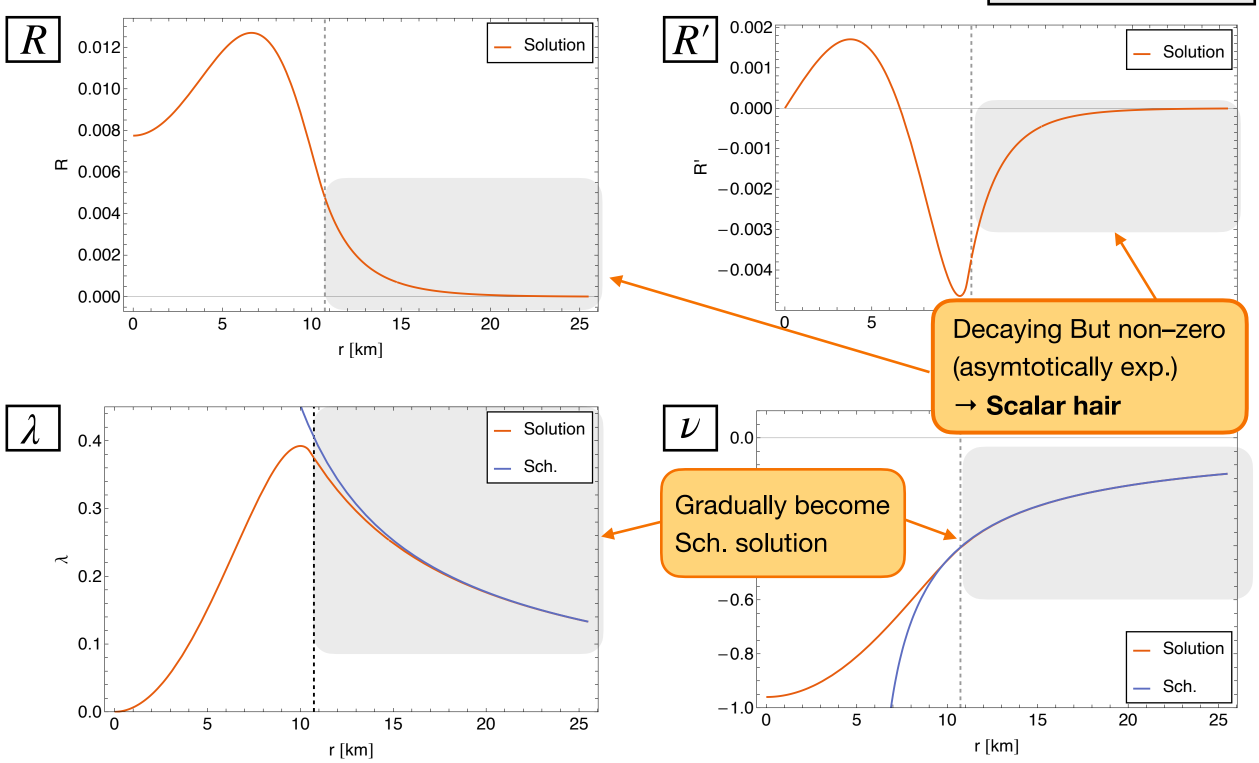

Results – Mass–Radius Relation

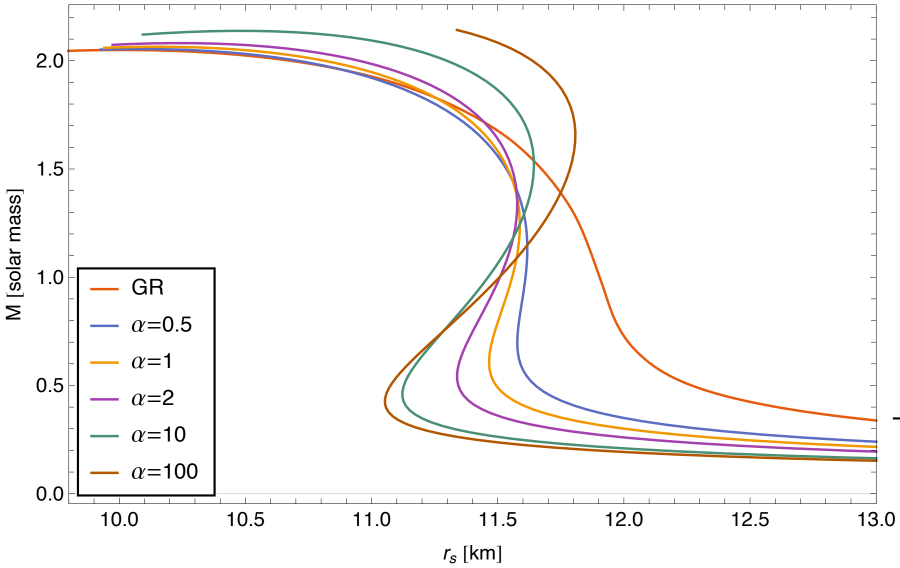

- Mass: Sch. mass at r_2
  Radius: Surface radius
- Curves "rotate clockwise" as α increases.
- Maximum mass increases about $\mathcal{O}(10^{-2} M_\odot)$ as α increases.

→ Consistent with prev. works.
[S. S. Yazadjiev+, 2014]
[A. V. Astashenok+, 2018]
Etc…

Results – Scalar Distribution

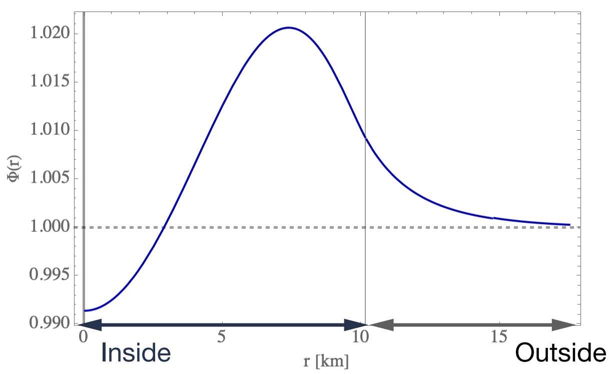

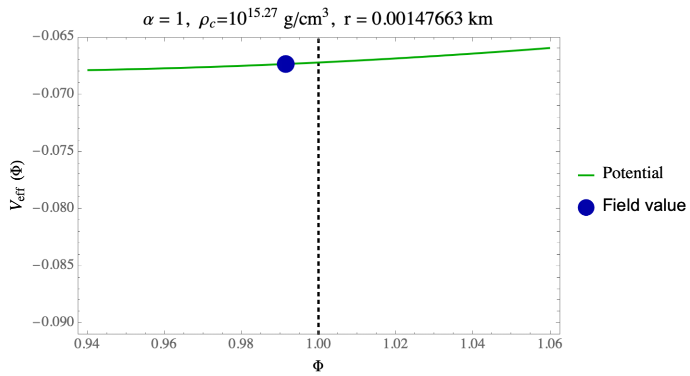

Scalar (=curvature) radial distribution can be understood from chameleon potential.
Scalar field "tries to get out" of the potential when it is traced from center.

$$\because \quad \Box\Phi = \frac{dV_{\mathrm{eff}}}{d\Phi} = m_\Phi^2(\Phi - \Phi_{\mathrm{min}}) \quad \text{where} \quad V_{\mathrm{eff}}(\Phi, T) = \frac{1}{12\alpha}\Phi\left(\Phi - 2 + 4\kappa^2\alpha T\right)$$

Now considering r dependence → metric: +

Results – Scalar Distribution

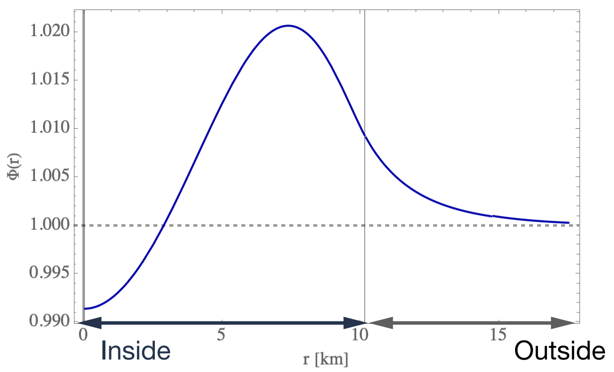

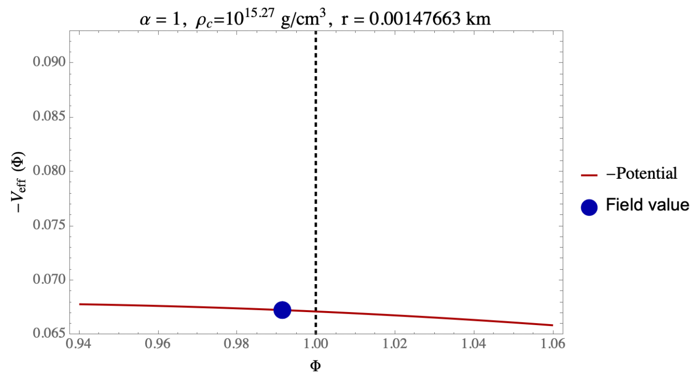

Scalar (=curvature) radial distribution can be understood from chameleon potential.

Scalar field "tries to get out" of the potential when it is traced from center.

$$\because \quad \Box\Phi = \frac{\mathrm{d}V_{\mathrm{eff}}}{\mathrm{d}\Phi} = m_\Phi^2(\Phi - \Phi_{\mathrm{min}}) \quad \text{where} \quad V_{\mathrm{eff}}(\Phi, T) = \frac{1}{12\alpha}\Phi\big(\Phi - 2 + 4\kappa^2\alpha T\big)$$

Now considering r dependence → metric: +

→ Radial distribution is **determined by $-V_{\mathrm{eff}}$** (concave func. now).
Asymp. flat sol is one that scalar gets to "potential maximum" for large r.

Summary

- We re–examined **TOV problem in R^2 gravity.**
- We especially focused on the **asymptotic behaviors** of solutions, and **scalar (=curvature) profile** including its effective potential (chameleon mechanism). These have not been well investigated.
- **By checking scalar effective mass**, the asymptotic solutions can be predicted. In other words, the calculated numerical solutions should be consistent with it.
- Radial distribution of scalar (=curvature) **is determined from sign–flipped chameleon potential.**

Future Work

- Other model of $F(R)$ gravity
  (now tackling on the non-integer power model, whose scalar is massless in vacuum.)
- Inverse–TOV problem
  (Reconstruction of IVs from the asymptotic solutions)

B–Slides

Chameleon Mechanism in R^2 Gravity

Jordan frame

$$V_{\text{eff}}(\Phi, T) = \frac{1}{12\alpha}\Phi\left(\Phi - 2 + 4\kappa^2\alpha T\right)$$

$$\left.\frac{\mathrm{d}^2 V_{\text{eff}}}{\mathrm{d}\Phi^2}\right|_{\Phi=\Phi_{\min}} = \frac{1}{6\alpha} \equiv m_\Phi^2$$

Constant anytime anywhere!

Einstein frame

$$U_{\text{eff}}(\tilde{\Phi}, T) = \frac{1}{8\kappa^2\alpha}\mathrm{e}^{-2\sqrt{\frac{2}{3}}\kappa\tilde{\Phi}}\left(2\,\mathrm{e}^{\sqrt{\frac{2}{3}}\kappa\tilde{\Phi}} - 1 + 2\kappa^2\alpha T\right)$$

$$m_{\tilde{\Phi}}^2 \equiv \left.\frac{\mathrm{d}^2 U_{\text{eff}}}{\mathrm{d}\tilde{\Phi}^2}\right|_{\tilde{\Phi}=\tilde{\Phi}_{\min}} = \frac{1}{6\alpha(1 - 2\kappa^2\alpha T)}$$

Depend on energy–momentum

→ It is up to frame whether mechanism works

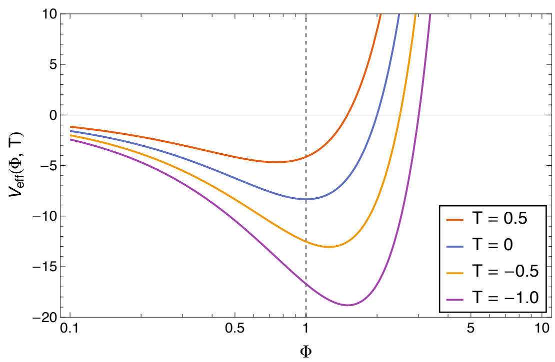

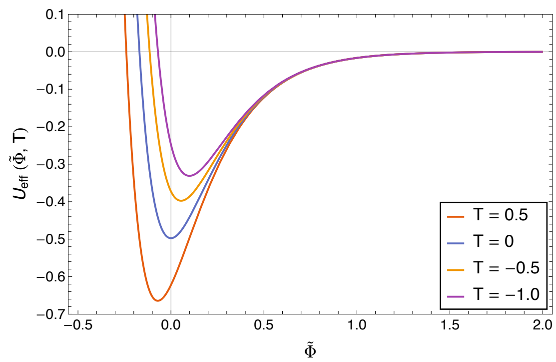

C16

Polarizations of gravitational waves in Palatini-Horndeski theory

Speaker: Yu-Qi Dong

With: Yu-Xiao Liu

Lanzhou University

2022.10.24

Y. Dong and Y. Liu, Phys. Rev. D 105, 064035 (2022) arXiv: 2111.07352

Content

- **1. Motivation**
- **2. Polarization modes**
- **3. Polarizations of Palatini-Horndeski theory**

Content

Why polarizations

The polarization modes allowed by various modified gravity theories are different [1].

Some of modified gravity could be excluded from the detection of polarization modes of gravitational waves in Lisa [2], Taiji [3] and TianQin [4] in the future.

[1] D. M. Eardley, D. L. Lee, and A. P. Lightman, Phys. Rev. D 8, 3308 (1973)
[2] P. Amaro-Seoane, et al. (LISA Team), arXiv:1702.00786
[3] Z. Luo, et al. , Prog. Theor. Exp. Phys. 2021, 05A108 (2021)
[4] J. Luo, et al., Classical Quantum Gravity 33, 035010 (2016)

Why Palatini-Horndeski theory

In 2021, a tentative indication for scalar transverse gravitational waves was reported [1].

In the metric formalism, the most general scalar-tensor theory that can obtain second-order field equations is Horndeski theory [2].

[1] Z. Chen, C. Yuan, and Q. Huang, Sci. China Phys. Mech. Astron. 64, 120412 (2021)
[2] G. W. Horndeski, Int. J Theor. Phys. 10, 363 (1974)

Action of Horndeski theory

$$S = \int d^4x\sqrt{-g}\left(\mathcal{L}_2+\mathcal{L}_3+\mathcal{L}_4+\mathcal{L}_5\right)$$

$$\begin{aligned}
\mathcal{L}_2 &= K(\phi, X),\\
\mathcal{L}_3 &= -G_3(\phi, X)\tilde{\Box}\phi,\\
\mathcal{L}_4 &= G_4(\phi, X)R + G_{4,X}(\phi, X)\left[\left(\tilde{\Box}\phi\right)^2 - \left(\nabla_\mu\nabla_\nu\phi\right)\left(\nabla^\mu\nabla^\nu\phi\right)\right],\\
\mathcal{L}_5 &= G_5(\phi, X)\left(R_{\mu\nu}-\frac{1}{2}g_{\mu\nu}R\right)\nabla^\mu\nabla^\nu\phi\\
&- \frac{1}{6}G_{5,X}(\phi, X)\left[\left(\tilde{\Box}\phi\right)^3 - 3\tilde{\Box}\phi\left(\nabla_\mu\nabla_\nu\phi\right)\left(\nabla^\mu\nabla^\nu\phi\right)\right.\\
&+ \left. 2\left(\nabla^\lambda\nabla_\rho\phi\right)\left(\nabla^\rho\nabla_\sigma\phi\right)\left(\nabla^\sigma\nabla_\lambda\phi\right)\right].
\end{aligned}$$

Where $\tilde{\Box} = \nabla^\mu\nabla_\mu$, $X = -\frac{1}{2}\nabla_\mu\phi\nabla^\mu\phi$。

GW 170817

GW170817 and GRB 170817A require that the speed of tensor mode gravitational wave is limited:

$$-3 \times 10^{-15} \leq \frac{c_{gw}}{c} - 1 \leq 7 \times 10^{-16}.$$

If in the FRW background, the speed of the tensor mode wave is c, then only

$$S = \int d^4x \sqrt{-g}\, [K(\phi, X) - G_3(\phi, X)\tilde{\Box}\phi + G_4(\phi)R]$$

meets the above condition.

[1] B. P. Abbottet et al. Astrophys. J. 848, L13 (2017); Phys. Rev. Lett. 123, 011102 (2019)
[2] P. Creminelli and F. Vernizzi, Phys. Rev. Lett. 119, 251302 (2017)

GW170817 / GRB 170817A severely constrain the possible parameter space of metric Horndeski theory.

Taking the Horndeski action in the Palatini formalism may be a way to beyond the metric Horndeski theory.

We consider the polarizations of gravitational waves in Palatini-Horndeski theory.

Content

- 1. Motivation
- 2. Polarization modes
- 3. Polarizations of Palatini-Horndeski theory

Consider

(1) weak gravitional field
(2) Minkowski background
(3) relative displacement η_μ of two test particles

$$\frac{d^2\eta_i}{dt^2} = -R_{i0j0}\eta^j \quad (\mathrm{i,j} = 1, 2, 3)$$

Gravitational Wave

$$R_{i0j0} = A\ \boxed{E_{ij}}\ e^{ikx}$$

polarization

Define $P_1, \dots, P_6$

$$E_{ij} = \begin{pmatrix} P_4 + P_6 & P_5 & P_2 \\ P_5 & -P_4 + P_6 & P_3 \\ P_2 & P_3 & P_1 \end{pmatrix}$$

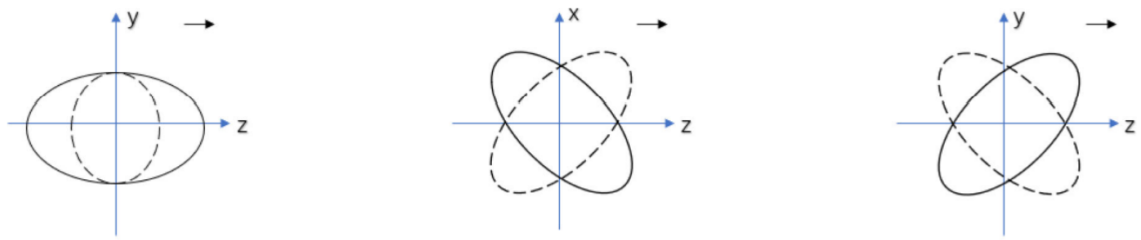

P_1: longitudinal mode **P_2: vector-x mode** **P_3: vector-y mode**

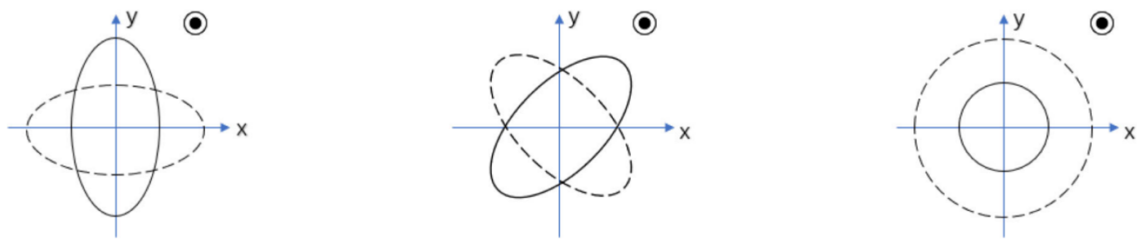

P_4: + mode **P_5: × mode** **P_6: breathing mode**

D. M. Eardley, D. L. Lee, and A. P. Lightman, Phys. Rev. D 8, 3308 (1973)

Polarizations of metric Horndeski theory

1. $+$ and $\times$ mode, speed is c

2. A mixed mode of breathing mode and longitudinal mode (when $\overset{0}{K}_{,\phi\phi} = 0$, degenerate to breathing mode)

S. Hou, Y. Gong and Y. Liu, Eur. Phys. J. C 78, 378 (2018)

Content

In the Palatini formalism, we assume the connection is torsion free:

$$\Gamma^{\lambda}_{\mu\nu} = \Gamma^{\lambda}_{\nu\mu}$$

For the action of the Palatini-Horndeski theory：

$$R_{\mu\nu} = \partial_\lambda \Gamma^{\lambda}_{\mu\nu} - \partial_\nu \Gamma^{\lambda}_{\mu\lambda} + \Gamma^{\lambda}_{\sigma\lambda}\Gamma^{\sigma}_{\mu\nu} - \Gamma^{\lambda}_{\sigma\nu}\Gamma^{\sigma}_{\mu\lambda}$$

$$\begin{aligned}\tilde{\Box}\phi &= g^{\mu\nu}\nabla_\mu\nabla_\nu\phi,\\ \nabla^\mu\nabla^\nu\phi &= g^{\mu\rho}\nabla_\rho\nabla^\nu\phi,\\ \nabla^\mu\nabla_\nu\phi &= g^{\mu\rho}\nabla_\rho\nabla_\nu\phi.\end{aligned}$$

Taking perturbations

$$g_{\mu\nu} = \eta_{\mu\nu} + h_{\mu\nu}, \quad \Gamma^{\lambda}_{\mu\nu} = \overset{0}{\Gamma}{}^{\lambda}_{\mu\nu} + \Sigma^{\lambda}_{\mu\nu}, \quad \phi = \phi_0 + \varphi$$

We obtain the linearized field equation

$$\overset{(g)}{R}_{\mu\nu} = \left(\overset{0}{G}{}_{4,\phi} / \overset{0}{G}_4\right)\left(\partial_\mu\partial_\nu\varphi + \frac{1}{2}\eta_{\mu\nu}\Box\varphi\right),$$

$$a\Box\Box\varphi + b\Box\varphi + c\varphi = 0.$$

Where

$$\begin{aligned}a &= \overset{0}{G}_5\,\overset{0}{G}_3 \,/\, \overset{0}{G}_4,\\ b &= \overset{0}{K}{}_{,X} - 2\,\overset{0}{G}{}_{3,\phi} + 2\,\overset{0}{G}{}_{4,\phi}\,\overset{0}{G}_3 \,/\, \overset{0}{G}_4 + \frac{2}{3}\left(\overset{0}{G}_3\right)^2 / \overset{0}{G}_4,\\ c &= \overset{0}{K}{}_{,\phi\phi}.\end{aligned}$$

The Newman-Penrose formalism can be used to analyze the polarizations

Cases	Conditions	$+$ mode	$\times$ mode	massless scalar mode	massive scalar mode
case 0	${G^0}_{4,\phi} = 0.$	1	1	0	0
case 1.1	${G^0}_{4,\phi} \neq 0, a = b = c = 0.$	-	-	-	-
case 1.2	${G^0}_{4,\phi} \neq 0, a = b = 0, c \neq 0.$	1	1	0	0
case 1.3	${G^0}_{4,\phi} \neq 0, a = c = 0, b \neq 0.$	1	1	1	0
case 1.4	${G^0}_{4,\phi} \neq 0, a = 0, b, c \neq 0.$	1	1	0	1
case 2.1	${G^0}_{4,\phi} \neq 0, a \neq 0, b^2 - 4ac < 0.$	1	1	0	0
case 2.2.1	${G^0}_{4,\phi} \neq 0, a \neq 0, b = c = 0.$	1	1	1	0
case 2.2.2	${G^0}_{4,\phi} \neq 0, a \neq 0, b, c \neq 0, b^2 - 4ac = 0.$	1	1	0	1
case 2.2.3	${G^0}_{4,\phi} \neq 0, a \neq 0, b^2 - 4ac > 0, c = 0.$	1	1	1	1
case 2.2.4	${G^0}_{4,\phi} \neq 0, a \neq 0, b^2 - 4ac > 0, c \neq 0.$	1	1	0	2

Future work

- Ostrogradsky instability
- Tensor gravitational wave speed in cosmological background

Thanks !

Scalar Gauss-Bonnet and dynamical Chern-Simons BHs in EFT extension of GR

in preparation

Shin'ichi Hirano (Titech: Tokyo inst. of Tech.)

with **M. Kimura** (Daiichi Inst. of Tech.), **M. Yamaguchi** (Titech)

JGRG31, October 24-28th 2022

GR and EFT

- **GWs from binary BHs merger (LIGO, VIRGO)**

  observed wave forms would correspond to that predicted by numerical relativity

  → general relativity (GR) is almost correct

- **GR might be corrected from UV physics**

  e.g.) GR is non-renormalizable. We need inflaton.

  → including higher curvature corrections (Effective Field Theory: **EFT**) e.g.) $R^2, \frac{1}{\Lambda^2}R^3$

EFT Black Holes

- **BH physics?**

  corrections become effective on small scale due to $r_{\rm H} \gg \dfrac{1}{\Lambda}$?   No!

- **BH solutions can be changed thanks to corrections: EFT BHs**

  → interesting to explore UV physics by using BH!

  $(\text{Riemann})^3$: de Rham+ (2020), Cano+ (2021)

  $(\text{Riemann})^4$: Cardoso+ (2018)

  Non-linear Maxwell: K. Nomura+ (2021)

Image

combination of $M_{\rm pl},\ \Lambda,\ r_{\rm g}\ (:= 2M)$

$$R_{\mu\nu} - \frac{1}{2} g_{\mu\nu} R = \epsilon\,(\text{corrections})$$

Solving above perturbatively as $g_{\mu\nu} = g^{\rm GR}_{\mu\nu} + \epsilon g^{\rm EFT1}_{\mu\nu} + \epsilon^2 g^{\rm EFT2}_{\mu\nu}$

Image

combination of $M_{\rm pl},\ \Lambda,\ r_{\rm g}\ (:= 2M)$

$$R_{\mu\nu} - \frac{1}{2} g_{\mu\nu} R = \epsilon\,(\text{corrections})$$

Solving above perturbatively as $g_{\mu\nu} = g^{\rm GR}_{\mu\nu} + \epsilon g^{\rm EFT1}_{\mu\nu} + \epsilon^2 g^{\rm EFT2}_{\mu\nu}$

$\mathcal{O}(\epsilon^0)$: $$R_{\mu\nu} - \frac{1}{2} g_{\mu\nu} R = 0 \longrightarrow g_{\mu\nu} = g^{\rm GR}_{\mu\nu}$$

Image

combination of $M_{\rm pl},\ \Lambda,\ r_{\rm g}\ (:= 2M)$

$$R_{\mu\nu} - \frac{1}{2} g_{\mu\nu} R = \epsilon\,(\text{corrections})$$

Solving above perturbatively as $g_{\mu\nu} = g^{\rm GR}_{\mu\nu} + \epsilon g^{\rm EFT1}_{\mu\nu} + \epsilon^2 g^{\rm EFT2}_{\mu\nu}$

$\mathcal{O}(\epsilon^0)$: $$R_{\mu\nu} - \frac{1}{2} g_{\mu\nu} R = 0 \longrightarrow g_{\mu\nu} = g^{\rm GR}_{\mu\nu}$$

$\mathcal{O}(\epsilon^1)$: $$R_{\mu\nu} - \frac{1}{2} g_{\mu\nu} R = \epsilon\,(\text{corrections})$$

$g_{\mu\nu} = \epsilon g^{\rm EFT1}_{\mu\nu}$ $\qquad$ $g_{\mu\nu} = g^{\rm GR}_{\mu\nu}$

Image

combination of $M_{\rm pl},\ \Lambda,\ r_{\rm g}\ (:= 2M)$

$$R_{\mu\nu} - \frac{1}{2} g_{\mu\nu} R = \epsilon\,(\text{corrections})$$

Solving above perturbatively as $g_{\mu\nu} = g^{\rm GR}_{\mu\nu} + \epsilon g^{\rm EFT1}_{\mu\nu} + \epsilon^2 g^{\rm EFT2}_{\mu\nu}$

$\mathcal{O}(\epsilon^0)$: $R_{\mu\nu} - \frac{1}{2} g_{\mu\nu} R = 0 \longrightarrow g_{\mu\nu} = g^{\rm GR}_{\mu\nu}$

$\mathcal{O}(\epsilon^1)$: $R_{\mu\nu} - \frac{1}{2} g_{\mu\nu} R = \epsilon\,(\text{corrections})$

$g_{\mu\nu} = \epsilon g^{\rm EFT1}_{\mu\nu}$ $\qquad$ $g_{\mu\nu} = g^{\rm GR}_{\mu\nu}$

$\mathcal{O}(\epsilon^2)$: $R_{\mu\nu} - \frac{1}{2} g_{\mu\nu} R = \epsilon\,(\text{corrections})$

$g_{\mu\nu} = \epsilon^2 g^{\rm EFT2}_{\mu\nu}$ $\qquad$ $g_{\mu\nu} = \epsilon g^{\rm EFT1}_{\mu\nu}$

Our work

Our work *Hirano, Kimura, Yamaguchi, in prep.*

- **additional DoFs** as EFT of GR
- **parity violating terms**

→ **scalar field & metric tensor couplings** as a first step

※ bonus: other terms outside modified gravity models

(1) action and leading operators

(2) static spherically symm. BH and perturbation (QNM)

construction of action

Hirano+

1. We can use Ricci flat (scalar vanishes in vacuum) at $\mathcal{O}(\epsilon^0)$

   → in EoM, we need not to consider R, $R_{\mu\nu}$, and its derivatives

   e.g.) $R_{\mu\nu}^2$, R^3, $RR_{\mu\nu}^2$ in action

2. RX, $R_{\mu\nu}Y^{\mu\nu}$ (X: scalar, $Y^{\mu\nu}$: tensor) can be pushed to higher order via $g_{\mu\nu} \to g_{\mu\nu} + \epsilon Z_{\mu\nu}$ ($Z_{\mu\nu}$: tensor)

3. We can choose one from terms proportional to same Weyl comp.

   e.g.) $R_{abcd}R^{cd\mu\nu}R_{\mu\nu}{}^{ab}$, $R_{abcd}R^{cd\mu\nu}R_{\mu}{}^{a}{}_{\nu}{}^{b} \propto W_{abcd}W^{cd\mu\nu}W_{\mu\nu}{}^{ab}$

Effective action

Hirano+

$$
\begin{aligned}
\frac{\mathcal{L}_{\mathrm{EFT}}}{\sqrt{-g}} = \; & \frac{M_{\mathrm{pl}}^2}{2}R - \frac{1}{2}(\partial_\mu\phi)^2 - \frac{1}{2}m^2\phi^2 \\
& + \frac{b_1}{\Lambda}\phi R_{\mu\nu\alpha\beta}^2 + \frac{b_2}{\Lambda}\phi \tilde{R}_{\mu\nu\alpha\beta}R^{\mu\nu\alpha\beta} \\
& + \frac{c_1}{\Lambda^3}\Box\phi R_{\mu\nu\rho\sigma}^2 + \frac{c_2}{\Lambda^3}\phi R_{\mu\nu\rho\sigma}^3 \\
& + \frac{d_1}{\Lambda^3}\Box\phi \tilde{R}^{\mu\nu}{}_{\alpha\beta}R^{\alpha\beta}{}_{\mu\nu} + \frac{d_2}{\Lambda^3}\phi \tilde{R}^{\mu\nu}{}_{\alpha\beta}R^{\alpha\beta}{}_{ab}R^{ab}{}_{\mu\nu} \\
& + \mathcal{O}\left(\frac{1}{\Lambda^4}\right)
\end{aligned}
$$

Effective action

Hirano+

$$\frac{\mathscr{L}_{\rm EFT}}{\sqrt{-g}} = \frac{M_{\rm pl}^2}{2}R - \frac{1}{2}(\partial_\mu\phi)^2 - \frac{1}{2}m^2\phi^2$$

converted to ϵ by combining with $M_{\rm pl}$ and r_g

$$+\frac{b_1}{\Lambda}\phi R^2_{\mu\nu\alpha\beta} + \frac{b_2}{\boxed{\Lambda}}\phi\tilde{R}_{\mu\nu\alpha\beta}R^{\mu\nu\alpha\beta} \leftarrow$$

leading operators: scalar Gauss-Bonnet /dynamical Chern-Simons

$$+\frac{c_1}{\Lambda^3}\Box\phi R^2_{\mu\nu\rho\sigma} + \frac{c_2}{\Lambda^3}\phi R^3_{\mu\nu\rho\sigma} \leftarrow$$

new sub-leading operators

$\downarrow$

$$+\frac{d_1}{\Lambda^3}\Box\phi\tilde{R}^{\mu\nu}{}_{\alpha\beta}R^{\alpha\beta}{}_{\mu\nu} + \frac{d_2}{\Lambda^3}\phi\tilde{R}^{\mu\nu}{}_{\alpha\beta}R^{\alpha\beta}{}_{ab}R^{ab}{}_{\mu\nu}$$

$$+\mathcal{O}\left(\frac{1}{\Lambda^4}\right)$$

Effective action

Hirano+

$$\frac{\mathscr{L}_{\rm EFT}}{\sqrt{-g}} = \frac{M_{\rm pl}^2}{2}R - \frac{1}{2}(\partial_\mu\phi)^2 - \frac{1}{2}m^2\phi^2$$

converted to ϵ by combining with $M_{\rm pl}$ and r_g

this talk

$$+\frac{b_1}{\Lambda}\phi R^2_{\mu\nu\alpha\beta} + \frac{b_2}{\boxed{\Lambda}}\phi\tilde{R}_{\mu\nu\alpha\beta}R^{\mu\nu\alpha\beta} \leftarrow$$

leading operators: scalar Gauss-Bonnet /dynamical Chern-Simons

$$+\frac{c_1}{\Lambda^3}\Box\phi R^2_{\mu\nu\rho\sigma} + \frac{c_2}{\Lambda^3}\phi R^3_{\mu\nu\rho\sigma} \leftarrow$$

new sub-leading operators

$\downarrow$

$$+\frac{d_1}{\Lambda^3}\Box\phi\tilde{R}^{\mu\nu}{}_{\alpha\beta}R^{\alpha\beta}{}_{\mu\nu} + \frac{d_2}{\Lambda^3}\phi\tilde{R}^{\mu\nu}{}_{\alpha\beta}R^{\alpha\beta}{}_{ab}R^{ab}{}_{\mu\nu}$$

$$+\mathcal{O}\left(\frac{1}{\Lambda^4}\right)$$

Static spherically sym. sol.

cf) Yunes+ (2008)

Hirano+

$$\boxed{\frac{b_1}{\Lambda}\phi R^2_{\mu\nu\rho\sigma},\quad \frac{b_2}{\Lambda}\phi \tilde{R}^{\mu\nu}{}_{\alpha\beta}R^{\alpha\beta}{}_{\mu\nu}}$$

- Ansatz $\quad ds^2 = -A(r)dt^2 + \dfrac{1}{B(r)}dr^2 + r^2(d\theta^2 + \sin^2\theta d\phi^2)$

$$A(r) = 1 - \frac{r_{\rm g}}{r} + \epsilon^2 f(r),\ B(r) = 1 - \frac{r_{\rm g}}{r} + \epsilon^2 g(r) \quad , \epsilon := \frac{1}{\Lambda M_{\rm pl}^2 r_{\rm g}^3}$$

$\phi = 0 + \epsilon\,\pi(r)$ (no hair at $\mathcal{O}(\epsilon^0)$)

Static spherically sym. sol.

cf) Yunes+ (2008)

Hirano+

$$\boxed{\frac{b_1}{\Lambda}\phi R^2_{\mu\nu\rho\sigma},\quad \frac{b_2}{\Lambda}\phi \tilde{R}^{\mu\nu}{}_{\alpha\beta}R^{\alpha\beta}{}_{\mu\nu}}$$

← ~~parity~~ term (no effect at BG)

- Ansatz $\quad ds^2 = -A(r)dt^2 + \dfrac{1}{B(r)}dr^2 + r^2(d\theta^2 + \sin^2\theta d\phi^2)$

$$A(r) = 1 - \frac{r_{\rm g}}{r} + \epsilon^2 f(r),\ B(r) = 1 - \frac{r_{\rm g}}{r} + \epsilon^2 g(r) \quad , \epsilon := \frac{1}{\Lambda M_{\rm pl}^2 r_{\rm g}^3}$$

$\phi = 0 + \epsilon\,\pi(r)$ (no hair at $\mathcal{O}(\epsilon^0)$)

Static spherically sym. sol.

cf) Yunes+ (2008)
Hirano+

$$\boxed{\frac{b_1}{\Lambda}\phi R^2_{\mu\nu\rho\sigma},\quad \frac{b_2}{\Lambda}\phi \tilde{R}^{\mu\nu}{}_{\alpha\beta}R^{\alpha\beta}{}_{\mu\nu}} \longleftarrow$$ ~~parity~~ term (no effect at BG)

- Ansatz $ds^2 = -A(r)dt^2 + \frac{1}{B(r)}dr^2 + r^2(d\theta^2 + \sin^2\theta d\phi^2)$

$$A(r) = 1 - \frac{r_g}{r} + \underbrace{\epsilon^2}_{\text{2nd}} f(r),\ B(r) = 1 - \frac{r_g}{r} + \underbrace{\epsilon^2}_{\text{2nd}} g(r) \quad , \epsilon := \frac{1}{\Lambda M_{pl}^2 r_g^3}$$

$\phi = 0 + \underbrace{\epsilon}_{\text{1st}}\pi(r)$ (no hair at $\mathcal{O}(\epsilon^0)$)

Static spherically sym. sol.

cf) Yunes+ (2008)
Hirano+

(field eq.) $$(\Box - m^2)\overset{\epsilon\,\pi(r)}{\phi} = \epsilon\,(R^{abcd}R_{abcd} + \cdots)\quad [R \leftarrow g^{\text{Sch}}_{\mu\nu}]$$

(EoMs) $$R_{\mu\nu} - \frac{1}{2}\overset{\epsilon^2 f(r),\ \epsilon^2 g(r)}{g_{\mu\nu}}R = \underbrace{\epsilon\,(\overset{\epsilon\,\pi(r)}{\phi} R^2_{abcd}\overset{g^{\text{Sch}}_{\mu\nu}}{g_{\mu\nu}} + \cdots)}_{\mathcal{O}(\epsilon^2)}$$

- Substituting ansatz into EoMs, we can determine unknown funcs.

$$\pi(r) = \frac{4b_1M_{pl}^2r_g^2}{r}\left(1 + \frac{r_g}{2r} + \frac{r_g^2}{3r^2}\right)$$ (massless, regular at $r \to r_g,\ \infty$)

$$f(r) = \frac{4b_1^2M_{pl}^2r_g^5}{3r^3}\left(1 + \frac{13r_g}{r} + \cdots\right),\ g(r) = \frac{8b_1^2M_{pl}^2r_g^4}{r^2}\left(1 + \frac{r_g}{2r} + \cdots\right)$$

scalar GB coupling

cf) Pani+ (2009)

Hirano+

- $g_{\mu\nu} = g_{\mu\nu}^{\text{Sch}} + \epsilon^2 \bar{g}_{\mu\nu}^{\text{sGB}} + h_{\mu\nu}^{\text{odd/even}}, \quad \phi = \epsilon \bar{\phi}^{\text{sGB}} + \delta\phi$
- scalar GB coupling $\quad \phi R_{\mu\nu\rho\sigma}^2$

scalar GB coupling

cf) Pani+ (2009)

Hirano+

- $g_{\mu\nu} = g_{\mu\nu}^{\text{Sch}} + \epsilon^2 \bar{g}_{\mu\nu}^{\text{sGB}} + h_{\mu\nu}^{\text{odd/even}}, \quad \phi = \epsilon \bar{\phi}^{\text{sGB}} + \delta\phi$
- scalar GB coupling $\quad \phi R_{\mu\nu\rho\sigma}^2$ $\quad$ scalar-even couplings

$\underline{\mathcal{O}(\epsilon)}$,

(field eq.) $$(\Box - m^2)\overset{\overset{\delta\phi}{\downarrow}}{\phi} = \epsilon\, \overset{\overset{h_{\mu\nu}^{\text{even}}}{\downarrow}}{R^{abcd}} R_{abcd}$$

(EoMs) $$R_{\mu\nu} - \frac{1}{2} \overset{\overset{h_{\mu\nu}^{\text{even}}}{\downarrow}}{g_{\mu\nu}} R = \epsilon(\overset{\overset{\delta\phi}{\downarrow}}{\phi} R_{abcd}^2 \overset{\overset{g_{\mu\nu}^{\text{Sch}}}{\downarrow}}{g_{\mu\nu}} + \cdots)$$

scalar GB coupling

cf) Pani+ (2009)
Hirano+

- $g_{\mu\nu} = g^{\rm Sch}_{\mu\nu} + \epsilon^2 \bar{g}^{\rm sGB}_{\mu\nu} + h^{\rm odd/even}_{\mu\nu}, \quad \phi = \epsilon \bar{\phi}^{\rm sGB} + \delta\phi$
- scalar GB coupling $\quad \phi R^2_{\mu\nu\rho\sigma}$ $\quad$ scalar-even couplings
  kinetic terms, potential terms

$\mathcal{O}(\epsilon)$, $\mathcal{O}(\epsilon^2)$

(field eq.) $\quad (\underbrace{\Box}_{\epsilon^2 \bar{g}^{\rm sGB}_{\mu\nu}} - m^2)\overbrace{\phi}^{\delta\phi} = \epsilon\, \overbrace{R^{abcd}}^{h^{\rm even}_{\mu\nu}\ +\epsilon\,\delta\phi} R_{abcd}$

(EoMs) $\quad \underbrace{R_{\mu\nu}}_{\epsilon^2 \bar{g}^{\rm sGB}_{\mu\nu},\ h^{\rm even}_{\mu\nu},\ h^{\rm odd}_{\mu\nu}} - \frac{1}{2} g_{\mu\nu} \overbrace{R}^{h^{\rm even}_{\mu\nu}} = \epsilon(\overbrace{\phi}^{\delta\phi\ +\epsilon\bar{\phi}^{\rm sGB} + \epsilon\, h^{\rm even}_{\mu\nu}} \underbrace{R^2_{abcd}}_{g^{\rm Sch}_{\mu\nu},\ h^{\rm even}_{\mu\nu},\ h^{\rm odd}_{\mu\nu}} g_{\mu\nu} + \cdots)$

scalar GB coupling

cf) Pani+ (2009)
Hirano+

- $g_{\mu\nu} = g^{\rm Sch}_{\mu\nu} + \epsilon^2 \bar{g}^{\rm sGB}_{\mu\nu} + h^{\rm odd/even}_{\mu\nu}, \quad \phi = \epsilon \bar{\phi}^{\rm sGB} + \delta\phi$
- scalar GB coupling $\quad \phi R^2_{\mu\nu\rho\sigma}$ $\quad$ scalar-even couplings
  kinetic terms, potential terms

$$\frac{d^2\Psi^{\rm o}}{dr_*^2} + \omega^2 c^2_{\rm odd}\Psi^{\rm o} - \left(1 - \frac{r_g}{r}\right)(V^{\rm o}_{\rm GR} + \epsilon^2 V^{\rm o}_{\rm EFT})\Psi^{\rm o} = 0,$$

$$\frac{d^2\mathbf{\Psi}}{dr_*^2} + \omega^2 \mathbf{c}^2 \mathbf{\Psi} - \left(1 - \frac{r_g}{r}\right)\mathbf{V}\mathbf{\Psi} = 0\ ,\ \mathbf{\Psi} = \begin{pmatrix}\Psi^{\rm s} \\ \Psi^{\rm e}\end{pmatrix},$$

$\Psi^{\rm o} \sim h^{\rm odd}_{\mu\nu}$
$\Psi^{\rm s} \sim \delta\phi$
$\Psi^{\rm e} \sim h^{\rm even}_{\mu\nu}$

$$\mathbf{c}^2 = \begin{pmatrix} 1 + \epsilon^2(1 - r_g/r)c_s^2 & 0 \\ 0 & 1 + \epsilon^2(1 - r_g/r)c_e^2 \end{pmatrix},\ \mathbf{V} = \begin{pmatrix} V_{\rm KG} + \epsilon^2 V^{\rm s}_{\rm EFT} & \epsilon V^{\rm s,e} \\ \epsilon V^{\rm s,e} & V^{\rm e}_{\rm GR} + \epsilon^2 V^{\rm e}_{\rm EFT} \end{pmatrix},$$

$$c^2_{\rm odd} = 1 + \epsilon^2(1 - r_g/r)(\cdots)\ ,\ \frac{dr}{dr_*} = 1 - \frac{r_g}{r} + \epsilon^2(\cdots)$$

dynamical CS coupling

cf) Kimura (2019)
Hirano+

- $g_{\mu\nu} = g^{\mathrm{Sch}}_{\mu\nu} \cancel{+ \epsilon^2 \bar{g}^{\mathrm{sGB}}_{\mu\nu}} + h^{\mathrm{odd/even}}_{\mu\nu}, \quad \phi = \cancel{\epsilon\bar{\phi}^{\mathrm{sGB}}} + \delta\phi$
- dynamical CS coupling $\phi \tilde{R}_{\mu\nu\rho\sigma} R^{\mu\nu\rho\sigma}$ **scalar-odd** couplings
  ~~kinetic terms~~, potential terms

$$\frac{d^2\Psi^{\mathrm{e}}}{dr_*^2} + \omega^2 \Psi^{\mathrm{e}} - \left(1 - \frac{r_g}{r}\right) V^{\mathrm{e}}_{\mathrm{GR}} \Psi^{\mathrm{e}} = 0,$$

$$\frac{d^2\mathbf{\Psi}}{dr_*^2} + \omega^2 \mathbf{\Psi} - \left(1 - \frac{r_g}{r}\right) \mathbf{V}\mathbf{\Psi} = 0\,,\ \mathbf{\Psi} = \begin{pmatrix} \Psi^{\mathrm{scalar}} \\ \Psi^{\mathrm{o}} \end{pmatrix},$$

$$\mathbf{V} = \begin{pmatrix} V_{\mathrm{KG}} + \boxed{\epsilon^2 V^{\mathrm{s}}_{\mathrm{EFT}}} & \boxed{\epsilon V^{\mathrm{s,o}}} \\ \boxed{\epsilon V^{\mathrm{s,o}}} & V^{\mathrm{o}}_{\mathrm{GR}} \end{pmatrix}, \quad \frac{dr}{dr_*} = 1 - \frac{r_g}{r}$$

sGB-dCS coupling

Hirano+

- $g_{\mu\nu} = g^{\mathrm{Sch}}_{\mu\nu} + \epsilon^2 \bar{g}^{\mathrm{sGB}}_{\mu\nu} + h^{\mathrm{odd/even}}_{\mu\nu}, \quad \phi = \epsilon\bar{\phi}^{\mathrm{sGB}} + \delta\phi$
- $\phi R^2_{\mu\nu\rho\sigma}, \ \phi \tilde{R}_{\mu\nu\rho\sigma} R^{\mu\nu\rho\sigma}$ scalar-odd/-even couplings, **kinetic terms**
  potential terms, new even-odd coupling

$$\frac{d^2\mathbf{\Psi}}{dr_*^2} + \omega^2 \mathbf{c}^2 \mathbf{\Psi} - \left(1 - \frac{r_g}{r}\right) \mathbf{V}\mathbf{\Psi} = 0\,,\ \mathbf{\Psi} = \begin{pmatrix} \Psi^{\mathrm{s}} \\ \Psi^{\mathrm{o}} \\ \Psi^{\mathrm{e}} \end{pmatrix},$$

$$\mathbf{c}^2 = \begin{pmatrix} 1 + \epsilon^2 (1 - r_g/r) c_s^2 & 0 & 0 \\ 0 & \boxed{1 + \epsilon^2 (1 - r_g/r) c_o^2} & 0 \\ 0 & 0 & 1 + \epsilon^2 (1 - r_g/r) c_e^2 \end{pmatrix}, \quad \frac{dr}{dr_*} = 1 - \frac{r_g}{r} + \epsilon^2 (\cdots)$$

$$\mathbf{V} = \begin{pmatrix} V_{\mathrm{KG}} + \epsilon^2 V^{\mathrm{s}}_{\mathrm{EFT}} & \epsilon V^{\mathrm{s,o}} & \epsilon V^{\mathrm{s,e}} \\ \epsilon V^{\mathrm{s,o}} & V^{\mathrm{o}}_{\mathrm{GR}} + \boxed{\epsilon^2 V^{\mathrm{o}}_{\mathrm{EFT}}} & \boxed{\epsilon^2 V^{\mathrm{o,e}}} \\ \epsilon V^{\mathrm{s,e}} & \boxed{\epsilon^2 V^{\mathrm{o,e}}} & V^{\mathrm{e}}_{\mathrm{GR}} + \epsilon^2 V^{\mathrm{e}}_{\mathrm{EFT}} \end{pmatrix}$$

leading order
in QMN!!!

QUASI-NORMAL MODE

Hirano+

eigenvalues ω of Master eqs. with B.C.s

e.g) quantum mechanics

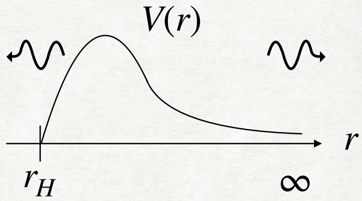

<u>scalar-odd/-even coupling</u> (i = o/e)

$$\begin{pmatrix} V_s & \epsilon V_{\mathrm{s,i}} \\ \epsilon V_{\mathrm{s,i}} & V_i \end{pmatrix} \text{:non-degenerate} \qquad V_{\mathrm{s}} - \frac{V_{\mathrm{s,i}}^2}{V_{\mathrm{s}} - V_{\mathrm{i}}}\boxed{\epsilon^2},\ V_{\mathrm{i}} + \frac{V_{\mathrm{s,i}}^2}{V_{\mathrm{s}} - V_{\mathrm{i}}}\boxed{\epsilon^2}\ (V_{\mathrm{s}} > V_{\mathrm{i}})$$

same (leading) order

<u>even-odd coupling</u>

$$\begin{pmatrix} V_{\mathrm{GR}} & \epsilon^2 V_{\mathrm{o,e}} \\ \epsilon^2 V_{\mathrm{o,e}} & V_{\mathrm{GR}} \end{pmatrix} \text{: degenerate} \qquad V_{\mathrm{GR}} \pm V_{\mathrm{o,e}}\boxed{\epsilon^2}$$

(iso-spectrality of V_{GR})

QUASI-NORMAL MODE

Hirano+

eigenvalues ω of Master eqs. with B.C.s

e.g) quantum mechanics

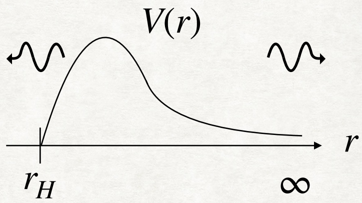

- **Demo**: parametrized QNM formula *Ryan+ (2019)*

$$l = 2,\quad V_{\mathrm{o,e}} = \frac{2b_1b_2\left(94080 + 199626r - 47306r^2 - 223293r^3 - 22080r^4 + 21760r^5 + 51840r^6\right)}{5r^9(4r+3)^2}$$

$(r_g = 1,\ M_{\mathrm{pl}} = 1)$

$$\rightarrow \quad \delta\omega = (-10.5681 + 95.996i)b_1b_2\epsilon^2 \qquad \text{(preliminary)}$$

For high precision, we are computing with continued fraction method
(multi ver. of Leaver's method) cf) Nomura+ (2021)

Summary

- **GR might be corrected from UV physics**

  BH solutions can be changed thanks to corrections: **EFT BH**

- **Our work**

  scalar-tensor couplings with parity violating terms

  ✔ action, leading operators: **sGB-dCS couplings**

  ✔ coupled Schrodinger eqs.: **new odd-even coupling**

  ✔ Quasi-normal mode: **leading effect from o-e coupling**

- **Future prospects**

  rotating case , overtone, fermion, ….

C18

Spin-2 dark matter from anisotropic Universe

Yusuke Manita
(Kyoto University)

Collaborators:Katsuki Aoki(YITP), Tomohiro Fujita(WIAS), and Shinji Mukohyama(YITP)

Overview

"Spin-2 dark matter"

Observation

Testing by GW detectors.

implication!

Theory

✓Spin-2 DM is regarded as a massive graviton.

✓DM production from the anisotropic Universe.

Ultra-light DM

[Ferreira, 2020]

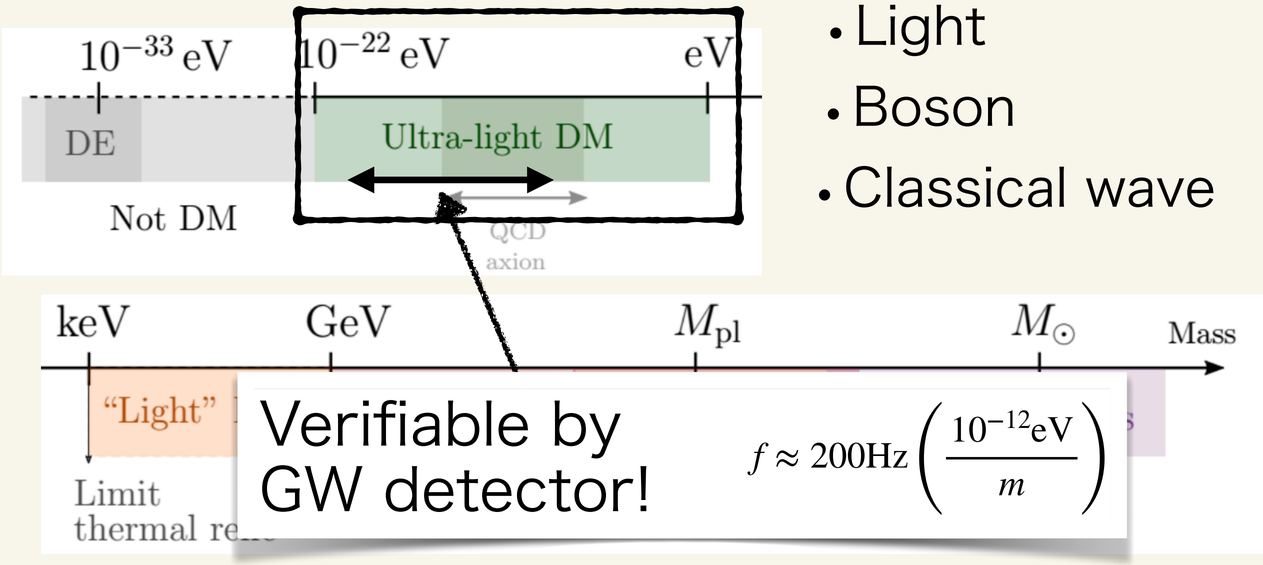

- Light
- Boson
- Classical wave

Ultraligh spin-2 DM can be tested by GW detector!

Spin-2 dark matter

- **Spin-2 DM** is a tensor dark matter originating from **bigravity**.

  Maeda, Volkov (2013), Aoki, Mukohyama (2017), Babichev et al. (2017)

- Spin-2 DM is regarded as a massive graviton.

$$\mathscr{L}_{\text{int}} \sim \frac{1}{M_G} \varphi_{\mu\nu} T^{\mu\nu}$$

→ Ultralight Spin-2 DM can be searched by the **GW detector**!

Armaleo, Nacir, Urban, (2021); YM, Aoki, Fujita, Mukohyama, in prep.

Production mechanism

Today's topic

- Production from

phase transition of anisotropy

Manita, Aoki, Fujita, Mukohyama in prep.

- Anisotropic perturbation of the massive graviton can be regarded as a spin-2 DM.

  ✓Anisotropy behaves as a dust fluid [Maeda, Volkov, 2013].

  ✓Structure formation [Aoki, Maeda, 2017].

Anisotropic fixed point in bigravity

Bigravity

- Bigravity is a gravity theory with two metrics $\{g_{\mu\nu}, f_{\mu\nu}\}$.

- It is a theory of massive graviton which couples to the massless graviton.
  $\rightarrow$ **Bigravity describes spin-2 particles in a gravitational field.**

$$S = \underbrace{\frac{1}{2\kappa_g^2}\int d^4x\sqrt{-g}R^{(g)}}_{\text{Einstein-Hilbert term}} + \underbrace{\frac{1}{2\kappa_f^2}\int d^4x\sqrt{-f}R^{(f)}}_{\text{Einstein-Hilbert term}} + \underbrace{\frac{m^2}{\kappa^2}\int d^4x\mathscr{L}_{\rm int}[g_{\mu\nu}, f_{\mu\nu}]}_{\text{Interaction term}}$$

Hassan-Rosen bigravity[Hassan, Rosen, 2012],
Minimal theory of bigravity [De Felice, Larrouturou, Mukohyama, Oliosi, 2020]

Set up

- **Homogeneous anisotropic Universe**
  $\rightarrow$ Bianchi type-I universe:

β_g, β_f are **anisotropy.**

$$g_{\mu\nu}dx^\mu dx^\nu = -N_g^2 dt^2 + a_g^2\left[e^{4\beta_g}dx^2 + e^{-2\beta_g}\left(dy^2 + dz^2\right)\right],$$
$$f_{\mu\nu}dx^\mu dx^\nu = -N_f^2 dt^2 + a_f^2\left[e^{4\beta_f}dx^2 + e^{-2\beta_f}\left(dy^2 + dz^2\right)\right]$$

- Anisotropies are relatively large.

- We assume **vacuum** configuration.

Background equation

Friedmann equation

$$H_g^2 = \sigma_g^2 + \frac{{m_g}^2}{3}\left[b_0 + b_1\left(e^{-2\beta} + 2e^{\beta}\right)\xi + b_2\left(2e^{-\beta} + e^{2\beta}\right)\xi^2 + b_3\xi^3\right],$$

$\sigma_g = \dot{\beta}_g$,
$\beta = \beta_g - \beta_f$

→ Cosmic expansion is sourced by anisotropy.

Equations of anisotropies

$$\frac{1}{a_g^3}\frac{d}{dt}\left(a_g^3\sigma_g\right) + \kappa_g^2\frac{\partial U}{\partial \beta} = 0, \quad \frac{1}{a_g^3}\frac{d}{dt}\left(a_f^3\sigma_f\right) - \kappa_f^2\frac{\partial U}{\partial \beta} = 0$$

U is a potential of β

→ The anisotropies behave as two fluids.

Constraint equation

The background equation are nonlinear ODE.
→ First, let's look at the fixed point!

Anisotropic fixed point

[Condition of fixed point]

$$\dot{H}_g = \dot{H}_f = \dot{\beta}_g = \dot{\beta}_f = \dot{\xi} = 0$$

→ stationary solution

[result]

Isotropic fixed point $\beta = 0$	Anisotropic fixed point $\beta \neq 0$ (NEW)
$(H_g - H_f\xi)(b_1 + 2b_2\xi + b_3\xi^2) = 0$	$c_4 e^{12\beta} + c_3 e^{9\beta} + c_2 e^{6\beta} + c_1 e^{3\beta} + c_0 = 0$
• Normal branch	$\xi =$ (Function of β)
• Self-accelerating branch	$H_g, H_f =$ (Function of β and ξ)
Strauss+, 2012, De Felice+, 2020, etc.	

Local stability

Linearizing around each fixed point,

$$H_g \to H_{g0} + \epsilon H_{g1}\,, \quad \beta \to \beta_0 + \epsilon \beta_1\,, \cdots$$

- Equation of the massive anisotropy

$$\Rightarrow \quad \ddot{\beta}_1 + 3H_{g0}\dot{\beta}_1 + M^2\beta_1 = 0\,.$$

M is determined for each fixed point.

Stability condition: $\quad M^2 > 0$

	stable spiral (damped-oscillation)	stable node (over-damping)	saddle point (unstable)
M^2	$+$	$+$	$-$
$9H_{g0}^2 - 4M^2$	$-$	$+$	$+$

Isotropic fixed point

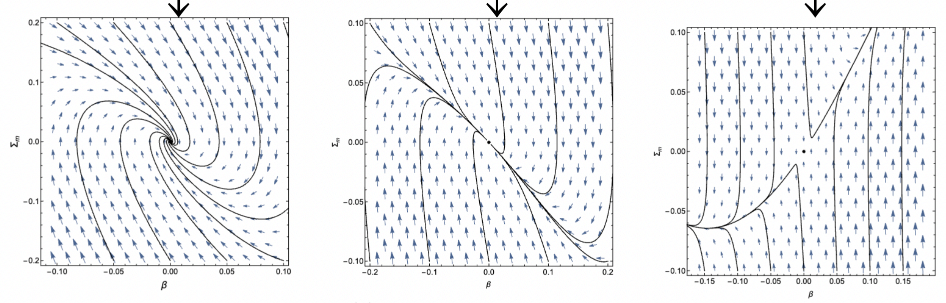

(a) $b_0 = 9.32, b_1 = -0.0162, b_2 = -0.0479, b_3 = 0.0122, b_4 = 0.00549, \alpha = 1.$

(b) $b_0 = 6.61, b_1 = -0.0542, b_2 = -0.00258, b_3 = 0.00320, b_4 = 0.00357, \alpha = 1.$

(c) $b_0 = 50, b_1 = 1, b_2 = 8.15, b_3 = -12.0, b_4 = 26.6, \alpha = 1.$

Anisotropic fixed point

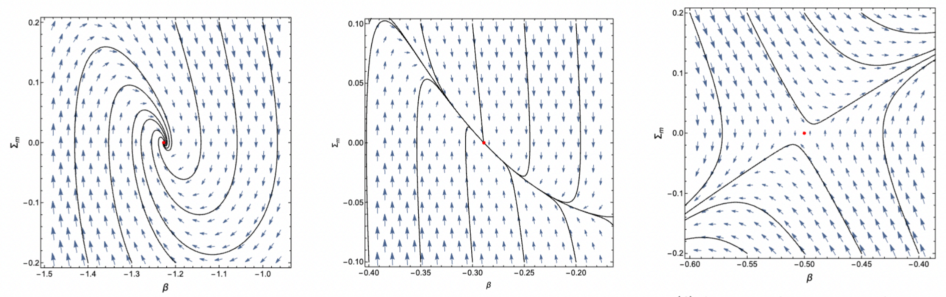

(d) $b_0 = -6.8, b_1 = 4, b_2 = -1.9, b_3 = 0.95, b_4 = -1, \alpha = 1.$

(e) $b_0 = 50, b_1 = 1, b_2 = 8.15, b_3 = -12.0, b_4 = 26.6, \alpha = 1.$

(f) $b_0 = 9.32, b_1 = -0.0162, b_2 = -0.0479, b_3 = 0.0122, b_4 = 0.00549, \alpha = 1.$

Global behavior

Anisotropic fixed point — saddle(unstable)

Isotropic fixed point — stable-spiral (damped-oscillation)

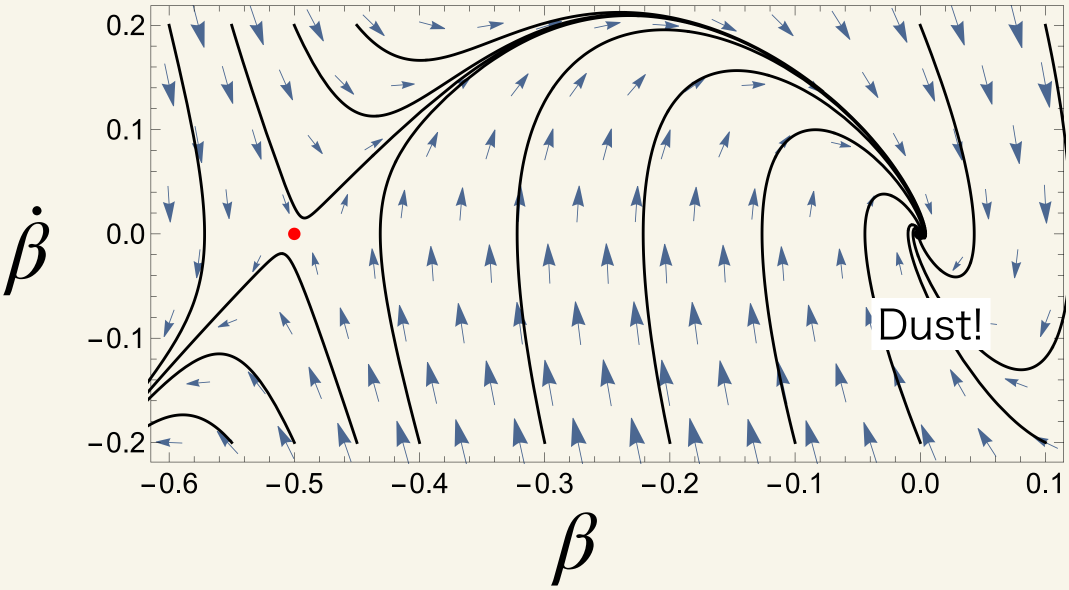

Spin-2 dark matter production

DM from anisotropic Universe

The **external fields** (inflaton, radiation) occurs a phase transition from Isotropic to anisotropic FP.

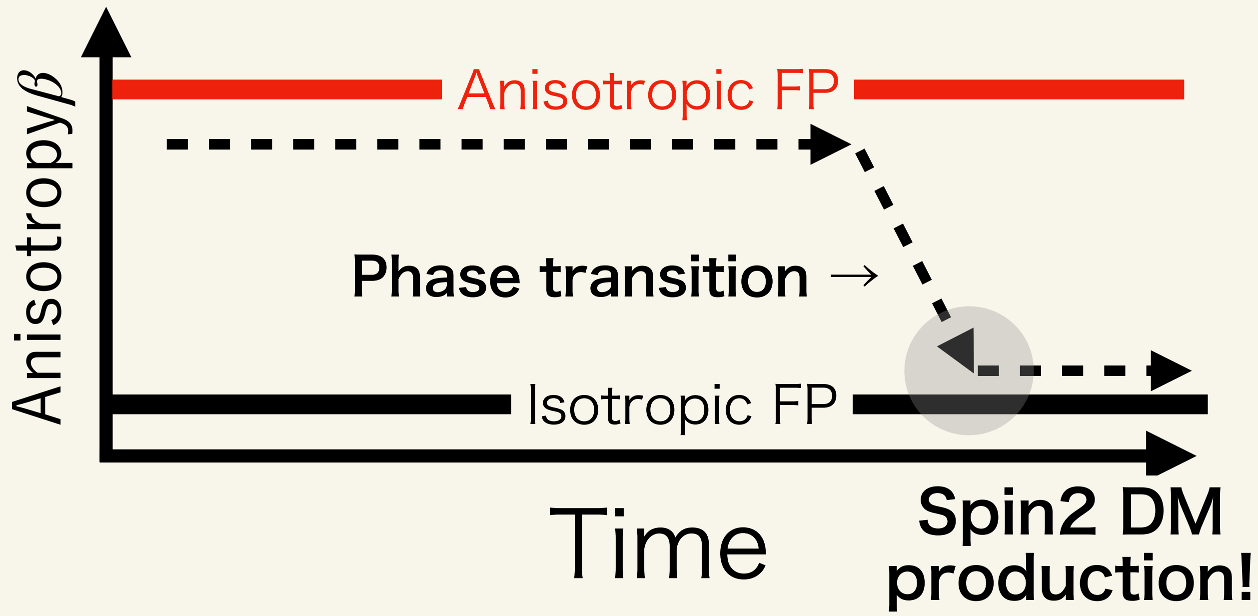

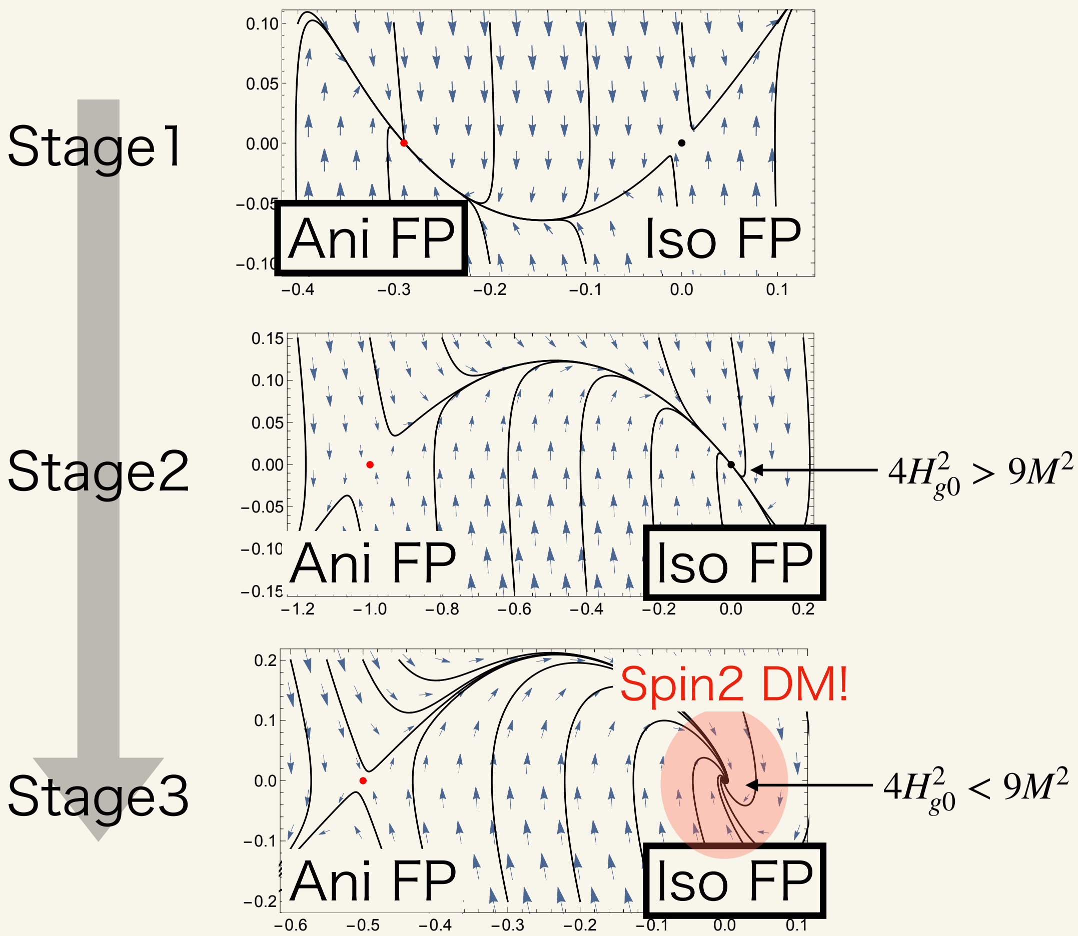

Estimate of DM abundance

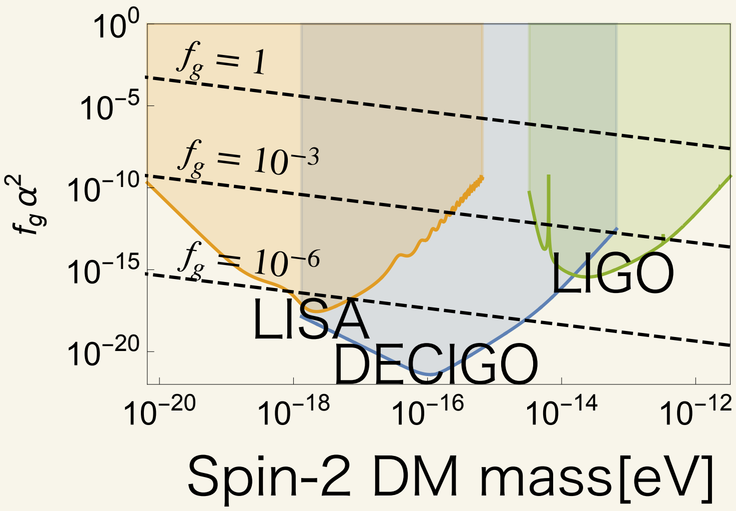

- Order estimate.
  The exact abundance cannot be determined without solving for the time evolution of the outer field.
- [asumption]
  Phase transition occurs at radiation dominant.
  $\beta(a_{\rm tr}) = \mathcal{O}(1)$。

$$f_g \equiv \frac{\Omega_{\rm spin-2}}{\Omega_{\rm DM}} \sim \alpha^2 \Omega_{r,0}^{3/4} \left(\frac{m}{H_0}\right)^{1/2}$$

$\alpha := \frac{\kappa_g}{\kappa_f}$ is a coupling constant.

TAKE HOME MESSAGE

The spin-2 DM can be produced by the phase transition of the anisotropic Universe!

It can be Verified by the GW detectors!

C19

25th Oct. 2022 @ JGRG31

Hybrid metric-Palatini Higgs inflation

Yuichiro TADA IAR, Nagoya, KEK

w/ Minxi He & Yusuke Mikura 2209.11051

(Mikura & YT '21)

Higgs inflation

Bezrukov & Shaposhnikov '07, Barvinsky, Kamenshchick, & Starobinsky '08

non-minimal coupling

$$S = \int \mathrm{d}^4x\sqrt{-g}\left[\frac{1}{2}(M_{\mathrm{Pl}}^2 + \boxed{\xi|\mathscr{H}|^2})R - \frac{1}{2}|\partial_\mu\mathscr{H}|^2 - \frac{\lambda}{4}|\mathscr{H}|^4\right]$$

$$\begin{cases} \tilde{g}_{\mu\nu} &= \left(1+\xi\dfrac{|\mathscr{H}|^2}{M_{\mathrm{Pl}}^2}\right)g_{\mu\nu} \\ \tilde{V}(\mathscr{H}) &= \dfrac{\lambda}{4}\dfrac{|\mathscr{H}|^4}{(1+\xi|\mathscr{H}|^2/M_{\mathrm{Pl}}^2)^2} \end{cases}$$

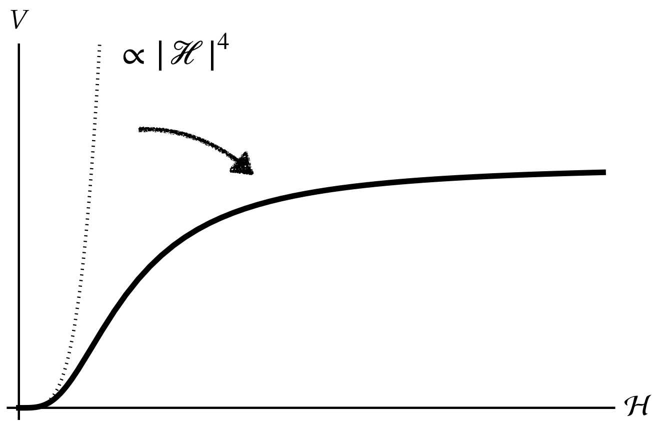

Higgs inflation

Bezrukov & Shaposhnikov '07, Barvinsky, Kamenshchick, & Starobinsky '08

non-minimal coupling

$$S = \int d^4x\sqrt{-g}\left[\frac{1}{2}(M_{\rm Pl}^2 + \boxed{\xi\,|\mathscr{H}|^2})R - \frac{1}{2}|\partial_\mu\mathscr{H}|^2 - \frac{\lambda}{4}|\mathscr{H}|^4\right]$$

- Unique scalar we really found
- $n_{\rm s} \simeq 0.96, \quad r \sim 10^{-3}$
- no free param. → full predictable

????

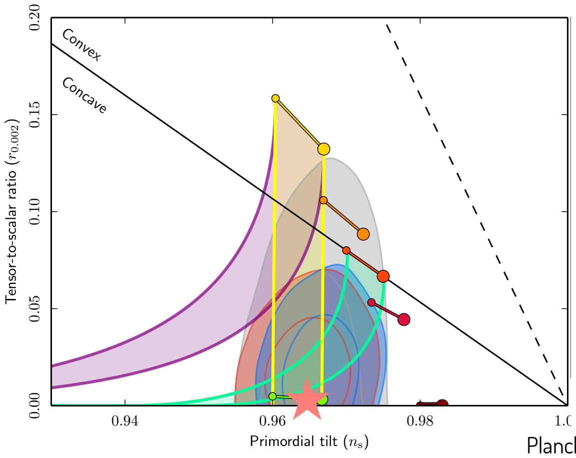

Planck '18

Unitarity issue

- large non-minimal coupling

$$\xi \simeq \sqrt{\frac{\lambda}{72\pi^2\mathscr{P}_\zeta}}N \sim 5\times 10^4\sqrt{\lambda}$$

- 4 real scalar d.o.f.

curved target space

$$\mathscr{H} = \frac{1}{\sqrt{2}}\begin{pmatrix}\phi_1 + i\phi_2\\ \phi_3 + i\phi_4\end{pmatrix} \quad \Rightarrow \quad \tilde{g}_{\mu\nu} = \left(1 + \xi\frac{|\mathscr{H}|^2}{M_{\rm Pl}^2}\right)g_{\mu\nu} \to -\frac{1}{2}\boxed{G_{ij}(\phi)}\partial_\mu\phi_i\partial^\mu\phi_j$$

PTB UV cutoff | dynamical scale

$$\mathscr{R}_G^{-1/2}\Big|_{\phi\sim 0} \sim \frac{M_{\rm Pl}}{\xi} \quad \ll \quad V_{\rm end}^{1/4} \sim \frac{M_{\rm Pl}}{\sqrt{\xi}}$$

PTB QFT breaks down!!

Ema+ '16

R^2 as σ meson

Ema+ '20

$\xi\phi^2 R$ $\qquad$ $\xi^2 R^2$

e.g., Salvio & Mazumdar '15

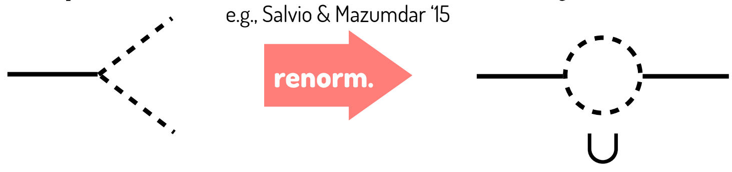

$\cup$

dynamical scalaron σ

$$V_{\rm eff}(\sigma,\phi) \;\to\; \sigma = \sigma_{\rm sur}(\phi)$$

scalars can deviate from the hypersurface @ high E

regularized

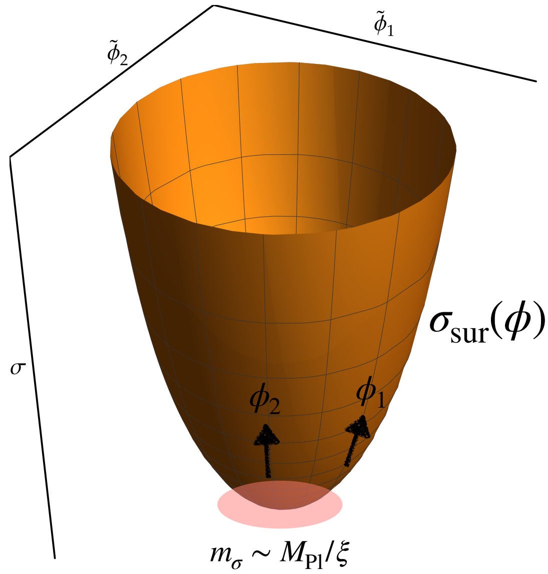

Palatini variation

Bauer & Demir '08

$$S = \int d^4x\sqrt{-g}\left[\frac{1}{2}(M_{\rm Pl}^2 + \xi|\mathscr{H}|^2)R(g,\Gamma) - \frac{1}{2}|\partial_\mu\mathscr{H}|^2 - \frac{\lambda}{4}|\mathscr{H}|^4\right]$$

$$\cancel{\Gamma^{\mu}_{\nu\rho} =} \frac{1}{2}g^{\mu\sigma}\left(g_{\nu\sigma,\rho} + g_{\rho\sigma,\nu} - g_{\nu\rho,\sigma}\right)$$

Γ s.t. $\dfrac{\partial\mathscr{L}}{\partial\Gamma} = 0$ (Palatini)

- $n_{\rm s} \simeq 0.96, \quad r \ll 10^{-3}$
- $\mathscr{R}_G^{-1/2} \sim \dfrac{M_{\rm Pl}}{\sqrt{\xi}} \quad \sim \quad V_{\rm end}^{1/4} \sim \dfrac{M_{\rm Pl}}{\sqrt{\xi}}$

marginal?

Direct embedding

Mikura & YT '21

$S \nearrow G_{ij}^{\mathrm{metric}}(\phi) \longrightarrow$

$S \searrow G_{ij}^{\mathrm{Palatini}}(\phi) \longrightarrow$

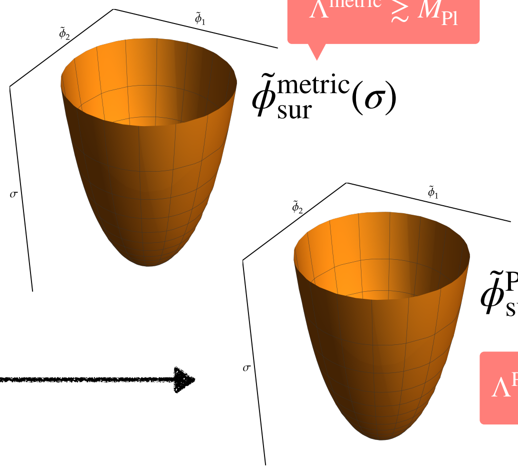

$\checkmark$ $\Lambda^{\mathrm{metric}} \gtrsim M_{\mathrm{Pl}}$

$\tilde{\phi}_{\mathrm{sur}}^{\mathrm{metric}}(\sigma)$

$\tilde{\phi}_{\mathrm{sur}}^{\mathrm{Palatini}}(\sigma)$

$\Lambda^{\mathrm{Palatini}} \sim M_{\mathrm{Pl}}/\sqrt{\xi}$ ✗

$$\frac{\tilde{\lambda}}{4}\left(\tilde{\phi}^2 - \boxed{\tilde{\phi}_{\mathrm{sur}}^2(\sigma)}\right)^2$$

renorm. up to M_{Pl}-suppressed op.?

Hybrid metric-Palatini

$$S = \int \mathrm{d}^4x\sqrt{-g}\left[\frac{1}{2}M_{\mathrm{Pl}}^2 R^{\mathrm{Palatini}} + \frac{1}{2}(\xi_g R^{\mathrm{metric}} + \xi_\Gamma R^{\mathrm{Palatini}})\,|\mathscr{H}|^2 - \frac{1}{2}|\partial_\mu \mathscr{H}|^2 - \frac{\lambda}{4}|\mathscr{H}|^4\right]$$

- $\xi_g = 0 \quad \rightarrow$ Palatini Higgs inflation
- $\xi_\Gamma = 0$

$$S \supset \int \mathrm{d}^4x\sqrt{-g}\left[\frac{1}{2}M_{\mathrm{Pl}}^2 \boxed{R^{\mathrm{Palatini}}} + \frac{1}{2}\xi_g R^{\mathrm{metric}}|\mathscr{H}|^2\right] \qquad \text{metric Higgs inflation}$$

EL const. $\rightarrow R^{\mathrm{metric}}$

Inf. pheno. COBE norm.

$n_{\mathrm{s}} \simeq 0.96, \quad r \lesssim 10^{-3}$

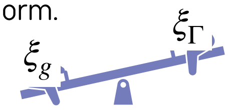

Hybrid metric-Palatini

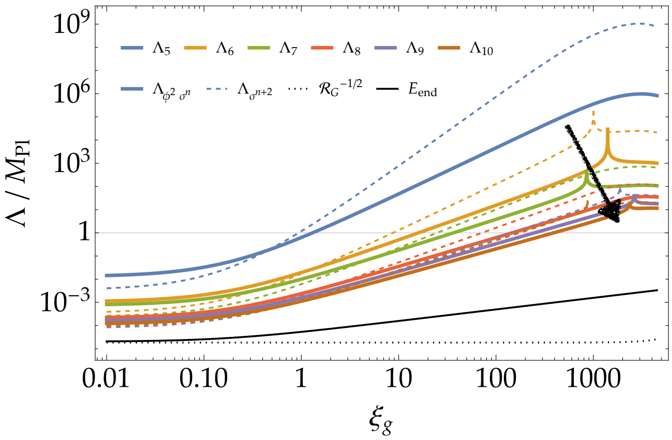

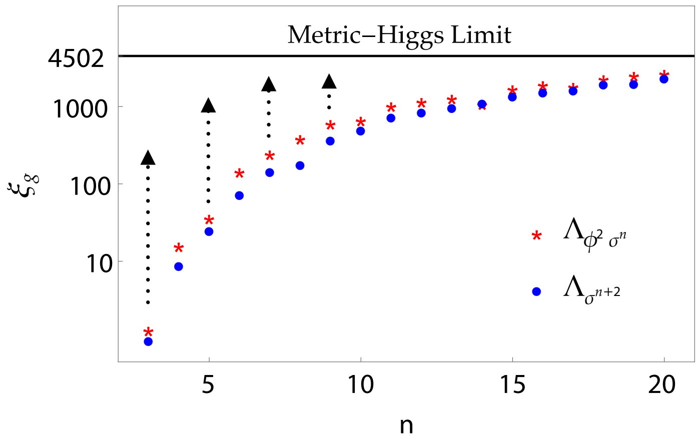

Conclusions

by direct embedding

- metric Higgs is UV-completed up to $M_{\rm Pl}$
- cutoff in Palatini Higgs does not change so much
- cutoff in hybrid mP Higgs can be uplifted,

  but $M_{\rm Pl}$-completion is realized only in the metric limit

C20

Anisotropic warm inflation

Ann Nakato
Kobe university Cosmology group

Ref. Sugumi Kanno, **Ann Nakato**, Jiro Soda, Kazushige Ueda, [arXiv:2209.05776]

Contents

1. Background
   - Cosmic no-hair theorem
   - Anisotropic inflation
   - Warm inflation
2. Motivation
3. Anisotropic warm inflation
4. Analysis
   - Dynamical system approach
5. Summary
6. Next step

Cosmic no-hair theorem

[Wald'1983]

Irrespective of initial conditions, rapid cosmic expansion driven by a positive cosmological constant makes

1. the energy density of ordinary matter vanish
2. anisotropy of the spacetime vanish
3. spatial curvature vanish

Anisotropic inflation and warm inflation

Anisotropic inflation

[Watanabe-Kanno-Soda'09]

$$S = \int d^4x\sqrt{-g}\left[\frac{M_{\rm pl}^2}{2}R - \frac{1}{2}(\partial_\mu\phi)(\partial^\mu\phi) - V(\phi) - \underline{\frac{1}{4}f^2(\phi)F_{\mu\nu}F^{\mu\nu}}\right]$$

- A dynamical cosmological constant due to a gauge field can make anisotropic universe
- Anisotropic inflation predicts statistical anisotropy

Warm inflation

$$S = \int d^4x\sqrt{-g}\left[\frac{M_{\rm pl}^2}{2}R - \frac{1}{2}(\partial_\mu\phi)(\partial^\mu\phi) - V(\phi) + \underline{\mathscr{L}_{\rm free}\left(\psi_{\rm matter}\right) + \mathscr{L}_{\rm int}\left(\phi, \psi_{\rm matter}\right)}\right]$$

- A coupling between inflaton and ordinary matter cause to the decay of the inflaton during inflation
- Warm inflation provides an automatic reheating

Motivation

Counterexamples give the following situation

	Isotropy	Anisotropy
Cold (No dissipation)	○ Standard inflation	○ Anisotropic inflation
Warm (dissipation)	○ Warm inflation	?

We study whether **anisotropic warm inflation** can occur

Warm inflation review

[Berghaus_Graham_Kaplan'20]

Warm inflation set up

$$S = \int d^4x\sqrt{-g}\left[\frac{M_{\rm pl}^2}{2}R - \frac{1}{2}(\partial_\mu\phi)(\partial^\mu\phi) - V(\phi) + \underline{\mathcal{L}_{\rm free}\left(\psi_{\rm matter}\right) + \mathcal{L}_{\rm int}\left(\phi, \psi_{\rm matter}\right)}\right]$$

$$ds^2 = -dt^2 + a(t)^2\,\delta_{ij}\,dx^i dx^j$$

Basic equation

- "Q" is a dissipation term for the dissipation caused by the decay of the inflaton into matter
- In general, Q depends on Inflaton field, temperature, etc. , but we analyze it as a constant.

$$\ddot{\phi} + 3H\left(1 + \underline{Q}\right)\dot{\phi} + V'\left(\phi\right) = 0$$

$$H^2 = \frac{1}{3M_{\rm pl}^2}\left(V(\phi) + \frac{1}{2}\dot{\phi}^2 + \underline{\rho_{\rm R}}\right)$$

$$\dot{\rho}_{\rm R} + 4H\rho_{\rm R} = \underline{\Upsilon\dot{\phi}^2}$$

ρ_R Radiation by inflaton decay

$\Upsilon = 3HQ$

Anisotropic warm inflation

- A combination of anisotropic inflation and warm inflation
- A gauge $A_0 = 0$, $A_\mu = (0, A(t), 0, 0)$ and the direction does not change during inflation
- The metric is also anisotropic in the x-axis direction

Anisotropic warm inflation set up

$$S = \int d^4x\sqrt{-g}\left[\frac{M_{\rm pl}^2}{2}R - \frac{1}{2}(\partial_\mu\phi)(\partial^\mu\phi) - V(\phi) \underbrace{- \frac{1}{4}f^2(\phi)F_{\mu\nu}F^{\mu\nu}}_{\text{Gauge field}} + \underbrace{\mathscr{L}_{\rm free}\left(\psi_{\rm matter}\right) + \mathscr{L}_{\rm int}\left(\phi, \psi_{\rm matter}\right)}_{\text{Ordinary matter field}}\right]$$

$$ds^2 = -dt^2 + e^{2\alpha(t)}\left[\underline{e^{-4\sigma(t)}}dx^2 + \underline{e^{2\sigma(t)}}(dy^2 + dz^2)\right]$$

Gauge kinetic function

$$f(\phi) = \exp\left[\frac{2c}{M_{\rm pl}^2}\int\frac{V}{V'}d\phi\right]$$

c : Coupling constant of gauge field

Evolution of anisotropy of anisotropic warm inflation

By solving the basic equation series, under the condition of $c > 1 + Q$, degree of anisotropy is

$$\frac{\Sigma}{H} \equiv \frac{\dot\sigma}{\dot\alpha} = \frac{2}{3}\frac{\rho_A}{V(\phi)} \xrightarrow{\alpha\to\infty} \frac{1}{3}\frac{(c-1-Q)(1+Q)}{c^2}\epsilon_V$$

$\dot\sigma$ Expansion rate of anisotropy
$\dot\alpha$ Hubble parameter

Anisotropy exists under the condition

No dissipation Q=0	$c > 1$
Dissipation Q≠0	$c > 1 + Q$

c : Coupling constant of gauge field

→The condition for anisotropy growth gets tight in the presence of dissipation

Dynamical system approach for power-law potential

dimensionless variables

$$X = \frac{\dot{\sigma}}{\dot{\alpha}} \qquad Y = \frac{1}{M_{\rm pl}}\frac{\dot{\phi}}{\dot{\alpha}} \qquad Z = p_A \frac{f^{-1}(\phi)}{M_{\rm pl}\,\dot{\alpha}} e^{-2\alpha-2\sigma} \qquad W = \frac{\rho_{\rm R}}{M_{\rm pl}^2 \dot{\alpha}^2}$$

Anisotropy | velocity of Inflaton | Energy density of gauge field | Energy density of radiation

power-law potential

$$V(\phi) = V_0 \exp\left[\lambda \frac{\phi}{M_{\rm pl}}\right] \qquad f(\phi) = f_0 \exp\left[\kappa \frac{\phi}{M_{\rm pl}}\right] \qquad \kappa = \frac{2c}{\lambda}$$

Dynamical system approach for power-law potential

Basic equation

X	Anisotropy
Y	Velocity of Inflaton
Z	Energy density of gauge field
W	Energy density of radiation

$$\frac{dX}{d\alpha} = \frac{1}{3}Z^2(X+1) + X\left[3(X^2-1) + \frac{1}{2}Y^2 + \frac{2}{3}W\right]$$

$$\frac{dY}{d\alpha} = \kappa Z^2 + \lambda\left[3(X^2-1) + \frac{1}{2}Y^2 + \frac{1}{2}Z^2 + W\right] + Y\left[-3(1+Q) + 3X^2 + \frac{1}{2}Y^2 + \frac{1}{3}Z^2 + \frac{2}{3}W\right]$$

$$\frac{dZ}{d\alpha} = Z\left[-\kappa Y - 2(X+1) + 3X^2 + \frac{1}{2}Y^2 + \frac{1}{3}Z^2 + \frac{2}{3}W\right]$$

$$\frac{dW}{d\alpha} = 3QY^2 - 4W + 6WX^2 + WY^2 + \frac{2}{3}WZ^2 + \frac{4}{3}W^2$$

- Calculate fixed points

→Exact analytical solution was obtained and two fixed points were found, which are warm inflation and anisotropic warm inflation

Phase structure of anisotropic warm inflation under $c > 1 + Q$

Dissipation : Q=0.3
Gauge filed : κ=50
Inflaton potential : λ=0.1

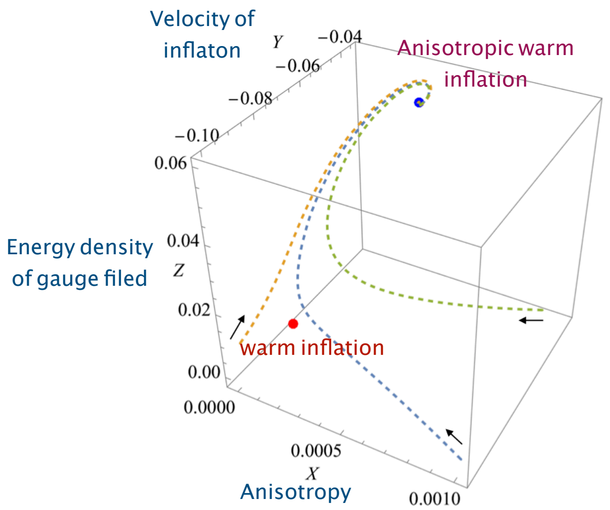

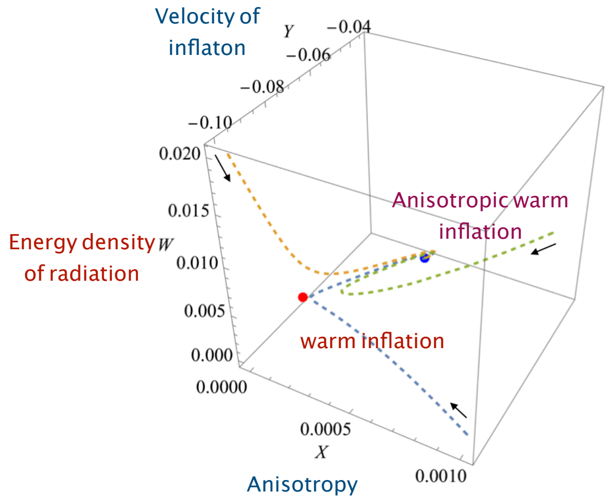

- Two fixed points appear
- Universe evolves to warm inflation first, after that, toward the anisotropic warm inflation
- If Inflation period is enough long, we can see anisotropic warm inflation

Phase structure of anisotropic warm inflation with large dissipation under $c < 1 + Q$

Dissipation : Q=3
Gauge filed : κ=50
Inflaton potential λ=0.1

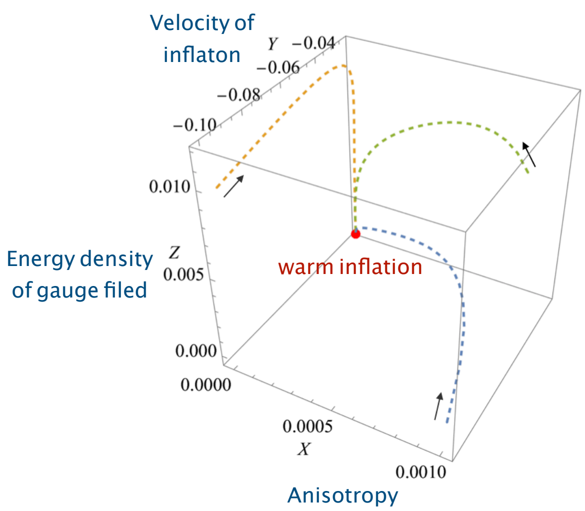

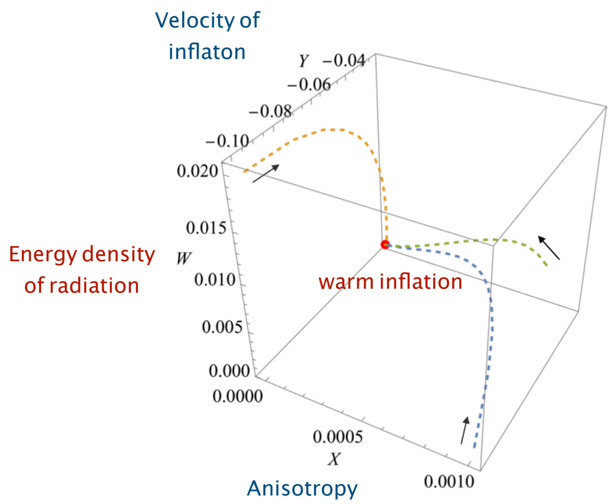

- The fixed point of anisotropic warm inflation disappears
- Warm inflation becomes attractor
- it was confirmed that large dissipation tends to erase the anisotropy

Summary

The following situation is updated

	Isotropy	**Anisotropy**
Cold (No dissipation)	○ **Standard inflation**	○ **Anisotropic inflation** c>1
Warm (dissipation)	○ **Warm inflation**	△ **Anisotropic warm inflation** c>1+Q

Phase space structure tells us that decay speed of inflaton is

Very slow Anisotropy is realized

Slow Anisotropy tend to be hard to grow enough within the duration of inflation

Rapid No anisotropic inflation occurs

Next step

- In this paper, we assumed the dissipation Q is constant. In general, the dissipation depends on the inflaton field, temperature and the mass of the inflaton field. It would be worth investigating more realistic models in detail
- Particle production during inflation produces a thermal bath. Therefore, the effect of thermal fluctuations should remain in the CMB on the top of the quantum fluctuations. So the spectrum of fluctuations should be calculated in future

End

SU(N)-natural inflation in axisymmetric background

Rikkyo University (D1) : Tomoaki Murata
Collaborator : Tomohiro Fujita (WIAS)
Tsutomu Kobayashi

Based on work with
・TM, T. Fujita, T. Kobayashi, arXiv:2211.xxxxx

JGRG31 2022/10/25

Introduction

■ Inflation: accelerated expansion in the early universe

■ Initial conditions of the standard big-bang model
…homogeneity, isotropy, spatially flat
→ Inflation can explain in a natural way

■ Starting from generic initial conditions?
…inhomogeneity, anisotropy, spatial curvature

Do **anisotropic** initial conditions lead to an isotropic solution?

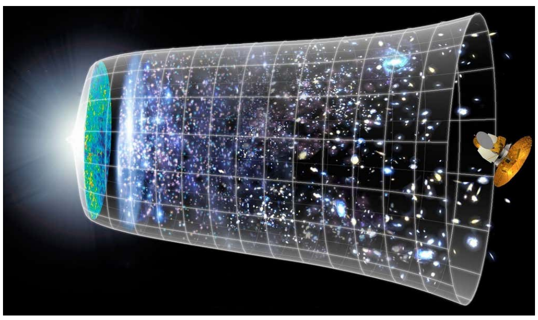

Introduction

Cosmic no-hair theorem [R. Wald(1983)]
Positive cosmological constant + standard matter
→ All Bianchi type (except type IX)
evolve toward de Sitter solution

- Scalar field + vector field [M. Watanabe, et al.(2009)]
  accelerated expansion but remain anisotropy

- SU(N)-natural inflation model [T. Fujita, et al.(2021)]
  Scalar field + SU(N) gauge field
  → It is non-trivial to isotropize

Motivation 1
Does SU(N)-natural model have an isotropic attractor solution?

Outline

- Introduction
- SU(N)-natural inflation model
  - SU(N)-natural inflation model
  - Isotropic solution
- Axisymmetric background
- Numerical result
- Conclusion

SU(N)-natural inflation

■ SU(N) gauge fields： $A = A^a_\mu \mathrm{d}x^\mu \underline{T^a}$

The SU(N) generator：$[T^a, T^b] = i f^{abc} T^c$

f^{abc} : Structure constant of SU(N)

$\mu, \nu, .. = 0, .., 3$
$i,\ j, .. = 1, .., 3$
$a, b, .. = 1, .., N^2 - 1$

■ Field strength of SU(N) gauge fields：

$$F^a_{\mu\nu} = \partial_\mu A^a_\nu - \partial_\nu A^a_\mu + g_A f^{abc} A^b_\mu A^c_\nu$$

g_A: gauge coupling

■ Lagrangian：

$$\mathcal{L} = \frac{M_{\rm Pl}^2}{2} R - \frac{1}{4} F^a_{\mu\nu} F^{\mu\nu}_a - \frac{1}{2} (\partial\phi)^2 - V(\phi) - \frac{\phi}{4f} F^a_{\mu\nu} \widetilde{F}^{\mu\nu}_a$$

(N=2 → axion-SU(2) model)

$c = \hbar = 1$

Isotropic solution

[T. Fujita, K. Murai & R. Namba(2022)]

■ The SU(2) subalgebra (SU(2) ⊂ SU(N))

$$\mathcal{T}_i := n^a_i T^a \longrightarrow [\mathcal{T}_i, \mathcal{T}_j] = i\,\underline{\lambda}\,\epsilon_{ijk} \mathcal{T}_k, \quad \mathrm{Tr}(\mathcal{T}_i \mathcal{T}_j) = \frac{1}{2}\delta_{ij}$$

λ is a value depending on the choice of the SU(2) subalgebra

Examples. SU(2) → 1
SU(3) → 1 or 1/2

■ Static solution of the gauge field ($A_0 = 0, \quad A_i = a\psi \mathcal{T}_i$)

$$\psi = \left(-\frac{f V_{,\phi}}{3 g_A \lambda H} \right)^{1/3} \propto \lambda^{-1/3}$$

→ The amplitude of the gauge field is characterized by λ

Isotropic solution

[T. Fujita, K. Murai & R. Namba(2022)]

■ The SU(2) subalgebra (SU(2) ⊂ SU(N))

$$\mathcal{T}_i := n_i^a T^a \longrightarrow [\mathcal{T}_i, \mathcal{T}_j] = i\,\underline{\lambda}\,\epsilon_{ijk}\mathcal{T}_k, \quad \mathrm{Tr}(\mathcal{T}_i\mathcal{T}_j) = \frac{1}{2}\delta_{ij}$$

λ is a value depending on the choice of the SU(2) subalgebra

Examples. SU(2) $\rightarrow$ 1
SU(3) $\rightarrow$ 1 or 1/2

■ Static solution of the gauge field ($A_0 = 0, \quad A_i = a\psi\mathcal{T}_i$)

$$\psi = \left(-\frac{fV_{,\phi}}{3g_A\lambda H}\right)^{1/3} \propto \lambda^{-1/3}$$

→ The amplitude of the gauge field is characterized by λ

Isotropic solution

[T. Fujita, K. Murai & R. Namba(2022)]

■ The SU(2) subalgebra (SU(2) ⊂ SU(N))

$$\mathcal{T}_i := n_i^a T^a \longrightarrow [\mathcal{T}_i, \mathcal{T}_j] = i\,\underline{\lambda}\,\epsilon_{ijk}\mathcal{T}_k, \quad \mathrm{Tr}(\mathcal{T}_i\mathcal{T}_j) = \frac{1}{2}\delta_{ij}$$

λ is a value depending on the choice of the SU(2) subalgebra

Examples. SU(2) $\rightarrow$ 1
SU(3) $\rightarrow$ 1 or 1/2

■ Static solution of the gauge field ($A_0 = 0, \quad A_i = a\psi\mathcal{T}_i$)

$$\psi = \left(-\frac{fV_{,\phi}}{3g_A\lambda H}\right)^{1/3} \propto \lambda^{-1/3}$$

→ The amplitude of the gauge field is characterized by λ

SU(N) vs SU(2) [T. Fujita, K. Murai & R. Namba(2022)]

■ However, g_A and λ are degenerated

$$F_{\mu\nu} = \partial_\mu A_\nu - \partial_\nu A_\mu - \underline{ig_A[A_\mu, A_\nu]}$$
$$\propto [\mathcal{T}_i, \mathcal{T}_j] = i\,\underline{\lambda}\,\epsilon_{ijk}\mathcal{T}_k$$

This degeneracy also occurs at the linear perturbation level
→ Qualitatively same as axion-SU(2) model $(g_A\lambda \to g_A)$

■ One way to break the degeneracy is
the **transition** of the SU(2) subalgebra

Motivation 2

Does SU(N)-natural model occur transitions?

SU(N) vs SU(2) [T. Fujita, K. Murai & R. Namba(2022)]

■ However, g_A and λ are degenerated

$$F_{\mu\nu} = \partial_\mu A_\nu - \partial_\nu A_\mu - \underline{ig_A[A_\mu, A_\nu]}$$
$$\propto [\mathcal{T}_i, \mathcal{T}_j] = i\,\underline{\lambda}\,\epsilon_{ijk}\mathcal{T}_k$$

This degeneracy also occurs at the linear perturbation level
→ Qualitatively same as axion-SU(2) model $(g_A\lambda \to g_A)$

■ One way to break the degeneracy is
the **transition** of the SU(2) subalgebra

Motivation 2

Does SU(N)-natural model occur transitions?

SU(N) vs SU(2) [T. Fujita, K. Murai & R. Namba(2022)]

■ However, g_A and λ are degenerated

$$F_{\mu\nu} = \partial_\mu A_\nu - \partial_\nu A_\mu - \underline{ig_A[A_\mu, A_\nu]}$$
$$\propto [\mathcal{T}_i, \mathcal{T}_j] = i\,\underline{\lambda}\,\epsilon_{ijk}\mathcal{T}_k$$

This degeneracy also occurs at the linear perturbation level
→ Qualitatively same as axion-SU(2) model $(g_A\lambda \to g_A)$

■ One way to break the degeneracy is
the **transition** of the SU(2) subalgebra

Motivation 2

Does SU(N)-natural model occur transitions?

Outline

■ Introduction

■ SU(N)-natural inflation model

■ Axisymmetric background

◆ Axisymmetric metric

◆ Axisymmetric SU(3) gauge field

■ Numerical result

■ Conclusion

Anisotropic metric

■ Axisymmetric Bianchi type-I metric

$$\mathrm{d}s^2 = -\mathrm{d}t^2 + a^2(t)\left[e^{-4\sigma(t)}\mathrm{d}x^2 + e^{2\sigma(t)}\left(\mathrm{d}y^2 + \mathrm{d}z^2\right)\right]$$

a : scale factor

σ : anisotropy of metric

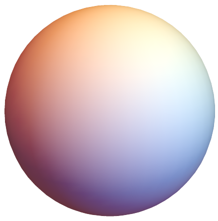

isotropic ($\sigma = 0$)

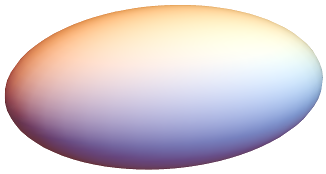

Bianchi Type-I

Axisymmetric SU(3) gauge field

■ Configurations

$$\begin{aligned} A_x &= ae^{-2\sigma}\psi_x \\ A_y &= ae^{\sigma}\psi_y \\ A_z &= ae^{\sigma}\psi_z \end{aligned} \quad \longrightarrow \quad \begin{aligned} \psi_x &= \psi_1 T^1 + \psi_8 T^8 \\ \psi_y &= \psi_4 T^4 + \psi_5 T^5 + \psi_6 T^6 + \psi_7 T^7 \\ \psi_z &= -\psi_7 T^4 + \psi_6 T^5 - \psi_5 T^6 + \psi_4 T^7 \end{aligned}$$

■ The isotropic subset of this configuration has two branches

$$\boxed{\begin{aligned} &\lambda = \frac{1}{2} \quad \rightarrow \quad \psi_8 = 0 \quad \text{and} \quad \psi_4\psi_6 + \psi_5\psi_7 = 0 \\ &\lambda = 1 \quad \rightarrow \quad \text{Otherwise} \end{aligned}}$$

Axisymmetric SU(3) gauge field

■ Configurations

$$A_x = ae^{-2\sigma}\psi_x \qquad \psi_x = \psi_1 T^1 + \psi_8 T^8$$
$$A_y = ae^{\sigma}\psi_y \quad \longrightarrow \quad \psi_y = \psi_4 T^4 + \psi_5 T^5 + \psi_6 T^6 + \psi_7 T^7$$
$$A_z = ae^{\sigma}\psi_z \qquad \psi_z = -\psi_7 T^4 + \psi_6 T^5 - \psi_5 T^6 + \psi_4 T^7$$

■ The isotropic subset of this configuration has two branches

$$\boxed{\begin{array}{lll} \lambda = \frac{1}{2} & \rightarrow & \psi_8 = 0 \;\; \text{and} \;\; \psi_4\psi_6 + \psi_5\psi_7 = 0 \\ \lambda = 1 & \rightarrow & \text{Otherwise} \end{array}}$$

Outline

■ Introduction

■ SU(N)-natural inflation model

■ Axisymmetric background

■ Numerical result

◆ Setup

◆ Result

■ Conclusion

Numerical setup

■ Normalized mean amplitude of the gauge field

$$\Psi^2(t) := \left(\frac{3g_A H(t)}{\mu^4}\right)^{2/3} \sum_a \frac{[\psi_a(t)]^2}{3} \qquad (a = 1,4,5,6,7,8)$$

$\Psi(t)$ converges to $\lambda^{-1/3}$ when isotropic

$$\lambda = 1 \quad \rightarrow \quad \Psi = 1$$

$$\lambda = \frac{1}{2} \quad \rightarrow \quad \Psi \simeq 1.26$$

Time evolution of the gauge field

Ψ : Normalized mean amplitude of the gauge field

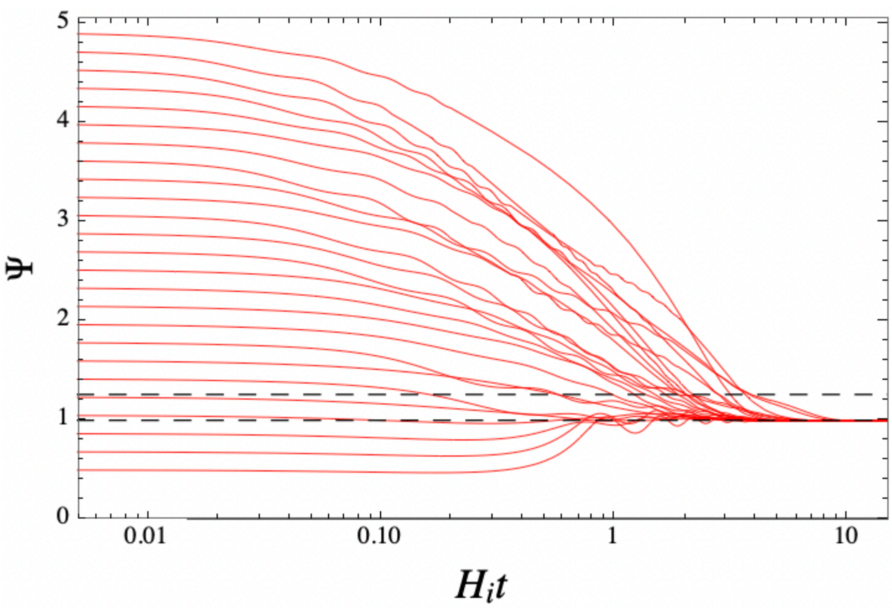

$\lambda = \frac{1}{2}$

$\lambda = 1$

Time evolution of the gauge field

Ψ : Normalized mean amplitude of the gauge field

Blue line: random initial conditions with

$$\begin{cases} \psi_8 = 0 \\ \psi_4\psi_6 + \psi_5\psi_7 = 0 \end{cases}$$

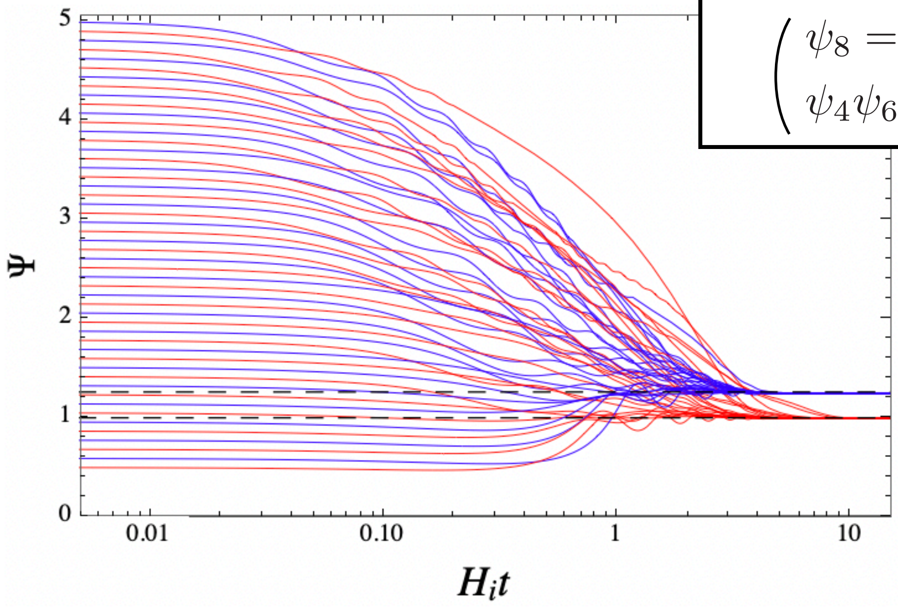

$\lambda = \frac{1}{2}$

$\lambda = 1$

Time evolution of the gauge field

Ψ : Normalized mean amplitude of the gauge field

Blue line: random initial conditions with

$$\begin{cases} \psi_8 = 0 \\ \psi_4\psi_6 + \psi_5\psi_7 = 0 \end{cases}$$

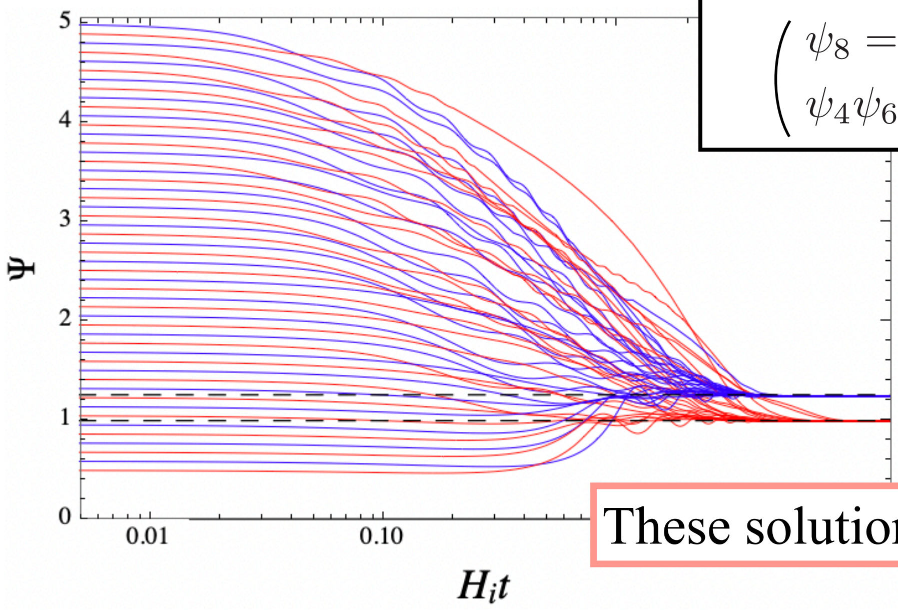

$\lambda = \frac{1}{2}$

$\lambda = 1$

These solutions are isotropize!

Transition of SU(2) subalgebra

$$\lambda = \frac{1}{2} \quad \longrightarrow \left(\begin{array}{l} \psi_8 = 0 \\ \psi_4 \psi_6 + \psi_5 \psi_7 = 0 \end{array} \right.$$

Transition of SU(2) subalgebra

$$\lambda = \frac{1}{2} \quad \longrightarrow \left(\begin{array}{l} \psi_8 = 0 \quad \leftarrow \text{perturbative} \\ \psi_4 \psi_6 + \psi_5 \psi_7 = 0 \end{array} \right.$$

Transition of SU(2) subalgebra

$$\lambda = \frac{1}{2} \quad \longrightarrow \quad \left(\begin{array}{l} \psi_8 = 0 \quad \leftarrow \text{perturbative} \\ \psi_4\psi_6 + \psi_5\psi_7 = 0 \end{array} \right.$$

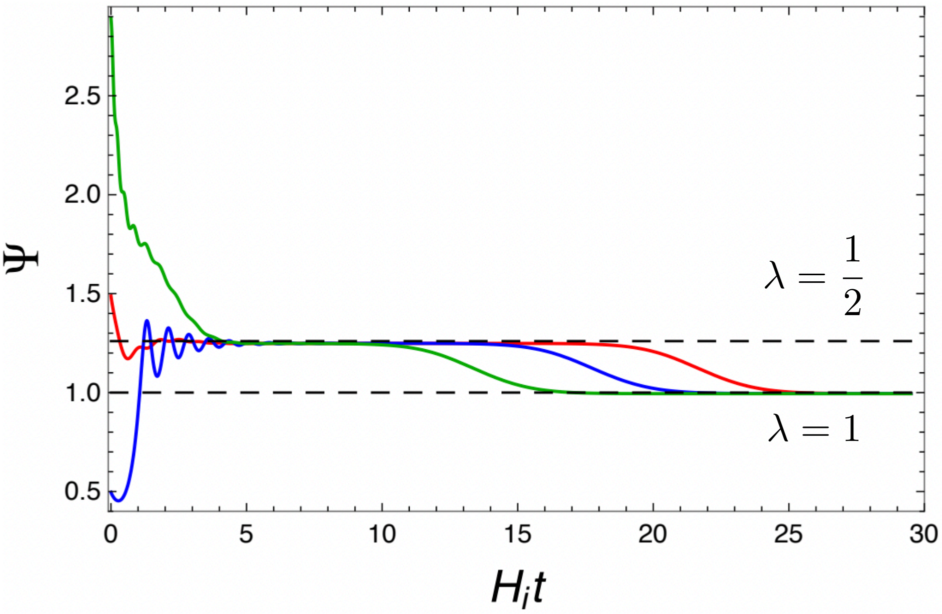

Stability analysis

■ The background gauge field realize $\lambda = 1/2$

$$\psi_1,\ \psi_4,\ \psi_7 \simeq \frac{2H}{g_A} m_\psi$$

m_ψ : dimensionless gauge field amplitude

■ Add the perturbation that breaking **the condition of λ=1/2**

$$\psi_5 = \delta\psi_5 \qquad \left(\begin{array}{l} \psi_8 = 0 \\ \psi_4\psi_6 + \psi_5\psi_7 = 0 \end{array} \right.$$

$$\psi_6 = \delta\psi_6$$

$$\psi_8 = \delta\psi_8$$

$$\rightarrow \quad \delta\psi_{5,6,8} \propto a^{-\frac{3}{2}+\frac{1}{2}\sqrt{25-24m_\psi^2}}$$

$$\simeq a \quad (m_\psi \sim 0.07)$$

Stability analysis

- The background gauge field realize $\lambda = 1/2$

$$\psi_1,\ \psi_4,\ \psi_7 \simeq \frac{2H}{g_A} m_\psi$$

m_ψ : dimensionless gauge field amplitude

- Add the <u>perturbation</u> that breaking <u>**the condition of λ=1/2**</u>

$$\psi_5 = \delta\psi_5 \qquad \psi_6 = \delta\psi_6 \qquad \psi_8 = \delta\psi_8$$

$$\left(\begin{array}{l} \psi_8 = 0 \\ \psi_4\psi_6 + \psi_5\psi_7 = 0 \end{array} \right.$$

$$\rightarrow \quad \delta\psi_{5,6,8} \propto a^{-\frac{3}{2}+\frac{1}{2}\sqrt{25-24m_\psi^2}}$$

$$\simeq a \quad (m_\psi \sim 0.07)$$

Stability analysis

- The background gauge field realize $\lambda = 1/2$

$$\psi_1,\ \psi_4,\ \psi_7 \simeq \frac{2H}{g_A} m_\psi$$

m_ψ : dimensionless gauge field amplitude

- Add the <u>perturbation</u> that breaking <u>**the condition of λ=1/2**</u>

$$\psi_5 = \delta\psi_5 \qquad \psi_6 = \delta\psi_6 \qquad \psi_8 = \delta\psi_8$$

$$\left(\begin{array}{l} \psi_8 = 0 \\ \psi_4\psi_6 + \psi_5\psi_7 = 0 \end{array} \right.$$

$$\rightarrow \quad \delta\psi_{5,6,8} \propto a^{-\frac{3}{2}+\frac{1}{2}\sqrt{25-24m_\psi^2}}$$

$$\simeq a \quad (m_\psi \sim 0.07)$$

Stability analysis

- The background gauge field realize $\lambda = 1/2$

$$\psi_1,\ \psi_4,\ \psi_7 \simeq \frac{2H}{g_A} m_\psi$$

m_ψ : dimensionless gauge field amplitude

- Add the <u>perturbation</u> that breaking **<u>the condition of λ=1/2</u>**

$$\psi_5 = \delta\psi_5 \qquad \psi_6 = \delta\psi_6 \qquad \psi_8 = \delta\psi_8$$

$$\left(\begin{array}{l} \psi_8 = 0 \\ \psi_4\psi_6 + \psi_5\psi_7 = 0 \end{array} \right.$$

$$\rightarrow\ \delta\psi_{5,6,8} \propto a^{-\frac{3}{2}+\frac{1}{2}\sqrt{25-24m_\psi^2}}$$

$$\simeq a \quad (m_\psi \sim 0.07)$$

Exist the growing mode!

Numerical result

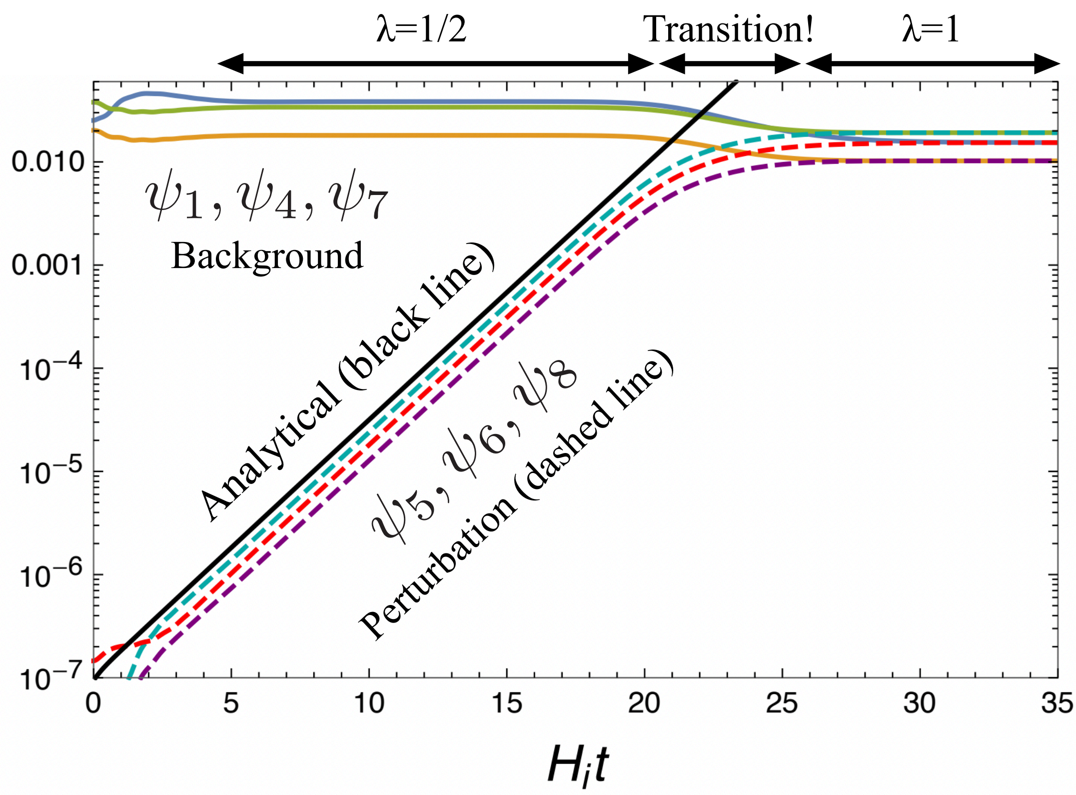

Numerical result

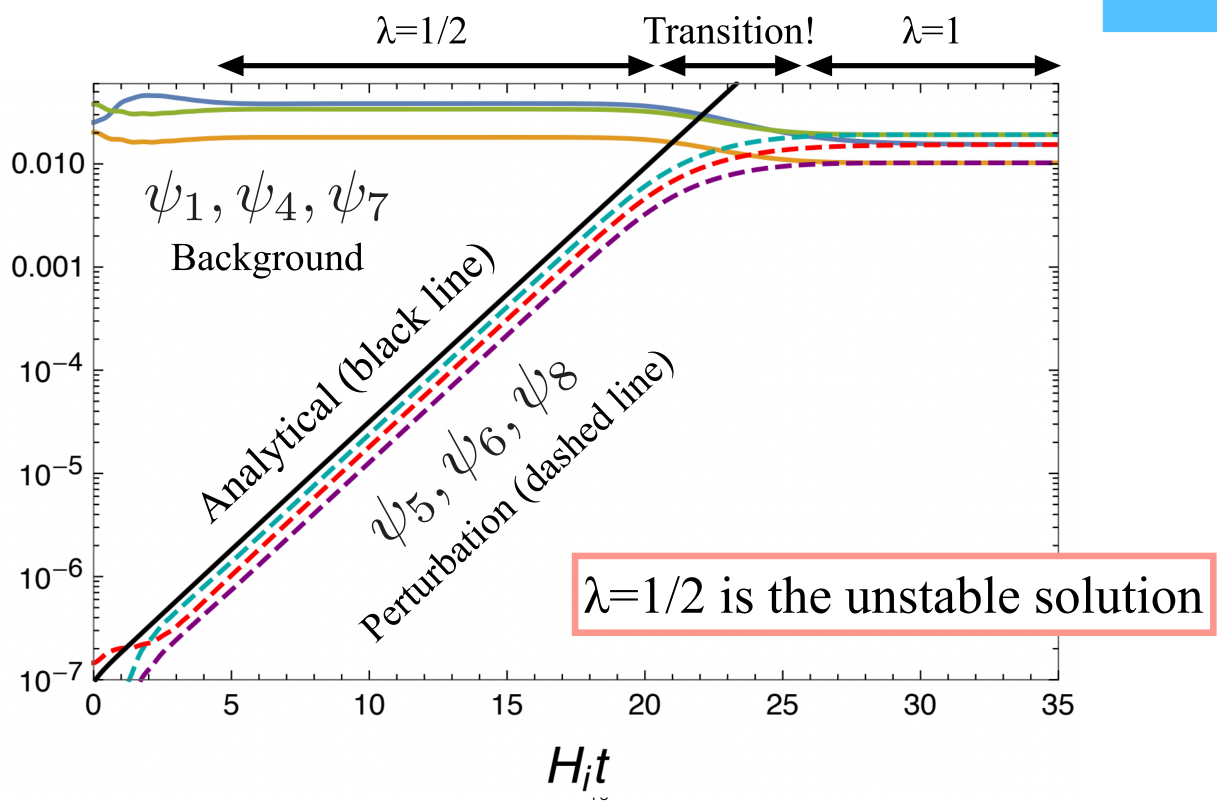

Conclusion

- SU(N)-natural inflation model constructs isotropic solutions with SU(2) subalgebra
- Isotropic solutions can be obtained even starting from axisymmetric configurations
- λ=1/2 is the unstable solution
- We found the possibility of transition
  → It would be a distinctive signal of SU(N)-natural inflation
- Future work:
  Primordial gravitational waves with transitions

ika yobi

Numerical result

Ψ : Normalized mean amplitude of the gauge field

Random initial conditions

$$\begin{cases} A_x^8 = 0 \\ A_y^4 A_y^6 + A_y^5 A_y^7 = 0 \end{cases}$$

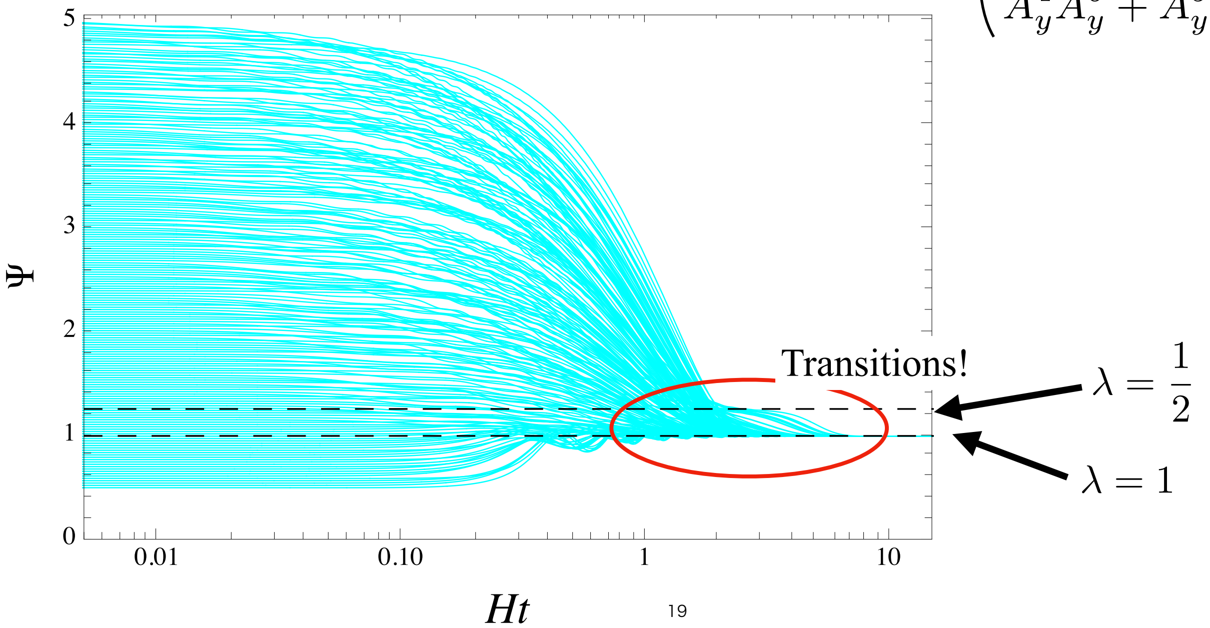

Commutation relation

■ Isotropic solution and the SU(2) subalgebra

$$A_i = \sqrt{2}|A|\mathcal{T}_i \qquad [\mathcal{T}_i, \mathcal{T}_j] = i\,\lambda\,\epsilon_{ijk}\mathcal{T}_k$$

■ The isotropic gauge field satisfies the commutation relation:

$$[A_i, A_j] = \sqrt{2}i\lambda|A|\epsilon_{ijk}A_k$$

■ We solve algebraic equations

$$[A_x, A_y] - \sqrt{2}i\lambda|A|A_z = 0$$

$$[A_y, A_z] - \sqrt{2}i\lambda|A|A_x = 0$$

$$\boxed{\begin{aligned} A_x &= A_x^1T^1 + A_x^8T^8 \\ A_y &= A_y^4T^4 + A_y^5T^5 + A_y^6T^6 + A_y^7T^7 \\ A_z &= -A_y^7T^4 + A_y^6T^5 - A_y^5T^6 + A_y^4T^7 \end{aligned}}$$

※ Due to axisymmetric, we only consider these two equations

C22

One-loop perturbativity bound in single-field inflation

Jason Kristiano (PhD student in The University of Tokyo)
References: JCAP 07 (2022) 007 and PRL 128, 061301 (2022)

The 31st Workshop on General Relativity and Gravitation in Japan

Introduction

Quantum fluctuations stretched by cosmic inflation is currently the leading theory to explain the origin of CMB fluctuations and large scale structure.

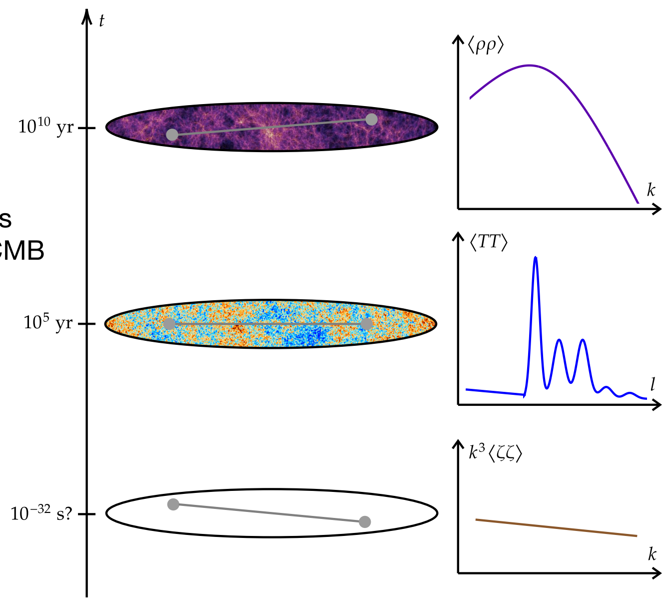

Fluctuations in CMB

Observed by Planck 2018:

- Almost normally distributed (Gaussian).
- Almost scale-invariant.
- Correlated over super-horizon scale.

Fluctuation: $\zeta \approx \sqrt{\left\langle \frac{\delta T^2}{T^2} \right\rangle} \sim 10^{-5}$

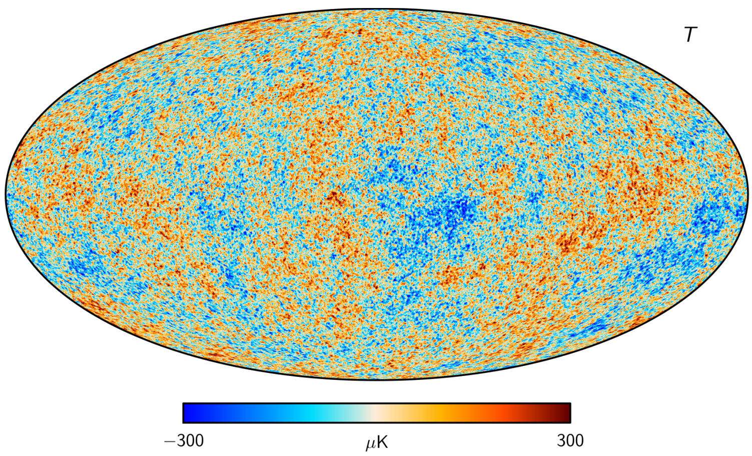

Model building of inflation

Physical mechanism of inflation is still unknown. How to determine it?

Top-down approach:

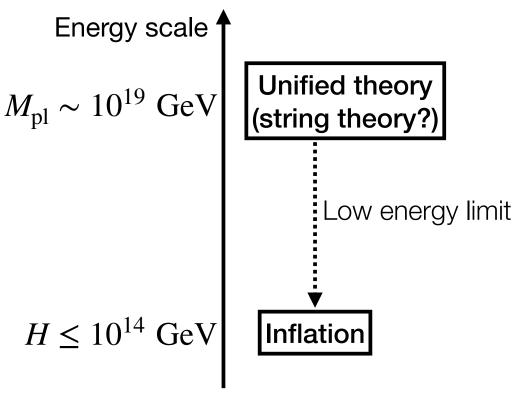

Bottom-up approach:

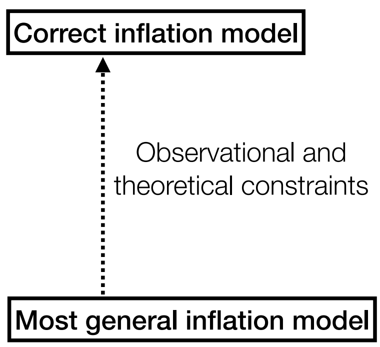

Model building of inflation

An inflation model predicts:

- Deviation from scale-invariant (spectral tilt).
- Deviation from Gaussian distribution (non-Gaussianity).

Observational detection (or bound) of such deviations constrain parameters in an inflation model.

Can we constrain those parameters theoretically by requiring self-consistency of the theory?

In this talk, I will show that requiring perturbativity of higher-order correction to the fluctuations power spectrum leads to a constraint on inflationary parameter space.

k-inflation

Consider k-inflation, the simplest model which can generate large spectrum of non-Gaussianity, with action

$$S = \frac{1}{2}\int \mathrm{d}^4x\sqrt{-g}\left[M_{\mathrm{pl}}^2 R + 2P(X,\phi)\right],$$

where $g = \det\, g_{\mu\nu}$, $g_{\mu\nu}$ is spacetime metric, R is Ricci scalar, ϕ is inflaton, and $X = -\frac{1}{2}\partial^\mu\phi\partial_\mu\phi$.

Armendariz-Picon et. al., PLB 1998

Cosmological perturbations

Small perturbations:

$$\phi(\mathbf{x}, t) = \bar{\phi}(t) + \delta\phi(\mathbf{x}, t),$$

$$\mathrm{d}s^2 = g_{\mu\nu}\mathrm{d}x^\mu \mathrm{d}x^\nu = -N^2\mathrm{d}t^2 + \gamma_{ij}(\mathrm{d}x^i + N^i\mathrm{d}t)(\mathrm{d}x^j + N^j\mathrm{d}t)$$

Gauge fixing condition (comoving gauge): $\delta\phi = 0$ and $\gamma_{ij} = a^2(1+2\zeta)\delta_{ij}$

Some parameters ($\epsilon, \eta, s \ll 1$): $\epsilon = -\dfrac{\dot{H}}{H^2}, \eta = \dfrac{\dot{\epsilon}}{\epsilon H}, s = \dfrac{\dot{c}_s}{c_s H}$, and $c_s^2 = \dfrac{P_{,X}}{P_{,X} + 2XP_{,XX}}$

Two-point functions

Second-order action: $S^{(2)} = M_{\mathrm{pl}}^2 \displaystyle\int \mathrm{d}t\ \mathrm{d}^3x \frac{\epsilon}{c_s^2} a^3 \left[\dot{\zeta}^2 - \frac{c_s^2}{a^2}(\partial_i\zeta)^2\right]$.

Quantization: $\zeta(\mathbf{k}, \tau) = \zeta_k(\tau)a_{\mathbf{k}} + \zeta_k^*(\tau)a^\dagger_{-\mathbf{k}}$ where $\zeta_k(\tau) = \left(\dfrac{H^2}{4M_{\mathrm{pl}}^2\epsilon c_s}\right)_H^{\frac{1}{2}} \dfrac{e^{-ic_sk\tau}}{k^{3/2}}(1 + ic_sk\tau)$ and τ is conformal time defined as $\mathrm{d}t = a\ \mathrm{d}\tau$ with domain $(-\infty, 0)$.

Power spectrum: $\Delta^2_{s(0)}(k) = \dfrac{k^3}{2\pi^2}\langle\zeta(\mathbf{k},0)\zeta(-\mathbf{k},0)\rangle = \left(\dfrac{H^2}{8\pi^2 M_{\mathrm{pl}}^2 c_s\epsilon}\right)_H = \Delta^2_{s(0)}(k_*)\left(\dfrac{k}{k_*}\right)^{n_s-1}$,

where subscript H denotes horizon crossing $c_sk = aH$ and $n_s - 1 = -2\epsilon - \eta - s$.

Feynman-Witten diagram

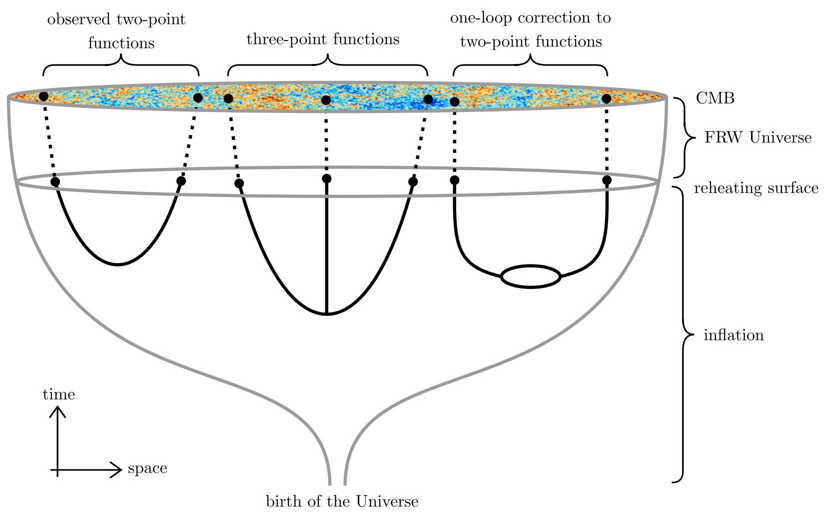

Three-point functions

Leading cubic-order action:

$$S_{\text{int}} = \int \mathrm{d}t\ \mathrm{d}^3x \frac{\epsilon M_{\text{pl}}^2}{H c_s^2} \left[\frac{2\tilde{c}_3}{3c_s^2} a^3 \dot{\zeta}^3 + a\dot{\zeta}(\partial_i \zeta)^2 \right], \text{ where } \frac{\epsilon M_{\text{pl}}^2 H^2}{3c_s^4} \tilde{c}_3 = -X^2 P_{,XX} - (2/3) X^3 P_{,XXX}.$$

Three-point functions: $f_{NL}^{\text{equil}} = \dfrac{5\langle \zeta\zeta\zeta \rangle}{18\langle \zeta\zeta \rangle^2} = \dfrac{1}{c_s^2}(-0.275 - 0.520\tilde{c}_3).$

Chen et. al., JCAP 2009 and Cheung et. al., JHEP 2008

One-loop correction

One-loop correction generated by cubic-order action is computed using in-in perturbation theory:

$$\langle \mathcal{O}(\tau) \rangle = \langle \mathcal{O}(\tau) \rangle^{\dagger}_{(0,2)} + \langle \mathcal{O}(\tau) \rangle_{(1,1)} + \langle \mathcal{O}(\tau) \rangle_{(0,2)}$$

$$\langle \mathcal{O}(\tau) \rangle_{(1,1)} = \int_{-\infty}^{\tau} \mathrm{d}\tau_1 \int_{-\infty}^{\tau} \mathrm{d}\tau_2 \left\langle H_{\mathrm{int}}(\tau_1) \hat{\mathcal{O}}(\tau) H_{\mathrm{int}}(\tau_2) \right\rangle$$

$$\langle \mathcal{O}(\tau) \rangle_{(0,2)} = -\int_{-\infty}^{\tau} \mathrm{d}\tau_1 \int_{-\infty}^{\tau_1} \mathrm{d}\tau_2 \left\langle \hat{\mathcal{O}}(\tau) H_{\mathrm{int}}(\tau_1) H_{\mathrm{int}}(\tau_2) \right\rangle$$

Operator: $\mathcal{O}(\tau_0) = \zeta(\mathbf{p}, \tau_0)\zeta(-\mathbf{p}, \tau_0)$ where $\tau_0 \to 0$.

One-loop correction

Performing loop momentum integration over two regions:

$k \ll p$: $\langle \zeta(\mathbf{p})\zeta(-\mathbf{p}) \rangle_{(1)} \propto \int_0^p \frac{\mathrm{d}^3k}{(2\pi)^3} k \to 0$, means no infrared (IR) divergence.

$k \gg p$: $\langle \zeta(\mathbf{p})\zeta(-\mathbf{p}) \rangle_{(1)} \propto \int_p^{\infty} \frac{\mathrm{d}^3k}{(2\pi)^3} \langle \zeta(\mathbf{k})\zeta(-\mathbf{k}) \rangle_{(0)}$

$$= \int_p^{\infty} \mathrm{d}k\, k^2 \frac{1}{k^3} \Delta^2_{s(0)}(k_*) \left(\frac{k}{k_*} \right)^{n_s - 1} = \frac{\Delta^2_{s(0)}(p)}{1 - n_s}$$

converge for $n_s - 1 < 0$, based on observation $n_s = 0.97$

Kristiano and Yokoyama, PRL 2022

Constraint on parameter space

Total one-loop correction: $\Delta^2_{s(1)}(p) = \dfrac{[\Delta^2_{s(0)}(p)]^2}{1-n_s}\left[\dfrac{51}{40c_s^4} + \dfrac{3}{10c_s^2}\left(\dfrac{\tilde{c}_3}{c_s^2}\right) + \dfrac{1}{15}\left(\dfrac{\tilde{c}_3}{c_s^2}\right)^2\right].$

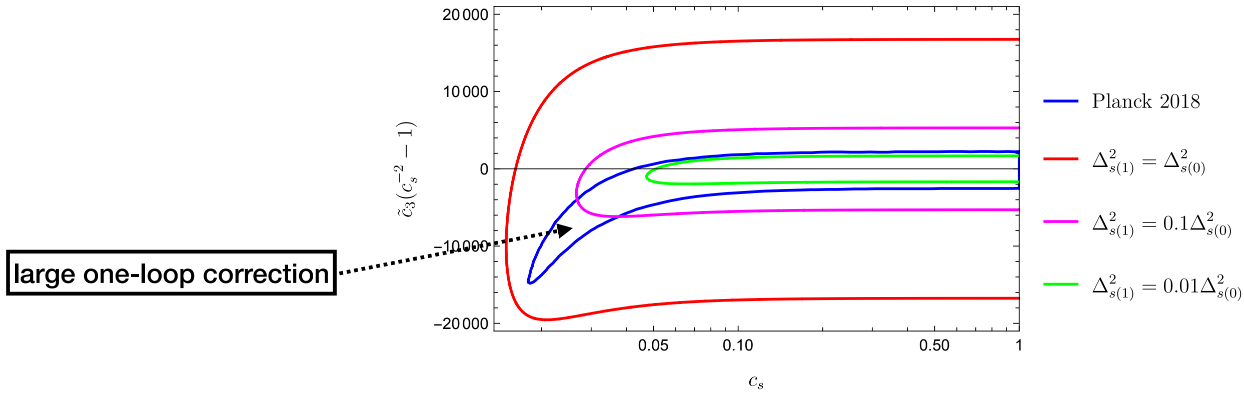

Kristiano and Yokoyama, JCAP 2022

Corrected spectral index

Total power spectrum: $\Delta^2_s(p) = \Delta^2_{s(0)}(p)\left\{1 + \dfrac{\Delta^2_{s(0)}(p)}{1-n_s}\left[\dfrac{51}{40c_s^4} + \dfrac{3}{10c_s^2}\left(\dfrac{\tilde{c}_3}{c_s^2}\right) + \dfrac{1}{15}\left(\dfrac{\tilde{c}_3}{c_s^2}\right)^2\right]\right\}.$

Explicit momentum dependence: $\Delta^2_s(p) = \Delta^2_s(p_*)\left(\dfrac{p}{p_*}\right)^{N_s-1},$

where $N_s - 1 = \dfrac{\mathrm{d}\log\Delta^2_s}{\mathrm{d}\log p} = n_s - 1 - \Delta^2_{s(0)}\left[\dfrac{51}{40c_s^4} + \dfrac{3}{10c_s^2}\left(\dfrac{\tilde{c}_3}{c_s^2}\right) + \dfrac{1}{15}\left(\dfrac{\tilde{c}_3}{c_s^2}\right)^2\right].$

Kristiano and Yokoyama, JCAP 2022

Conclusion

Perturbativity of a theory may not be taken for granted.

Imposing perturbativity leads to a non-trivial constraints to the theory.

Even within the observationally allowed region of non-Gaussianity, one-loop correction can be greater than 0.1 times tree-level contribution, although still smaller than the tree-level itself. If future observation find non-Gaussianity inside this region, it will be important to consider one-loop correction in the cosmological perturbation theory.

The End. Thank You!

Backup slides

Exact scale-invariant limit

Performing dynamical dimensional regularization: $\int \frac{\mathrm{d}^3k}{(2\pi)^3k^3} \to \mu^\epsilon \int \frac{\mathrm{d}^3k}{(2\pi)^3k^{3+\epsilon}} \approx \frac{1}{2\pi^2}\left(\frac{1}{\epsilon} - \log\frac{p}{\mu}\right)$.

Total power spectrum: $\Delta_s^2(p) = \Delta_{s(0)}^2 \left\{1 + \left(\frac{1}{\epsilon} - \log\frac{p}{\mu}\right)\Delta_{s(0)}^2\left[\frac{51}{40c_s^4} + \frac{3}{10c_s^2}\left(\frac{\tilde{c}_3}{c_s^2}\right) + \frac{1}{15}\left(\frac{\tilde{c}_3}{c_s^2}\right)^2\right]\right\}$.

Introducing renormalization factor $\tilde{\Delta}_s^2(p) = Z\Delta_s^2(p)$ with

$Z = 1 - \left(\frac{1}{\epsilon} - \log\frac{\tilde{p}}{\mu}\right)\Delta_{s(0)}^2\left[\frac{51}{40c_s^4} + \frac{3}{10c_s^2}\left(\frac{\tilde{c}_3}{c_s^2}\right) + \frac{1}{15}\left(\frac{\tilde{c}_3}{c_s^2}\right)^2\right]$, and perform renormalization

$$\tilde{\Delta}_s^2(p) = \Delta_{s(0)}^2\left\{1 - \Delta_{s(0)}^2\left[\frac{51}{40c_s^4} + \frac{3}{10c_s^2}\left(\frac{\tilde{c}_3}{c_s^2}\right) + \frac{1}{15}\left(\frac{\tilde{c}_3}{c_s^2}\right)^2\right]\log\frac{p}{\tilde{p}}\right\}.$$

Exact scale-invariant limit

Requiring the total power spectrum to be independent of $\tilde{p}$: $0 = \frac{\partial}{\partial\log\tilde{p}}\log\tilde{\Delta}_s^2(p)$

$$\frac{\partial\log\Delta_{s(0)}^2}{\partial\log\tilde{p}} = -\Delta_{s(0)}^2\left[\frac{51}{40c_s^4} + \frac{3}{10c_s^2}\left(\frac{\tilde{c}_3}{c_s^2}\right) + \frac{1}{15}\left(\frac{\tilde{c}_3}{c_s^2}\right)^2\right].$$

Identifying $\Delta_{s(0)}^2 = \tilde{\Delta}_s^2(\tilde{p})$ and redefining $\tilde{p} \to p$: $\tilde{\Delta}_s^2(p) = \tilde{\Delta}_s^2(p_*)\left(\frac{p}{p_*}\right)^{N_s-1}$,

where $N_s - 1 = -\Delta_{s(0)}^2\left[\frac{51}{40c_s^4} + \frac{3}{10c_s^2}\left(\frac{\tilde{c}_3}{c_s^2}\right) + \frac{1}{15}\left(\frac{\tilde{c}_3}{c_s^2}\right)^2\right]$.

C23

Multi-field inflation with non-minimal coupling in the metric /Palatini formalism

Tatsuki Kodama

in corroboration with

Sang Chul Hyun (Yonsei .U), **Jinsu Kim** (Tongji U.),
Seong Chan Park (Yonsei U.), **Tomo Takahashi** (Saga U.)

(S. C. Hyun, J. Kim, **TK**, S. C. Park, T. Takahashi in preparation)

JGRG31 @ U. of Tokyo 2022/10/25

Introduction

✓ Many minimal single field slow-roll inflation models are excluded by current observational constraints.

(chaotic inf., natural inf. ⇨)

However...

✓ Introducing a scalar field with non-minimal coupling to gravity, some models can be alleviated.

(Higgs inf. / F. L. Bezrukov, M. E. Shaposhnikov [0710.3755]
Non-minimal natural inf. / R. Z. Ferreira et al. [1806,05511])

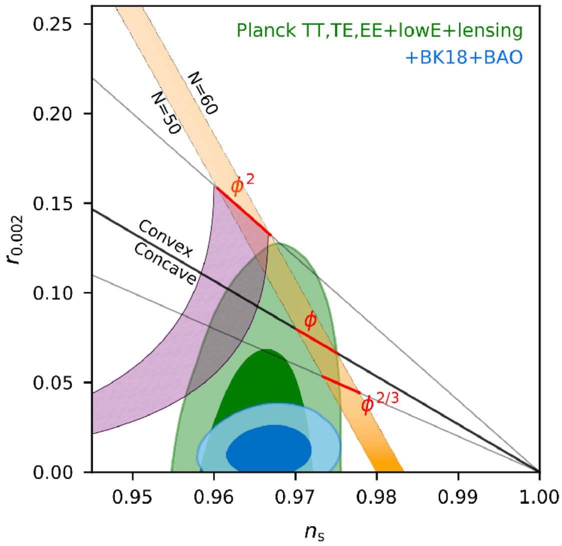

P. A. R. Ade et al. 2110.00483

Introduction

✓ Many minimal single field slow-roll inflation models are excluded by current observational constraints.

(chaotic inf., natural inf. ⇨)

However…

✓ Introducing a scalar field with non-minimal coupling to gravity, some models can be alleviated.

(Higgs inf. / F. L. Bezrukov, M. E. Shaposhnikov [0710.3755]
Non-minimal natural inf. / R. Z. Ferreira et al. [1806,05511])

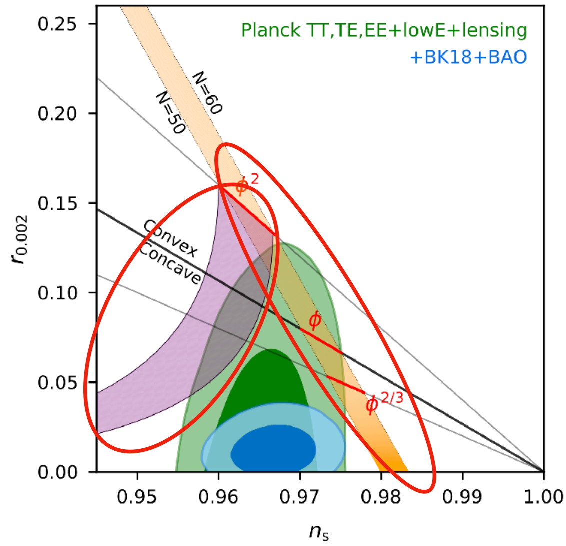

P. A. R. Ade et al. 2110.00483

Introduction

TK, T. Takahashi [2112.05283]

✓ If we consider the potential in the Einstein frame has a plateau,

- **The Metric formalism** n_s and r approach some attractor points.
- **The Palatini formalism** r is suppressed.

(Single field inflation)

However…

✓ Many high energy physics models involves **multiple scalar fields**.

Non-minimal coupling Multi-field inflation Metric vs Palatini	How inflationary predictions change?

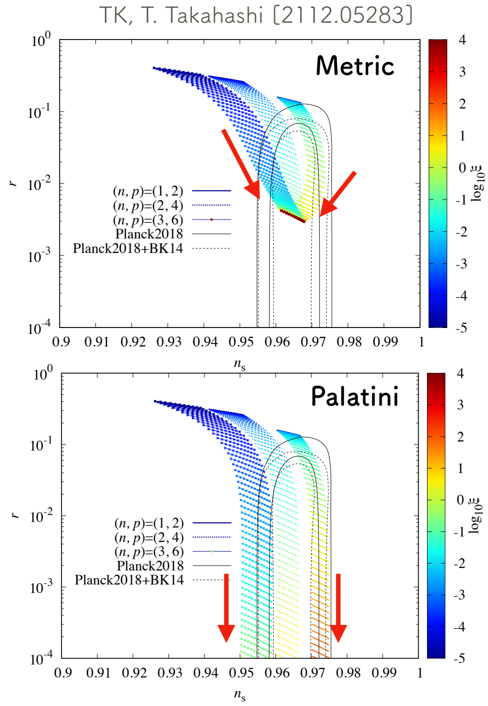

Multi-filed inflation with non-minimal coupling

✓ Action in the Jordan frame (multi-field)

$$S_J = \int d^4x \left[A(\phi^I) g^{\mu\nu} R_{\mu\nu}(\Gamma, g_{\mu\nu}) - \frac{1}{2} G_{IJ} g^{\mu\nu} \partial_\mu \phi^I \partial_\nu \phi^J - V(\phi^I)\right] \quad (M_{\rm Pl} = 1)$$

Conformal trans. $g_{\mu\nu} \to \Omega^2(x) g_{\mu\nu}\,, \quad \Omega^2 = A$

✓ Action in the Einstein frame

$$S_E = \int d^4x \left[\frac{1}{2} g^{\mu\nu} R_{\mu\nu}(\Gamma, g_{\mu\nu}) - \frac{1}{2} \tilde{G}_{IJ} g^{\mu\nu} \partial_\mu \phi^I \partial_\nu \phi^J - U(\phi^I)\right]$$

$$\tilde{G}_{IJ} = \frac{1}{2A}\left(G_{IJ} + 3\kappa \frac{A_{,I} A_{,J}}{A}\right)$$

Multi-filed inflation with non-minimal coupling

✓ Action in the Jordan frame (two-field)

$$S_J = \int dx^4 \sqrt{-g} \left[\frac{1}{2} A(\phi_J, \chi_J) g^{\mu\nu} R_{\mu\nu}(\Gamma, g_{\mu\nu}) - \frac{1}{2}(\partial \phi_J) - \frac{1}{2}(\partial \chi_J)^2 - V_J(\phi_J, \chi_J)\right] \quad (M_{\rm Pl} = 1)$$

Conformal trans. $g_{\mu\nu} \to \Omega^2(x) g_{\mu\nu}\,, \quad \Omega^2 = A$

✓ Action (in the Einstein frame)

$$S_E = \int dx^4 \left[\frac{1}{2} g^{\mu\nu} R_{\mu\nu}(\Gamma) - \frac{1}{2}\left\{\frac{1}{A} + \frac{3}{2}\kappa \left(\frac{A_{,\phi_J}}{A}\right)^2\right\}(\partial \phi_J)^2 - \frac{1}{2}\left\{\frac{1}{A} + \frac{3}{2}\kappa \left(\frac{A_{,\chi_J}}{A}\right)^2\right\}(\partial \chi_J)^2 - \frac{3}{2}\kappa \frac{A_{,\phi_J} A_{,\chi_J}}{A^2}(\partial \phi_J) \cdot (\partial \chi_J) - \frac{V_J(\phi_J, \chi_J)}{A^2}\right]$$

- In this talk, we consider the case that the only field ϕ_J is non-minimal coupling to gravity.
- $\kappa = 1$: the metric formalism $\left(\Gamma^\lambda{}_{\mu\nu} = \frac{1}{2} g^{\lambda\rho}(\partial_\mu g_{\rho\nu} + \partial_\nu g_{\mu\rho} - \partial_\rho g_{\mu\nu})\right)$
  $\kappa = 0$: the Palatini formalism ($g_{\mu\nu}$ and $\Gamma^\lambda{}_{\mu\nu}$ are independent from each other)

Multi-filed inflation with non-minimal coupling

✓ Action in the Jordan frame (two-field)

$$S_J = \int dx^4 \sqrt{-g}\left[\frac{1}{2}A(\phi_J,\chi_J)g^{\mu\nu}R_{\mu\nu}(\Gamma, g_{\mu\nu}) - \frac{1}{2}(\partial\phi_J) - \frac{1}{2}(\partial\chi_J)^2 - V_J(\phi_J,\chi_J)\right] \qquad (M_{\rm Pl}=1)$$

Conformal trans. $g_{\mu\nu} \to \Omega^2(x) g_{\mu\nu}\,,\ \ \Omega^2 = A$

✓ Action (in the Einstein frame)

$$S_E = \int dx^4 \left[\frac{1}{2}g^{\mu\nu}R_{\mu\nu}(\Gamma) - \frac{1}{2}\left\{\frac{1}{A} + \frac{3}{2}\kappa\left(\frac{A_{,\phi_J}}{A}\right)^2\right\}(\partial\phi_J)^2 - \frac{1}{2}\left\{\frac{1}{A} + \cancel{\frac{3}{2}\kappa\left(\frac{A_{,\chi_J}}{A}\right)^2}\right\}(\partial\chi_J)^2 \cancel{- \frac{3}{2}\kappa\frac{A_{,\phi_J}A_{,\chi_J}}{A^2}(\partial\phi_J)\cdot(\partial\chi_J)} - \frac{V_J(\phi_J,\chi_J)}{A^2}\right]$$

- In this talk, we consider the case that the only field ϕ_J is non-minimal coupling to gravity.
- $\kappa = 1$: the metric formalism $\left(\Gamma^{\lambda}{}_{\mu\nu} = \frac{1}{2}g^{\lambda\rho}(\partial_\mu g_{\rho\nu} + \partial_\nu g_{\mu\rho} - \partial_\rho g_{\mu\nu})\right)$
  $\kappa = 0$: the Palatini formalism ($g_{\mu\nu}$ and $\Gamma^{\lambda}{}_{\mu\nu}$ are independent from each other)

Multi-filed inflation with non-minimal coupling

✓ Action (in the Einstein frame)

$$S_E = \int dx^4 \left[\frac{1}{2}g^{\mu\nu}R_{\mu\nu}(\Gamma) - \frac{1}{2}\left\{\frac{1}{A} + \frac{3}{2}\kappa\left(\frac{A_{,\phi_J}}{A}\right)^2\right\}(\partial\phi_J)^2 - \frac{1}{2}\left\{\frac{1}{A} + \cancel{\frac{3}{2}\kappa\left(\frac{A_{,\chi_J}}{A}\right)^2}\right\}(\partial\chi_J)^2 \cancel{- \frac{3}{2}\kappa\frac{A_{,\phi_J}A_{,\chi_J}}{A^2}(\partial\phi_J)\cdot(\partial\chi_J)} - \frac{V_J(\phi_J,\chi_J)}{A^2}\right]$$

Multi-filed inflation with non-minimal coupling

✓ Action (in the Einstein frame)

$$\boxed{S_E = \int dx^4 \left[\frac{1}{2} g^{\mu\nu} R_{\mu\nu}(\Gamma) - \frac{1}{2}\left\{ \frac{1}{A} + \frac{3}{2}\kappa \left(\frac{A_{,\phi_J}}{A}\right)^2 \right\}(\partial\phi_J)^2 - \frac{1}{2}\left\{ \frac{1}{A} + \cancel{\frac{3}{2}\kappa \left(\frac{A_{,\chi_J}}{A}\right)^2} \right\}(\partial\chi_J)^2 - \cancel{\frac{3}{2}\kappa\frac{A_{,\phi_J}A_{,\chi_J}}{A^2}(\partial\phi_J)\cdot(\partial\chi_J)} - \frac{V_J(\phi_J,\chi_J)}{A^2} \right]}$$

The kinetic term for ϕ_J is complicated… ➡ Canonicalize!

$$\boxed{P(\phi_J) \equiv \frac{d\phi_J}{d\phi_E} = \sqrt{\frac{2A^2}{2A + 3\kappa(A')^2}}}$$

(The difference between the **metric** formalism and the **Palatini** formalism, one is appeared in $P(\phi_J)$)

➡

$$\boxed{S_E = \int d^4x \left[g^{\mu\nu} R_{\mu\nu}(\Gamma) - \frac{1}{2}(\partial\phi_E)^2 - \frac{e^{2b(\phi)}}{2}(\partial\chi_E)^2 - U(\phi_E,\chi_E) \right]}$$

$$U(\phi,\chi) = \frac{V(\phi,\chi)}{A^2(\phi)}$$

$$b^{2b(\phi)} = \frac{1}{A(\phi)}$$

Slow-roll analysis

✓ Equation of motions

$$\boxed{\begin{aligned} &\ddot{\phi} + 3H\dot{\phi} + U_{,\phi} = b_{,\phi} e^{2b(\phi)} \dot{\chi}^2 \\ &\ddot{\chi} + (3H + 2b_{,\phi}\dot{\phi})\dot{\chi} + e^{-2b(\phi)} U_{,\chi} = 0 \end{aligned}}$$

$$U = \frac{V}{A^2}$$

$$e^{-2b(\phi_J)} = A(\phi_J)$$

Prediction is modified
in slow-roll approx.

✓single field slow-roll inflation

Slow-roll parameter

$$\epsilon = \frac{1}{2}\left(\frac{V'^2}{V}\right), \quad \eta = \frac{V''}{V}$$

➡ Spectral index $n_s = 1 - 6\epsilon + 2\eta$

Tensor-to-scalar ratio $r = 16\epsilon$ ➡

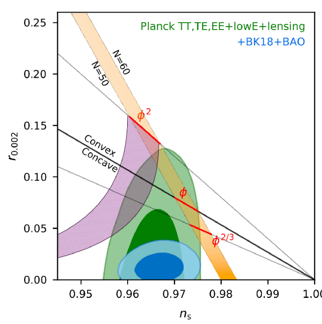

P. A. R. Ade et al. 2110.00483

Slow-roll analysis

✓ **Two-field** slow-roll inflation

$$\epsilon^\phi = \frac{1}{2}\frac{U_{,\phi}}{U}, \quad \epsilon^\chi = \frac{1}{2}\frac{U_{,\chi}}{U}e^{-2b(\phi)}, \quad \epsilon^b = 8b_{,\phi}^2$$

$$\eta^\phi = \frac{U_{,\phi\phi}}{U}, \quad \eta^\chi = \frac{U_{,\chi\chi}}{U}e^{-2b(\phi)}, \quad \eta^b = 16b_{,\phi\phi} \qquad \longrightarrow \quad U = U_1(\phi)U_2(\chi) = \frac{V_1(\phi_J)}{A^2(\phi_J)} \cdot V_2(\chi_J)$$

Now, we will focus on the case of the product-separable potential $V = V_1(\phi)V_2(\chi)$ below.

$$\epsilon^\phi = P^2(\phi_J)\left[\epsilon_J^\phi - 2\frac{A'}{A}\frac{V_1'}{V_1} + 2\left(\frac{A'^2}{A}\right)\right], \quad \epsilon^\chi = \frac{1}{2}\left(\frac{V_2'}{V_2}\right) \quad e^{-2b(\phi_J)}, \quad \epsilon^b = 2P^2\left(\frac{A'}{A}\right)^2, \quad \epsilon = \epsilon^\phi + \epsilon^\chi$$

$$\eta^\phi = P^2(\phi_J)\left[\eta_J^\phi - 4\frac{A'}{A}\frac{V_1'}{V_1} + 6\left(\frac{A'}{A}\right)^2 - 2\frac{A''}{A} + \frac{P'}{P}\left(-2\frac{A'}{A} + \frac{V_1'}{V_1}\right)\right]$$

$$\eta^\chi = \frac{V_2''}{V_2}e^{-2b(\phi_J)}, \quad \eta^b = 8P^2(\phi_J)\left[\frac{P'}{P}\frac{A'}{A} + \left(\frac{A'}{A}\right)^2 - \frac{A''}{A}\right]$$

$$\left(\begin{array}{c} \epsilon_J^\phi = \frac{1}{2}\left(\frac{V_1'}{V_1}\right)^2 \\ \eta_J^\phi = \frac{V_1''}{V_1} \end{array}\right)$$

(This expression is only product-separable case)

Slow-roll analysis

✓ **Two-field** slow-roll inflation

$$\epsilon^\phi = \frac{1}{2}\frac{U_{,\phi}}{U}, \quad \epsilon^\chi = \frac{1}{2}\frac{U_{,\chi}}{U}e^{-2b(\phi)}, \quad \epsilon^b = 8b_{,\phi}^2$$

$$\eta^\phi = \frac{U_{,\phi\phi}}{U}, \quad \eta^\chi = \frac{U_{,\chi\chi}}{U}e^{-2b(\phi)}, \quad \eta^b = 16b_{,\phi\phi} \qquad \longrightarrow \quad U = U_1(\phi)U_2(\chi) = \frac{V_1(\phi_J)}{A^2(\phi_J)} \cdot V_2(\chi_J)$$

Now, we will focus on the case of the product-separable potential $V = V_1(\phi)V_2(\chi)$ below.

$$\epsilon^\phi = P^2(\phi_J)\left[\epsilon_J^\phi - 2\frac{A'}{A}\frac{V_1'}{V_1} + 2\left(\frac{A'^2}{A}\right)\right], \quad \epsilon^\chi = \frac{1}{2}\left(\frac{V_2'}{V_2}\right) \quad e^{-2b(\phi_J)}, \quad \epsilon^b = 2P^2\left(\frac{A'}{A}\right)^2, \quad \epsilon = \epsilon^\phi + \epsilon^\chi$$

$$\eta^\phi = P^2(\phi_J)\left[\eta_J^\phi - 4\frac{A'}{A}\frac{V_1'}{V_1} + 6\left(\frac{A'}{A}\right)^2 - 2\frac{A''}{A} + \frac{P'}{P}\left(-2\frac{A'}{A} + \frac{V_1'}{V_1}\right)\right]$$

$$\eta^\chi = \frac{V_2''}{V_2}e^{-2b(\phi_J)}, \quad \eta^b = 8P^2(\phi_J)\left[\frac{P'}{P}\frac{A'}{A} + \left(\frac{A'}{A}\right)^2 - \frac{A''}{A}\right]$$

$$P(\phi_J) \equiv \frac{d\phi_J}{d\phi_E} = \sqrt{\frac{2A^2}{2A + 3\kappa(A')^2}}$$

The difference between the metric and the Palatini formulation are included in P

(This expression is only product-separable case)

Slow-roll analysis

✓ ϕ_J vs ϕ_E

Non-minimal function $\cdots$ $A = 1 + \xi\phi_J$

$$P(\phi_J) \equiv \frac{d\phi_J}{d\phi_E} = \sqrt{\frac{2A^2}{2A + 3\kappa(A')^2}}$$

$$= \sqrt{\frac{2(1+\xi\phi_J)^2}{2(1+\xi\phi_J) + 3\kappa\xi^2}}$$

$$\Big\downarrow \quad \phi_J \gg \xi$$

$$\simeq \sqrt{\xi\phi_J}$$

$$\phi_E = \frac{2}{\sqrt{\xi}}\phi_J$$

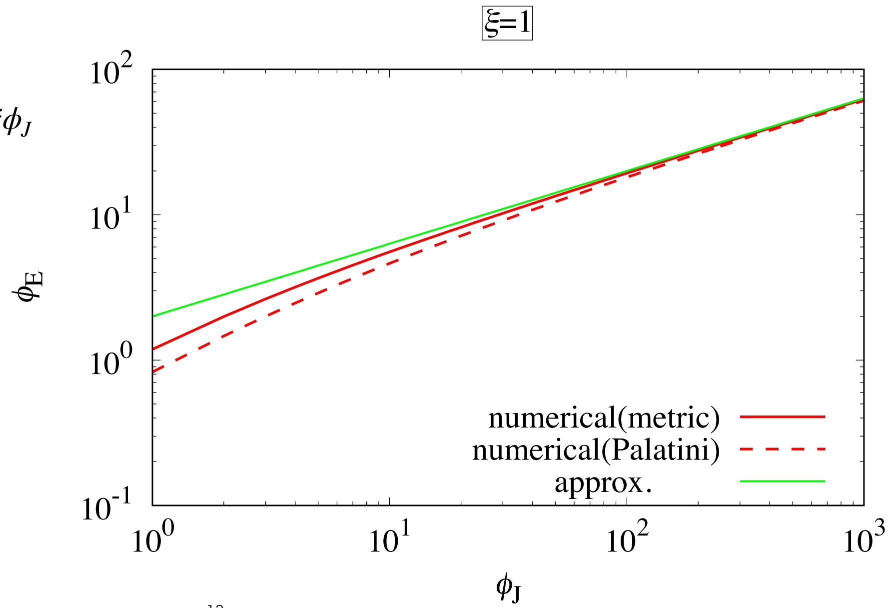

Inflationary Observables

✓ The spectral index n_s and the Tensor-to-scalar ratio r

$$u = \frac{\epsilon^\phi}{\epsilon}, \quad v = \frac{\epsilon^\chi}{\epsilon}$$

$$\alpha = e^{-2b_e+2b_*}\left[1 + \frac{\epsilon_e^\chi}{\epsilon_e^\phi}(1 - e^{2b_e-2b_*})\right]$$

$$\mathcal{P}_\zeta(k) = A_s\left(\frac{k}{k_*}\right)^{n_s-1} \qquad \mathcal{P}_h(k) = A_T\left(\frac{k}{k_*}\right)^{n_T} \qquad r = \frac{\mathcal{P}_T}{\mathcal{P}_\zeta}$$

$$\boxed{\begin{aligned} n_s - 1 = &-2\epsilon_* - \frac{4e^{-2b_e+4b_*}}{u^2\alpha^2/\epsilon_*^\phi + v^2/\epsilon_*^\chi} - \frac{1}{12}\frac{\left(\sqrt{\frac{\epsilon_*^\chi}{\epsilon_*^\phi}}u\alpha - \sqrt{\frac{\epsilon_*^\phi}{\epsilon_*^\chi}}v\right)^2}{u^2\alpha^2/\epsilon_*^\phi + v^2/\epsilon_*^\chi} \\ &+ \frac{2}{u^2\alpha^2/\epsilon_*^\phi + v^2/\epsilon_*^\chi}\left[\frac{u^2\alpha^2}{\epsilon_*^\phi}\eta_*^\phi + \frac{v^2}{\epsilon_*^\chi}\eta_*^\chi + 4uv\alpha + \frac{s^\phi s^b}{2}v\sqrt{\epsilon_*^\phi\epsilon_*^b}\left(\frac{v}{\epsilon_*^\chi} - \frac{2u\alpha}{\epsilon_*^\phi}\right)\right] \\ r = &\ \frac{16e^{-4b_e+4b_*}}{u^2\alpha^2/\epsilon_*^\phi + v^2/\epsilon_*^\chi} \end{aligned}}$$

(M. Sasaki, E. D. Stewart. astro-ph/9507001)
(J. Kim et al. 1301.5472)

An example model

✓ Minimal case

$$V(\phi_J,\chi_J) = \mu^2\phi_J^2\left[1+\cos\left(\frac{\chi_J}{f}\right)\right]$$

$$\left[\;V_1(\phi_J)=\mu^2\phi^2,\;\; V_2(\chi_J)=1+\cos\left(\frac{\chi_J}{f}\right)\;\right]$$

Chaotic Natural

Non-minimal function

$$A = 1+\xi\phi_J$$

✓ the potential in the Einstein frame

$$\boxed{U(\phi_J,\chi_J) = \frac{\mu^2\phi_J^2}{(1+\xi\phi_J)^2}\left[1+\cos\left(\frac{\chi_J}{f}\right)\right]}$$

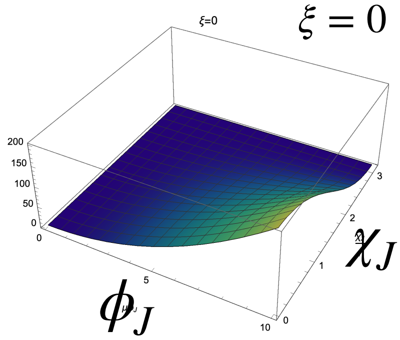

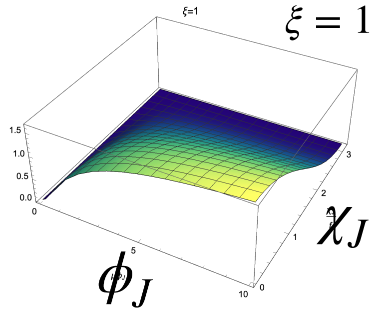

$$\boxed{U(\phi_J,\chi_J) = \frac{\mu^2\phi_J^2}{(1+\xi\phi_J)^2}\left[1+\cos\left(\frac{\chi_J}{f}\right)\right]}$$

Result

✓ n_s - r plane

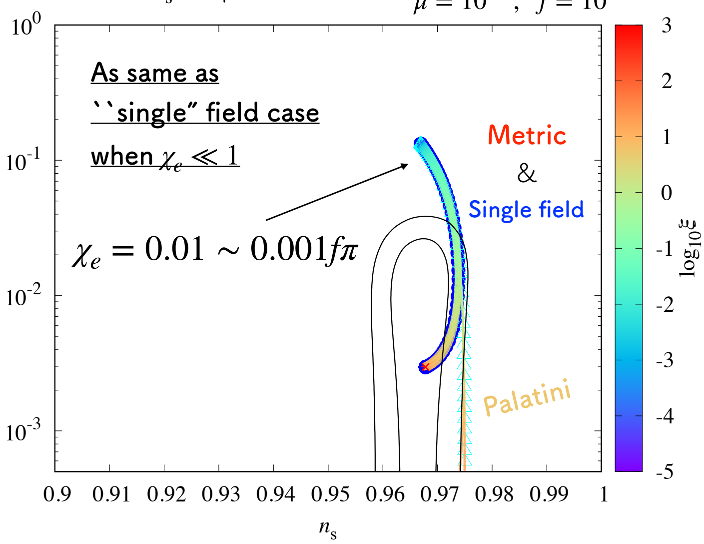

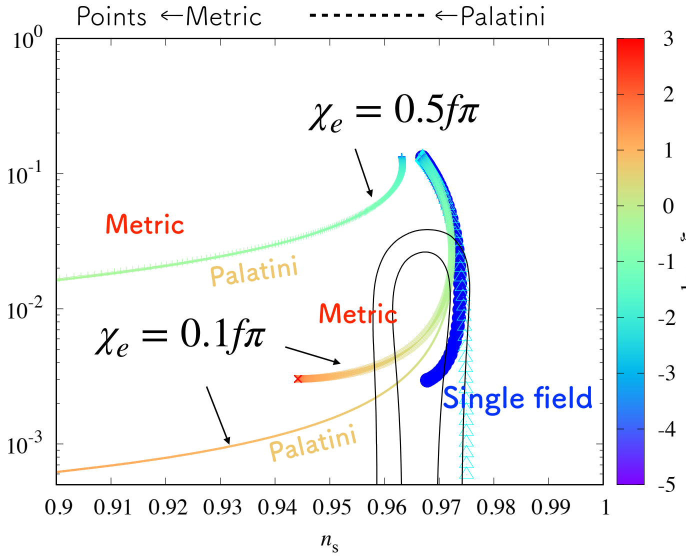

Inflation predictions are getting broken due to the effects of the multi-field model.

$$U(\phi_J,\chi_J) = \frac{\frac{1}{4}\lambda\phi_J^4}{(1+\xi\phi_J^2)^2}\left[1+\cos\left(\frac{\chi_J}{f}\right)\right]$$

Result

✓ n_s - r plane $\lambda = 1$, $f = 10$

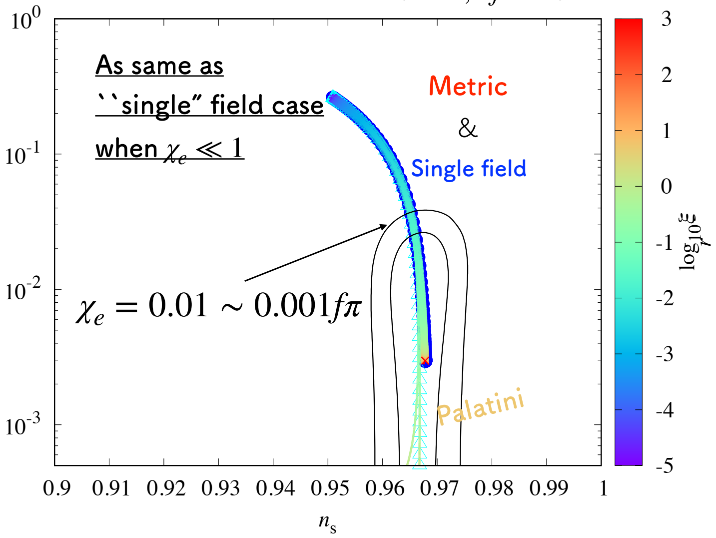

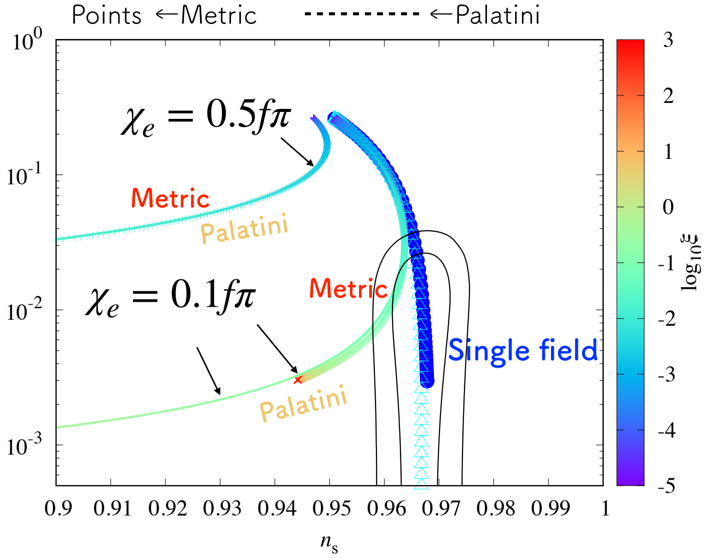

Inflation predictions are getting broken due to the effects of the multi-field model.

Summary

- We have investigated the multi-field inflation with non-minimal coupling in the metric formalism & the Palatini formalism.
- The difference between the metric & the Palatini depends not only on ξ but also the field values.
- Predictions of non-minimal inflation (even for the attractor case) can be affected by the existence of multiple field.
- The predictions of non-minimal multi-field inflation should be more systematically and analytically explored.

$$S_E = \int d^4x \left[g^{\mu\nu}R_{\mu\nu}(\Gamma) - \frac{1}{2}(\partial\phi_E)^2 - \frac{e^{2b(\phi)}}{2}(\partial\chi_E)^2 - U(\phi_E,\chi_E)\right]$$

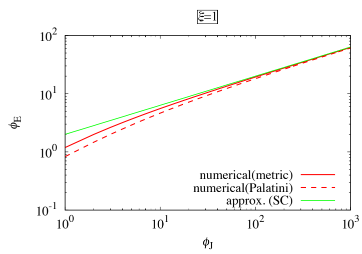

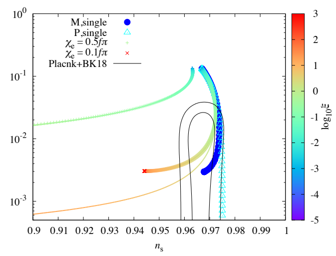

C24

Inflation with 2-form field:

the production of primordial black holes and gravitational waves

Ippei Obata (MPA, Germany → Kavli IPMU (2022.10.1-))

JCAP 09 (2022) 017 [arXiv: 2202.02401]

In collaboration with
Tomohiro Fujita, Hiromasa Nakatsuka, Sam Young

科研費 KAKENHI

ダークマターの正体は何か？
広大なディスカバリースペースの網羅的研究
What is dark matter? - Comprehensive study of the huge discovery space in dark matter
文部科学省 科学研究費助成事業 学術変革領域研究 (2020–2024)

2022.10.25 JGRG31, Hongo

Standard prediction from inflation

- Primordial density perturbation (curvature perturbation)

$$dl^2 = a(t)^2 \left[1 + 2\zeta(t,\boldsymbol{x})\right] \left[\delta_{ij} + h_{ij}(t,\boldsymbol{x})\right] dx^i dx^j$$

provides a **nearly scale-invariant** power spectrum: $\langle \zeta_{\boldsymbol{k}} \zeta_{\boldsymbol{k}'} \rangle \equiv (2\pi)^3 \delta(\boldsymbol{k}+\boldsymbol{k}') \frac{2\pi^2}{k^3} \mathcal{P}_\zeta(k)$

$$\mathcal{P}_\zeta = \frac{H^2}{8\pi^2 M_p^2 \epsilon_H}\bigg|_{k=aH} \equiv A_s \left(\frac{k}{k_*}\right)^{n_s - 1}$$

(CMB scales)

$$\boxed{A_s \simeq 2 \times 10^{-9} \ , \ n_s \simeq 0.96}$$

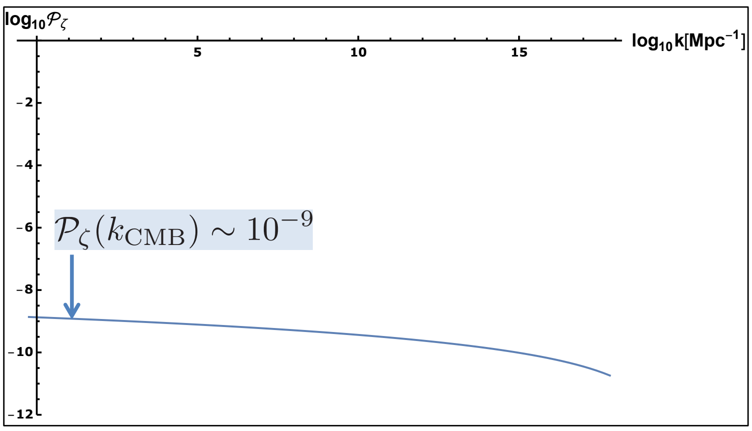

- Obtained by the **vacuum fluctuation**

(no matter sectors are included)

Inflation with form fields

- In higher dimensional theories, scalar sectors are naturally coupled to matter sectors (e.g. form fields):

$$\boxed{\mathcal{L} \supset I(\varphi)^2 F_{\mu\nu}F^{\mu\nu}, \ \ I(\varphi)^2 H_{\mu\nu\rho}H^{\mu\nu\rho}}$$

$F_{\mu\nu} = \partial_\mu A_\nu - \partial_\nu A_\mu$: vector field (1-form field)

$H_{\mu\nu\rho} = \partial_\mu B_{\nu\rho} + \partial_\nu B_{\rho\mu} + \partial_\rho B_{\mu\nu}$: antisymmetric tensor field (2-form field)

- **Time variation of the kinetic function** could trigger the **particle production of form fields** during inflation
→ enhance the coupled cosmological perturbations

Rich cosmological phenomena

$\boxed{I^2FF \text{ model}}$

- Generation of primordial magnetic fields ***Ratra (1992); Martin, Yokoyama (2008); Fujita, Mukohyama (2012);… (a lot)***
- Anisotropic inflation models ***Watanabe, Kanno, Soda (2009)…; Ito, Soda (2015);***
- Statistically-anisotropic primordial GWs ***Fujita, IO, Tanaka, Yokoyama (2018); Hiramatsu, Murai, IO, Yokoyama (2020);***
- Generation of primordial BHs & GWs ***Kawasaki, Nakatsuka, IO (2019)***

$\boxed{I^2HH \text{ model}}$

- Anisotropic inflation models ***Ohashi, Tsujikawa, Soda (2013)…; Ito, Soda (2015);***
- Statistically-anisotropic primordial GWs ***IO, Fujita (2018);***
- **Generation of Primordial BHs & GWs** ***Fujita, Nakatsuka, IO, Young (2022);***

Inflation with two-form field

■ Consider the two-form field kinetically coupled to inflaton

$$\boxed{\mathcal{L} = \frac{1}{2}M_p^2 R - \frac{1}{2}(\partial_\mu \varphi)^2 - V(\varphi) - \frac{1}{12} I(\varphi)^2 H_{\mu\nu\rho} H^{\mu\nu\rho}}$$

FLRW Metric: $ds^2 = -dt^2 + a(t)^2 d\boldsymbol{x}^2 = a(\tau)^2(-d\tau^2 + d\boldsymbol{x}^2)$

Gauge conditions: $\partial_i B_{ij} = 0\ , \quad \partial_i B_{0i} = 0$

■ Consider the Fourier decomposition of dynamical component:

$$B_{ij}(t, \boldsymbol{x}) = \int \frac{d\boldsymbol{k}}{(2\pi)^3} \hat{B}_{\boldsymbol{k}} \epsilon_{ij}(\hat{\boldsymbol{k}}) e^{i\boldsymbol{k}\cdot\boldsymbol{x}}$$

$k_i \epsilon_{ij}(\hat{\boldsymbol{k}}) = 0\ , \quad \epsilon_{ij}(-\hat{\boldsymbol{k}}) = \epsilon_{ij}^*(\hat{\boldsymbol{k}})\ , \quad \epsilon_{ij}(\hat{\boldsymbol{k}})\epsilon_{ij}^*(\hat{\boldsymbol{k}}) = 2$

$$\hat{B}_{\boldsymbol{k}} = B_k a_{\boldsymbol{k}} + B_k^* a_{-\boldsymbol{k}}^\dagger$$

$[a_{\boldsymbol{k}},\ a_{-\boldsymbol{k}'}^\dagger] = (2\pi)^3 \delta(\boldsymbol{k} + \boldsymbol{k}')$

↑ find a solution of mode function

Solution of mode function (1)

■ EOM for the mode function:

$$\left[\partial_\tau^2 + k^2 - \frac{\partial_\tau^2 I}{I} - \frac{2\partial_\tau I}{\tau I}\right]\left(\frac{I B_k}{a}\right) = 0$$

■ Define the following index: $n \equiv -\frac{\dot{I}}{HI}$ → $I(\varphi(\tau)) \propto a(\tau)^{-n}$

when $n = n_0$ (const.), EOM leads to

$$\left[\partial_\tau^2 + k^2 - \frac{n_0(n_0+1)}{\tau^2}\right]\left(\frac{I B_k}{a}\right) = 0$$ (Bessel-type equation)

Then, we obtain $\frac{I B_k}{a} = \frac{e^{i(n_0+1)\pi/2}}{\sqrt{2k}} \sqrt{\frac{-\pi k \tau}{2}} H_{n_0+1/2}^{(1)}(-k\tau)$

(Banch-Davies initial condition is chosen)

Solution of mode function (2)

- Then, using the following asymptotic form in the super-horizon limit:

$$H^{(1)}_{\nu>0}(x) \to -\frac{i}{\pi}\Gamma(\nu)\left(\frac{2}{x}\right)^{\nu} \qquad (x \equiv -k\tau \to 0)$$

The "electromagnetic-like" component of two-form field

$$E_k = \frac{I\dot{B}_k}{a^2}\ , \qquad M_k = \frac{kIB_k}{a^3}$$

are computed as

$$\boxed{\begin{aligned} E_k &= \frac{H^2 e^{i\frac{n_0+1}{2}\pi}}{\sqrt{2k^3}}\sqrt{\frac{\pi x^5}{2}}H^{(1)}_{n_0+3/2}(x) \propto \left(\frac{a_k}{a}\right)^{1-n_0} \\ M_k &= \frac{H^2 e^{i\frac{n_0+1}{2}\pi}}{\sqrt{2k^3}}\sqrt{\frac{\pi x^5}{2}}H^{(1)}_{n_0+1/2}(x) \propto \left(\frac{a_k}{a}\right)^{2-n_0} \end{aligned}} \qquad (a_k \equiv k/H \ll a)$$

- Electric (magnetic) field is amplified when $\boxed{n_0 > 1\ (n_0 > 2)}$

However…

- **In most cases, the index "n" is not a constant but a dynamical value**

Ex) consider the simplest configuration

$$\boxed{I(\varphi) = I_0 \exp\left(\frac{\varphi}{\Lambda}\right)} \quad \to \quad n = \frac{\dot{\varphi}}{H\Lambda} \neq \text{const.}$$

Since the speed of scalar field naturally increases in time,
we need to solve the EOM with dynamical "n":

$$\boxed{\partial_\tau^2 V_k + \left(k^2 - \frac{n(\tau)(n(\tau)+1)}{\tau^2}\right)V_k = 0}$$

- The occurrence of particle production could be scale-dependent depending on the time evolution of $n(t)$

Model setup

Fujita, Nakatsuka, IO, Young (2022);

Inflaton potential

$$V(\varphi) = \mu^4 (1 - e^{-\gamma\varphi})^2 \, , \qquad \gamma = \sqrt{\frac{2}{3}} M_{\rm Pl}^{-1}$$

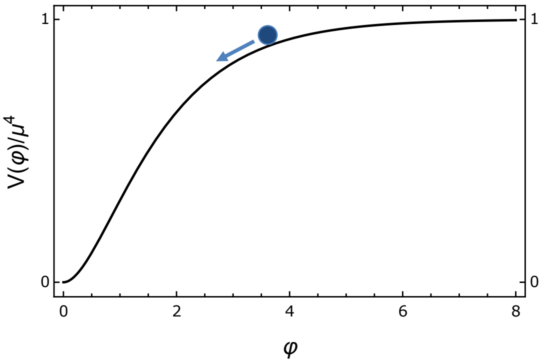

Kinetic function

$$I(\varphi) = B_1 \exp\left(c_1 \frac{\varphi}{M_{\rm Pl}}\right) + B_2$$

$$n(t) \equiv \frac{d \ln \bar{I}}{dN} = -\frac{\bar{I}_\varphi}{\bar{I}} \frac{\dot{\bar{\varphi}}}{H}$$

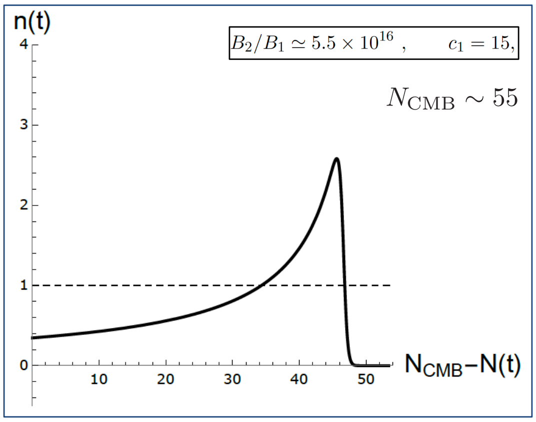

Perturbation dynamics

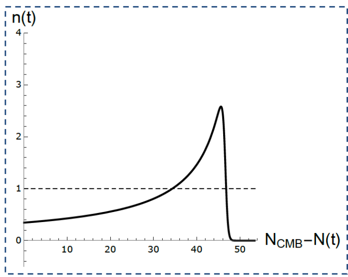

Evolutions of the electric field component on super-horizon regime

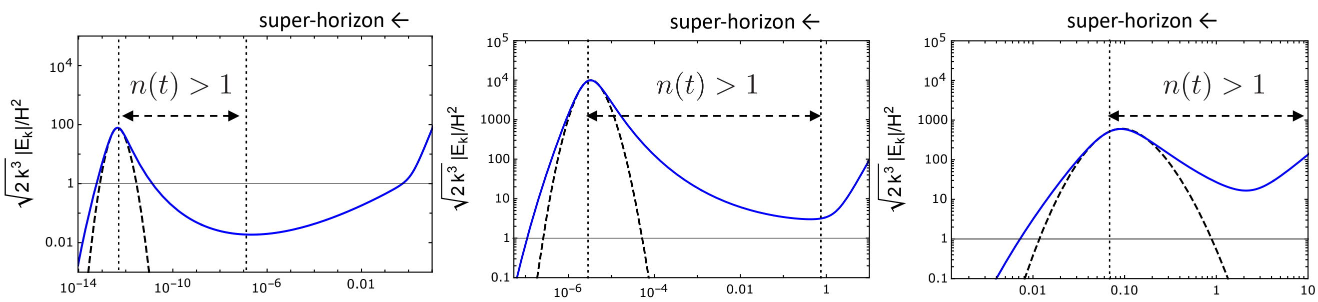

exiting horizon at $N \sim 35$ $N \sim 20$ $N \sim 10$

around peak: $E_k \simeq \frac{H^2}{\sqrt{2k^3}} E_{\rm peak}(k) \exp\left[-\frac{(\ln(\tau/\tau_{\rm peak}))^2}{\sigma^2}\right]$

Generation of scalar mode

- Curvature perturbation is sourced by the two-form field at second-order level

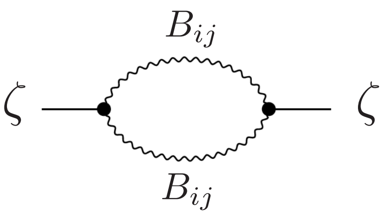

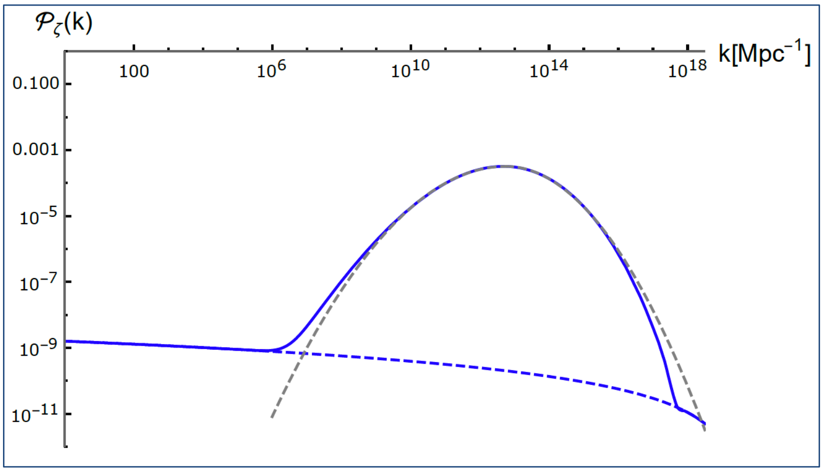

The fitting function around the peak:

$$\mathcal{P}_\zeta(k) \simeq A \exp\left[-\frac{(\ln(k/k_p))^2}{\sigma_\zeta^2}\right]$$

$A \simeq 3.2 \times 10^{-4}$, $k_p \simeq 5.6 \times 10^{12}\mathrm{Mpc}^{-1}$, $\sigma_\zeta^2 \simeq 3.7^2\Theta(k_p - k) + 3.1^2\Theta(k - k_p)$

Generation of PBHs as DM

Hawking (1971); Carr, Hawking (1974); …

- Assuming ζ obeys χ-squared distribution: $\zeta = \chi^2$

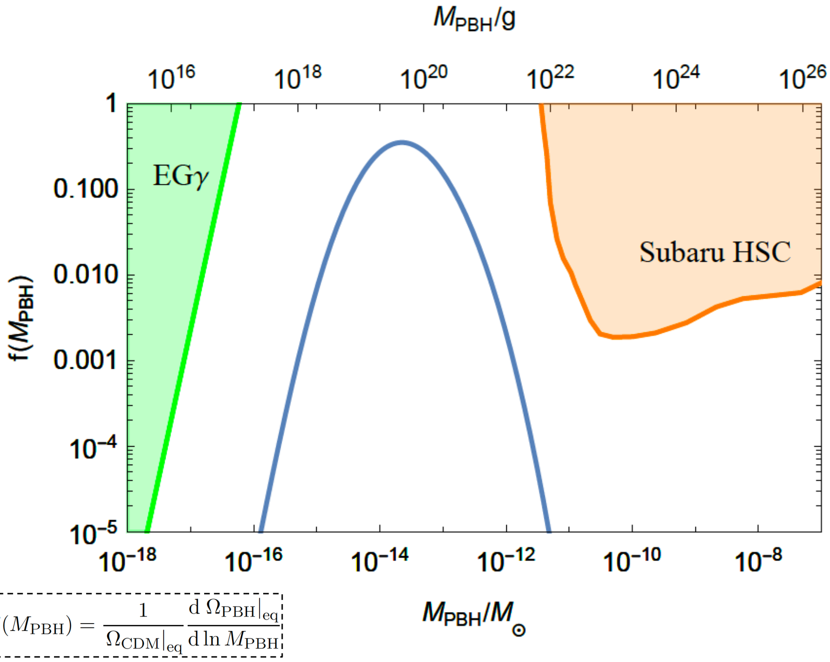

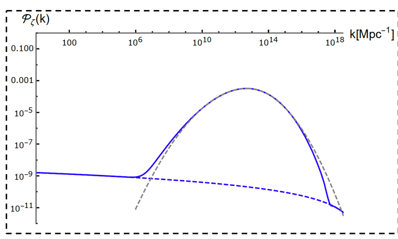

$$f(M_{\rm PBH}) = \frac{1}{\Omega_{\rm CDM}|_{\rm eq}} \frac{{\rm d}\,\Omega_{\rm PBH}|_{\rm eq}}{{\rm d}\ln M_{\rm PBH}}$$

Generation of tensor modes

Induced GWs by PBHs ***Saito, Yokoyama (2008);…***

- Secondary GWs are sourced by scalar perturbations after re-entering the horizon

$$\left[\partial_\tau^2 - \nabla^2\right](ah_{ij}) = -4a\Pi_{ij}^{lm}\mathcal{S}_{lm} \ ,$$

$$\mathcal{S}_{ij} \equiv 4\Psi\partial_i\partial_j\Psi + 2\partial_i\Psi\partial_j\Psi - \frac{1}{\mathcal{H}^2}\partial_i(\Psi' + \mathcal{H}\Psi)\partial_j(\Psi' + \mathcal{H}\Psi) \qquad \boxed{\Psi_{\boldsymbol{k}}(\tau) = -\frac{2}{3}\zeta_{\boldsymbol{k}}\Psi(k\tau)}$$

- 2-point function of induced GWs is given by the 8-point function of two-form field

$$\langle hh\rangle \propto \langle\zeta\zeta\zeta\zeta\rangle \propto \langle BBBBBBBB\rangle$$

→ Three diagram contributes the spectrum

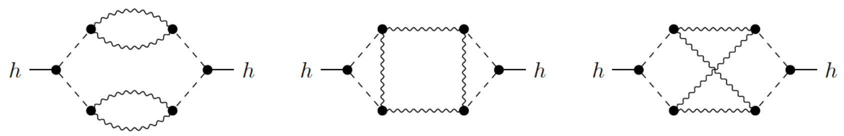

"Reducible" "Planar" "Non-Planar"

Garcia-Bellido, Peloso, Unal (2017);
Cai, Pi, Sasaki (2019);
Adshead, Lozanov, Weiner (2021);

Power spectrum of indued GWs

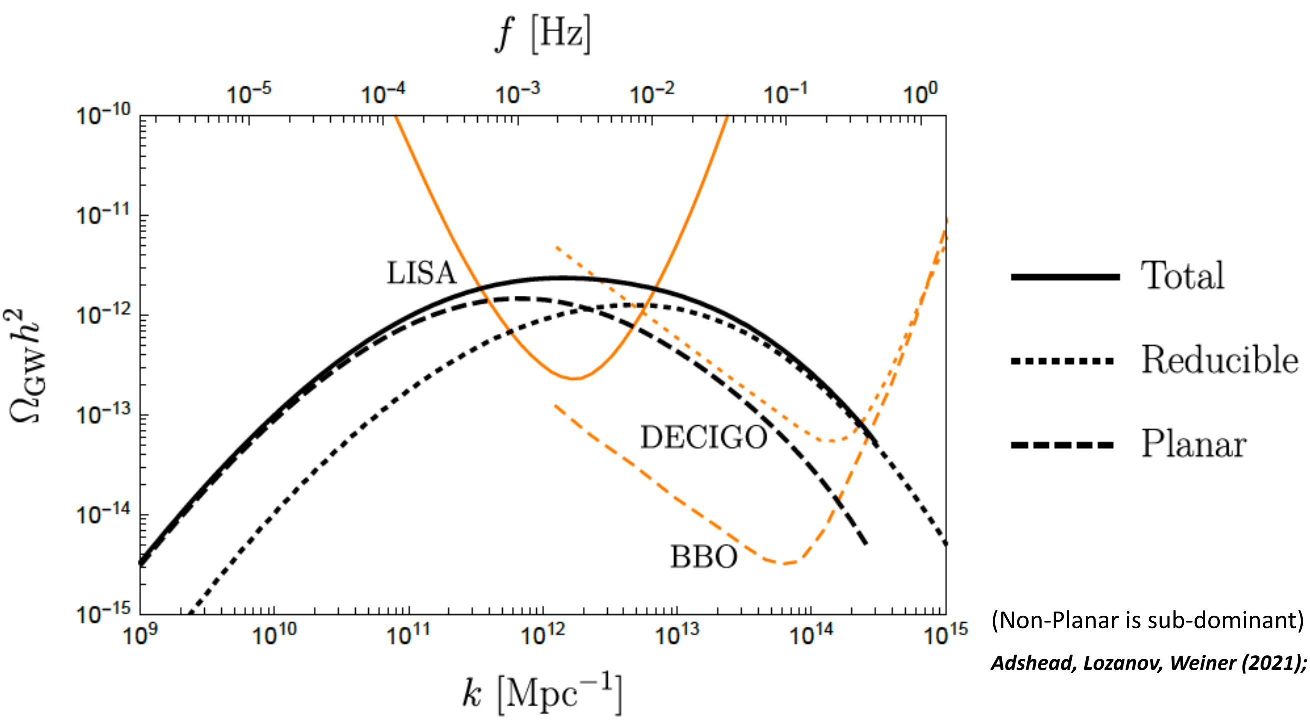

(Non-Planar is sub-dominant)

Adshead, Lozanov, Weiner (2021);

Summary

- We proposed an inflationary model where a two-form field is kinetically coupled with an inflaton, and explored the particle production of two-form field occurring at an intermediate scale during inflation.
- The amplified two-form field enhances the curvature perturbation at second order and produces the sizable amount of PBHs as dark matter after inflation.
- The enhanced curvature perturbation also provides induced GWs after inflation and the spectral amplitudes are potentially testable with future laser interferometers.

C25

Resummed formulation of particle production as a source of observables

Ryo Namba

RIKEN iTHEMS

JGRG 31

25 October 2022

RN & Motoo Suzuki, 2211.XXXXX

Outline

1. Introduction
2. Particle Production via **exact WKB**
   - Borel summation and exact WKB
3. Application to more realistic scenarios (*work in progress*)
   - Connection to observables from particle production
4. Summary & Outlook

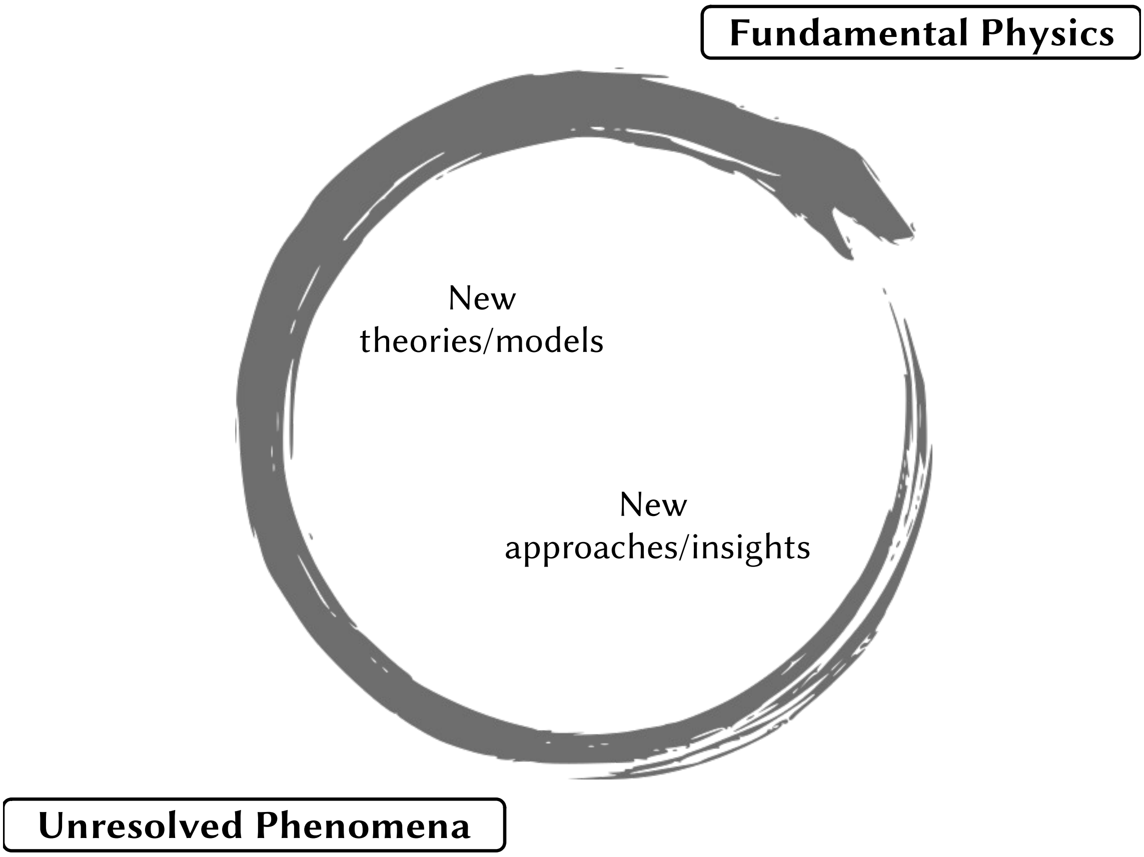

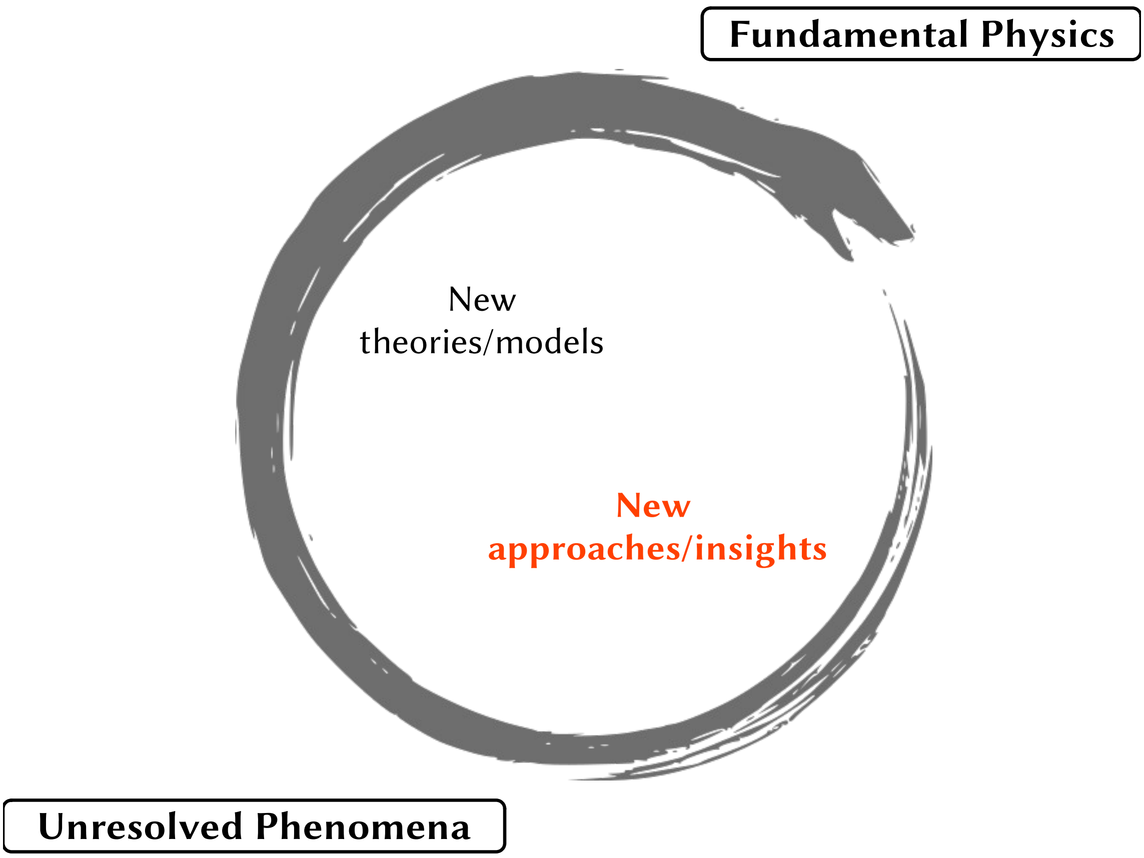

Ryo Namba (RIKEN iTHEMS) Particle production & exact WKB 3 / 23

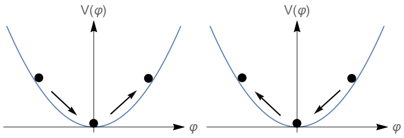

Time-dependent background of fields

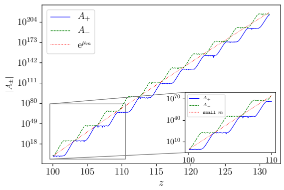

Resonant/tachyonic particle production

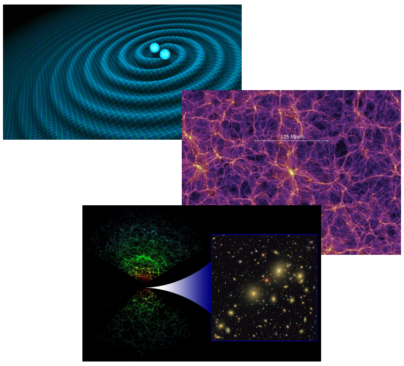

Observable remnants

- Gravitational waves
- Density fluctuations
- Dark matter abundance
- ...

Universal form of equation describing particle production

$$\boxed{\mathcal{L}_{\text{scalar-vector}} = e A_\mu J^\mu_{\text{scalar}}}$$

$$\boxed{\mathcal{L}_{\text{scalar-scalar}} = -g\,\varphi^2 \chi^2}$$

$$\boxed{\mathcal{L}_{\text{scalar-tensor}} = \xi\,\varphi^2 R}$$

Schrödinger-type equation

$$\left[\frac{\partial^2}{\partial t^2} + \omega^2(t,\eta)\right] \Psi(t) = 0$$

$$\langle \varphi \rangle = \varphi(t)$$

$$\boxed{\mathcal{L}_{\text{EFT, scalar-vector}} = -\frac{I^2(\varphi)}{4} F_{\mu\nu} F^{\mu\nu}}$$

$$\boxed{\mathcal{L}_{\text{EFT, pseudo S-tensor}} = \frac{\varphi}{8f} R_{\mu\nu\rho\sigma} \tilde{R}^{\mu\nu\rho\sigma}}$$

$$\boxed{\mathcal{L}_{\text{EFT, pseudo S-vector}} = \frac{\varphi}{4f} F_{\mu\nu} \tilde{F}^{\mu\nu}}$$

Broad goals

- **Analytical approach to strong couplings and/or nonlinear regimes**
  - ▷ Clear parameter dependence
  - ▷ Broader parameter space
  - ▷ Most of phenomena in nature are nonlinear after all
- **Backreaction of particle production onto the background dynamics**
  - ▷ Naïve perturbative analysis may break down
  - ▷ Particle production $\sim$ coupled system of multiple fields by nature

Outline

Standard WKB technology

1-D Schrödinger-type equation

$$\left[-\frac{\partial^2}{\partial x^2} + \eta^2 Q(x)\right]\psi(x,\eta) = 0$$

- $\eta \equiv \hbar^{-1}$: Small $\hbar$ = large η expansion
- WKB ((Jeffreys-)Wentzel-Kramers-Brillouin) series solution

Standard WKB technology

1-D Schrödinger-type equation

$$\left[-\frac{\partial^2}{\partial x^2} + \eta^2 Q(x)\right]\psi(x,\eta) = 0$$

- $\eta \equiv \hbar^{-1}$: Small $\hbar$ = large η expansion
- WKB ((Jeffreys-)Wentzel-Kramers-Brillouin) series solution

Formal WKB solution

$$\psi_\pm(x,\eta) = \frac{1}{\sqrt{|S_{\rm odd}|}} \exp\left[\pm\int^x {\rm d}x' \, S_{\rm odd}(x',\eta)\right]$$

$$S_{\rm odd} = \eta^1 S_{-1} + \eta^{-1} S_1 + \eta^{-3} S_3 + \ldots$$

$$S_{-1}(x) = \pm\sqrt{Q(x)}\,, \quad S_{-1}S_0 = -\frac{1}{2}\frac{\partial S_{-1}}{\partial x}\,, \quad S_{-1}S_j = -\frac{1}{2}\left(\frac{\partial S_{j-1}}{\partial x} + \sum_{n+m=j-1,n,m\geq 0} S_n S_m\right)$$

The standard WKB is divergent

Formal WKB solution

$$\psi_\pm(x,\eta) = \frac{1}{\sqrt{|S_{\mathrm{odd}}|}} \exp\left[\pm \int^x \mathrm{d}x' \, S_{\mathrm{odd}}(x',\eta)\right]$$

The standard WKB solution is often a divergent series around $Q(x) = 0$

$$S_{\mathrm{odd}} = \eta S_{-1} + \eta^{-1} S_1 + \eta^{-3} S_3 + \ldots \,, \qquad S_{-1} = \sqrt{Q(x)}$$

The standard WKB is divergent

Formal WKB solution

$$\psi_\pm(x,\eta) = \frac{1}{\sqrt{|S_{\mathrm{odd}}|}} \exp\left[\pm \int^x \mathrm{d}x' \, S_{\mathrm{odd}}(x',\eta)\right]$$

The standard WKB solution is often a divergent series around $Q(x) = 0$

$$S_{\mathrm{odd}} = \eta S_{-1} + \eta^{-1} S_1 + \eta^{-3} S_3 + \ldots \,, \qquad S_{-1} = \sqrt{Q(x)}$$

- Textbook solution is to expand $Q(x) \approx x - x_c$ around $Q(x_c) = 0$
  - ▷ Solve the equation using the Airy functions $A_i(x)$, $B_i(x)$
  - ▷ Connect WKB and Airy solutions
- More general, sophisticated approach?

The standard WKB is divergent

Formal WKB solution

$$\psi_{\pm}(x,\eta) = \frac{1}{\sqrt{|S_{\text{odd}}|}} \exp\left[\pm \int^{x} \mathrm{d}x'\, S_{\text{odd}}(x',\eta)\right]$$

The standard WKB solution is often a divergent series around $\boldsymbol{Q(x) = 0}$

$$S_{\text{odd}} = \eta S_{-1} + \eta^{-1} S_1 + \eta^{-3} S_3 + \dots\ , \qquad S_{-1} = \sqrt{Q(x)}$$

- Textbook solution is to expand $Q(x) \approx x - x_c$ around $Q(x_c) = 0$
  - ▷ Solve the equation using the Airy functions $A_i(x),\ B_i(x)$
  - ▷ Connect WKB and Airy solutions
- More general, sophisticated approach?

↓

Borel sum

Some applications of **Borel sum** in physics

- **Instantons**: some singularities of $\mathcal{B}[\psi]$ are associated with instanton solutions
- **Resurgence**: “unification of perturbation theory and non-perturbative physics”
  by G. Dunne’s talk
  - ▷ Quantum mechanics: degenerate vacua, level splitting (∼ instantons)
  - ▷ Quantum field theory: asymptotically free renormalons ?
- **Schwinger effect**: pair creation in strong electric fields

$$\mathrm{Im} S \sim \exp\left(-\frac{m^2\pi}{eE}\right)$$

- $\boxed{\textbf{Exact WKB}}$

Borel re-summation of the standard WKB solution

Formal WKB solution

$$\psi_\pm(x,\eta) = \mathrm{e}^{\pm s(x)\,\eta} \sum_{j=0}^{\infty} \psi_{\pm,j}(x)\,\eta^{-j-\frac{1}{2}} \qquad s(x) \equiv \int^x \mathrm{d}x' \sqrt{Q(x')}$$

Borel re-summation of the standard WKB solution

Formal WKB solution

$$\psi_\pm(x,\eta) = \mathrm{e}^{\pm s(x)\,\eta} \sum_{j=0}^{\infty} \psi_{\pm,j}(x)\,\eta^{-j-\frac{1}{2}} \qquad s(x) \equiv \int^x \mathrm{d}x' \sqrt{Q(x')}$$

Method of Borel sum

- **Borel transform:**

$$\mathcal{B}\left[\psi_\pm\right] \equiv \psi_{\pm,B}(x,y) = \sum_{j=0}^{\infty} \frac{\psi_{\pm,j}(x)}{\boldsymbol{\Gamma(j+1/2)}} \left[y \pm s(x)\right]^{j-1/2}$$

- **Laplase integration:**

$$\Psi_\pm(x,\eta) \equiv \int_{\mp s(x)}^{\infty} \mathrm{e}^{-y\eta}\,\psi_{\pm,B}(x,y)\,\mathrm{d}y$$

Borel re-summation of the standard WKB solution

Formal WKB solution

$$\psi_\pm(x,\eta) = \mathrm{e}^{\pm s(x)\eta} \sum_{j=0}^{\infty} \psi_{\pm,j}(x)\,\eta^{-j-\frac{1}{2}} \qquad s(x) \equiv \int^x \mathrm{d}x' \sqrt{Q(x')}$$

Method of Borel sum

- **Borel transform:**

$$\mathcal{B}\left[\psi_\pm\right] \equiv \psi_{\pm,B}(x,y) = \sum_{j=0}^{\infty} \frac{\psi_{\pm,j}(x)}{\boldsymbol{\Gamma(j+1/2)}} \left[y \pm s(x)\right]^{j-1/2}$$

- **Laplace integration:**

$$\Psi_\pm(x,\eta) \equiv \int_{\mp s(x)}^{\infty} \mathrm{e}^{-y\eta}\, \psi_{\pm,B}(x,y)\,\mathrm{d}y$$

Ψ is called the **Borel sum** of the original series ψ

❇ **Borel sum** = a representation of inverse Laplace transform

Borel summation of the standard WKB solution

$$\left[-\frac{\partial^2}{\partial x^2} + \eta^2 Q(x)\right] \psi(x,\eta) = 0$$

- **Turning points $x_{\rm tp}$:**

$$Q(x_{\rm tp}) = 0$$

- **Simple turning points:**

$$\left.\frac{\mathrm{d}Q}{\mathrm{d}x}\right|_{x=x_{\rm tp}} \neq 0$$

- **Stokes curves:**

$$\mathrm{Im} \int_{x_{\rm tp}}^{x} \sqrt{Q(x')}\,\mathrm{d}x' = 0$$

Borel summation of the standard WKB solution

Stokes curves

$$\mathrm{Im} \underbrace{\int_{x_{\mathrm{tp}}}^{x} \sqrt{Q(x')}\,\mathrm{d}x'}_{s(x)} = 0$$

Borel transform

$$\psi_{\pm,B}(x,y) = \sum_{j=0} \frac{\psi_{\pm,j}(x)}{\Gamma(j+1/2)} \left[y \pm s(x)\right]^{j-1/2}$$

Laplase integration

$$\Psi_{\pm}(x,\eta) \equiv \int_{\mp s(x)}^{\infty} \mathrm{e}^{-y\eta}\, \psi_{\pm,B}(x,y)\,\mathrm{d}y$$

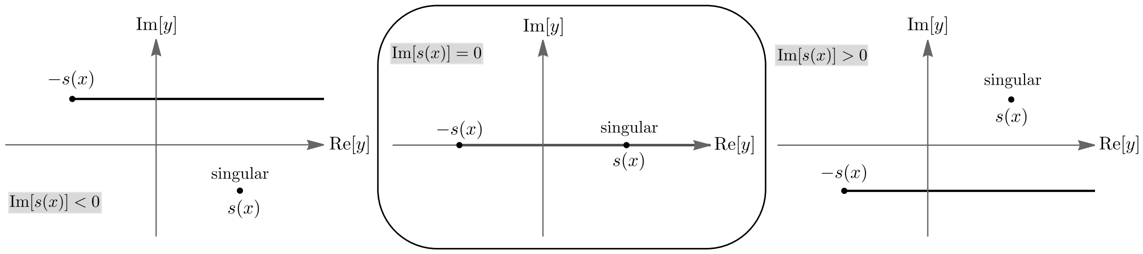

Crossing Stokes curves

What happens if crossing a Stokes curve?

Original x-space

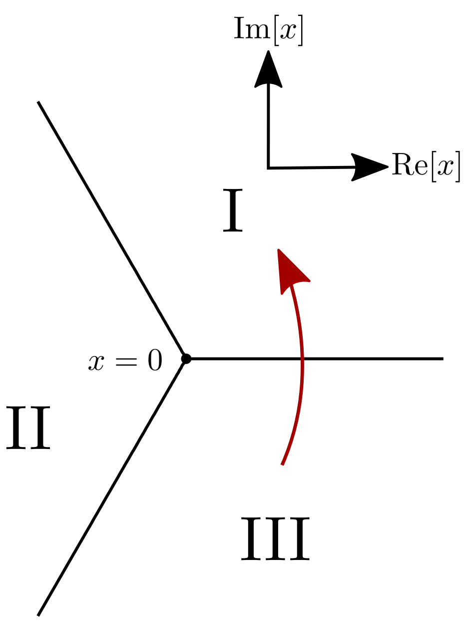

Borel y-space

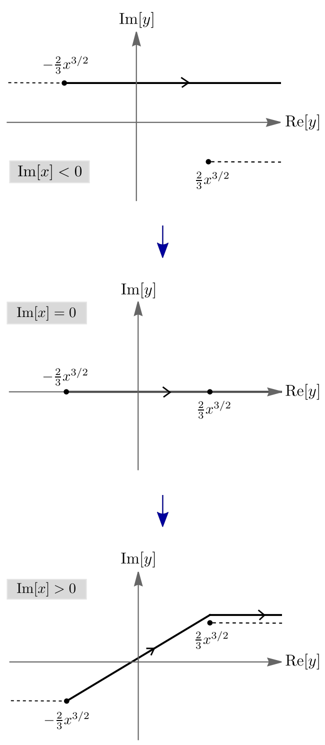

Crossing Stokes curves

What happens if crossing a Stokes curve?

Original x-space

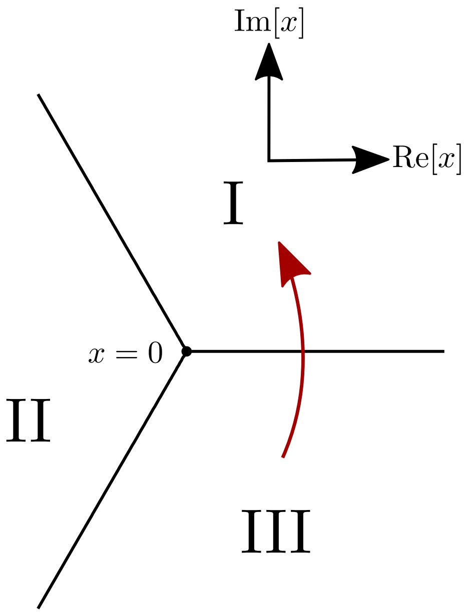

Borel y-space

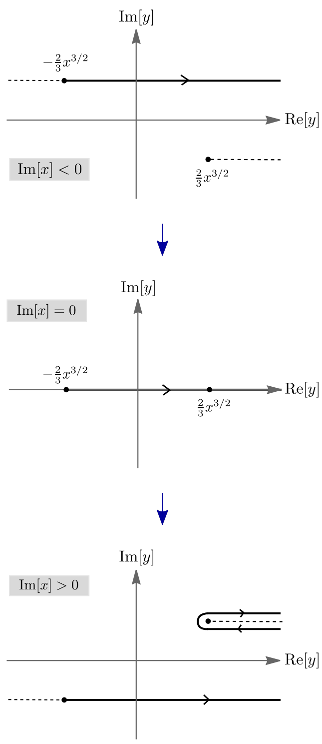

Crossing Stokes curves

What happens if crossing a Stokes curve?

Original x-space

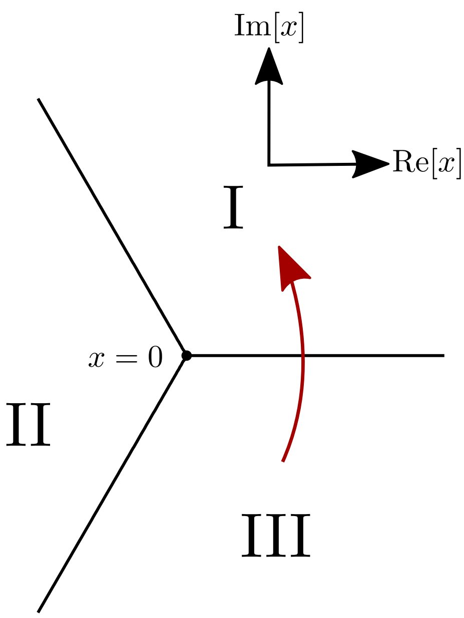

Borel y-space

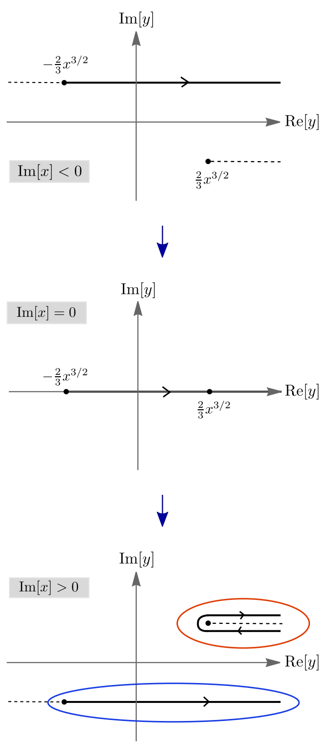

Connection formula

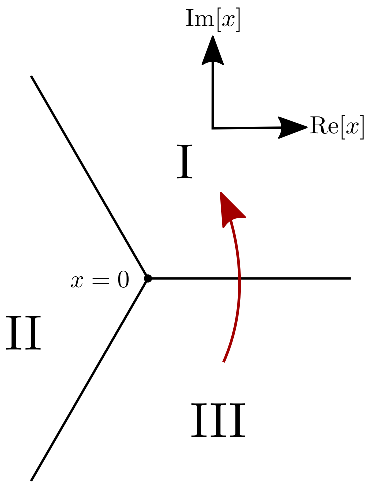

Connection formula

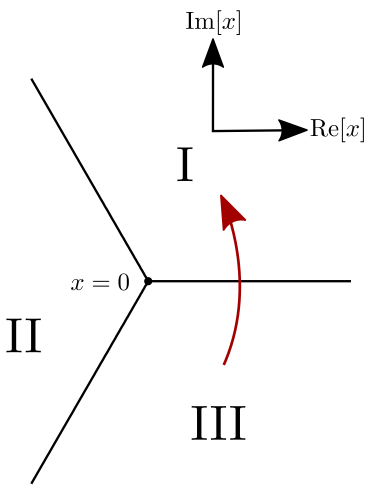

$\Rightarrow$

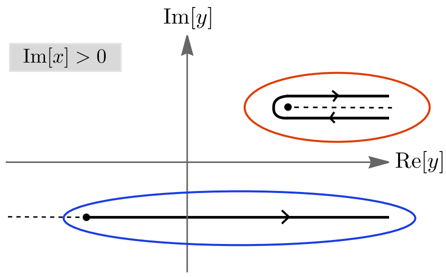

$$\underbrace{\psi_+^{(\mathrm{III})}(x,\eta)}_{\mathrm{Im}[x]<0} = \underbrace{\psi_+^{(\mathrm{I})}(x,\eta) + i\,\psi_-^{(\mathrm{I})}(x,\eta)}_{\mathrm{Im}[x]>0}$$

Connection formula

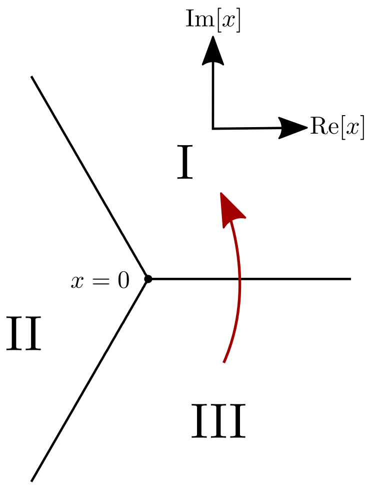

$\Rightarrow$

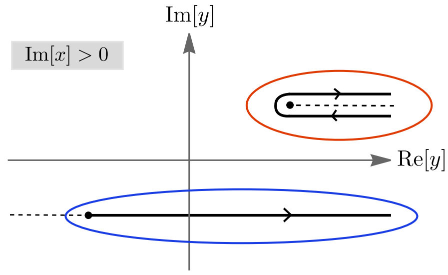

$$\underbrace{\psi_+^{(\mathrm{III})}(x,\eta)}_{\mathrm{Im}[x]<0} = \underbrace{\psi_+^{(\mathrm{I})}(x,\eta) + i\,\psi_-^{(\mathrm{I})}(x,\eta)}_{\mathrm{Im}[x]>0}$$

- In the limit $x \to \pm\infty$, $\psi_\pm$ correspond to the Bogolyubov coefficients α, β

$$\alpha = 1\,, \quad \beta = 0 \qquad \Longrightarrow \qquad \alpha \neq 0\,, \quad \beta \neq 0$$

- This connection formula implies **particle production is equivalent to the crossings of the Stokes curve**

Limitation of the connection formulae

An assumption: Turning points are never connected by Stokes lines

$Q(x) = x$

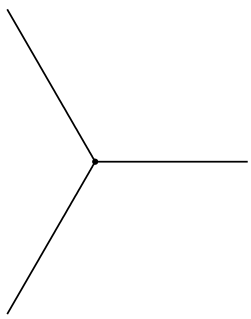

OK

$Q(x) = E - x^2/4 \;\; (\mathrm{Re}[E] > 0)$

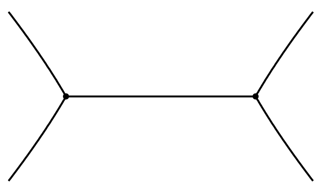

Not OK

An assumption: Turning points are never connected by Stokes lines

$Q(x) = x$

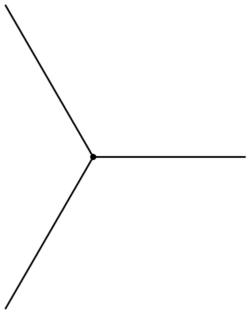

OK

$Q(x) = E - x^2/4 \ \ (\mathrm{Re}[E] > 0)$

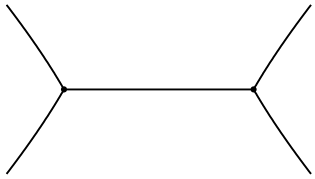

Not OK

Q.: What goes wrong with connected T.P.'s ?

An assumption: Turning points are never connected by Stokes lines

$Q(x) = x$

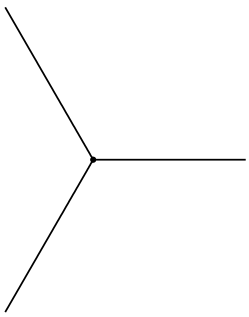

OK

$Q(x) = E - x^2/4 \ \ (\mathrm{Re}[E] > 0)$

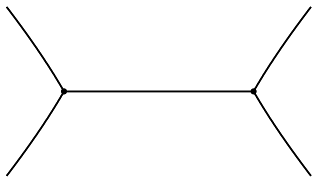

Not OK

Q.: What goes wrong with connected T.P.'s ?

A.: **Non-conservation of** $|\alpha|^2 - |\beta|^2$

Limitation of the connection formulae

An assumption: Turning points are never connected by Stokes lines

$Q(x) = x$

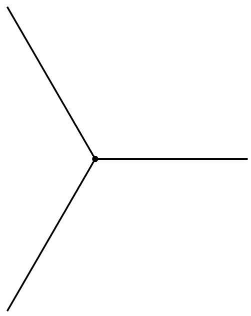

OK

$Q(x) = E - x^2/4 \;\; (\mathrm{Re}[E] > 0)$

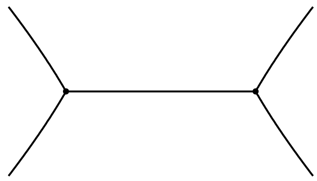

Not OK

Q.: What goes wrong with connected T.P.'s ?

A.: Non-conservation of $|\alpha|^2 - |\beta|^2$

- Equation of motion guarantees the conservation of **Bogolyubov coefficients**

$$\partial_x \left(|\alpha|^2 - |\beta|^2 \right) = 0$$

- Connected T.P.'s with the above connection formulae **do not** respect E.o.M. 😔

Outline

Oscillating field

Coherent oscillation of fields in the universe

- Inflaton
- Axion (dark matter)
- Higgs field ? (BSM)
- Electroweak/QCD phase transition ? (BSM)
- Fluid in neutron stars ?
- ...

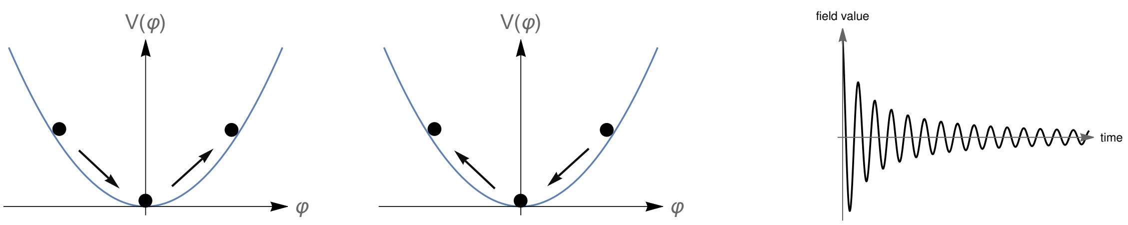

$$Q(x) = -A - 2q\cos 2x$$

Repeated crossings of Stokes lines

$$Q(x) = -A - 2q\cos 2x$$

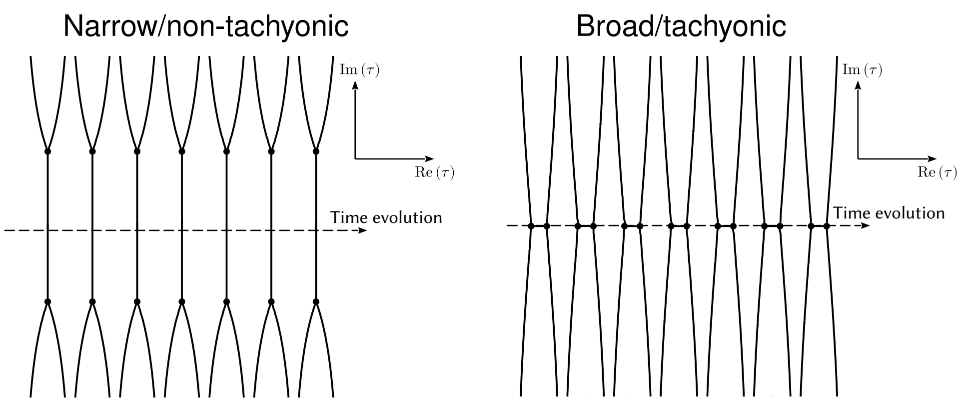

$$\begin{pmatrix} \alpha_{n+1} \\ \beta_{n+1} \end{pmatrix} = \mathcal{U}_n \begin{pmatrix} \alpha_n \\ \beta_n \end{pmatrix} = \mathcal{U}_n \mathcal{U}_{n-1} \begin{pmatrix} \alpha_{n-1} \\ \beta_{n-1} \end{pmatrix} = \cdots = \mathcal{V}_n \begin{pmatrix} \alpha_0 \\ \beta_0 \end{pmatrix} , \qquad \mathcal{V}_n \equiv \prod_{j=0}^{n} \mathcal{U}_j$$

General consideration of sourcing effects from particle production

Sourced equation

$$\Box\varphi_I = S_I$$

- **Curvature perturbations:** $\varphi_I = \zeta$
- **Gravitational wave:** $\varphi_I = h_{ij}$

Linear sourcing (mixing)

$$S_I = \mathcal{O}_I \otimes \psi$$

Quadratic sourcing (3-point vertex)

$$S_I = \mathcal{O}_I \otimes \psi\psi$$

Formal solution using Green function

$$\varphi_{I,\boldsymbol{k}} = \int_{-\infty}^{\infty} \mathrm{d}t'\, G_k(t,t')\, \tilde{S}_{I,\boldsymbol{k}}(t')$$

$$\Box_t G_k(t,t') = \delta(t-t')$$

Outline

Summary

Resonant/tachyonic production is ubiquitous in cosmology

- ▷ Reheating, dark matter production, phase transition, Schwinger effect, ...

WKB method – a systematic approach to Schrödinger-type equations

- ▷ Infinite series is often divergent around $Q(x) = 0$

Summary

Resonant/tachyonic production is ubiquitous in cosmology

- ▷ Reheating, dark matter production, phase transition, Schwinger effect, ...

WKB method – a systematic approach to Schrödinger-type equations

- ▷ Infinite series is often divergent around $Q(x) = 0$

Exact WKB = WKB + Borel sum

- ▷ **Particle production = crossing Stokes curves**

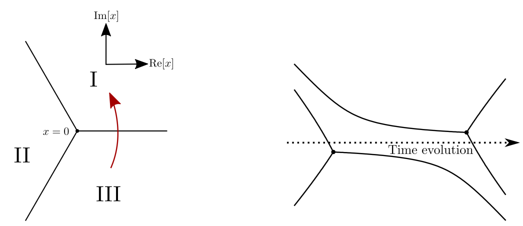

Connection formulae

$$\begin{pmatrix} \psi_+^{(\mathrm{III})} \\ \psi_-^{(\mathrm{III})} \end{pmatrix} = \begin{pmatrix} 1 & i \\ 0 & 1 \end{pmatrix} \begin{pmatrix} \psi_+^{(\mathrm{I})} \\ \psi_-^{(\mathrm{I})} \end{pmatrix}$$

Ryo Namba (RIKEN iTHEMS) Particle production & exact WKB 22 / 23

Issues & Outlook

- More rigorous, more "exact" calculation for periodic $Q(x)$

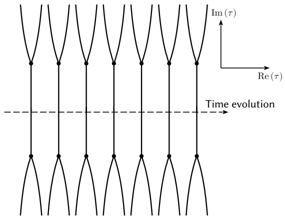

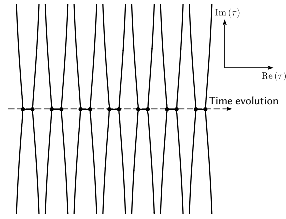

- More complete framework for generation of observables, e.g. gravitational waves

$$\Box \varphi_I = S_I \ , \qquad S_I = \mathcal{O}_I \otimes \psi \ , \ \mathcal{O}_I \otimes \psi\psi$$

- Consistent treatment of backreaction from particle production
  - ▷ To other fields coupled to ψ
  - ▷ To spacetime geometry
- Strong coupling regime
  - ▷ Resurgence framework
- Other applications
  - ▷ Hawking radiation, vacuum decay, strong gravity phenomena, ...

C26

Ruling out Interacting Holographic Dark Energy with Hubble scale cutoff
+
New constraints on Interacting dark energy

Ricardo G. Landim

Technical University of Munich

JGRG 31 – October 25, 2022

Based on 2206.10205 [Phys.Rev.D 106 (2022)] and work in progress (in collaboration with F. Abdalla, G. Hoerning, L. Ponte)

The best theories so far . . .

Gravitational interaction:

- General Relativity is running well . . . `[GR-Result: 0 Errors, xx Warnings, yy Bad Boxes]`

Strong and Electro-Weak interactions:

- Standard Model of particle physics is running . . . `[SM-Result: xx Errors, yy Warnings, zz Bad Boxes]` (+ neutrino masses + . . .)

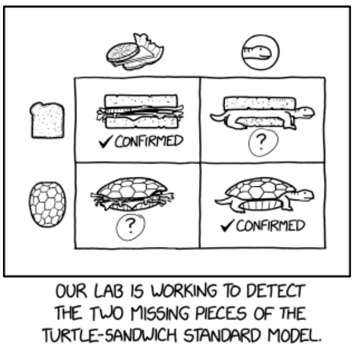

https://xkcd.com/2301/

The best theories so far . . .

Gravitational interaction:

- General Relativity is running well . . . `[GR-Result: 0 Errors, xx Warnings, yy Bad Boxes]`

Strong and Electro-Weak interactions:

- Standard Model of particle physics is running . . . `[SM-Result: xx Errors, yy Warnings, zz Bad Boxes]` (+ neutrino masses + . . .)

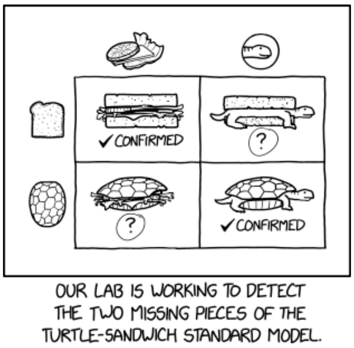

https://xkcd.com/2301/

- \make{ theory SM+GR} . . . `[fatal error occurred! no output produced ]`

The best theories so far . . .

Gravitational interaction:

- General Relativity is running well . . . `[GR-Result: 0 Errors, xx Warnings, yy Bad Boxes]`

Strong and Electro-Weak interactions:

- Standard Model of particle physics is running . . . `[SM-Result: xx Errors, yy Warnings, zz Bad Boxes]` (+ neutrino masses + . . .)

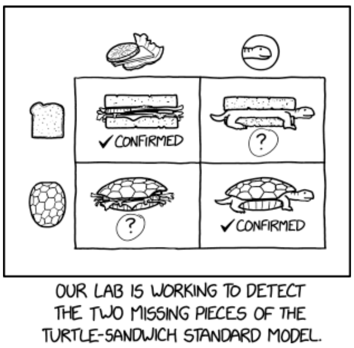

https://xkcd.com/2301/

- \make{ theory SM+GR} . . . `[fatal error occurred! no output produced ]`

BUT there is not only light, there is the dark side

- $SU(3) \times SU(2) \times U(1)$ (5%)
- Universe is expanding at accelerated rate (68%)
- Dark matter (27%)

Cosmological constant problem

- Universe expanding at an accelerated rate.
- $\rho_\Lambda^{(obs)} \approx 10^{-47}\text{GeV}^4$.
- $\rho_{vac} \approx 10^{74}\text{GeV}^4$.
- Famous 120-orders-of-magnitude discrepancy.
- Coincidence 'problem' - why are dark energy and matter densities of the same order today?

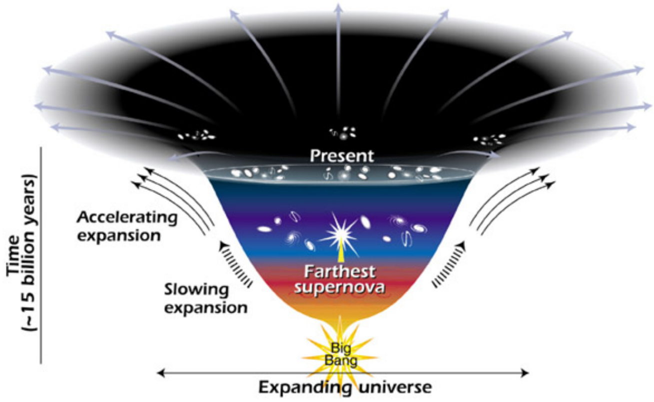

Source: Wikipedia

Dark energy models

Long list:

- Scalar or vector fields
- Modified gravity
- Metastable DE
- Extra dimensions
- Exotic fluids
- etc

Interacting dark energy

$$\dot{\rho_d} + 3H(\rho_d + p_d) = -\mathcal{Q}, \tag{1}$$

$$\dot{\rho_m} + 3H\rho_m = \mathcal{Q}, \tag{2}$$

$$\dot{\rho_r} + 4H\rho_r = 0, \tag{3}$$

The case of $\mathcal{Q} > 0$ corresponds to dark energy transformation into dark matter, while $\mathcal{Q} < 0$ is the transformation in the opposite direction.

Holographic principle

Degrees of freedom of a physical system scales with its boundary area rather than its volume.

- 't Hooft
- Susskind
- Thorn and Bekenstein

Cohen, Kaplan & Nelson [1998] suggested the following relationship:

$$L^3\Lambda^4 \lesssim LM_P^2 \tag{4}$$

$$\rho_D = 3c^2 M_{pl}^2 L^{-2} \tag{5}$$

HDE Hubble cutoff

- First (obvious)choice [Hsu, 2004]: $L \sim H^{-1}$, BUT

$$3H^2 = \rho_D + \rho_m = 3c^2H^2 + \rho_m \tag{6}$$
$$\rho_m = 3H^2(1 - c^2) \tag{7}$$

ρ_m **scales with** a^{-3}**, as so** $\rho_D \quad \rightarrow w_D = 0$

Holographic dark energy

HDE Particle horizon

- $L = R_H$

$$\rho_D = 3c^2M_{pl}^2L^{-2}, \quad R_H = a\int_0^t \frac{dt}{a}, \quad w_D = -\frac{1}{3} + \frac{2}{3c} > -\frac{1}{3} \tag{8}$$

HDE Future event horizon

- $L = R_E$ [Li 2004]

$$\rho_D = 3c^2 M_{pl}^2 L^{-2}, \quad R_E = a\int_t^\infty \frac{dt}{a}, \quad w_D = -\frac{1}{3} - \frac{2}{3c} \tag{9}$$

Interacting HDE

$$\rho_d = 3c^2 M_{pl}^2 H^2 \tag{10}$$

Constant c.

- $\mathcal{Q} = H(\lambda_1 \rho_{\rm dm} + \lambda_2 \rho_{\rm de})$

$$w = -\frac{1}{3}\left(\lambda_1 + \frac{\lambda_2}{r}\right)(1+r)\,. \tag{11}$$

$r \equiv \rho_m/\rho_d = (1-c^2)/c^2 \rightarrow c^2 = (1+r_0)^{-1}$

- Equation of state is no longer a free parameter
- When the coupling constants are zero, a pressureless fluid is recovered

$$\rho_{\rm dm} = \rho_{\rm dm,0}a^{-3+\lambda_1+\frac{\lambda_2}{r_0}} , \tag{12}$$

$$\rho_{\rm de} = \rho_{\rm de,0}a^{-3+\lambda_1+\frac{\lambda_2}{r_0}} . \tag{13}$$

$$\Rightarrow w_{\rm de}^{\rm eff} = w_{\rm dm}^{\rm eff} = -1/3(\lambda_1 + \lambda_2/r_0)$$

- Both fluids will have the same evolution
  - CDM (with $\lambda_1 = \lambda_2 \simeq 0$)   (*remember previous slides*)
  - DE ($w_{\rm de}^{\rm eff} < -1/3$)

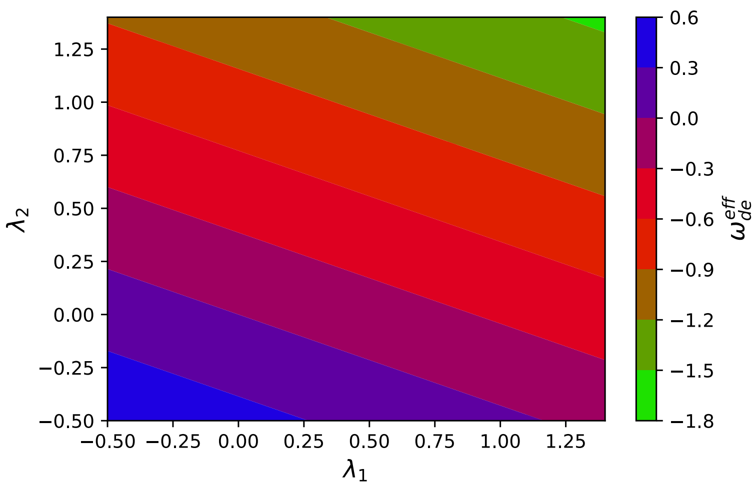

$$\dot{\delta}_{\rm dm} = -\theta_{\rm dm} - \frac{\dot{h}}{2} + \mathcal{H}\lambda_2 \frac{\rho_{\rm de,0}}{\rho_{\rm dm,0}}(\delta_{\rm de} - \delta_{\rm dm}) + \left(\lambda_1 + \lambda_2 \frac{\rho_{\rm de,0}}{\rho_{\rm dm,0}}\right)\left(\frac{k v_T}{3} + \frac{\dot{h}}{6}\right), \quad (14)$$

$$\dot{\theta}_{\rm dm} = -\mathcal{H}\theta_{\rm dm} - \left(\lambda_1 + \lambda_2 \frac{\rho_{\rm de,0}}{\rho_{\rm dm,0}}\right)\mathcal{H}\theta_{\rm dm}\,, \quad (15)$$

$$\dot{\delta}_{\rm de} = -(1+w)\left(\theta_{\rm de} + \frac{\dot{h}}{2}\right) - 3\mathcal{H}(1-w)\delta_{\rm de} + \mathcal{H}\lambda_1 \frac{\rho_{\rm dm,0}}{\rho_{\rm de,0}}(\delta_{\rm de} - \delta_{\rm dm})$$
$$- 3\mathcal{H}(1-w)\left[3(1+w) + \lambda_1 \frac{\rho_{\rm dm,0}}{\rho_{\rm de,0}} + \lambda_2\right]\frac{\mathcal{H}\theta_{\rm de}}{k^2} - \left(\lambda_1 \frac{\rho_{\rm dm,0}}{\rho_{\rm de,0}} + \lambda_2\right)\left(\frac{k v_T}{3} + \frac{\dot{h}}{6}\right), \quad (16)$$

$$\dot{\theta}_{\rm de} = 2\mathcal{H}\theta_{\rm de}\left[1 + \frac{1}{1+w}\left(\lambda_1 \frac{\rho_{\rm dm,0}}{\rho_{\rm de,0}} + \lambda_2\right)\right] + \frac{k^2}{1+w}\delta_{\rm de}\,, \quad (17)$$

$$(1+w_T)v_T = \sum_a (1+w_a)\Omega_a v_a\,. \quad (18)$$

Inclusion of term δH for interaction (*absent in other works!*)

$$\delta^{(i)}_{\rm de} = \delta^{(i)}_{\rm dm} = \frac{3}{4}\delta^{(i)}_r\left(1 - \frac{\lambda_1}{3} - \frac{\lambda_2}{3}\frac{1}{r_0}\right), \quad (19)$$

$$v^{(i)}_{\rm de} = v^{(i)}_r\,, \quad (20)$$

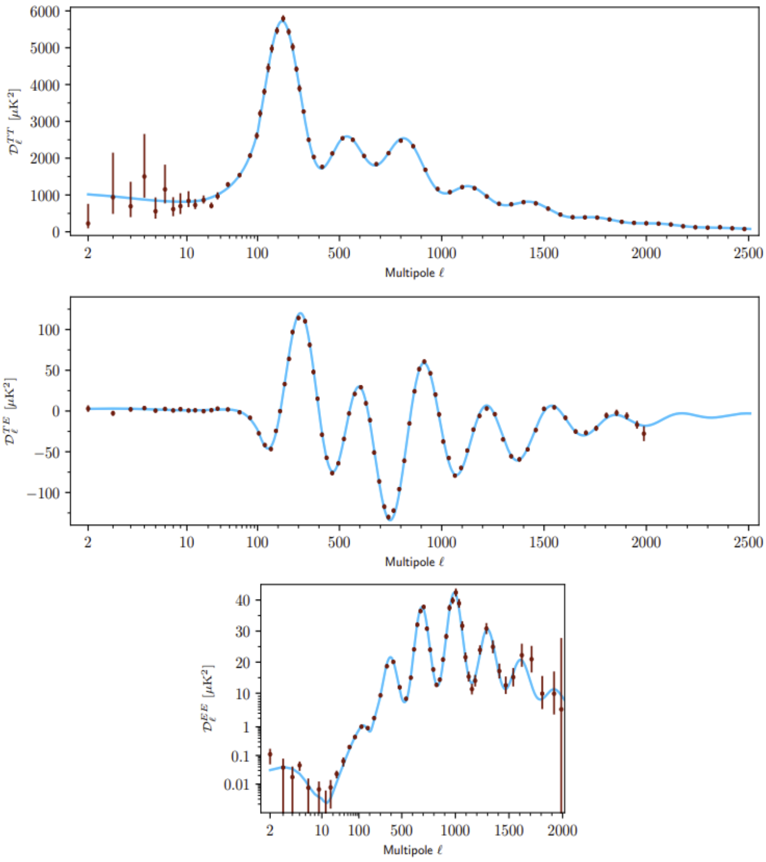

Planck 2018

Results

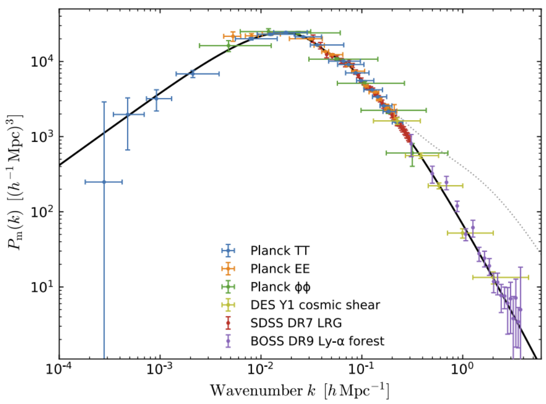

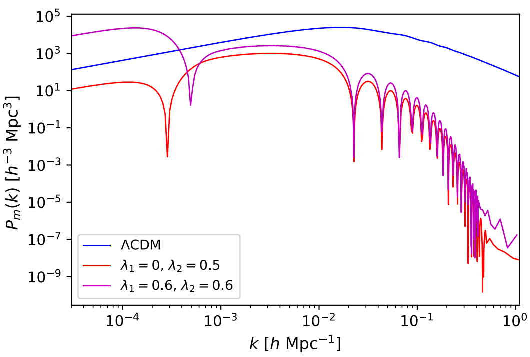

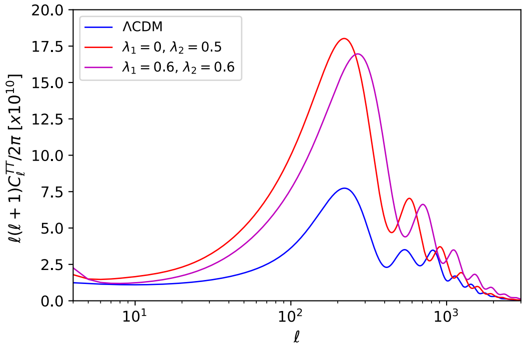
ΛCDM
$\lambda_1 = 0, \lambda_2 = 0.5$
$\lambda_1 = 0.6, \lambda_2 = 0.6$
$\ell(\ell+1)C_\ell^{TT}/2\pi$ [x10^{10}]
ℓ

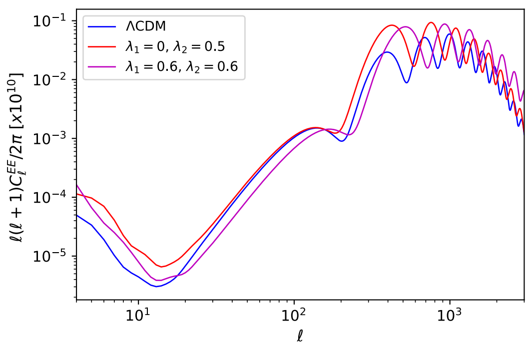
ΛCDM
$\lambda_1 = 0, \lambda_2 = 0.5$
$\lambda_1 = 0.6, \lambda_2 = 0.6$
$\ell(\ell+1)C_\ell^{EE}/2\pi$ [x10^{10}]
ℓ

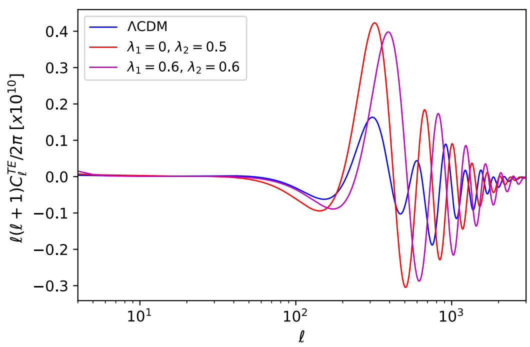
ΛCDM
$\lambda_1 = 0, \lambda_2 = 0.5$
$\lambda_1 = 0.6, \lambda_2 = 0.6$
$\ell(\ell+1)C_\ell^{TE}/2\pi$ [x10^{10}]
ℓ

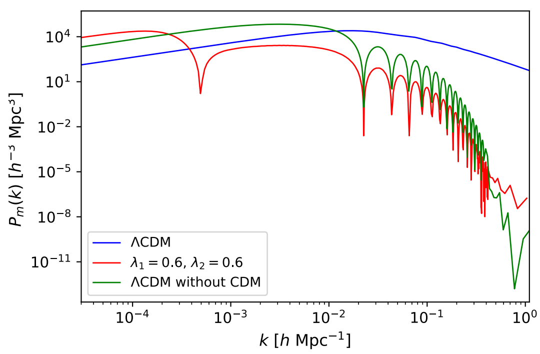
ΛCDM
$\lambda_1 = 0.6, \lambda_2 = 0.6$
ΛCDM without CDM
$P_m(k)$ [h^{-3} Mpc^3]
k [h Mpc^{-1}]

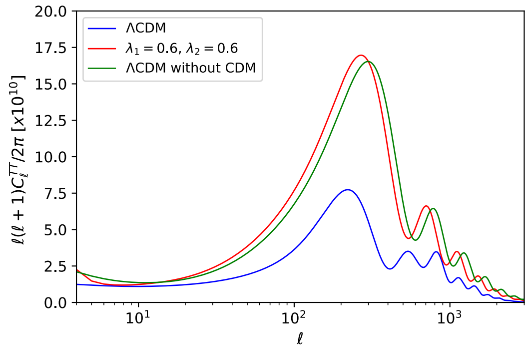
ΛCDM
$\lambda_1 = 0.6, \lambda_2 = 0.6$
ΛCDM without CDM
$\ell(\ell+1)C_\ell^{TT}/2\pi$ [x10^{10}]
ℓ

- Why new constraints?

New constraints on IDE

- Why new constraints?
- – (Not very) New data (Planck 2018, BAO, Pantheon)

Ricardo G. Landim October 20, 2022 19 / 25

- Why new constraints?
- – (Not very) New data (Planck 2018, BAO, Pantheon)
- – Inclusion of term δH for interaction (*absent in other works!*)

New constraints on IDE

- Why new constraints?
- – (Not very) New data (Planck 2018, BAO, Pantheon)
- – Inclusion of term δH for interaction (*absent in other works!*)

$$\dot{\rho}_{\rm dm} + 3\mathcal{H}\rho_{\rm dm} = a^2 Q^0_{\rm dm} = aQ\,, \tag{21}$$

$$\dot{\rho}_{\rm de} + 3\mathcal{H}(1+w)\rho_{\rm de} = a^2 Q^0_{\rm de} = -aQ\,, \tag{22}$$

$$Q = H(\lambda_1\rho_{\rm dm} + \lambda_2\rho_{\rm de})$$

- $\lambda_1 \neq 0$, $\lambda_2 = 0$
- $\lambda_1 = 0$, $\lambda_2 \neq 0$
- $\lambda_1 = \lambda_2$

- $\lambda_1 \neq 0,\ \lambda_2 = 0$

$$\rho_{\rm dm} = \rho_{\rm dm,0} a^{-3(1+w_1^{\rm eff})}\,, \tag{23}$$
$$\rho_{\rm de} = \rho_{\rm de,0} a^{-3(1+w)} + \lambda_1 \frac{\rho_{\rm dm,0} a^{-3(1+w)}}{3(w - w_1^{\rm eff})}\left[1 - a^{3(w-w_1^{\rm eff})}\right], \tag{24}$$

where $w_1^{\rm eff} = -\lambda_1/3$.

- $\lambda_1 = 0,\ \lambda_2 \neq 0$ [Lucca, 2020]

$$\rho_{\rm dm} = \rho_{\rm dm,0} a^{-3} + \lambda_2 \frac{\rho_{\rm de,0} a^{-3}}{3 w_2^{\rm eff}}\left[1 - a^{-3 w_2^{\rm eff}}\right], \tag{25}$$
$$\rho_{\rm de} = \rho_{\rm de,0} a^{-3(1+w_2^{\rm eff})}\,, \tag{26}$$

where $w_2^{\rm eff} = w + \lambda_2/3$.

- $\lambda_1 = \lambda_2$ [Olivares, 2005]

$$\rho_{\rm dm} = w_{\rm eff}^{-1}\left\{\left[\left(1 + w + \frac{\lambda}{3}\right)\rho_{\rm dm,0} + \frac{\lambda}{3}\rho_{\rm de,0}\right](a^{S_-} - a^{S_+}) + \rho_{\rm dm,0}(S_- a^{S_-} - S_+ a^{S_+})\right\}, \tag{27}$$
$$\rho_{\rm de} = w_{\rm eff}^{-1}\left\{\left[\frac{\lambda}{3}\rho_{\rm dm,0} - \left(1 - \frac{\lambda}{3}\right)\rho_{\rm de,0}\right](a^{S_+} - a^{S_-}) + \rho_{\rm de,0}(S_- a^{S_-} - S_+ a^{S_+})\right\}, \tag{28}$$

where $w_{\rm eff} = (w^2 + 4\lambda w/3)^{1/2}$ and $S_\pm = -(1 + w/2) \mp w_{\rm eff}/2$.

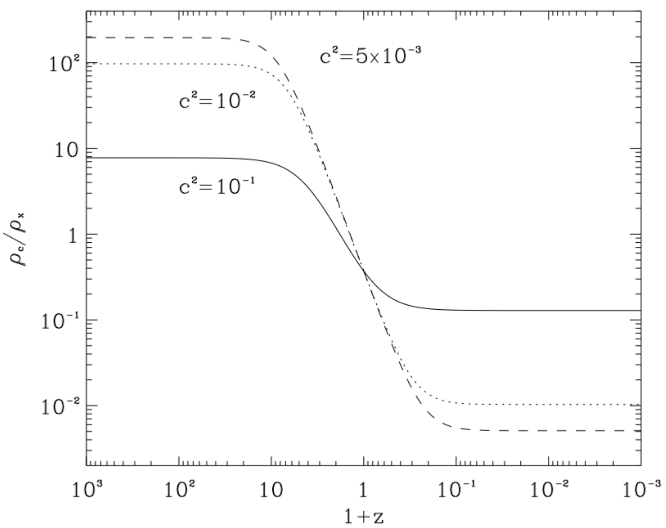

Olivares 2005

$\Rightarrow \dot{r} = 0$

$$\lambda_1 r_+ = -\frac{3}{2}\left(w + \frac{\lambda_1}{3} + \frac{\lambda_2}{3}\right) + \frac{3}{2}\sqrt{w^2 + \frac{2}{3}w(\lambda_1 + \lambda_2) + \frac{1}{9}(\lambda_1 - \lambda_2)^2}\,, \tag{29}$$

$$\lambda_1 r_- = -\frac{3}{2}\left(w + \frac{\lambda_1}{3} + \frac{\lambda_2}{3}\right) - \frac{3}{2}\sqrt{w^2 + \frac{2}{3}w(\lambda_1 + \lambda_2) + \frac{1}{9}(\lambda_1 - \lambda_2)^2}\,. \tag{30}$$

$$\dot{\delta}_{\rm dm} = -\theta_{\rm dm} - \frac{\dot{h}}{2} + \mathcal{H}\lambda_2\frac{\rho_{\rm de}}{\rho_{\rm dm}}(\delta_{\rm de} - \delta_{\rm dm}) + \left(\lambda_1 + \lambda_2\frac{\rho_{\rm de}}{\rho_{\rm dm}}\right)\underbrace{\left(\frac{kv_T}{3} + \frac{\dot{h}}{6}\right)}_{\propto\,\delta H}, \tag{31}$$

$$\dot{\theta}_{\rm dm} = -\mathcal{H}\theta_{\rm dm} - \left(\lambda_1 + \lambda_2\frac{\rho_{\rm de}}{\rho_{\rm dm}}\right)\mathcal{H}\theta_{\rm dm}\,, \tag{32}$$

$$\begin{aligned}\dot{\delta}_{\rm de} =& -(1+w)\left(\theta_{\rm de} + \frac{\dot{h}}{2}\right) - 3\mathcal{H}(1-w)\delta_{\rm de} + \mathcal{H}\lambda_1\frac{\rho_{\rm dm}}{\rho_{\rm de}}(\delta_{\rm de} - \delta_{\rm dm})\\ & - 3\mathcal{H}(1-w)\left[3(1+w) + \lambda_1\frac{\rho_{\rm dm}}{\rho_{\rm de}} + \lambda_2\right]\frac{\mathcal{H}\theta_{\rm de}}{k^2} - \left(\lambda_1\frac{\rho_{\rm dm}}{\rho_{\rm de}} + \lambda_2\right)\underbrace{\left(\frac{kv_T}{3} + \frac{\dot{h}}{6}\right)}_{\propto\,\delta H}, \end{aligned} \tag{33}$$

$$\dot{\theta}_{\rm de} = 2\mathcal{H}\theta_{\rm de}\left[1 + \frac{1}{1+w}\left(\lambda_1\frac{\rho_{\rm dm}}{\rho_{\rm de}} + \lambda_2\right)\right] + \frac{k^2}{1+w}\delta_{\rm de}\,, \tag{34}$$

$Q \propto \rho_{\rm dm} + \rho_{\rm de}$

$$\delta_{\rm de}^{(i)} = \frac{3}{4}\delta_r^{(i)}\left(1 + w + \frac{\lambda_1}{3}r + \frac{\lambda_2}{3}\right), \tag{35}$$

$$\delta_{\rm dm}^{(i)} = \frac{3}{4}\delta_r^{(i)}\left(1 - \frac{\lambda_1}{3} - \frac{\lambda_2}{3}\frac{1}{r}\right), \tag{36}$$

$$v_{\rm de}^{(i)} = v_r^{(i)}\,, \tag{37}$$

$Q \propto \rho_{\rm dm}$

$$\delta_{\rm de}^{(i)} = \delta_{\rm dm}^{(i)} = \frac{3}{4}\delta_r^{(i)}\left(1 - \frac{\lambda_1}{3}\right), \tag{38}$$

$Q \propto \rho_{\rm de}$

$$\delta_{\rm de}^{(i)} = \frac{3}{4}\delta_r^{(i)}\left(1 + w + \frac{\lambda_2}{3}\right), \tag{39}$$

$$\delta_{\rm dm}^{(i)} = \frac{3}{4}\delta_r^{(i)}\,. \tag{40}$$

- $Q \propto \rho_{\rm dm}$: $0 \leq \lambda_1 < -3w$ and $w < -1$
- $Q \propto \rho_{\rm de}$: $\lambda_2 < -w$
- $Q \propto \rho_{\rm dm} + \rho_{\rm de}$: $\lambda \leq -3w/4$ and $w < -1$

Preliminary

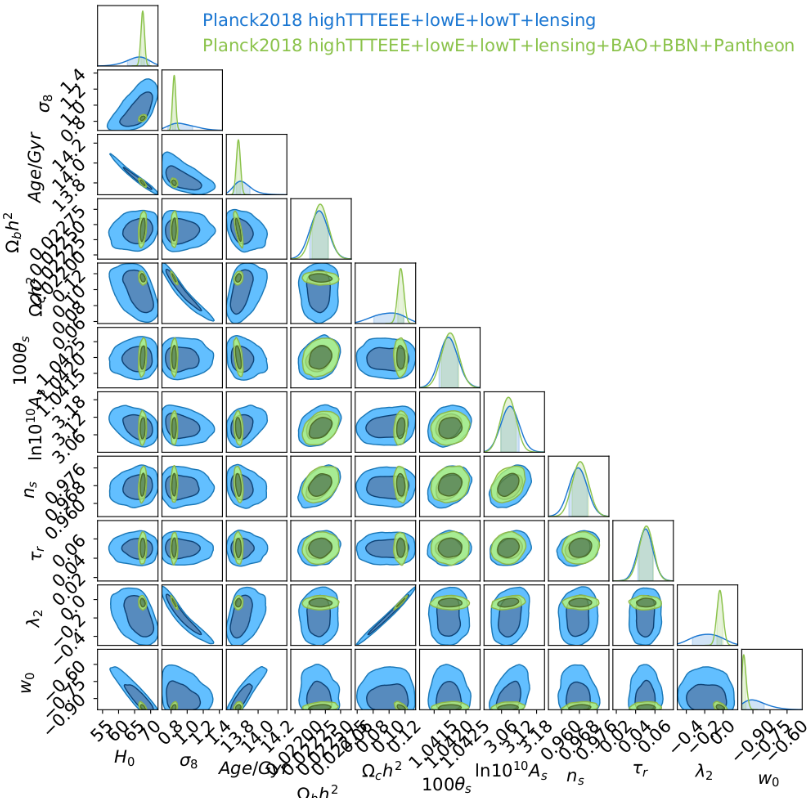

Thank you very much for your attention!

ご清聴ありがとうございました

ricardo.landim@tum.de

Neutrino Lines from MeV Dark Matter Annihilation and Decay in JUNO

Michiru NIIBO (TiTech., Ochanomizu Univ.)
2022/10/25, JGRG31(c27)@Univ. of Tokyo

Based on: [arXiv: 2206.06755], accepted for publication in JCAP, with
K.Akita, G.Lambiase(Salerno Univ., Italy) , M.Yamaguchi(TiTech, Japan)

Outline

- Introduction:
  - Dark matter detection strategies
- Analysis
  - Neutrino lines from dark matter
  - Current constraints
  - JUNO experiment and detection principle
- Results
- Summary

Dark matter(DM) detection strategies

(1) Direct Detection

Scatter DM particles with atoms (nuclei, electrons...)

(2) Optical Detection

Detect photons from DM or from standard model particles produced from DM

⇨ Unfortunately, we have not detected any signals of DM and strong constraints on DM- standard model particle interactions are discovered.

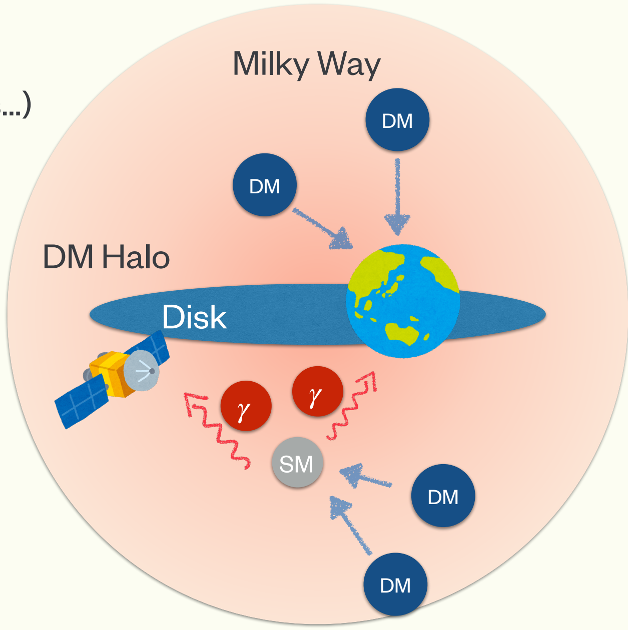

Detection strategy (3) Neutrino observation

- **Complementary strengths of neutrino detection**
  - Detectable on the ground
  - Less background than optical signals
  - Electrically neutral -> stable, straight signal
- **Next-generation neutrino detectors**
  - JUNO (2023 ? -)
  - Super - Kamiokande (+ Gd)(2020 -)
  - Hyper - Kamiokande (2027 -)

⇨ Would undiscovered DM signals be finally found through neutrino observation?

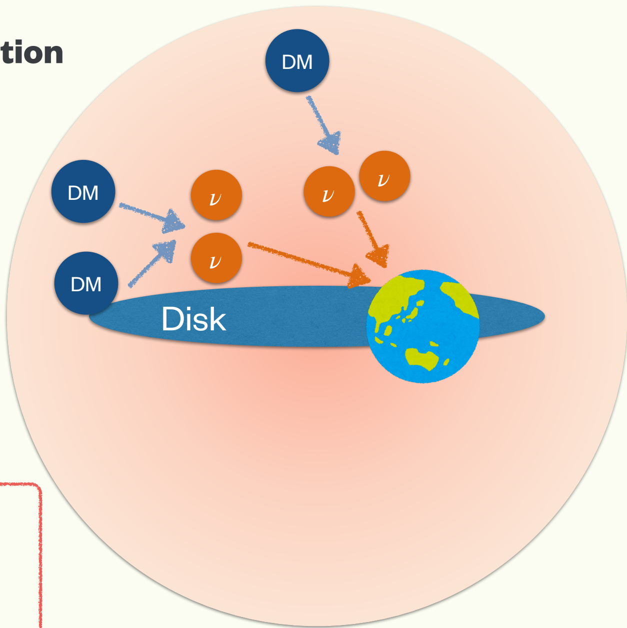

Neutrino lines from DM

Neutrino productions in Milky Way (MW)

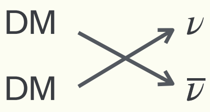

$$\frac{d\Phi_{\text{anni}}}{dE_\nu} = \Phi_{\text{anni}}\delta\left(E_\nu - m_{\text{DM}}\right)$$

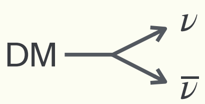

$$\frac{d\Phi_{\text{dec}}}{dE_\nu} = \Phi_{\text{dec}}\delta\left(E_\nu - \frac{m_{\text{DM}}}{2}\right)$$

One to one correspondence

between E_ν and m_{DM}

Neutrino production in the whole MW

$$\Phi_{\text{anni}} = \frac{1}{6}\int \frac{ds\, d\Omega}{4\pi}\langle\sigma_{\text{anni}}v\rangle\, n_{\text{DM}}^2 \propto m_{\text{DM}}^{-2}$$

$$\Phi_{\text{dec}} = \frac{1}{6}\int \frac{ds\, d\Omega}{4\pi}\, 2\tau^{-1}\, n_{\text{DM}}^1 \propto m_{\text{DM}}^{-1}$$

$n_{\text{DM}} = \frac{\rho_{\text{DM}}}{m_{\text{DM}}}$: DM number density $\quad \rho_{\text{DM}}$: DM profile

Φ gets smaller as m_{DM} gets larger.

The largest uncertainty of our work: DM profile $\rho = \rho(r)$

$$\Phi_{\text{anni}} = \frac{1}{6}\int \frac{ds\, d\Omega}{4\pi}\langle\sigma_{\text{anni}}v\rangle\, n_{\text{DM}}^2,$$

$$\Phi_{\text{dec}} = \frac{1}{6}\int \frac{ds\, d\Omega}{4\pi}\, 2\tau^{-1}\, n_{\text{DM}}^1,$$

$$\mathcal{J} = \int ds\, d\Omega\, \rho_{\text{DM}}^2, \quad \text{...Annihilation}$$

$$\mathcal{D} = \int ds\, d\Omega\, \rho_{\text{DM}}. \quad \text{...Decay}$$

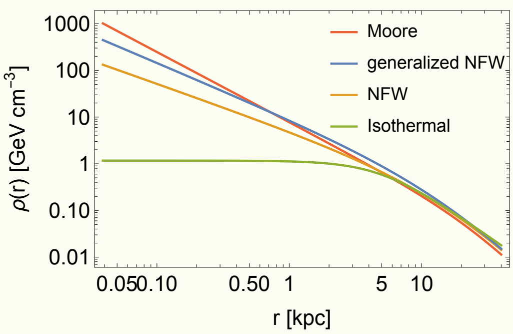

$\mathcal{J}$ $[10^{23}\,\text{GeV}^2\text{cm}^{-5}]$, $\mathcal{D}$ $[10^{23}\,\text{GeV}\text{cm}^{-2}]$

	$\mathcal{J}$	$\mathcal{D}$
Generalized NFW	2.3	2.5
NFW	0.88	1.9
Moore	2.7	2.5
Isothermal	0.53	1.9

Factor 5 of uncertainty in annihilation case

Current constraint on annihilation

DM → ν
DM → $\overline{\nu}$

Colored areas:
constraints from the current observations

Dashed lines:
anticipated constraints from the future observations

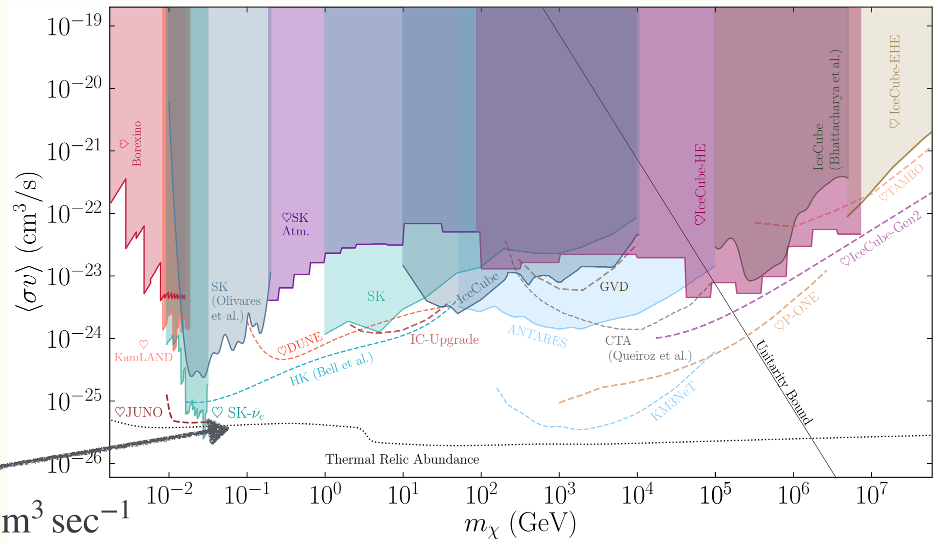

Dotted line: (WIMP)
Thermal Relic Abundance

$$\langle \sigma_{\rm anni} v \rangle \sim (3-4) \times 10^{-26}\, {\rm cm}^3\, {\rm sec}^{-1}$$

... Has NOT been tested

[Arguelles et al. [1912.09486]]

Current constraint on decay

DM → ν $\overline{\nu}$

[Palomares-Ruiz [0712.1937]]

Super-Kamiokande

Shaded area: [0209028]
Colored : [0501064]

$\tau \geq 10^{23}$ sec
Current constraint in MeV

$\tau > t_U \simeq 4 \times 10^{17}$sec
Age of our universe

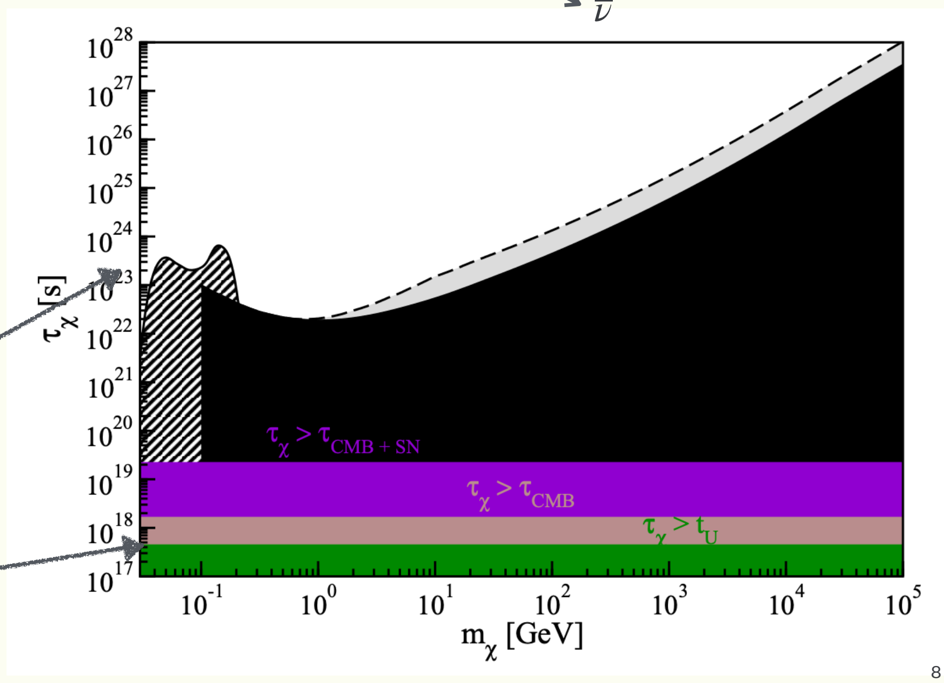

JUNO experiment

	Super Kamiokande	JUNO
Detection	Water	liquid scintillator
Volume	$\simeq 22.5\,\mathrm{kton}$	$17\,\mathrm{kton}$
Resolution	$\simeq 40\,\%$ at $1\,\mathrm{MeV}$ [Palomares-Ruiz et al. [0710.5420]]	$3\,\%$ at $1\,\mathrm{MeV}$

Wikipedia

- **Channel** : Inverse beta decay (IBD) $\bar{\nu}_e + p \to n + e^+$
  - Main channel in $10\,\mathrm{MeV} < E_\nu < 100\,\mathrm{MeV}$
  - Little smearing effect $\Delta E_{e^+} \equiv E_{\max} - E_{\min} \sim 5\,\mathrm{MeV}\left(\frac{E_\nu}{50\,\mathrm{MeV}}\right)^2$

⇨ Easy to distinguish signals from background

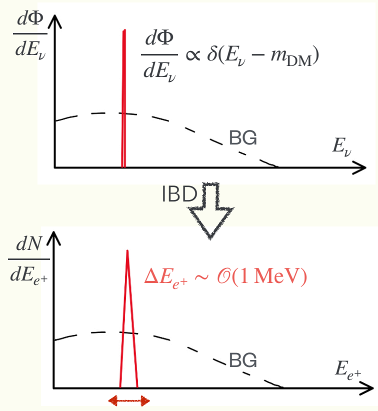

Annihilation cross section (20years, 90% C.L.)

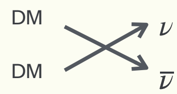

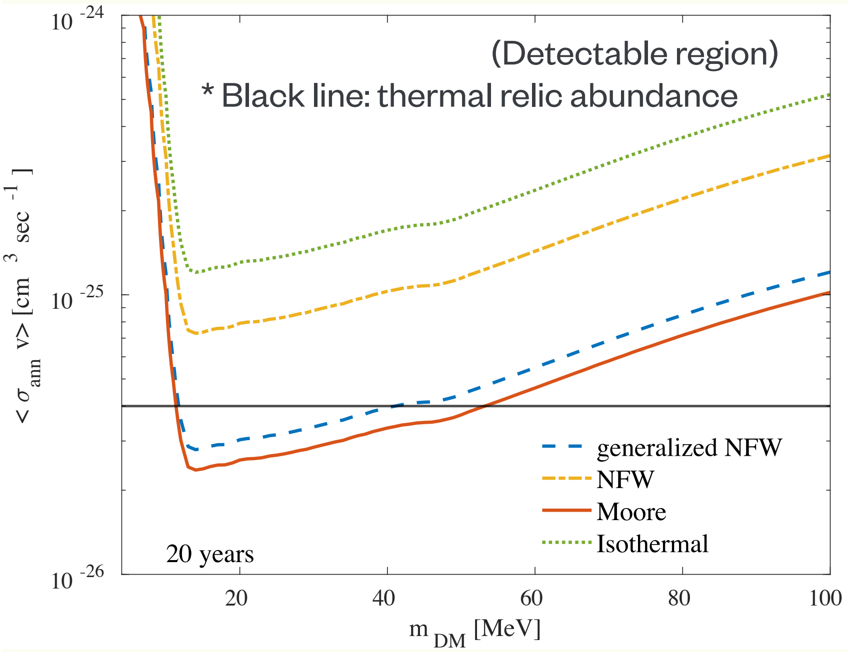

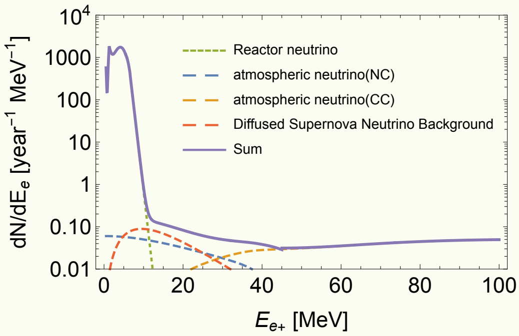

- JUNO may test the thermal relic abundance in $10\,\mathrm{MeV} \leq m_{\mathrm{DM}} \leq 60\,\mathrm{MeV}$
- Factor 5 of uncertainty due to DM profile
- $\Phi_{\mathrm{anni}} \propto m_{\mathrm{DM}}^{-2}$:

  weaker constraint in the higher energy

Lifetime (20years, 90% C.L.)

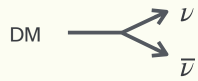

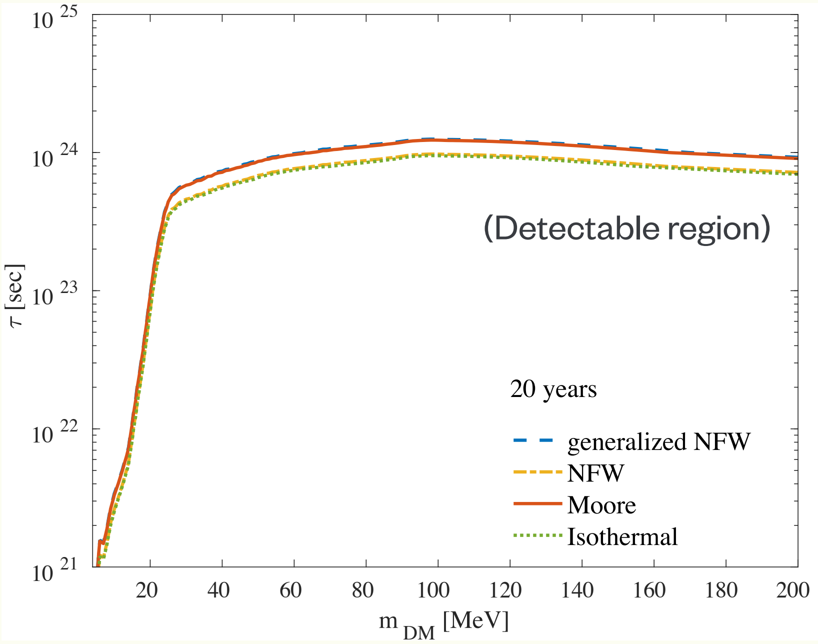

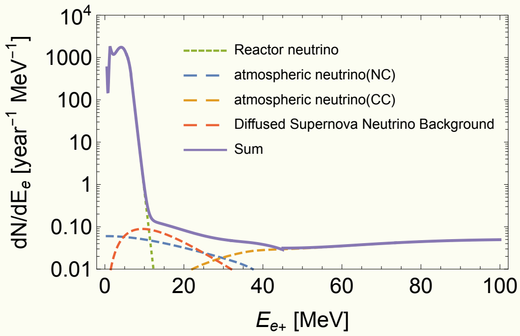

- $\tau \simeq 1 \times 10^{24}$ sec in
  $30\,\mathrm{MeV} \lesssim m_{\mathrm{DM}} \lesssim 200\,\mathrm{MeV}$
- Factor 2 of uncertainty due to DM profile
- $\Phi_{\mathrm{dec}} \propto m_{\mathrm{DM}}^{-1}$:
  weaker constraint in the higher energy
  … Compared to annihilation, weakening effect is little

Summery

- **Dark Matter (DM)**
  - Unknown massive substances which contribute to the structure formation
  - Thermal relic abundance

$$\langle \sigma_{\mathrm{anni}} v \rangle \sim (3-4) \times 10^{-26} \mathrm{cm}^2\,\mathrm{sec}^{-1}$$

- **JUNO experiment :**

	Super Kamiokande	JUNO
Detection	Water	liquid scintillator
Volume	$\simeq 22.5$ kton	17 kton
Resolution	$\simeq 40\,\%$ at 1 MeV	$3\,\%$ at 1 MeV

[Palomares-Ruiz et al. [0710.5420]]

- **Channel : Inverse beta decay**
  - Main channel in MeV region
  - Little smearing effect
- **Discussion and results**
  - Neutrino lines in Milky Way

1. Successfully update the constraints
   JUNO may detect DM signals!!
2. Test thermal relic abundance ?
3. Profile uncertainty : factor 2-5
4. Constraints get weaker as m_{DM} gets larger.

C28

Superheavy Dark Matter Production from Symmetry Restoration First-Order Phase Transition During Inflation

Siyi Zhou
Kobe University
with Haipeng An, Xi Tong
arXiv:2208.14857 [hep-ph]

Outline

- Superheavy Dark Matter
- Symmetry Restoration First-Order Phase Transition During Inflation
- Observational Signatures: Stochastic gravitational wave background
- Conclusion and Outlook

Dark Matter

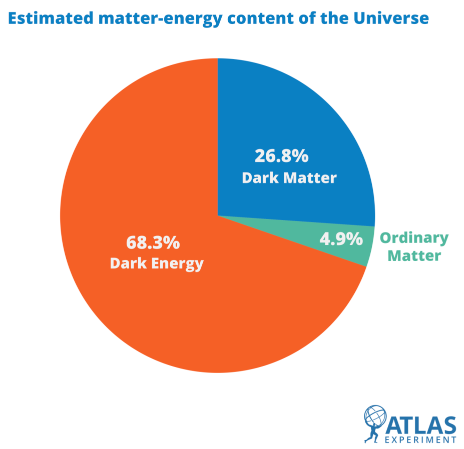

Most (85%) of the matter in our universe is made of dark matter

Does not interact with the electromagnetic field

Has huge influence on cosmology & large scale structure

We know its existence through its gravitational effects

ΛCDM Cosmology
68.3% Dark Energy
26.8% Dark Matter
4.9% Ordinary Matter

Dark Matter

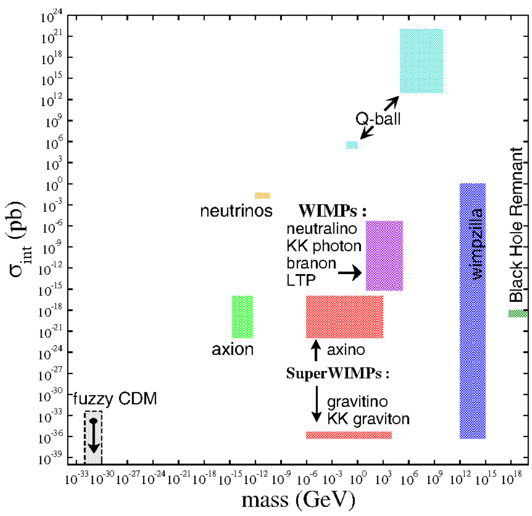

Many dark matter candidates

Wide range of masses & cross sections

The nature of dark matter and its production mechanism remains unknown

Particle vs wave?

Most popular dark matter model
Weakly Interacting Massive Particles (WIMPs)

WIMPs are produced from the early universe through the freeze out mechanism

Superheavy Dark Matter

Many WIMP models are strictly constrained by direct detection experiments
Search for dark matter heavier than **Griest-Kamionkowski bound**
Different dark matter production mechanism
Freeze in
E. Kolb, D. Chung, A. Riotto, AIP Conf. Proc. 484 (1999) 91-105
D. J. H. Chung, P. Crotty, E. W. Kolb, A. Riotto, Phys. Rev. D 64 (2001) 043503
Phase transitions
D. Marfatia, P. Y. Tseng JHEP 02 (2021) 022
A. Azatov, M. Vanvlasselaer, W. Yin, JHEP 03 (2021) 288

Freeze in

Production Time

During inflation from vacuum

At inflation to matter dominated/radiation dominated era

Production Rate

$m_\sigma \ll H$ $\quad n_\sigma \sim H$ $\quad$ Ford 1987

$m_\sigma \gg H$ $\quad n_\sigma \sim \exp(-\# m_\sigma / H)$ $\quad$ Chung 2003

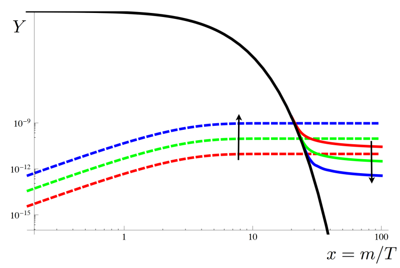

Production mechanism freeze in

Properties

Stable a lifetime much greater than the age of the universe
Non-thermal it must not have been in equilibrium when it froze out

Phase transitions

A more efficient superheavy dark matter production mechanism during inflation

Symmetry restoration first order phase transition during inflation

Enough dark matter can be produced from large latent heat during first order phase transition

Outline

Superheavy Dark Matter

Symmetry Restoration First-Order Phase Transition During Inflation

Observational Signatures

Conclusion and Outlook

First Order Phase Transition

Inflation begins
Symmetry broken phase

Symmetry restoration first order
phase transition happens GW generated

Dark matter is produced, relativistic

Dark matter becomes non-relativistic

Inflation ends
Symmetry restoration phase

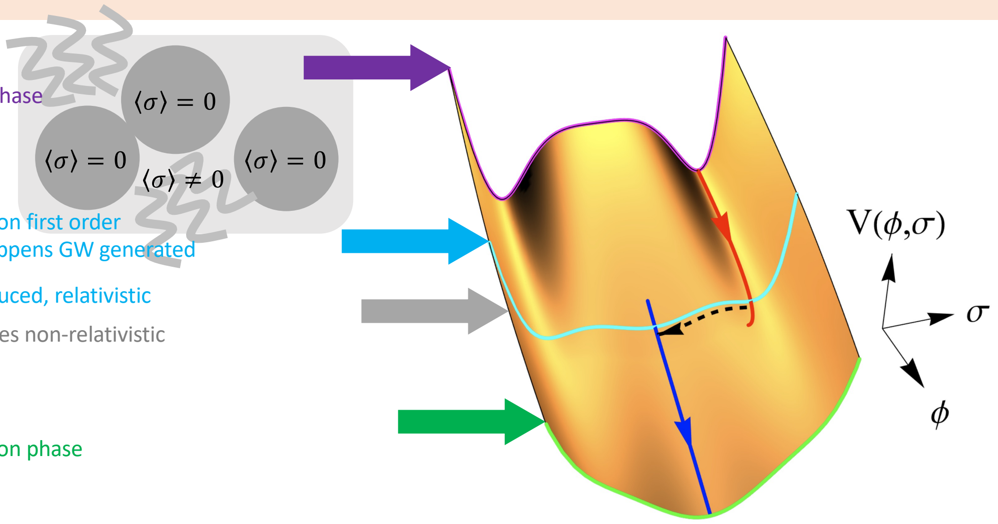

First Order Phase Transition

During inflation, the inflaton field typically travels $\Delta\phi \sim N_e\sqrt{\epsilon}\, M_{pl}$

The change in the inflaton field value will induce the change in the effective potential in the σ sector

$$S \equiv \int d^4x\sqrt{-g}[-\frac{1}{2}(\partial\phi)^2 - \frac{1}{2}(\partial\sigma)^2 - U(\phi,\sigma)]$$

$$U(\phi,\sigma) \equiv V(\phi,\sigma) + V_{sr}(\phi)$$

$$V(\phi,\sigma) \equiv \frac{1}{2}\mu_{eff}^2(\phi)\sigma^2 + \frac{\lambda}{4}\sigma^4 + \frac{1}{8\Lambda^2}\sigma^6$$

$$\mu_{eff}^2(\phi) \equiv \mu^2 - c^2\phi^2$$

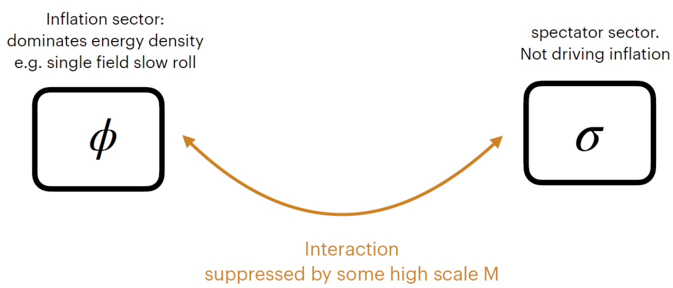

First Order Phase Transition

Typical mass scale of the σ particle is m_σ

The bubble nucleation rate per physical volume

$$\frac{\Gamma}{V_{phys}} = O(1) \times m_\sigma^4 e^{-S_4}$$

S_4 is the classical action of the bounce solution

Bubble nucleate at t', the comoving radius at t is

$$R(t,t') = \frac{1}{H}(e^{-Ht'} - e^{-Ht})$$

The fraction of the space that remains at the false vacuum at time t

$$P(t) = \exp(-\int_{-\infty} dt' \frac{4\pi}{3H^3}\left(e^{-Ht'} - e^{-Ht}\right)^3 e^{3Ht'} C m_\sigma e^{-S_4}) \sim O(1)$$

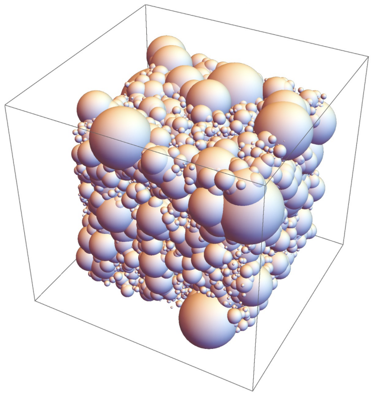

First Order Phase Transition

Conditions on the parameter space

- Phase transition is strong first order $S_4 \gg 1$

$$m_\sigma^4 \gg \beta^4$$

- The energy density of the spectator sector is subdominant

$$m_\sigma^4 \sim V(\phi,\sigma) \ll V_{sr}(\phi) \sim M_{pl}^2 H^2$$

We need

$$\left[\left(\frac{\beta}{H}\right)^4 H^2\right] H^2 \ll m_\sigma^4 \ll M_{pl}^2 H^2$$

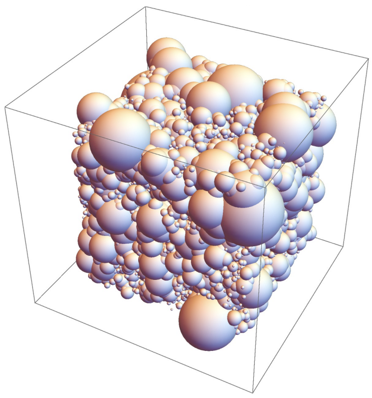

First Order Phase Transition

β describes how fast the phase transition happens

$$\beta \equiv -\frac{dS_4}{dt} = O(100)\left|\frac{\dot{\phi}}{\phi - \frac{\mu^2}{c^2\phi}}\right|$$

$\beta \gg H$ phase transition completes during inflation

β also determines the bubble radius

$$R_{bubble} \sim \beta^{-1} \ll H^{-1}$$

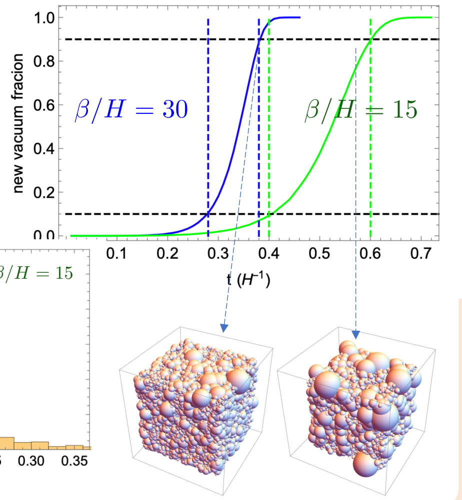

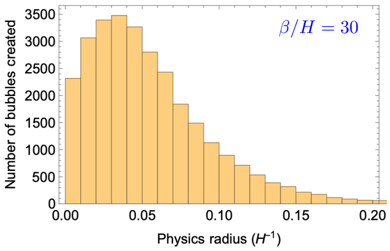

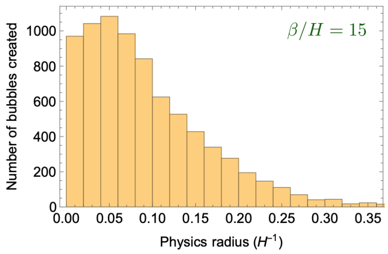

First Order Phase Transition

After the phase transition

σ particles are formed in the Z_2 symmetric phase

σ particles are stable and can be the dark matter candidate

First Order Phase Transition

Latent heat $L \equiv \gamma_{PT} m_\sigma^4$ $\gamma_{PT} \le 0.6$

$$\gamma_{PT} m_\sigma^4 = \int \frac{d^3\mathbf{p}}{(2\pi)^3} \sqrt{m_\sigma^2 + \mathbf{p}^2}\, e^{-\frac{\sqrt{m_\sigma^2+\mathbf{p}^2}}{T}}$$

Just after the phase transition ends

Highly relativistic $\gamma_{PT} \le 0.6$ $\mathrm{T} = 1.2 m_\sigma$ $\bar{E} = 4 m_\sigma$

After a while, Marginal relativistic $\bar{E} = 2 m_\sigma$ $\mathrm{T} = 0.48 m_\sigma$ $\gamma_* \simeq 0.01$

Dark matter relic abundance

$$\rho_{DM}^{(0)} = \Omega_\sigma \rho_0 = \frac{0.11923}{0.68^2}\left(3 M_p^2 H_0^2\right) \hbar^2 c^4 = (1.76\times 10^{-12}\mathrm{GeV})^4$$

The energy density of dark matter today

$$\rho_\sigma^{(0)} \sim \gamma_* \times m_\sigma^4 e^{-3\left(N_{today} + N_{PT} - \frac{1}{4}\ln(\gamma_{PT}/\gamma_*)\right)} \qquad \rho_\sigma^{(0)} = \rho_{DM}^{(0)}$$

Typical parameter choice $H = 10^{12}\mathrm{GeV}$ The e-folding number from end of inflation to today is $N_{today} = 65$ The e-folding number from phase transition to end of inflation is $N_{PT} = 18$

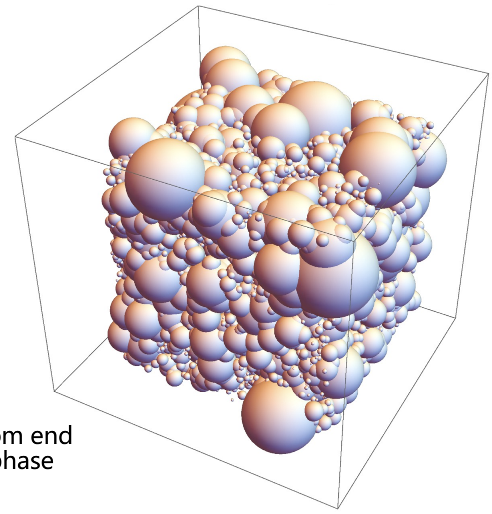

Dark Matter Decay Rate

Particle number decreases! Decay channels

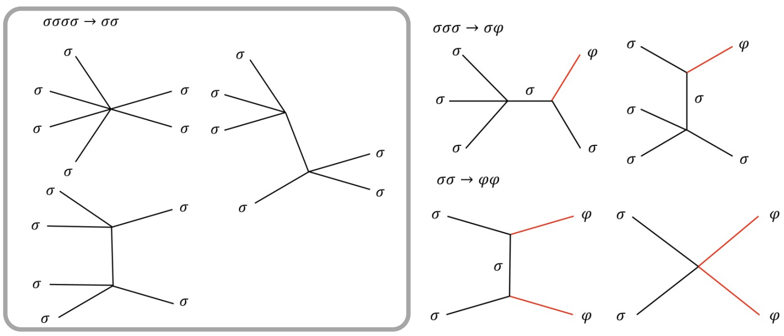

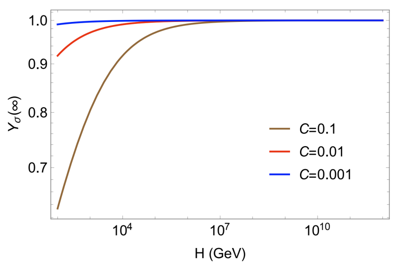

$$Y_\sigma(t) = \frac{n_\sigma(t) a^3(t)}{n_\sigma(t_*) a^3(t_*)}$$

$$\frac{dY_\sigma}{dt} \sim C \frac{Y_\sigma^4 n_\sigma^3(t_*)}{m_\sigma^8} e^{-9H(t-t_*)} - \frac{Y_\sigma^4 n_\sigma^2(t_*)}{m_\sigma^3 M_{pl}^2} e^{-6H(t-t_*)} - \frac{Y_\sigma^2 n_\sigma(t_*)}{M_{pl}^4} e^{-3H(t-t_*)}$$

Most dominant contribution

Dark Matter Decay Rate

Dark matter decay is protected by global Z_2 symmetry via symmetry restoration first order phase transition

What about symmetry broken first order phase transition?

As long as there are Z_2 symmetry left, there are will be enough dark matter left after the phase transition

Dark Matter Decay Rate

No global symmetry in quantum gravity

σ particles will decay, unable to serve as dark matter

Local Z_2 symmetry

$$S = \int d^4x \sqrt{-g}[-\frac{1}{2}(\partial\phi)^2 + |\partial\eta - 2igA\eta|^2 - W(\phi, |\eta|) - |\partial\sigma - igA\sigma|^2 - m_\sigma^2|\sigma|^2 - \frac{1}{4}F_{\mu\nu}F^{\mu\nu}]$$

Rolling of ϕ generates a VEV for η

Symmetry breaking phase transition, σ particle production

$$U(1) \to \text{local } Z_2$$
$$\sigma \to e^{i\alpha(x)}\sigma = \pm\sigma$$
$$\eta \to e^{2i\alpha(x)}\eta = \eta$$

$$A \to A + \frac{1}{g}\partial\alpha(x) \quad \alpha(x) = 0, \pi$$

σ can serve as dark matter $H \ll m_\sigma \ll m_\eta, m_A$

Outline

Superheavy Dark Matter

Symmetry Restoration First-Order Phase Transition During Inflation

Observational Signatures

Conclusion and Outlook

Stochastic Gravitational Wave

Very low frequency: CMB B mode

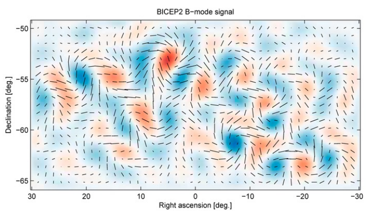

Middle frequency: LISA

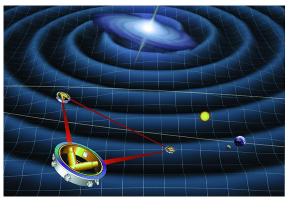

Low frequency: Pulsar timing array

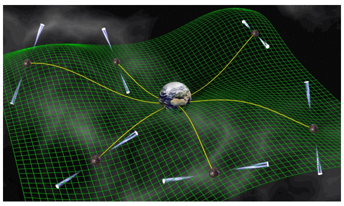

High frequency: LIGO, VIRGO

Stochastic Gravitational Wave

Sources that can generate stochastic gravitational wave

Inflation Quantum fluctuations of GW that went outside horizon and became classical

Cosmic strings one-dimensional topological defects

First order phase transitions GW from bubble nucleations

Pre big bang models an extension of the standard inflationary cosmology

Binary black holes GWs

Binary neutron stars GWs

Supernovae if a supernova has some asymmetry, then GWs will be produced

Pulsar and magnetars Non-axisymmetric spinning neutron stars are expected to be a detectable source of GWs

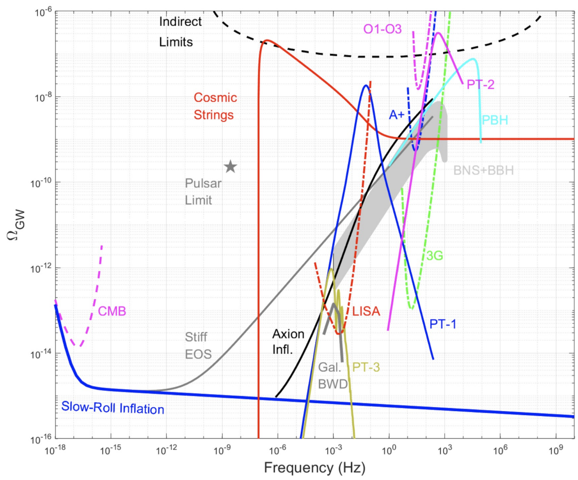

Gravitational wave from first order phase transitions

The UV spectrum decreases as $f^{-1.8}$

Arthur Kowsowsky, Michael S. Turner
PRD Volume 47, Number 10
Two bubbles

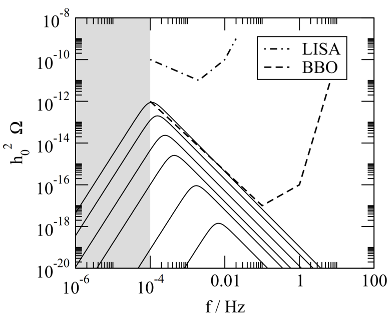

The IR spectrum rises as f^3
The UV spectrum decreases as f^{-1}

Stephan J. Huber, Thomas Konstandin
JCAP 0809:022,2008
More bubbles

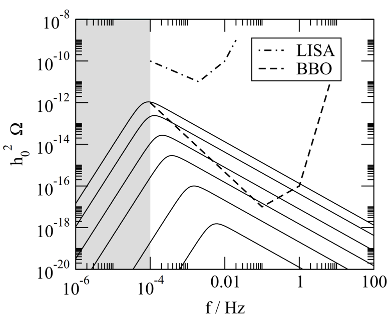

Gravitational wave from first order phase transitions during inflation

First order phase transition happen during inflation. The first order phase transition will produce bubbles. Bubbles will collide and thus generate gravitational waves.

H. Jiang, T. Liu, S. Sun, Y. Wang Physics Letters B, Volume 765, Pages 339-343

First order phase transition at the beginning of inflation and its detectability at cosmic microwave background (CMB)

Y. Wang, Y. Cai, Y. Piao Phys.Lett.B789(2019)191-196

First order phase transition during inflation and its detectability at gravitational wave interferometers, such as LISA and LIGO

H. An, K. Lyu, L. Wang, S. Zhou Chin.Phys.C 46 (2022) 10, 101001

First order phase transition during inflation, its associated gravitational wave signal and how it can be distinguished from the first order phase transition after inflation

H. An, K. Lyu, L. Wang, S. Zhou JHEP 06 (2022) 050

First order phase transition during inflation, its associated gravitational wave signal and how it can reflect the cosmological time evolution

How GW propagates in spacetime

The equation of motion of the transverse and traceless GW perturbation is

$$h_{ij}'' + \frac{2a'}{a}h_{ij}' - \nabla^2 h_{ij} = \boxed{16\pi G_N a^2 \sigma_{ij}}$$

Bubble wall collisions
Sound waves
MHD turbulence

FRW metric $ds^2 = a^2(\tau)(-d\tau^2 + (\delta_{ij} + h_{ij})dx^i dx^j)$ During inflation $a(\tau) = -\frac{1}{H\tau}$

Typical time scale of the problem

1. The phase transition happens at conformal time τ_*
2. The duration of the phase transition is $\Delta_\tau \ll \tau_*$

Separate the problem into three regimes

1. IR $k < |\tau_*|^{-1}$
2. Intermediate $|\tau_*|^{-1} < k < \Delta_\tau^{-1}$

ignore the details of the gravitational wave source, treat it as a delta function source $\widetilde{\sigma_{ij}} \sim \widetilde{T_{ij}^{(0)}} a^{-3}(\tau_*)\delta(\tau - \tau_*)$

Solution is $h \simeq -\frac{16\pi G_N H\tilde{T}\tau}{k}\left[\left(\frac{1}{k\tau} - \frac{1}{k\tau_*}\right)\cos k(\tau - \tau_*) + \left(1 + \frac{1}{k^2\tau\tau_*}\right)\sin k(\tau - \tau_*)\right] \to -\frac{16\pi G_N H\tilde{T}}{k^2}(\cos k\tau_* - \sin k\tau_* / k\tau_*)$

3. UV $k > \Delta_\tau^{-1}$ The details of bubble collision is essential

How GW propagates in spacetime

If inflation is connected to a radiation dominated universe immediately after inflation

$$h_k = h_k \frac{\sin k\tau}{k\tau}$$

The energy density of the gravitational wave has the form

$$\rho_{GW} \sim \frac{1}{a^2}\int \frac{d^3k}{(2\pi)^3}|h'(\tau)|^2$$

Deeply inside the horizon $k\tau \gg 1$

$$\boxed{\frac{d\rho_{GW}}{d\log k} \sim \frac{1}{k}\left(\cos k\tau_* - \frac{\sin k\tau_*}{k\tau_*}\right)^2}$$

1. IR regime $k < |\tau_*|^{-1}$ $\frac{d\rho_{GW}}{d\log k} \sim k^3$ similar to GW signal from instantaneous source in radiation domination

R. Cai, S. Pi, M. Sasaki Phys. Rev. D 102, 083528 (2020)

C. Caprini, R. Durrer, T. Konstandin, and G. Servant, Phys. Rev. D 79, 083519 (2009)

2. Intermediate regime oscillation

3. UV regime $\frac{d\rho_{GW}}{d\log k} \sim k^{-4}\frac{d\rho_{GW}^{flat}}{d\log k_p}$

Gravitational wave from first order phase transitions during inflation

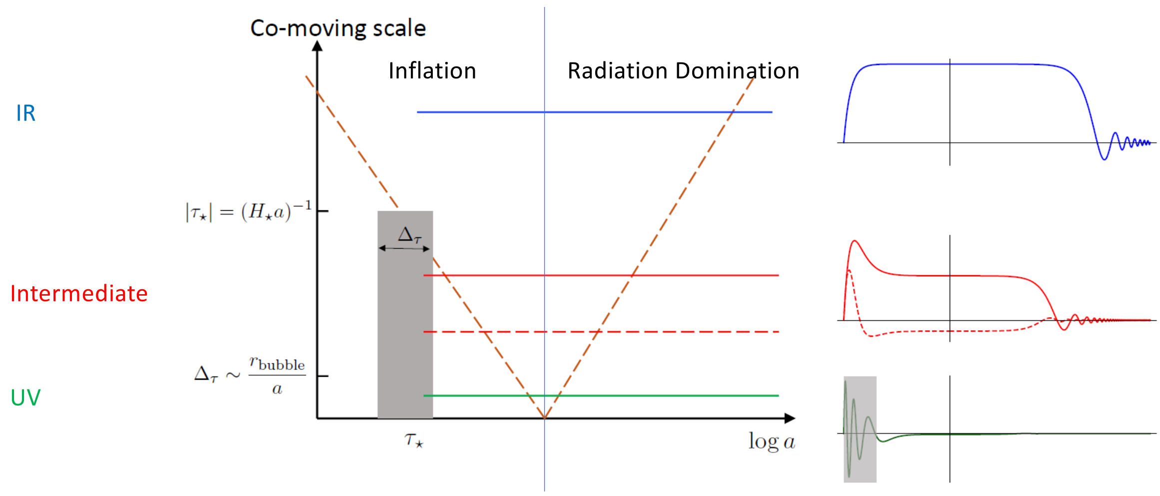

Gravitational wave from first order phase transitions during inflation

Final spectrum

$$\Omega_{GW}(k_{today}) = \Omega_R S(2\pi f_*) \left(\frac{L}{\rho_{\inf}}\right) \frac{d\rho_{GW}^{flat}}{L\, d\ln f_p} \qquad L = \gamma_{PT} m_\sigma^4\text{: Latent heat}$$

GW spectrum in flat space

$$\frac{d\rho_{GW}^{flat}}{L\, d\ln f_p} = \kappa^2 \left(\frac{L}{\rho_{\inf}}\right) \left(\frac{H}{\beta}\right)^2 \Delta(2\pi f_p) \qquad \Delta(2\pi f_p) = \tilde{\Delta}\times 3.8\ \frac{\widetilde{k_p} k_p^{2.8}}{\widetilde{k_p}^{3.8} + 2.8\, k_p^{3.8}}$$

GW frequency

$$f_{today} = f_{PT}\, e^{-N_{PT} - N_{today}} \quad e^{-N_{today}} = \frac{T_{CMB}}{\left(\left(\frac{30}{g_*^{(R)}\pi^2}\right)\left(\frac{3H_r^2}{8\pi G_N}\right)\right)^{\frac{1}{4}}}$$

Due to the distortion from inflation, highest peak

$$f_*^{peak} \simeq \frac{H}{2\pi}$$

If σ particles constitute all the dark matter today $f_{today}^{peak} = \frac{1}{2\pi}\left(\frac{\gamma_{PT}}{\gamma_*}\right)^{\frac{1}{12}} \left(\frac{L}{\rho_{\inf}}\right)^{-\frac{1}{3}} \left(\frac{\Omega_{DM} H\, H_0^2}{Y_\sigma(\infty)}\right)^{1/3}$

Gravitational wave frequency

Low scale inflation

$H = 10^{-18} \sim 10^{-14} GeV$

Signal may be detected by PTA

Intermediate scale inflation

$H = 10^{2} \sim 10^{12} GeV$

Signal may be detected by Space-based GW detectors

High scale inflation

$H = 10^{12} \sim 10^{14} GeV$

Signal may be detected by Terrestrial detectors

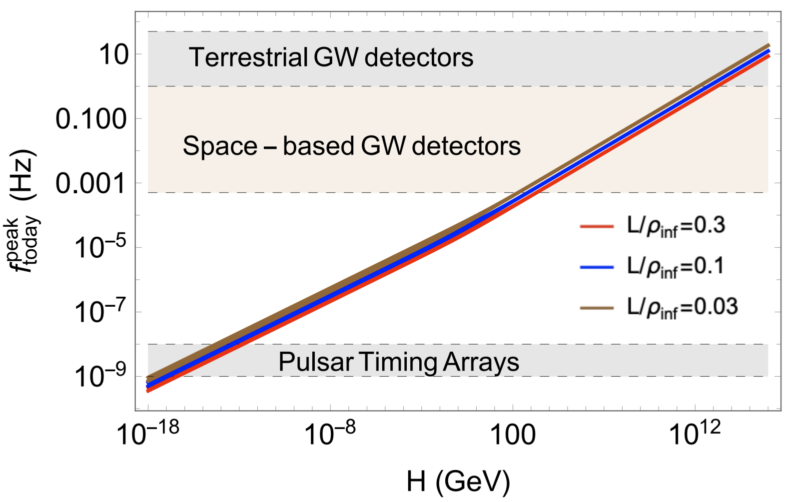

Gravitational wave signature

Magnitude of the signal is controlled by the latent heat released during first order phase transition
The frequency of the gravitational wave is linked to the Hubble parameter during inflation

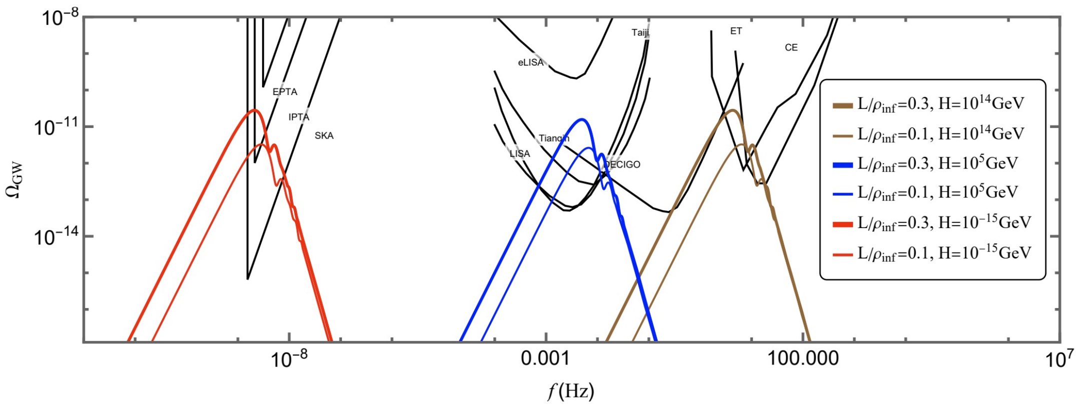

Outline

Superheavy Dark Matter

Symmetry Restoration First-Order Phase Transition During Inflation

Observational Signatures

Conclusion and Outlook

Conclusion and Outlook

Dark matter can be heavy, the production rate is generically small

A mechanism to produce enough superheavy dark matter during inflation via symmetry restoration first order phase transition

Complementary gravitational wave signals

25 October 2022

A Proposal for Simple Model of Acoustic Black Hole

Chuo University
Ren Tsuda

With Shinya Tomizawa* and Ryotaku Suzuki*
* Toyota Technological Institute

The 31st Workshop on General Relativity and Gravitation in Japan - JGRG31
24 - 28 October, 2022 @Kobayashi Hall, The University of Tokyo

What is "Acoustic Black Hole" ?

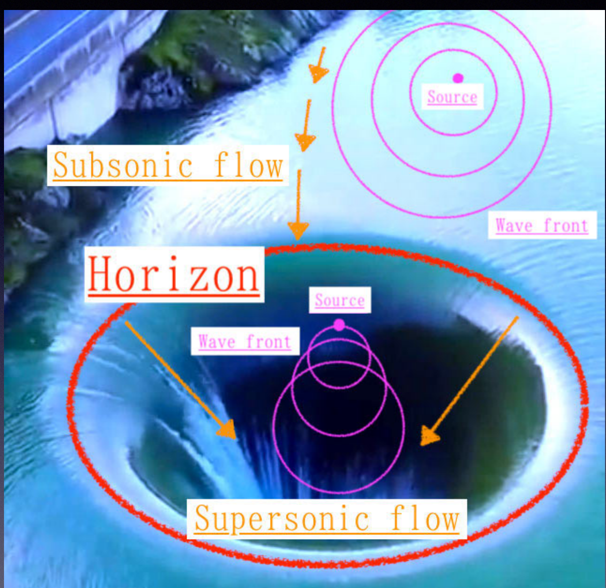

- Subsonic region
  Flow speed < Sonic speed
- Sonic horizon
  Flow speed = Sonic speed
- Supersonic region
  Flow speed > Sonic speed

"Transonic flow" is considered as Acoustic analogue of black hole

Sound wave equation

Wave equation of $\tilde{\phi}$

$$\left(\partial_0 + \partial_i v^i_{\rm bg} + v^i_{\rm bg}\partial_i\right)\left[\frac{\rho_{\rm bg}}{c_{\rm s}^2}\left(\partial_0\tilde{\phi} + v^j_{\rm bg}\partial_j\tilde{\phi}\right)\right] - \delta^{ij}\partial_i\left(\rho_{\rm bg}\partial_j\tilde{\phi}\right) = 0$$

Background flow velocity

$$v^i_{\rm bg} = -\delta^{ij}\partial_j\phi_{\rm bg}$$

Perturbation of flow velocity potential

$$\phi_{\rm bg} \to \phi_{\rm bg} + \tilde{\phi}$$

Acoustic metric

Regarding the sound wave equation

as a Klein-Gordon equation

$$0 = \Box\tilde{\phi} = \left(\partial_0 + \partial_i v^i_{\rm bg} + v^i_{\rm bg}\partial_i\right)\left[\frac{\rho_{\rm bg}}{c_{\rm s}^2}\left(\partial_0\tilde{\phi} + v^j_{\rm bg}\partial_j\tilde{\phi}\right)\right] - \delta^{ij}\partial_i\left(\rho_{\rm bg}\partial_j\tilde{\phi}\right)$$

yields “the acoustic metric” as

$$ds^2_{\rm (ac)} = \frac{\alpha\rho_{\rm bg}(x)}{c_{\rm s}(x)}\left[-\left(c_{\rm s}^2(x) - v_{\rm bg}^2(x)\right)dt^2 - 2v_{\rm bg}(x)\,dtdx + dx^2 + dy^2 + dz^2\right]$$

Acoustic metric can be interpreted as representing a space-time for a sound wave

Black hole can be examined in the laboratory

How to make transonic flow in laboratory

Laval nozzle:

Major equipment for transonic flow model which makes use of the Bernoulli theorem

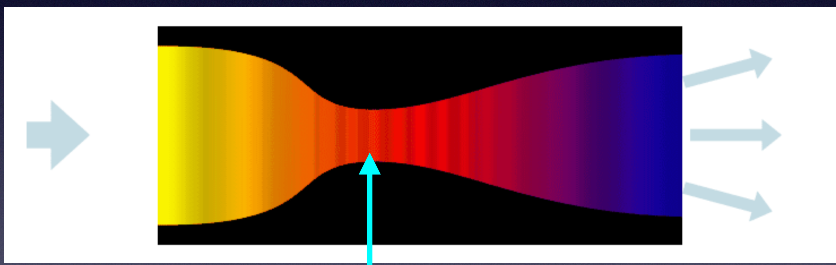

$M < 1$ $M = 1$ $M > 1$

M is the Mach number

$$M = \frac{\text{flow speed}}{\text{sonic speed}}$$

At the throat, fluid velocity locally becomes sonic

Today we propose an another model without a throat

Our proposal:
Wavy toroidal waterway model

1. Consider a tube with the length $2\pi L$

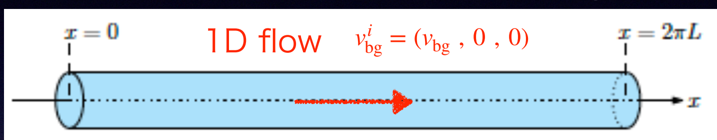

x-axis is drawn along the tube

2. Bend the tube with the height given by

$$h\,(x) = \lambda \sin^2 \frac{x}{L} + h_{\rm min}$$

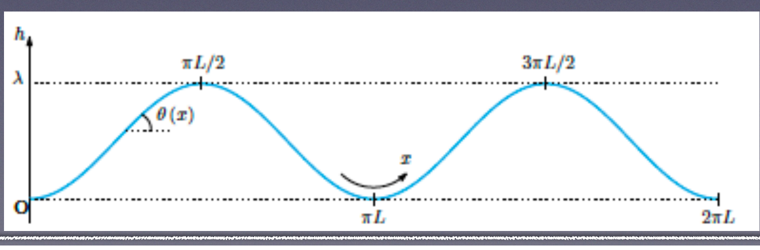

3. Assume periodicity of $2\pi L$

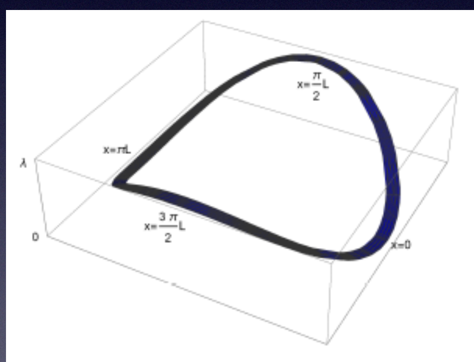

Equation of motion for the model

Euler equation: E.O.M of fluid dynamics

$$\partial_0 v_{\rm bg} + v_{\rm bg}\partial_1 v_{\rm bg} = -\frac{1}{\rho_{\rm bg}}\partial_1 p + \mu$$

where μ is the external force acting along the waterway

$$\mu = -g\frac{dh}{dx} = -g\frac{\lambda}{L}\sin\frac{2x}{L}$$

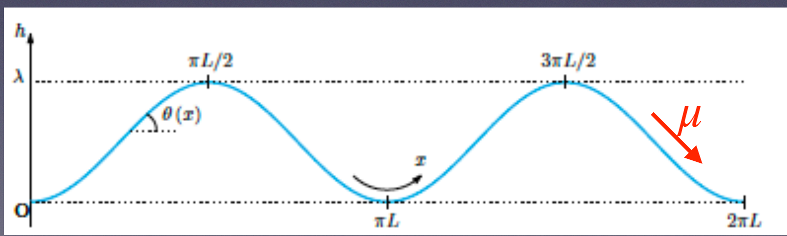

$$h(x) = \lambda\sin^2\frac{x}{L} + h_{\rm min}$$

Transonic flow solution

$$v_{\rm bg} = \hat{c}_s\sqrt{-2\sqrt{\cos^3\frac{\phi}{3}} + 3\sqrt{\cos\phi} - \frac{\sqrt{\cos^2\frac{x}{L}}}{\cos\frac{x}{L}}\sqrt{-3\cos\frac{\phi}{3} + \cos\phi\left(2+\sqrt{\cos\phi\sec^3\frac{\phi}{3}}\right)}}$$

with $\phi = \arccos\left[\left(1+\frac{g\lambda}{\hat{c}_s^2}\cos^2\frac{x}{L}\right)^2\right]$

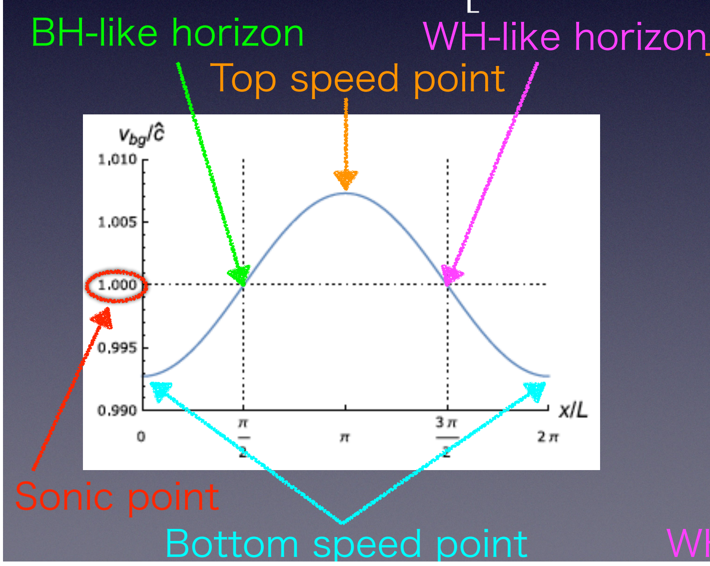

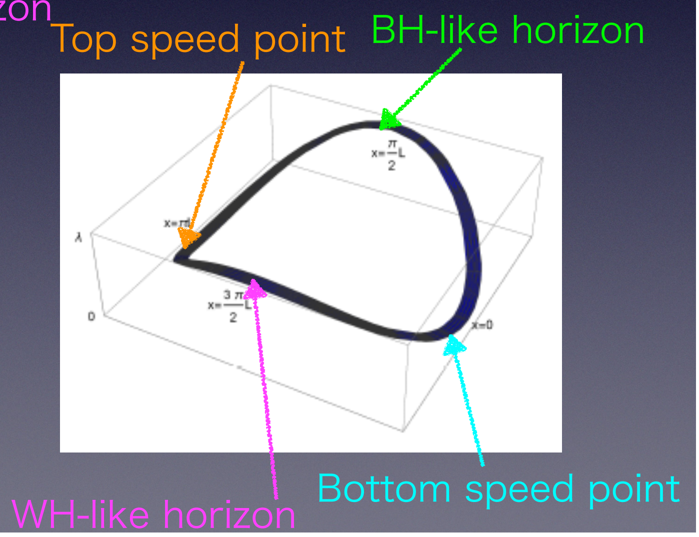

Solving sound wave equation on the model

Sound wave equation

$$\left(\partial_0 + \partial_i v^i_{\mathrm{bg}} + v^i_{\mathrm{bg}}\partial_i\right)\left[\frac{\rho_{\mathrm{bg}}}{c_s^2}\left(\partial_0\tilde{\phi} + v^j_{\mathrm{bg}}\partial_j\tilde{\phi}\right)\right] - \delta^{ij}\partial_i\left(\rho_{\mathrm{bg}}\partial_j\tilde{\phi}\right) = 0$$

v_{bg} : background solution ρ_{bg}, c_s are given by v_{bg}

Ansatz

- Forward propagation・・・goes the same direction with v_{bg}

$$\tilde{\phi}^{(\mathrm{for})}(t,x) = A(x)\exp\left[-i\left(\omega t - k(x)\,x\right)\right]$$

- Backward propagation・・goes the opposite

$$\tilde{\phi}^{(\mathrm{back})}(t,x) = B(x)\exp\left[-i\left(\omega t + k(x)\,x\right)\right]$$

Assumption $c_s \approx v_{\mathrm{bg}}$

Appearances of the propagations

Forward propagation Backward propagation

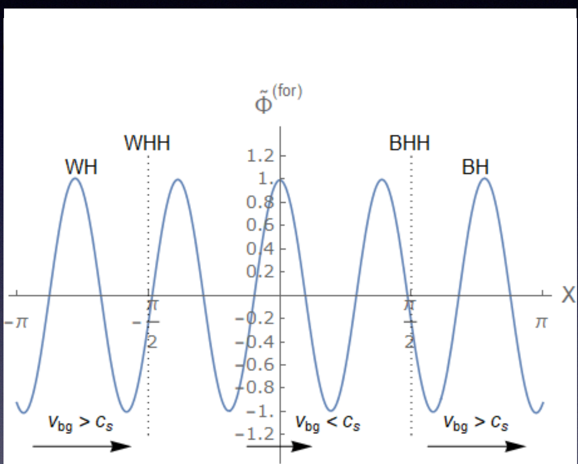

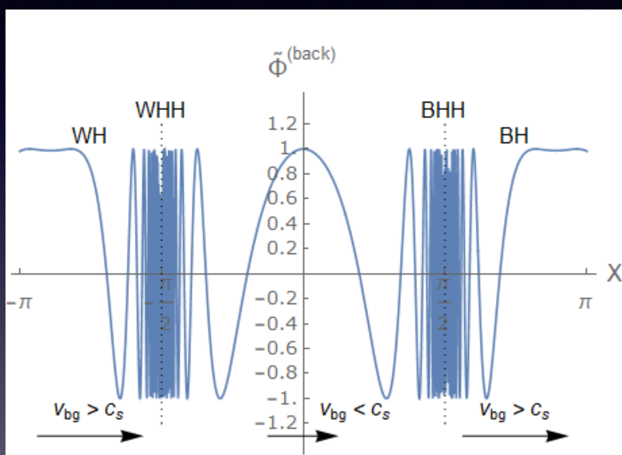

In the case of backward propagation,
the propagation is trapped across the BH horizon
and WH horizon.

Summary

We have proposed a wavy toroidal waterway model

- Stationary 1D flow
- Possesses two sonic points corresponding to BH horizon and WH horizons
- Background is easily solved analytically
- Forward and backward propagation are solved analytically under the assumption of the near-sonic flow

Future work

- Exploring causal structure of a space-time represented by an acoustic metric

C30

Generating quantum entanglement between macroscopic objects with continuous measurement and feedback control

Kyushu University*

Daisuke Miki

Collaborators

A.Matsumura*, T.Shichijo*, Y.Sugiyama*, K.Yamamoto*

N.Matsumoto(Gakushuin), N.Yamamoto(Keio)

arXiv:2210.13169

Contents

1. Introduction
2. Optomechanical system
3. Macroscopic entanglement
4. Conclusion

2022/10/25/JGRG31

Main conclusion

We investigate the feasibility of generating entanglement between two mg-scale mirror in optomechanical system.

We will show that it is possible to detect the entanglement between such massive objects experimentally in the near future.

This study will be a first step towards verifying the quantum nature of gravity.

1. Introduction

- Is a superposition of gravitational field realized?

The region where both the effects of gravity and quantum mechanics appear is important.

However, because gravity is weak, we must realize macroscopic object in quantum state to test the quantum nature of gravity.

- Current measurement in quantum mechanics and gravity

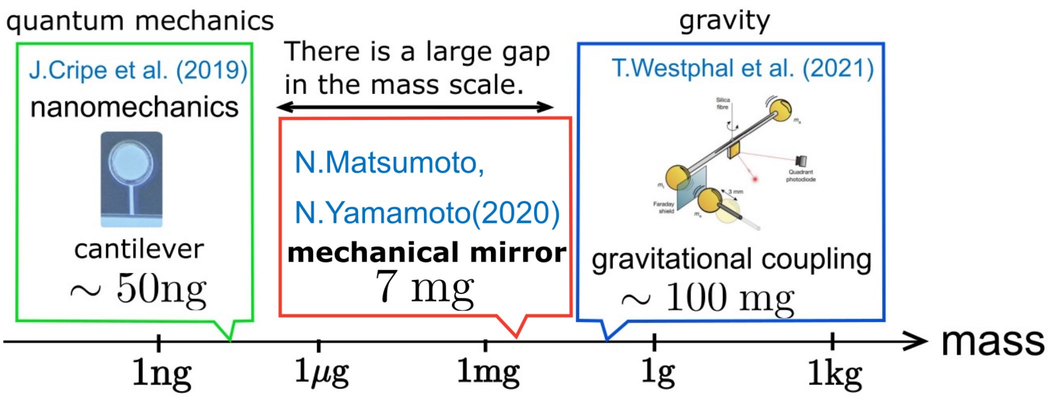

Macroscopic quantum state of mirror

N.Matsumoto and N.Yamamoto (2020)

- Quantum control of mirror in optomechanical system

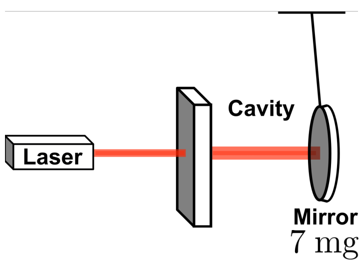

The mg-scale mirror is squeezed near quantum regime through the photon measurement.

- When we measure the mirror's position through the photons, the position uncertainty is small.

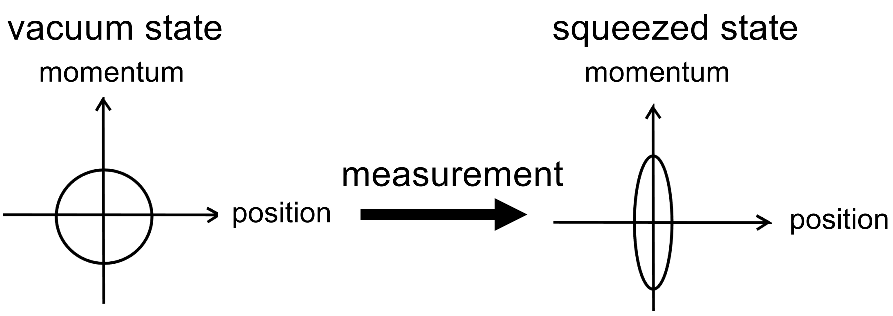

2. Optomechanical system

- Hamiltonian

$$H = \frac{\hbar\Omega}{4}(q^2+p^2) + \hbar\omega_p a^\dagger a - \underline{\hbar G q a^\dagger a} + i\hbar E(a^\dagger e^{-i\omega_0 t} - a e^{i\omega_0 t})$$

mirror photon interaction laser

coupling

$$G = \frac{\omega_p}{l}\sqrt{\frac{\hbar}{2m\Omega}}$$

- Langevin equation for fluctuation part

linearization $q \to \bar{q} + q \quad p \to \bar{p} + p \quad a \to \bar{a} + a$

$$\left.\begin{aligned} \dot{q} &= \Omega p \\ \dot{p} &= -\Omega q \underline{- \Gamma p} + \underline{\sqrt{2\Gamma} p_{\mathrm{in}}} \underline{- 2g(a' + a'^\dagger)} \end{aligned}\right\} \text{mirror}$$

$$\left.\dot{a}' = i\Delta a' \underline{- \frac{\kappa}{2} a'} + \underline{\sqrt{\kappa} a_{\mathrm{in}}} \underline{- igq}\right\} \text{photon}$$

decay noise interaction

$$a' = e^{i\omega_0 t} a \qquad g = |\bar{a}| G$$

$$\Delta = \omega_0 - \omega_p + 2g^2/\Omega$$

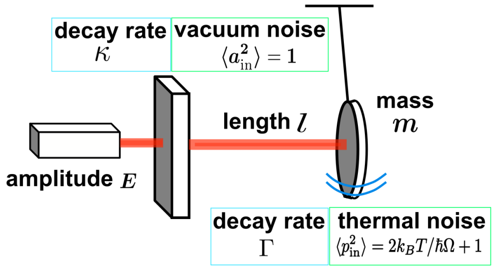

Continuous measurement and feedback

- optical decay $\kappa \gg$ frequency Ω

We continuously get the information of mirror position through the measurements of output photons.

- The feedback control effectively lowers the bath temperature.

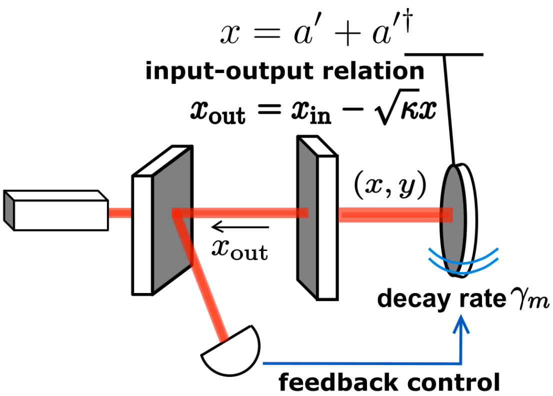

- Langevin equation

$$\begin{cases} \dot{q} = \omega_m p \\ \dot{p} = -\omega_m q \underline{- \gamma_m p} + (\text{noise}) \\ x_{\mathrm{out}} = \boxed{-\chi q} + (\text{noise}) \end{cases}$$

$$\omega_m = \sqrt{\Omega^2 + \Omega\frac{16g^2\Delta}{\kappa^2 + 4\Delta^2}}$$

$$\chi = \frac{8g\Delta}{\kappa^2 + 4\Delta^2}\sqrt{\frac{\kappa\eta\Omega}{\omega_m}}$$

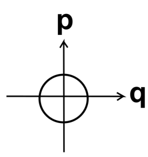

The mirror position is estimated by observation signal. → Squeezing

3. Macroscopic entanglement

H. Müller-Hebhardt, et al. (2013)

- Fabry-Perot-Michelson interferometer

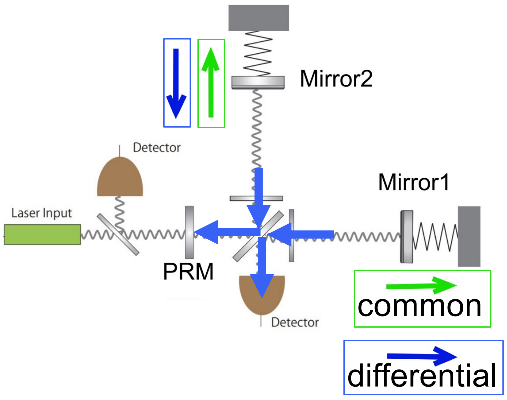

When the different squeezed states pass the HBS, the state 1 and 2 is entangled.

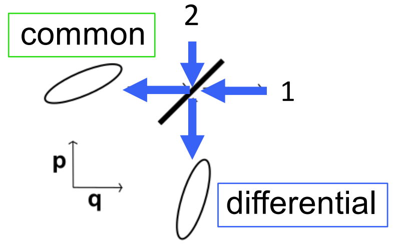

We measure the common and differential modes of two mirrors.

Power-Recycled Mirror (PMR) makes the asymmetry between the common and differential modes.

When the common mode and the differential mode are in different squeezed states, the mirrors 1 and 2 are entangled.

Covariance matrix of mirror 1 and 2

- Covariance matrix: second-order moments of (q,p)

$$V = \frac{1}{2}\begin{pmatrix} \overset{\text{mirror1}}{\boxed{\mathcal{V}_{\text{comm}} + \mathcal{V}_{\text{diff}}}} & \overset{\text{correlation}}{\boxed{\mathcal{V}_{\text{comm}} - \mathcal{V}_{\text{diff}}}} \\ \mathcal{V}_{\text{comm}} - \mathcal{V}_{\text{diff}} & \underset{\text{mirror2}}{\boxed{\mathcal{V}_{\text{comm}} + \mathcal{V}_{\text{diff}}}} \end{pmatrix}$$: 4×4 matrix

$$\mathcal{V}_{\text{comm}} = \begin{pmatrix} V_{qq}^{\text{comm}} & V_{qp}^{\text{comm}} \\ V_{pq}^{\text{comm}} & V_{pp}^{\text{comm}} \end{pmatrix} \quad \mathcal{V}_{\text{diff}} = \begin{pmatrix} V_{qq}^{\text{diff}} & V_{qp}^{\text{diff}} \\ V_{pq}^{\text{diff}} & V_{pp}^{\text{diff}} \end{pmatrix}$$: 2×2 matrix

Both matrices are exactly derived from the Langevin equation.

- When the common mode and differential mode are symmetrical, the correlation $\mathcal{V}_{\text{comm}} - \mathcal{V}_{\text{diff}} = 0$.

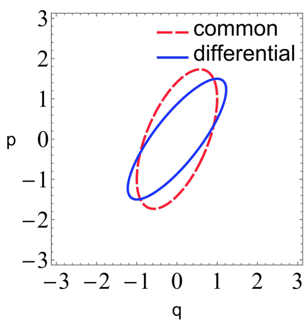

Generation of the entanglement between mirror 1 and mirror 2 requires the asymmetry of the common mode and differential mode.

Entanglement between mirror 1 and 2

- Logarithmic negativity $\boxed{\epsilon_{\rm cr}(\boldsymbol{V}) > 0}$ $\longleftrightarrow$ The state is entangled.

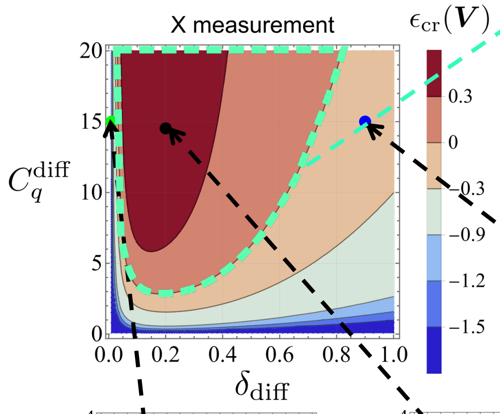

$C_q^{\rm diff}$: quantum cooperativity
characterize the quantumness of the system

$\delta_{\rm diff}$: detuning

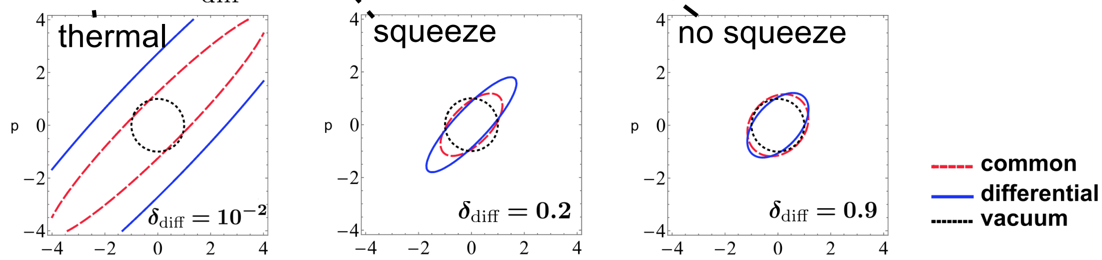

$\delta_{\rm diff} \simeq 0.1 \sim 0.2$ is advantageous in generating entanglement.

Entanglement between mirror 1 and 2

- Logarithmic negativity $\epsilon_{\rm cr}(\boldsymbol{V}) > 0$ $\longleftrightarrow$ The state is entangled.

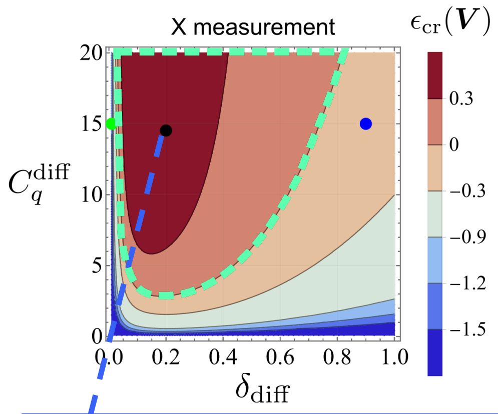

Experimentally feasible parameter

N.Matsumoto and N.Yamamoto (2020)
S.B.Catano-Lopez et al. (2020)

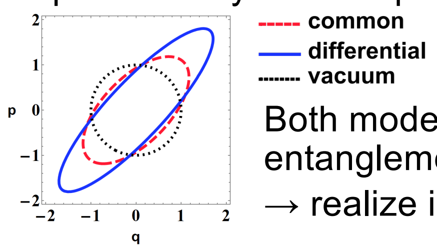

Both modes are in different squeezed states and the entanglement is generated.
→ realize in near future

4. Conclusion

- We investigated the feasibility of generating a macroscopic entanglement between mechanical mirrors coupled with cavity photons under continuous measurement and feedback control.

- We analyzed the logarithmic negativity, assuming tabletop experiments with the experimentally feasible parameters.

- This study is a first step to verify the quantum nature of gravity.

Entanglement between mirror 1 and 2

- Logarithmic negativity $\epsilon_{\rm cr}(\boldsymbol{V}) > 0 \longleftrightarrow$ The state is entangled.

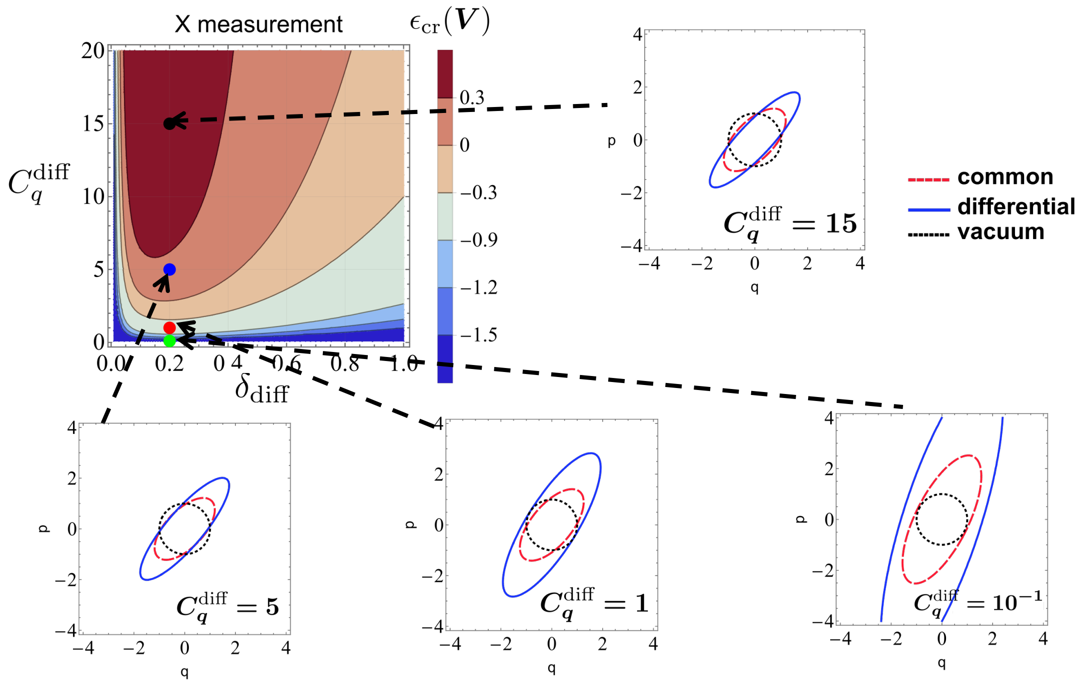

Gravitational effects

Signatures of the quantum nature of gravity in the differential motion of two masses A.Datta and H.Miao (2021)

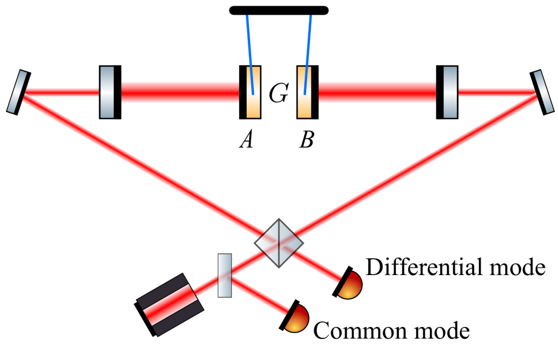

Optomechanical interaction

- Interaction

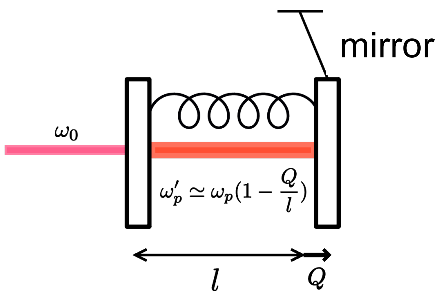

$$H_{\rm cav} = \hbar\omega'_p a^\dagger a \simeq \hbar\omega_p a^\dagger a - \hbar\frac{\omega_p}{l}Qa^\dagger a$$

coupling

Experimental parameters

Experimentally feasible parameter expected from [1,2]

Symbol	Name	Value
Ω	Mechanical frequency	$2\pi \times 2.2$ Hz
$\Gamma(\Omega)$	Mechanical decay rate	$2\pi \times 10^{-6}$ Hz
γ_m	Effective mechanical decay rate under feedback control	$2\pi \times 6.9 \times 10^{-3}$ Hz
T	Bath temperature	300 K
$\delta_- = \Delta/\kappa_-$	(Normalized) detuning	0.2
ζ	Normalized detuning ratio of differential mode to common mode	3
η	Detection efficiency	0.92
$N_{\rm th}$	Thermal photon number	0
$Q_- = \omega_m^-/\gamma_m$	Quality factor	7.5×10^4
Q_+ is defined by Eq. (52)		1.6×10^5
$C_- = 4(g_m^-)^2/\gamma_m\kappa_-$	Cooperativity	1.1×10^5
C_+ is defined by Eq. (53)		1.6×10^5
$n_{\rm th}^-$	Thermal phonon number	7.5×10^3
$n_{\rm th}^+$ is defined by Eq. (54)		1.8×10^3
m	Mirror mass	7.71×10^{-6} kg
ℓ	Cavity length	10^{-1} m
ω_L	Laser frequency	$2\pi \times 300 \times 10^{12}$ Hz
κ_-	Optical decay rate	$2\pi \times 1.64 \times 10^6$ Hz
$\lvert\bar{a}\rvert$	Expectation value of cavity photon quadrature	1.27×10^5
$g = \lvert\bar{a}\rvert(\omega_c/\ell)\sqrt{\hbar/2m\Omega}$	Optomechanical coupling	1.69×10^6 Hz
$F = 2\pi c/\ell\kappa_-$	Finesse	1.8×10^3
P_{in}	Input laser power	30 mW

C31

JGRG31

Quantum gravity witness of harmonic oscillator system using Leggett-Garg inequality

Youka Kaku (Nagoya Univ.)

Collaborators: Shin'ya Maeda, Yasusada Nambu, Osawa Yuki

In progress

Introduction

Introduction

- We need experimental evidence to explore quantum gravity
- Quantum gravity theory ∋ non-relativistic gravity in QM regime

Our focus

How to test the quantum nature of non-relativistic gravity?

First proposed by **B**ose, **M**arletto, **V**ederal, et al.

⇒ BMV proposal

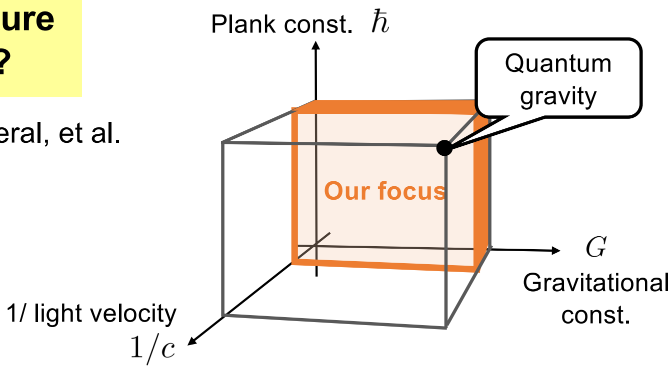

Quantum Gravity witness

Feynman (1957)
Marletto, Vedral (2017), Bose et al. (2017)

- **"Is gravity also superposed when the quantum state of mass source is superposed?"**

If Yes, Quantized Gravity (QG)

$$V_{\mathrm{QG}}(\hat{x},\hat{X}) = -\frac{GmM}{|\hat{x}-\hat{X}|}$$

Operator of the source system

Probe: $m,\ \hat{x}$ Mass source: $M,\ \hat{X}$

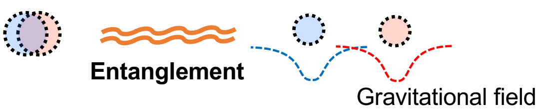

If No, Semiclassical Gravity (CG)

$$V_{\mathrm{CG}}(\hat{x}) = \left\langle -\frac{GmM}{|\hat{x}-\hat{X}|} \right\rangle_{\mathrm{source}}$$

c-number of the source system

Probe: $m,\ \hat{x}$ Mass source: $M,\ \hat{X}$

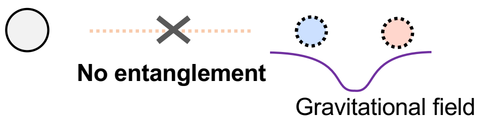

– Observation of gravity-induced entanglement is good criteria to judge superposed gravity.
– How to observe entanglement? —— Interference experiment etc.⋯
– We propose an alternative way to test gravity-induced entanglement using Leggett-Garg inequality.

Bell inequality

Clauser, Horne, Shimony, Holt (1965)

- Bell inequality (CHSH inequality)
  - Measurement on 2 observables at 2 **spacelike** points

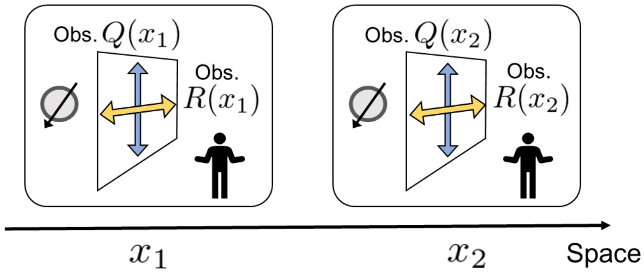

  - Macroscopic realism: Probability is defined locally, and the system is fundamentally classical.

$$-2 \leq \langle Q(x_1)Q(x_2)\rangle + \langle Q(x_1)R(x_2)\rangle + \langle R(x_1)Q(x_2)\rangle - \langle R(x_1)R(x_2)\rangle \leq 2$$

Bell inequality: Inequality of correlations between **spacelike** points

Leggett-Garg inequality (LGI)

Leggett, Garg (1985), Haustein (2017)

- LGI (Modified version): Timelike version of Bell inequality
  - Measurement on 1 observable at 2 **timelike** points
  - Assume
    - Non-invasive measurement
      : the measurement does not affect the future
    - Causality
  - Macroscopic realism: the system is fundamentally classical

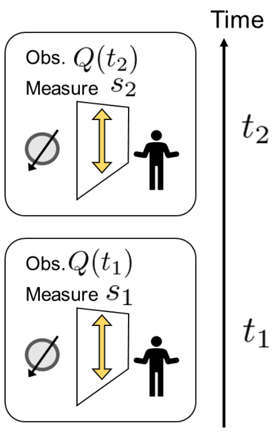

$q_{s_1,s_2}(t_1,t_2) \geq 0$ **LGI**: Inequality of correlations between **timelike** points

Here,

$$q_{s_1,s_2}(t_1,t_2) := \frac{1}{4}\left(1 + s_1\langle Q(t_1)\rangle + s_2\langle Q(t_2)\rangle + s_1 s_2\langle Q(t_1)Q(t_2)\rangle\right)$$

Quasi-probability: Similar to the conditional probability to measure s_1 at t_1 and s_2 at t_2 .

Our work:

Quantum gravity witness
in harmonic oscillator system using LGI

Quantum gravity witness using LGI

- Why do we consider LGI?
  - Violation of LGI in quantum system has been investigated well experimentally. Knee et al. (2012)
  - We can capture unique feature of gravity by post-Newtonian calculation (as future work!)
    → LGI contains timelike correlation, so it maybe interesting observable!
- What do we expect to see?

QG

Probe: $m,\ \hat{x}$ Mass source: $M,\ \hat{X}$

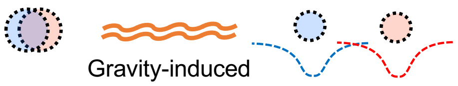

Gravity-induced Entanglement

Particle decoheres (loss quantum coherence) due to gravity-induced entanglement.

→ LGI of probe tends to be less-violated.

CG

Probe: $m,\ \hat{x}$ Mass source: $M,\ \hat{X}$

No entanglement

Particle does not decohere.

→ LGI of probe is still violated.

Can we distinguish QG and CG by observing how much LGI is violated??

Setup

- Gravitational interacting hybrid system on 2 dim space

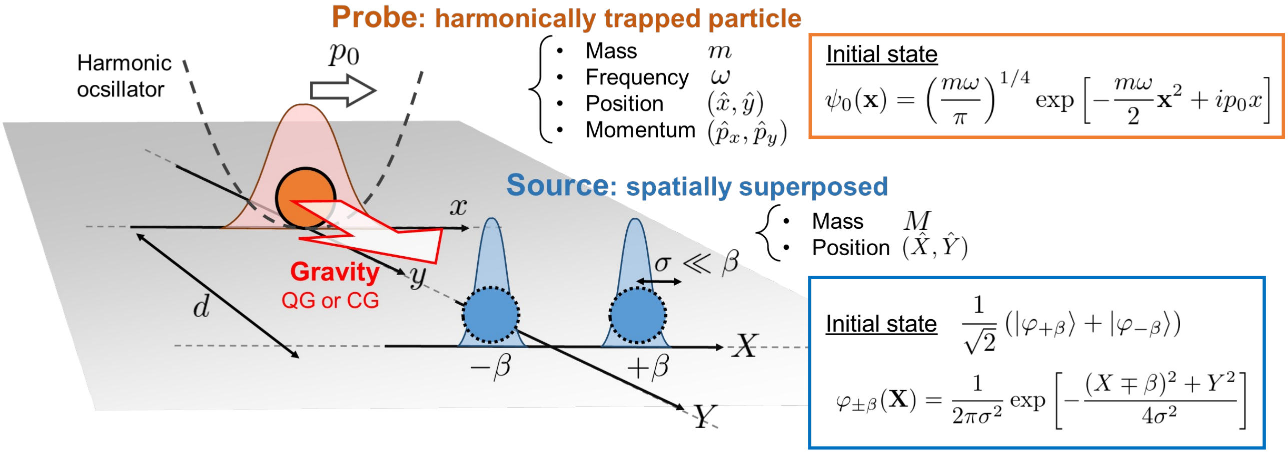

– Hamiltonian: $\hat{H} = \frac{1}{2m}\hat{\mathbf{p}}^2 + \frac{1}{2}m\omega^2\hat{\mathbf{x}}^2 + \underline{\hat{V}}$ Gravity: QG or CG

Measurement

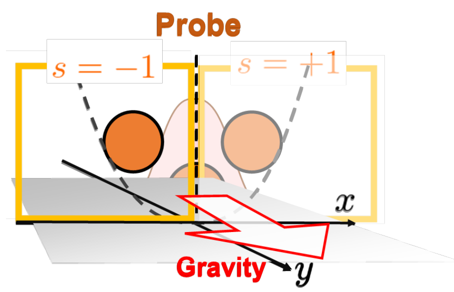

- Projective measurement: $+1$ for $x > 0$, -1 for $x < 0$
  - Observable $\hat{Q}(t) = 2\theta(\hat{x}(t)) - 1$
  - Measurement value $s = \pm 1$
  - Projection op. $\hat{P}_s(t) \equiv \theta(s\hat{x}(t))$

- Calculate quasi-probability and estimate LGI violation

$$q_{s_1,s_2}(t_1,t_2) \equiv \frac{1}{4}\left(1 + s_1\langle\hat{Q}(t_1)\rangle + s_2\langle\hat{Q}(t_2)\rangle + s_1 s_2\langle\hat{Q}(t_1)\hat{Q}(t_2)\rangle\right)$$
$$= \mathrm{Re}\left[\mathrm{Tr}_{\mathrm{source}}\left[|\hat{P}_{s_2}(t_2)\hat{P}_{s_1}(t_1)|\Psi_0\rangle\langle\Psi_0|\right]\right]$$

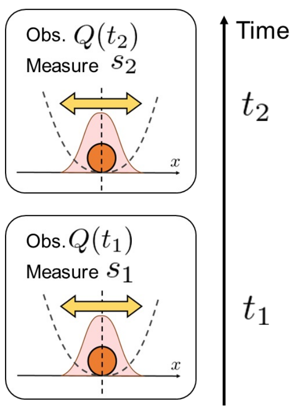

Quantum system violates LGI $q_{s_1,s_2}(t_1,t_2) \geq 0$

How does LGI violation differs w.r.t. quantumness of gravity?

Results

- Typical behavior of quasi-probability

$s_1 = +1,\ s_2 = -1,\ t_1 = 0,\ t_2 = \Delta t,\ \kappa_{p_0} = 1,\ \kappa_G = 1/4$

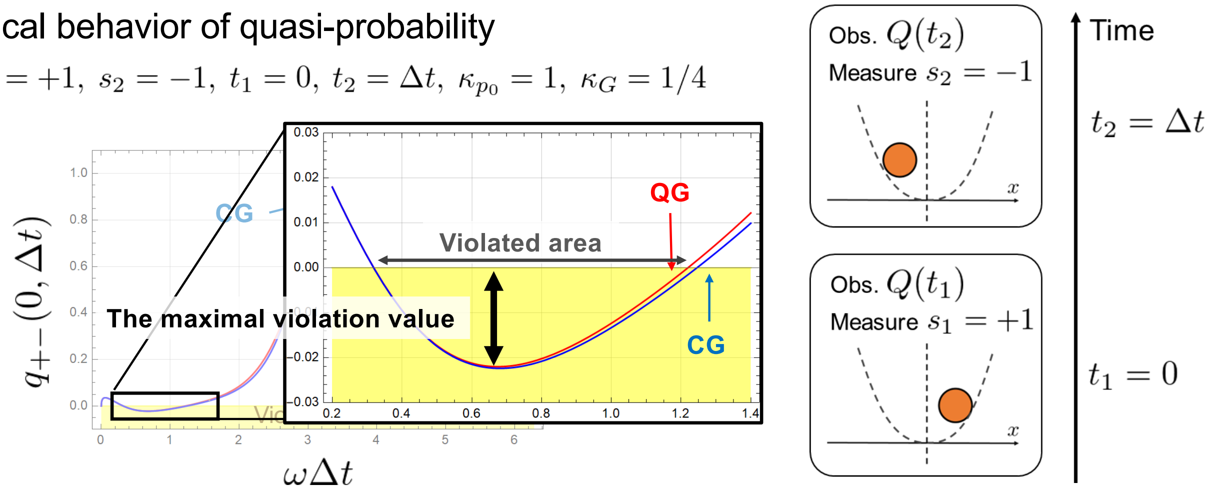

- QG suppress the LGI violation compared to CG in this case: Gravity-induced decoherence
- We analyzed the behavior of the maximal violation value and the violated area.

We focus only on this today.

Results: Maximal violation point

- Difference of maximal violation value: $\mathrm{Min}[q^{(\mathrm{QG})}_{s_1,s_2}(t_1,t_2)] - \mathrm{Min}[q^{(\mathrm{CG})}_{s_1,s_2}(t_1,t_2)]$
  - Default parameters: $s_1 = +1,\ s_1 = -1,\ t_1 = 0,\ \kappa_{p_0} = 1,\ \kappa_G = 1/4$

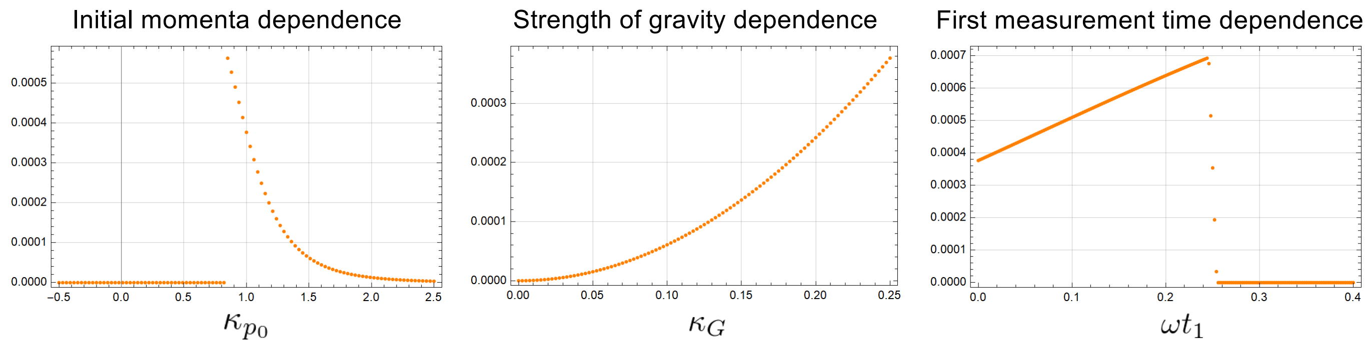

- Difference of maximal violation value (QG−CG) is always positive.
- QG always suppress the maximal violation of LGI because of gravity-induced decoherence.
- Observation of the maximal violation value of LGI is a good criteria to distinguish QG and CG.

Conclusion

- Summary
  - We investigated the gravity interacting hybrid system of the harmonically trapped particle and the mass source in a cat state.
  - We estimated the LGI violation for 2 cases; QG & CG.
  - The maximal violation is always suppressed in QG case compared to CG case due to gravity-induced decoherence of the particle system.
- On-going work: The analysis of violation area also gives interesting results.
  - There is a slight region where QG promote the violation counterintuitively!
  - This results from the quantum effect called quantum backflow.
  - LGI violation is determined by the balance of decoherence and quantum backflow.

Backup

Setup

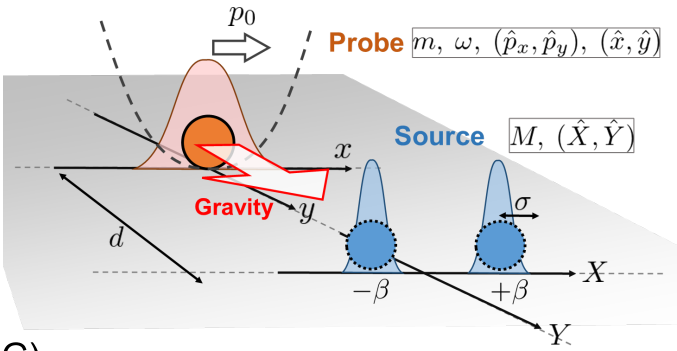

- Hamiltonian

$$\hat{H} = \frac{1}{2m}\hat{\mathbf{p}}^2 + \frac{1}{2}m\omega^2\hat{\mathbf{x}}^2 + \hat{V}$$

We calculated 2 cases;
when gravity is superposed (QG), or not (CG).

$$V_{\mathrm{QG}}(\hat{\boldsymbol{x}}, \hat{\boldsymbol{X}}) = -\frac{GmM}{\sqrt{(\hat{x}-\hat{X})^2 + (\hat{y}-\hat{Y}-d)^2}} \qquad V_{\mathrm{CG}}(\hat{\boldsymbol{x}}) = \left\langle -\frac{GmM}{\sqrt{(\hat{x}-\hat{X})^2 + (\hat{y}-\hat{Y}-d)^2}} \right\rangle_{\mathrm{source}}$$

- Initial state $|\Psi_0\rangle = |\psi_0\rangle \otimes \frac{1}{\sqrt{2}}\left(|\varphi_{+\beta}\rangle + |\varphi_{-\beta}\rangle\right)$
  - Probe: Ground state with initial momenta $\psi_0(\mathbf{x}) = \left(\frac{m\omega}{\pi}\right)^{1/4} \exp\left[-\frac{m\omega}{2}\mathbf{x}^2 + ip_0 x\right]$
  - Source: Well-localized cat state $\varphi_{\pm\beta}(\mathbf{X}) = \frac{1}{2\pi\sigma^2} \exp\left[-\frac{(X \mp \beta)^2 + Y^2}{4\sigma^2}\right] \quad (\sigma \ll \beta)$

Results: Violation area

- Violated region on $(\omega t_1,\ \omega \Delta t)$ plane

$\kappa_{p_0} = 1,\ \kappa_G = 1/4$

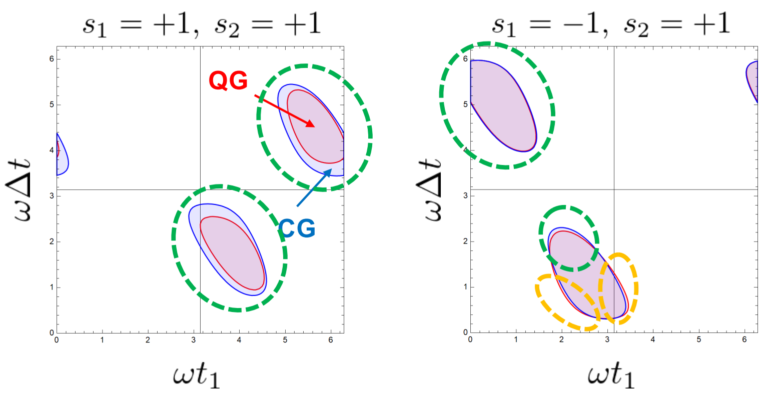

- Area of QG is smaller than CG
  - QG suppress the violation;
    Gravity induced decoherence
- Area of QG is smaller than CG
  - QG promote the violation;
    Counterintuitive!

- Surprisingly, there is a slight parameter region where QG promote the LGI violation.
- This results from quantum backflow effect.

Quantum backflow

Yearsly, Halliwell (2015)
Halliwell(2019)

- Quantum backflow
  - Quantum effect that the state with positive momenta has a negative current.

    e.g. The superposition of 2 Gaussian states with initial positive momenta

Time evolution of wave function **The probability to exist at $x > 0$**

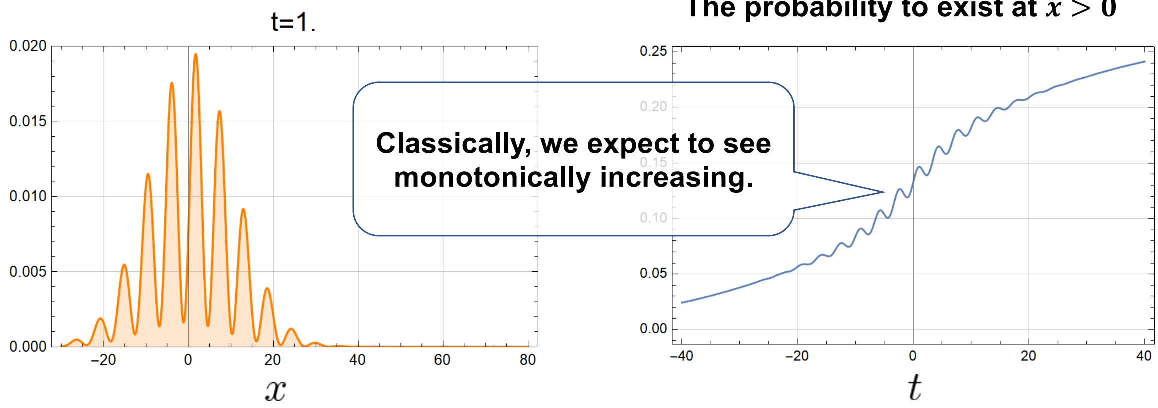

Quantum backflow

Yearsly, Halliwell (2015)
Halliwell(2019)

- Formulation of quantum backflow
  - Current op. $\hat{J} = \frac{d}{dt}\hat{P}_+$
  - Flux op. $\hat{F}(t_1, t_2) = \int_{t_1}^{t_2} dt \hat{J}(t) = \hat{P}_+(t_2) - \hat{P}_+(t_1) = \frac{1}{2}(\theta_{t_2}(\hat{x}) - \theta_{t_1}(\hat{x}))$
  - Backflow op. $\hat{\lambda} \equiv \theta(\hat{p})\hat{F}(t_1, t_2)$
  - The state with $\langle\hat{\lambda}\rangle < 0$ is in backflow.

    For instance, consider the state with positive momenta: $\theta(\hat{p})|\psi\rangle = |\psi\rangle$

    Then, $\langle\lambda\rangle = \langle\psi|\theta(\hat{p})\hat{F}|\psi\rangle = \langle\psi|\hat{F}|\psi\rangle < 0$

    This means that the state with positive momenta has a negative flux, namely backflow.
  - Backflow is also related to negative Wigner function.
  - The spectrum of backflow eigenvalue takes $-0.04 \sim 1$. Bracken, Melloy (1994)

Quantum backflow

Halliwell(2019)

- Relation between quasi-probability

Suppose $|\psi_0\rangle$ to be an eigenstate of backflow op. with a positive momenta.

$$q_{-+}(t_1,t_2) = \frac{1}{8}\langle\psi_0|(1-\hat{Q}(t_1)+\hat{Q}(t_2))^2-1|\psi_0\rangle \qquad \theta(\hat{p})|\psi_0\rangle = |\psi_0\rangle$$

$$= \frac{1}{8}\langle\psi_0|\{1+\theta(\hat{p})(\hat{Q}(t_2)-\hat{Q}(t_1))\}\{1+(\hat{Q}(t_2)-\hat{Q}(t_1))\theta(\hat{p})\}|\psi_0\rangle$$

$$= \frac{1}{8}\langle\psi_0|(1+2\lambda^*)(1+2\lambda)-1|\psi_0\rangle \qquad \hat{\lambda}|\psi_0\rangle = \lambda|\psi_0\rangle$$

$$= \frac{1}{2}\lambda(\lambda+1)$$

When $s_1=-s_2$, quasi-probability is rewritten using the backflow eigenvalue.
When the state is in backflow, the backflow eigenvalue takes $-0.04 \lesssim \lambda < 0$ and quasi-probability will be violated.

Results: Violation area

- The expectation value of backflow operator

$s_1=-1,\ s_2=+1,\ \kappa_{p_0}=1,\ \kappa_G=1/4$

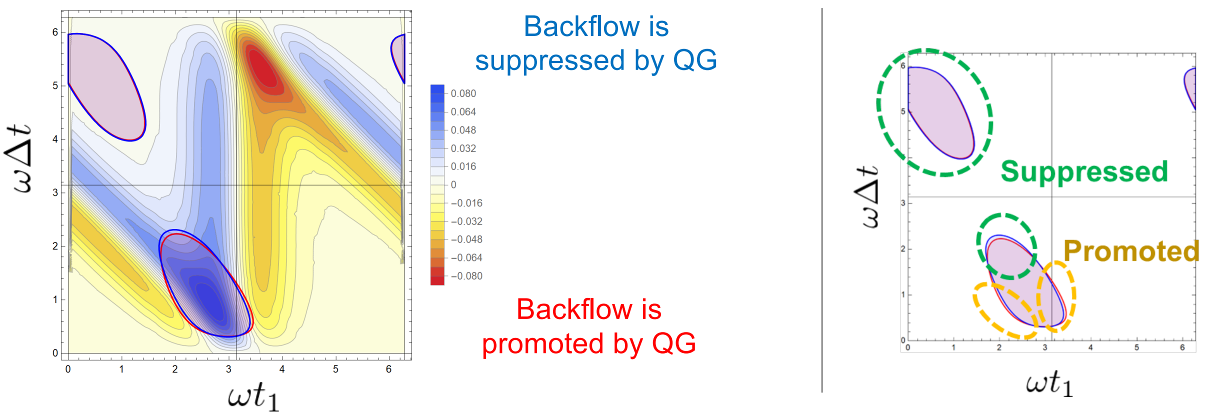

– Since backflow is also related with negative Wigner function, backflow promotion by QG implies the cat state of a particle state in QG case.
– More backflow effect by QG leads to LGI violation.

Results: Violation area

$s_1 = -1,\ s_2 = +1,\ \kappa_{p_0} = 1,\ \kappa_G = 1/4$

Backflow expectation value

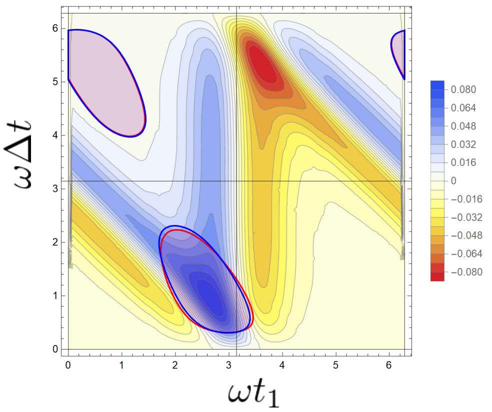

Log negativity of QG

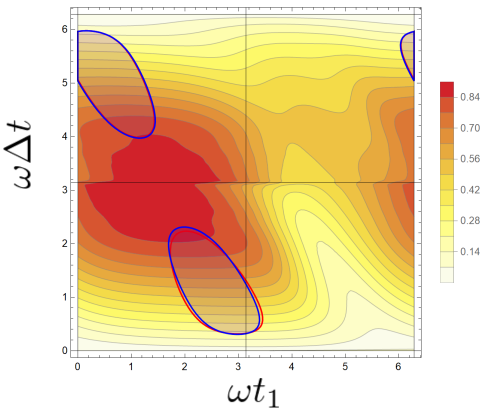

- Suppression of violation by QG corresponds to the region where entanglement is created.
- The LGI violation is determined by the balance of backflow and decoherence.

Results: Violated area

- Log-negativity and violated area

$\kappa_{p_0} = 1,\ \kappa_G = 1/4$

$s_1 = -1,\ s_2 = +1$

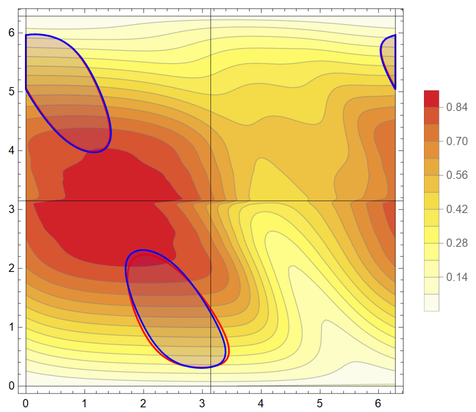

$s_1 = +1,\ s_2 = +1$

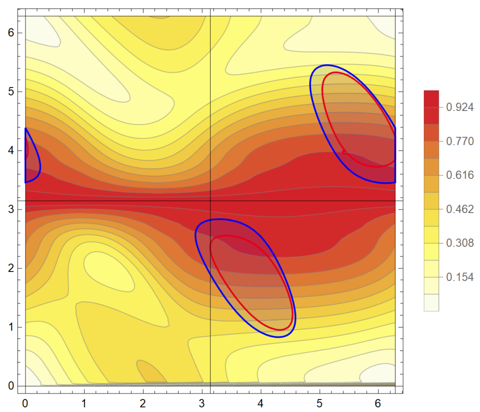

Feasibility

- We evaluated the maximal violation value with realistic parameters.
  - Parameters are set as follows.

$$s_1 = +1,\ s_2 = -1,\ \lambda_{p_0} = 1,\ m = 10^{-14}[kg],\ \omega = 10^6[Hz],$$
$$M = 10[ng],\ d = 100[\mu m],\ \beta = 10[\mu m]$$

  - The difference of the maximal violation value between QG and CG is given by

$$\Delta \mathrm{Min}[q_{+,+}] \sim 5.55112 \times 10^{-17}$$

  - This means that we can test quantumness of gravity if we can perform a 2-level measurement with an uncertainty below 10^{-17}.

$$\boxed{q_{s_1,s_2}(t_1,t_2) := \frac{1}{4}\left(1 + s_1\langle Q(t_1)\rangle + s_2\langle Q(t_2)\rangle + s_1 s_2\langle Q(t_1)Q(t_2)\rangle\right)}$$

Gravitational wave from the axion cloud

Hidetoshi Omiya(Kyoto U)
Ongoing Work with
T. Takahashi, T. Tanaka, and H. Yoshino

2022/10/25@JGRG

Introduction

- Axion is attracting many interests!
  - Possible solution to strong CP problem
  - Dark Matter candidates
  - Appears in low energy effective theory of string theory
  - Can be observed by cosmological/astrophysical phenomena

Signature of the axion

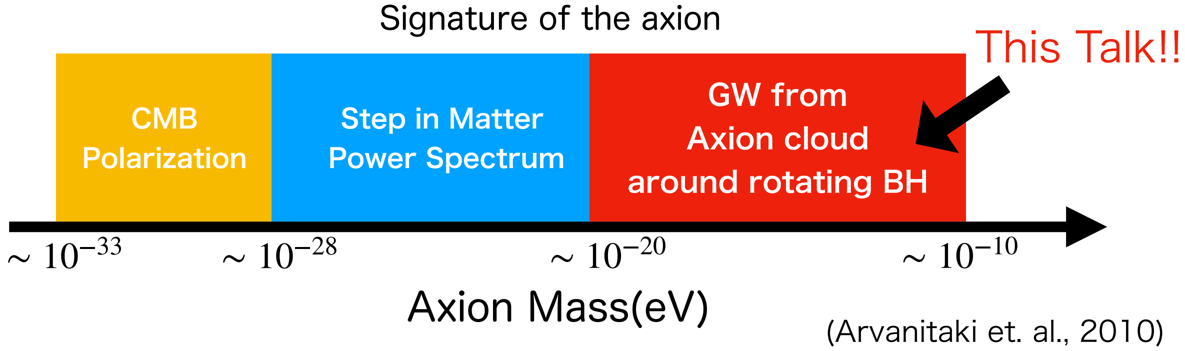

(Arvanitaki et. al., 2010)

Axion cloud

Axion cloud = Condensate of axion around rotating BH spontaneously formed by superradiance

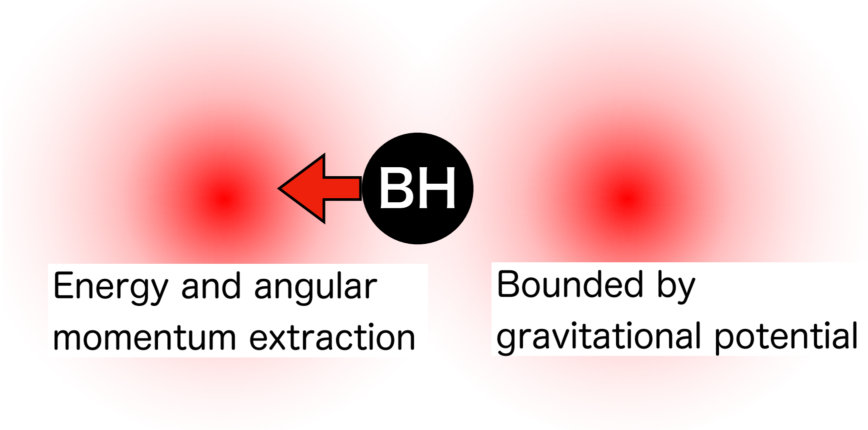

Observable Signal

- GW from the cloud
- Characteristic distribution of BH spin

$$\phi = R_{lm\omega}(r) S_{lm\omega}(\theta) e^{-i(\omega t - m\varphi)} + \text{c.c.}$$

$$\omega = \omega_R + i\omega_I \qquad \tau = \omega_I^{-1} \sim 1\text{min}(M = M_\odot)$$

$$\underbrace{\omega_I > 0}_{\text{Instability}}, \ \omega_R \sim \mu \gg \omega_I, \ \underbrace{\omega_R - m\Omega_H < 0}_{\text{Superradiance condition}}$$

Self-interaction

After the cloud gets dense, self-interaction plays important role.

(Arvanitaki et. al.,2010)

$$S = \int d^4x \sqrt{-g} \left[-\frac{1}{2}(\partial_\mu \phi)^2 - \mu^2 F_a^2 \left(1 - \boxed{\cos \frac{\phi}{F_a}} \right) \right] ,$$

$$\sim \frac{1}{2}\mu^2 \phi^2 - \underbrace{\frac{\mu^2}{4! F_a^2}\phi^4}_{\text{Attractive}} + \dots$$

1. Excitation of dissipative modes. Saturate instability.
2. Collapse of cloud and burst of GW (Bosenova). Accelerate instability.

1.

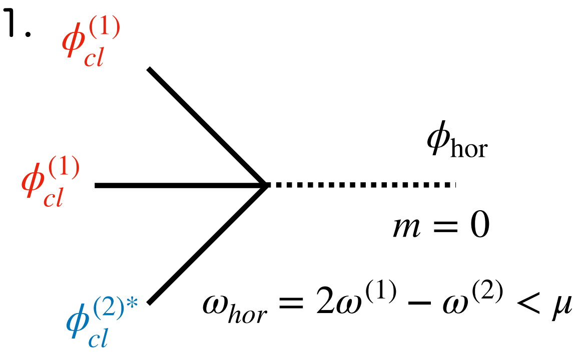

Dissipation by Multiple mode

Mode coupling induce efficient dissipation channel

(Baryakhtar et. al. 2020)

$\phi_{cl}^{(1)} : l = m = 1, \omega_R^{(1)} < \mu$

$\phi_{cl}^{(2)} : l = m = 2, \omega_R^{(1)} < \omega_R^{(2)} < \mu$

※$m = -1, \omega = -\omega^{(1)*}$ is also excited since ϕ is real

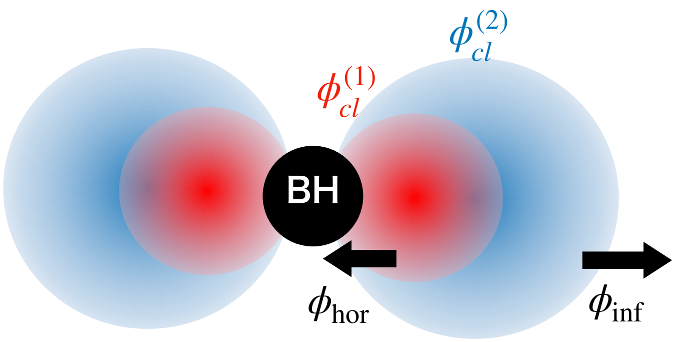

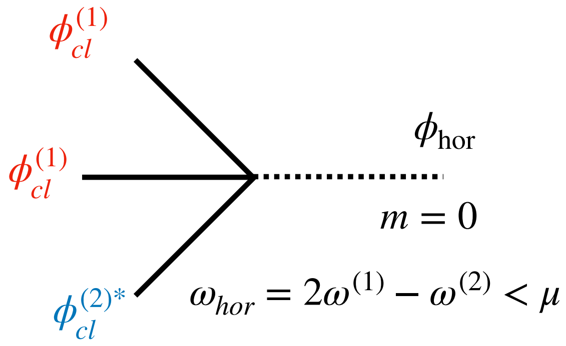

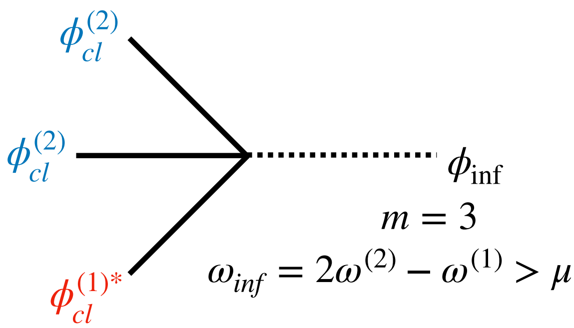

Evolution with self-interaction

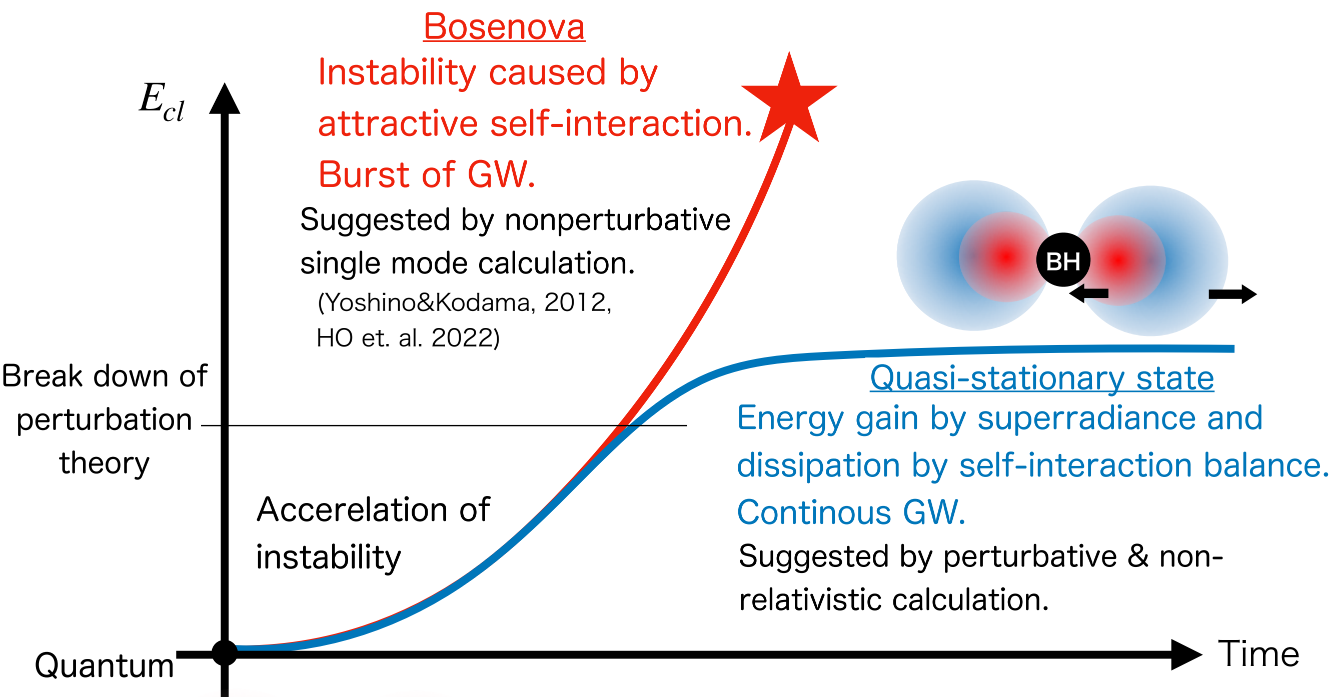

Q:Which one is expected in realistic situation?

Time evolution with multiple mode

Under the adiabatic approximation

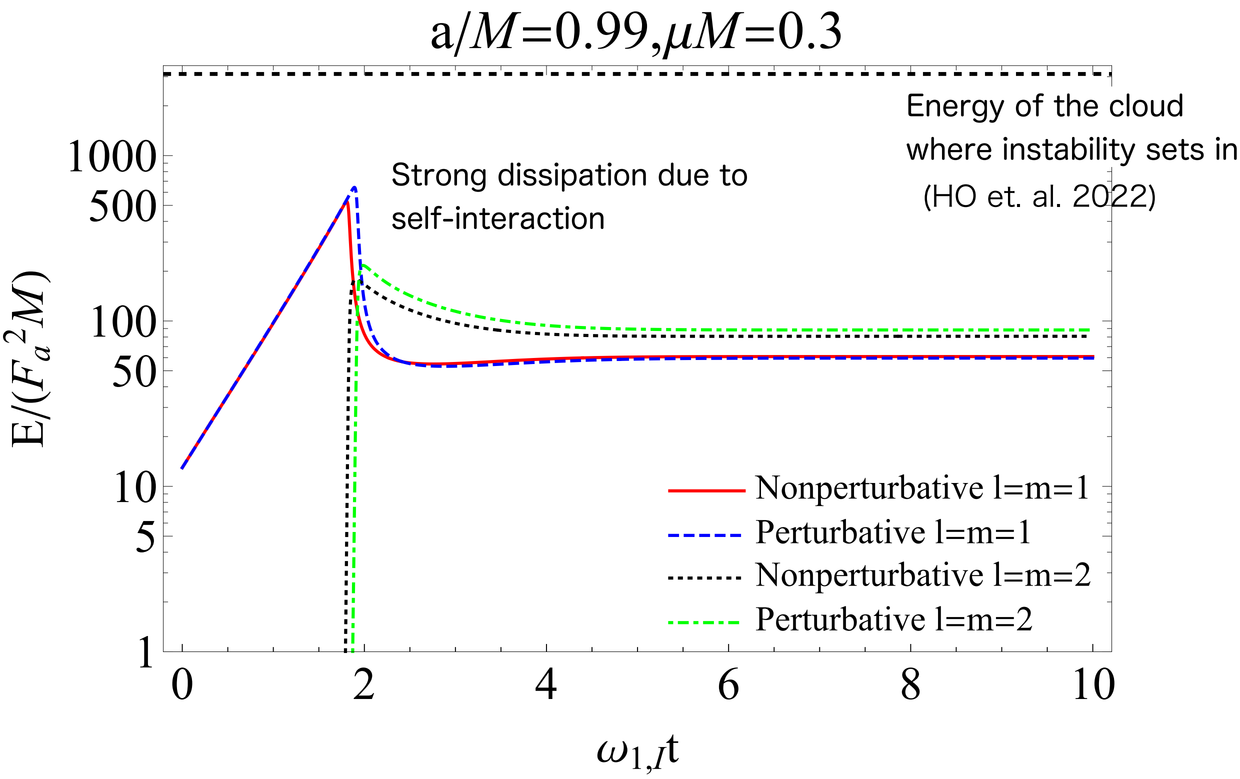

Dependence on initial energy

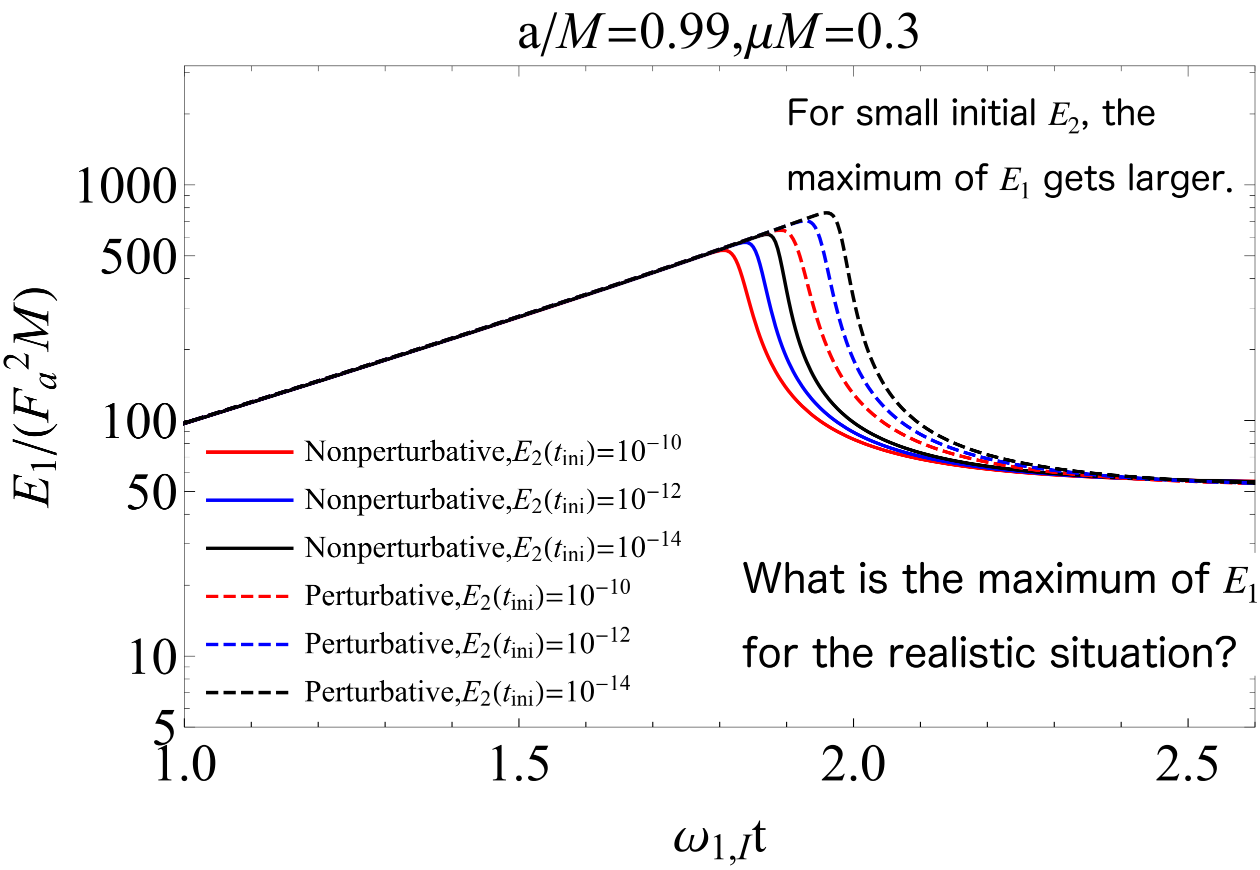

Estimation of maximum energy

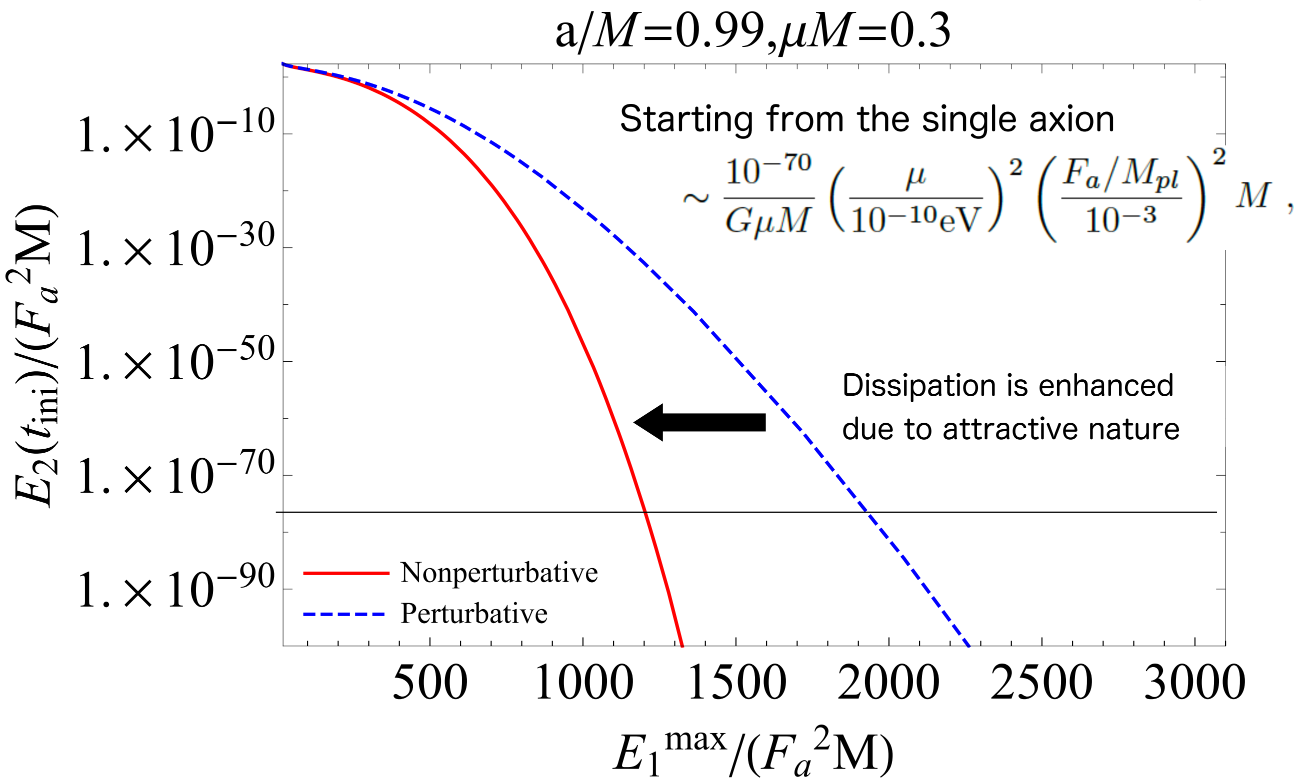

Saturation occurs even starting with quantum fluctuation.

Higher multipole cloud

Let's consider case starting with $l = m = 2$ ($G\mu M \gtrsim 0.45$)

$\phi_{cl}^{(1)} : l = m = 2, \omega_R^{(1)} < \mu$

$\phi_{cl}^{(2)} : l = m = 3, \omega_R^{(1)} < \omega_R^{(2)} < \mu$

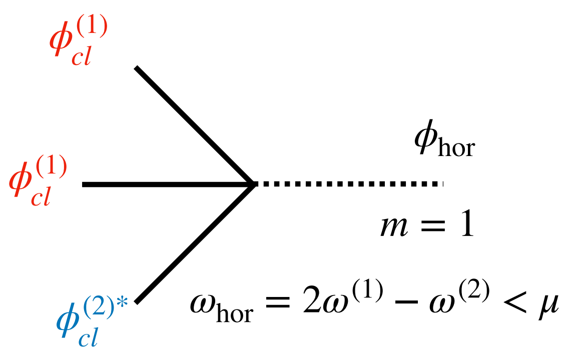

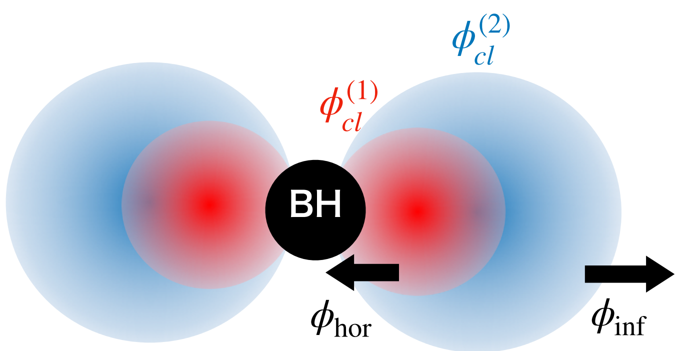

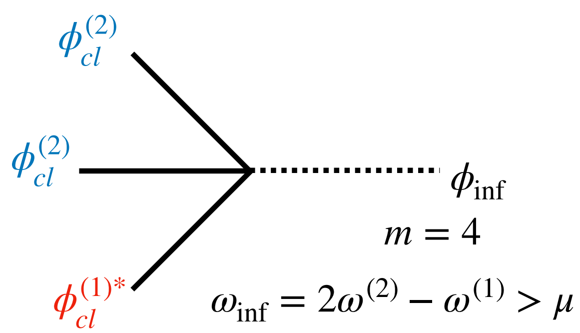

Higher multipole cloud

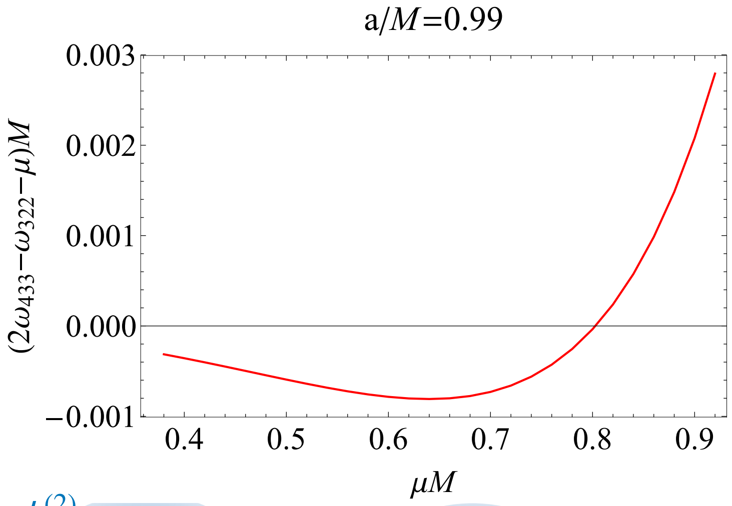

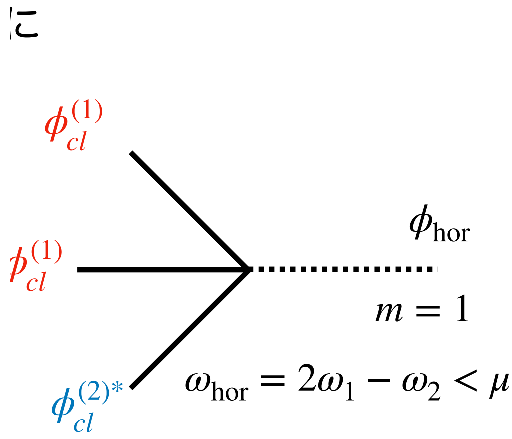

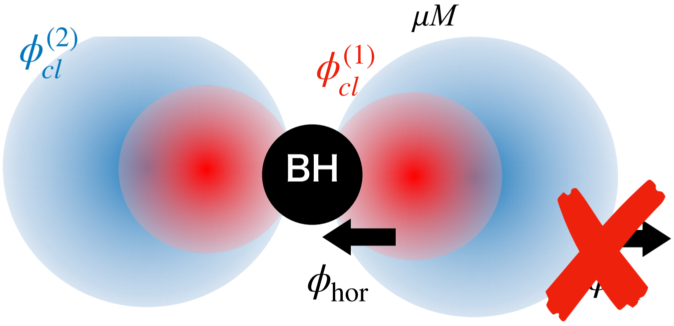

For $\mu \lesssim 0.8$

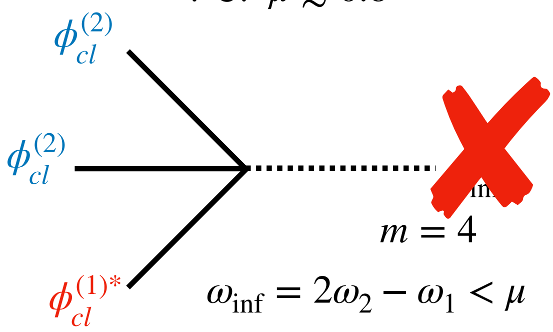

Higher multipole cloud

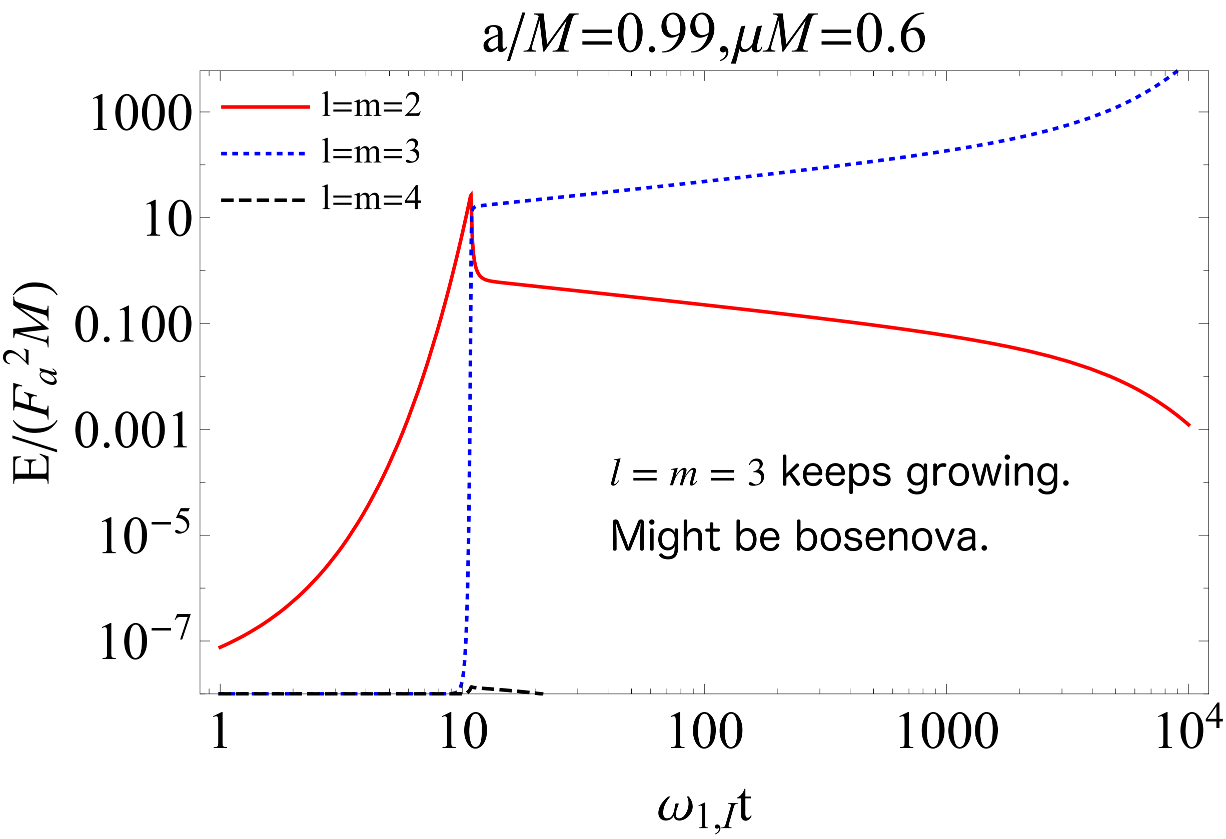

Higher multipole cloud

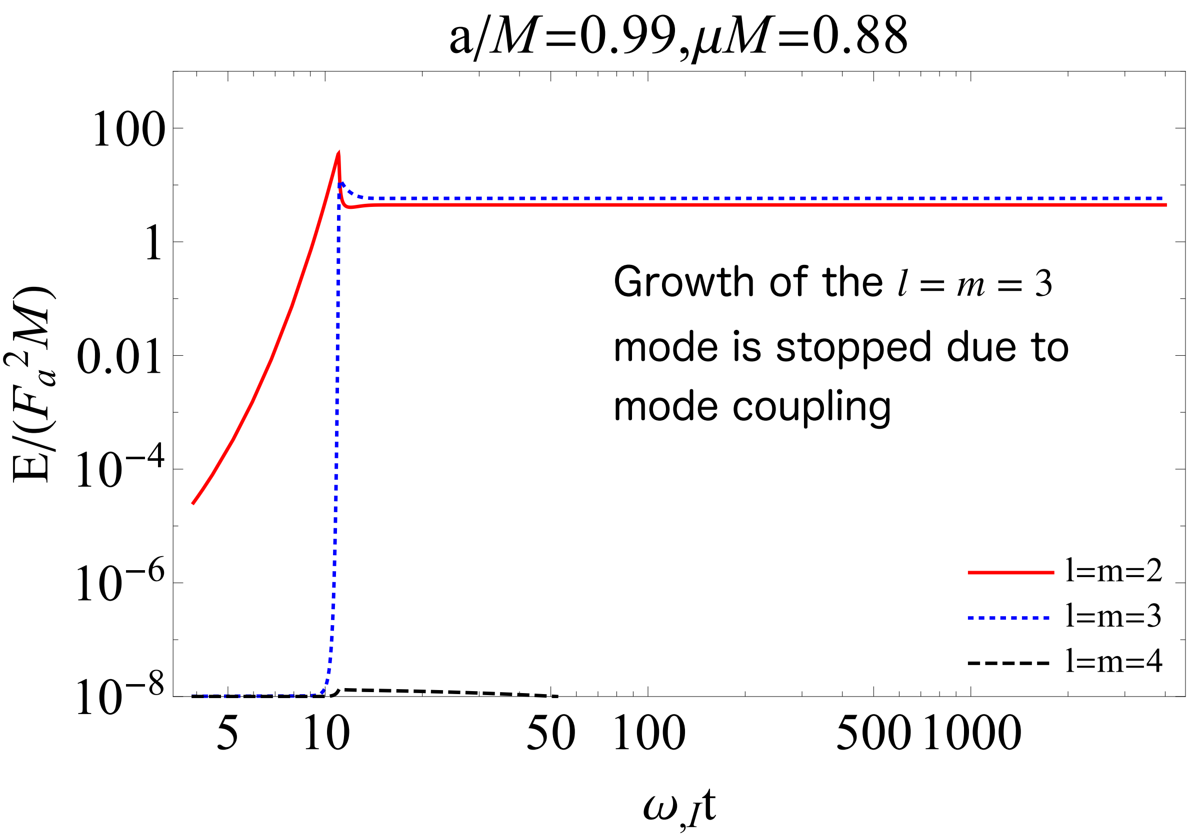

GW from saturated configuration

Two types of GWs are expected from the quasi-stationary configuration.

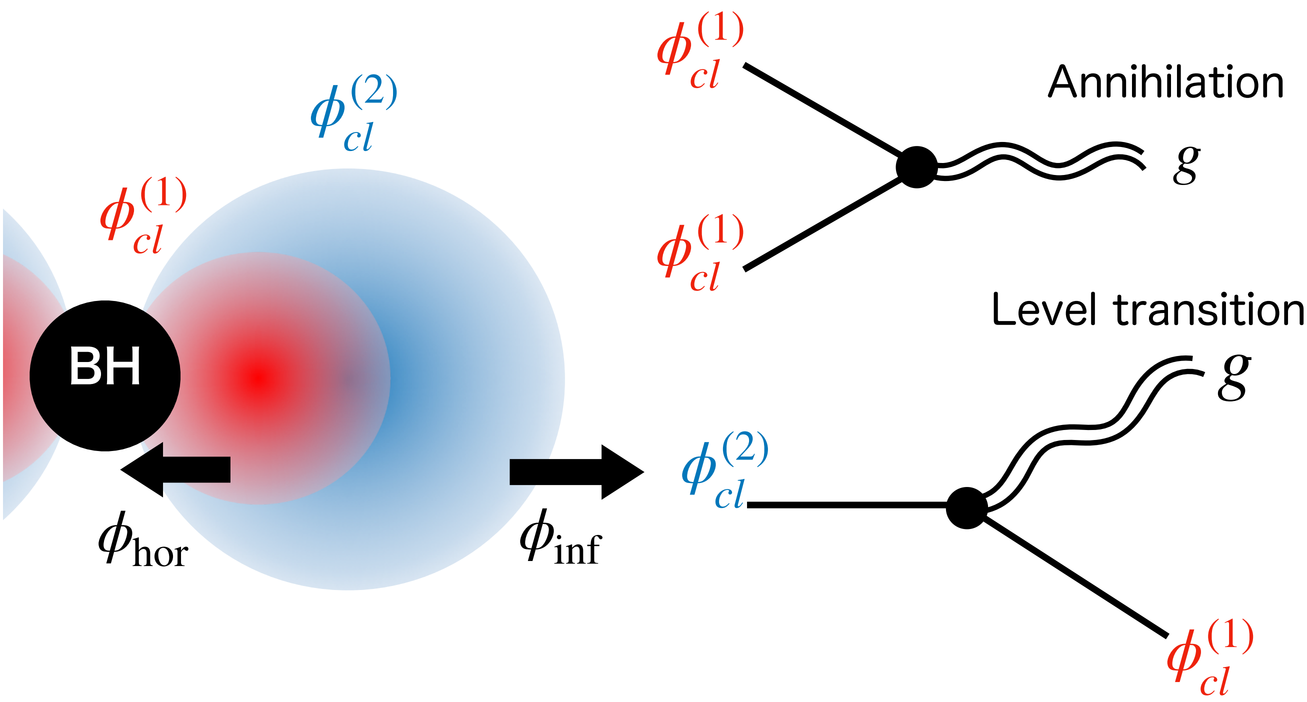

GW from saturated configuration

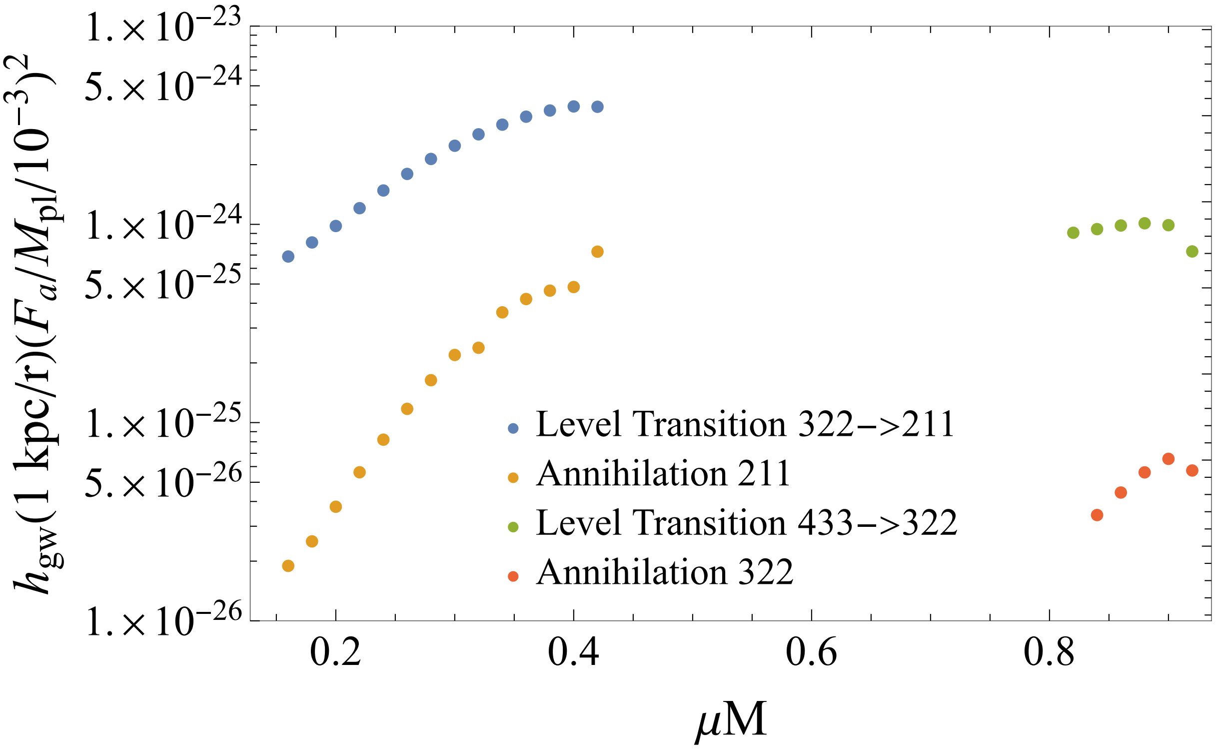

GW from saturated configuration

Multi-frequency continuous GW from same place!

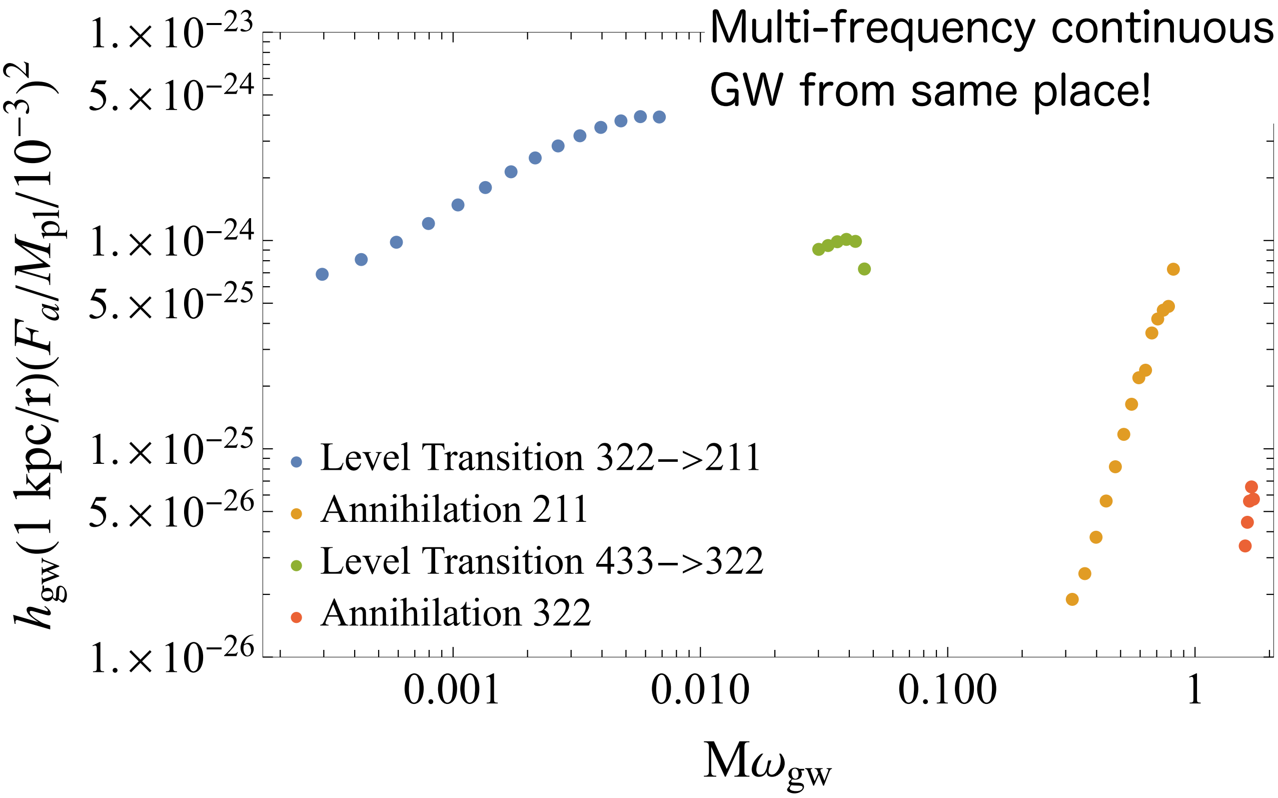

Summary

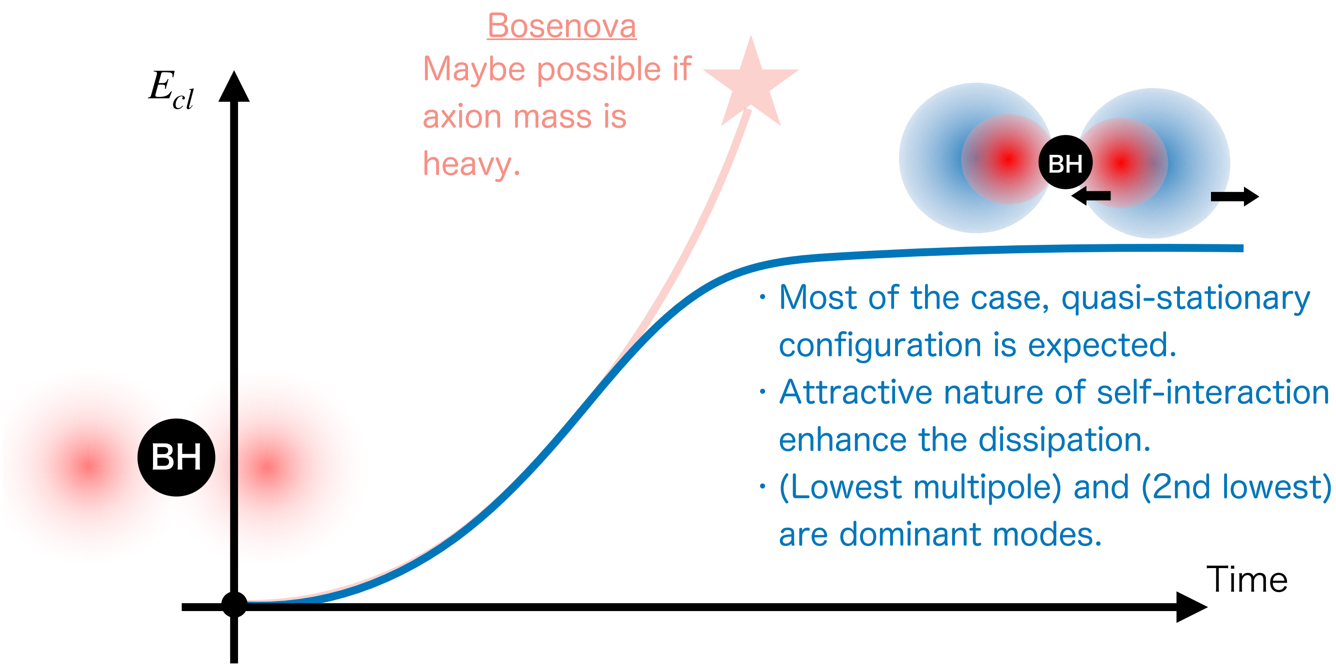

- Continuous GWs with different frequencies are expected from the same sky position.

Back up

Non-Perturbative analysis of cloud evolution

(Omiya et. al.,2022)

- Because of adiabatic growth ($\omega_R \gg \omega_I$), locally ($\Delta t \ll \omega_I^{-1}$), cloud can be approximated to be stationary

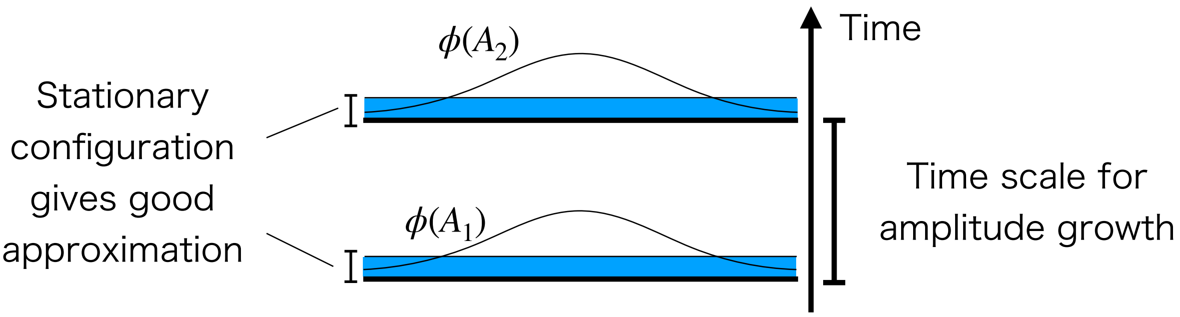

Impose $\dfrac{\mathrm{d}E(A_0)}{\mathrm{d}A_0}\dfrac{\mathrm{d}A_0}{\mathrm{d}t} = -F_{tot}(A_0)$

$E(A_0)$:Energy of $\phi(A_0)$

$F_{tot}(A_0)$:Total Energy flux

Main Idea

Construct the one parameter family of stationary configuration $\{\phi(A_0)\}_{A_0}$ by varying amplitude A_0 and join them by energy conservation.

Non-perturbative analysis with multiple mode

(Work in progress)

- Growth is adiabatic
  →Extension of single mode calculation is possible.
- Assume 2nd mode do not grow so much
  →Configuration of 1st mode is not altered by 2nd mode.

Self-interaction of second mode can be neglected.

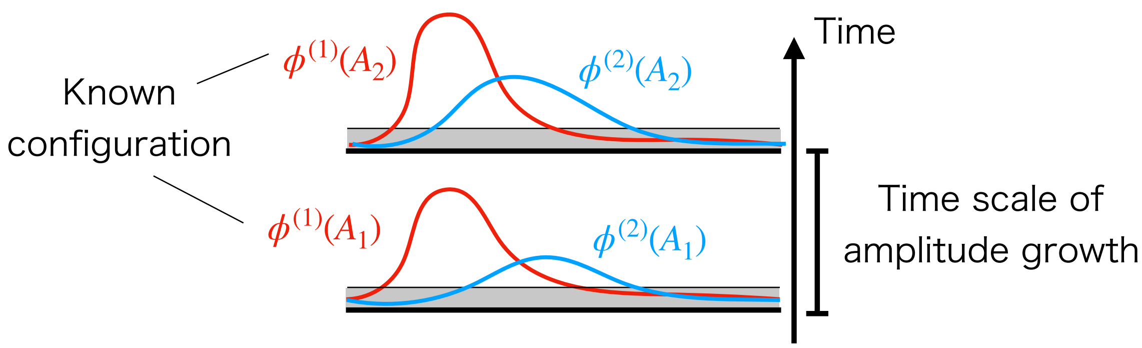

Configuration of 2nd mode: $(\Box_g - \mu^2\cos(\phi^{(1)}(A_0)))\phi^{(2)}(A_0) = 0$

Impose energy conservation + angular momentum conservation

Estimation of maximum energy

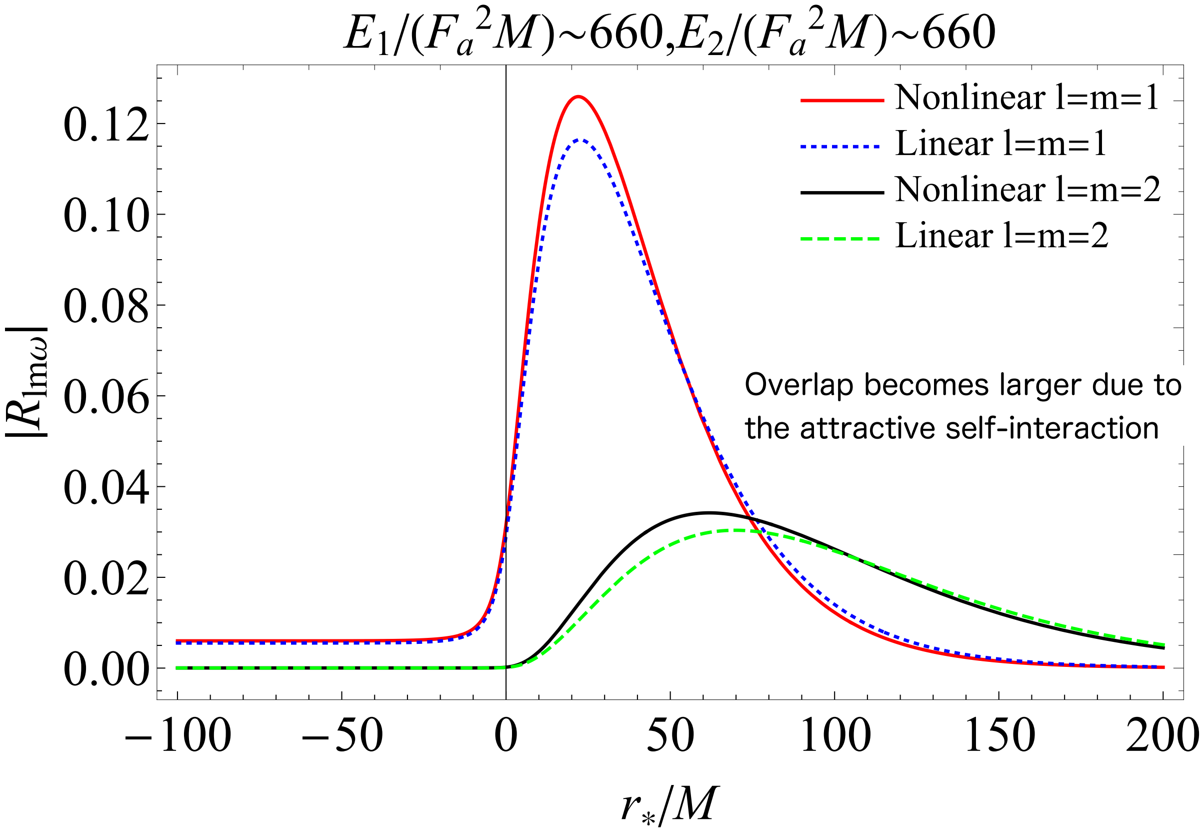

C33

Can we detect the signature of axion clouds in extreme mass ratio inspirals?

Takuya Takahashi (Kyoto University)

with Hidetoshi Omiya and Takahiro Tanaka

Based on [arXiv: 2211.xxxxx]

JGRG31, Oct 25th, 2022

- Introduction
- Formulation
- Results
- Summary

- **Introduction**
- Formulation
- Results
- Summary

Axion Clouds around BHs

Ultralight bosons are closely related to the phenomena in the universe.

axion, axion-like particles,…

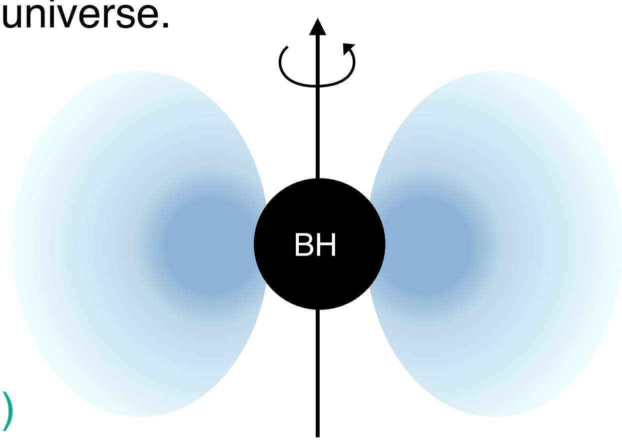

Superradiant instability

Energy and angular momentum extraction from the rotating BH

(Compton wavelength) ~ (BH radius)

$$\alpha \equiv \frac{r_g}{\lambda_c} = \frac{GM\mu}{\hbar c} \simeq 0.2 \left(\frac{M}{30M_\odot}\right)\left(\frac{\mu}{10^{-12}\mathrm{eV}}\right)$$

BH mass M axion mass μ

Axions can form a cloud around a BH.

Observational Signatures

① Gravitational Wave

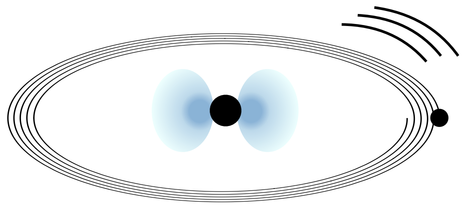

Modification of the waveform
due to the presence of axion clouds

② BH parameter

"Forbidden region" in mass and spin distribution of BHs due to the extraction of angular momentum

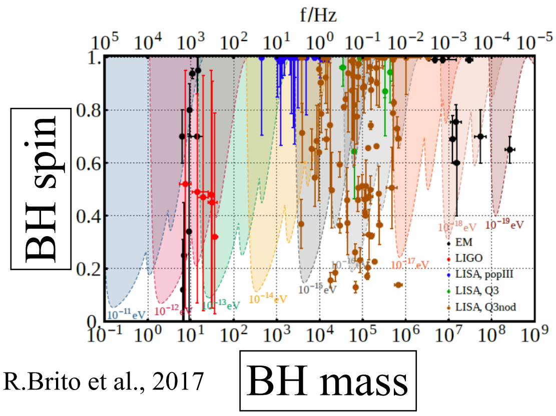

R.Brito et al., 2017

It is important for observations to consider binary systems.

Resonance in the Binary Inspiral

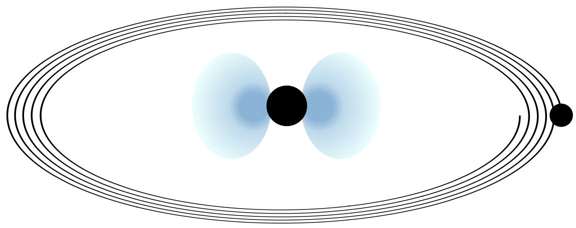

Clouds are described by the bound state solutions

$$\psi_{nlm} = e^{-i(\omega_{nlm}-\mu)t} R_{nl}(r) Y_{lm}(\theta,\varphi)$$

$$\boxed{\omega_{nlm} = (\omega_R)_{nlm} + i(\omega_I)_{nlm}}$$

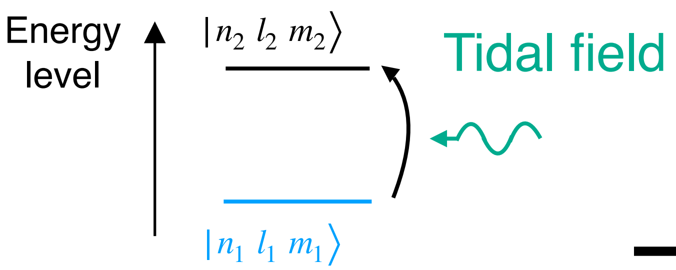

(Energy gap)
= (Orbital frequency)

→ Resonant Transition

D.Baumann et al., 2019

Our Work

Previously, we investigated equal mass binaries

- Hyperfine resonance can be neglected
- Axion clouds evaporate through the emission

T.Takahashi et al., 2021

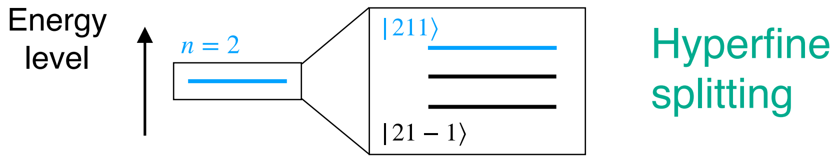

This talk

- **Extreme (or small) mass ratio inspiral**
- **Hyperfine resonance**

  - Long timescales
  - Backreaction to the orbital motion and the BH
  - Impacts on observational signatures

Background

EoM for axions $(g^{\mu\nu}\nabla_\mu\nabla_\nu - \mu^2)\phi = A^\nu(h)\nabla_\nu\phi$

Background part

- Non-relativistic approx.

$$\phi = \frac{1}{\sqrt{2\mu}}\left(e^{-i\mu t}\psi + e^{i\mu t}\psi^*\right)$$

$$\boxed{i\frac{\partial}{\partial t}\psi = H_0\psi\ , \quad H_0 = -\frac{1}{2\mu}\nabla^2 - \frac{\alpha}{r} + \mathcal{O}(\alpha^2)}$$

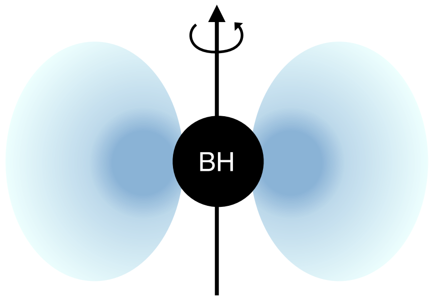

Gravitational coupling $\boxed{\alpha = M\mu}$ BH mass M , axion mass μ

- Hydrogen atom-like structure
- This approximation is good for $\alpha \ll 1$

Perturbation

EoM for axions $(g^{\mu\nu}\nabla_\mu\nabla_\nu - \mu^2)\phi = A^\nu(h)\nabla_\nu\phi$

① Tidal interaction

$$i\frac{\partial}{\partial t}\psi = \left(-\frac{1}{2\mu}\nabla^2 - \frac{\alpha}{r} + V_*(t)\right)\psi$$ Tidal potential

Two level system $\boxed{\psi = c_1(t)\varphi_1 + c_2(t)\varphi_2}$

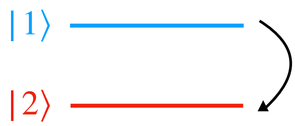

$$\boxed{i\frac{d}{dt}\begin{pmatrix} c_1 \\ c_2 \end{pmatrix} = \begin{pmatrix} -(\Omega - \Omega_{\rm res}) + i\omega_I^{(1)} & \eta \\ \eta & (\Omega - \Omega_{\rm res}) + i\omega_I^{(2)} \end{pmatrix}\begin{pmatrix} c_1 \\ c_2 \end{pmatrix}}$$

② GW emission

H.Yoshino & H.Kodama, 2013

Axions pair-annihilation $\frac{dE_{\rm GW}}{dt} = C\left(\frac{M_c}{M}\right)^2\alpha^{14}$

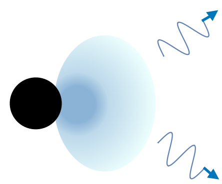

$$\boxed{\frac{dn_1}{dt} = -\frac{C}{M_{c,0}}\left(\frac{M_{c,0}}{M}\right)^2 n_1^2\alpha^{14}}$$ $n_1(t) = |c_1(t)|^2/(M_{c,0}\mu)$

Evolutions of the System

(timescales involved in transition) $\gg \tau_{BH} = M$

$\longrightarrow$ Adiabatic approximation

Variables $\{M, J, \Omega, c_1, c_2\}$

1. Energy flux balance at the horizon	$\frac{dM}{dt} + 2\omega_I^{(1)} M_c^{(1)} + 2\omega_I^{(2)} M_c^{(2)} = 0 \ ,$
2. Angular momentum flux balance at the horizon	$\frac{dJ}{dt} + \frac{2\omega_I^{(1)}}{\mu} M_c^{(1)} - \frac{2\omega_I^{(2)}}{\mu} M_c^{(2)} = 0 \ ,$
3. Total angular momentum conservation	$\frac{d}{dt}\left(J_{\rm orb} + J + J_c\right) + \frac{1}{\mu}\frac{dE_{\rm GW}}{dt} = -\mathcal{T}_{\rm GW}$
4,5. Time evolution of the number of particles in each mode	$i\frac{dc_1}{dt} = \left(-(\Omega - \Omega_{\rm res}) + i\omega_I^{(1)} - i\Gamma_{\rm GW}\right) c_1 + \eta c_2 \ ,$ $i\frac{dc_2}{dt} = \eta c_1 + \left((\Omega - \Omega_{\rm res}) + i\omega_I^{(2)}\right) c_2 \ ,$

All backreactions, decaying process, GW emission are included!

7/13

Evolutions of the System

(timescales involved in transition) $\gg \tau_{BH} = M$

$\longrightarrow$ Adiabatic approximation

Variables $\{M, J, \Omega, c_1, c_2\}$

Difficulty:

Long timescales & Oscillating behavior

4,5. Time evolution of the number of particles in each mode

$$i\frac{dc_1}{dt} = \left(-(\Omega - \Omega_{\rm res}) + i\omega_I^{(1)} - i\Gamma_{\rm GW}\right) c_1 + \eta c_2 \ ,$$
$$i\frac{dc_2}{dt} = \eta c_1 + \left((\Omega - \Omega_{\rm res}) + i\omega_I^{(2)}\right) c_2 \ ,$$

All backreactions, decaying process, GW emission are included!

Adiabatic Elimination

The decay rate $|\omega_I^{(2)}|$ is large compared to the tidal mixing term η

Transferred axions are immediately absorbed by the BH

You can effectively discuss only with the particle number in the first mode

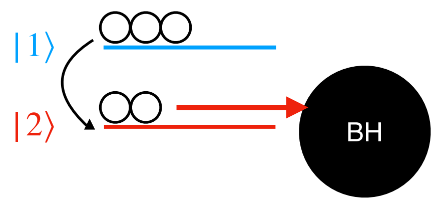

$$i\frac{d\tilde{c}_i}{dt} = \sum_{j=1,2} \tilde{\mathcal{H}}_{ij}\tilde{c}_j \ , \quad \tilde{\mathcal{H}} = \begin{pmatrix} 0 & \eta(t) \\ \eta(t) & \Delta(t) + i\Gamma(t) \end{pmatrix}$$

$$\Delta(t) = 2(\Omega(t) - \Omega_{\rm res}(t)) \ ,$$
$$\Gamma(t) = \omega_I^{(2)}(t) - \omega_I^{(1)}(t) + \Gamma_{\rm GW}(t)$$

$$\boxed{|\tilde{c}_1(t)|^2 = \exp\left(2\int_{-\infty}^{t} dt' \frac{\Gamma\eta^2}{\Delta^2 + \Gamma^2}\right) ,} \quad \boxed{|\tilde{c}_2(t)|^2 = \frac{\eta^2}{\Delta^2 + \Gamma^2}|\tilde{c}_1(t)|^2}$$

$\longrightarrow$ Equation not for $c_1(t)$ but for $n_1(t)$!

Evolutions of the System ~Improved ver.~

Variables $\{M, J, \Omega, n_1\}$

BH mass,
BH angular momentum,
Binary orbital frequency,
Particle number

1. Energy flux balance at the horizon
$$\frac{dM}{dt} + 2\omega_I^{(1)} M_c^{(1)} + 2\omega_I^{(2)} M_c^{(2)} = 0 \ ,$$
2. Angular momentum flux balance at the horizon
$$\frac{dJ}{dt} + \frac{2\omega_I^{(1)}}{\mu} M_c^{(1)} - \frac{2\omega_I^{(2)}}{\mu} M_c^{(2)} = 0 \ ,$$
3. Total angular momentum conservation
$$\frac{d}{dt}(J_{\rm orb} + J + J_c) + \frac{1}{\mu}\frac{dE_{\rm GW}}{dt} = -\mathcal{T}_{\rm GW}$$
4. Time evolution of the number of particles in each mode
$$\frac{dn_1}{dt} = 2\omega_I^{(1)} n_1 + \frac{2\Gamma\eta^2}{\Delta^2 + \Gamma^2} n_1 - \frac{1}{M_{c,0}}\frac{dE_{\rm GW}}{dt}$$

Now, we can solve them for wide parameter region!

- Introduction
- Formulation
- **Results**
- Summary

Setup

Parameters

- (Initial) gravitational coupling $\alpha = M\mu$
- Mass ratio $q = M_*/M$
- Initial cloud mass $M_{\mathrm{c},0}$

Initial conditions

- The cloud is composed of $|211\rangle$
- BH spin is saturated at the critical spin

Evolution of the system around the hyperfine transition $|211\rangle \rightarrow |21-1\rangle$

Evolution of the Cloud

Normalized particle number

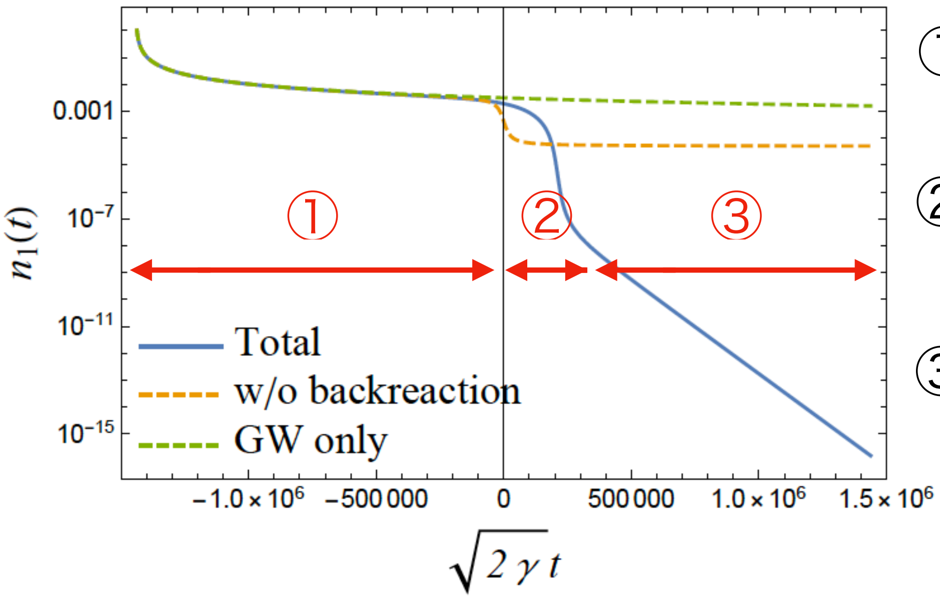

$\{q = 10^{-4}, \alpha_0 = 0.1, M_{c,0} = 10^{-3}\}$

① GW emission

② Transition

Tidal effect

③ BH absorption

BH spin down

BH spin

Deviation from the critical spin

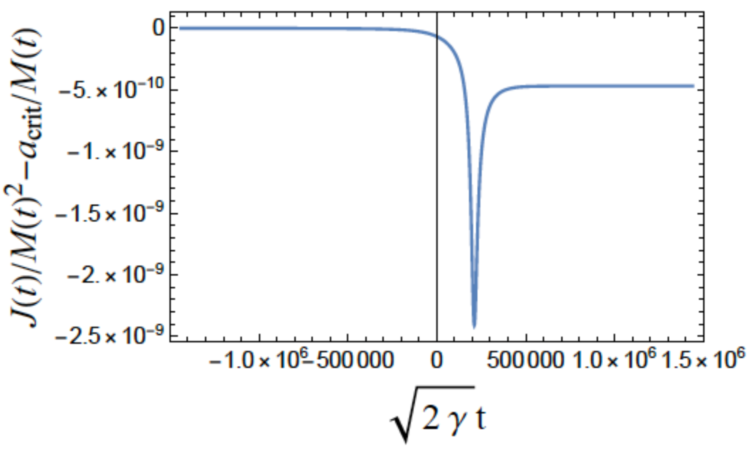

Superradiance condition

$$\omega < m\Omega_H$$

$$M_c(0) \simeq \frac{M_{c,0}}{1 + M_{c,0}(C/M^2)\alpha_0^{14} t_s}$$
$$< \frac{M}{C\alpha_0^{14}\omega_I^{(2)}/(2M\gamma)}$$
$$\simeq 1.4 \times 10^{-4}\, M \left(\frac{q}{10^{-4}}\right)\left(\frac{\alpha_0}{0.1}\right)^{8/3}$$

- Almost clouds are dissipated through GW emission
- The spin-down due to the absorption can be large to deplete the cloud, but would not affect the constraints on axions from the spin measurements

GW form the binary orbital motion

Angular momentum is transferred to the orbital motion

Stagnation around the resonance frequency

$$f_{\rm res} = \frac{\Omega_{\rm res}}{\pi} = 2.2\ {\rm mHz}\ \frac{1}{1+4\alpha_0^2}\left(\frac{\alpha_0}{0.1}\right)^7\left(\frac{10M_\odot}{M}\right)$$

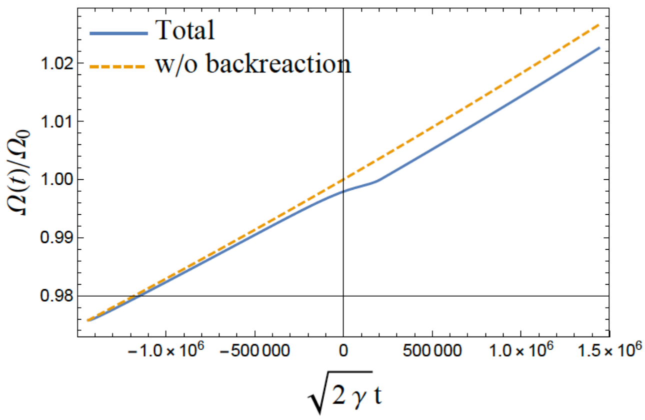

- Timescale of the binary evolution is large
- $f\ddot{f}/\dot{f}^2$ can be largely affected

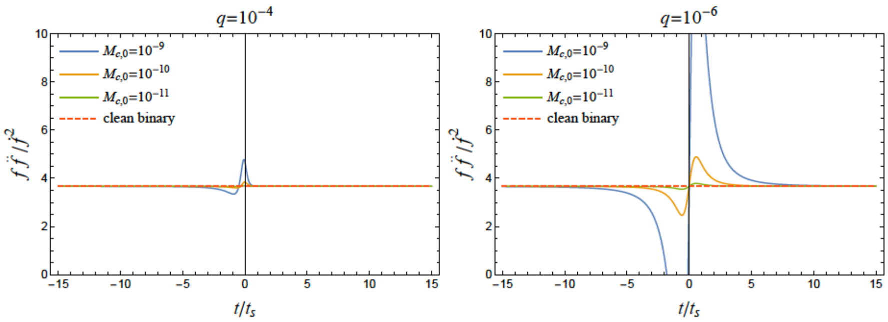

- Introduction
- Formulation
- Results
- **Summary**

Summary

The evolution of binary systems associated with axion clouds inspiraling around the hyperfine resonance frequency, for small mass ratio case.

Formulation:

- Adiabatic approximation
- All backreactions, decaying process, GW emission

Results:

- If tidal effect works, the cloud disappear
- Impact on the BH spin is tiny
- $f\ddot{f}/\dot{f}^2$ can be largely affected

Parameter dependence

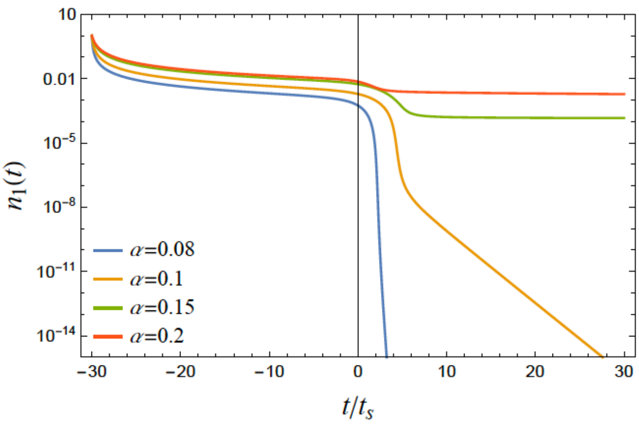

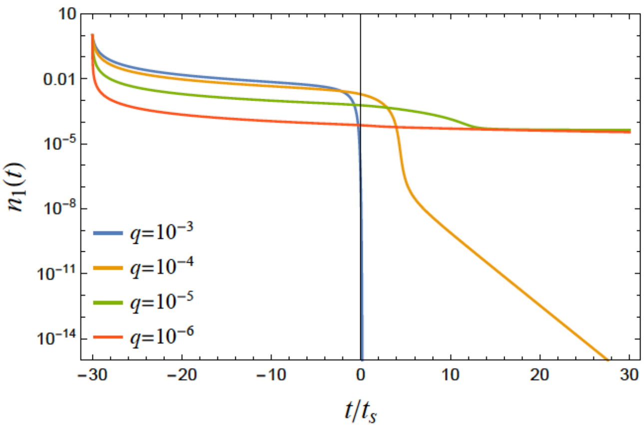

(Tidal effect) ~ (Tidal coupling)
× (Time passing through the resonance)

C34

Axion emission from photon spheres of black holes due to photon–axion conversion

Kimihiro Nomura (D2, Kobe Univ.)

KN, Kaishu Saito, Jiro Soda, in preparation

JGRG31, Oct 25, 2022, @Koshiba Hall, Univ. of Tokyo

Introduction

- **Axion (or axion-like particle): hypothetical scalar particle**
  - explains strong CP: QCD axion [Peccei, Quinn 1977] [Weinberg 1978] [Wilczek 1978] ...

$$m_a \sim 10^{-9}\,\mathrm{eV}\left(\frac{10^{16}\,\mathrm{GeV}}{f_a}\right)$$

decay constant: $\cancel{U(1)}_{\mathrm{PQ}}$ scale

  - from string theory [Arvanitaki+ 2010]

$\mu^2 \sim \cancel{\Lambda_{\mathrm{SUSY}}} M_{\mathrm{Pl}}$

$$m_a \sim \frac{\mu^2}{f_a} e^{-S/2} \lesssim 10^{-10}\,\mathrm{eV}$$

$f_a \sim M_{\mathrm{Pl}}/S$ instanton action $S \gtrsim 200$

  - roles in cosmology
    - inflation
    - dark matter
    - dark energy

Introduction

- **Photons are converted to axions in a magnetic field.**

$$\mathscr{L}_{\rm int} = -\frac{1}{4} g_{a\gamma}\, \phi\, F_{\mu\nu}\tilde{F}^{\mu\nu}$$

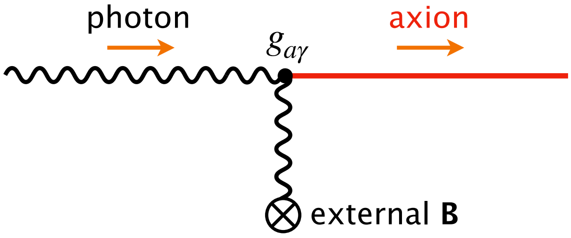

- **Conversion becomes efficient under**
  - Strong magnetic field
  - Long distance propagation

Introduction

- **Photons are converted to axions in a magnetic field.**

$$\mathscr{L}_{\rm int} = -\frac{1}{4} g_{a\gamma}\, \phi\, F_{\mu\nu}\tilde{F}^{\mu\nu}$$

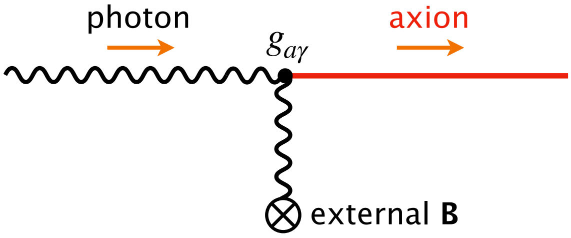

This talk

- **Conversion becomes efficient around black holes because**
  - Strong magnetic field
    - induced by flows of ionized gas.
  - Long distance propagation
    - holds for photons orbiting around BHs.

➡ **What is the signal?**
- **Modification of photon's spectrum?**
- **Axion emission?**

Photon–Axion Conversion

Photon–Axion Conversion

- Consider an electromagnetic wave propagating in a magnetic field:

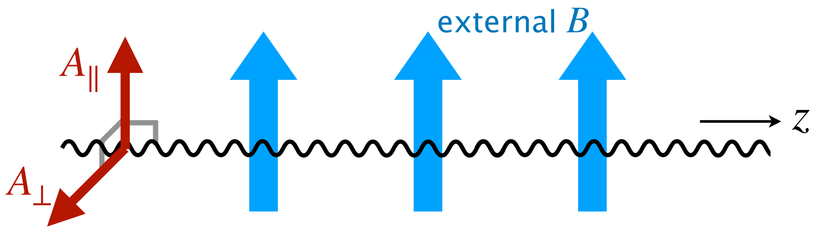

✓ We assume a background magnetic field, not background axions.

- One of the polarizations $A_\parallel$ mixes with the axion.

plane wave with frequency ω

$$\text{photon:} \quad A_\parallel(t,z) = \tilde{A}(z)\, e^{-i\omega(t-z)} + \text{h.c.}$$

$$\text{(relativistic) axion:} \quad \phi(t,z) = \tilde{\phi}(z)\, e^{-i\omega(t-z)} + \text{h.c.}$$

amplitudes vary by interaction

Photon–Axion Conversion

- Evolution of $\tilde{A}(z)$ and $\tilde{\phi}(z)$:

$$i\frac{d}{dz}\begin{pmatrix}\tilde{A}(z)\\ \tilde{\phi}(z)\end{pmatrix} = \begin{pmatrix}\Delta_{\rm pla}-\Delta_{\rm vac} & -\Delta_{\rm M}\\ -\Delta_{\rm M} & \Delta_a\end{pmatrix}\begin{pmatrix}\tilde{A}(z)\\ \tilde{\phi}(z)\end{pmatrix}$$

[Raffelt, Stodolsky 1988]

$\Delta_{\rm M} \equiv \frac{1}{2}g_{a\gamma}B$: photon–axion mixing effect

$\Delta_{\rm pla} \equiv \frac{2\pi\alpha n_e}{\omega\, m_e}$: photon's effective mass due to surrounding plasma

$\Delta_{\rm vac} \equiv \frac{14\alpha^2}{45 m_e^4}\omega B^2$: electron's 1-loop correction in an external B

$\Delta_a \equiv \frac{m_a^2}{2\omega}$: effect from axion mass

α : fine-structure constant, n_e : electron number density,
m_e : electron mass, m_a : axion mass

Conversion Probability [Raffelt, Stodolsky 1988]

$$P_{\gamma\to a}(z;\omega) = |\langle\phi(z)|A(0)\rangle|^2 = \left(\frac{\Delta_{\rm M}}{\Delta_{\rm osc}/2}\right)^2 \sin^2\left(\frac{\Delta_{\rm osc}}{2}z\right)$$

$$\Delta_{\rm osc} = \sqrt{(\Delta_{\rm pla}-\Delta_{\rm vac}-\Delta_a)^2 + 4\Delta_{\rm M}^2}$$

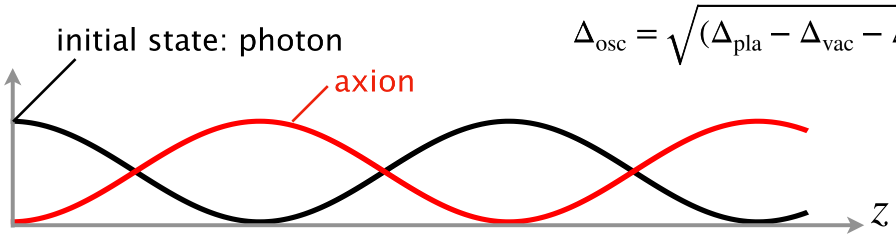

Conversion Probability

[Raffelt, Stodolsky 1988]

$$P_{\gamma\to a}(z;\omega) = |\langle\phi(z)|A(0)\rangle|^2 = \boxed{\left(\frac{\Delta_M}{\Delta_{osc}/2}\right)^2} \sin^2\left(\frac{\Delta_{osc}}{2} z\right)$$

$$\Delta_{osc} = \sqrt{(\Delta_{pla} - \Delta_{vac} - \Delta_a)^2 + 4\Delta_M^2}$$

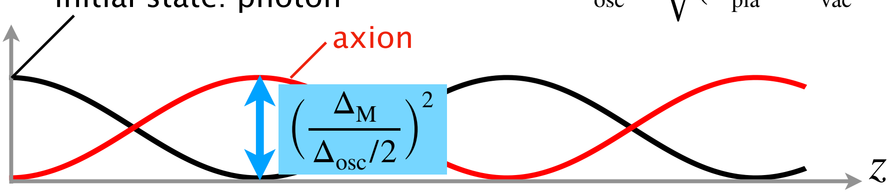

- Maximum of $P_{\gamma\to a}$ becomes unity (at least) if $\Delta_M \gg \Delta_{pla}, \Delta_{vac}, \Delta_a$.
  - Vicinity of BHs can be the case for hard X-rays ($\omega \gtrsim 10\,\mathrm{keV}$).

$$\Delta_M = 3\times 10^{-21}\,\mathrm{eV}\left(\frac{g_{a\gamma}}{10^{-11}\,\mathrm{GeV}^{-1}}\right)\left(\frac{B}{30\,\mathrm{G}}\right) \gg \begin{cases} \Delta_{pla} = 7\times 10^{-22}\,\mathrm{eV}\left(\frac{n_e}{10^4\,\mathrm{cm}^{-3}}\right)\left(\frac{10\,\mathrm{keV}}{\omega}\right) \\ \Delta_{vac} = 8\times 10^{-25}\,\mathrm{eV}\left(\frac{\omega}{10\,\mathrm{keV}}\right)\left(\frac{B}{30\,\mathrm{G}}\right)^2 \\ \Delta_a = 5\times 10^{-23}\,\mathrm{eV}\left(\frac{m_a}{\mathrm{neV}}\right)^2\left(\frac{10\,\mathrm{keV}}{\omega}\right) \end{cases}$$

(Parameters are for M87* from Event Horizon Telescope.)

Conversion Probability

[Raffelt, Stodolsky 1988]

$$P_{\gamma\to a}(z;\omega) = |\langle\phi(z)|A(0)\rangle|^2 = \left(\frac{\Delta_M}{\Delta_{osc}/2}\right)^2 \sin^2\left(\boxed{\frac{\Delta_{osc}}{2} z}\right)$$

$$\Delta_{osc} = \sqrt{(\Delta_{pla} - \Delta_{vac} - \Delta_a)^2 + 4\Delta_M^2}$$

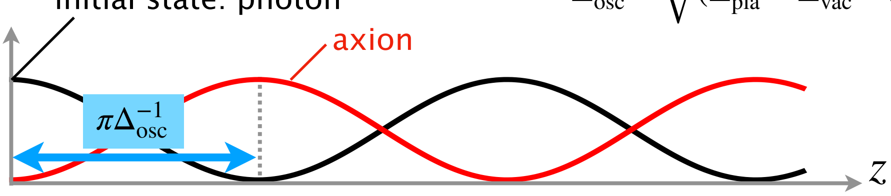

- Conversion length for M87*:

$$\pi\Delta_{osc}^{-1} \simeq 11\times(6.2\times 10^9 GM_\odot)\left(\frac{30\,\mathrm{G}}{B}\right)\left(\frac{10^{-11}\,\mathrm{GeV}^{-1}}{g_{a\gamma}}\right)$$

  - longer than Schwarzschild radius.
  - but, photons can orbit near the BH (strong magnetic field) for a long period.

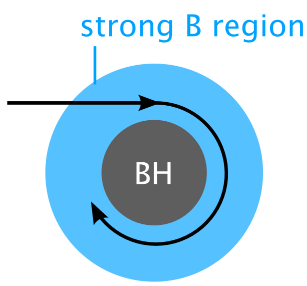

Orbits around Photon Sphere

- Photon sphere: $r = 3GM$ — unstable circular orbits exist.

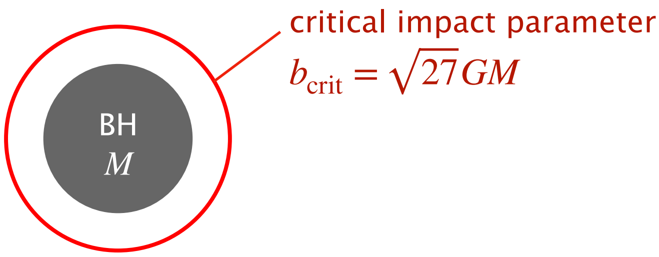

Orbits around Photon Sphere

- Photon sphere: $r = 3GM$ — unstable circular orbits exist.

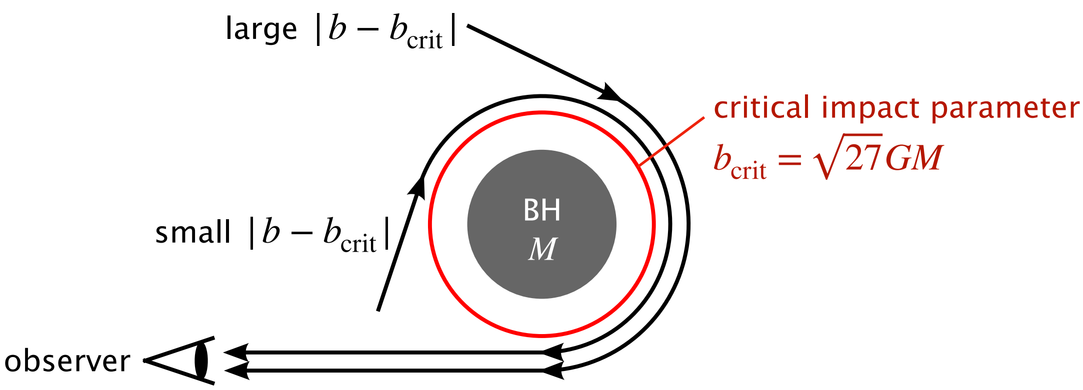

- Photons with impact parameter b (close to b_{crit}) can stay in $3GM < r < (3+\epsilon)GM$ for a distance $z(b) = 3GM \ln \dfrac{\sqrt{3}\,\epsilon^2 GM}{2\,|b - b_{\text{crit}}|}$.

[Yoshino, Takahashi, Nakao 2019]

➡ $P_{\gamma\to a}(z(b);\omega) = \left(\dfrac{\Delta_{\text{M}}}{\Delta_{\text{osc}}/2}\right)^2 \sin^2\!\left(\dfrac{\Delta_{\text{osc}}}{2}\, z(b)\right)$

Observables

Spectra

- Number of photons decreases by conversion to axions.
  ➡ The image near the photon sphere becomes dark.
- We assume that the source of photons approaching the photon sphere is thermal bremsstrahlung of surrounding plasma.

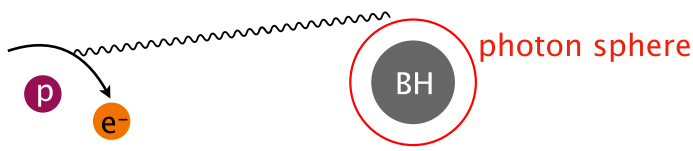

– Spectra from the photon sphere of M87*

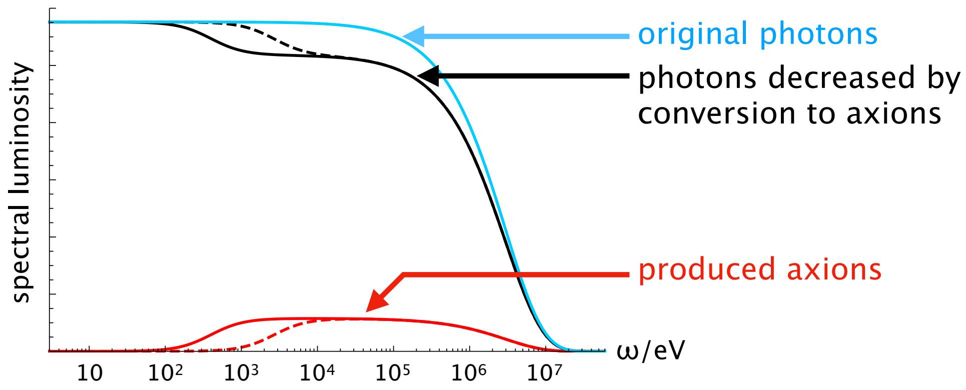

Spectra

- Number of photons decreases by conversion to axions.
  ➡ The image near the photon sphere becomes dark.
- We assume that the source of photons approaching the photon sphere is thermal bremsstrahlung of surrounding plasma.

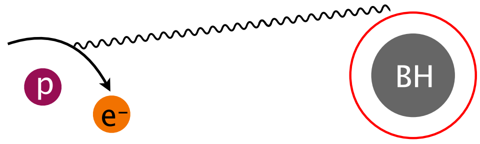

– Spectra from the photon sphere of M87*

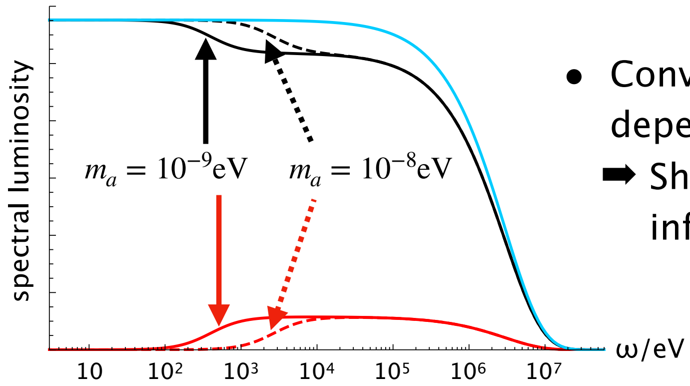

- Conversion frequency depends on axion mass.
  ➡ Shape of spectra has information on axion mass.

Summary

- **Photon-axion conversion can efficiently occur in the vicinity of black holes.**
  – Strong magnetic field is present.
  – Photons can propagate over a long distance by orbiting around the photon sphere.
- **Number of photons decreases by conversion to axions.**
  ➡ The image near the photon sphere becomes dark.

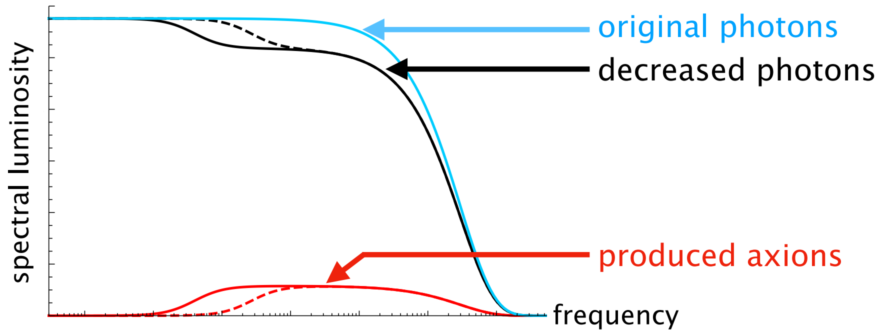

- **Shape of spectra has information on axion mass.**

Backup

Conversion Probability

$$P_{\gamma\to a}(z;\omega) = |\langle \phi(z)|A(0)\rangle|^2 = \left(\frac{\Delta_{\mathrm{M}}}{\Delta_{\mathrm{osc}}/2}\right)^2 \sin^2\left(\frac{\Delta_{\mathrm{osc}}}{2}z\right)$$

$$\Delta_{\mathrm{osc}}(\omega) = \sqrt{(\Delta_{\mathrm{pla}} - \Delta_{\mathrm{vac}} - \Delta_a)^2 + 4\Delta_{\mathrm{M}}^2}$$

- $\left(\frac{\Delta_{\mathrm{M}}}{\Delta_{\mathrm{osc}}/2}\right)^2$ in the ω-nₑ plane

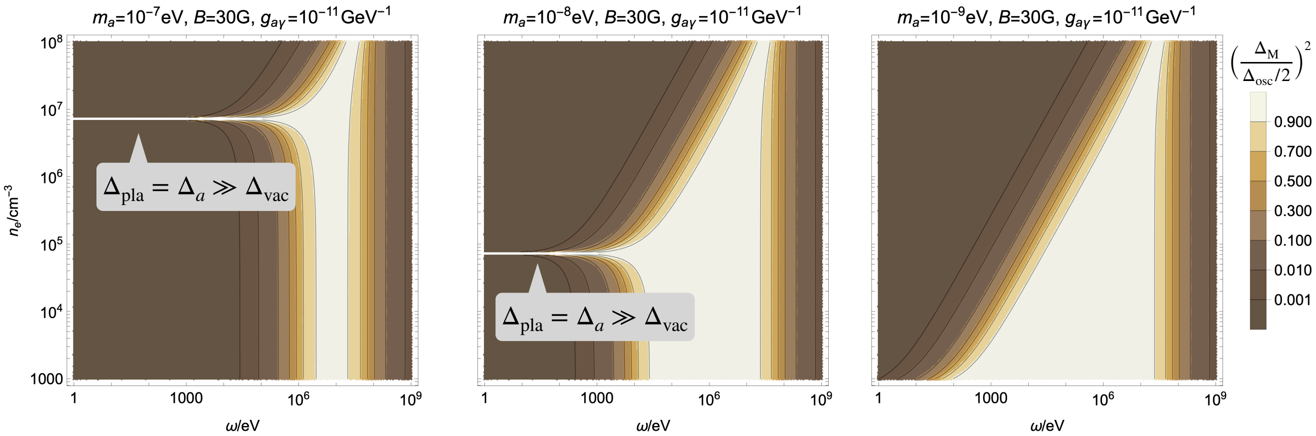

Orbits around Photon Sphere

- Photons with impact parameter b (close to b_{crit}) can stay in $3GM < r < (3+\epsilon)GM$ for a distance $z(b) = 3GM \ln \dfrac{\sqrt{3}\,\epsilon^2 GM}{2|b - b_{\mathrm{crit}}|}$.

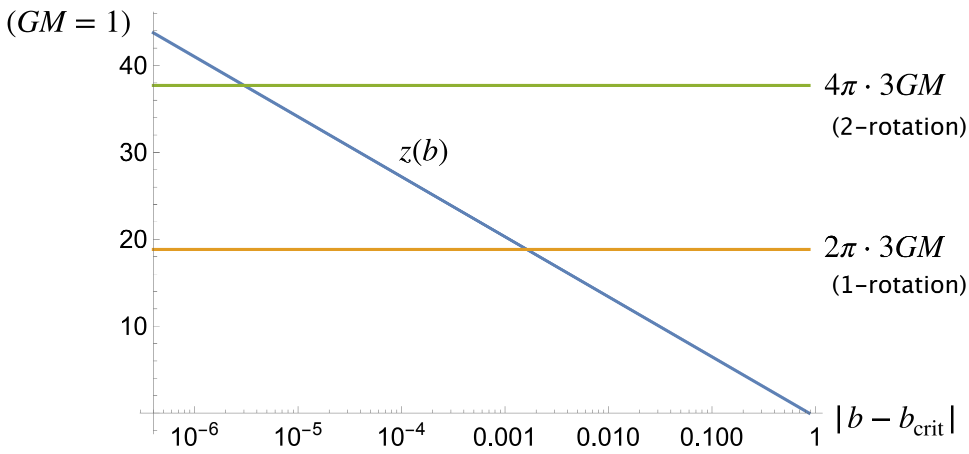

Dimming of Photon Sphere

- Let $\dfrac{d^3N_\gamma}{dt\,d\omega\,db}$ be the number of photons approaching the photon sphere per unit time t, unit frequency ω, unit impact parameter b.

- Number of photons converted to axions reads

$$\frac{d^2N_{\gamma\to a}}{dt\,d\omega} = \int db\ \frac{1}{2}\ \frac{d^3N_\gamma}{dt\,d\omega\,db}\ P_{\gamma\to a}(z(b);\omega)$$

conversion probability

Only one polarization $A_\parallel$ converts to axions.

- Number of photons decreases:

$$\frac{d^2N_{\gamma\to a}}{dt\,d\omega}\bigg/\frac{d^2N_\gamma}{dt\,d\omega} = \left(\frac{\Delta_{\mathrm{M}}}{\Delta_{\mathrm{osc}}/2}\right)^2 \frac{(3GM\Delta_{\mathrm{osc}})^2}{1+(3GM\Delta_{\mathrm{osc}})^2} \times 25\% \xrightarrow[\text{in M87*}]{\text{for X-ray}} 10\%.$$

Dimming of Photon Sphere

- Number of photons decreases:

$$\frac{d^2N_{\gamma\to a}}{dt\,d\omega}\bigg/\frac{d^2N_\gamma}{dt\,d\omega} = \left(\frac{\Delta_{\mathrm{M}}}{\Delta_{\mathrm{osc}}/2}\right)^2 \frac{(3GM\Delta_{\mathrm{osc}})^2}{1+(3GM\Delta_{\mathrm{osc}})^2} \times 25\%$$

$$\xrightarrow[\textbf{most efficient case}]{\Delta_{\mathrm{M}}=\Delta_{\mathrm{osc}}/2} \frac{(6GM\Delta_{\mathrm{M}})^2}{1+(6GM\Delta_{\mathrm{M}})^2} \times 25\%$$

$$6GM\Delta_{\mathrm{M}} = 0.8\left(\frac{M}{6.2\times10^9 M_\odot}\right)\left(\frac{B}{30\,\mathrm{G}}\right)\left(\frac{g_{a\gamma}}{10^{-11}\,\mathrm{GeV}^{-1}}\right)$$

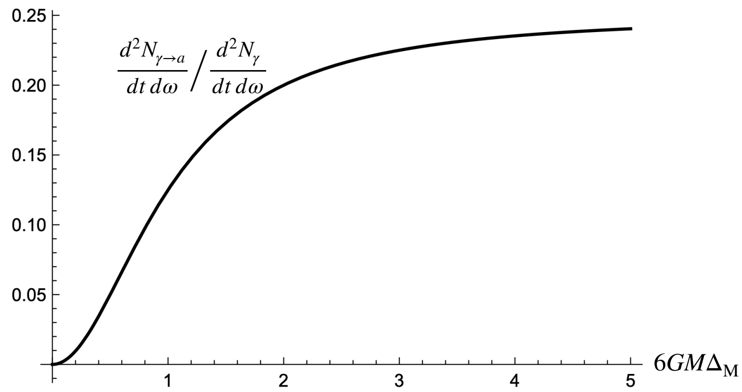

Computation of Spectra

- Assuming a spherical source of photons surrounding the BH,

$$\frac{d^3N_\gamma}{dt\,d\omega\,db} = \frac{4\pi^2}{\sqrt{3}}\int_{r_{\rm in}}^{r_{\rm out}} dr\, J^{(N)}\left(\frac{\omega}{\sqrt{3f(r)}}, r\right)\frac{b\,r}{\sqrt{(r^2/f(r)) - b^2}}$$

$f(r) = 1 - \frac{2GM}{r}$, $J^{(N)}$ = Emitted photon number per unit time, frequency, volume, solid angle

- Assuming thermal bremsstrahlung,

$$J^{(N)}(\omega, r) = \frac{4\alpha^3}{3\pi m_e}\left(\frac{2\pi}{3m_e}\right)^{1/2}\omega^{-1}T_e^{-1/2}n_e^2 e^{-\omega/T_e}\bar{g}_{ff}$$

T_e = electron temperature, n_e = electron number density,
$\bar{g}_{ff}(\sim 1)$ = velocity averaged Gaunt factor

- Furthermore, we assume
  - $T_e \propto r^{-1}$: virial temperature
  - $n_e \propto r^{-3/2}$: free-fall

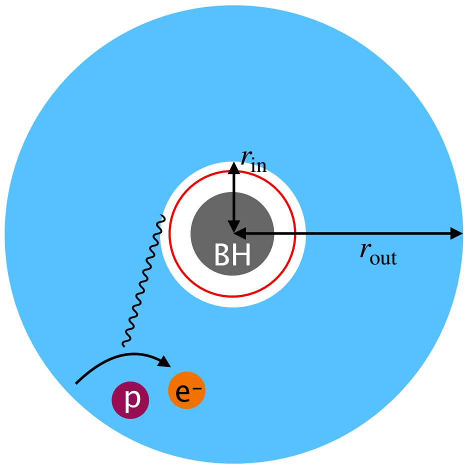

Luminosity

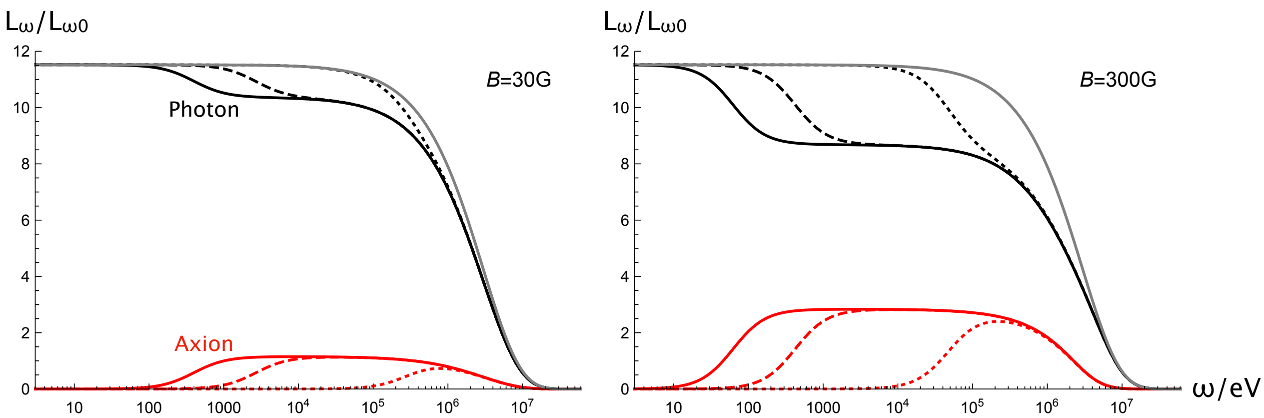

- From $3GM < r < (3+\epsilon)GM$,

$$L_{\omega 0} = 1.6\times 10^{34}\epsilon^2\left(\frac{M}{10^9 M_\odot}\right)^3\left(\frac{T_e}{10^{11}\ \mathrm{K}}\right)^{-1/2}\left(\frac{n_e}{10^4\ \mathrm{cm}^{-3}}\right)^2\bar{g}_{ff}\ \mathrm{keV}\cdot\mathrm{sec}^{-1}\cdot\mathrm{keV}^{-1}$$

(T_e, n_e are electron temperature, number density on the photon sphere.)

Axion Number Flux

- From $3GM < r < (3+\epsilon)GM$,

$$F_{a,\omega}^{(N)} \sim 1.4 \times 10^{-16} \epsilon^2 \left(\frac{\mathrm{Mpc}}{D}\right)^2 \left(\frac{M}{10^9 M_\odot}\right)^3 \left(\frac{T_e}{10^{11}\ \mathrm{K}}\right)^{-1/2}$$

$$\times \left(\frac{n_e}{10^4\ \mathrm{cm}^{-3}}\right)^2 \left(\frac{\mathrm{keV}}{\omega}\right)\ \mathrm{cm}^{-2} \cdot \mathrm{sec}^{-1} \cdot \mathrm{keV}^{-1}$$

(T_e, n_e are electron temperature, number density on the photon sphere.)

C35

C35

Microlensing constraints on axion stars including finite lens and source size effects

JGRG31(2022/10/25)

Kohei Fujikura (Kobe U.)

In collaboration with:

Mark P. Hertzberg (Tufts U.)

Enrico D. Schiappacasse (Rice U.)

Masahide Yamaguchi (TiTech)

This talk is based on arXiv:2109.04283 [Phys. Rev. D 104, 123012]

Axions in the early Universe

- The QCD axion is introduced to solve the strong CP problem.

[Peccei, Quinn (1977)]

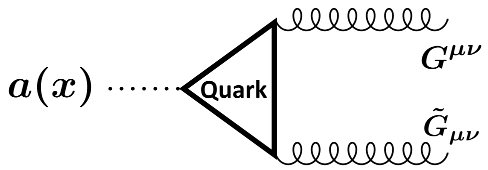

$a(x)$: the QCD axion, $G_{\mu\nu}$:Field strength of $SU(3)_C$

$$V(a) \simeq \Lambda_{\rm QCD}^4\left(1-\cos(a/F_a)\right)$$

F_a :Decay constant $\Lambda_{\rm QCD} \sim 0.1\,\mathrm{GeV}$

$$\simeq \frac{1}{2}m_a^2 a^2 - \frac{\lambda}{4}a^4$$

- Axions are produced with high occupancy and can be DM!

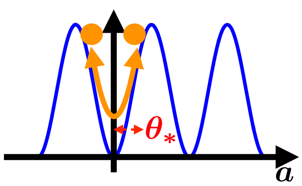

$$\Omega_{\rm osc}h^2 \sim \theta_*^2\left(\frac{F_a}{10^{12}\,\mathrm{GeV}}\right)^{1.19}$$

θ_*: initial misalignment angle [Kawasaki, Nakayama (2013)]

[Preskill, Wise, Wilczek (1983); Abbott, Sikivie (1983) ; Dine, Fischler (1983)]

- Axion Bose-Einstein condensate (BEC) may take place.

[Sikivie, Yang (2009); Erken, Sikivie, Tam, Yang (2011); Saikawa, Yamaguchi (2013); Noumi, Saikawa, Sato, Yamaguchi (2014)]

… and so many works …

Axion Stars

A consequence of BEC dark matter:

“Localized clumps” made of axions bounded by gravity (axion stars) are formed.

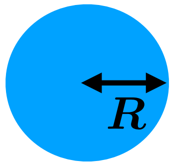

[Guth, Hertzberg, Weinstein (2014)]

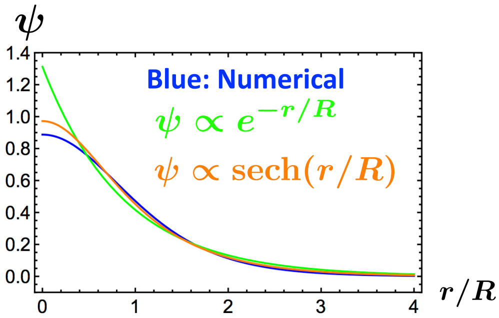

[Schiappacasse, Hertzberg (2017)]

Equation of motion:

$$i\dot{\psi} = \underbrace{-\frac{1}{2m_a}\nabla^2\psi}_{\text{Pressure}} \underbrace{- Gm_a^2\psi\int d^3x'\frac{|\psi(x')|^2}{|x-x'|}}_{\text{Gravity}} \underbrace{-\frac{\lambda}{8m_a^2}|\psi|^2\psi}_{\text{Self-coupling}}$$

ψ: The wavefunction of the ground state

Typical radius and mass of (QCD) axion stars

- **Total number of axions in axion stars**

α **: axion clump density**

$$N \simeq 1.7\times 10^{60}\times\alpha\left(\frac{10^{-5}\mathrm{eV}}{m_a}\right)^2\times\left(\frac{F_a}{10^{12}\mathrm{GeV}}\right) \qquad 0\le\alpha\le 1$$

- **Length scale of axion stars**

$$R \simeq 1.8\times 10^4\ \mathrm{m}\times\left(\frac{1+\sqrt{1-\alpha^2}}{\alpha}\right)\times\left(\frac{10^{-5}\mathrm{eV}}{m_a}\right)\times\left(\frac{10^{12}\mathrm{GeV}}{F_a}\right)$$

- **Mass of axion stars (not axion itself!)**

$$M_{\mathrm{clump}} = Nm_a \simeq 1.5\times 10^{-11}M_\odot\times\alpha\left(\frac{10^{-5}\mathrm{eV}}{m_a}\right)\times\left(\frac{F_a}{10^{12}\mathrm{GeV}}\right)$$

$$M_{\rm clump} = N m_a \simeq 1.5 \times 10^{-11} M_\odot \times \alpha \left(\frac{10^{-5}{\rm eV}}{m_a}\right) \times \left(\frac{F_a}{10^{12}{\rm GeV}}\right)$$

Microlensing constraints?

Microlensing events

Image of a background source star is distorted when massive objects pass close to its line-of-sight.

One can observe time varying amplification of the source star. (Microlensing events)

Massive compact objects are constrained by microlensing events!

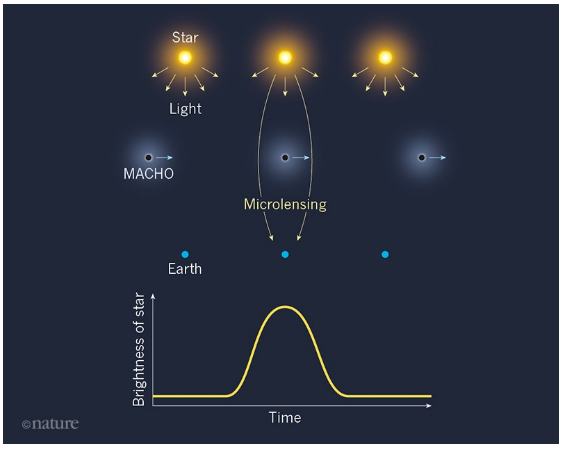

Microlensing constraints on compact object

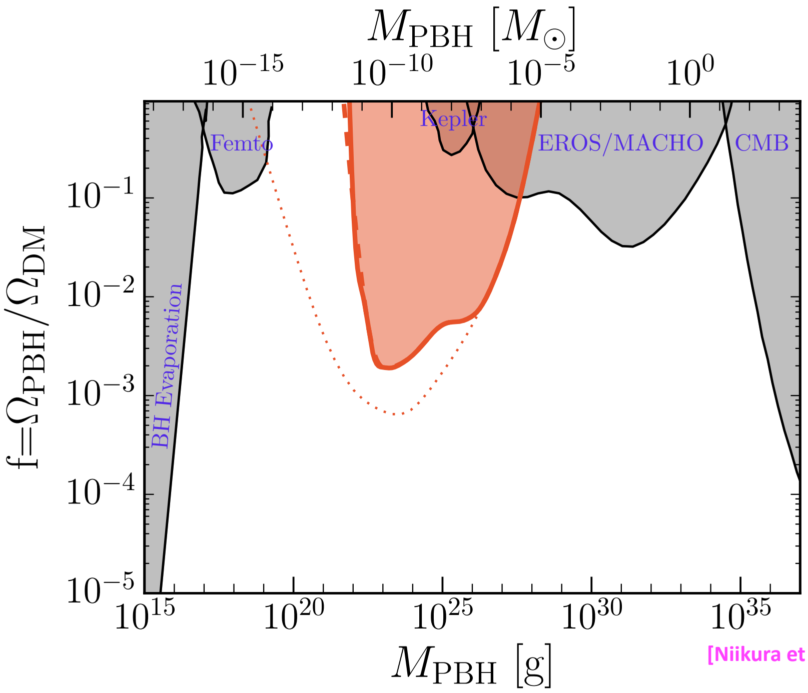

[Niikura et al. (2017)]

How about axion stars?

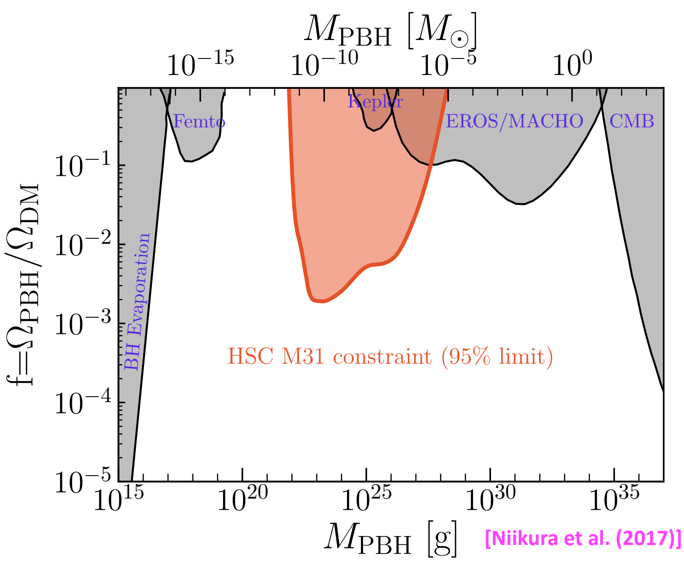

[Niikura et al. (2017)]

Microlensing constraints on axion stars?

$$M_{\rm PBH} \to M_{\rm clump}(m_a, F_a, \alpha)$$

$$\Omega_{\rm PBH}/\Omega_{\rm DM} \to \Omega_{\rm clump}/\Omega_{\rm DM}$$

We are not satisfied this argument since…

Axion Stars may not be “compact”

A detectable amplification occurs when compact object enters “microlensing tube”.

Radius of tube (point-like Einstein ring radius):

$R_E \sim \sqrt{GMD_L}$ ~(Schwarzschild radius of compact object × distance from source)$^{1/2}$

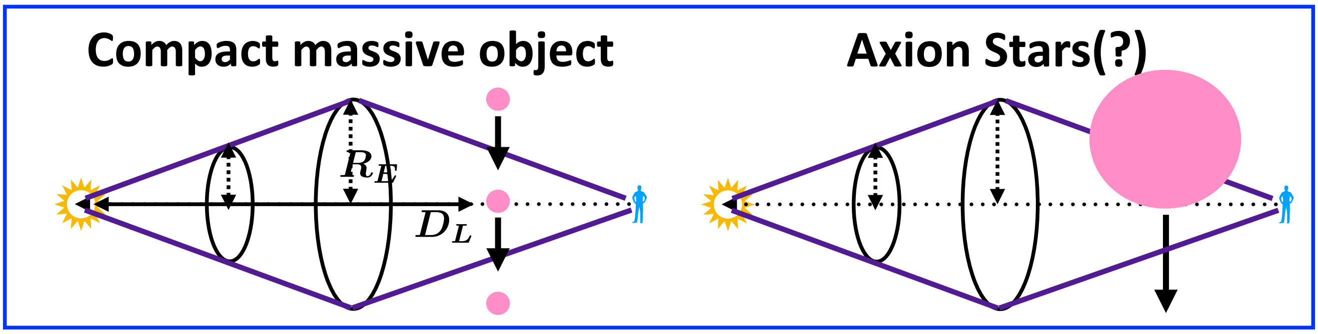

Our numerical detailed analysis shows that microlensing events do not occur for $R_E \lesssim R$!

Answer: How about axion stars?

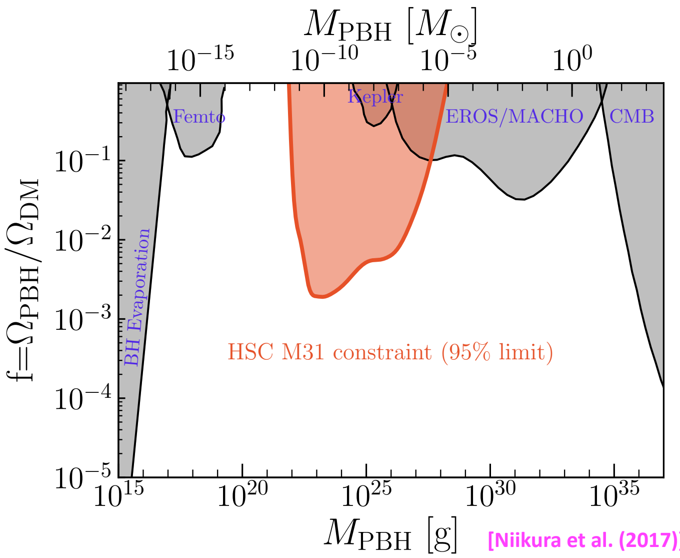

[Niikura et al. (2017)]

Microlensing constraints on axion stars:

$$M_{\rm PBH} \to M_{\rm clump}(m_a, F_a, \alpha)$$

$$\Omega_{\rm PBH}/\Omega_{\rm DM} \to \Omega_{\rm clump}/\Omega_{\rm DM}$$

$$R_E(M_{\rm clump}) \gtrsim R(m_a, F_a, \alpha)$$

Very roughly speaking, this is (one of the) main conclusions of our paper.

I would like to show you results obtained by detailed numerical calculations.

We focus on EROS-2 and Subaru HSC observations.

Free Parameters:

F_a : the breaking scale of axion
m_a : the axion mass

$m_a \sim \Lambda_{\rm QCD}^2/F_a$ for the QCD axion

α : the clump density

$\Omega_{\rm clump}/\Omega_{\rm DM}$: Fraction of dark matter collapsed into clumps

Result1

$(M_{\rm clump}(m_a),\ F_a,\ \Omega_{\rm clump}/\Omega_{\rm DM},\ \alpha)$ with fixed F_a, α.

Subaru HSC

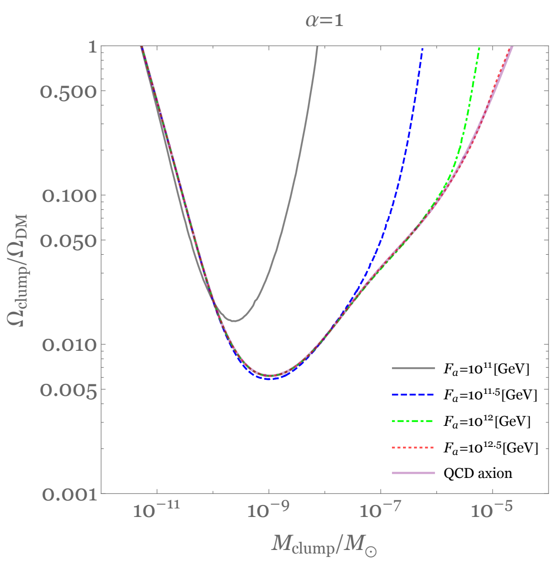

EROS-2

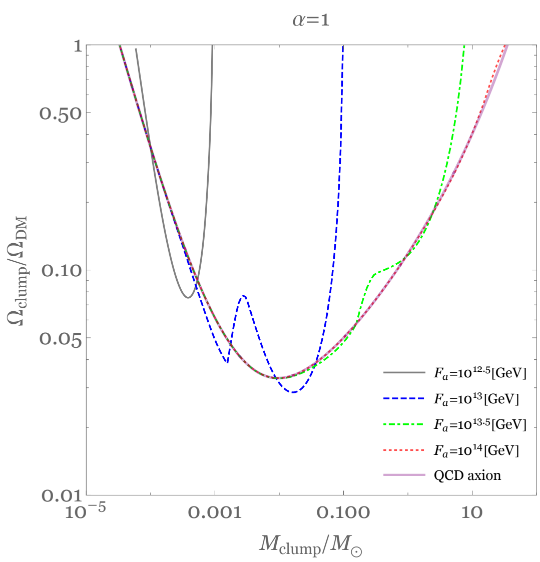

Result2 (1)

$(M_{\mathrm{clump}}(m_a),\ F_a,\ \Omega_{\mathrm{clump}}/\Omega_{\mathrm{DM}},\ \alpha)$ **with fixed $\Omega_{\mathrm{clump}}/\Omega_{\mathrm{DM}}, \alpha$.**

Subaru HSC

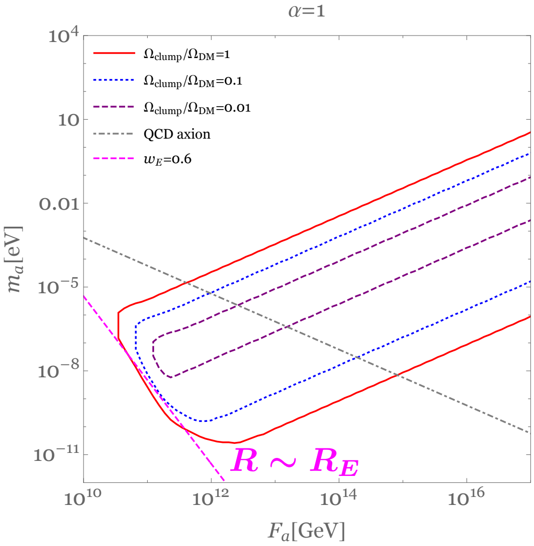

EROS-2

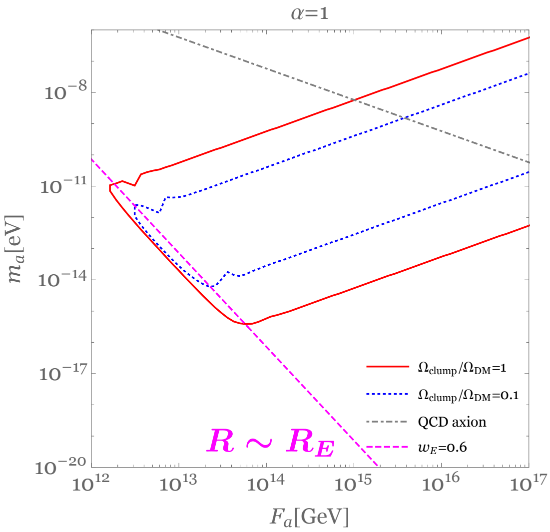

Result2 (2)

High breaking scale $F_a \gtrsim 10^{12}\,\mathrm{GeV}$ can be constrained!

Subaru HSC

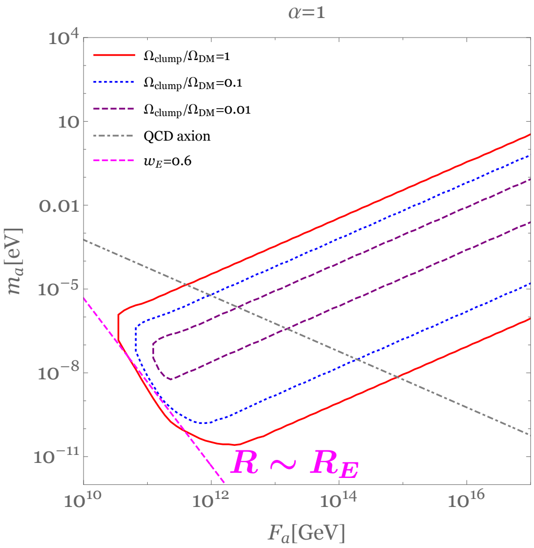

EROS-2

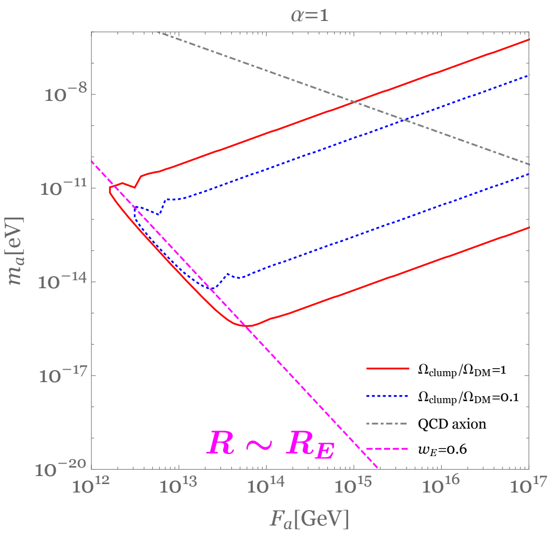

Conclusions

- **In the early Universe, axions may form localized clumps called axion stars.**
- **We give microlensing constraints on axion stars including an effect of the finite extent.**
- **A finite lens size effect can be neglected when a radius of the axion star is much shorter than the point-like Einstein ring radius.**

C36

Interaction between cosmic strings with point sources approximation

Siyao Li
Department of Physics, Tokyo Institute of Technology

Based on ongoing work in collaboration with Kohei Fujikura, Masahide Yamaguchi

JGRG31

2022.10.25

Contents

- Introduction
- Apply source method* to derive interaction energy of two strings for:
  - Bosonic Superconducting Cosmic Strings
  - Global cosmic string
  - Fermionic Superconducting Cosmic Strings

  *originated by J. M. Speight in Phys. Rev. D 55, 3830 (1997) for abelian-Higgs model
- Numerical results for two-string system
- Summary

Introduction

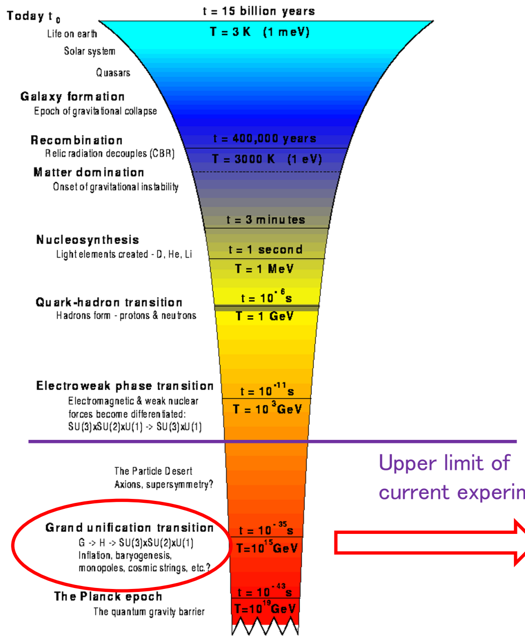

Upper limit of current experiment

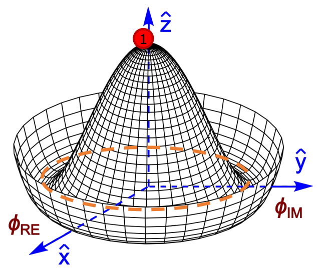

Spontaneous symmetry breaking during phase transition

Natural high energy experiment lab

Independent regions

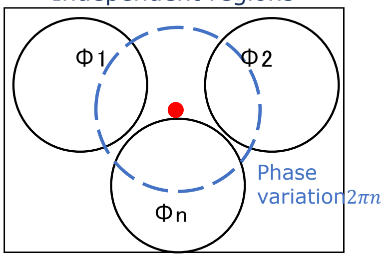

$\xi(t)$: Correlation length

Cosmic strings (topological defects)

Introduction

Purpose of this work: to investigate interaction between two cosmic strings

Cosmic strings network

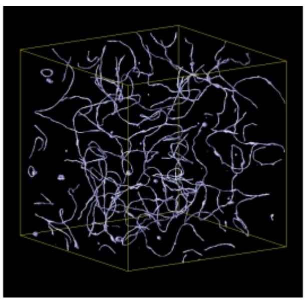

[Takashi.H et al. 2013]

interactions, dynamics… → reconnect, collapse··· → kinks, cusps, Y-junctions

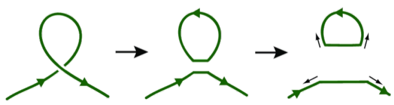

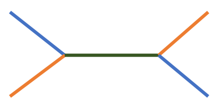

Y-junction

stochastic gravitational wave + gravitational wave burst

Local string models

Abelian-Higgs model

$$\mathcal{L}_{AH} = -\frac{1}{4}F^{\mu\nu}F_{\mu\nu} + |D_\mu\phi|^2 - V(\phi),$$

$$V(\phi) = \frac{1}{4}\lambda(|\phi|^2 - \eta^2)^2$$

$U(1)$ gauge symmetry

Bosonic superconducting model

$$\mathcal{L}_{BC} = -\frac{1}{4}F^{\mu\nu}F_{\mu\nu} + |D_\mu\phi|^2 - \frac{1}{4}\widetilde{F^{\mu\nu}}\widetilde{F_{\mu\nu}} + |\widetilde{D_\mu}\tilde{\phi}|^2 - V(\phi,\tilde{\phi}),$$

$$V(\phi,\tilde{\phi}) = \frac{1}{4}\lambda_\phi(|\phi|^2 - \eta_\phi{}^2)^2 + \frac{1}{4}\lambda_{\tilde{\phi}}\left(|\tilde{\phi}|^2 - \eta_{\tilde{\phi}}{}^2\right)^2 + \beta|\phi|^2|\tilde{\phi}|^2$$

[Witten, Nuclear Physics B, 1985]

static, straight, circular symmetric

Abrikosov–Nielsen–Olsen(ANO) string solution:

$$\phi = |\phi(r)|e^{in\theta},$$

$$A_\mu = A_\mu(r)\delta_\theta^\mu$$

in cylindrical coordinate system (r,θ,z)

[Nielsen, Olesen P. Nuclear Physics B, 1973]

$U(1)\times\tilde{U}(1)$ gauge symmetry

- $U(1)$ symmetry to be spontaneously broken ⇩ giving rise to ANO string
- $\tilde{U}(1)$ symmetry to be unbroken outside the string ⇩ making the string carry persistent current

Bosonic superconducting strings

Parameter space:

- $\tilde{U}(1)$ symmetry unbroken outside string

$$m_{\tilde{\phi}}^2(\infty) = \beta\eta_\phi^2 - \frac{1}{2}\lambda_{\tilde{\phi}}\eta_{\tilde{\phi}}^2 > 0$$

- $|\phi| = \eta_\phi$, $|\tilde{\phi}| = 0$ should be global minimum

$$\lambda_\phi\eta_\phi^4 > \lambda_{\tilde{\phi}}\eta_{\tilde{\phi}}^4$$

- To make $|\tilde{\phi}| \neq 0$ energy favorable rather than trivial solution $|\tilde{\phi}| = 0$

(existence of negative energy state)

$$\beta < \lambda_{\tilde{\phi}}\eta_{\tilde{\phi}}^2/\eta_\phi^2$$

static, straight, circular symmetric

Note the lowest energy solutions as $\tilde{\phi} = \tilde{\phi}_r(r), \widetilde{A_\mu} = 0$.

Then a general ansatz is

[Alford M, Benson K, Coleman S, et al. Nuclear Physics B, 1991]

$$\tilde{\phi} = \tilde{\phi}_r(r)e^{-is(r)\alpha(z)}, \widetilde{A_\mu} = -\frac{1}{g}\alpha(z)\partial_\mu s(r).$$

zero mode, modulation of gauge transformation

⇩ gauge transformation

$$\tilde{\phi} = \tilde{\phi}_r(r), \widetilde{A_\mu} = \frac{1}{g}s(r)\partial_\mu\alpha(z).$$

$$r\partial_r s\partial_z^2\alpha = 0$$

$$\frac{1}{r}\partial_r(r\partial_r)s(r) - 2g^2 s(r)\tilde{\phi}_r^2 = 0$$

⇨ $\alpha(z) = \omega z$

London equation with penetration depth $\delta_A(r) = 1/g\tilde{\phi}_r(r)$

$$J_z = \int d^2x[-2g\omega s(r)\tilde{\phi}_r^2]$$

Asymptotic solutions

Boundary conditions:

- Regularity at the origin

$$|\phi| = 0, A_\mu = 0, \partial_r|\widetilde{\phi}| \to 0, \partial_r\tilde{s}(r) \to 0, \quad \text{at } r = 0$$

- Finite energy

$$|\phi| \to \eta_\phi,\ D_\mu\phi \to 0, |\tilde{\phi}| \to 0\ , \quad \text{at } r \to \infty$$

Asymptotic solutions at large distance:

$$\sigma(r) = k_\phi K_0(m_\phi r)$$

$$\mathrm{U}_\theta(r) = k_e r K_1(m_e r)$$

$$\tilde{\phi}_r(r) = k_{\tilde{\phi}} K_0(m_{\tilde{\phi}} r)$$

$$s(r) = k_s \ln r$$

modified Bessel function $K_i(mx) \propto e^{-mx}$ at $x \to \infty$

$k_\phi \propto |n|$

$k_e \propto -n$

$k_{\tilde{\phi}} \propto |\omega|$

$k_s \propto \omega$

$m_\phi \equiv \sqrt{\lambda}\eta$

$m_e \equiv \sqrt{2}e\eta$

with parameterization

$$\phi(r) = \left(\eta_\phi + \frac{\sigma(r)}{\sqrt{2}}\right)e^{in\theta},\ A_\theta(r) = \mathrm{U}_\theta(r) + \frac{n}{e}$$

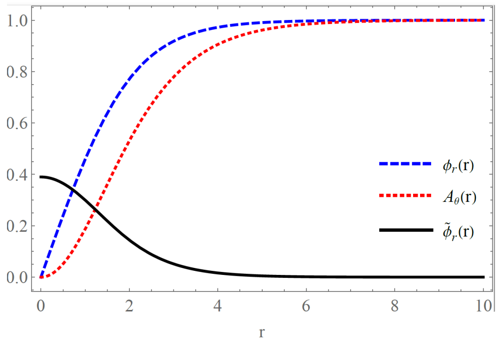

Field configurations

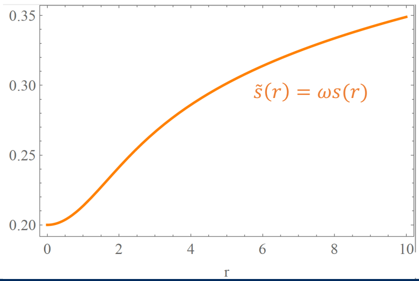

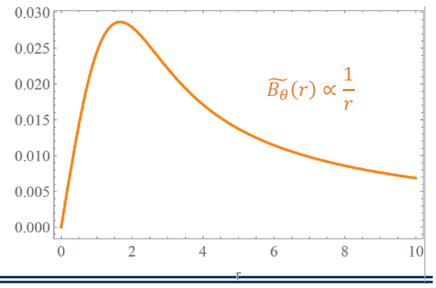

Interaction with source method

We look for the external sources representing the asymptotic fields by linearized field theory,

$$\mathcal{L} = \frac{1}{2}(\partial_\mu\sigma)^2 - \frac{1}{2}m_\phi^2\sigma^2 - \frac{1}{4}F^{\mu\nu}F_{\mu\nu} + \frac{1}{2}m_e^2 U_\mu U^\mu - J_\sigma\sigma - j_\mu U^\mu$$
$$+ \frac{1}{2}(\partial_\mu\tilde{\phi}_r)^2 - \frac{1}{2}m_{\tilde{\phi}}^2\tilde{\phi}_r^{\ 2} - \frac{1}{4}\widetilde{F^{\mu\nu}}\widetilde{F_{\mu\nu}} - J_{\tilde{\phi}}\tilde{\phi}_r - \widetilde{j_\mu}\widetilde{\mathrm{A}^\mu}$$

$$J_\sigma = -2\pi k_\phi \delta^{(2)}(\boldsymbol{x})$$

$$j_\theta = -2\pi\frac{k_e}{m_e}\partial_r\delta^{(2)}(\boldsymbol{x})$$

$$J_{\tilde{\phi}} = -2\pi k_{\tilde{\phi}}\delta^{(2)}(\boldsymbol{x})$$

$$\widetilde{j_\mu} = -2\pi\frac{k_s}{g}\delta^{(2)}(\boldsymbol{x})$$

point-like sources in 2-dimensions

$k_\phi \propto |n|$

$k_e \propto -n$

$k_{\tilde{\phi}} \propto |\omega|$

$k_s \propto \omega$

parallel, well-separated strings

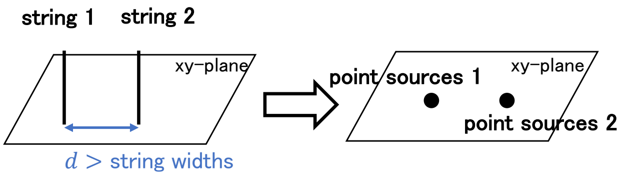

We assume superposition of two sources

$$J_{total}(\boldsymbol{x}) = J_1(\boldsymbol{x} - \boldsymbol{x}_1) + J_2(\boldsymbol{x} - \boldsymbol{x}_2)$$

determined by winding direction of vortex

$$E_{int} = 2\pi\int dz \left[\boxed{\begin{matrix} -k_{\phi 1}k_{\phi 2}K_0(m_\phi d) \\ -k_{\tilde{\phi}1}k_{\tilde{\phi}2}K_0(m_{\tilde{\phi}} d) \end{matrix}} \begin{matrix} + \boxed{k_{A1}k_{A2}K_0(m_e d)} \\ + \boxed{k_{\tilde{A}1}k_{\tilde{A}2}\ln d} \end{matrix} \right]$$

always attractive contribution

determined by direction of flowing current

Numerical calculation

- The solutions we are looking for are the static, lowest energy states of the system.
- Method: Gradient Flow
  - initial guess satisfying boundary conditions
  - evolve the fields with time

    field $X_i(r,\theta) \rightarrow X_i(t,r,\theta)$

    $EOM\ of\ X_i = 0\ \rightarrow EOM\ of\ X_i = \partial_t X_i$

  - converge symbol: $\partial_t X_i = 0$
  - fix the string centers by hand (two-string system)

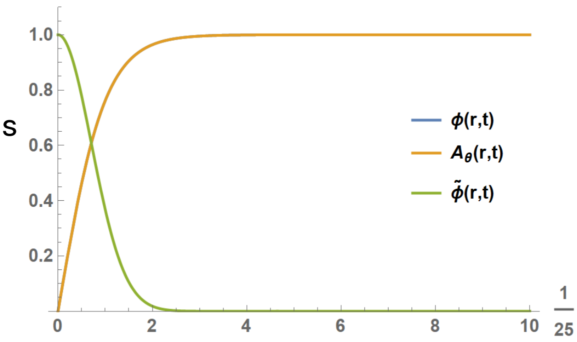

Numerical result for two-string system

Field configurations of a two bosonic superconducting string system without current ($\tilde{A}_\mu = 0$) , with $n = 1$.

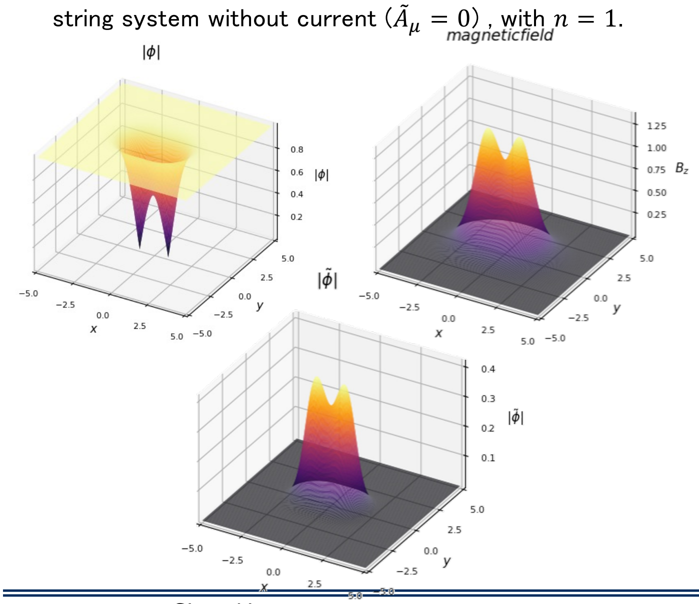

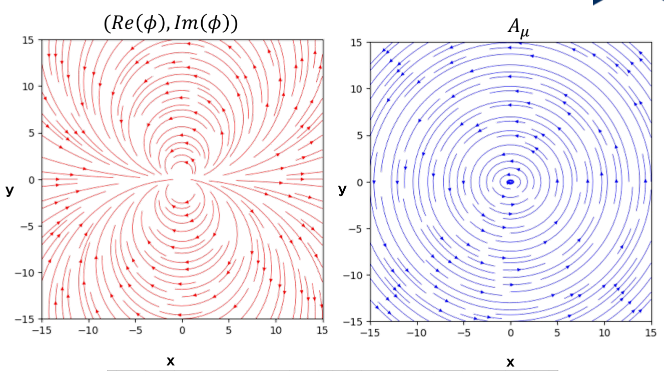

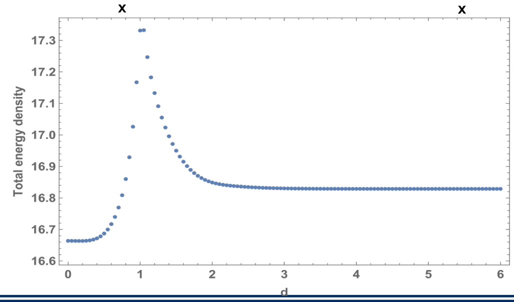

Global string

$$\mathcal{L} = |\partial_\mu \phi|^2 - V(\phi),$$
$$V(\phi) = \frac{1}{4}\lambda(|\phi|^2 - \eta^2)^2$$

global $U(1)$ symmetry

$$\phi(r) = \left(\eta + \frac{\sigma(r)}{\sqrt{2}}\right) e^{i\pi(\theta)}, \qquad \pi(\theta) = n\theta$$

massless Nambu−Goldston boson

$$\sigma(r) = -\frac{\sqrt{2}n^2\eta}{m^2 r^2} \qquad \mathrm{m} \equiv \sqrt{\lambda}\eta$$

$$J_\sigma = \frac{\sqrt{2}n^2\eta}{r^2}$$
$$J_\pi = 2\pi n\eta\delta^{(2)}(\boldsymbol{x})$$

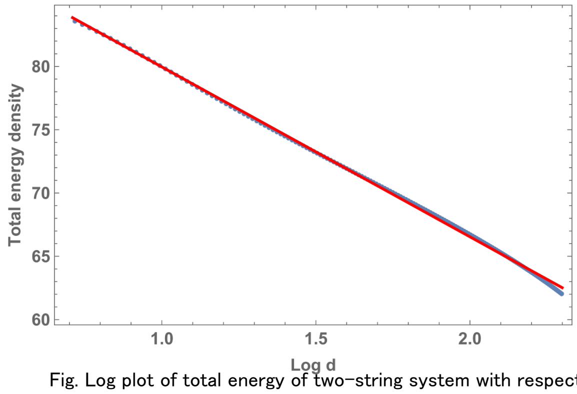

Fig. Log plot of total energy of two−string system with respective to separation d. Blue line is the numerical results , while red line is source method result.

$$E_\pi = 2\pi\eta^2 \int dz\ [-n_1 n_2 \ln(\epsilon d)\ ]$$

cutoff at $\delta = \frac{1}{m}$

$$E_{int} = 2\pi\eta^2 \int dz\ [\underline{-n_1 n_2 \ln(md)} - \frac{1}{\lambda} n_1^2 n_2^2 \frac{1}{d^2} \ln(m^2 d^2)]$$

suppressed at large distance

Fermionic superconducting strings

$$\mathcal{L} = |\partial_\mu \phi|^2 + i\bar{\psi}_L \gamma^\mu \partial_\mu \psi_R + i\bar{\psi}_R \gamma^\mu \partial_\mu \psi_L$$
$$-g\phi\bar{\psi}_L\psi_R - g\phi^*\bar{\psi}_L\psi_R - V(\phi),$$
$$V(\phi) = \frac{1}{4}\lambda(|\phi|^2 - \eta^2)^2$$

The fermion is defined as

$$\gamma^5 \psi_{L,R} = \pm\psi_{L,R}$$

A zero−mode solution is found as

$$\psi_L(r) = \tau \exp(-g \int_0^r |\phi|(r') dr')$$
$$\psi_R = -i\gamma^1 \psi_L$$

the solutions are eigenstates of two−dimensional chirality operator

$$\Gamma^5 \equiv i\gamma^1\gamma^2$$
$$\Gamma^5 \psi_{L,R} = \pm\psi_{L,R}$$

[Callan & Harvey, Nuclear Physics B, 1985]

$$\bar{\psi}_L \psi_R = -\psi_L^\dagger \gamma^0 \Gamma^5 \psi_R = -\bar{\psi}_L \psi_R = 0$$
$$[\Gamma^5, \gamma^0] = 0$$

Solution to ϕ remains the same as global string

at large distance

$$\psi_L(r) = \tau \exp(-g\eta r)$$
$$\psi_R = -i\gamma^1 \psi_L$$

source current $J_F = 0$
no contribution to interaction

Summary

- We investigated interaction between two straight, static, cylindrical symmetric cosmic strings .
- Method

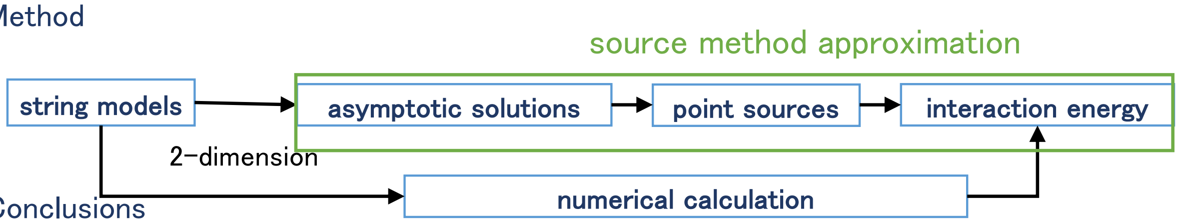

- Conclusions
  - Bosonic superconducting string: asymptotic configurations can be represented by **scalar monopoles** at string center and **a static current flowing along string**. Long-distance force is dominated by the **logarithmic contributions** from massless gauge field.
  - Global string: dominant by **logarithmic contributions** from NG-boson
  - Fermionic superconducting: fermionic zero mode has no contribution, interaction same as global string
- Future work
  - Numerical calculation of bosonic superconducting strings with currents
  - Cosmic string dynamics; Formation and distribution of substructures; Prospective observations…

Thank you very much for attention.

SSB and Topological defects

Goldstone model for real scalar field

$$\mathcal{L} = \frac{1}{2}(\partial_\mu \phi)^2 - V(\phi)$$

$$V(\phi) = \frac{1}{4}\lambda(\phi^2 - \eta^2)^2$$

invariant for $\phi \to -\phi$

Topological solution:

$$\phi(x) = \pm\eta \tanh\left(\sqrt{\frac{\lambda}{2}}\eta x\right)$$

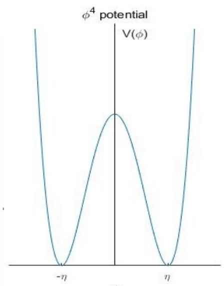

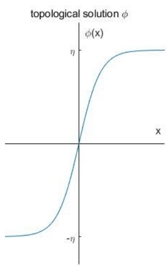

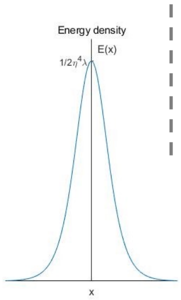

Complex scalar field

$$\mathcal{L} = (\partial^\mu \phi^*)(\partial_\mu \phi) - V(\phi), \;\; V(\phi) = \frac{1}{4}\lambda(\phi^2 - \eta^2)^2$$

global U(1) symmetry $\qquad \phi \to \phi' = \phi e^{i\theta}$

Topological solution:

$$\phi \approx \eta e^{in\theta} \quad at\; r \to \infty$$

ϕ = 0 at center ⇨ high energy ⇨ cosmic strings

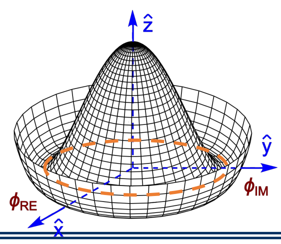

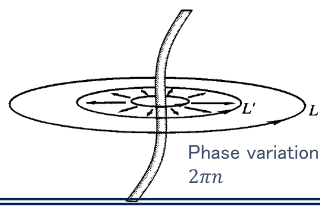

Abelian-Higgs Cosmic Strings

Continuous symmetry: abelian–Higgs model

$$\mathcal{L} = -\frac{1}{4}F^{\mu\nu}F_{\mu\nu} + (D^{\mu}\phi)^{*}D_{\mu}\phi - V(\phi), \qquad V(\phi) = \frac{1}{4}\lambda(\phi^{*}\phi - \eta^{2})^{2}$$

$F_{\mu\nu} = \partial_{\mu}A_{\nu} - \partial_{\nu}A_{\mu}$, $D_{\mu} \equiv \partial_{\mu} - ieA_{\mu}$. Local U(1) symmetry.

Cylinder symmetric static solutions are found to be Nielson–Olesen vortices

$$\phi(\boldsymbol{r}) = \phi_{r}(r)e^{in\theta}, \boldsymbol{A}(\boldsymbol{r}) = \frac{\boldsymbol{r}\times\boldsymbol{e}_{z}}{r}|\boldsymbol{A}(\boldsymbol{r})|$$

Finite energy conditions:

$$V(\phi) \to 0,\ D_{\mu}\phi \to 0\ \ at\ r \to \infty$$

Boundary conditions:

$$\boxed{\begin{array}{c}\phi_{r} \to \eta,\ \alpha(r) \to 1,\ r \to \infty \\ \phi_{r}(0) = \alpha(0) = 0,\ r = 0\end{array}} \qquad A_{\theta}(r) = \frac{n}{er}\alpha(r)$$

EOM:

$$\frac{\partial^{2}}{\partial r^{2}}\phi_{r}(r) + \frac{1}{r}\frac{\partial}{\partial r}\phi_{r}(r) - \frac{n^{2}}{r^{2}}(\alpha - 1)^{2}\phi_{r} - \frac{1}{2}\lambda\phi_{r}(\phi_{r}^{2} - \eta^{2}) = 0,$$

$$\frac{\partial^{2}}{\partial r^{2}}\alpha - \frac{1}{r}\frac{\partial}{\partial r}\alpha - 2e^{2}\phi_{r}^{2}(\alpha - 1) = 0$$

Mass of scalar and gauge fields

$$m_{S} \equiv \sqrt{\lambda}\eta$$

$$m_{A} \equiv \sqrt{2}e\eta$$

(m_{A} comes from absorption of Goldstone boson by Higgs mechanism)

Width of string core

$$\delta_{S} \approx m_{S}^{-1}$$

$$\delta_{A} \approx m_{A}^{-1}$$

Analogous to superconductor

$$\beta \equiv \lambda/2e^{2} = (\delta_{A}/\delta_{S})^{2}$$

$\beta < 1$, Type–I cosmic string

$\beta > 1$, Type–II cosmic string

Abelian-Higgs Cosmic Strings

$$\frac{\partial^{2}}{\partial r^{2}}\phi_{r}(r) + \frac{1}{r}\frac{\partial}{\partial r}\phi_{r}(r) - \frac{n^{2}}{r^{2}}(\alpha - 1)^{2}\phi_{r} - \frac{1}{2}\lambda\phi_{r}(\phi_{r}^{2} - \eta^{2}) = 0,$$

$$\frac{\partial^{2}}{\partial r^{2}}\alpha - \frac{1}{r}\frac{\partial}{\partial r}\alpha - 2e^{2}\phi_{r}^{2}(\alpha - 1) = 0$$

$$\phi_{r} \to \eta,\ \alpha(r) \to 1,\ r \to \infty$$
$$\phi_{r}(0) = \alpha(0) = 0,\ r = 0$$

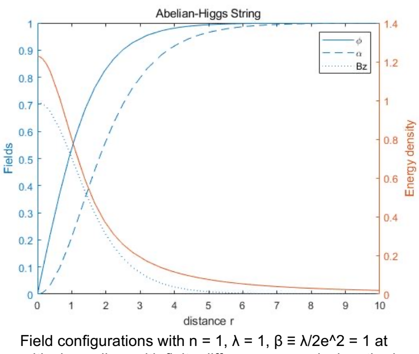

Field configurations with n = 1, λ = 1, β ≡ λ/2e^2 = 1 at critical coupling, with finite difference numerical method

Asymptotic behavior at r ⟶∞

$$\alpha(r) \approx 1 - k_{A}rK_{1}(m_{A}r) \sim 1 - \mathcal{O}(\sqrt{r}e^{-m_{A}r})$$

$$\phi_{r}(r) \approx 1 - k_{\phi}K_{0}(m_{S}r) \sim 1 - \mathcal{O}(e^{-m_{S}r}/\sqrt{r})$$

K_{n}: second kind of modified Bessel functions

Asymptotic behavior at r ⟶0

$$\phi_{r}(r) \approx a_{1}r + \mathcal{O}(r^{3})$$

$$\alpha(r) \approx b_{2}r^{2} + \mathcal{O}(r^{4})$$

In a special case, critical coupling, $\beta = 1$, it is found

$$k_{\phi} = \sqrt{2}|n|\eta,\ \ k_{A} = \sqrt{2}n\eta$$

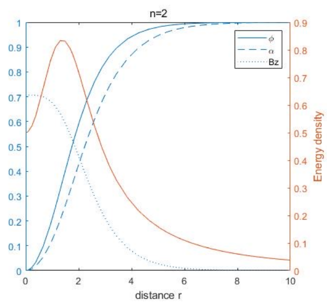

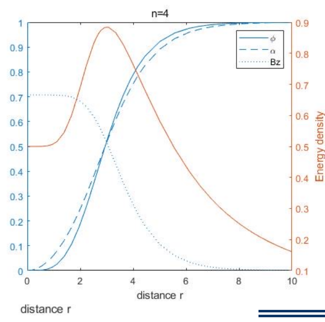

Fitting with the asymptotic solution

C37

Regge-Wheeler equation

Regge, Wheeler (1957)

$$\Psi = \sum_{\ell,m} \frac{\psi_\ell(t,r)}{r} Y_{\ell m}(\theta,\varphi)$$

$$\left(-\frac{\partial^2}{\partial t^2} + \frac{\partial^2}{\partial r_*^2} - V_{\rm RW}(r)\right)\psi_\ell(t,r) = 0$$

$$V_{\rm RW}(r) = \left(1 - \frac{2M}{r}\right)\left(\frac{\ell(\ell+1)}{r^2} - \frac{6M}{r^3}\right)$$

$r_* \to -\infty$
(Event horizon)

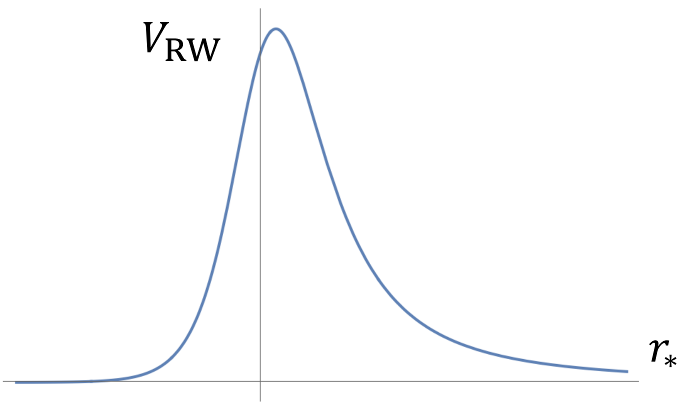

$r_* \to \infty$
$(r \to \infty)$

Ringdown

Vishveshwara (1970)

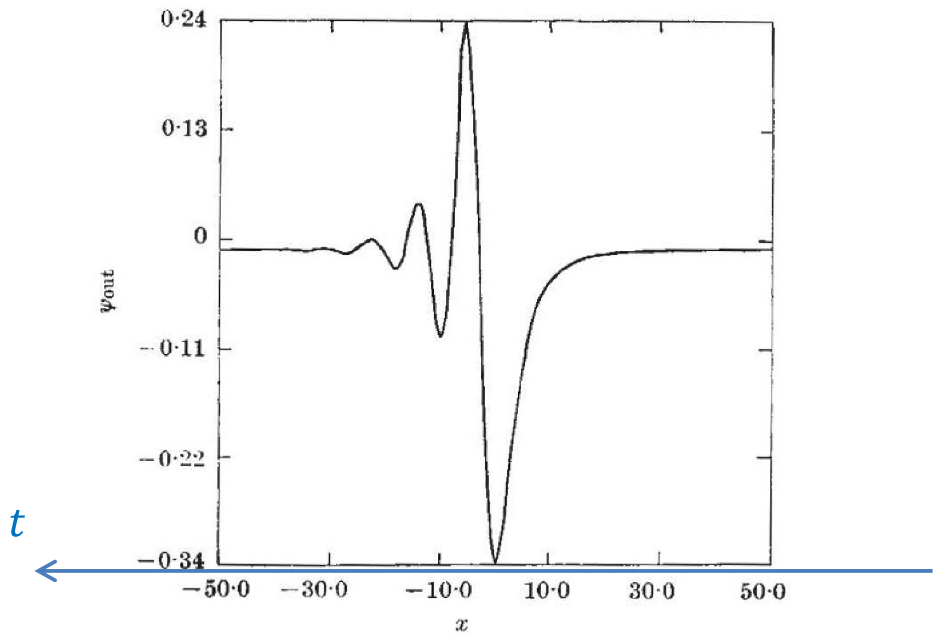

Fig. 3. The outgoing wave packet $\psi_{out}(x)$ at spatial infinity corresponding to the incident Gaussian wave packet $\psi_{in}(x) = e^{-ax^2}$ with $a = 1$.

$$\psi \sim e^{-\Gamma t/2} \sin \omega_R t$$

Ringdown

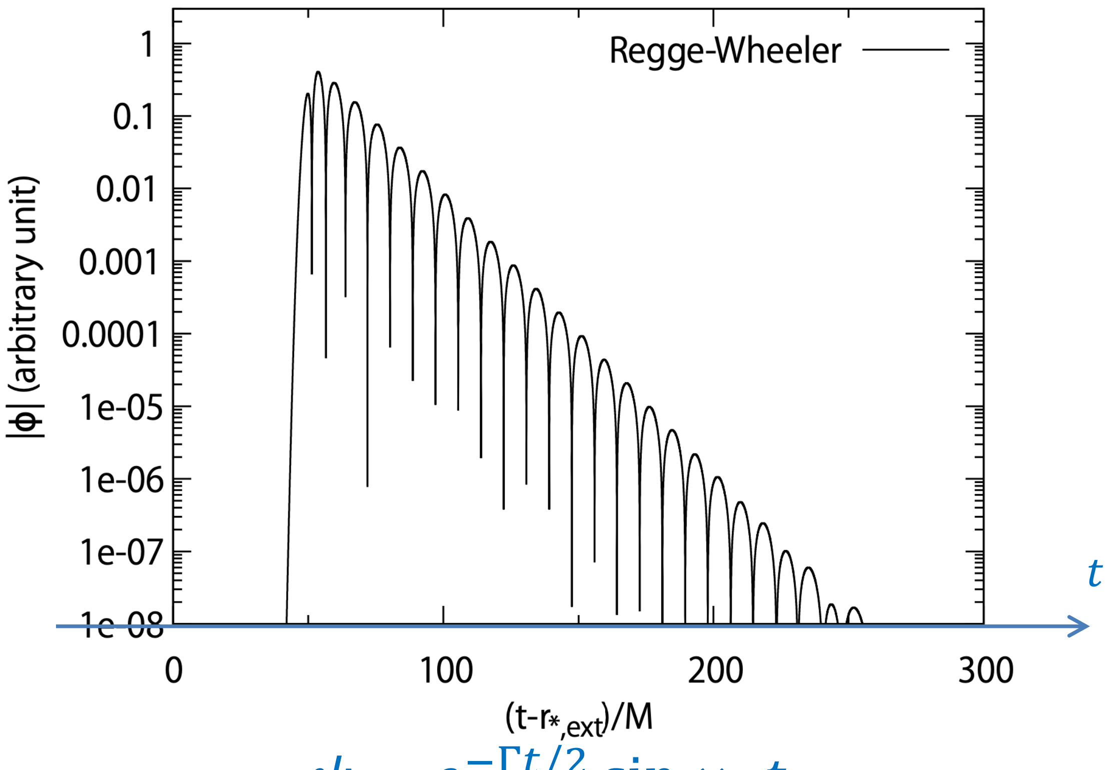

$$\psi \sim e^{-\Gamma t/2} \sin \omega_R t$$

Ringdown

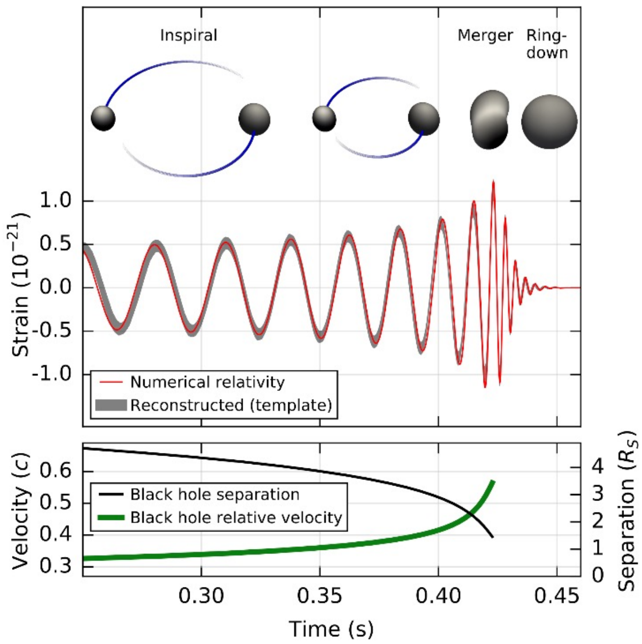

LIGO Collaboration

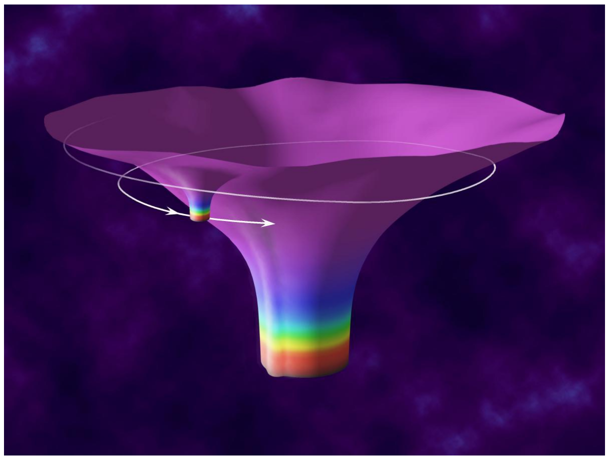

Credit: NASA

Quasinormal modes (QNMs)

$$\left(\frac{\partial^2}{\partial r_*^2} + \omega^2 - V_{\mathrm{RW}}(r)\right)\psi(\omega, r) = 0$$

Review papers:
Kokkotas, Schmidt, gr-qc/9909058
Berti, Cardoso, Starinets, 0905.2975
Konoplya, Zhidenko, 1102.4014

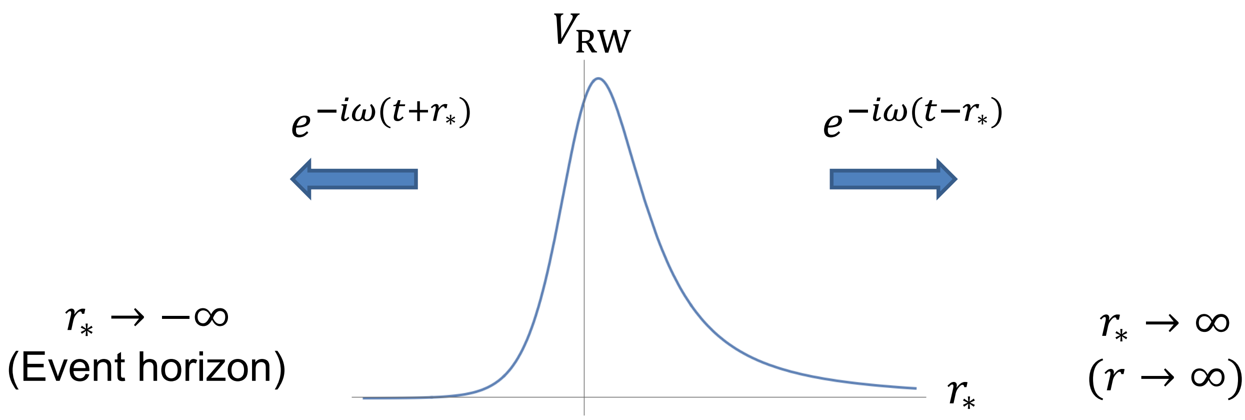

QNMs: $\omega_n = \omega_{nR} - i\Gamma_n/2$
Discrete complex eigenvalues satisfying the boundary condition.
Poles of the Green's function.

Schwarzschild QNMs

Leaver (1985)

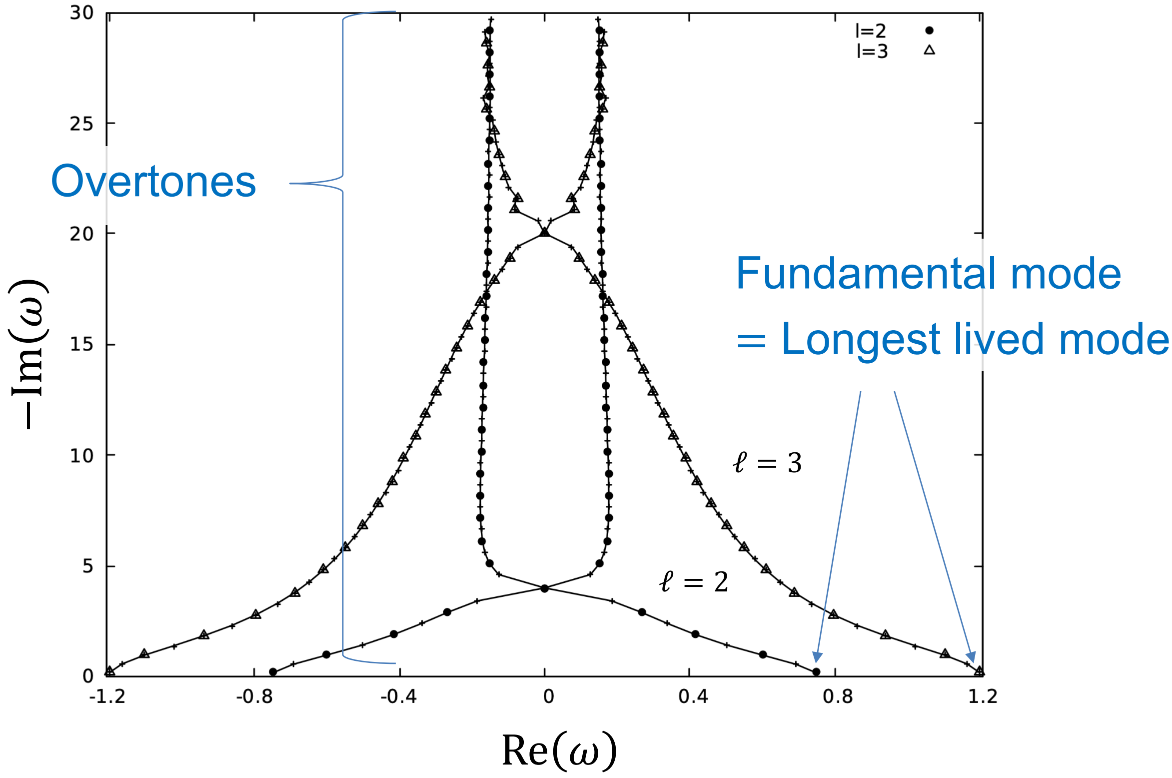

Potential

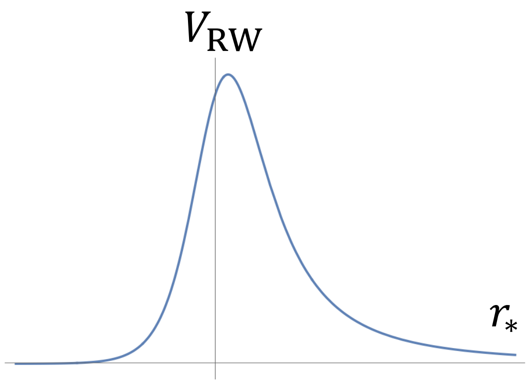

QNM spectrum

Ringdown signal

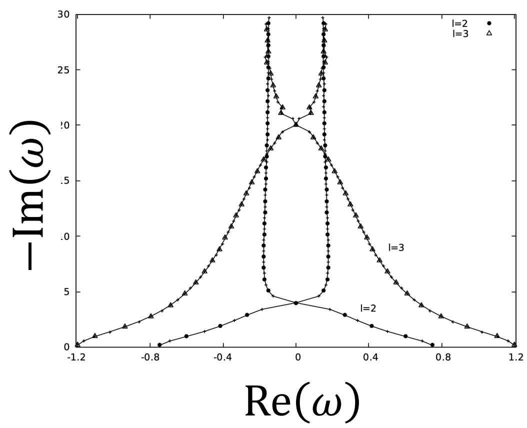

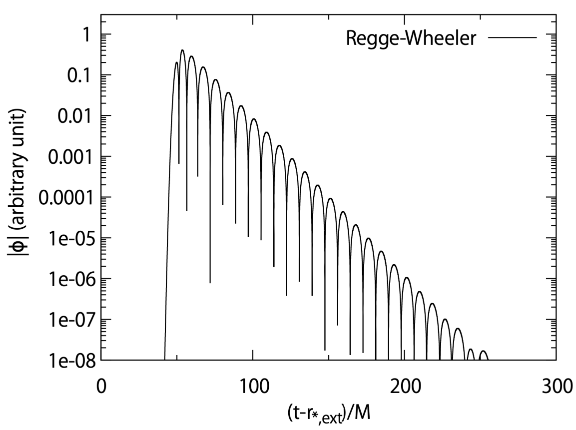

Potential ← “Small” change

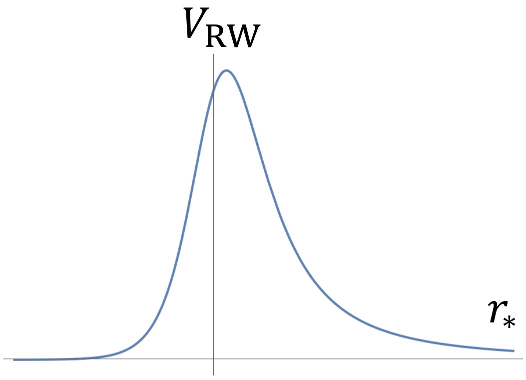

QNM spectrum

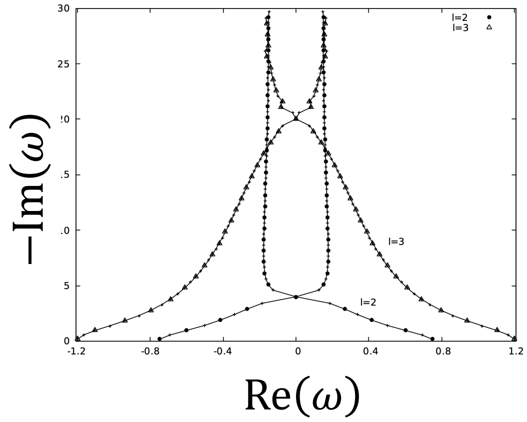

Ringdown signal

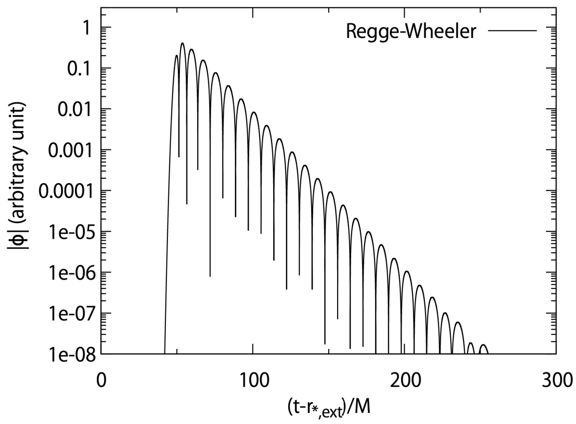

Potential ← “Small” change

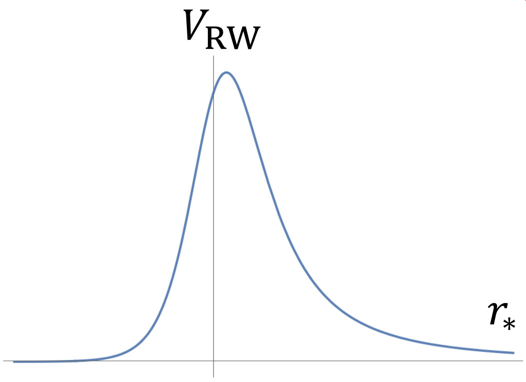

QNM spectrum

→ Large change

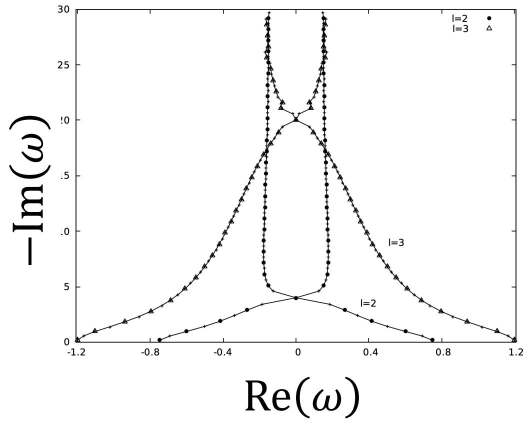

Ringdown signal

→ Change at late time only

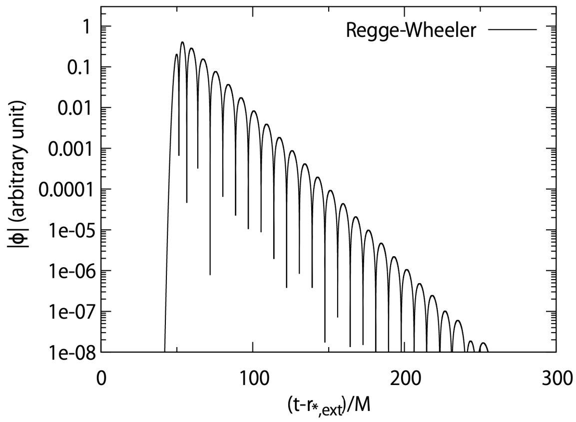

“Elephant & flea”

Cheung, Destounis, Macedo, Berti, Cardoso, PRL 128, 111103 (2022), [arXiv:2111.05415]

Potential ← “Small” change

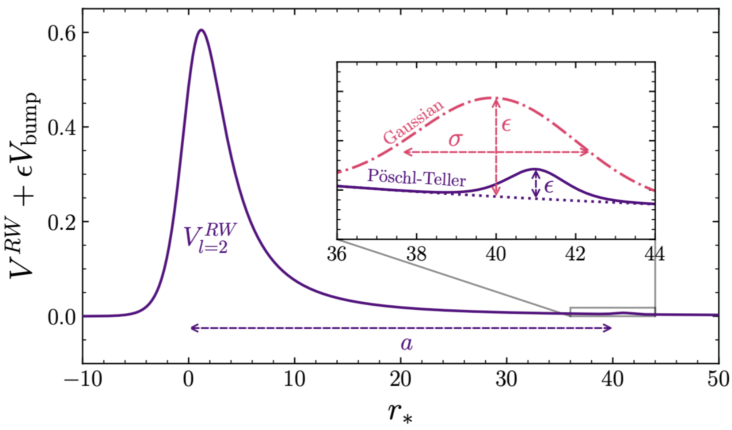

QNM spectrum
→ Large change

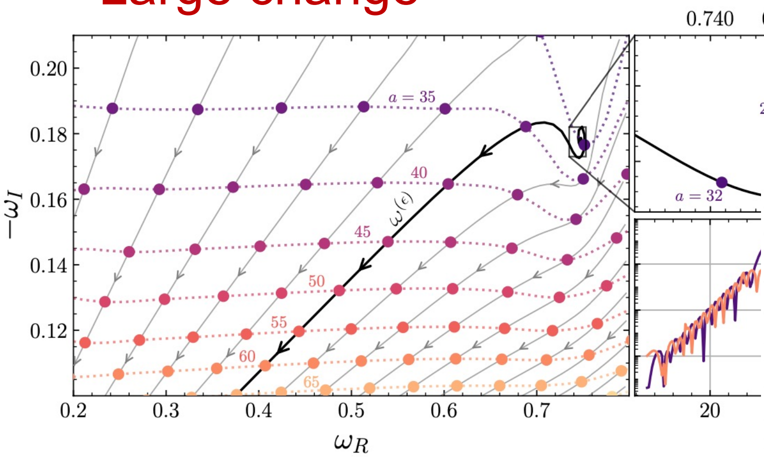

extremal Kerr BHs [58]? What are the implications of our results for modeling the ringdown of BHs surrounded by matter or other forms of “hair”? Is this instability a threat to the BH spectroscopy program in GW astronomy [40], and can it circumvent the failure of determinism in GR [52, 59]? More fundamentally, do infrared and/or ultraviolet corrections to general relativity affect at a fundamental level the meaning of the QNM spectrum and BH stability? These are important questions that must be addressed through numerical simulations and further theoretical work (see Ref. [60] for first steps in this direction).

QNM spectral instability

However, the instability of exact QNM spectrum does ***not*** destabilize observable ringdown signals.

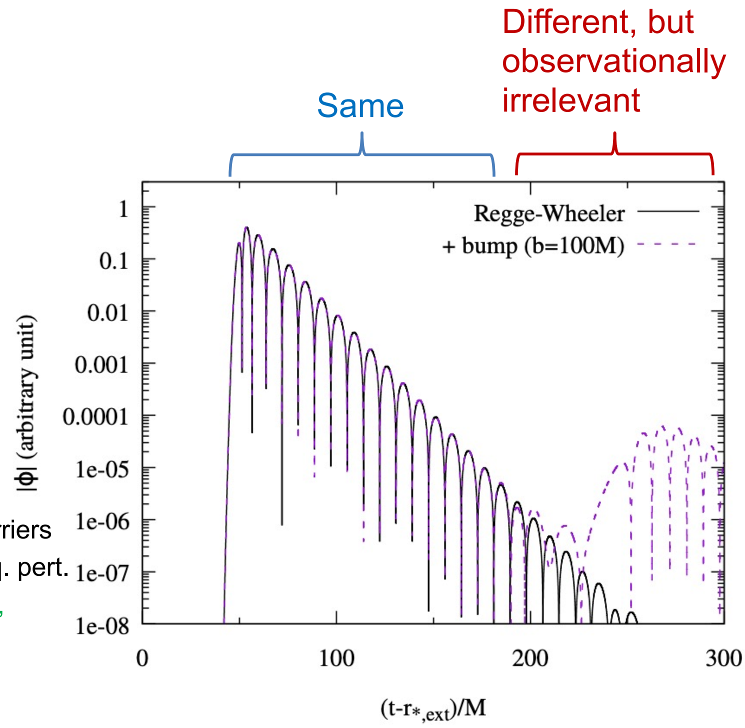

Nollert, gr-qc/9602032 Step potential
Nollert, Price, gr-qc/9810074 δ function
Barausse et al, 1404.7149 Double rectangular barriers
Jaramillo et al, 2004.06434, 2105.03451 High freq. pert.
Cheung et al, 2111.05415, Berti et al, 2205.08547,
Kyutoku, HM, Tanaka, 2206.00671 Tiny bump

But why?

Green's function

$$G(r,r') \sim \int_{-\infty}^{\infty} \frac{d\omega}{2\pi} e^{-i\omega t} \frac{\psi_{\rm in}(r)\psi_{\rm up}(r')}{W(\omega)}$$

$\boxed{\text{Integral along the real axis}}$

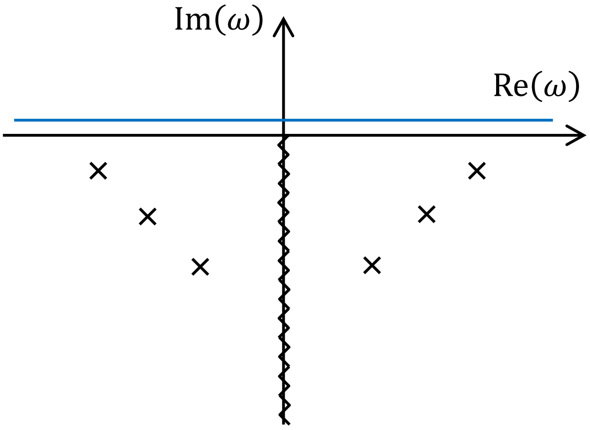

Sum of infinite residues

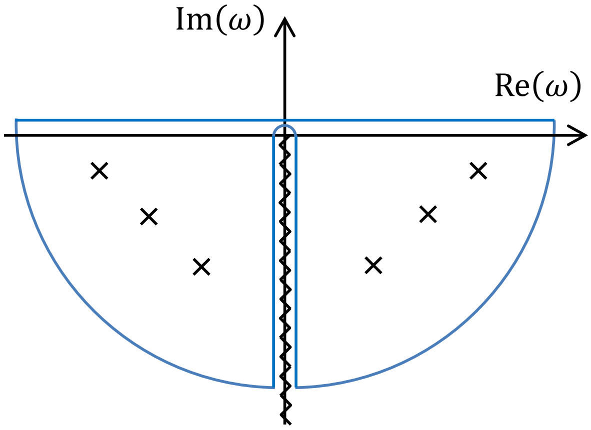

Green's function

$$G(r,r') \sim \int_{-\infty}^{\infty} \frac{d\omega}{2\pi} e^{-i\omega t} \frac{\psi_{\rm in}(r)\psi_{\rm up}(r')}{W(\omega)}$$

$W(\omega) = 2i\omega A_{\rm in}$ on the real axis is almost unchanged.

$$\psi_{\rm in} = \begin{cases} e^{-i\omega r_*} & (r_* \to -\infty) \\ A_{\rm in} e^{-i\omega r_*} + A_{\rm out} e^{-i\omega r_*} & (r_* \to \infty) \end{cases}$$

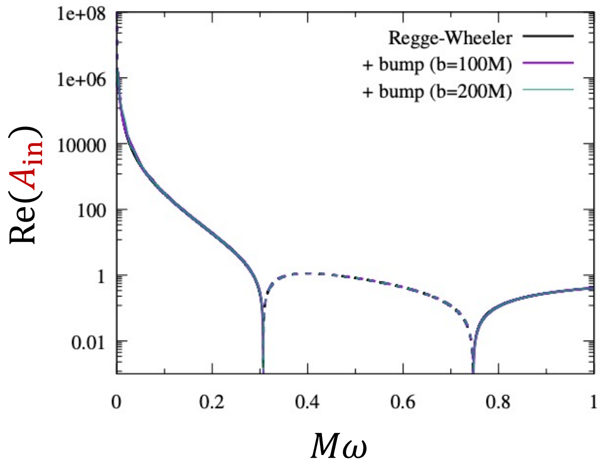

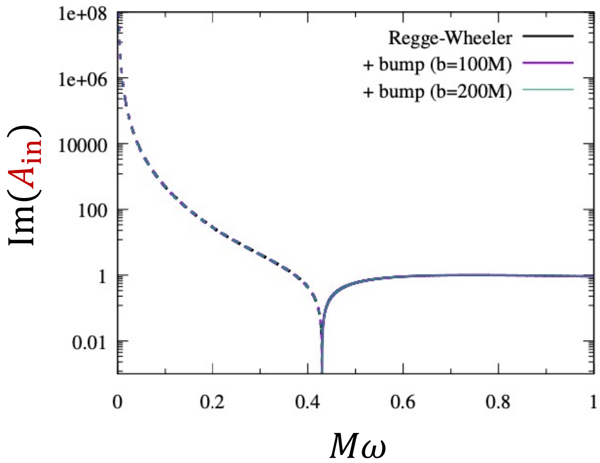

Kyutoku, HM, Tanaka, 2206.00671

Quantum resonance

$$\left[-\frac{\hbar^2}{2m}\left(\frac{d^2}{dr^2}-\frac{\ell(\ell+1)}{r^2}\right)+V(r)\right]\phi_\ell = E\phi_\ell$$

$$\phi_\ell \to \frac{i}{2}[f_\ell(p)e^{-i(pr-\ell\pi/2)} - f_\ell(p)^* e^{i(pr-\ell\pi/2)}]$$

$f_\ell(p)$: Jost function

$S_\ell = f_\ell(p)^*/f_\ell(p)$: S matrix

$e^{-i\delta_\ell} = f_\ell(p)/|f_\ell(p)|$: phase shift

Breit-Wigner peak around

$E = E_R - i\Gamma/2$

$$\frac{d\delta_\ell}{dE} \approx \frac{\Gamma/2}{(E-E_\mathrm{R})+(\Gamma/2)^2}$$

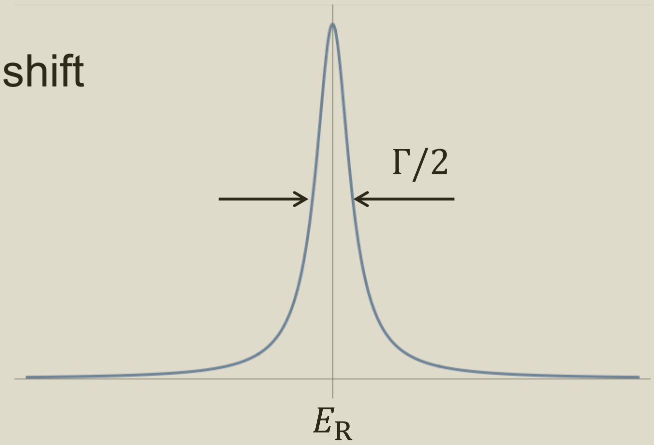

Phase shift for QNM

Analogously, let us introduce a phase shift by

$$e^{-i\delta} = A_\mathrm{in}/|A_\mathrm{in}|$$

We then expect that around QNM $\omega = \omega_R - i\Gamma/2$

$$\frac{d\delta}{d\omega} \approx \frac{\Gamma/2}{(E-\omega_\mathrm{R})+(\Gamma/2)^2}$$

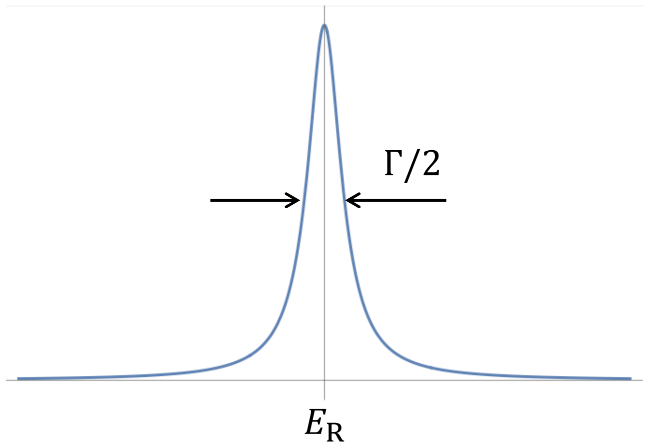

Phase shift for QNM

$d\delta/d\omega$ captures the unperturbed fundamental mode.

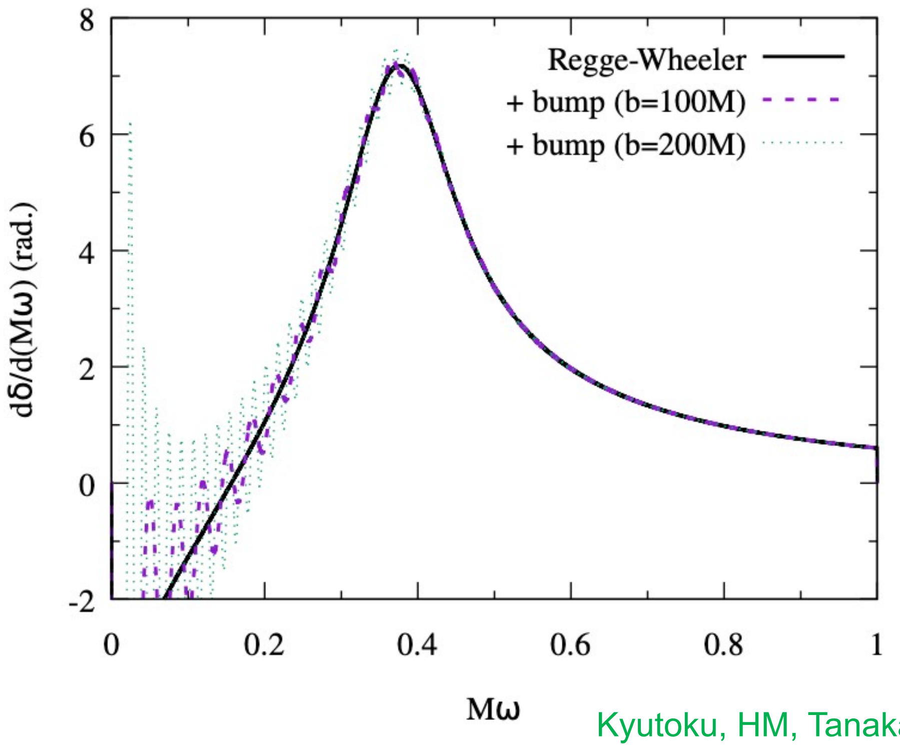

Kyutoku, HM, Tanaka, 2206.00671

Summary

- While perturbations to the potential causes the QNM spectral instability, the observable ringdown signal is stably characterized by unperturbed QNMs, except for very late-time echo signals.
- One way to understand the difference between the frequency- and time-domain analyses is to focus on the real axis values of the Wronskian, which we confirmed is almost unaltered in the presence of the perturbations.
- Using analogy from quantum resonance, we introduced a phase shift analysis to extract the QNM characterizing observable ringdown signals in an approximate but stable manner.

C38

Stability of the Fundamental Quasinormal Mode in Time-Domain Observations

Paul Martens

Center for Gravitational Physics and Quantum Information (CGPQI),
Yukawa Institute for Theoretical Physics (YITP), Kyoto University

JGRG 31

October, the 25th, 2022 — Phys. Rev. D 106, 084011 — arXiv:2205.08547

in collaboration with Emmanuele Berti, Vitor Cardoso, Mark Ho-Yeuk Cheung, Francesco Di Filippo, Francisco Duque & Shinji Mukohyama

Context, motivation and goal

Quasinormal modes (QNMs)

The late-time gravitational wave signal produced by binary mergers. These ringdown waves are described by damped exponentials with complex frequencies.

- QNMs can be used to test predictions of GR, provided they remain spectrally stable
- Some studies —*e.g.* arXiv:2111.05415— have asserted that they are unstable under small perturbations, but... these were looking at the frequency domain

Goal of this study

Consider the time-domain as the signal-to-noise ratio may hide the above differences beyond current observational capabilities

Initial conditions

Wave equation

$$\frac{\partial^2\Psi}{\partial r_\star^2} - \frac{\partial^2\Psi}{\partial t^2} - VZ = 0$$

Initial wavepacket

$$\Psi(t=0,r) = 0$$

$$\frac{\partial\Psi}{\partial t}(t=0,r) = \exp\left(-\frac{(r_\star - 5)^2}{2}\right)$$

Setup

Choice of potential

$$V = V_{\text{RW}} + \epsilon V_{\text{bump}}$$

where

$$V_{\text{RW}} = 3\left(1 - \frac{1}{r}\right)\left(\frac{2}{r^2} - \frac{1}{r^3}\right) \qquad V_{\text{bump}} = \exp\left(-\frac{(r_\star - a)^2}{2\sigma^2}\right)$$

Potential profile

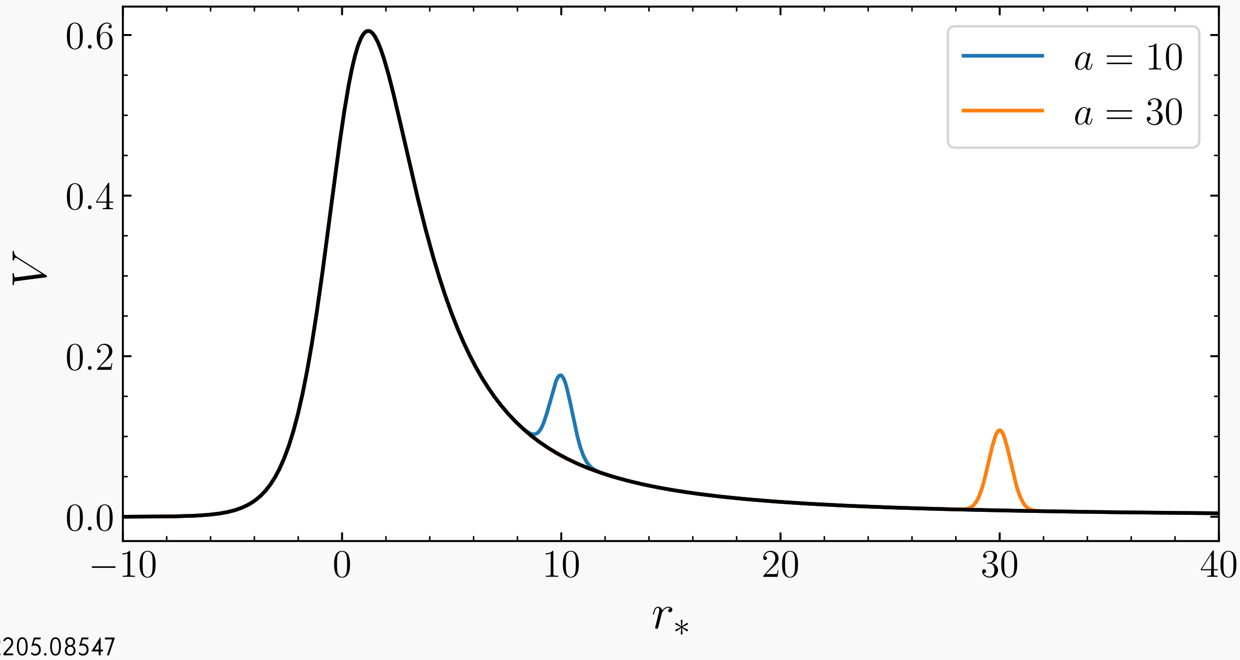

arXiv:2205.08547

Part I
The time domain observations

Different parameters a

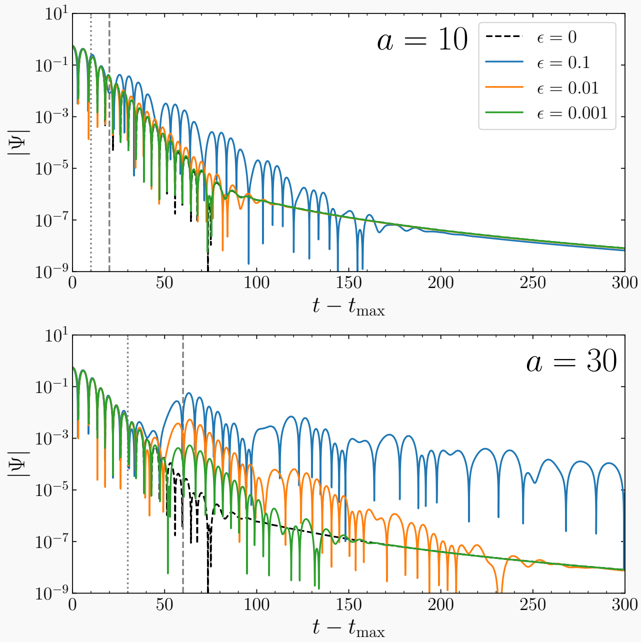

Observation 1

If a increases, the damping time increases

Stability with respect to th perturbation amplitude ϵ

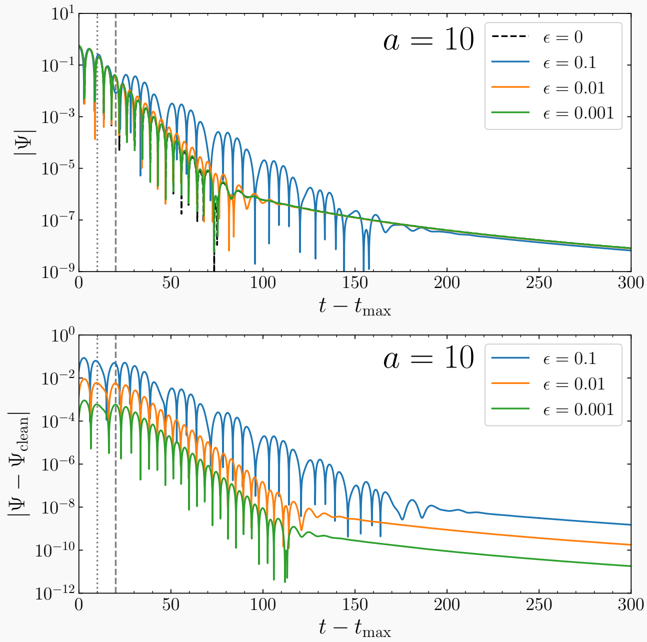

Observation 2

A bump of size ϵ entails a proportionately sized perturbation of order ϵ on the ringdown waves

Part II
The frequency-domain observations

Comparison procedure

Frequency ω_n inferred theoretically

Eigenfrequencies computed directly from the wave equation

Frequency ω_n given by the fit of the numerical results

$$\Psi(t) = \sum_{n=0}^{N-1} A_n \exp(-\imath(\underline{\omega_n} t - \phi_n))$$
$$= \sum_{n=0}^{N-1} A_n \exp(\underline{\omega_{nI}} t) \cos(\underline{\omega_{nR}} t - \phi_n)$$

Fitting range highlight

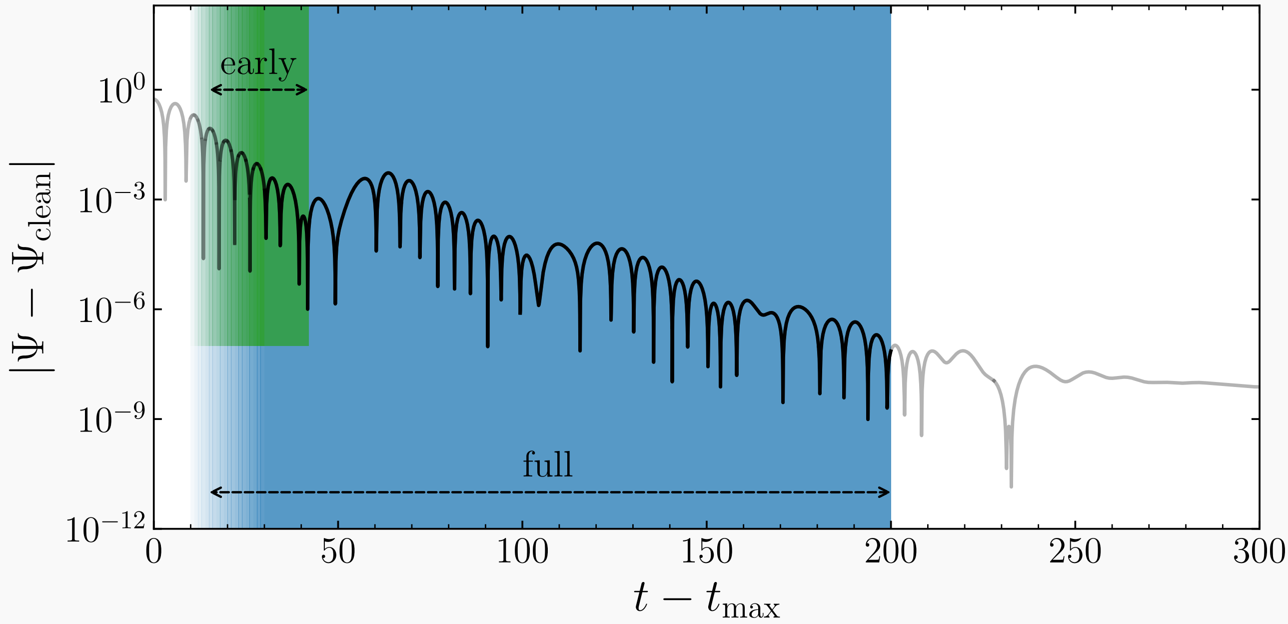

QNMs fitted on the first train of the initial ringdown only

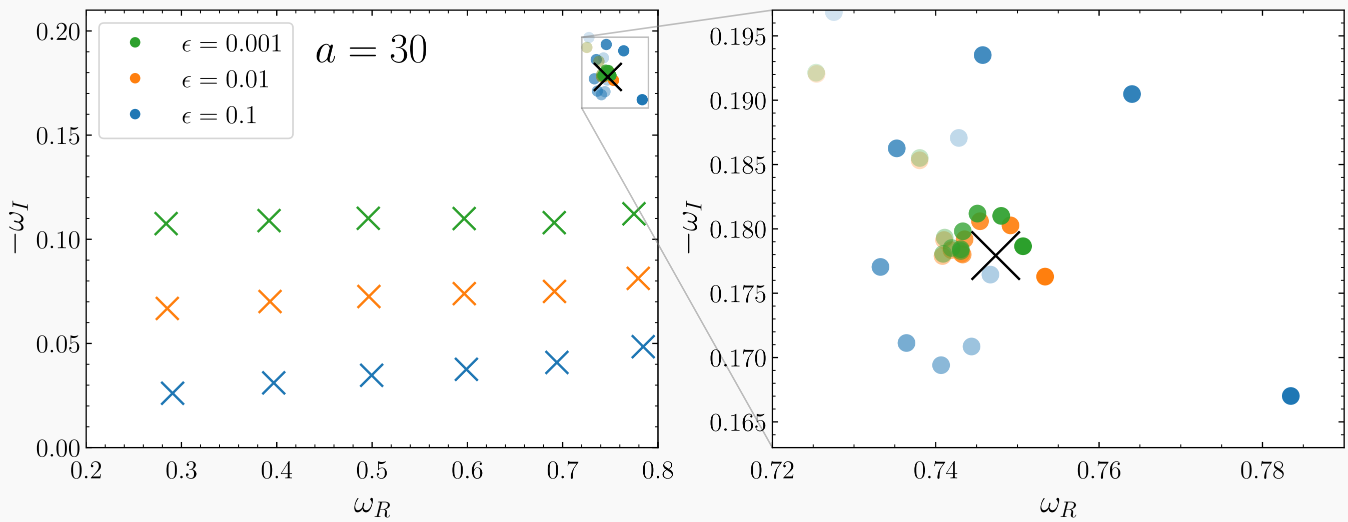

QNMs fitted on the full range

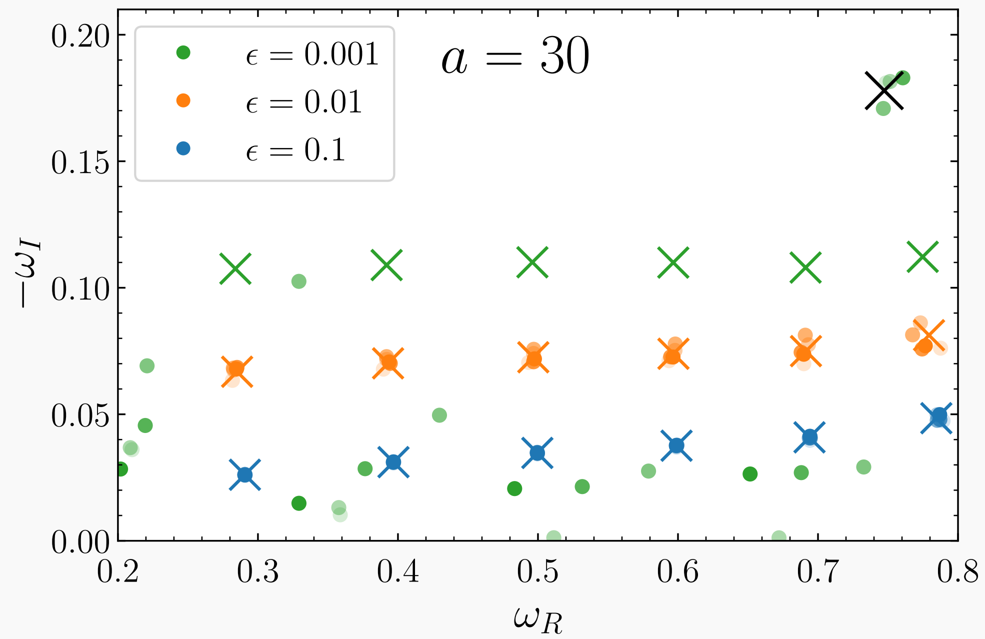

Conclusion and outlook

Main message

- Spectral instability results obtained in the frequency domain should not be used naively in the interpretation of time-domain signals.
- In particular, the spectral instability of the fundamental QNM does not imply an instability of the "physical" fundamental ringdown QNM.

Outlook

- Overtones may exhibit a different behaviour and shall be investigated in another study

Thank you! 😃

Phys. Rev. D 106, 084011 — arXiv:2205.08547

. . .

arXiv:2205.08547

Summary of the plots obtained in the time-domain

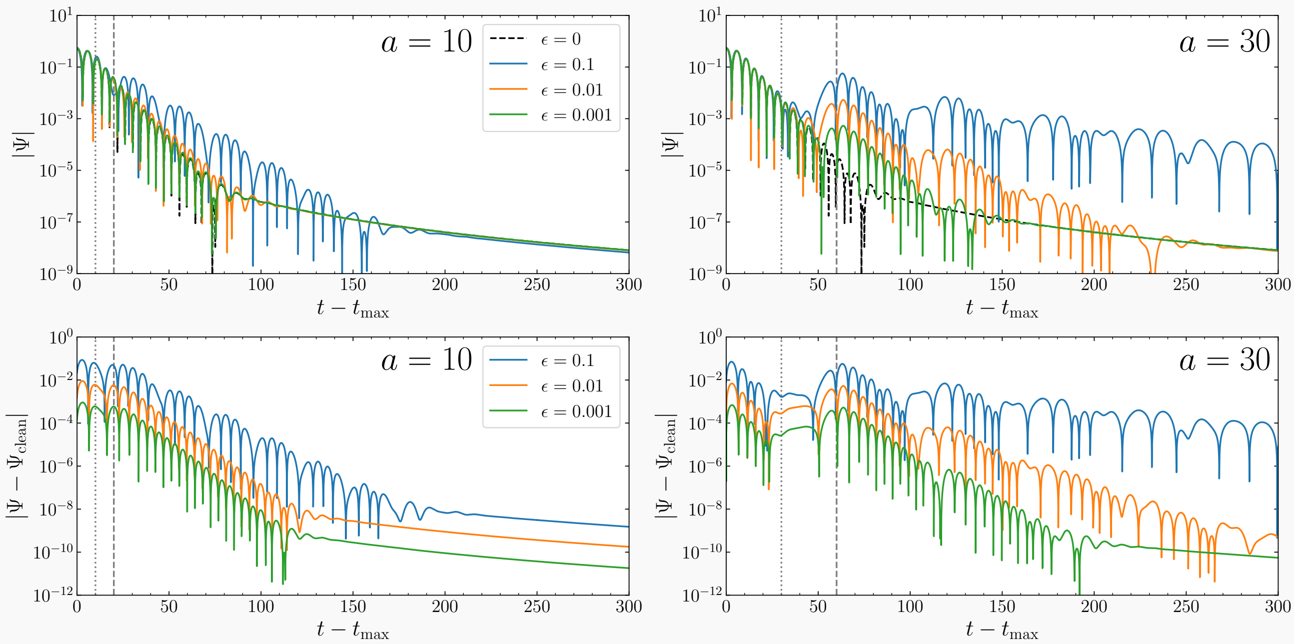

Shooting method

- The eigenfrequencies ω_n can be computed directly from the wave equation with a Laplace transform, *i.e.* by solving the equation

$$\frac{\partial^2 \Psi}{\partial r_\star^2} + \left(\omega^2 - V\right)\Psi = 0$$

- The QNM frequencies ω_n correspond to the poles of the Green's function of the above equation, with the appropriate boundary conditions of ingoing waves at $r_\star = -\infty$ and outgoing waves at $r_\star = +\infty$.
- The frequencies can be found by a shooting method: we start from each of the two boundaries and numerically integrate inwards or outwards iteratively, searching for the roots of the Wronskian *i.e.* the values of ω for which the two solutions match smoothly in an intermediate region.

QNMs obtained via fitting the full range, at $a = 10$ and $a = 30$

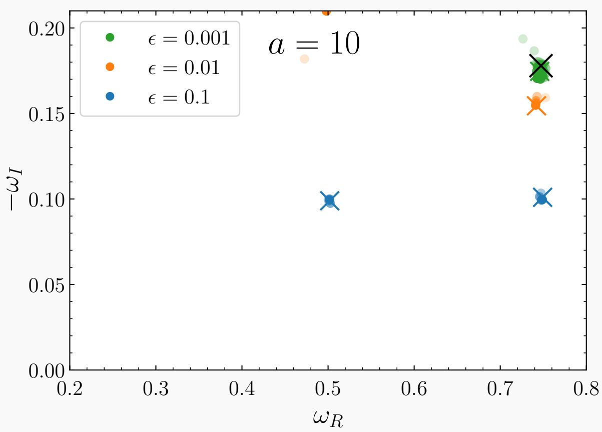

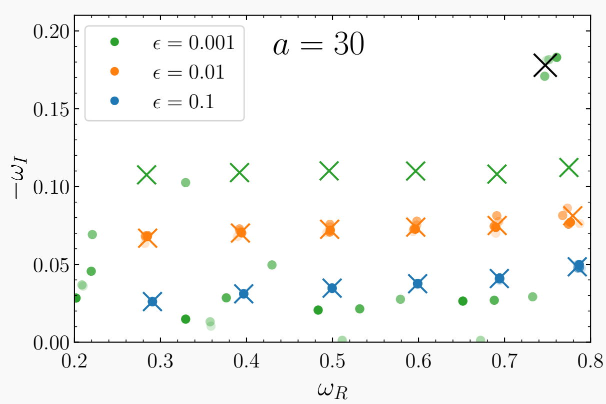

QNMs obtained via improved fitting and the shooting method, for $\epsilon = 0.001$

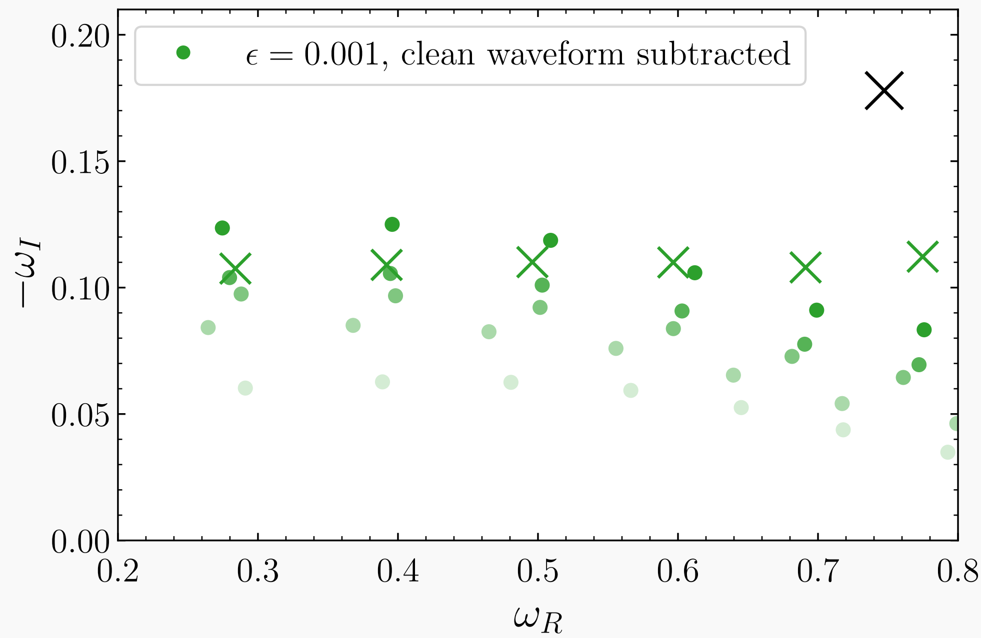

Observation of quasi-normal mode overtones in ringdown gravitational waves

Norichika Sago (Kyoto U./Osaka Metropolitan U.)
Collaborator: Takahiro Tanaka, Hiroyuki Nakano

2022.10.25 JGRG31 (online)

Ringdown (RD) GW

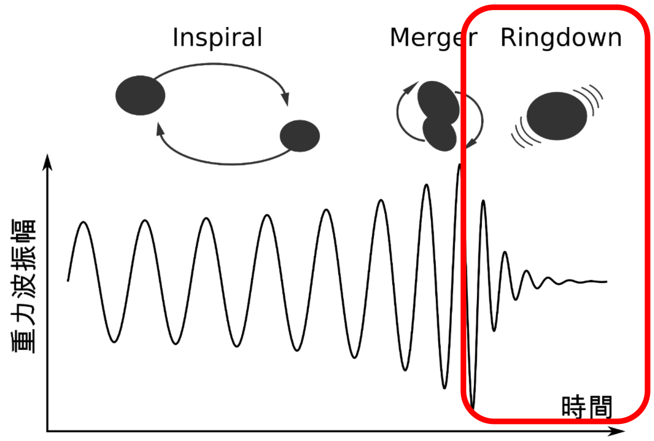

- Damped oscillation GW just after the merger phase.
- Expressed well by quasi-normal modes (QNMs).

$$h(t) = Ae^{-(t-t_0)/\tau}\cos[2\pi f_0(t-t_0)+\phi_0]$$

- The frequency and decay time (f_0, τ) are determined by the mass and spin of the remnant BH.

Effects of overtones on RD

Giesler et al. (2019)

Waveform model (l=m=2)
fundamental tone + N overtones

$$h^N(t) = \sum_{n=0}^{N} A_n \exp[-i\omega_n(t-t_p) + \phi_n]$$

ω_n : (complex) QNM frequency
t_c : starting time of fit
A_n, ϕ_n : model parameters

The RD part of SXS data is expressed well by the model with overtones even near the peak time.
Overtones cannot be negligible.

[arXiv:1903.08284]

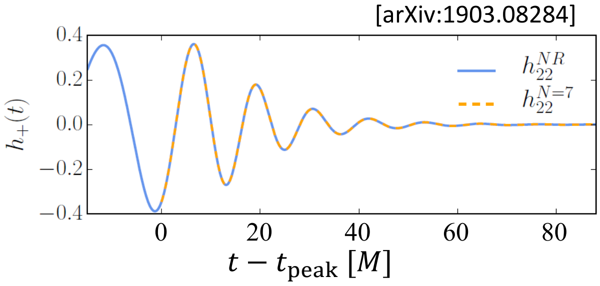

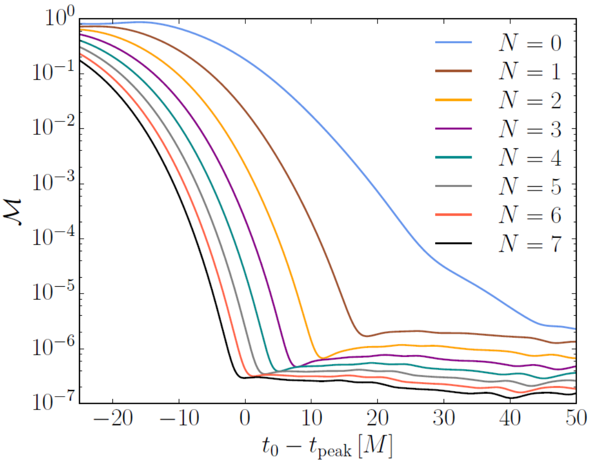

Aim of this work

Question
How accurately can we determine the model parameters from the real data of GW observation?

Errors in the model parameters
- Systematic errors due to
  - Ambiguity of the model (how many overtones included in the model)
  - Effect of source/non-linearity.
- Statistical error due to the detector noise.

Robustness of the model parameters

If the linear perturbation is relevant, the model parameters are constant, regardless of the starting time of fit.

<u>Mock data (fundamental + 1st and 2nd overtones)</u>

$$h_{\mathrm{mock}} = W(t-t_p)\sum_{n=0}^{2} e^{-(t-t_p)/\tau_n}\cos[\omega_n(t-t_p)]$$

Window func.

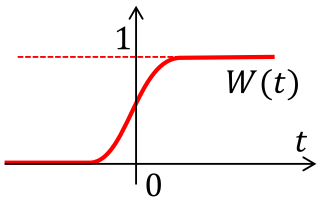

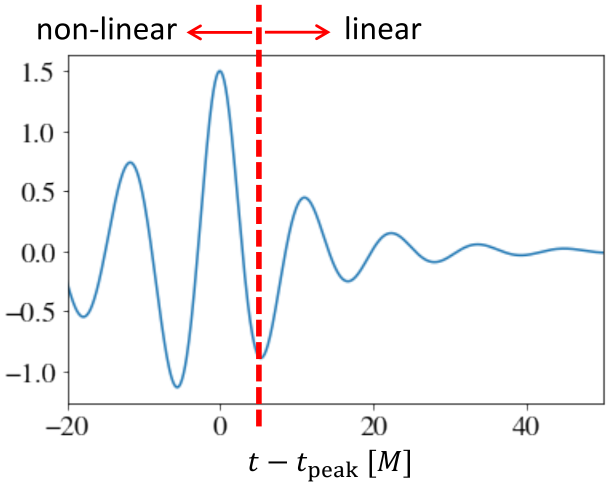

Dependence on the starting time (Mock data)

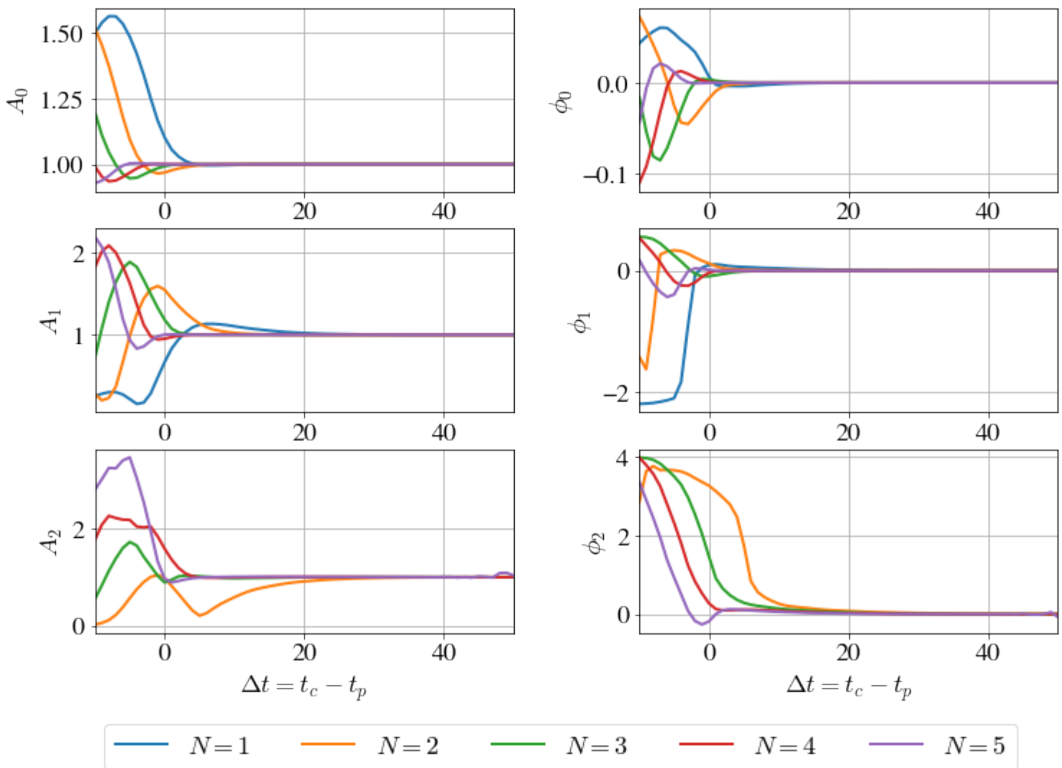

NR data

ID	Mass ($M_{\rm rem}/M$)	Spin ($\chi_{\rm rem}$)	Reference
SXS:BBH:0305	0.952032939704	0.6920851868180025	[66,124,125]

- SXS:BBH:0305 ⋯ GW150914-like data
- We focus only on $(l, m) = (2,2)$ mode.

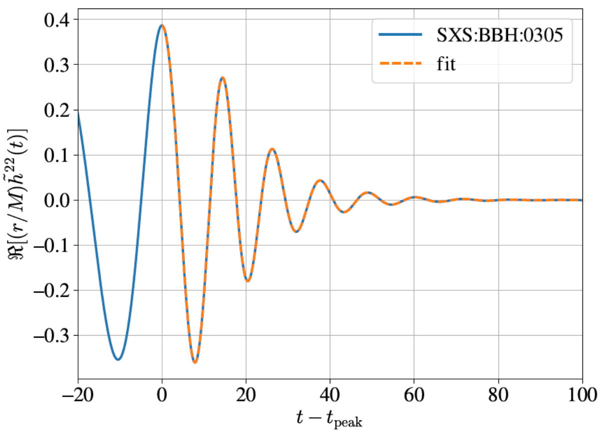

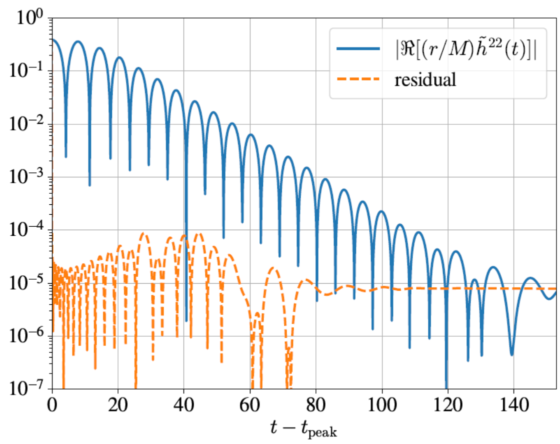

[NS, Isoyama, Nakano (2021)]

Dependence on t_c (SXS:BBH:0305)

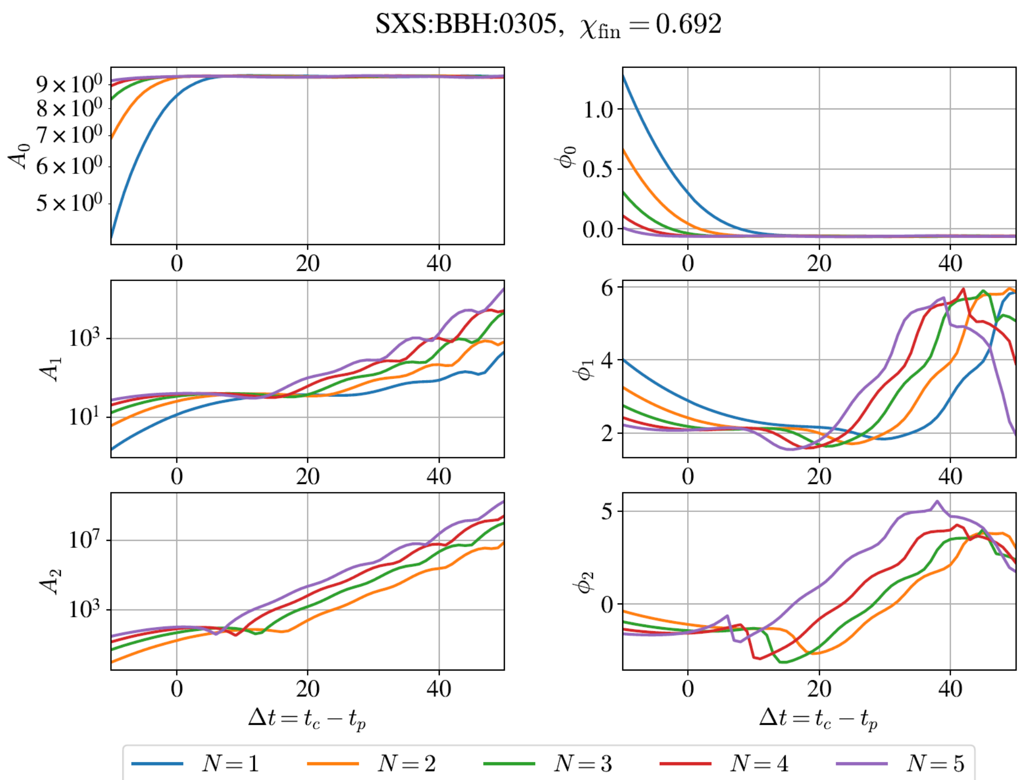

Dependence on t_c (SXS:BBH:0305)

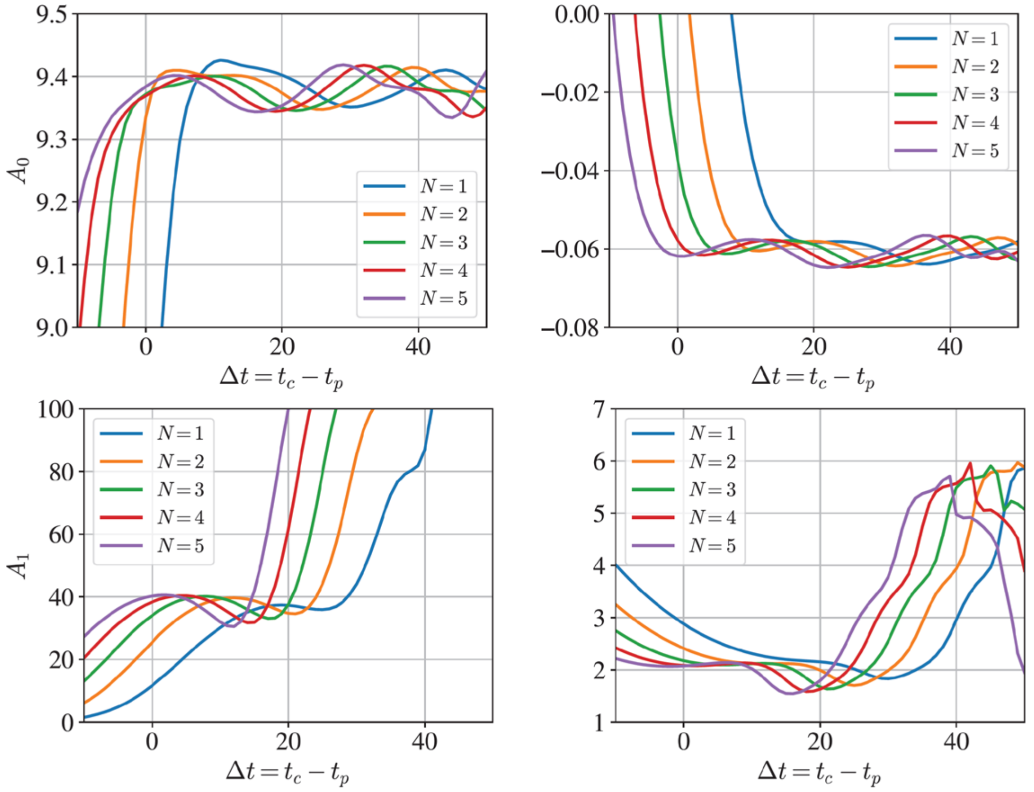

Estimate the model parameters

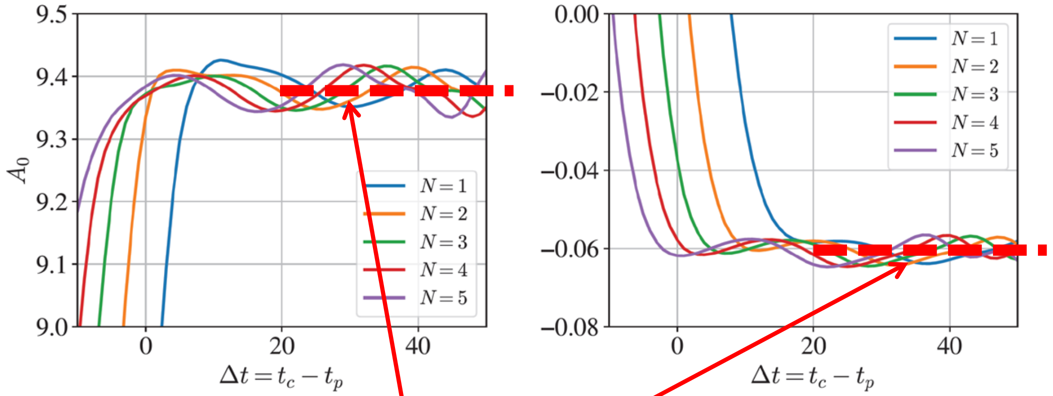

We estimate the model parameters, $\bar{A}_n, \bar{\phi}_n$, by taking the average in late time ($20 \leq t_c - t_p \leq 50$).

<u>Systematic errors</u>

$$\Delta A_n \equiv A_n - \bar{A}_n$$
$$\Delta \phi_n \equiv \phi_n - \bar{\phi}_n$$

Estimate the systematic error

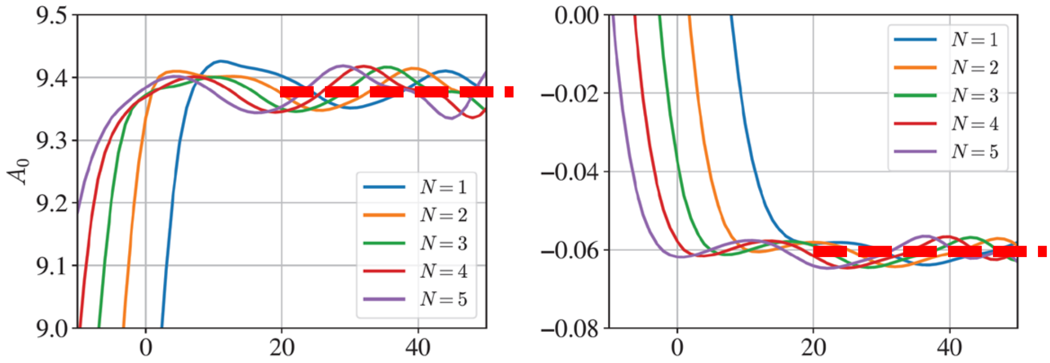

$\Delta A_n \equiv A_n - \bar{A}_n$ $\qquad$ $\Delta\phi_n \equiv \phi_n - \bar{\phi}_n$

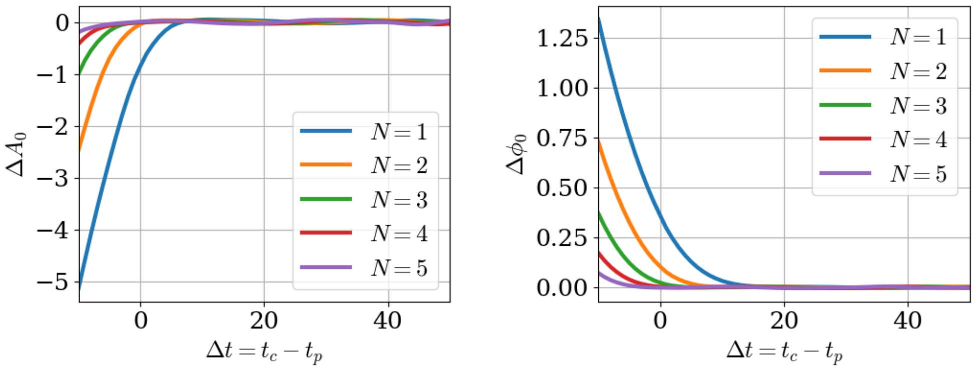

Statistical errors of the model parameters

Estimate the statistical errors assuming the white noise of detector.

$$\langle n(t)n(t')\rangle = \delta(t-t')$$

Black solid line:
ΔA_0 (systematic error)

Shaded region:
δA_0 (statistical error)

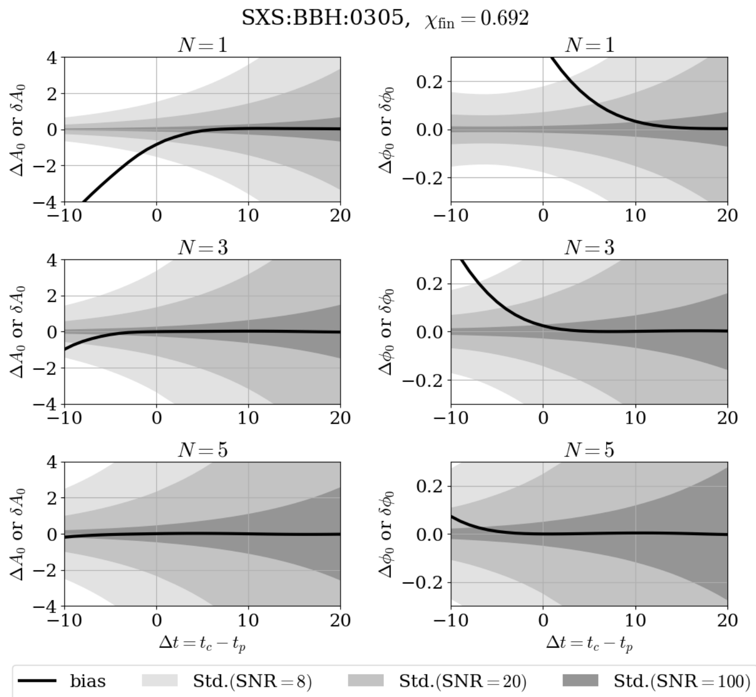

Optimal starting time for fit

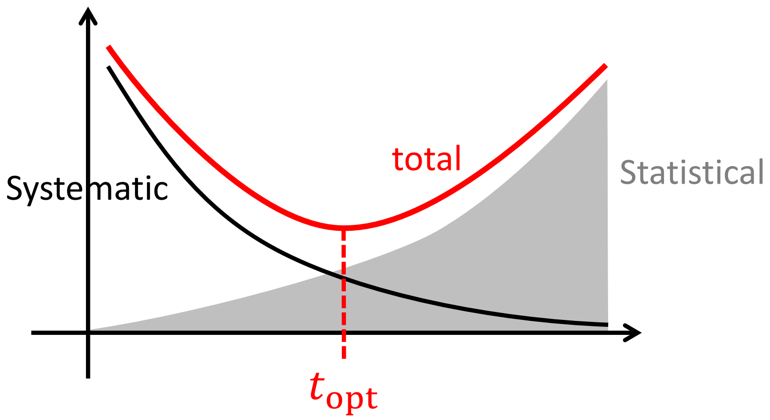

We find the optimal starting time, $t_{\rm opt}$, at which the total error of the parameter is minimized.

$$\mathrm{Err}[A_0] = \sqrt{(\Delta A_0)^2 + (\delta A_0)^2}$$
$$\mathrm{Err}[\phi_0] = \sqrt{(\Delta \phi_0)^2 + (\delta \phi_0)^2}$$

Parameter estimation error

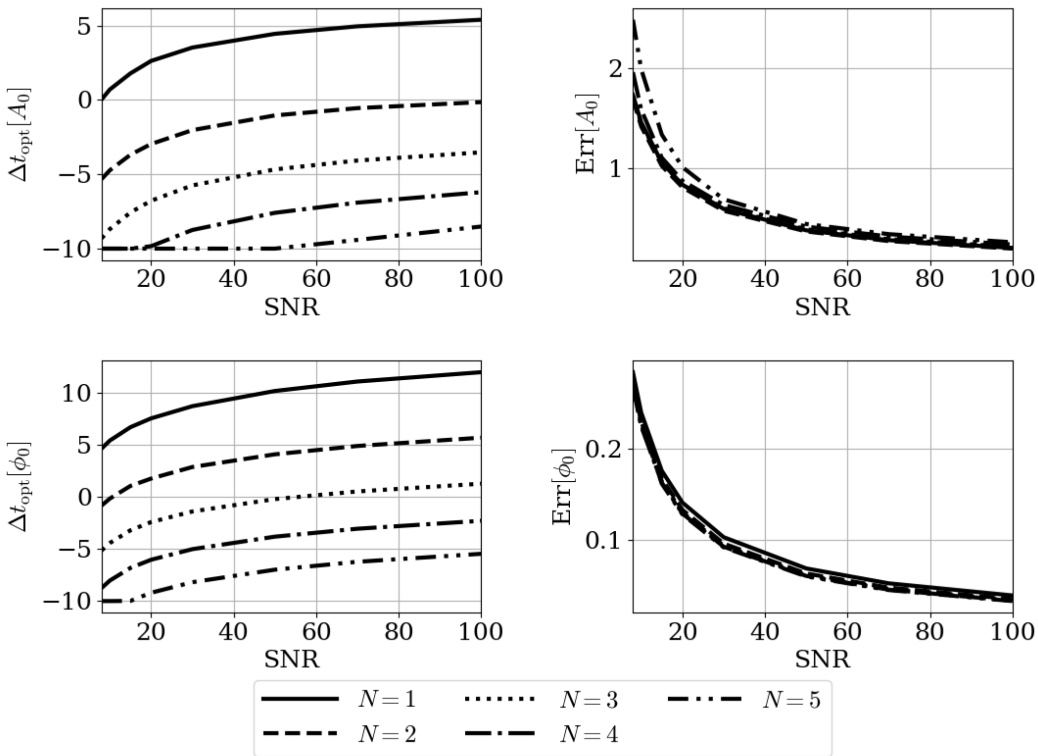

Summary

- We try to read the model parameters of QNM fit from GW150914-like signal (SXS:BBH:0305).
  Fundamental mode: OK   Overtones: Difficult?
- We estimate the systematic, statistical and total errors of the model parameters for the fundamental tone.
  total error～10% (amplitude) and ～4% (phase) for SNR=20

Open issues

- The model parameters of the overtones cannot be determined?
  (even in the case that the spin of the remnant BH is large)
  higher multipoles, late-time tail, changes of mass/spin …
- Analysis for more realistic noise of detectors
  (non-Gaussian, frequency dependence, etc)

C40

Searching for gravitational wave echoes from binary black hole mergers

Nami Uchikata (ICRR)

Hiroyuki Nakano (Ryukoku Univ.), Tatsuya Narikawa (ICRR), Norichika Sago (Kyoto Univ.), Hideyuki Tagoshi (ICRR), and Takahiro Tanaka (Kyoto Univ.)

JGRG31 October 25, 2022

Introduction

- ~ 90 gravitational wave signals from binary black hole (BBH) mergers (LIGO-Virgo-KAGRA collaborations 2021)
- Any possibility of other compact objects?
- Search for possible sequences of pulse-like signals after the compact binary coalescence

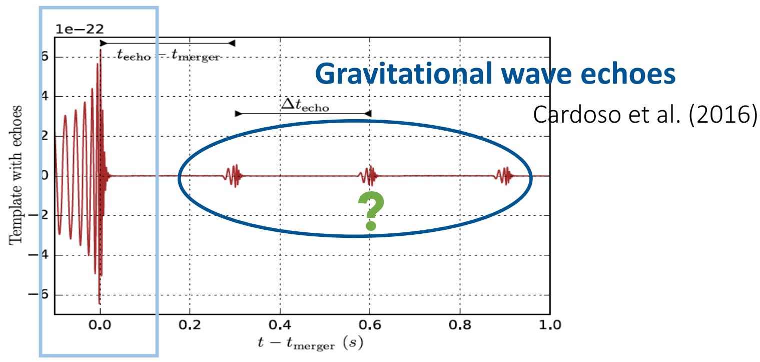

Binary black hole merger

Abedi et al. (2017)

Possible source objects

- Theoretical compact object models

Ex) Boson stars, gravastars, wormholes, …

- (Quantum black holes)

- Existence of unstable photon orbit
- Absence of the event horizon

- Observation

→ the modification of the classical horizon?

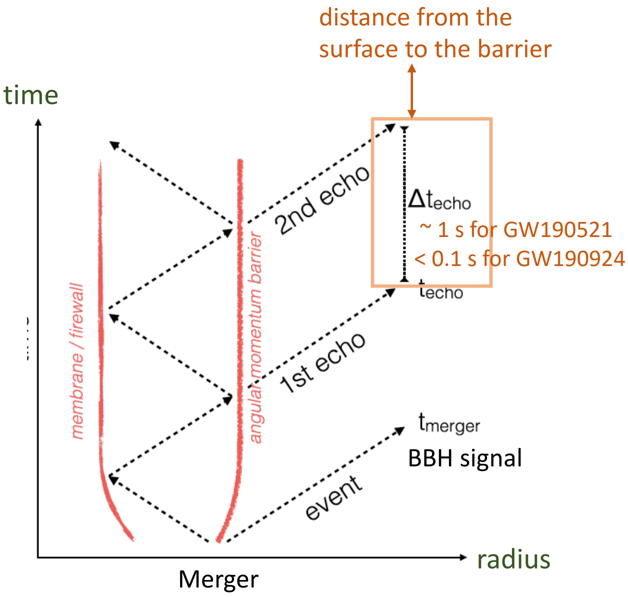

Abedi et al. (2017)

Previous analyses:

Search method	O1	O2	O3a	O3b
Template based	• 2.5 σ evidence (Abedi et al. 2017) • Low significance (Westerweck et al. 2017, **Uchikata et al. 2018**, Nielsen et al. 2019)	• Low significance (LVC 2021, **Uchikata et al. 2018**)	• Low significance (LVC 2021) • Bayes factor = 7 for GW190521 (Abedi et al. 2022) • **This study**	• **This study**
Model independent	• Low significance (Salemi et al. 2019, Tsang et al. 2020)	• 4.2 σ evidence for GW170817 (Abedi & Afshordi 2019) • Low significance (Salemi et al. 2019, Tsang et al. 2020)	• 2.5 σ evidence but inconclusive for GW190521 (Abedi et al. 2022)	• Low significance (LVK 2022)

This study

Search for echo signals in O1 ~ O3 events using two templates:

1. Originally given by Abedi et al. 2017: Simple model

2. Taking into account physical effects (black hole perturbations) (Nakano et al. 2017): BHP model

Common assumptions:

- The spacetime is Kerr with a modification in the vicinity of the horizon. (Mass M and spin a)
- Perfect reflection at the surface of the object.

Method of analysis : templates (Abedi et al. 2017, Nakano et al. 2017)

Inspiral-merger-ringdown

1. Simple model: repetition of a cutoff IMR waveform with a constant reflection rate γ and an interval of each echo Δt_{echo}

$$\tilde{h}_1(f) = \underbrace{\tilde{h}_0(f)}_{\Theta(t_0) h_{IMR}(t)} \sum_{n=1}^{N} \gamma^{n-1} \underbrace{(-1)^{n-1}}_{\text{phase shift}} e^{-i[2\pi f \Delta t_{\mathrm{echo}}](n-1)}$$

cutoff function

Search parameters: $(\gamma, \Delta t_{\mathrm{echo}}(a, M))$
Initial phase is fixed to 0.

Black hole perturbation

2. BHP model: Frequency dependent reflection rate $R(f; a, M)$

$$\tilde{h}_2(f) = \sqrt{1 - R^2(f)}\, \tilde{h}_0(f) \times \sum_{n=1}^{N} R(f)^{n-1} e^{-i[2\pi f \Delta t_{\mathrm{echo}} + \underbrace{\phi(f)}_{\text{phase shift}}](n-1)}$$

Search parameters: $(a, M, \phi(f) \approx \phi_0)$
Optimize the initial phase.

N: Number of echoes depends on the length of Δt_{echo} , (10, 15, 20, 30).

Examples: best fit templates for GW190412

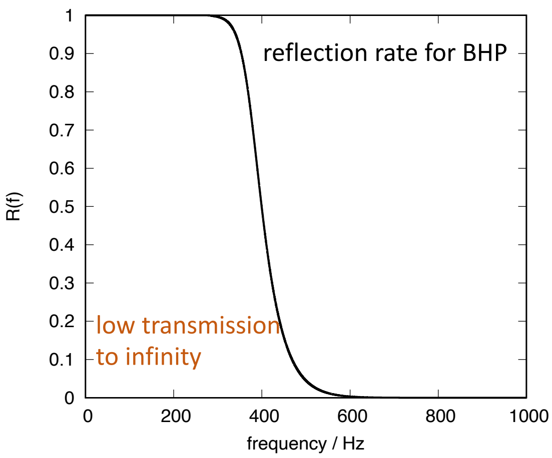

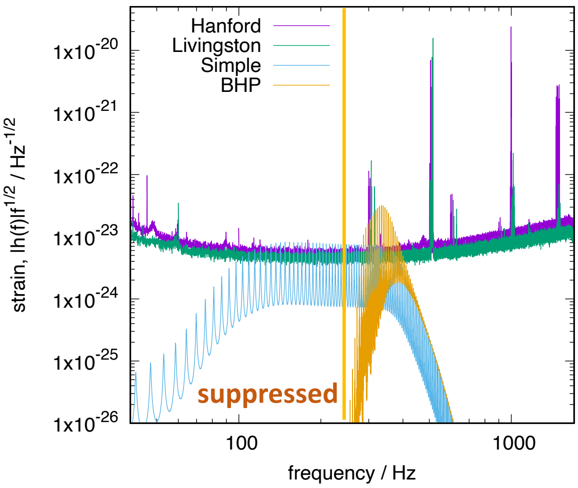

Method of analysis : Evaluation of significance (Abedi et al. 2017)

- Search for the maximum of matched filter signal-to-noise ratio (SNR)

$$\rho \equiv (x, s_t) = 4\,\mathrm{Re}\left(\int_0^\infty \frac{\tilde{x}(f)\tilde{s_t}^*(f)}{S_n(f)} df\right),$$

$\tilde{x}$: data
$\tilde{s_t}$: template (Simple/BHP)
S_n: noise power spectrum

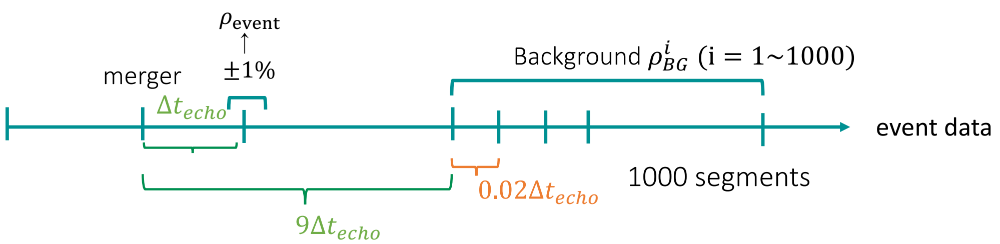

P-value: $P = \frac{\#(\rho_{BG}^i \geq \rho_{\mathrm{event}})}{1000}$

Larger p-value: likely to be noise

Events and data

- O1, O2 and O3 events
  - with FAR < 10^{-3} yr^{-1} (cf. LVK testing GR papers)
  - Observed by Livingston and Hanford.
  - Compute p-value for each event.
- Data are from GWOSC. (https://www.gw-openscience.org/eventapi/html/allevents/)

- Data length: 32 or 64 seconds for each event. (depends on the length of Δt_{echo})
- Welch's method for estimation of power spectrum density.

- KAGALI is partly used.

Results: Distribution of p-values for all events

- Consistent with noise = uniform distribution (null hypothesis)
- On source data: search for echo signals
- Off source data: do not contain possible GW signals. (subsequent data)

Slight deviation from the Null hypothesis for both templates.

But consistent with the off source data (noise only data).

No evidence of echo signals.

On source data

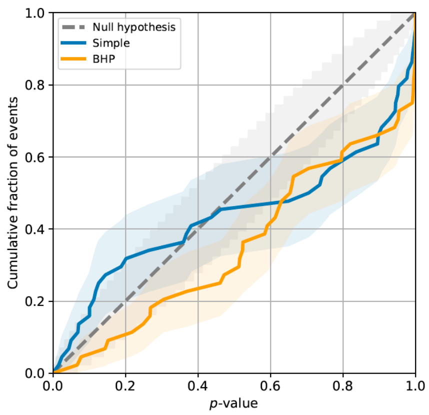

Off source data

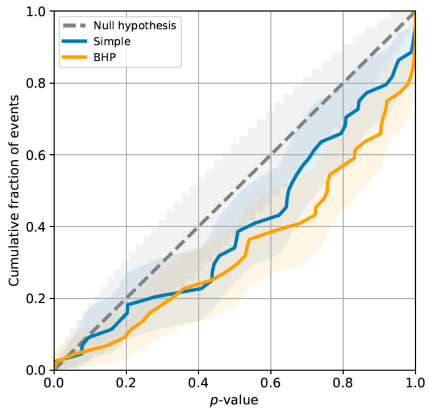

Summary

- We have analyzed gravitational wave echo signals from O1, O2 and O3 events using two templates.
  - Simple model: Repetition of the same waveform.
  - BHP model: Includes black hole perturbations. Suppresses lower frequency signals.

- P-value distributions slightly deviate from the null hypothesis, but consistent with the distributions obtained from the noise only data.

- No evidence for echo signals modeled by Simple/BHP models.